World Journal of Gastroenterology®

Volume 13 Number 7
February 21, 2007

National Journal Award
2005

The WJG Press

The WJG Press, Apartment 1066 Yishou Garden, 58 North Langxinzhuang Road, PO Box 2345, Beijing 100023, China
Telephone: +86-10-85381892
Fax: +86-10-85381893
E-mail: wjg@wjgnet.com
http: //www.wjgnet.com

ISSN 1007-9327 CN 14-1219/R Local Post Offices Code No. 82-261

World Journal of Gastroenterology www.wjgnet.com Volume 13 Number 7 Feb 21 2007

ISSN 1007-9327
CN 14-1219/R

WJG

World Journal of Gastroenterology®

Indexed and Abstracted in:

Current Contents®/Clinical Medicine, Science Citation Index Expanded (also known as SciSearch®) and Journal Citation Reports/Science Edition, *Index Medicus*, MEDLINE and PubMed, Chemical Abstracts, EMBASE/Excerpta Medica, Abstracts Journals, *Nature Clinical Practice Gastroenterology and Hepatology*, CAB Abstracts and Global Health.
ISI JCR 2003-2000 IF: 3.318, 2.532, 1.445 and 0.993.

Volume 13 Number 7
February 21, 2007

World J Gastroenterol
2007 February 21; 13(7): 985-1148
Online Submissions
www.wjgnet.com/wjg/index.jsp
www.wjgnet.com
Printed on Acid-free Paper

A Weekly Journal of Gastroenterology and Hepatology

National Journal Award
2005

World Journal of Gastroenterology®

Volume 13 Number 7
February 21, 2007

The WJG Press

Contents

REVIEW

985 p53 gene in treatment of hepatic carcinoma: *Status quo*
Guan YS, La Z, Yang L, He Q, Li P

993 Metallothionein: An overview
Thirumoorthy N, Manisenthil Kumar KT, Shyam Sundar A, Panayappan L, Chatterjee M

ESOPHAGEAL CANCER

997 Cytochrome P450 levels are altered in patients with esophageal squamous-cell carcinoma
Bergheim I, Wolfgarten E, Bollschweiler E, Hölscher AH, Bode C, Parlesak A

LIVER CANCER

1003 Successful initial ablation therapy contributes to survival in patients with hepatocellular carcinoma
Morimoto M, Numata K, Sugimori K, Shirato K, Kokawa A, Oka H, Hirasawa K, Koh R, Nihommatsu H, Tanaka K

1010 Rab23 is a potential biological target for treating hepatocellular carcinoma
Liu YJ, Wang Q, Li W, Huang XH, Zhen MC, Huang SH, Chen LZ, Xue L, Zhang HW

COLORECTAL CANCER

1018 Decreased fragile histidine triad expression in colorectal cancer and its association with apoptosis inhibition
Cao J, Chen XP, Li WL, Xia J, Du H, Tang WB, Wang H, Chen XW, Xiao HQ, Li YY

VIRAL HEPATITIS

1027 Hepatitis B virus infection and replication in primarily cultured human fetal hepatocytes
Lin M, Chen Q, Yang LY, Li WY, Cao XB, Wu JR, Peng YP, Chen MR

BASIC RESEARCH

1032 Role of soluble factors and three-dimensional culture in *in vitro* differentiation of intestinal macrophages
Spoettl T, Hausmann M, Menzel K, Piberger H, Herfarth H, Schoelmerich J, Bataille F, Rogler G

1042 Evidence for a sequential transfer of iron amongst ferritin, transferrin and transferrin receptor during duodenal absorption of iron in rat and human
Kolachala VL, Sesikeran B, Nair KM

1053 Influence of heme oxygenase-1 gene transfer on the viability and function of rat islets in *in vitro* culture
Chen XB, Li YX, Jiao Y, Dong WP, Li G, Chen J, Tan JM

1060 Uric acid enhances T cell immune responses to hepatitis B surface antigen-pulsed-dendritic cells in mice
Ma XJ, Tian DY, Xu D, Yang DF, Zhu HF, Liang ZH, Zhang ZG

CLINICAL RESEARCH

1067 Feasibility and safety of autologous bone marrow mononuclear cell transplantation in patients with advanced chronic liver disease
Lyra AC, Soares MBP, da Silva LFM, Fortes MF, Silva AGP, Mota ACA, Oliveira SA, Braga EL, de Carvalho WA, Genser B, dos Santos RR, Lyra LGC

World Journal of Gastroenterology
Volume 13 **Number** 7 **February** 21, 2007

Contents

RAPID COMMUNICATION

1074 Hepatitis C risk assessment, testing and referral for treatment in urban primary care: Role of race and ethnicity
Trooskin SB, Navarro VJ, Winn RJ, Axelrod DJ, McNeal AS, Velez M, Herrine SK, Rossi S

1079 A new oral formulation for the release of sodium butyrate in the ileo-cecal region and colon
Roda A, Simoni P, Magliulo M, Nanni P, Baraldini M, Roda G, Roda E

1085 Possible role of human cytomegalovirus in pouchitis after proctocolectomy with ileal pouch-anal anastomosis in patients with ulcerative colitis
Casadesus D, Tani T, Wakai T, Maruyama S, Iiai T, Okamoto H, Hatakeyama K

1090 Frequent loss of heterozygosity in two distinct regions, 8p23.1 and 8p22, in hepatocellular carcinoma
Lu T, Hano H, Meng C, Nagatsuma K, Chiba S, Ikegami M

1098 KIT-negative gastrointestinal stromal tumors with a long term follow-up: A new subgroup does exist
Kontogianni-Katsarou K, Lariou C, Tsompanaki E, Vourlakou C, Kairi-Vassilatou E, Mastoris C, Pantazi G, Kondi-Pafiti A

1103 NCB-02 (standardized Curcumin preparation) protects dinitrochlorobenzene-induced colitis through down-regulation of NF_{κ}-B and iNOS
Venkataranganna MV, Rafiq Md, Gopumadhavan S, Peer G, Babu UV, Mitra SK

1108 Primary duodenal neoplasms: A retrospective clinico-pathological analysis
Bal A, Joshi K, Vaiphei K, Wig JD

1112 Aqueous suspension of anise "*Pimpinella anisum*" protects rats against chemically induced gastric ulcers
Al Mofleh IA, Alhaider AA, Mossa JS, Al-Sohaibani MO, Rafatullah S

1119 *H pylori* are associated with chronic cholecystitis
Chen DF, Hu L, Yi P, Liu WW, Fang DC, Cao H

1123 Effect of parenteral and early intrajejunal nutrition on pancreatic digestive enzyme synthesis, storage and discharge in dog models of acute pancreatitis
Qin HL, Su ZD, Hu LG, Ding ZX, Lin QT

1129 Mechanisms involved in ceramide-induced cell cycle arrest in human hepatocarcinoma cells
Wang J, Lv XW, Shi JP, Hu XS

CASE REPORTS

1135 Pancreatic metastasis of leiomyosarcoma in the right thigh: A case report
Koh YS, Chul J, Cho CK, Kim HJ

1138 A prophylactic approach for bone marrow transplantation from a hepatitis B surface antigen-positive donor
Sobhonslidsuk A, Ungkanont A

1141 Lipoma within inverted Meckel's diverticulum as a cause of recurrent partial intestinal obstruction and hemorrhage: A case report and review of literature
Karadeniz Cakmak G, Emre AU, Tascilar O, Bektaş S, Ucan BH, Irkorucu O, Karakaya K, Ustundag Y, Comert M

ACKNOWLEDGMENTS

1144 Acknowledgments to Reviewers of *World Journal of Gastroenterology*

APPENDIX

1145 Meetings

1146 Instructions to authors

World Journal of Gastroenterology
Volume 13 **Number** 7 **February** 21, 2007

Contents

FLYLEAF	I-V	Editorial Board
INSIDE FRONT COVER		Online Submissions
INSIDE BACK COVER		International Subscription

Responsible E-Editor for this issue: Wen-Hua Ma

C-Editor for this issue: Dr. Osman Cavit Ozdogan

Responsible S-Editor for this issue: Jing Wang

World Journal of Gastroenterology (*World J Gastroenterol , WJG*), a leading international journal in gastroenterology and hepatology, has an established reputation for publishing first class research on esophageal cancer, gastric cancer, liver cancer, viral hepatitis, colorectal cancer, and *H pylori* infection, providing a forum for both clinicians and scientists, and has been indexed and abstracted in Current Contents®/Clinical Medicine, Science Citation Index Expanded (also known as SciSearch®) and Journal Citation Reports/Science Edition, *Index Medicus*, MEDLINE and PubMed, Chemical Abstracts, EMBASE/Excerpta Medica, Abstracts Journals, *Nature Clinical Practice Gastroenterology and Hepatology*, CAB Abstracts and Global Health. ISI JCR 2003-2000 IF: 3.318, 2.532, 1.445 and 0.993. *WJG* is a weekly journal published by The WJG Press. The publication date is on 7th, 14th, 21st, and 28th every month. The *WJG* is supported by The National Natural Science Foundation of China, No. 30224801 and No.30424812, which was founded with a name of *China National Journal of New Gastroenterology* on October 1,1995, and renamed as *WJG* on January 25, 1998.

PUBLISHED BY
The WJG Press

PRINTED BY
Printed in Beijing on acid-free paper by Beijing Kexin Printing House

Print ISSN 1007-9327
CN 14-1219/R

EDITORIAL OFFICE
World Journal of Gastroenterology,
The WJG Press, Apartment 1066 Yishou Garden, 58 North Langxinzhuang Road, PO Box 2345, Beijing 100023, China
Telephone: +86-10-85381892
Fax: +86-10-85381893
E-mail: wjg@wjgnet.com
http://www.wjgnet.com

SUBSCRIPTION AND AUTHOR REPRINTS
Jing Wang
The WJG Press, Apartment 1066 Yishou Garden, 58 North Langxinzhuang Road, PO Box 2345, Beijing 100023, China
Telephone: +86-10-85381892
Fax: +86-10-85381893
E-mail: j.wang@wjgnet.com
http://www.wjgnet.com

SUBSCRIPTION INFORMATION
Institutional Price 2007: USD 1500.00
Personal Price 2007: USD 700.00

INSTRUCTIONS TO AUTHORS
Full instructions are available online at http://www.wjgnet.com/wjg/help/instructions.jsp. If you do not have web access please contact the editorial office.

World Journal of Gastroenterology®

Editorial Board

2007-2009

Published by The WJG Press, PO Box 2345, Beijing 100023, China
Fax: +86-10-85381893 E-mail: wjg@wjgnet.com http://www.wjgnet.com

The *World Journal of Gastroenterology* Editorial Board consists of 916 members, representing a team of worldwide experts in gastroenterology and hepatology. They are from 55 countries, including Albania (1), Argentina (2), Australia (26), Austria (9), Belarus (1), Belgium (13), Brazil (1), Bulgaria (1), Canada (23), Chile (1), China (49), Croatia (2), Cuba (1), Czech (1), Denmark (5), Egypt (3), Finland (4), France (36), Germany (96), Greece (3), Hungary (2), Iceland (1), India (6), Iran (2), Ireland (4), Israel (6), Italy (71), Japan (163), Lebanon (3), Lithuania (1), Macedonia (1), Malaysia (3), Mexico (3), Monaco (1), Netherlands (21), New Zealand (1), Nigeria (1), Norway (3), Pakistan (1), Poland (6), Portugal (2), Russia (3), Serbia (1), Singapore (3), Slovakia (1), Slovenia (1), South Africa (1), South Korea (13), Spain (29), Sweden (9), Switzerland (12), Turkey (8), United Arab Emirates (1), United Kingdom (61), and United States (192).

Louis Libbrecht, *Leuven*
Etienne M Sokal, *Brussels*
Gert A Van Assche, *Leuven*
Yvan Vandenplas, *Brussels*
Eddie Wisse, *Keerbergen*

Brazil
Heitor Rosa, *Goiania*

Bulgaria
Zahariy Krastev, *Sofia*

Canada
Fernando Alvarez, *Québec*
David Armstrong, *Ontario*
Olivier Barbier, *Québec*
Nancy Baxter, *Toronto*
Matthew Bjerknes, *Toronto*
Frank J Burczynski, *Winnipeg*
Michael F Byrne, *Vancouver*
Wang-Xue Chen, *Ottawa*
Hugh J Freeman, *Vancouver*
Chantal Guillemette, *Québec*
Samuel S Lee, *Calgary*
Gary A Levy, *Toronto*
John K Marshall, *Ontario*
Donna-Marie McCafferty, *Calgary*
Thomas I Michalak, *St. John's*
Gerald Y Minuk, *Manitoba*
Paul Moayyedi, *Hamilton*
Eldon Shaffer, *Calgary*
Morris Sherman, *Toronto*
Alan BR Thomson, *Edmonton*
EF Verdu, *Ontario*
John L Wallace, *Calgary*
Eric M Yoshida, *Vancouver*

Chile
Silvana Zanlungo, *Santiago*

China
Henry LY Chan, *Hongkong*
Xiao-Ping Chen, *Wuhan*
Zong-Jie Cui, *Beijing*
Da-Jun Deng, *Beijing*
Sheung-Tat Fan, *Hong Kong*
Jin Gu, *Beijing*
De-Wu Han, *Taiyuan*
Ming-Liang He, *Hong Kong*
Wayne HC Hu, *Hong Kong*
Chee-Kin Hui, *Hong Kong*
Ching Lung Lai, *Hong Kong*
Kam Chuen Lai, *Hong Kong*
James YW Lau, *Hong Kong*
Yuk Tong Lee, *Hong Kong*
Suet Yi Leung, *Hong Kong*
Wai-Keung Leung, *Hong Kong*
Jing-Yun Ma, *Beijing*
Lun-Xiu Qin, *Shanghai*
Qin Su, *Beijing*
Wai-Man Wong, *Hong Kong*
Hong Xiao, *Beijing*
Dong-Liang Yang, *Wuhan*
Winnie Yeo, *Hong Kong*
Yuan Yuan, *Shenyang*
Man-Fung Yuen, *Hong Kong*
Jian-Zhong Zhang, *Beijing*
Xin-Xin Zhang, *Shanghai*
Shu Zheng, *Hangzhou*

Croatia
Tamara Cacev, *Zagreb*
Marko Duvnjak, *Zagreb*

Cuba
Damian Casadesus Rodriguez, *Havana*

Czech
Milan Jirsa, *Praha*

Denmark
Peter Bytzer, *Copenhagen*
Hans Gregersen, *Aalborg*
Jens H Henriksen, *Hvidovre*
Fin Stolze Larsen, *Copenhagen*
SØren MØller, *Hvidovre*

Egypt
Abdel-Rahman El-Zayadi, *Giza*
Sanaa Moharram Kamal, *Cairo*
Ayman Yosry, *Cairo*

Finland
Irma Elisabet Jarvela, *Helsinki*
Katri Maria Kaukinen, *Tampere*
Minna Nyström, *Helsinki*
Pentti Sipponen, *Espoo*

France
Bettaieb Ali, *Dijon*
Corlu Anne, *Rennes*
Denis Ardid, *Clermont-Ferrand*
Charles Paul Balabaud, *Bordeaux*
Soumeya Bekri, *Rouen*
Jacques Belghiti, *Clichy*
Pierre Brissot, *Rennes*
Patrice Philippe Cacoub, *Paris*
Franck Carbonnel, *Besancon*
Laurent Castera, *Pessac*
Bruno Clément, *Rennes*
Jacques Cosnes, *Paris*
Thomas Decaens, *Cedex*
Francoise Lunel Fabiani, *Angers*
Gérard Feldmann, *Paris*
Jean Fioramonti, *Toulouse*
Catherine Guettier, *Villejuif*
Chantal Housset, *Paris*
Juan Lucio Iovanna, *Marseille*
Rene Lambert, *Lyon*
Philippe Mathurin, *Lille*
Tamara Matysiak–Budnik, *Paris*
Francis Mégraud, *Bordeaux*
Richard Moreau, *Clichy*
Thierry Piche, *Nice*
Raoul Poupon, *Paris*
Jean Rosenbaum, *Bordeaux*
Jose Sahel, *Marseille*
Jean-Philippe Salier, *Rouen*
Jean-Yves Scoazec, *Lyon*
Khalid Ahnini Tazi, *Clichy*
Baumert F Thomas, *Strasbourg*
Emmanuel Tiret, *Paris*
MC Vozenin-brotons, *Villejuif*
Jean-Pierre Henri Zarski, *Grenoble*
Jessica Zucman-Rossi, *Paris*

Germany
HD Allescher, *Garmisch-Partenkirchen*
Martin Anlauf, *Kiel*
Rudolf Arnold, *Marburg*
Max G Bachem, *Ulm*
Thomas F Baumert, *Freiburg*
Daniel C Baumgart, *Berlin*
Hubert Blum, *Freiburg*
Thomas Bock, *Tuebingen*
Katja Breitkopf, *Mannheim*
Dunja Bruder, *Braunschweig*
Markus W Büchler, *Heidelberg*
Christa Buechler, *Regensburg*
Reinhard Buettner, *Bonn*
Elke Cario, *Essen*
Uta Dahmen, *Essen*
CF Dietrich, *Bad Mergentheim*
Rainer Josef Duchmann, *Berlin*
Paul Enck, *Tuebingen*
Fred Fändrich, *Kiel*
Ulrich Robert Fölsch, *Kiel*
Helmut Friess, *Heidelberg*
Peter R Galle, *Mainz*
Nikolaus Gassler, *Aachen*
Andreas Geier, *Aachen*
Dieter Glebe, *Giessen*
Burkhard Göke, *Munich*
Florian Graepler, *Tuebingen*
Axel M Gressner, *Aachen*
Veit Gülberg, *Munich*
Rainer Haas, *Munich*
Eckhart Georg Hahn, *Erlangen*
Stephan Hellmig, *Kiel*
Martin Hennenberg, *Bonn*
Johannes Herkel, *Hamburg*
Klaus Herrlinger, *Stuttgart*
Eberhard Hildt, *Berlin*
Joerg C Hoffmann, *Berlin*
Ferdinand Hofstaedter, *Regensburg*
Werner Hohenberger, *Erlangen*
RG Jakobs, *Ludwigshafen*
Jutta Keller, *Hamburg*
Andrej Khandoga, *Munich*
Sibylle Koletzko, *München*
Stefan Kubicka, *Hannover*
Joachim Labenz, *Siegen*
Frank Lammert, *Bonn*
Thomas Langmann, *Regensburg*
Christian Liedtke, *Aachen*
Matthias Löhr, *Mannheim*
Christian Maaser, *Muenster*
Ahmed Madisch, *Dresden*
Michael Peter Manns, *Hannover*
Stephan Miehlke, *Dresden*
Sabine Mihm, *Göttingen*
Silvio Nadalin, *Essen*
Markus F Neurath, *Mainz*
Johann Ockenga, *Berlin*
Florian Obermeier, *Regensburg*
Gustav Paumgartner, *Munich*
Ulrich Ks Peitz, *Magdeburg*
Markus Reiser, *Bochum*
Steffen Rickes, *Magdeburg*
Gerhard Rogler, *Regensburg*
Tilman Sauerbruch, *Bonn*
Dieter Saur, *Munich*
Andreas Schäffler, *Regensburg*
Hans Scherubl, *Berlin*
Joerg Schirra, *Munich*
Volker Schmitz, *Bonn*
Roland M Schmid, *München*
AG Schreyer, *Regensburg*
Tobias Schroeder, *Essen*
Hans Seifert, *Oldenburg*
Manfred V Singer, *Mannheim*
Gisela Sparmann, *Rostock*
Jurgen M Stein, *Frankfurt*
Ulrike Susanne Stein, *Berlin*
Manfred Stolte, *Bayreuth*
Christian P Strassburg, *Hannover*
WR Stremmel, *Heidelberg*
Harald F Teutsch, *Ulm*
Robert Thimme, *Freiburg*
HL Tillmann, *Leipzig*
Tung-Yu Tsui, *Regensburg*
Axel Ulsenheimer, *Munich*
Patrick Veit, *Essen*
Claudia Veltkamp, *Heidelberg*
Siegfried Wagner, *Deggendorf*
Henning Walczak, *Heidelberg*
Fritz von Weizsacker, *Berlin*
Jens Werner, *Heidelberg*
Bertram Wiedenmann, *Berlin*
Reiner Wiest, *Regensburg*
Stefan Wirth, *Wuppertal*
Stefan JP Zeuzem, *Homburg*

Greece

Elias A Kouroumalis, *Heraklion*
Ioannis E Koutroubakis, *Heraklion*
Spiros Sgouros, *Athens*

Hungary

Peter Laszlo Lakatos, *Budapest*
Zsuzsa Szondy, *Debrecen*

Iceland

H Gudjonsson, *Reykjavik*

India

KA Balasubramanian, *Vellore*
Sujit K Bhattacharya, *Kolkata*
Yogesh K Chawla, *Chandigarh*
Radha K Dhiman, *Chandigarh*
Sri Prakash Misra, *Allahabad*
ND Reddy, *Hyderabad*

Iran

Reza Malekzadeh, *Tehran*
Seyed Alireza Taghavi, *Shiraz*

Ireland

Billy Bourke, *Dublin*
Ronan A Cahill, *Cork*
Anthony P Moran, *Galway*

Israel

Simon Bar-Meir, *Hashomer*
Abraham Rami Eliakim, *Haifa*
Yaron Ilan, *Jerusalem*
Avidan U Neumann, *Ramat-Gan*
Yaron Niv, *Pardesia*
Ran Oren, *Tel Aviv*

Italy

Giovanni Addolorato, *Roma*
Luigi E Adinolfi, *Naples*
Domenico Alvaro, *Rome*
V Annese, *San Giovanni Rotond*
Adolfo Francesco Attili, *Roma*
Giovanni Barbara, *Bologna*
Gabrio Bassotti, *Perugia*
Pier Maria Battezzati, *Milan*
Stefano Bellentani, *Carpi*
Luca Saverioq Belli, *Milan*
Antomio Benedetti, *Ancona*
Mauro Bernardi, *Bologna*
Livia Biancone, *Rome*
Luigi Bonavina, *Milano*
Flavia Bortolotti, *Padova*
Giuseppe Brisinda, *Rome*
Giovanni Cammarota, *Roma*
Antonino Cavallari, *Bologna*
Giuseppe Chiarioni, *Valeggio*
Michele Cicala, *Rome*
Amedeo Columbano, *Cagliari*
Massimo Conio, *Sanremo*
Dario Conte, *Milano*
Gino Roberto Corazza, *Pavia*
Francesco Costa, *Pisa*
Antonio Craxi, *Palermo*
Roberto De Giorgio, *Bologna*
Giovanni D De Palma, *Naples*
Fabio Farinati, *Padua*
Francesco Feo, *Sassari*
Stefano Fiorucci, *Perugia*
Andrea Galli, *Firenze*
Valeria Ghisett, *Turin*
Gianluigi Giannelli, *Bari*
Edoardo G Giannini, *Genoa*
Paolo Gionchetti, *Bologna*
Mario Guslandi, *Milano*
Pietro Invernizzi, *Milan*
Giacomo Laffi, *Firenze*
Giovanni Maconi, *Milan*
Lucia Malaguarnera, *Catania*
ED Mangoni, *Napoli*
Giulio Marchesini, *Bologna*
Fabio Marra, *Florence*
Marco Marzioni, *Ancona*
Giuseppe Montalto, *Palermo*
Giovanni Monteleone, *Rome*
Giovanni Musso, *Torino*
Gerardo Nardone, *Napoli*
Valerio Nobili, *Rome*
Luisi Pagliaro, *Palermo*
Fabrizio R Parente, *Milan*
F Perri, *San Giovanni Rotondo*
Raffaele Pezzilli, *Bologna*
A Pilotto, *San Giovanni Rotondo*
Mario Pirisi, *Novara*
Paolo Del Poggio, *Treviglio*
Gabriele Bianchi Porro, *Milano*
Piero Portincasa, *Bari*
Bernardino Rampone, *Siena*
Claudio Romano, *Messina*
Marco Romano, *Napoli*
Gerardo Rosati, *Potenza*
Mario Del Tacca, *Pisa*
Pier Alberto Testoni, *Milan*
Enrico Roda, *Bologna*
Domenico Sansonno, *Bari*
Vincenzo Savarino, *Genova*
Roberto Testa, *Genoa*
Dino Vaira, *Bologna*

Japan

Kyoichi Adachi, *Izumo*
Yasushi Adachi, *Sapporo*
Taiji Akamatsu, *Matsumoto*
Sk Md Fazle Akbar, *Ehime*
Takafumi Ando, *Nagoya*
Akira Andoh, *Otsu*
Taku Aoki, *Tokyo*
Masahiro Arai, *Tokyo*
Tetsuo Arakawa, *Osaka*
Yasuji Arase, *Tokyo*
Masahiro Asaka, *Sapporo*
Hitoshi Asakura, *Tokyo*
Takeshi Azuma, *Fukui*
Yoichi Chida, *Fukuoka*
Takahiro Fujimori, *Tochigi*
Jiro Fujimoto, *Hyogo*
Kazuma Fujimoto, *Saga*
Mitsuhiro Fujishiro, *Tokyo*
Yoshihide Fujiyama, *Otsu*
Hirokazu Fukui, *Tochigi*
Hiroyuki Hanai, *Hamamatsu*
Kazuhiro Hanazaki, *Kochi*
Naohiko Harada, *Fukuoka*
Makoto Hashizume, *Fukuoka*
Tetsuo Hayakawa, *Nagoya*
Kazuhide Higuchi, *Osaka*
Keisuke Hino, *Ube*
Keiji Hirata, *Kitakyushu*
Yuji Iimuro, *Nishinomiya*
Kenji Ikeda, *Tokyo*
Fumio Imazeki, *Chiba*
Yutaka Inagaki, *Kanagawa*
Yasuhiro Inokuchi, *Yokohama*
Haruhiro Inoue, *Yokohama*
Masayasu Inoue, *Osaka*
Akio Inui, *Kagoshima*
Hiromi Ishibashi, *Nagasaki*
Shunji Ishihara, *Izumo*
Toru Ishikawa, *Niigata*
Kei Ito, *Sendai*
Masayoshi Ito, *Tokyo*
Hiroaki Itoh, *Akita*
Ryuichi Iwakiri, *Saga*
Yoshiaki Iwasaki, *Okayama*
Terumi Kamisawa, *Tokyo*
Hiroshi Kaneko, *Aichi-Gun*
Shuichi Kaneko, *Kanazawa*
Takashi Kanematsu, *Nagasaki*
Mitsuo Katano, *Fukuoka*
Junji Kato, *Sapporo*
Mototsugu Kato, *Sapporo*
Shinzo Kato, *Tokyo*
Norifumi Kawada, *Osaka*
Sunao Kawano, *Osaka*
Mitsuhiro Kida, *Kanagawa*
Yoshikazu Kinoshita, *Izumo*
Tsuneo Kitamura, *Chiba*
Seigo Kitano, *Oita*
Kazuhiko Koike, *Tokyo*
Norihiro Kokudo, *Tokyo*
Satoshi Kondo, *Sapporo*
Shoji Kubo, *Osaka*
Shigeki Kuriyama, *Kagawa*
Masato Kusunoki, *Tsu Mie*
Katsunori Iijima, *Sendai*
Shin Maeda, *Tokyo*
Masatoshi Makuuchi, *Tokyo*
Osamu Matsui, *Kanazawa*
Yasuhiro Matsumura, *Chiba*
Yasushi Matsuzaki, *Tsukuba*
Kiyoshi Migita, *Omura*
Tetsuya Mine, *Kanagawa*
Hiroto Miwa, *Hyogo*
Masashi Mizokami, *Nagoya*
Yoshiaki Mizuguchi, *Tokyo*
Motowo Mizuno, *Hiroshima*
Morito Monden, *Suita*
Hisataka S Moriwaki, *Gifu*
Yasuaki Motomura, *Iizuka*
Yoshiharu Motoo, *Kanazawa*
Kazunari Murakami, *Oita*
Kunihiko Murase, *Tusima*
Masahito Nagaki, *Gifu*
Masaki Nagaya, *Kawasaki*
Yuji Naito, *Kyoto*
Hisato Nakajima, *Tokyo*
Hiroki Nakamura, *Yamaguchi*
Shotaro Nakamura, *Fukuoka*
Mikio Nishioka, *Niihama*
Shuji Nomoto, *Nagoya*
Susumu Ohmada, *Maebashi*
Masayuki Ohta, *Oita*
Tetsuo Ohta, *Kanazawa*
Kazuichi Okazaki, *Osaka*
Katsuhisa Omagari, *Nagasaki*
Saburo Onishi, *Nankoku*
Morikazu Onji, *Ehime*
Satoshi Osawa, *Hamamatsu*
Masanobu Oshima, *Kanazawa*
Hiromitsu Saisho, *Chiba*
Hidetsugu Saito, *Tokyo*
Yutaka Saito, *Tokyo*
Isao Sakaida, *Yamaguchi*
Michiie Sakamoto, *Tokyo*
Yasushi Sano, *Chiba*
Hiroki Sasaki, *Tokyo*
Iwao Sasaki, *Sendai*
Motoko Sasaki, *Kanazawa*
Chifumi Sato, *Tokyo*
Shuichi Seki, *Osaka*
Hiroshi Shimada, *Yokohama*
Mitsuo Shimada, *Tokushima*
Tomohiko Shimatan, *Hiroshima*
Hiroaki Shimizu, *Chiba*
Ichiro Shimizu, *Tokushima*
Yukihiro Shimizu, *Kyoto*
Shinji Shimoda, *Fukuoka*
Tooru Shimosegawa, *Sendai*
Tadashi Shimoyama, *Hirosaki*
Ken Shirabe, *Iizuka*
Yoshio Shirai, *Niigata*
Katsuya Shiraki, *Mie*
Yasushi Shiratori, *Okayama*

Masayuki Sho, *Nara*
Yasuhiko Sugawara, *Tokyo*
Hidekazu Suzuki, *Tokyo*
Minoru Tada, *Tokyo*
Tadatoshi Takayama, *Tokyo*
Tadashi Takeda, *Osaka*
Koji Takeuchi, *Kyoto*
Kiichi Tamada, *Tochigi*
Akira Tanaka, *Kyoto*
Eiji Tanaka, *Matsumoto*
Noriaki Tanaka, *Okayama*
Shinji Tanaka, *Hiroshima*
Wei Tang, *Tokyo*
Hideki Taniguchi, *Yokohama*
Kyuichi Tanikawa, *Kurume*
Akira Terano, *Shimotsugagun*
Hitoshi Togash, *Yamagata*
Kazunari Tominaga, *Osaka*
Takuji Torimura, *Fukuoka*
Minoru Toyota, *Sapporo*
Akihito Tsubota, *Chiba*
Shingo Tsuji, *Osaka*
Takato Ueno, *Kurume*
Shinichi Wada, *Tochigi*
Hiroyuki Watanabe, *Kanazawa*
Toshio Watanabe, *Osaka*
Yuji Watanabe, *Ehime*
Chun-Yang Wen, *Nagasaki*
Koji Yamaguchi, *Fukuoka*
Takayuki Yamamoto, *Yokkaichi*
Takashi Yao, *Fukuoka*
Masashi Yoneda, *Tochigi*
Hiroshi Yoshida, *Tokyo*
Masashi Yoshida, *Tokyo*
Norimasa Yoshida, *Kyoto*
Kentaro Yoshika, *Toyoake*
Masahide Yoshikawa, *Kashihara*

Lebanon
Bassam N Abboud, *Beirut*
Ala I Sharara, *Beirut*
Joseph Daoud Boujaoude, *Beirut*

Lithuania
Limas Kupcinskas, *Kaunas*

Macedonia
Vladimir Cirko Serafimoski, *Skopje*

Malaysia
Andrew Seng Boon Chua, *Ipoh*
Khean-Lee Goh, *Kuala Lumpur*
Jayaram Menon, *Sabah*

Mexico
Garcia-Compean Diego, *Monterrey*
Saúl Villa-Treviño, *México*
JK Yamamoto-Furusho, *México*

Monaco
Patrick Rampal, *Monaco*

Netherlands
Ulrich Beuers, *Amsterdam*
Gerd Bouma, *Amsterdam*
Lee Bouwman, *Leiden*
J Bart A Crusius, *Amsterdam*
Rick Greupink, *Groningen*
Janine K Kruit, *Groningen*
Ernst Johan Kuipers, *Rotterdam*
Ton Lisman, *Utrecht*
Yi Liu, *Amsterdam*
Servaas Morré, *Amsterdam*
Chris JJ Mulder, *Amsterdam*
Michael Müller, *Wageningen*
Amado Salvador Peña, *Amsterdam*
Robert J Porte, *Groningen*
Ingrid B Renes, *Rotterdam*
Andreas Smout, *Utrecht*
RW Stockbrugger, *Maastricht*
Luc JW van der Laan, *Rotterdam*
Karel van Erpecum, *Utrecht*
GP VanBerge-Henegouwen, *Utrecht*

New Zealand
Ian David Wallace, *Auckland*

Nigeria
Samuel Babafemi Olaleye, *Ibadan*

Norway
Trond Berg, *Oslo*
Tom Hemming Karlsen, *Oslo*
Helge Lyder Waldum, *Trondheim*

Pakistan
Muhammad S Khokhar, *Lahore*

Poland
Tomasz Brzozowski, *Cracow*
Robert Flisiak, *Bialystok*
Hanna Gregorek, *Warsaw*
DM Lebensztejn, *Bialystok*
Wojciech G Polak, *Wroclaw*
Marek Hartleb, *Katowice*

Portugal
MP Cecília, *Lisbon*
Miguel Carneiro De Moura, *Lisbon*

Russia
Vladimir T Ivashkin, *Moscow*
Leonid Lazebnik, *Moscow*
Vasiliy I Reshetnyak, *Moscow*

Serbia
DM Jovanovic, *Sremska Kamenica*

Singapore
Bow Ho, *Kent Ridge*
Khek-Yu Ho, *Singapore*
Francis Seow-Choen, *Singapore*

Slovakia
Anton Vavrecka, *Bratislava*

Slovenia
Sasa Markovic, *Ljubljana*

South Africa
Michael C Kew, *Parktown*

South Korea
Byung Ihn Choi, *Seoul*
Ho Soon Choi, *Seoul*
M Yeo, *Suwon*
Sun Pyo Hong, *Gyeonggi-do*
Jae J Kim, *Seoul*
Jin-Hong Kim, *Suwon*
Myung-Hwan Kim, *Seoul*
Chang Hong Lee, *Seoul*
Jong Kyun Lee, *Seoul*
Eun-Yi Moon, *Seoul*
Jae-Gahb Park, *Seoul*
Dong Wan Seo, *Seoul*
Dong jin Suh, *Seoul*

Spain
Juan G Abraldes, *Barcelona*
Agustin Albillos, *Madrid*
Raul J Andrade, *Málaga*
Luis Aparisi, *Valencia*
Fernando Azpiroz, *Barcelona*
Ramon Bataller, *Barcelona*
Josep M Bordas, *Barcelona*
Xavier Calvet, *Sabadell*
Andres Cardenas, *Barcelona*
Vicente Carreño, *Madrid*
Jose Castellote, *Barcelona*
Antoni Castells, *Barcelona*
Vicente Felipo, *Valencia*
Juan C Garcia-Pagán, *Barcelona*
Jaime Bosch Genover, *Barcelona*
Jaime Guardia, *Barcelona*
Angel Lanas, *Zaragoza*
María Isabel Torres López, *Jaén*
José M Mato, *Derio*
Juan F Medina, *Pamplona*
MA Muñoz-Navas, *Pamplona*
Julian Panes, *Barcelona*
Miguel Minguez Perez, *Valencia*
Miguel Perez-Mateo, *Alicante*
Josep M Pique, *Barcelona*
Jesus M Prieto, *Pamplona*
Sabino Riestra, *Pola De Siero*
Luis Rodrigo, *Oviedo*
Manuel Romero-Gómez, *Sevilla*

Sweden
Curt Einarsson, *Huddinge*
Ulf Hindorf, *Lund*
Hanns-Ulrich Marschall, *Stockholm*
Lars Christer Olbe, *Molndal*
Matti Sallberg, *Stockholm*
Magnus Simrén, *Göteborg*
Xiao-Feng Sun, *Linköping*
Ervin Tóth, *Malmö*
Weimin Ye, *Stockholm*

Switzerland
Chrish Beglinger, *Basel*
Pierre A Clavien, Zurich
Jean-Francois Dufour, *Bern*
Franco Fortunato, *Zürich*
Jean Louis Frossard, *Geneva*
Gerd A Kullak-Ublick, *Zurich*
Pierre Michetti, *Lausanne*
Francesco Negro, *Genève*
Bruno Stieger, *Zurich*
Arthur Zimmermann, *Berne*
Radu Tutuian, *Zurich*
Stephan Robert Vavricka, *Zurich*

Turkey
Yusuf Bayraktar, *Ankara*
Figen Gurakan, *Ankara*
Aydin Karabacakoglu, *Konya*
Serdar Karakose, *Konya*
Hizir Kurtel, *Istanbu*
Osman Cavit Ozdogan, *Istanbul*
Özlem Yilmaz, *Izmir*
Cihan Yurdaydin, *Ankara*

United Arab Emirates
Sherif M Karam, *Al-Ain*

United Kingdom
David Adams, *Birmingham*
NK Ahluwalia, *Stockport*
CG Antoniades, *London*
Anthony TR Axon, *Leeds*
Qasim Aziz, *Manchester*
Nicholas M Barnes, *Birmingham*
Jim D Bell, *London*
Mairi Brittan, *London*
Simon Scott Campbell, *Manchester*
Simon R Carding, *Leeds*
Paul Jonathan Ciclitira, *London*

Tatjana Crnogorac-Jurcevic, *London*
Amar Paul Dhillon, *London*
Emad M El-Omar, *Aberdeen*
Annette Fristscher-Ravens, *London*
Elizabeth Furrie, *Dundee*
Daniel Richard Gaya, *Edinburgh*
Subrata Ghosh, *London*
William Greenhalf, *Liverpool*
Indra Neil Guha, *Southampton*
Peter Clive Hayes, *Edinburgh*
Gwo-Tzer Ho, *Edinburgh*
Anthony R Hobson, *Salford*
Stefan G Hübscher, *Birmingham*
Robin Hughes, *London*
Pali Hungin, *Stockton*
David Paul Hurlstone, *Sheffield*
Janusz AZ Jankowski, *Oxford*
Brian T Johnston, *Belfast*
David EJ Jones, *Newcastle*
Michael A Kamm, *Harrow*
Peter Karayiannis, *London*
Laurens Kruidenier, *Harlow*
Patricia F Lalor, *Birmingham*
Hong-Xiang Liu, *Cambridge*
K E L McColl, *Glasgow*
Stuart AC McDonald, *London*
Dermot Patrick Mcgovern, *Oxford*
Giorgina Mieli-Vergani, *London*
Nikolai V Naoumov, *London*
John P Neoptolemos, *Liverpool*
James Neuberger, *Birmingham*
Mark S Pearce, *Newcastle Upon Tyne*
D Mark Pritchard, *Liverpool*
Stephen E Roberts, *Swansea*
Marco Senzolo, *Padova*
Soraya Shirazi-Beechey, *Liverpool*
Robert Sutton, *Liverpool*
Simon D Taylor-Robinson, *London*
Ulrich Thalheimer, *London*
Nick Paul Thompson, *Newcastle*
David Tosh, *Bath*
Frank Ivor Tovey, *London*
Chris Tselepis, *Birmingham*
Diego Vergani, *London*
Geoffrey Warhurst, *Salford*
Peter James Whorwell, *Manchester*
Karen Leslie Wright, *Bath*
Min Zhao, *Foresterhill*

United States

Gary A Abrams, *Birmingham*
Golo Ahlenstiel, *Bethesda*
BS Anand, *Houston*
Frank A Anania, *Atlanta*
Gavin Edward Arteel, *Louisville*
Jasmohan Singh Bajaj, *Milwaukee*
Jamie S Barkin, *Miami Beach*
Kim Elaine Barrett, *San Diego*
Marc Basson, *Detroit*
Timothy R Billiar, *Pittsburgh*
Edmund J Bini, *New York*
Jennifer D Black, *Buffalo*
Herbert L Bonkovsky, *Farmington*
Andrea D Branch, *New York*
Robert S Bresalier, *Houston*
Alan L Buchman, *Chicago*
Alan Cahill, *Philadelphia*
John M Carethers, *San Diego*
David L Carr-Locke, *Boston*
Ravi S Chari, *Nashville*
Jiande Chen, *Galveston*
Xian-Ming Chen, *Rochester*
Ramsey Chi-man Cheung, *Palo Alto*
William D Chey, *Ann Arbor*
John Y Chiang, *Rootstown*
Parimal Chowdhury, *Arkansas*
Raymond T Chung, *Boston*
James M Church, *Cleveland*
Mark G Clemens, *Charlotte*
Vincent Coghlan, *Beaverton*
David Cronin II, *New Haven*
John Cuppoletti, *Cincinnati*
Peter V Danenberg, *Los Angeles*
Kiron Moy Das, *New Brunswick*
Sharon DeMorrow, *Temple*
Deborah L Diamond, *Seattle*
Peter Draganov, *Florida*
Bijan Eghtesad, *Cleveland*
Hala El-Zimaity, *Houston*
Michelle Embree-Ku, *Providence*
Ronnie Fass, *Tucson*
Mark A Feitelson, *Philadelphia*
Ariel E Feldstein, *Cleveland*
Alessandro Fichera, *Chicago*
Chris E Forsmark, *Gainesville*
Chandrashekhar R Gandhi, *Pittsburgh*
Susan L Gearhart, *Baltimore*
Xupeng Ge, *Boston*
John P Geibel, *New Haven*
Xin Geng, *New Brunswick*
Jean-Francois Geschwind, *Baltimore*
Ignacio Gil-Bazo, *New York*
Shannon S Glaser, *Temple*
Ajay Goel, *Dallas*
Julia Butler Greer, *Pittsburgh*
David R Graham, *Houston*
Anna S Gukovskaya, *Los Angeles*
Sanjeev Gupta, *Bronx*
David J Hackam, *Pittsburgh*
Stephen B Hanauer, *Chicago*
Gavin Harewood, *Rochester*
Alan W Hemming, *Gainesville*
Samuel B Ho, *San Diego*
Hongjin Huang, *Alameda*
Jamal A Ibdah, *Columbia*
Atif Iqbal, *Omaha*
Hajime Isomoto, *Rochester*
Hartmut Jaeschke, *Tucson*
Dennis M Jensen, *Los Angeles*
Leonard R Johnson, *Memphis*
Peter James Kahrilas, *Chicago*
AN Kalloo, *Baltimore*
Neil Kaplowitz, *Los Angeles*
Rashmi Kaul, *Tulsa*
Jonathan D Kaunitz, *Los Angeles*
Ali Keshavarzian, *Chicago*
Miran Kim, *Providence*
Joseph B Kirsner, *Chicago*
Leonidas G Koniaris, *Miami*
Burton I Korelitz, *New York*
Robert J Korst, *New York*
Richard A Kozarek, *Seattle*
Michael Kremer, *Chapel Hill*
Shiu-Ming Kuo, *Buffalo*
Daryl Tan Yeung Lau, *Galvesto*
Joel E Lavine, *San Diego*
Dirk J van Leeuwen, *Lebanon*
Glen A Lehman, *Indianapolis*
Alex B Lentsch, *Cincinnati*
Andreas Leodolter, *La Jolla*
Gene LeSage, *Houston*
Ming Li, *New Orleans*
Zhiping Li, *Baltimore*
LM Lichtenberger, *Houston*
GR Lichtenstein, *Philadelphia*
Otto Schiueh-Tzang Lin, *Seattle*
Martin Lipkin, *New York*
Edward V Loftus, *Rocheste*
Robin G Lorenz, *Birmingham*
JD Luketich, *Pittsburgh*
Henry Thomson Lynch, *Omaha*
Patrick M Lynch, *Houston*
Peter J Mannon, *Bethesda*
John Frank Di Mari, *Texas*
John M Mariadason, *Bronx*
WM Mars, *Pittsburgh*
Laura E Matarese, *Pittsburgh*
Lynne V McFarland, *Washington*
Kevin McGrath, *Pittsburgh*
Harihara Mehendale, *Monroe*
Howard Mertz, *Nashville*
George W Meyer, *Sacramento*
G Michalopoulos, *Pittsburgh*
James Michael Millis, *Chicago*
Smruti Ranjan Mohanty, *Chicago*
Satdarshan Singh Monga, *Pittsburgh*
Timothy H Moran, *Baltimore*
Steven F Moss, *Providence*
Masaki Nagaya, *Boston*
Laura Eleanor Nagy, *Cleveland*
Hiroshi Nakagawa, *Philadelphia*
Douglas B Nelson, *Minneaplis*
Brant K Oelschlager, *Washington*
Curtis T Okamoto, *Los Angeles*
Stephen JD O'Keefe, *Pittsburgh*
Dimitry Oleynikov, *Omaha*
Natalia A Osna, *Omaha*
Stephen J Pandol, *Los Angeles*
Pankaj Jay Pasricha, *Gaveston*
Zhiheng Pei, *New York*
Michael A Pezzone, *Pittsburgh*
CS Pitchumoni, *New Brunswiuc*
Jay Pravda, *Gainesville*
M Raimondo, *Jacksonville*
GS Raju, *Galveston*
Murray B Resnick, *Providence*
Adrian Reuben, *Charleston*
Douglas K Rex, *Indianapolis*
Victor E Reyes, *Galveston*
Richard A Rippe, *Chapel Hill*
Marcos Rojkind, *Washington*
Hemant Kumar Roy, *Evanston*
Shawn David Safford, *Norfolk*
NJ Shaheen, *Chapel Hill*
Stuart Sherman, *Indianapolis*
Shivendra Shukla, *Columbia*
Alphonse E Sirica, *Virginia*
Shanthi V Sitaraman, *Atlanta*
Shanthi Srinivasan, *Atlanta*
Michael Steer, *Boston*
Gary D Stoner, *Columbus*
Liping Su, *Chicago*
Christina Surawicz, *Seattle*
Gyongyi Szabo, *Worcester*
Yvette Taché, *Los Angeles*
Seng-Lai Tan, *Seattle*
Andrzej Tarnawski, *Long Beach*
Andrzej S Tarnawski, *Orange*
K-M Tchou-Wong, *New York*
Neil D Theise, *New York*
PJ Thuluvath, *Baltimore*
Swan Nio Thung, *New York*
Natalie J Torok, *Sacramento*
RA Travagli, *Baton Rouge*
G Triadafilopoulos, *Stanford*
James F Trotter, *Denver*
Chung-Jyi Tsai, *Lexington*
Hugo E Vargas, *Scottsdale*
Scott A Waldman, *Philadelphia*
Jian-Ying Wang, *Baltimore*
Steven David Wexner, *Weston*
Keith Tucker Wilson, *Baltimore*
Jacqueline L Wolf, *Boston*
Jackie Wood, *Ohio*
George Y Wu, *Farmington*
Jian Wu, *Sacramento*
Samuel Wyllie, *Houston*
Wen Xie, *Pittsburgh*
Yoshio Yamaoka, *Houston*
Francis Y Yao, *San Francisco*
Min You, *Tampa*
Zobair M Younossi, *Virginia*
Liqing Yu, *Winston-Salem*
David Yule, *Rochester*
Ruben Zamora, *Pittsburgh*
Michael E Zenilman, *New York*
Zhi Zhong, *Chapel Hill*

PO Box 2345, Beijing 100023, China
www.wjgnet.com
wjg@wjgnet.com

World J Gastroenterol 2007 February 21; 13(7): 985-992
World Journal of Gastroenterology ISSN 1007-9327

REVIEW

p53 gene in treatment of hepatic carcinoma: *Status quo*

Yong-Song Guan, Zi La, Lin Yang, Qing He, Ping Li

Yong-Song Guan, Zi La, Lin Yang, Qing He, Ping Li, Department of Radiology and Oncology, West China Hospital of Sichuan University, Chengdu 610041, Sichuan Province, China
Correspondence to: Dr. Yong-Song Guan, State Key Laboratory of Biotherapy, West China Hospital, West China Medical School, Sichuan University-Gaopeng Street, Keyuan Road 4, Chengdu 610041, Sichuan Province, China. yongsongguan@yahoo.com
Telephone: +86-28-85422601 Fax: +86-28-85538359
Received: 2006-11-30 Accepted: 2007-01-16

Abstract

Hepatocellular carcinoma (HCC) is one of the 10 most common cancers worldwide. There is no ideal treatment for HCC yet and many researchers are trying to improve the effects of treatment by changing therapeutic strategies. As the majority of human cancers seem to exhibit either abnormal p53 gene or disrupted p53 gene activation pathways, intervention to restore wild-type p53 (wt-p53) activities is an attractive anti-cancer therapy including HCC. Abnormalities of p53 are also considered a predisposition factor for hepatocarcinogenesis. p53 is frequently mutated in HCC. Most HCCs have defects in the p53-mediated apoptotic pathway although they carry wt-p53. High expression of p53 *in vivo* may exert therapeutic effects on HCC in two aspects: (1) High expression of exogenous p53 protein induces apoptosis of tumor cells by inhibiting proliferation of cells through several biologic pathways and (2) Exogenous p53 renders HCC more sensitive to some chemotherapeutic agents. Several approaches have been designed for the treatment of HCC *via* the p53 pathway by restoring the tumor suppression function from inactivation, rescuing the mutated p53 gene from instability, or delivering therapeutic exogenous p53. Products with p53 status as the target have been studied extensively *in vitro* and *in vivo*. This review elaborates some therapeutic mechanisms and advances in using recombinant human adenovirus p53 and oncolytic virus products for the treatment of HCC.

Key words: p53 gene; Hepatocellular carcinoma; Therapeutic strategies; Advances; Prospects

Guan YS, La Z, Yang L, He Q, Li P. p53 gene in treatment of hepatic carcinoma: *Status quo*. *World J Gastroenterol* 2007; 13(7): 985-992

http://www.wjgnet.com/1007-9327/13/985.asp

INTRODUCTION

The concept of human gene therapy[1,2] derives from fundamental discoveries[3,4] on the nature and working[5] of the gene. Since the essential principles of molecular genetics and gene transfer in bacteria were established in the 1960s, gene transfer into animals and humans using either viral vector and/or genetically modified cultured cells has become inevitable[6]. Since then, this concept has promoted thousands of researchers to attempt to realize their long-cherished dreams of eradicating some of the obstinate human diseases. Broadly defined, the concept of gene therapy involves transfer of genetic materials[6] into cells, tissues, or whole organs, with the goal of eliminating diseases or at least improving the clinical condition of patients[7]. As a milestone of gene therapy, the first approved clinical protocol started trials in September, 1990[8]. Gene therapy provides great opportunities for treating diseases due to genetic disorders, infections and cancer[9]. Hepatocellular carcinoma (HCC) is one of the 10 most common cancers worldwide with its highest prevalence in Southeast Asia and sub-Saharan Africa[10]. Although great efforts have been made to overcome this cancer, no ideal treatment is available at present[11]. In recent years, many researchers are trying to improve the effects of treatment by changing therapeutic strategies[12]. As the majority of human cancers seem to exhibit either abnormal p53 gene[13] or disrupted p53 gene activation pathways[14], intervention to restore wild-type p53 (wt-p53) activities is an attractive anti-cancer therapy[14,15]. This review elaborates some therapeutic mechanisms and advances in using recombinant human adenovirus p53[16] and oncolytic virus[17] products for the treatment of HCC.

CARCINOGENESIS OF LIVER CELLS AND p53 GENE

Cancer predisposition, onset and therapeutic response can be critically determined by the integrity of tumor suppressor p53[15]. Tumor suppressor protein p53 can protect cells from growth and division[18], thus mediating cell-cycle arrest[19], DNA repair[20] and apoptosis[13,14,19,21] after its activation by multiple forms of cellular stresses[19]. p53 mutations[22] in plasma DNA are associated with several cancers, and abnormalities of p53 are also considered a predisposition factor for HCC (Table 1). Mutant p53 (mt-p53) may be a marker of HCC carcinogen exposure[22]. For example, in aflatoxin B1-exposed patients[23], R249S tumor protein p53[24], one of the cancer-associated mutants, encodes p53, and is considered a

Table 1 Abnormal p53 status detected in HCC with probable mechanisms

Endogenous status of p53 or its pathways	Probable mechanisms
Mutation of p53 gene	Point mutation, allele deletion, insertion, *etc.*
Loss of or decrease in wt-p53 expression	Enhanced p53 degradation, complex formation
Hyperactivities of negative regulators of p53	No p53 mutation, over-expressed negative regulators of p53 attenuate its function
Increased diversity of p53 aberration	Progression of HCC
Presence of serum anti-p53 antibodies	Over-expression of wt-p53, presence of mt-p53, or both

Table 2 Approaches for restoring tumor suppression function of p53 in the treatment of HCC

Strategies	Therapeutic effects
Chemotherapy or radiotherapy	Inducing p53-dependent apoptosis in tumor cells with wt-p53
Supplying exogenous wt-p53 by gene delivery	Suppressing growth of both mutant and wild-type p53-containing tumor cells
Overexpression of ARF	Blocking p53 degradation pathways to induce p53 triggered tumor cell death
Interruption of MDM2-p53 interaction	Preventing MDM2-mediated p53 ubiquitinationand degradation to restore transactivation
Molecules stabilizing the active conformation of the protein	Rescuing mt-p53 to restore p53 function

genetic alteration during hepatocarcinogenesis[23]. Here R249S as a mutant of p53 core domain, is a structural mutation[25], and constitutes one of the "hot spots" associated with cancer.

There is evidence that the level of p53 alterations is high in HCC, since it was reported that p53 increases the frequency of HCC prediction from 79.5% to 86.3%[26], showing that serum concentration of p53 protein may be a convenient and useful non-invasive screening test for prediction of HCC. A study[27] showed that attenuated p53 function and telomere-induced chromosomal instability play a critical and cooperative role in the progression of chronic liver damage to hepatocellular carcinoma. Loss of p53 expression or presence of abnormal forms of the protein is frequently associated with HCC cell lines. Bressac *et al*[28] studied the p53 gene at the DNA, RNA, and protein level in seven human HCC-derived cell lines, and found that six of them show p53 abnormalities, suggesting that alterations in p53 may be important events in the transformation of hepatocytes[29] into the malignant phenotype. p53 gene is frequently mutated in high-grade[30] HCC. Inactivation of this multiple tumor suppressor gene plays an important role in the progression of chronic liver damage to hepatocellular carcinoma by directly or indirectly inducing chromosome instability, cell proliferation and neovascularization[31]. Kondo *et al*[32] performed dual-color fluorescence *in situ* hybridization to evaluate loss of the p53 gene, and revealed that loss of the p53 gene occurs in HCC, and diversity of the p53 gene aberration increases with the progression of chronic liver damage to HCC.

Other factors for hepatocarcinogenesis are correlated with abnormal functioning of p53, such as hepatitis B virus (HBV)[23,33] and hepatitis C virus (HCV)[34]. HBV gene encodes HBV protein x (HBx)[33], a protein as a transcriptional activator[35] and plays an important role in viral replication in HBV-infected cells. HBx as an oncoprotein[36], can bind to the C terminus of p53 and inhibit several critical p53-mediated cellular processes, including DNA sequence-specific binding, transcriptional transactivation, and apoptosis[37]. HBx integration and inactivation of p53 by mutations and regional allelic deletions are frequently found in tumors associated with HBV infection[38]. HBx up-regulates survivin[39] expression in hepatoma tissues. Survivin is an inhibitor of apoptosis and found in many common human cancers but not in normal tissues. Survivin is suppressed by wt-p53 and over-expressed in 41%-70% of HCCs from Asia, its over-expression is associated with aberrant p53 nuclear positivity[40].

In addition to its aberration, as p53 responds to a variety of genotoxic[34] and cytotoxic[41] agents in the presence of a potent inhibitor[42] of p53, the liver's ability to handle such toxic agents is influenced, thus inducing hepatocarcinogenesis.

Anti-p53 antibodies (p53-Abs) are products triggered by accumulation of a mutated form of p53 protein and probably a large quantity of wt-p53 protein[43]. As a specific serological marker for p53 gene expression changes in HCC, the presence of p53-Abs is independent of serum alpha fetoprotein and other conventional tumor markers[44]. It was reported that serum p53-Abs have a specificity of 100% for detecting malignancy[44], suggesting that its use in combination with markers may increase the diagnostic sensitivity of cancer.

MECHANISMS OF p53 THERAPY FOR HCC

Restoration of tumor suppression function of p53 has been speculated in several clinical lines for the treatment of HCC (Table 2).

p53 is frequently mutated in HCC[31]. Most HCCs have defects in the p53-mediated[37] apoptotic pathway although they carry wt-p53. Sometimes, p53 in HCC is wild-type but has inactive function[45]. Signal to and activation of p53 can lead to wt-p53 expression, thus suppressing the transformed phenotype of hepatocytes and increasing the effects of both chemotherapeutic agents and radiation therapy[46]. Repression of p53 can be partial or complete[45] in HCC, and activation of p53 can be achieved by single small molecules, such as the well known antimalaria drug quinacrine[45]. Supplying exogenous wt-p53 in cancer cells by gene delivery is effective in suppressing tumor growth of both mutant and wild-type p53-containing tumors[14]. The murine double minute 2 gene (MDM2) is an oncogene and contains a p53-DNA binding site and produces a phosphoprotein that forms a tight complex with both mutant and wild-type p53 protein, thus inhibiting p53-mediated transactivation and inducing p53 degradation[47]. There is a MDM2-p53 auto-regulatory feedback loop[48] that regulates the function of p53 protein and expression

of the MDM2 gene. Expression of the MDM2 gene can be regulated by the level of wild-type p53 protein, while the MDM2 protein, in turn, can form a complex with p53 and decrease its ability to act as a positive transcription factor at the MDM2 gene-responsive element. Several approaches have now been used to interrupt MDM2-p53 interaction to increase functional p53 levels and p53-mediated therapeutic effectiveness[49]. ADP-ribosylation factor (ARF) proteins are critical regulators of the protein secreting pathway[50]. In a human HCC cell line[51], adenosine diphosphate (ADP) and adenosine triphosphate (ATP) are degraded to adenosine and treatment of HCC cells with adenosine can inhibit growth of HCC cells and activate caspase-3, indicating that adenosine is an apoptotic agent with cytotoxicity. ARF is considered a tumor suppressor[52], and can initiate cellular response to aberrant oncogene activation by binding to and inhibiting the activity of MDM2. The human counterpart[53] of MDM2 (HDM2), like the murine protein, can inactivate the transactivation ability of human p53. ARF and p53 bind to MDM2 on different sites. ARF-p53 complex is formed depending on the mediation by MDM2 and can enhance p53 stability[54]. Blockage of p53 degradation pathways either by over-expression of ARF or interruption of MDM2-p53 interaction can effectively induce p53-triggered tumor cell death[14].

High expression of p53[55] *in vivo* may exert therapeutic effects on HCC in two aspects: (1) High expression of exogenous p53 protein induces apoptosis of tumor cells by inhibiting proliferation of cells through several biologic pathways and (2) exogenous p53 renders HCC more sensitive to some chemotherapeutic agents.

In addition, p53 down-regulates the expression of genes involved in angiogenesis[56], by the angiogenesis-inhibiting properties of wt-p53 protein[13].

It is very difficult to treat HCC due to drug resistance. It is necessary to reverse multiple drug resistance to human HCC cells and to find out the related mechanisms. The expression and activity of P-glycoprotein as well as the multiple drug resistance gene (MDR) products, are elevated in HCC cells with mt-p53[57]. Expression of mt-p53 enhances drug resistance to HCC cells and reduces their uptake of chemotherapeutic agents. In contrast to the increased expression of MDR by mt-p53, wt-p53 inhibits transcription of MDR[58]. Therefore, restoration of wt-p53 activity in HCC cells leads to the sensitivity of HCC cells to chemotherapeutic agents because of the decreased expression of P-glycoprotein encoded by MDR.

APPROACHES OF p53 THERAPY FOR HCC

Studies indicate that it is necessary to deliver therapeutic genes into cells with high specificity and efficiency in order to increase the effect of gene therapy against cancer[5,7,9,11]. A key factor for the success of gene therapy is the development of delivery systems[5,7,9] that are capable of efficiently transferring genes into a variety of tissues, without any associated pathogenic effects[7]. These techniques permit the isolation and insertion of genes into the recombinant delivery systems[5]. Two kinds of gene transfer vectors, namely viral and non-viral, are available at present.

Viruses are recognized natural gene carriers[5] and provide inspiration of gene therapy. Viruses have been engineered as gene delivery vectors[59]. However, their limits such as selective disadvantage[60], immunogenicity and toxicity[61], inefficient gene transfer and short-lived[62] or inadequate expression in transfected liver cells[63], require us to search other delivery systems.

Non-viral vectors have several advantages over viral vectors[61]. The transferred gene is in the form of a plasmid[64] that is on the surface or in the interior of the vector. Such vectors include liposome[61], molecular conjugates[65], nanoparticles[66] with strong anti-tumor effect on human HCC, naked DNA[67] and complexed DNA[68]. Better transfection efficiency can be achieved with delivery systems such as cationic lipids and cationic polymers[63].

To date, tissue-specific expression[69], self-replicating[70] and integrating plasmid[71] systems have been reported for gene therapy of HCC. Iodized oil emulsion[72] has a particular affinity to hypervascular hepatic tumors and is now commonly used in HCC chemoembolization, suggesting that it can be applied to the liver as a non-viral gene transfer system for intra-arterial gene delivery with selective gene expression in tumor cells.

THERAPEUTIC PRODUCTS WITH p53 STATUS AS TARGET

Recombinant adenovirus p53 (rAd-p53) and oncolytic virus are the promising therapeutic products for the treatment of HCC mostly applied *in vitro* and *in vivo* at present. With the introduction of exogenous wt-p53 expressed by the recombinant adenoviral vector, the expression of both p53 and p21 proteins is found to be up-regulated in cells[55]. Inhibition of cell growth and apoptosis can be achieved[55]. Oncolytic viruses[73,74] are a number of defective viruses, which cannot replicate in normal cells but are able to grow in tumor cells, finally leading to their lysis.

The two kinds of viruses and their characteristics were compared (Table 3).

Recombinant adenovirus p53 (rAd-p53)

Since human adenovirus vector systems have a lager host range and lower pathogenicity to humans[75], and the binding affinity for epithelium[76] is important because most of human tumors are of the epithelial origin, and serotype 4 of species E[77,78] shows a specific binding affinity for HCC cells[76], they are generally used for the expression of proteins in human beings or other species with some advantages. The E1 region of adenovirus has been identified as a subregion of the viral genome present in transformed cells and is responsible for transformation[79]. Recombinant human adenoviruses constructed with the E1 region replaced by exogenous DNA become replication-defective and yield a relatively low degree of acute toxicity[80]. Since recombinant adenoviral vector expresses wt-p53 (Ad-p53), p53 gene can be transfected into HCC cell lines[55]. Experiments showed that tumor cells transduced with the wt-p53 gene can inhibit *in vivo*

Table 3 Comparison of several characteristics of rAd-p53 with oncolytic virus products

Products	Characteristics
rAd-p53	p53 gene is transfected into HCC cells with recombinant adenoviral vector expressing wt-p53
Advexin	Larger host range, low pathogenicity to human, replication-impaired adenoviral vector carrying the p53 gene
Gendicine	The first commercial gene therapy product in the world approved by SFDA
SCH58500	Replication-deficient type 5 adenovirus vector expressing human wt-p53 under control of cytomegalovirus promoter
Oncolytic viruses	Incapable of replicating in normal cells but selectively replicating in p53-defective tumor cells to lyse them
ONYX-015	Tumor-selective replicating virus, the prototype for oncolytic adenoviral therapy
CNHK300-mE	Replication-competent with advantages of both gene and virus therapies

tumor growth of adjacent nontransduced cells, suggesting that Ad-p53 is also anti-angiogenic[81], partially by the bystander effect induced by the wt-p53 gene transfer on adjacent tumor cells.

Oncolytic viruses

As HCC cells with p53 defects have lost their cellular surveillance mechanisms, oncolytic viruses interfering with the main surveillance pathways such as those controlled by p53[73], could replicate selectively in them and cause lysis. E1A gene of adenovirus is an apoptosis-inducing gene and E1B gene of adenovirus is an apoptosis-inhibiting gene. The 55-kilodalton (55kDa) protein from the E1B-region of adenovirus binds to and inactivates the p53 gene[82]. Because of a deletion in E1B, the 55-kDa E1B protein is not expressed and the mutant adenovirus, termed ONYX-015[83], is able to replicate only in wt-p53 deficient cells. The E1B55K-defective adenovirus ONYX-015 is a prototype[73,82,83] of oncolytic viruses and can selectively replicate in and kill p53-deficient HCC cells, the success of cancer gene therapy is not promising unless it is carefully designed based on the biology of a specific[84] tumor type. To enhance the efficiency of such oncolytic viruses, another E1B 55kDa-deficient adenovirus armed with a mouse endostatin gene has been constructed for anti-tumor activities against HCC, and termed as CNHK200-mE[85]. With the synergistic effect of carrier virus and therapeutic gene, a novel approach has been established with the vector system termed as gene-viral vector[86] or gene-viral therapeutic system wherein an anti-tumor gene is inserted into the genome of a replicative virus specific for tumor cells to combine the advantages of gene and virus therapies. Using the human telomerase reverse transcriptase (hTERT) promoter to drive the expression of adenovirus E1A gene and clone the therapeutic gene mouse endostatin into the adenovirus genome, CNHK300-murine endostatin (CNHK300-mE)[87] is constructed, showing potential effects in the treatment of HCC.

EMPIRICAL STUDIES OF p53 THERAPY FOR HCC

Activation of p53 by either chemotherapy or radiotherapy induces p53-dependent apoptosis in tumor cells with wt-p53[14].

In the treatment of HCC, p53 products are injected into liver tissue by a variety of routes[55,72,82,88-92]. When p53 products are injected intratumorally[55,88,89], introduction of exogenous wt-p53 can inhibit cell growth, the expression of both p53 and p21 proteins is up-regulated in tumor cells. Intraarterial gene delivery into animal hepatic tumors can lead to selective gene expression in tumor cells[72]. Antegrade intraportal and retrograde intrabiliary routes are compared, induce transgene expression in periportal areas of liver with no significant difference in transduction efficacy, and no apparent complications are observed apart from very mild elevation of serum biochemical parameters[90]. The effect of bile and pancreatic juice on gene delivery has been studied under the guide of endoscopic retrograde cholangiopancreatography (ERCP)[92], showing that neither bile nor pancreatic juice affects transgene expression. Intrasplenic injection of p53 products can transfer gene into the portal venous circulation. When p53 products are injected intravenously, barriers such as the endothelial lining of tumor vasculature impair the efficiency of adenoviral vectors for gene delivery into HCCs[65,82], which can be overcome by direct injection of p53 products into tumor tissues[89]. Other gene delivery routes have also been reported[91].

High-volume hydrodynamic injection of a gene *via* the hepatic artery with inferior vena cava/portal vein occlusion can achieve a high level of gene expression in HCC rat model[67]. This gene transfer technique may have potential in clinical gene therapy for HCC. Oncolytic adenovirus-mediated gene therapy induces tumor-cell apoptosis and reduces tumor angiogenesis, leading to inhibition of HCC growth in animal model[88]. Because CNHK200-mE is capable of selectively replicating in HCC cells, thus suppressing tumor growth and antiangiogenic activity in nude mice[85], it can be used as a potential agent in the treatment of HCC.

CLINICAL RESEARCHES OF p53 THERAPY FOR HCC

After *in vitro* and *in vivo* experiments, different adenovirus-mediated p53 gene therapies for various tumors have been evaluated[46]. It was reported that when recombinant adenovirus p53 (SCH 58500) is administered by hepatic arterial infusion, and it distributes more predominantly in liver tissues than in tumors[93].

Intratumoural injection of Ad-p53 can lead to over-expression of p53 in cancer cells by inducing cell growth arrest and apoptosis, and overcome resistance or increase the effectiveness of radiation therapy and chemotherapy[94].

Hepatic artery embolization for the treatment of HCC was first reported in 1979[95]. Since the 1980s, transcatheter arterial chemo-embolization (TACE) has been applied

to various HCCs apart from those with humoral hypercalcemia[96]. TACE as a local ablative treatment is able to control local disease and prolong a similar survival to that of surgical resection[11]. However, the recurrence of HCC after successful control of local tumor spread is high due to the non-curative procedure. In contrast to necrosis resulting from TACE, apoptosis is not commonly accompanied with inflammation that causes collateral cell damage, suggesting that the effects of intra-tumoral or intraarterial injection of p53 products in combination with TACE, on tumor tissue ischemia and necrosis, may be synergic and can improve survival.

In addition, inhibitors of p53-mediated apoptosis might be used to transiently decrease apoptosis in normal tissues when patients receive high doses of radiation or chemotherapy[97]. Emulsion of iodized oil and contrast medium can be used as a nonviral gene transfer system for intraarterial gene delivery[72].

CHALLENGES AND PROSPECTS

p53 is an ideal target for anti-cancer drug design[14]. Blockage of p53 degradation pathways can effectively induce p53 triggered tumor cell death[14]. Since unlike most other tumor suppressor genes, mt-p53 is over-expressed in tumor cells, a promising approach involving reactivation of tumor-suppressing function to mt-p53[21,25]. Further understanding of the mechanisms of how to restore p53 activity, may lead to discovery of more potent analogs and new strategies[11,73,91] for p53-targeting in tumor therapy.

More genes previously unknown have been identified that are involved in the regulation of p53 transcriptional activity and their over-expression inhibits p53 target promoters and p53-mediated apoptosis, suggesting that these genes play a role as p53 inhibitors and may have oncogenic activity[98].

As hepatocarcinogenesis is a multistage process involving a number of genes[99,100], attention should be paid to the target genes whose altered expression actually mediates neoplastic phenotype. There is an urgent need to establish simple and low-cost tests for detecting expression of p53-related genes in HCC[99,100] that are hallmarks of HCC development. Continuous monitoring of serum p53 protein is important in early detection of recurrence of HCC, and immunodetection of serum p53 is valuable[101] for post-operative monitoring during follow-up in preoperatively positive patients.

Nevertheless, about 40% of cancers retain wt-p53, and there may be mutations of other genes in cells with p53 mutations. Therefore, the mechanisms of p53 in HCC therapies should be further studied.

It was reported that hepatic arterial administration of p53 products cannot substantially increase transduction of tumor cells, and ligation of the hepatic artery following infusion of adenovirus or addition of lipiodol infusion has no effect on the transduction of tumor cells[102], suggesting that better administration approaches must be developed for more efficient transduction of tumor cells.

Safety and research ethics must be emphasized. Human gene therapy can lead to serious adverse effects and even death[103]. In a gene therapy experiment in 1999[104], death of Jesse Gelsinger was found to be directly linked to the viral vector used for the treatment. This tragic event has raised new questions about the prospects for human gene therapy, which not only achieves a therapeutic effect but also has potential adverse effects.

Another task at present is to find out the key points of tumor resistance to rAd-p53[105-108]. Since exogenous wt-p53 was introduced, inhibition of tumor growth has become unnecessary for human cancer cells carrying mt-p53[105]. In some cancer cells, wt-p53 is inactivated by different mechanisms. Since the presence of mt-p53 may induce genome instability of human cancer cells and mutator ability, they can escape the effects of exogenous wt-p53 and contribute to the failure of wt-p53 gene therapy. On the contrary, exogenous wt-p53 in other cancers can have effects only on those expressing wt-p53. For example, alterations of p53 gene are uncommon in differentiated thyroid neoplasm but can be frequently detected in anaplastic thyroid carcinoma[107], suggesting that impaired p53 function may contribute to the undifferentiated and highly aggressive phenotype of these tumors. It was reported that exogenous expression of wt-p53 has influence on thyroid tumorigenic properties only in cells bearing altered p53, whereas it has no effect on cells expressing wt-p53 activity[106], indicating that the endogenous p53 status seems to be essential for the effectiveness of p53-based gene therapy for some cancers. Another study[108] evaluated the therapeutic effects of truncated Bid gene (tBid) on p53-resistent HCC and demonstrated that this gene only targets AFP-producing cells but not non-AFP producing ones[109]. The introduction of tBid can not only significantly but also specifically kill HCC cells that produce AFP, indicating that death of HCC cells is induced by an apoptotic pathway independent of p53 status[108].

CONCLUSION

p53 is an ideal target for the design of anti-cancer therapeutic strategies. p53 is frequently mutated in a significant portion of HCCs, and can mediate defective apoptotic pathways in HCC carrying wild type of p53. Several approaches have been designed for the treatment of HCC *via* the p53 pathway by restoring tumor suppression function from inactivation, rescuing mutated p53 gene from instability, or delivering therapeutic exogenous p53. Products with p53 status as the target have been studied extensively *in vitro* and *in vivo*. Although their therapeutic effects are limited, further study is needed to elucidate the mechanisms of p53 in HCC therapies, the role of endogenous p53 status, novel genes involved in the regulation of p53 transcriptional activity, the establishment of simple and low-cost tests for detecting expression of p53-related genes in HCC, better administration approaches of exogenous p53, safety and research ethics, and the key points of resistance to rAd-p53 in HCC.

COMMENTS

Background

Hepatocellular carcinoma (HCC) is one of the 10 most common cancers

worldwide. There are no ideal therapies for advanced HCC so far, and many researchers are trying to improve the effects of treatment by changing therapeutic strategies including application of gene therapy.

Research frontiers

About 50% of human cancers are associated with mutations in the core domain of tumor suppressor p53, thus p53 is regarded as the most frequently mutated gene. It is an attractive approach to the treatment of HCC by restoring wild type p53 activity.

Innovations and breakthroughs

Several approaches have been designed for the treatment of HCC *via* the p53 pathway by restoring tumor suppression function from inactivation, rescuing the mutated p53 gene from instability, or delivering therapeutic exogenous p53. Products with p53 status as the target have been studied extensively *in vitro* and *in vivo*.

Applications

p53 pathway can be used as a target in the treatment of HCC.

Terminology

Gene Therapy: The treatment of certain disorders, especially those caused by genetic anomalies or deficiencies, by introducing specifically engineered genes into patient cells. **p53 gene**: It is a tumor suppressor gene providing instructions for making a protein called tumor protein 53 (TP53). Through the effect of the protein it produces, *TP53* is a tumor suppressor gene regulating the cycle of cell division by protecting cells from growing and dividing too fast or in an uncontrolled way. The p53 protein is located in the nuclei of cells throughout the body and can bind directly to DNA. When the DNA in cells becomes damaged, this protein plays a critical role in determining whether the DNA is repaired or the cells undergo programmed cell death (apoptosis). If the DNA can be repaired, p53 activates other genes to repair the damage. If the DNA cannot be repaired, the p53 tumor protein protects cells from dividing and signals it to undergo apoptosis. This process protects cells with mutated or damaged DNA from dividing, which helps prevent the development of tumors. Because the p53 tumor protein is essential for regulating cell division, it has been nicknamed the "guardian of the genome. **Vector**: Any device of transportation or movement. In this article, it denotes "a virus used to deliver genetic material into cells" or "a piece of DNA carrying DNA fragments into host cells".

Peer review

This review elaborates some therapeutic mechanisms and advances in using recombinant human adenovirus p53 and oncolytic virus products in the treatment of HCC. This review is helpful for many readers. The prospects should be expanded.

REFERENCES

1 **Editorial: Playing with genes**. *Br Med J* 1976; **1**: 302
2 **Stetten D**. What men fear. *Perspect Biol Med* 1978; **21**: 515-523
3 **Friedmann T**. Progress toward human gene therapy. *Science* 1989; **244**: 1275-1281
4 **Friedmann T**. The evolving concept of gene therapy. *Hum Gene Ther* 1990; **1**: 175-181
5 **Gonçalves MA**. A concise peer into the background, initial thoughts and practices of human gene therapy. *Bioessays* 2005; **27**: 506-517
6 **Wolff JA**, Lederberg J. An early history of gene transfer and therapy. *Hum Gene Ther* 1994; **5**: 469-480
7 **Verma IM**, Weitzman MD. Gene therapy: twenty-first century medicine. *Annu Rev Biochem* 2005; **74**: 711-738
8 **Blaese RM**, Culver KW, Miller AD, Carter CS, Fleisher T, Clerici M, Shearer G, Chang L, Chiang Y, Tolstoshev P, Greenblatt JJ, Rosenberg SA, Klein H, Berger M, Mullen CA, Ramsey WJ, Muul L, Morgan RA, Anderson WF. T lymphocyte-directed gene therapy for ADA- SCID: initial trial results after 4 years. *Science* 1995; **270**: 475-480
9 **Park TG**, Jeong JH, Kim SW. Current status of polymeric gene delivery systems. *Adv Drug Deliv Rev* 2006; **58**: 467-486
10 **Seeff LB**, Hoofnagle JH. Epidemiology of hepatocellular carcinoma in areas of low hepatitis B and hepatitis C endemicity. *Oncogene* 2006; **25**: 3771-3777
11 **Müller C**. Hepatocellular carcinoma--rising incidence, changing therapeutic strategies. *Wien Med Wochenschr* 2006; **156**: 404-409
12 **Llovet JM**. Updated treatment approach to hepatocellular carcinoma. *J Gastroenterol* 2005; **40**: 225-235
13 **Cheah PL**, Looi LM. p53: an overview of over two decades of study. *Malays J Pathol* 2001; **23**: 9-16
14 **Wang W**, Rastinejad F, El-Deiry WS. Restoring p53-dependent tumor suppression. *Cancer Biol Ther* 2003; **2**: S55-S63
15 **Haupt S**, Haupt Y. Importance of p53 for cancer onset and therapy. *Anticancer Drugs* 2006; **17**: 725-732
16 **Peng Z**. Current status of gendicine in China: recombinant human Ad-p53 agent for treatment of cancers. *Hum Gene Ther* 2005; **16**: 1016-1027
17 **Ries SJ**. Elucidation of the molecular mechanism underlying tumor-selective replication of the oncolytic adenovirus mutant ONYX-015. *Future Oncol* 2005; **1**: 763-766
18 **Levine AJ**. p53, the cellular gatekeeper for growth and division. *Cell* 1997; **88**: 323-331
19 **Bálint E E**, Vousden KH. Activation and activities of the p53 tumour suppressor protein. *Br J Cancer* 2001; **85**: 1813-1823
20 **Selivanova G**, Wiman KG. p53: a cell cycle regulator activated by DNA damage. *Adv Cancer Res* 1995; **66**: 143-180
21 **Bykov VJ**, Wiman KG. Novel cancer therapy by reactivation of the p53 apoptosis pathway. *Ann Med* 2003; **35**: 458-465
22 **Hagiwara N**, Mechanic LE, Trivers GE, Cawley HL, Taga M, Bowman ED, Kumamoto K, He P, Bernard M, Doja S, Miyashita M, Tajiri T, Sasajima K, Nomura T, Makino H, Takahashi K, Hussain SP, Harris CC. Quantitative detection of p53 mutations in plasma DNA from tobacco smokers. *Cancer Res* 2006; **66**: 8309-8317
23 **Laurent-Puig P**, Zucman-Rossi J. Genetics of hepatocellular tumors. *Oncogene* 2006; **25**: 3778-3786
24 **Friedler A**, DeDecker BS, Freund SM, Blair C, Rüdiger S, Fersht AR. Structural distortion of p53 by the mutation R249S and its rescue by a designed peptide: implications for "mutant conformation". *J Mol Biol* 2004; **336**: 187-196
25 **Bullock AN**, Henckel J, DeDecker BS, Johnson CM, Nikolova PV, Proctor MR, Lane DP, Fersht AR. Thermodynamic stability of wild-type and mutant p53 core domain. *Proc Natl Acad Sci USA* 1997; **94**: 14338-14342
26 **El Far MA**, Atwa MA, Yahya RS, El Basuni MA. Evaluation of serum levels of p53 in hepatocellular carcinoma in Egypt. *Clin Chem Lab Med* 2006; **44**: 653-656
27 **Farazi PA**, Glickman J, Horner J, Depinho RA. Cooperative interactions of p53 mutation, telomere dysfunction, and chronic liver damage in hepatocellular carcinoma progression. *Cancer Res* 2006; **66**: 4766-4773
28 **Bressac B**, Galvin KM, Liang TJ, Isselbacher KJ, Wands JR, Ozturk M. Abnormal structure and expression of p53 gene in human hepatocellular carcinoma. *Proc Natl Acad Sci USA* 1990; **87**: 1973-1977
29 **Nagao M**, Nakajima Y, Hisanaga M, Kayagaki N, Kanehiro H, Aomatsu Y, Ko S, Yagita H, Yamada T, Okumura K, Nakano H. The alteration of Fas receptor and ligand system in hepatocellular carcinomas: how do hepatoma cells escape from the host immune surveillance in vivo? *Hepatology* 1999; **30**: 413-421
30 **Jeng YM**, Peng SY, Lin CY, Hsu HC. Overexpression and amplification of Aurora-A in hepatocellular carcinoma. *Clin Cancer Res* 2004; **10**: 2065-2071
31 **Hirohashi S**. Pathology and molecular mechanisms of multistage human hepatocarcinogenesis. *Princess Takamatsu Symp* 1991; **22**: 87-93
32 **Kondo M**, Marusawa H, Ueda Y, Katsurada A, Kawasome C, Takami S, Kinoshita M, Ikai I, Yamaoka Y, Chiba T. Diverse p53 gene aberration in hepatocellular carcinoma detected by dual-color fluorescence in situ hybridization. *J Gastroenterol Hepatol* 2004; **19**: 1066-1073
33 **Dewantoro O**, Gani RA, Akbar N. Hepatocarcinogenesis in viral Hepatitis B infection: the role of HBx and p53. *Acta Med*

Indones 2006; **38**: 154-159
34 **Cho JW**, Park K, Kweon GR, Park JC, Lee JC, Baek WK, Jang BC, Suh SI, Suh MH. Modulation of cell death sensitivity by mutant p53 in HCV core-expressing cells. *Int J Mol Med* 2005; **15**: 475-480
35 **Wu CG**, Salvay DM, Forgues M, Valerie K, Farnsworth J, Markin RS, Wang XW. Distinctive gene expression profiles associated with Hepatitis B virus x protein. *Oncogene* 2001; **20**: 3674-3682
36 **Mathonnet G**, Lachance S, Alaoui-Jamali M, Drobetsky EA. Expression of hepatitis B virus X oncoprotein inhibits transcription-coupled nucleotide excision repair in human cells. *Mutat Res* 2004; **554**: 305-318
37 **Elmore LW**, Hancock AR, Chang SF, Wang XW, Chang S, Callahan CP, Geller DA, Will H, Harris CC. Hepatitis B virus X protein and p53 tumor suppressor interactions in the modulation of apoptosis. *Proc Natl Acad Sci USA* 1997; **94**: 14707-14712
38 **Cougot D**, Neuveut C, Buendia MA. HBV induced carcinogenesis. *J Clin Virol* 2005; **34** Suppl 1: S75-S78
39 **Zhang X**, Dong N, Yin L, Cai N, Ma H, You J, Zhang H, Wang H, He R, Ye L. Hepatitis B virus X protein upregulates survivin expression in hepatoma tissues. *J Med Virol* 2005; **77**: 374-381
40 **Kannangai R**, Wang J, Liu QZ, Sahin F, Torbenson M. Survivin overexpression in hepatocellular carcinoma is associated with p53 dysregulation. *Int J Gastrointest Cancer* 2005; **35**: 53-60
41 **Lacabanne V**, Viguier M, Guillet JG, Choppin J. A wild-type p53 cytotoxic T cell epitope is presented by mouse hepatocarcinoma cells. *Eur J Immunol* 1996; **26**: 2635-2639
42 **Eipel C**, Schuett H, Glawe C, Bordel R, Menger MD, Vollmar B. Pifithrin-alpha induced p53 inhibition does not affect liver regeneration after partial hepatectomy in mice. *J Hepatol* 2005; **43**: 829-835
43 **Lutz W**, Nowakowska-Swirta E. Gene p53 mutations, protein p53, and anti-p53 antibodies as biomarkers of cancer process. *Int J Occup Med Environ Health* 2002; **15**: 209-218
44 **Müller M**, Meyer M, Schilling T, Ulsperger E, Lehnert T, Zentgraf H, Stremmel W, Volkmann M, Galle PR. Testing for anti-p53 antibodies increases the diagnostic sensitivity of conventional tumor markers. *Int J Oncol* 2006; **29**: 973-980
45 **Gurova KV**, Hill JE, Guo C, Prokvolit A, Burdelya LG, Samoylova E, Khodyakova AV, Ganapathi R, Ganapathi M, Tararova ND, Bosykh D, Lvovskiy D, Webb TR, Stark GR, Gudkov AV. Small molecules that reactivate p53 in renal cell carcinoma reveal a NF-kappaB-dependent mechanism of p53 suppression in tumors. *Proc Natl Acad Sci USA* 2005; **102**: 17448-17453
46 **Horowitz J**. Adenovirus-mediated p53 gene therapy: overview of preclinical studies and potential clinical applications. *Curr Opin Mol Ther* 1999; **1**: 500-509
47 **Momand J**, Zambetti GP, Olson DC, George D, Levine AJ. The mdm-2 oncogene product forms a complex with the p53 protein and inhibits p53-mediated transactivation. *Cell* 1992; **69**: 1237-1245
48 **Wu X**, Bayle JH, Olson D, Levine AJ. The p53-mdm-2 autoregulatory feedback loop. *Genes Dev* 1993; **7**: 1126-1132
49 **Zhang** H. MDM2 oncogene as a novel target for human cancer therapy. *Curr Pharm Des* 2000; **6**: 393-416
50 **Stearns T**, Willingham MC, Botstein D, Kahn RA. ADP-ribosylation factor is functionally and physically associated with the Golgi complex. *Proc Natl Acad Sci USA* 1990; **87**: 1238-1242
51 **Wen LT**, Knowles AF. Extracellular ATP and adenosine induce cell apoptosis of human hepatoma Li-7A cells via the A3 adenosine receptor. *Br J Pharmacol* 2003; **140**: 1009-1018
52 **Rocha S**, Perkins ND. ARF the integrator: linking NF-kappaB, p53 and checkpoint kinases. *Cell Cycle* 2005; **4**: 756-759
53 **Brown DR**, Deb S, Muñoz RM, Subler MA, Deb SP. The tumor suppressor p53 and the oncoprotein simian virus 40 T antigen bind to overlapping domains on the MDM2 protein. *Mol Cell Biol* 1993; **13**: 6849-6857
54 **Lin J**, Zhu MH. Interactive pathway of ARF-mdm2-p53. *Ai Zheng* 2003; **22**: 328-330
55 **Guo Y**, Zeng Y, Wang K, Zhu X, Luo H, Zheng M, Li M, Chen J. Therapeutic potential of recombinant adenovirus expressing p53 in hepatocellular carcinoma cell lines. *Zhonghua Ganzangbing Zazhi* 2001; **9** Suppl: 43-45
56 **Oliveira AM**, Ross JS, Fletcher JA. Tumor suppressor genes in breast cancer: the gatekeepers and the caretakers. *Am J Clin Pathol* 2005; **124** Suppl: S16-S28
57 **Chan KT**, Lung ML. Mutant p53 expression enhances drug resistance in a hepatocellular carcinoma cell line. *Cancer Chemother Pharmacol* 2004; **53**: 519-526
58 **Li YX**, Lin ZB, Tan HR. Wild type p53 increased chemo-sensitivity of drug-resistant human hepatocellular carcinoma Bel7402/5-FU cells. *Acta Pharmacol Sin* 2004; **25**: 76-82
59 **Zhang X**, Godbey WT. Viral vectors for gene delivery in tissue engineering. *Adv Drug Deliv Rev* 2006; **58**: 515-534
60 **Büning H**, Ried MU, Perabo L, Gerner FM, Huttner NA, Enssle J, Hallek M. Receptor targeting of adeno-associated virus vectors. *Gene Ther* 2003; **10**: 1142-1151
61 **Miyazaki M**, Obata Y, Abe K, Furusu A, Koji T, Tabata Y, Kohno S. Gene transfer using nonviral delivery systems. *Perit Dial Int* 2006; **26**: 633-640
62 **Palmer DH**, Mautner V, Mirza D, Oliff S, Gerritsen W, van der Sijp JR, Hubscher S, Reynolds G, Bonney S, Rajaratnam R, Hull D, Horne M, Ellis J, Mountain A, Hill S, Harris PA, Searle PF, Young LS, James ND, Kerr DJ. Virus-directed enzyme prodrug therapy: intratumoral administration of a replication-deficient adenovirus encoding nitroreductase to patients with resectable liver cancer. *J Clin Oncol* 2004; **22**: 1546-1552
63 **Kodama K**, Katayama Y, Shoji Y, Nakashima H. The features and shortcomings for gene delivery of current non-viral carriers. *Curr Med Chem* 2006; **13**: 2155-2161
64 **Noireaux V**, Libchaber A. A vesicle bioreactor as a step toward an artificial cell assembly. *Proc Natl Acad Sci USA* 2004; **101**: 17669-17674
65 **Kim JW**, Lee HS. Tumor targeting by doxorubicin-RGD-4C peptide conjugate in an orthotopic mouse hepatoma model. *Int J Mol Med* 2004; **14**: 529-535
66 **Barraud L**, Merle P, Soma E, Lefrançois L, Guerret S, Chevallier M, Dubernet C, Couvreur P, Trépo C, Vitvitski L. Increase of doxorubicin sensitivity by doxorubicin-loading into nanoparticles for hepatocellular carcinoma cells in vitro and in vivo. *J Hepatol* 2005; **42**: 736-743
67 **Tada M**, Hatano E, Taura K, Nitta T, Koizumi N, Ikai I, Shimahara Y. High volume hydrodynamic injection of plasmid DNA via the hepatic artery results in a high level of gene expression in rat hepatocellular carcinoma induced by diethylnitrosamine. *J Gene Med* 2006; **8**: 1018-1026
68 **Meyer F**, Ball V, Schaaf P, Voegel JC, Ogier J. Polyplex-embedding in polyelectrolyte multilayers for gene delivery. *Biochim Biophys Acta* 2006; **1758**: 419-422
69 **Uto H**, Ido A, Hori T, Hirono S, Hayashi K, Tamaoki T, Tsubouchi H. Hepatoma-specific gene therapy through retrovirus-mediated and targeted gene transfer using an adenovirus carrying the ecotropic receptor gene. *Biochem Biophys Res Commun* 1999; **265**: 550-555
70 **Min KA**, Lee SK, Kim CK. Improved gene expression pattern using Epstein-Barr virus (EBV)-based plasmid and cationic emulsion. *Biomaterials* 2005; **26**: 1063-1070
71 **Wilson GM**, Deeley RG. An episomal expression vector system for monitoring sequence-specific effects on mRNA stability in human cell lines. *Plasmid* 1995; **33**: 198-207
72 **Kim YI**, Chung JW, Park JH, Han JK, Hong JW, Chung H. Intraarterial gene delivery in rabbit hepatic tumors: transfection with nonviral vector by using iodized oil emulsion. *Radiology* 2006; **240**: 771-777
73 **Cherubini G**, Petouchoff T, Grossi M, Piersanti S, Cundari E, Saggio I. E1B55K-deleted adenovirus (ONYX-015) overrides G1/S and G2/M checkpoints and causes mitotic catastrophe and endoreduplication in p53-proficient normal cells. *Cell Cycle* 2006; **5**: 2244-2252
74 **O'Shea CC**, Johnson L, Bagus B, Choi S, Nicholas C, Shen

A, Boyle L, Pandey K, Soria C, Kunich J, Shen Y, Habets G, Ginzinger D, McCormick F. Late viral RNA export, rather than p53 inactivation, determines ONYX-015 tumor selectivity. *Cancer Cell* 2004; **6**: 611-623

75 **Gonçalves MA**, de Vries AA. Adenovirus: from foe to friend. *Rev Med Virol* 2006; **16**: 167-186

76 **Zhang LQ**, Mei YF, Wadell G. Human adenovirus serotypes 4 and 11 show higher binding affinity and infectivity for endothelial and carcinoma cell lines than serotype 5. *J Gen Virol* 2003; **84**: 687-695

77 **Ebner K**, Rauch M, Preuner S, Lion T. Typing of human adenoviruses in specimens from immunosuppressed patients by PCR-fragment length analysis and real-time quantitative PCR. *J Clin Microbiol* 2006; **44**: 2808-2815

78 **Jacobs SC**, Davison AJ, Carr S, Bennett AM, Phillpotts R, Wilkinson GW. Characterization and manipulation of the human adenovirus 4 genome. *J Gen Virol* 2004; **85**: 3361-3366

79 **Bos JL**, Jochemsen AG, Bernards R, Schrier PI, van Ormondt H, van der Eb AJ. Deletion mutants of region E1a of AD12 E1 plasmids: effect on oncogenic transformation. *Virology* 1983; **129**: 393-400

80 **Wills KN**, Maneval DC, Menzel P, Harris MP, Sutjipto S, Vaillancourt MT, Huang WM, Johnson DE, Anderson SC, Wen SF. Development and characterization of recombinant adenoviruses encoding human p53 for gene therapy of cancer. *Hum Gene Ther* 1994; **5**: 1079-1088

81 **Nishizaki M**, Fujiwara T, Tanida T, Hizuta A, Nishimori H, Tokino T, Nakamura Y, Bouvet M, Roth JA, Tanaka N. Recombinant adenovirus expressing wild-type p53 is antiangiogenic: a proposed mechanism for bystander effect. *Clin Cancer Res* 1999; **5**: 1015-1023

82 **Heise C**, Sampson-Johannes A, Williams A, McCormick F, Von Hoff DD, Kirn DH. ONYX-015, an E1B gene-attenuated adenovirus, causes tumor-specific cytolysis and antitumoral efficacy that can be augmented by standard chemotherapeutic agents. *Nat Med* 1997; **3**: 639-645

83 **Rothmann T**, Hengstermann A, Whitaker NJ, Scheffner M, zur Hausen H. Replication of ONYX-015, a potential anticancer adenovirus, is independent of p53 status in tumor cells. *J Virol* 1998; **72**: 9470-9478

84 **Stoff-Khalili MA**, Dall P, Curiel DT. Gene therapy for carcinoma of the breast. *Cancer Gene Ther* 2006; **13**: 633-647

85 **Li G**, Sham J, Yang J, Su C, Xue H, Chua D, Sun L, Zhang Q, Cui Z, Wu M, Qian Q. Potent antitumor efficacy of an E1B 55kDa-deficient adenovirus carrying murine endostatin in hepatocellular carcinoma. *Int J Cancer* 2005; **113**: 640-648

86 **Qian Q**, Sham J, Che X, Xu J, Xue H, Cui Z, Zhu B, Wu M. Gene-viral vectors: a promising way to target tumor cells and express anticancer genes simultaneously. *Chin Med J (Engl)* 2002; **115**: 1213-1217

87 **Li GC**, Yang JM, Nie MM, Su CG, Sun LC, Qian YZ, Fang GE, Sham J, Wu MC, Qian QJ. Potent antitumoral effects of a novel gene-viral therapeutic system CNHK300-mEndostatin in hepatocellular carcinoma. *Chin Med J (Engl)* 2005; **118**: 179-185

88 **Ye Z**, Wang X, Hao S, Zhong J, Xiang J, Yang J. Oncolytic adenovirus-mediated E1A gene therapy induces tumor-cell apoptosis and reduces tumor angiogenesis leading to inhibition of hepatocellular carcinoma growth in animal model. *Cancer Biother Radiopharm* 2006; **21**: 225-234

89 **Yoon SK**, Armentano D, Wands JR, Mohr L. Adenovirus-mediated gene transfer to orthotopic hepatocellular carcinomas in athymic nude mice. *Cancer Gene Ther* 2001; **8**: 573-579

90 **Kuriyama S**, Yoshiji H, Nakai S, Deguchi A, Uchida N, Kimura Y, Inoue H, Kinekawa F, Ogawa M, Nonomura T, Masaki T, Kurokohchi K, Watanabe S. Adenovirus-mediated gene transfer into rat livers: comparative study of retrograde intrabiliary and antegrade intraportal administration. *Oncol Rep* 2005; **13**: 69-74

91 **White SA**, LoBuglio AF, Arani RB, Pike MJ, Moore SE, Barlow DL, Conry RM. Induction of anti-tumor immunity by intrasplenic administration of a carcinoembryonic antigen DNA vaccine. *J Gene Med* 2000; **2**: 135-140

92 **Xie X**, Forsmark CE, Lau JY. Effect of bile and pancreatic juice on adenoviral-mediated gene delivery: implications on the feasibility of gene delivery through ERCP. *Dig Dis Sci* 2000; **45**: 230-236

93 **Atencio IA**, Grace M, Bordens R, Fritz M, Horowitz JA, Hutchins B, Indelicato S, Jacobs S, Kolz K, Maneval D, Musco ML, Shinoda J, Venook A, Wen S, Warren R. Biological activities of a recombinant adenovirus p53 (SCH 58500) administered by hepatic arterial infusion in a Phase 1 colorectal cancer trial. *Cancer Gene Ther* 2006; **13**: 169-181

94 **Roth JA**. Adenovirus p53 gene therapy. *Expert Opin Biol Ther* 2006; **6**: 55-61

95 **Roche A**, Franco D, Dhumeaux D, Bismuth H, Doyon D. Emergency hepatic arterial embolization for secondary hypercalcemia in hepatocellular carcinoma. *Radiology* 1979; **133**: 315-316

96 **Suzuki K**, Kono N, Ono A, Osuga Y, Kiyokawa H, Mineo I, Matsuda Y, Miyoshi S, Kawata S, Minami Y. Transcatheter arterial chemo-embolization for humoral hypercalcemia of hepatocellular carcinoma. *Gastroenterol Jpn* 1988; **23**: 29-36

97 **Strom E**, Sathe S, Komarov PG, Chernova OB, Pavlovska I, Shyshynova I, Bosykh DA, Burdelya LG, Macklis RM, Skaliter R, Komarova EA, Gudkov AV. Small-molecule inhibitor of p53 binding to mitochondria protects mice from gamma radiation. *Nat Chem Biol* 2006; **2**: 474-479

98 **Llanos S**, Efeyan A, Monsech J, Dominguez O, Serrano M. A high-throughput loss-of-function screening identifies novel p53 regulators. *Cell Cycle* 2006; **5**: 1880-1885

99 **Feitelson MA**, Pan J, Lian Z. Early molecular and genetic determinants of primary liver malignancy. *Surg Clin North Am* 2004; **84**: 339-354

100 **Zhu MH**, Ni CR, Zhu Z, Li FM, Zhang SM. Determination of expression of eight p53-related genes in hepatocellular carcinoma with tissue microarrays. *Ai Zheng* 2003; **22**: 680-685

101 **Attallah AM**, Abdel-Aziz MM, El-Sayed AM, Tabll AA. Detection of serum p53 protein in patients with different gastrointestinal cancers. *Cancer Detect Prev* 2003; **27**: 127-131

102 **Maron DJ**, Tada H, Moscioni AD, Tazelaar J, Fraker DL, Wilson JM, Spitz FR. Intra-arterial delivery of a recombinant adenovirus does not increase gene transfer to tumor cells in a rat model of metastatic colorectal carcinoma. *Mol Ther* 2001; **4**: 29-35

103 **Smith L**, Byers JF. Gene therapy in the post-Gelsinger era. *JONAS Healthc Law Ethics Regul* 2002; **4**: 104-110

104 **Walters J**. Why did Jesse die? *Update* 2001; **17**: E1

105 **Vinyals A**, Peinado MA, Gonzalez-Garrigues M, Monzó M, Bonfil RD, Fabra A. Failure of wild-type p53 gene therapy in human cancer cells expressing a mutant p53 protein. *Gene Ther* 1999; **6**: 22-33

106 **Moretti F**, Nanni S, Farsetti A, Narducci M, Crescenzi M, Giuliacci S, Sacchi A, Pontecorvi A. Effects of exogenous p53 transduction in thyroid tumor cells with different p53 status. *J Clin Endocrinol Metab* 2000; **85**: 302-308

107 **Moretti F**, Farsetti A, Soddu S, Misiti S, Crescenzi M, Filetti S, Andreoli M, Sacchi A, Pontecorvi A. p53 re-expression inhibits proliferation and restores differentiation of human thyroid anaplastic carcinoma cells. *Oncogene* 1997; **14**: 729-740

108 **Miao J**, Chen GG, Chun SY, Yun JP, Chak EC, Ho RL, Lai PB. Adenovirus-mediated tBid overexpression results in therapeutic effects on p53-resistant hepatocellular carcinoma. *Int J Cancer* 2006; **119**: 1985-1993

109 **Luo X**, Budihardjo I, Zou H, Slaughter C, Wang X. Bid, a Bcl2 interacting protein, mediates cytochrome c release from mitochondria in response to activation of cell surface death receptors. *Cell* 1998; **94**: 481-490

S- Editor Liu Y **L- Editor** Wang XL **E- Editor** Lu W

PO Box 2345, Beijing 100023, China
www.wjgnet.com
wjg@wjgnet.com

World J Gastroenterol 2007 February 21; 13(7): 993-996
World Journal of Gastroenterology ISSN 1007-9327

REVIEW

Metallothionein: An overview

N Thirumoorthy, KT Manisenthil Kumar, A Shyam Sundar, L Panayappan, Malay Chatterjee

N Thirumoorthy, College of Pharmacy, Kovai Estate, Kalapatti Road, Tamilnadu, India
KT Manisenthil Kumar, A Shyam Sundar, L Panayappan, Malay Chatterjee, Department of Pharmaceutical Technology, Jadavpur University, Kolkata, India
Correspondence to: N Thirumoorthy, KMCH, College of Pharmacy, Kovai Estate, Kalapatti Road, Coimbatore 641 035, Tamilnadu, India. tmoorthyn@yahoo.com
Telephone: +91-98-43255552 Fax: +91-422-2628645
Received: 2006-07-27 Accepted: 2007-01-10

Abstract

Metallothioneins (MTs) were discovered in 1957 by Margoshes and Vallee and identified as low-molecular weight and sulphydryl rich proteins. It is not surprising that most mammalian tissues contain age related basal levels of MTs since they are involved in metalloregulatory processes that include cell growth and multiplication. In an effort to understand the biology of this intriguing tumor, various biomarkers such as oncogenes, p53 tumor suppressor gene, waf 1 protein, proliferating cell nuclear antigen, telomerase, microsatellite markers and cytogenetic changes have been examined. One biomarker which has recently shown to be expressed in various human tumors but still less reported in carcinoma is MT. Immunohistochemical detection of MT proteins in cold acetone-fixed paraffin embedded liver sections was performed by the streptavidin-avidin-biotin immuno-peroxidase complex method.

Key words: Metallothioneins; Protective function; Immuno-histochemical detection; Anti-oxidant character; Metal regulatory gene; Oncogene; Apoptosis; Genotoxic; Non-genotoxic environment; Detoxification

Thirumoorthy N, Manisenthil Kumar KT, Shyam Sundar A, Panayappan L, Chatterjee M. Metallothionein: An overview. *World J Gastroenterol* 2007; 13(7): 993-996

http://www.wjgnet.com/1007-9327/13/993.asp

INTRODUCTION

Metallothioneins (MTs) were discovered in 1957 by Margoshes and Vallee and identified as low-molecular weight sulphydryl rich proteins. Due to their high metal content and unusual bioinorganic structure, they are distinguished as metalloproteins. It is not surprising that most mammalian tissues contain age related basal levels of MTs since they are involved in metalloregulatory processes that include cell growth and multiplication. The presence of high levels of MTs in developing mammalian cells is well documented and it has been suggested that the MT-expressed protein is similar to onco-developmental gene products such as alpha-fetoprotein[1].

Classification of MTs

MT is a small protein with a high affinity for divalent heavy metal ions. MTs are a family of Mr 6000 proteins comprised of MT-Ⅰ, MT-Ⅱ, MT-Ⅲ and MT-Ⅳ classes with multiple isoforms within each class. MT-Ⅰ and MT-Ⅱ are ubiquitously expressed and are stress inducible. MT-Ⅰ isoform inducibility is reported to depend on the embryonic germ layer from which a tumor is derived[2].

MTs are a group of ubiquitous low molecular mass cysteine-rich intracellular metal binding proteins. In human, MTs are encoded by a family of genes consisting of 10 functional MT isoforms and the encoded proteins are conventionally subdivided into four groups: MT-1, MT-2, MT-3 and MT-4 proteins. While a single MT-2A gene encodes MT-2 protein, MT-1 protein comprises many subtypes encoded by a set of MT-1 genes (MT-1A, MT-1B, MT-1E, MT-1F, MT-1G, MT-1H and MT-1X), accounting for the micro-heterogeneity of the MT-1 protein. Different MT genes in humans possibly play different functional roles during development or under various physiological conditions[3,4].

The known functions of MTs include metalloregulatory roles in cell growth and differentiation, and enhanced synthesis of MTs in rapidly proliferating tissues suggests its crucial role in normal and neoplastic cell growth[5].

Characteristics of MTs

These intracellular proteins are characterized by their unusual high cysteine content (30%) and lack of aromatic amino acids. Because of their rich thiol content, MTs bind a number of trace metals including cadmium, mercury, platinum and silver, and also protect cells and tissues against heavy metal toxicity. Additionally MTs are among the most abundant intracellular aspects for biologically essential metals, zinc and copper. MT metal-thiolate fractions being dynamic and of high affinity also facilitate metal exchange in tissues[6].

They are present in a great variety of eukaryotes[3], functioning as anti-oxidants; they also play a protective role against hydroxyl free radicals. This is relevant in tumors (nasopharyngeal carcinoma) which are known to be

markedly radio-sensitive, where radiotherapy (which kills cells *via* free-radical-induced apoptosis) is the treatment of choice[7].

MT AS TUMOR MARKER

Alteration in MT function due to carcinogenesis

Development of carcinogenesis is a dynamic process in which irregulation of gene function occurs. Time is crucial in this process. During a latency period of several years or even decades, the genetic material of cells is subject to multiple 'hits' by damaged substances, carcinogens, etc. Accumulation of damage leads to altered gene function and colonal expansion of mutated cells. However, most of these early lesions never develop into more aggressive and invasive states, but disappear spontaneously. This feature of carcinogenesis does not solely influence the initial phase of this process but actively intervenes and changes the course of the disease[5].

Protective functions of MT

MTs have a high binding affinity to bivalent metal ions. A number of studies have demonstrated the presence or enhanced synthesis of MT in rapidly proliferating normal cells, regenerating cells and cancer cells. The studies have suggested a relationship between high expression of MT protein and aggressive neoplastic cell growth. Due to their nucleophilicity, MTs have been shown to protect cells against the cytotoxic effects of electrophilic anticancer drugs. However, protection of cells by MT from the cytotoxic effect of agents such as 1-β-D-arabinofuranosyl cytosine and nuclear factor DF-α must involve mechanisms other than simple covalent binding[8].

Relation between MT and apoptosis

Recent reports of various studies have shown that the enhanced expression of MT in cells induces the anti-apoptotic effects and a lack of MT in MT null cells increases the susceptibility to apoptic cell death after exposure to certain anticancer drugs. The down-regulation of MT in MCF-7 cells within 18-mer antisense has not only shown inhibition in growth but also initiated apoptosis[8].

MTs INVOLVED IN PATHOPHYSIOLOGICAL PROCESSES IN HUMAN

Role of MT in detoxification

MTs play a homeostatic role in the control and detoxification of the heavy metals; several evidences indicate that MT has the capacity to scavenge reactive oxygen metabolite (ROM), particularly the hydroxyl radical. These substances which are produced continuously during normal aerobic metabolism may become noxious in situations of imbalance with endogenous antioxidants and then can induce DNA damage, lipid peroxidation, enzyme oxidation, *etc.*, leading to cellular destruction, chromosomal aberrations and finally to cancer. Paradoxically, by anticancer treatment such as radiotherapy, chemotherapy and photodynamic therapy, tumor cells are killed by generating toxic amounts of ROM[2].

MT was considered as a potential prognostic marker in invasive ductal carcinoma of the breast[9], skin[10], cervix[11] and pancreas[12]. Irregular cell growth, due to increased cell proliferation or failure of cells to undergo apoptosis is recognized as a major contributory factor to the malignant process.

Dual functions of MT

MTs appear to perform dual functions of influencing the growth and survival of tumor cells as they are known to have metallo-regulatory functions in cellular repair processes, growth and differentiation and to play a protective role in oxidative stress by scavenging free radicals, thus protecting the cell against apoptosis induced by oxidative stress. MT can be induced by a number of endogenous and exogenous stimuli including glucocorticoids, interferon, interleukin-1, progesterone, vitamin D_3 endotoxins, serum factors, and heavy metals, storage of metal ions and regulation of cellular zinc[1].

MT and its response to anti-cancer drugs

The association of MT expression with spontaneous mutagenesis response to anti-cancer drugs and tumor progression has emerged in recent years. This has been more significant in the later stage, with reliable methods for detecting the two isoforms of MT-Ⅰ and MT-Ⅱ by immunohistochemistry in archival tissues. MT over expression has been associated with more malignant and higher grade tumors in some cancers and with more differentiated lower grade tumors in others[6].

Over expression of MT

The *in vitro* studies suggest that MT over expression in ovarian cancer may induce chemo-resistance. It has been proposed that the sequestration of drugs or their metabolites may prevent the reaction of these compounds with the respective intracellular target, thus decreasing the efficacy of certain anti-cancer drugs.

Recurrence of drug resistant ovarian tumors that initially appear to respond well to chemotherapy may be explained by over expression of drug resistance proteins such as MT.

Another opinion of the same investigators is that growth factor signals might activate transcription factors that control the expression of drug-resistant enzymes and proteins. However, two independent groups of investigators were unable to find a direct causal relationship between MT expression and chemo-resistance[1].

Genotoxic and non-genotoxic effects

Humans are exposed to mixtures of genotoxic and non-genotoxic environmental chemicals that may be linked to cancer. Robust biomarkers of somatic stem cell mutation and mutant clonal expansion may provide cancer surrogates that are useful for risk assessment. Acquired mutation of a selectable endogenous reporter gene like glucose-6-phosphate dehydrogenase (G6PD) within a colonic crypt stem cell induces a crypt-restricted phenotype change.

Stem cell mutation

Stable crypt-restricted immunopositivity for MT is a recently described stem cell mutation marker for mouse colon that can be assayed in paraffin-fixed tissue sections and has been validated against the G6PD assay. MT-immunopositive crypt frequency has shown a dose response to three different chemical mutagens that further confirmed the evidence that it is a somatic mutation marker[13].

Low levels of MTs and their susceptibility

Accumulating evidence indicates that cells with low levels of intracellular MT are more susceptible to DNA damage and apoptotic death after exposure to stress stimuli including oxidative stress, whereas prior induction of MT appears to confer protection. The findings of changes in unicellular localization of MT from cytoplasm to the nucleus during early differention of myoblasts coincide with increased apoptosis of newly formed myotubes[14].

Markers of carcinogenesis

The basal expression of MT in normal cells has generally been associated with heavy metal detoxification, intracellular trace elements storage and scavenging of free radicals. Authors Tridip and Thirumoorthy studied the roles of alterations of hepatic levels of trace elements and significance of the expression of MT and Ki-67 proteins as important markers of carcinogenesis in the development of pre-malignant phenotype and the reported dose (0.5 ppm) of vanadium in suppressing 2-AAF-induced carcinogenicity. Several reports are available to show that, over expression and up-regulation of MT and Ki-67 proteins are associated with the carcinogenic processes. But the reports documenting the anti-neoplastic potential of chemo-preventive agents in modulating these indicts are meager.

It was reported that the chemo-preventive potential of vanadium is suppressing in MT and Ki-67 expression in preneoplastic rat liver. The role of vanadium on p53 expression and induction of apoptosis in a defined rat model of experimental hepato-carcinogenesis has also been brought into focus[15].

MT as anti-oxidants

MTs can function as antioxidants. It has been suggested that intracellular oxidants may play a role in anticancer drug mediated programmed cell death and it was observed that MT expression can be regulated by ambient oxygen levels. This has led to speculation that MT may be an inducible anti-apoptotic gene product[6].

Proteins like MT may play an important role in carcinogenesis, including tumor cell pathology and drug resistance. It was shown that colorectal and gastric carcinogenesis was associated with a significant increase in the level of manganese (Mn-SOD) containing superoxide dismutase, an antioxidant enzyme that detoxifies superoxide to hydrogen peroxide[2].

Factors influencing synthesis of MT

The synthesis of MT is regulated by polymorphic genes and induced by many factors such as metals, hormones, cytokinen, drugs and physical and oxidative stresses. Tumor MT levels have also been reported to correlate with resistance to anticancer reagent[16].

MT regulates intracellular concentration of zinc and other metal ions. MT over expression can influence transcription, replication and protein synthesis, and might explain why MT over expression is associated with high-grade tumors, including carcinomas of the head and neck[17].

IMMUNOSTAINING OF MT

Positive control

Immunohistochemical detection of MT protein in cold acetone-fixed paraffin embedded liver sections was performed by the streptavidin-avidin-biotin-immuno peroxidase complex method (Jin *et al*, 2002). Briefly, 5 μm thin sections on poly-L-lysine coated slides were deparaffinized and rehydrated. Endogenous peroxidase activity was blocked with 1% H_2O_2 in 0.1 mol/L Tris-NaCl (pH 7.6) for 30 min. After incubation with 5% normal goat serum for 1 h at 37℃, sections were incubated overnight at 40C with the primary antibody rabbit anti-rat MT-1 in 1% BSA using 1:50 dilution. Sections were then incubated with a bio-tinylated secondary antibody goat anti-rabbit IgG (Sigma) for 30 min at 37℃ with 1:200 dilutions.

This was followed by incubation with streptavidin peroxidase (1:100) for 1 h and subsequent chromogen development with 0.5% of 3, 3'-diamino benzedrine tetra hydrochloride (DAB) and 0.33% H_2O_2 in 0.5 mol/L Tris-NaCl as substrate. The sections were then counterstained with Harris haematoxylin (H&E), then dehydrated, mounted and served as positive control.

Negative control

Negative control was prepared following the above steps but by omitting the primary antibody. MT immuno-staining was considered positive when the nuclei and cytoplasm of the hepatocytes were stained prominently (purplish brown/reddish brown). MT immunoreactivity was expressed as percentage of immuno-positive cells. A total of 10 high power fields were randomly chosen. The numbers of positive cells were determined in relation to the total number of cells in the field[15].

REFERENCES

1 **Tan Y**, Sinniah R, Bay BH, Singh G. Metallothionein expression and nuclear size in benign, borderline, and malignant serous ovarian tumours. *J Pathol* 1999; **189**: 60-65

2 **Janssen AM**, van Duijn W, Kubben FJ, Griffioen G, Lamers CB, van Krieken JH, van de Velde CJ, Verspaget HW. Prognostic significance of metallothionein in human gastrointestinal cancer. *Clin Cancer Res* 2002; **8**: 1889-1896

3 **Kägi JH**, Schäffer A. Biochemistry of metallothionein. *Biochemistry* 1988; **27**: 8509-8515

4 **Jin R**, Bay BH, Chow VT, Tan PH, Lin VC. Metallothionein 1E mRNA is highly expressed in oestrogen receptor-negative human invasive ductal breast cancer. *Br J Cancer* 2000; **83**: 319-323

5 **Jin R**, Chow VT, Tan PH, Dheen ST, Duan W, Bay BH. Metallothionein 2A expression is associated with cell proliferation in breast cancer. *Carcinogenesis* 2002; **23**: 81-86

6 **Kondo Y**, Woo ES, Michalska AE, Choo KH, Lazo JS. Metallothionein null cells have increased sensitivity to anticancer drugs. *Cancer Res* 1995; **55**: 2021-2023
7 **Jayasurya A**, Bay BH, Yap WM, Tan NG. Correlation of metallothionein expression with apoptosis in nasopharyngeal carcinoma. *Br J Cancer* 2000; **82**: 1198-1203
8 **Abdel-Mageed AB**, Agrawal KC. Activation of nuclear factor kappaB: potential role in metallothionein-mediated mitogenic response. *Cancer Res* 1998; **58**: 2335-2338
9 **Schmid KW**, Ellis IO, Gee JM, Darke BM, Lees WE, Kay J, Cryer A, Stark JM, Hittmair A, Ofner D. Presence and possible significance of immunocytochemically demonstrable metallothionein over-expression in primary invasive ductal carcinoma of the breast. *Virchows Arch A Pathol Anat Histopathol* 1993; **422**: 153-159
10 **Zelger B**, Hittmair A, Schir M, Ofner C, Ofner D, Fritsch PO, Böcker W, Jasani B, Schmid KW. Immunohistochemically demonstrated metallothionein expression in malignant melanoma. *Histopathology* 1993; **23**: 257-263
11 **Lim K**, Evans A, Adams M, Fish R, Dhundee J, Dallimone N, Jasani B. Association of immunohistochemically detachable metallothionein (IDMT) expression with malignant transformation in cervical neoplasia. *J pathol* 1996; **178**: 48A
12 **Ohshio G**, Imamura T, Okada N, Wang ZH, Yamaki K, Kyogoku T, Suwa H, Yamabe H, Imamura M. Immunohistochemical study of metallothionein in pancreatic carcinomas. *J Cancer Res Clin Oncol* 1996; **122**: 351-355
13 **Donnelly ET**, Bardwell H, Thomas GA, Williams ED, Hoper M, Crowe P, McCluggage WG, Stevenson M, Phillips DH, Hewer A, Osborne MR, Campbell FC. Metallothionein crypt-restricted immunopositivity indices (MTCRII) correlate with aberrant crypt foci (ACF) in mouse colon. *Br J Cancer* 2005; **92**: 2160-2165
14 **Lewin B**, Genes VI. Oxford-NewYork-Tokyo: Oxford University Press, 1997: 849-850
15 **Chakraborty T**, Samanta S, Ghosh B, Thirumoorthy N, Chatterjee M. Vanadium induces apoptosis and modulates the expressions of metallothionein, Ki-67 nuclear antigen, and p53 during 2-acetylaminofluorene-induced rat liver preneoplasia. *J Cell Biochem* 2005; **94**: 744-762
16 **Hishikawa Y**, Koji T, Dhar DK, Kinugasa S, Yamaguchi M, Nagasue N. Metallothionein expression correlates with metastatic and proliferative potential in squamous cell carcinoma of the oesophagus. *Br J Cancer* 1999; **81**: 712-720
17 **Raleigh JA**, Chou SC, Calkins-Adams DP, Ballenger CA, Novotny DB, Varia MA. A clinical study of hypoxia and metallothionein protein expression in squamous cell carcinomas. *Clin Cancer Res* 2000; **6**: 855-862

S- Editor Liu Y **L- Editor** Ma JY **E- Editor** Lu W

PO Box 2345, Beijing 100023, China
www.wjgnet.com
wjg@wjgnet.com

World J Gastroenterol 2007 February 21; 13(7): 997-1002
World Journal of Gastroenterology ISSN 1007-9327

Cytochrome P450 levels are altered in patients with esophageal squamous-cell carcinoma

I Bergheim, E Wolfgarten, E Bollschweiler, AH Hölscher, C Bode, A Parlesak

I Bergheim, C Bode, A Parlesak, Department of Physiology of Nutrition, Hohenheim University (140e), Stuttgart 70599, Germany
E Wolfgarten, E Bollschweiler, AH Hölscher, Department of Visceral and Vascular Surgery, University of Cologne, Cologne, Germany
Correspondence to: Ina Bergheim, PhD, Hohenheim University (140b), Fruwirthstrasse 12, Stuttgart 70599, Germany. bergheim@uni-hohenheim.de
Telephone: +49-711-45924102 Fax: +49-711-45924343
Received: 2006-08-10 Accepted: 2007-01-23

Abstract

AIM: To investigate the role of cytochrome P450 (CYP) in the carcinogenesis of squamous-cell carcinoma (SCC) in human esophagus by determining expression patterns and protein levels of representative CYPs in esophageal tissue of patients with SCC and controls.

METHODS: mRNA expression of CYP2E1, CYP2C, CYP3A4, and CYP3A5 was determined using RT-PCR in both normal and malignant esophageal tissues of patients with untreated esophageal SCC (n = 21) and in controls (n = 10). Protein levels of CYP2E1, CYP2C8, CYP3A4, and CYP3A5 were measured by Western blot.

RESULTS: Within the group of SCC patients, mRNA expression of CYP 3A4 and CYP2C was significantly lower in malignant tissue (-39% and -74%, respectively, $P < 0.05$) than in normal tissue. Similar results were found in CYP3A4 protein levels. Between groups, CYP3A4, CYP3A5, and CYP2C8 protein concentration was significantly higher in non-malignant tissue of SCC patients (4.8-, 2.9-, and 1.9-fold elevation, $P < 0.05$) than in controls. In contrast, CYP2E1 protein levels were significantly higher in controls than in SCC patients (+46%, $P < 0.05$).

CONCLUSION: Significant differences exist in protein levels of certain CYPs in non-malignant esophageal tissue (e.g. CYP2C8, CYP3A4, CYP3A5, and CYP2E1) between SCC patients and healthy subjects and may contribute to the development of SCC in the esophagus.

Key words: Squamous-cell carcinoma; Cytochrome P450; Western blot; RT-PCR; Human

Bergheim I, Wolfgarten E, Bollschweiler E, Hölscher AH, Bode C, Parlesak A. Cytochrome P450 levels are altered in patients with esophageal squamous-cell carcinoma. *World J Gastroenterol* 2007; 13(7): 997-1002

http://www.wjgnet.com/1007-9327/13/997.asp

INTRODUCTION

Worldwide, esophageal cancer is one of the ten most common cancers[1] with an overall 5-year survival rate of 3%-10%[2]. Although the entity of adenocarcinoma is rising[3], the majority of carcinomas of the esophagus are squamous-cell carcinoma (SCC)[1]. Results of several epidemiological studies indicate that hot beverage, alcohol and tobacco are key risk factors for the development of carcinoma in the esophagus[1,4]. However, despite intense research[5], the role of xenobiotica-metabolizing enzymes in the development of esophageal SCC is not fully understood due to the lack of successful pharmacological therapies.

Cytochrome P450 (CYP) is a multi-gene superfamily of heme-containing enzymes catalyzing the oxidative metabolism of many compounds[6]. CYP families 1, 2, and 3, which are the main CYP families participating in the metabolism of xenobiotics, are highly expressed within the liver. However, several CYPs have been shown to be also expressed in extrahepatic tissues such as the esophagus[7]. CYPs not only function in the detoxification but may also be involved in the activation of potential (pro-) carcinogens. The alimentary tract is exposed to a large variety of compounds, including potential (pro-) carcinogens. Indeed, it has been proposed that extrahepatic tissue might play an important role in the CYP-mediated metabolism of xenobiotic compounds and therefore might affect the susceptibility of certain organs to the development of malignancies. However, knowledge on regulation and localization of CYPs outside the liver (i.e., the esophagus) is limited and should be clarified.

CYPs may play a critical role not only in the development of SCC in the esophagus but also in the treatment of SCC. Therefore, the aim of the present study was to determine mRNA expression and protein concentrations of representative CYPs (e.g., CYP2C, CYP2E1, CYP3A4, and CYP3A5) in macroscopically normal esophageal tissue of patients with untreated SCC and in disease-free controls. Furthermore, as the expression of CYPs may be altered throughout the development of carcinoma, levels of CYPs were also

measured in SCC and compared to those determined in macroscopically normal neighboring esophageal tissue of the same patients.

MATERIALS AND METHODS

Subjects and tissue specimens

The study was approved by the Ethics Committee of the Medical Clinic of the University of Cologne, Germany. Informed consent was obtained from all subjects included in the study. All subjects underwent endoscopy for medical screening. Of the 31 subjects enrolled, 21 had an untreated SCC of the esophagus. Ten subjects with a negative diagnosis of SCC in the esophagus or malignancies in the gastrointestinal tract and no history of esophageal SCC or other malignancies served as controls. Only subjects without medication known to affect expression of the investigated CYPs were included in the current study. All study participants completed a questionnaire concerning smoking and anthropometrical parameters (Table 1). Using a standard pinch forceps, two biopsies were obtained from macroscopically normal esophageal tissue of controls and patients with SCC. Furthermore, in SCC subjects two biopsies were taken from carcinoma. Biopsies were placed immediately in liquid nitrogen, and stored at -80℃ until analysis. Histopathological analysis of SCC was performed by an experienced pathologist. Tumor staging was based on differentiation and varied from poorly differentiated (G1: n = 2, G1-2: n = 2), moderately differentiated (G2: n = 8, G2-3: n = 4) to well differentiated (G3: n = 5). In controls, the absence of SCC, inflammation, and any other pathological changes of the esophagus were confirmed endoscopically by an experienced physician.

Table 1 Characteristics of untreated esophageal SCC patients and controls (mean ± SE)

Parameter	Patients	Controls	*P*
n	21	10	
Age	56.7 ± 1.9	51.1 ± 3.5	0.118
Sex (Female/Male)	7/14	5/5	0.425
BMI	23.8 ± 1.4	25.1 ± 0.6	0.370
Cigarette usage (Yes/No)	10/11	3/7	0.242

BMI: body mass index.

Isolation of total RNA-protein

Both total RNA and protein were isolated using Trizol reagent following the instructions of the manufacturer (Invitrogene, Gaithersburg, MD, USA). Briefly, tissue was homogenized in Trizol reagent, chloroform was added and phases were separated into RNA and protein phases. RNA was precipitated using isopropanol, washed with ethanol and resuspended in RNAase-free water. Protein was precipitated using isopropanol and washed three times in 0.3 mol/L guanidin hydrochlorid in 95% ethanol solution. The protein pellet was dried, resuspended and the concentration of protein in each sample was determined using a commercially available Bradford assay (BioRad, Munich, Germany).

Reverse transcription and PCR

Using a first-strand cDNA synthesis kit (Invitrogen, Gaithersburg, MD, USA) cDNA was synthesized from 200 ng of total RNA. For the amplification of CYPs the following primer sequences were used: CYP2C8-19, detecting CYP2C isoformes 8 to 19: sense GCTAAAGTCCAGGAAGAGATTGA and antisense TCCTGCTGAGAAAGGCATGAAGT[8]; CYP2E1: sense AGCACAACTCTGAGATATGG and antisense ATAGTCACTGTACTTGAACT[8]; CYP3A4: sense CCAAGCTATGCTCTTCACCG and antisense TCAGGCTCCACTTACGGTGC[9]; CYP3A5: sense TGTCCAGCAGAAACTGCAAA and antisense TTGAAGAAGTCCTTGCGTGTC [9] . The PCR reaction mixture consisted of 0.6 μL of cDNA, 10 × PCR buffer, 200 μmol/L dNTPs (Boehringer, Mannheim, Germany), BSA (0.25 mg/mL), DMSO (2% v/v), 0.5 μmol/LM of specific primer and 0.5 U Taq-polymerase (Promega, Madison, WI, USA), and water to a final volume of 10 μL. For amplification of the four cytochrome P450 cDNAs, PCR-conditions were as follows: at 94℃ for 3 s, at 45°C for 3 s, at 72℃ for 30 s, for 32 cycles. Amplification of histone 3.3 (primer sequences: sense CGTGCTAGCTGGATGTCTT and antisense CCACTGAACTTCTGATTCGC[10]) was performed applying the following conditions: at 94℃ for 3 s, at 45℃ for 3 s, and at 72℃ for 30 s, for 30 cycles. All measurements were carried out at least in duplicate in a rapid cycler (Idaho Tec., USA) within the linear range of the reaction. PCR products were separated in a 1.5% agarose gel, stained with ethidium bromide and photographed using a digital camera from Biometra (Goettingen, Germany). To ensure the success of PCR, human liver cDNA was used as a positive control. RT-PCR analysis was performed in triplicate, whenever possible. However, in case of a reduced mRNA availability, measurements were conducted in duplicate.

Immunoblot analysis

Antibodies used for the detection of CYP2E1 and CYP3A4 were a generous gift of Dr. M. Ingelman-Sundberg, Karolinska Institute, Stockholm, Sweden. Primary antibodies for the measurements of CYP2C8 and CYP3A5 were purchased from Chemicon, Inc. (Frankfurt, Germany).

On each blot, protein extracted from human liver was used as standard. Twenty to 30 μg of total protein and serial dilutions of standard protein (12.5, 25, and 50 μg) were separated by sodium dodecylsulphate-polyacryamide gel electrophoresis (SDS-PAGE) and transferred to nitrocellulose membranes. After blocked in 5% non-fat milk in Tris-buffered saline-Tween 20 (TBST, 0.01% v/v Tween 20), membranes were probed with dilutions of primary antibodies in TBS, followed by an incubation with the secondary antibody. The protein/antibody complex was visualized by enhanced chemiluminescence (SuperSignal® West Dura, Pierce, KTM, Bad Godesberg,

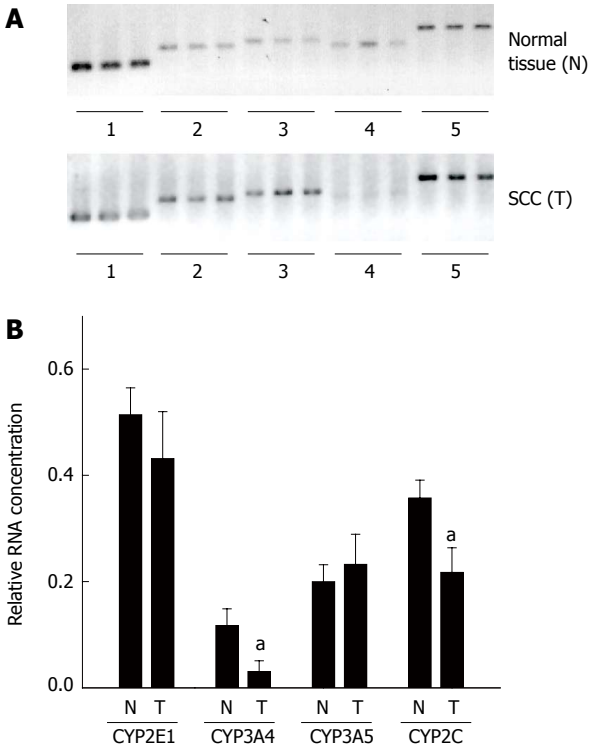

Figure 1 CYP3A5, CYP2E1, CYP3A4, and CYP2C mRNA expression in esophagus of untreated SCC patients. **A**: Representative photomicrograph of RT-PCR products of untreated esophageal SCC patients (N = normal esophageal tissue, T = tumor tissue obtained from SCC patients). Measurements were carried out either in triplicate or in case of reduced mRNA availability in duplicate. Lanes 1, 6: histone 3.3, lanes 2, 7: CYP2C, lanes 3, 8: CYP2E1, lanes 4, 9: CYP3A4, lanes 5, 10: CYP3A5; **B**: Densitometric analysis of CYP2C, CYP2E1, CYP3A4, and CYP3A5 mRNA expression in normal esophageal tissue and SCC. Results are normalized to histone 3.3 expression. Data are means ± SE. $^{a}P < 0.05$ *vs* normal tissue.

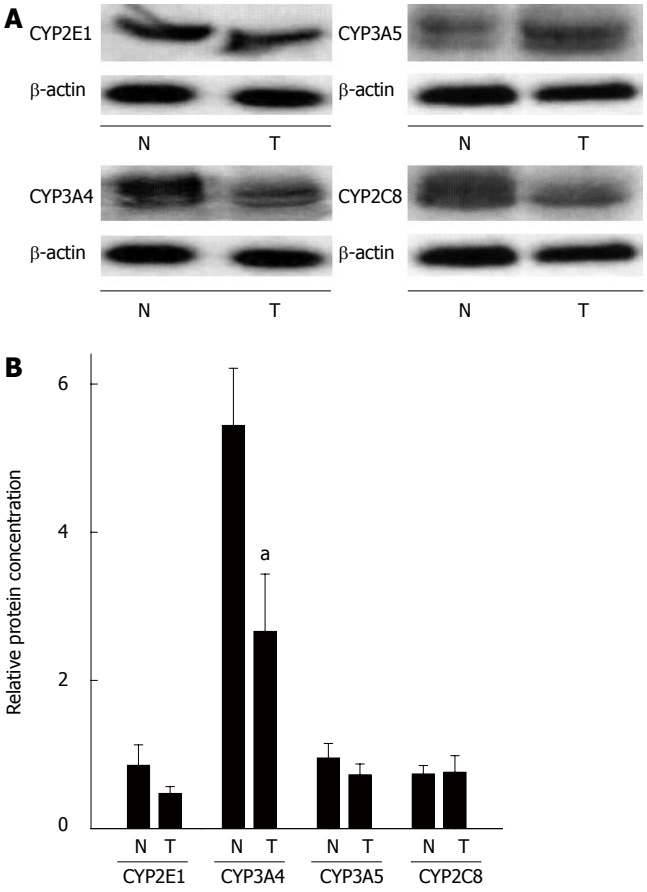

Figure 2 Protein levels of CYP2C8, CYP2E1, CYP3A4, and CYP3A5 in macroscopically normal tissue and SCC patients **A**: Representative Western blots of CYP2C8, CYP2E1, CYP3A4, and CYP3A5 in macroscopically normal esophageal tissue (N) and SCC (T) esophageal SCC patients; **B**: Quantitative analysis of blots. Results are normalized to β-actin. Data are means ± SE. $^{a}P < 0.05$ *vs* normal tissue.

Germany). Densitometric analysis was performed using the software AIDA (Raytest, Isotopenmessgeraete, Straubenhardt, Germany). Signal intensities of the samples were adjusted to the intensities of the serially diluted standards. To ensure equal loading, all blots were stained with Ponceau red. Haptene signals were normalized to β-actin using a commercially available antibody (Sigma Chemical Co., Munich, Germany).

Statistical analysis

Results are presented as means ± SE unless otherwise indicated. Fisher´s exact test was used to compare lifestyle data. The Mann-Whitney *U*-test was used for the comparison of relative mRNA concentration and protein levels measured in normal esophageal tissue obtained from patients with SCC and disease-free controls. Wilcoxon's *t*-test was used for the comparison of relative mRNA expression and protein concentration measured in normal esophageal tissue and SCC of the same patient. $P < 0.05$ was considered statistically significant.

RESULTS

The majority of the 31 patients were of normal weight and their age ranged from 38-71 years. No differences were found in smoking habits between patients and controls (Table 1).

CYP expression and protein levels in normal esophageal tissue and untreated esophageal SCC patients

High quality of undegraded mRNA from normal esophageal tissue and SCC was obtained from 12 out of 21 patients with esophageal SCC. Expression of histone 3.3 mRNA, used as housekeeping gene, was detected in all samples. The results of RT-PCR measurements are summarized in Figure 1. In addition to RNA measurements, protein levels of CYPs were determined in normal esophageal tissue and in patients with SCC (n = 21) (Figure 2).

CYP2E1: In SCC patients, expression of CYP2E1 did not differ between normal esophageal tissue and SCC. Similarly, no differences were found in CYP2E1 protein levels between normal tissue and SCC.

CYP 3A5: CYP3A5 mRNA expression and CYP3A5 protein levels were comparable in normal esophageal tissue and SCC.

CYP2 (8-19): Expression of CYP2C (8-19) was significantly lower in tissue obtained from SCC patients that in normal neighboring esophageal tissue. Specifically, mRNA expression of CYP2C (8-19) was about 39%

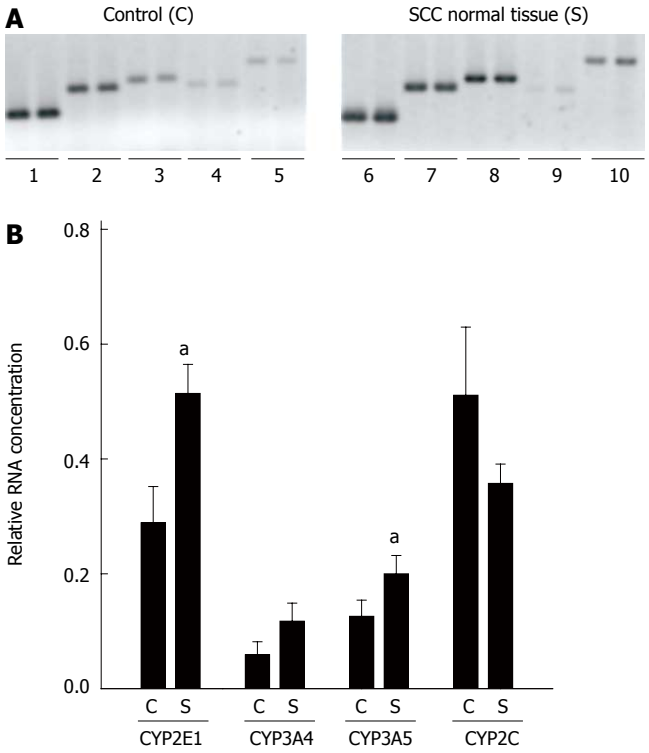

Figure 3 Expression of CYP2C8, CYP2E1, CYP3A4, and CYP3A5 in macroscopically normal tissue of SCC patients and controls. **A**: Representative photomicrograph of RT-PCR products determined in normal tissue of patients with untreated esophageal SCC (S) and controls (C). All measurements were carried out in dupilcate. Lanes 1, 6: histone 3.3, lanes 2, 7: CYP2C, lanes 3, 8: CYP2E1, lanes 4, 9: CYP3A4, lanes 5, 10: CYP3A5; **B**: Quantitative analysis of CYP2C, CYP2E1, CYP3A4, and CYP3A5 mRNA expression in normal esophageal tissue of SCC patients and controls. Results are normalized to histone 3.3 expression. Data are means ± SE. $^aP < 0.05$ *vs* normal tissue.

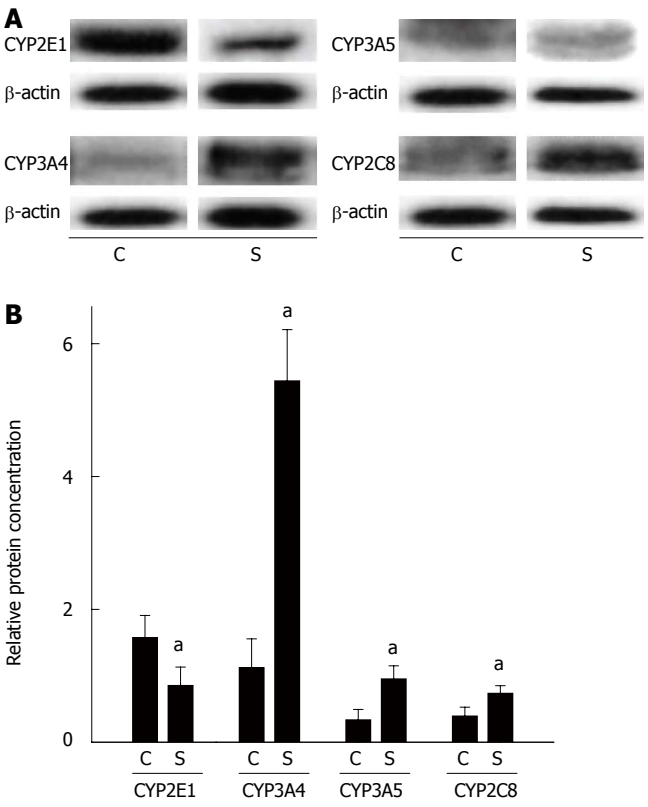

Figure 4 CYP3A5, CYP2E1, CYP3A4, and CYP2C protein levels in esophagus of SCC patients and disease-free controls. **A**: Representative Western blot of CYPs determined in normal tissue of untreated esophageal SCC patients (S) and disease-free controls (C); **B**: Quantitative analysis of CYP2C, CYP2E1, CYP3A4, and CYP3A5 protein levels in normal esophageal tissue of SCC patients and disease-free controls. Results are normalized to β-actin. Data are means ± SE. $^aP < 0.05$ *vs* disease-free controls.

lower ($P < 0.05$) in tissue of SCC patients than in normal tissue. In addition, protein concentration of CYP2C8 was determined, however no differences were found between SCC and normal tissue.

CYP3A4: CYP3A4 mRNA expression was significantly lower in SCC than in normal neighboring esophageal tissue. Specifically, mRNA expression of CYP3A4 was about 74 % lower in SCC than in normal tissue ($P < 0.05$). Furthermore, protein levels of CYP3A4 were significantly lower (by about 51%) in SCC than in normal esophageal tissue ($P < 0.05$).

Expression and protein levels of CYPs in normal esophageal tissue of SCC patients and controls

Furthermore, expression of CYP2C, CYP2E1, CYP3A4, and CYP3A5 mRNA and CYP2C8, CYP2E1, CYP3A4, as well as CYP3A5 protein concentrations were determined in normal esophageal tissue of untreated SCC patients ($n = 21$) and compared with those in 10 disease-free controls. Representative agarose gels depicting RT-PCR measurements and semiquantitative analysis of RT-PCR are shown in Figure 3. Expression of the housekeeping gene histone 3.3 was detected in all samples. Results of the comparisons of protein levels are summarized in Figure 4.

CYP2E1: Expression of CYP2E1 was found to be significantly higher by about 43 % in normal tissue obtained from patients with esophageal SCC than in disease-free controls ($P < 0.05$). Interestingly, CYP2E1 protein levels were significantly lower in normal tissue of SCC patients than in esophageal tissue obtained from disease-free controls (about -46%, $P < 0.05$).

CYP3A5: Expression of CYP3A5 mRNA in normal esophageal tissue was about 37 % higher in tissue obtained from SCC patients than in controls. Similar differences were found in protein levels, with protein levels of CYP3A5 being significantly higher by about 2.9-fold in normal esophageal tissue obtained from patients with esophageal SCC than in controls ($P < 0.05$).

CYP2C (8-19): No differences were found in CYP2C (8-19) mRNA expression between normal tissue of patients with esophageal SCC and controls. CYP2C8 protein levels were about 1.9-fold higher in normal tissue of SCC patients than in controls ($P < 0.05$).

CYP3A4: Similar to CYP2C (8-19), mRNA expression did not differ between normal tissue of patients with SCC and controls. However, when protein levels of CYP3A4 were compared between normal tissue of patients with SCC and controls, CYP3A4 protein concentration was found to be about 4.8-fold higher in normal tissue of SCC patients than in controls ($P < 0.05$).

Table 2 Correlation between mRNA expression and protein levels of CYP2E1, CYP3A4, CYP3A5, and CYP2C8 in normal esophageal tissue and SCC

Normal esophageal tissue	Spearmen R	*P*
CYP2E1	-0.09	0.72
CYP3A4	0.07	0.76
CYP3A5	0.19	0.41
CYP2C8	0.07	0.76
Esophageal SCC		
CYP2E1	0.02	0.96
CYP3A4	0.16	0.65
CYP3A5	0.49	0.15
CYP2C8	-0.22	0.53

Relation of protein levels and mRNA expression of CYPs in normal esophageal mucosa of SCC patients and disease-free controls

Since it has been shown before by others and our group[11-13] that mRNA expression and protein concentration of CYP450 are not related in tissues of some digestive organs (e.g. colon), non-parametric correlation analysis of mRNA expression and protein levels for each CYP investigated was performed. Indeed, no significant correlations were found between mRNA expression and protein levels in any of the CYPs investigated (Table 2).

DISCUSSION

Different protein levels of CYPs in normal tissue of untreated esophageal SCC patients and controls

Esophageal cancer is the third most common gastrointestinal cancer[1] with the majority of tumors being SCC[4]. It was reported that interindividual differences in CYP gene expression may contribute to the interindividual susceptibility to environmental (pro-) carcinogens and subsequently the development of malignancies[14]. Despite this hypothesis, only a few extensive studies have determined mRNA and/or protein expression of CYPs in esophageal tissue and esophageal carcinoma of humans, respectively[14-17] and most of these studies did not distinguish between adenocarcinoma and SCC. The presence of CYP2C-, CYP2E- and CYP3A- in normal esophageal tissue and SCC has been shown by others before[14-17]. However, some of the available data are contradictory and most studies determined either the expression or the protein levels in normal esophageal tissue and SCC. For example, using immunohistochemistry Murray *et al*[16] detected CYP3A, CYP1A, and CYP2C9 in most of the malignant tissue from patients with esophageal malignancies, but only CYP1A was detected in unaffected normal tissue of patients. Lechevrel *et al*[14] detected CYP3A4/5 and CYP2E1 protein and mRNA in some patients with adenocarcinoma or SCC in the esophagus. However, CYPs levels varied considerably between individuals and only CYP3A5 and CYP2E1 mRNA could be identified by RT-PCR. In the current study, CYP3A4 protein levels and CYP3A4 and CYP2C mRNA expression were found to be significantly lower in SCC than in its neighboring normal tissue. However, even more important, protein concentrations of CYP3A4, CYP3A5, and CYP2C8 were significantly higher in non-malignant esophageal tissue of patients with SCC than in tissues of healthy controls, while those of CYP2E1 were moderately reduced. At the level of mRNA expression, only CYP2E1 and CYP3A5 expression differed between groups. This finding can be considered to be of higher importance in carcinogenesis of the esophagus, as perpetually modified metabolism patterns of xenobiotics might result either in reduced detoxification of carcinogens or in elevated production of carcinogens from pro-carcinogens. The latter case might be of special importance due to strikingly increased amounts of CYP3A4 and CYP3A5 protein in non-malignant specimens from patients with SCC. These data suggest that the amount of CYPs might not only vary extensively between SCC and normal surrounding tissue but also between patients with SCC and healthy subjects. However, as in the present study CYP levels were only determined in SCC, it remains to be determined if expression and protein levels of CPYs are also altered in earlier stages of the disease (e.g., intraepithelial neoplasia of low and high grade). Furthermore, protein concentration of some CYPs (e.g., CYP2E1, CP2C8, CYP3A4, and CYP3A5) is considerably altered in normal tissue of patients with SCC compared to control subjects without malignancies. Hence, significant differences in protein concentration of these CYPs appear to be present before the development of malignancies in patients with SCC, suggesting that these enzymes are likely associated with the development of malignancies in the esophagus.

CYP mRNA is not related to protein levels either in normal esophageal tissue or in esophageal SCC

It has been suggested that expression of CYPs is not solely regulated at the level of gene transcription[18]. For instance, several studies performed in rodents and humans have reported a dissociation of mRNA expression and protein levels of CYP2C8 and CYP2E1, CYP3A4 and CYP3A5 in colon, duodenum and kidney, respectively[12,13,18]. Furthermore, *in vitro* studies performed in rat hepatocytes indicate that CYP2E1 is regulated by posttranscriptional ligand-dependent stabilization of the enzyme[19]. Similar mechanisms have been described for CYP3A in rats and humans[20,21]. Using cultured hepatocytes it also has been shown that only 60%-70% of mRNAs encoding for CYP2E1 are translated[22]. Indeed, in the present study, no correlation was found between protein and mRNA levels, suggesting that expression of certain CYPs (e.g., CYP2C8, CYP2E1, CYP3A4, and CYP3A5) in esophageal musoca might not solely be regulated at the level of transcription.

In conclusion, similar to the findings of others[14-17] interindividual variability along with a substantial dissociation of mRNA expression pattern and protein levels seems to be a characteristic of CYP expression. Although it is difficult to interpret the higher and lower levels of CYPs found in the present study, continued work focussing on the CYPs identified to have differential expression in pa-

tients with SCC is needed to determine their metabolic implications.

ACKNOWLEDGMENTS

The antibodies against human CYP2E1 and CYP3A4 were kindly provided by Dr. M Ingelman-Sundberg.

REFERENCES

1 **Glade MJ**. Food, nutrition, and the prevention of cancer: a global perspective. American Institute for Cancer Research/ World Cancer Research Fund, American Institute for Cancer Research, 1997. *Nutrition* 1999; **15**: 523-526
2 **Eloubeidi MA**, Desmond R, Arguedas MR, Reed CE, Wilcox CM. Prognostic factors for the survival of patients with esophageal carcinoma in the U.S.: the importance of tumor length and lymph node status. *Cancer* 2002; **95**: 1434-1443
3 **Bollschweiler E**, Wolfgarten E, Gutschow C, Hölscher AH. Demographic variations in the rising incidence of esophageal adenocarcinoma in white males. *Cancer* 2001; **92**: 549-555
4 **Bollschweiler E**, Wolfgarten E, Nowroth T, Rosendahl U, Mönig SP, Hölscher AH. Vitamin intake and risk of subtypes of esophageal cancer in Germany. *J Cancer Res Clin Oncol* 2002; **128**: 575-580
5 **Metzger R**, Schneider PM, Warnecke-Eberz U, Brabender J, Hölscher AH. Molecular biology of esophageal cancer. *Onkologie* 2004; **27**: 200-206
6 **Sheweita SA**. Drug-metabolizing enzymes: mechanisms and functions. *Curr Drug Metab* 2000; **1**: 107-132
7 **Ding X**, Kaminsky LS. Human extrahepatic cytochromes P450: function in xenobiotic metabolism and tissue-selective chemical toxicity in the respiratory and gastrointestinal tracts. *Annu Rev Pharmacol Toxicol* 2003; **43**: 149-173
8 **Hakkola J**, Pasanen M, Purkunen R, Saarikoski S, Pelkonen O, Mäenpää J, Rane A, Raunio H. Expression of xenobiotic-metabolizing cytochrome P450 forms in human adult and fetal liver. *Biochem Pharmacol* 1994; **48**: 59-64
9 **Kivistö KT**, Griese EU, Fritz P, Linder A, Hakkola J, Raunio H, Beaune P, Kroemer HK. Expression of cytochrome P 450 3A enzymes in human lung: a combined RT-PCR and immunohistochemical analysis of normal tissue and lung tumours. *Naunyn Schmiedebergs Arch Pharmacol* 1996; **353**: 207-212
10 **Futscher BW**, Blake LL, Gerlach JH, Grogan TM, Dalton WS. Quantitative polymerase chain reaction analysis of mdr1 mRNA in multiple myeloma cell lines and clinical specimens. *Anal Biochem* 1993; **213**: 414-421
11 **Eliasson E**, Johansson I, Ingelman-Sundberg M. Substrate-, hormone-, and cAMP-regulated cytochrome P450 degradation. *Proc Natl Acad Sci USA* 1990; **87**: 3225-3229
12 **Bergheim I**, Bode C, Parlesak A. Decreased expression of cytochrome P450 protein in non-malignant colonic tissue of patients with colonic adenoma. *BMC Gastroenterol* 2005; **5**: 34
13 **Bergheim I**, Bode C, Parlesak A. Distribution of cytochrome P450 2C, 2E1, 3A4, and 3A5 in human colon mucosa. *BMC Clin Pharmacol* 2005; **5**: 4
14 **Lechevrel M**, Casson AG, Wolf CR, Hardie LJ, Flinterman MB, Montesano R, Wild CP. Characterization of cytochrome P450 expression in human oesophageal mucosa. *Carcinogenesis* 1999; **20**: 243-248
15 **Ribeiro Pinto LF**, Teixeira Rossini AM, Albano RM, Felzenszwalb I, de Moura Gallo CV, Nunes RA, Andreollo NA. Mechanisms of esophageal cancer development in Brazilians. *Mutat Res* 2003; **544**: 365-373
16 **Murray GI**, Shaw D, Weaver RJ, McKay JA, Ewen SW, Melvin WT, Burke MD. Cytochrome P450 expression in oesophageal cancer. *Gut* 1994; **35**: 599-603
17 **Nakajima T**, Wang RS, Nimura Y, Pin YM, He M, Vainio H, Murayama N, Aoyama T, Iida F. Expression of cytochrome P450s and glutathione S-transferases in human esophagus with squamous-cell carcinomas. *Carcinogenesis* 1996; **17**: 1477-1481
18 **Hakkak R**, Korourian S, Ronis MJ, Ingelman-Sundberg M, Badger TM. Effects of diet and ethanol on the expression and localization of cytochromes P450 2E1 and P450 2C7 in the colon of male rats. *Biochem Pharmacol* 1996; **51**: 61-69
19 **Eliasson E**, Mkrtchian S, Ingelman-Sundberg M. Hormone- and substrate-regulated intracellular degradation of cytochrome P450 (2E1) involving MgATP-activated rapid proteolysis in the endoplasmic reticulum membranes. *J Biol Chem* 1992; **267**: 15765-15769
20 **Feierman DE**, Melnikov Z, Zhang J. The paradoxical effect of acetaminophen on CYP3A4 activity and content in transfected HepG2 cells. *Arch Biochem Biophys* 2002; **398**: 109-117
21 **Zangar RC**, Hernandez M, Novak RF. Posttranscriptional elevation of cytochrome P450 3A expression. *Biochem Biophys Res Commun* 1997; **231**: 203-205
22 **Kocarek TA**, Zangar RC, Novak RF. Post-transcriptional regulation of rat CYP2E1 expression: role of CYP2E1 mRNA untranslated regions in control of translational efficiency and message stability. *Arch Biochem Biophys* 2000; **376**: 180-190

S- Editor Liu Y **L- Editor** Wang XL **E- Editor** Ma WH

PO Box 2345, Beijing 100023, China
www.wjgnet.com
wjg@wjgnet.com

World J Gastroenterol 2007 February 21; 13(7): 1003-1009
World Journal of Gastroenterology ISSN 1007-9327

Successful initial ablation therapy contributes to survival in patients with hepatocellular carcinoma

Manabu Morimoto, Kazushi Numata, Kazuya Sugimori, Kazuhito Shirato, Atsushi Kokawa, Hiroyuki Oka, Kingo Hirasawa, Ryonho Koh, Hiromi Nihommatsu, Katsuaki Tanaka

Manabu Morimoto, Kazushi Numata, Kazuya Sugimori, Kazuhito Shirato, Atsushi Kokawa, Hiroyuki Oka, Kingo Hirasawa, Ryonho Koh, Hiromi Nihommatsu, Katsuaki Tanaka, Gastroenterological Center, Yokohama City University Medical Center, 4-57 Urafune-cho, Minami-ku, Yokohama 232-0024, Japan
Correspondence to: Manabu Morimoto, MD, Gastroenterological Center, Yokohama City University Medical Center, 4-57, Urafunecho, Minami-ku, Yokohama City, 232-0024, Japan. morimoto@urahp.yokohama-cu.ac.jp
Telephone: +81-45-2615656 Fax: +81-45-2619492
Received: 2006-11-27 Accepted: 2007-01-15

Key words: Percutaneous ethanol injection; Radiofrequency ablation; Successful initial treatment; Overall survival; Prognostic factor

Morimoto M, Numata K, Sugimori K, Shirato K, Kokawa A, Oka H, Hirasawa K, Koh R, Nihommatsu H, Tanaka K. Successful initial ablation therapy contributes to survival in patients with hepatocellular carcinoma. *World J Gastroenterol* 2007; 13(7): 1003-1009

http://www.wjgnet.com/1007-9327/13/1003.asp

Abstract

AIM: To evaluate the outcome predictors of percutaneous ablation therapy in patients with unresectable hepatocellular carcinoma (HCC), especially to identify whether the initial treatment response contributes to the survival of the patients.

METHODS: The study cohort included 153 patients with single (102) and two or three (51) HCC nodules 5 cm or less in maximum diameter. As an initial treatment, 110 patients received radiofrequency ablation and 43 patients received percutaneous ethanol injection.

RESULTS: The Kaplan-Meier estimates of overall 3- and 5-year survival rates were 75% and 59%, respectively. The log-rank test revealed statistically significant differences in the overall survivals according to Child-Pugh class (P = 0.0275), tumor size (P = 0.0130), serum albumin level (P = 0.0060), serum protein induced by vitamin K absence or antagonist Ⅱ level (P = 0.0486), and initial treatment response (P = 0.0130). The independent predictors of survival were serum albumin level (risk ratio, 3.216; 95% CI, 1.407-7.353; P = 0.0056) and initial treatment response (risk ratio, 2.474; 95% CI, 1.076-5.692; P = 0.0330) based on the Cox proportional hazards regression models. The patients had a serum albumin level 3.5 g/dL and the 3- and 5-year survival rates of 86% and 82%.

CONCLUSION: In HCC patients treated with percutaneous ablation therapy, serum albumin level and initial treatment response are the independent outcome predictors.

INTRODUCTION

Hepatocellular carcinoma (HCC) is one of the most prevalent human cancers with an increasing incidence worldwide[1], and about 70% of HCC is found in Asia[2]. Surveillance with ultrasonography (US) and alpha-fetoprotein in cirrhosis can detect small HCC at an early stage. For early stage patients (single HCC ⩽ 5 cm or ⩽ 3 nodules ⩽ 3 cm), surgery is considered the first treatment option, however, because of accompanying chronic liver disease, many HCC patients can not undergo surgical resection[3-5]. As non-surgical treatment, various local ablation therapies such as percutaneous ethanol injection (PEI)[6,7] or percutaneous radiofrequency (RF) ablation have been proposed, and encouraging results of survival rates have been reported[8-10].

Although many reports of the prognostic predictors after surgical resection of early stage HCC have been reported[11-13], there have been few reports of the prognostic predictors after percutaneous ablation therapy. Sala *et al* in recent years reported that "Child-Pugh class" and "initial treatment response" as prognostic factors of the survival in those who received percutaneous ablation therapy[14]; however, most of the cases (83%) were treated with PEI. The current state of the main percutaneous ablation therapy changes from PEI to RF ablation; therefore, to establish an optimal therapeutic strategy based on the current state, we started this cohort study after 2000 when RF ablation was introduced in our institution.

In this study, we examined a group of HCC patients whose tumors were percutaneously treated using RF ablation or PEI and analyzed the factors pertinent to the prognosis. This approach permits (1) establishment of an

optimal protocol in the percutaneous ablation therapy; and (2) assessment of the prognostic factors in RF ablation and PEI.

MATERIALS AND METHODS

Patients

Between May 2000 and March 2005, 226 patients were diagnosed for the first time as having HCC lesions using US and contrast-enhanced CT and were hospitalized at Yokohama City University Medical Center. The criteria for entry in this study were (1) the presence of either a solitary lesion or up to three lesions, (2) a maximum tumor diameter of 5 cm or less, (3) patients who did not meet with the surgical criteria (resection or transplantation), (4) the lesion was detectable using US, and (5) no evidence existing of portal thrombosis, extrahepatic metastasis, or uncontrollable ascites. Seventy-three patients were excluded from the study and 153 patients were enrolled. The patients' characteristics are depicted in Table 1. Ninety-three of the enrolled patients were men and 60 were women, ranging in age from 51 to 87 years (mean, 69 years). One hundred and thirty-three patients were Child-Pugh class A, and 20 patients were Child-Pugh class B. All had underlying cirrhosis due to hepatitis C virus (n = 134), hepatitis B virus (n = 8), alcohol use (n = 7), or other factors (n = 4). One hundred and two patients presented with solitary tumors and 51 patients had 2-3 lesions. The greatest tumor diameters $\leqslant$ 3 cm were seen in 120 patients, and > 3 cm in 33 patients. A confirmed diagnosis of HCC was made by the pathological examination of biopsied specimens obtained using a 21-gauge fine needle (Sonopsy, Hakko, Tokyo, Japan) and/or the radiological criteria[15] in all patients. Patients with a tumor more than 3 cm in maximum diameter were treated with transcatheter arterial chemoembolization (TACE) followed by RF ablation or PEI.

The entire protocol was approved by the hospital ethics committee and was performed in compliance with the Helsinki Declaration. Written informed consent was obtained from all patients and relatives.

Table 1 Characteristics of patients

Variables	All patients (n = 153)	PEI (n = 43)	RF ablation (n = 110)	P
Age (yr)				
mean ± SD	69 ± 7	69 ± 7	68 ± 7	NS
Sex				
Male/Female	93/60	22/21	71/39	NS
Etiology				
HCV	134	38	96	
HBV	8	1	7	NS
Alcohol	7	2	5	
Others	4	2	2	
Child-Pugh class				
A/B	133/20	37/6	96/14	NS
Tumor size (cm)				
$\leqslant$ 3/> 3	120/33	33/10	87/23	NS
Tumor number				
Single/Multiple	102/51	19/24	83/27	< 0.05
Serum alpha-fetoprotein level (ng/mL)				
mean ± SD	781 ± 8180	2501 ± 15289	109 ± 282	NS
Serum PIVKA-II level (ng/mL)				
mean ± SD	347 ± 1258	565 ± 1467	262 ± 1169	NS
Serum albumin level (g/dL)				
mean ± SD	3.8 ± 0.5	3.7 ± 0.5	3.8 ± 0.5	NS
Initial treatment response				
Successful/Unsuccessful	125/28	35/8	90/20	NS

RF: radiofrequency; PEI: percutaneous ethanol injection; NS: not significant; HCV: hepatitis C virus; HBV: hepatitis B virus; PIVKA-Ⅱ: protein induced vitamin K absence or antagonist Ⅱ.

Treatment procedures

Percutaneous ethanol injection: Based on the reports of Llovet *et al*[16] and Livraghi *et al*[17], we selected PEI without selecting RF ablation when a tumor satisfied the following criteria: (1) existing in a subcapsular location, (2) existing in a location adjacent to a major vessel and another organ (heart, gallbladder, stomach and bowel), and (3) demonstrating poor differentiation. Patients with impaired clotting tests, or with a lower platelet count less than 5×10^{10}/L were considered as being contraindicated for RF ablation and were treated by PEI. Ten patients (23% of patients treated by PEI) with tumors more than 3 cm in diameter were treated with TACE followed by PEI[18].

We used a real-time convex scanner or linear-array scanner with 3.5-MHz probes and a lateral attachable apparatus for needle guidance (Core-Vision 6000™, Toshiba Medical Co., Tokyo, Japan). First, it was confirmed under US guidance that a 15- or 20-cm, 21-gauge puncture needle with a closed conical tip and three terminal side holes (PEIT needle; Hakko, Tokyo, Japan) was correctly positioned within the lesion, and 99.5% absolute ethyl alcohol was then slowly injected. Caution was taken to inject the deepest portions of the lesion first and then the more central and superficial portions, to prevent superficial spreading of the ethanol from masking the view for subsequent injections. We usually used one or more PEIT needles for each treatment session, and ethanol was injected into the tumor at one or more locations until the lesion was completely filled. Treatment was given twice a week. A treatment series usually consisted of six or more sessions, and the total dose of ethanol varied with the volume of the lesion, the texture, patient compliance, and distribution of the ethanol.

Radiofrequency ablation: We selected the RF ablation for the cases with low risks of tumor seeding and the hemorrhage based on the previous reports[16,17,19]. Twenty-three patients (21% of patients treated by RF ablation) with tumors more than 3 cm in diameter were treated with TACE followed by RF ablation[20].

At the beginning, grounding was achieved by attaching 2 or 4 pads to the patient's thighs. A conscious sedation, consisting of a combination of intramuscular

administration of pentazocine (Pentazin™ 15 mg, Sankyo Pharmaceuticals, Tokyo, Japan) and hydroxyzine chloride (Atarax-P™ 25 mg, Pfizer Japan, Tokyo, Japan), was administered before treatment. Local anesthesia was achieved by injecting 1% lidocaine hydrochloride (Xylocaine™, Astra Japan, Tokyo, Japan). Sixty-five of 112 patients were treated with hooked, 15-gauge, 25-cm-long electrodes, which are expandable by 10 hooks to a maximum dimension of 3 or 3.5 cm (Le Veen Needle Electrode; Radiotherapeutics, Mountain View, CA), and RF ablation was applied using a generator (RTC 2000; Boston Scientific Japan, Tokyo, Japan). For the remaining 47 tumors, 17-gauge, cooled electrodes with a dimention of 2 or 3 cm (Cool-tip needle; Radionics, Burlington, MA) were used, attached to a 500-kHz RF generator (Radionics, Burlington, MA) capable of producing power of 200 W. A peristaltic pump (Watson-Marlow, Wilmington, MA) was used to infuse 0℃ normal saline solution into the lumen of the electrodes to maintain the temperature below 25℃. For tumors more than 2 cm in diameter, several insertions were performed to obtain complete ablation of the entire tumors.

Transcatheter arterial chemoembolization: Thirty-three patients with tumors more than 3 cm in diameter were treated with TACE followed by RF ablation or PEI. We performed TACE by selectively introducing a microcatheter into the right or left hepatic artery or a segmental branch of the hepatic artery and injecting a mixture of iodized oil (Lipiodol; Andre Guerbet, Aulnay-sous-Bois, France) and epirubicin hydrochloride (30-50 mg per body surface) (Farmorubicin; Pharmacia and Upjohn, Tokyo, Japan) or styrene maleic acid neocarzinostatin (1.0-3.0 mg per body surface) (SMANCS; Yamanouchi Pharmaceutical, Tokyo, Japan). This was followed by introduction of a gelatin sponge (1 mm × 1 mm × 1 mm) (Spongel; Yamanouchi Pharmaceutical, Tokyo, Japan).

Evaluation of initial treatment response and follow-up

Initial treatment response was assessed by contrast-enhanced CT 1, 3, and 6 mo after initial treatment session. Successful initial treatment was defined as the absence of an enhanced area within the tumor assessed by contrast enhanced CT 6 mo after initial treatment session. If the presence of residual viable tumor within the treated area was defined by CT within 6 mo after initial treatment, the case was judged to be unsuccessful in the initial treatment. After the evaluation of initial treatment response, patients were followed up every 3 mo by contrast enhanced CT and/or US.

When the residual viable tumor and/or distant recurrence were detected by the follow-up CT, percutaneous ablation therapy was added if they were within 3 lesions, and TACE was selected for patients who were ineligible for percutaneous ablation therapy, with large and/or multifocal HCC who did not have vascular invasion or extrahepatic spread[15]. The above-mentioned treatment was repeated at once whenever the tumor recurrence was detected, until uncontrolled ascites or intravascular tumor thrombus appeared and serum bilirubin level reached 3 mg/dL or higher.

Statistical analysis

The end point of the study was the survival. The baseline characteristics of patients were expressed as mean ± standard deviation. Differences in proportions among the groups were analyzed by the Chi-square test. Mean quantitative values were compared by the Student's *t* test. Follow-up data was dealt with from the beginning of the treatment and was maintained until the death or the last visit of the patients before April 30, 2006. The Kaplan-Meier method was used to calculate the survival rate and the log-rank test was used to analyze differences.

As pretreatment factors, fifteen variables were assessed in the univariate analysis: age (< 70 *vs* ≥ 70 years); sex (male *vs* female); cause of underlying cirrhosis (HCV *vs* HBV *vs* alcohol *vs* others); Child-Pugh class (A *vs* B); tumor size (≤ 3 cm *vs* > 3 cm); tumor number (single *vs* multiple); serum alpha-fetoprotein levels (<400 *vs* ≥ 400 ng/mL); serum protein induced by vitamin K absence or antagonist Ⅱ (PIVKA-Ⅱ) level (< 300 *vs* ≥ 300 ng/mL); and serum albumin level (≤ 3.5 *vs* > 3.5g/dL); serum alanine aminotransferase (ALT) level (<80 *vs* ≥ 80 U/L); serum bilirubin level (<2 *vs* ≥ 2 mg/dL); serum platelet count (<9 *vs* ≥ 9 × 10^9/L); prothrombin activity (≤ 70 *vs* > 70%); encephalopathy (none *vs* yes); and ascites (none *vs* yes). As treatment factors, two variables were assessed in the univariate analysis: type of treatment (PEI *vs* RF ablation); and initial treatment response (successful *vs* unsuccessful). Significant variables ($P < 0.05$) were included in a stepwise Cox regression analysis. Data analyses were performed with SPSS software (version 10.0J; SPSS, Tokyo, Japan). All *P* values were derived from two-tailed tests and $P < 0.05$ was accepted as statistically significant.

RESULTS

Treatment response and survival

In general, the percutaneous ablation procedures were well tolerated in all the patients. Both cardiac and respiratory parameters remained stable throughout the treatment. The regimen of conscious sedation and local anesthesia used in this study was adequate for these ablation methods. None of the patients experienced bleeding as a result of these percutaneous ablation techniques.

No local tumor residue was found in 125 of 153 (82%) patients as assessed by contrast enhanced CT 6 mo after the initial treatment (defined as successful initial treatment) (Figure 1). The remaining 28 (18%) patients judged as having residual viable tumor by contrast enhanced CT within 6 mo after the initial treatment (defined as unsuccessful initial treatment), were re-treated by RF ablation or PEI until no vascularities could be recognized within the tumor by contrast enhanced CT. With regard to the type of treatment, successful initial treatment was obtained in 90 (82%) of 110 patients treated with RF ablation, and in 35 (81%) of 43 patients treated with PEI, and no significant difference was observed between the two types of treatment. After a median follow-up of 34 mo (range, 1-66), the 1-, 3-, and 5-year survival rates were 95%, 75%, and 59%, respectively (Figure 2). At the time of the analysis, 83 (54%) patients had tumor recurrence

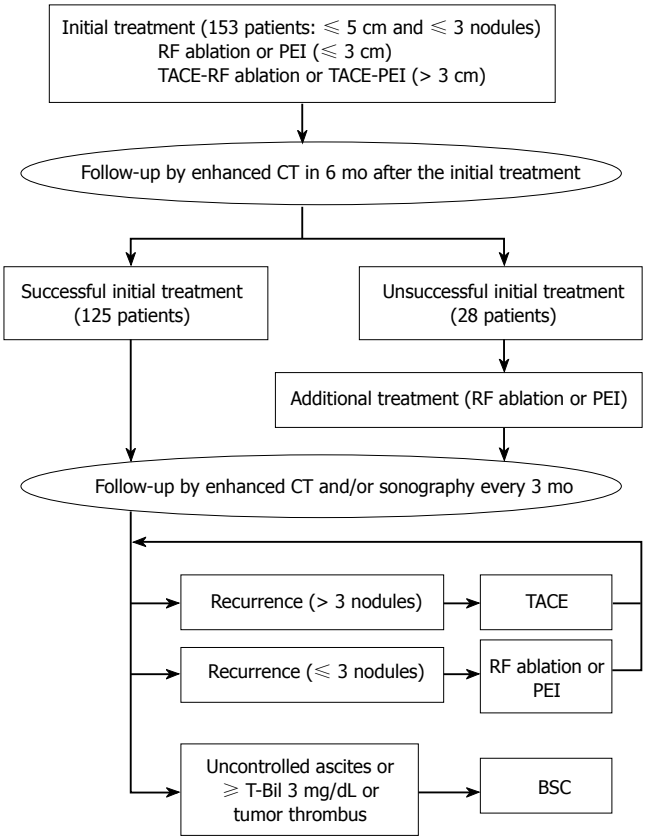

Figure 1 Follow-up chart of overall treatment design.

Table 2 Univariate analysis for factors associated with survival

Variables	Patients	*P*
Pre-treatment factors		
Age (yr)		
< 70/≥ 70	74/79	0.0923
Sex		
Male/Female	93/60	0.7284
Child-Pugh class		
A/B	133/20	0.0275
Tumor size (cm)		
≤ 3/> 3	120/33	0.0130
Tumor number		
Single/Multiple	102/51	0.6298
Serum alpha-fetoprotein level (ng/mL)		
< 400/≥ 400	142/11	0.0722
Serum PIVKA-Ⅱ level (ng/mL)		
< 300/≥ 300	133/20	0.0486
Serum albumin level (g/dL)		
≤ 3.5/> 3.5	50/103	0.0060
Treatment factors		
Type of ablation therapy		
RF ablation/PEI	110/43	0.9829
Initial treatment response		
Successful/Unsuccessful	125/28	0.0130

RF: radiofrequency; PEI: percutaneous ethanol injection; NS: not significant; PIVKA-Ⅱ: protein induced vitamin K absence or antagonist Ⅱ.

(incomplete local treatment and/or distant recurrence), 24 patients died and 3 were l lost to follow-up. With regard to the type of treatment, tumor recurrences were observed in 58 (53%) of 110 patients treated with RF ablation, and in 25 (58%) of 43 patients treated with PEI. Death was due to tumor progression in 18 patients and due to liver failure in 6 patients.

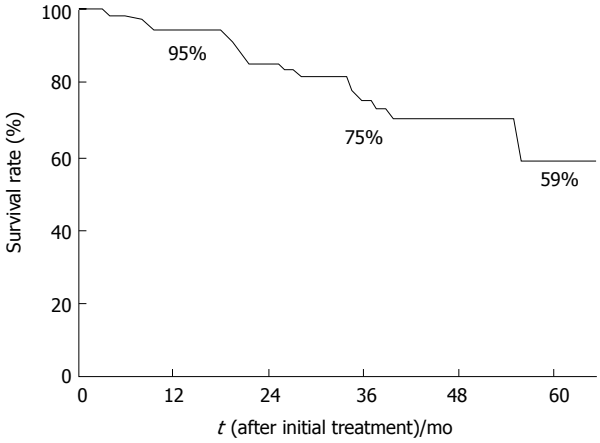

Figure 2 Overall probability of survival.

Table 3 Multivariate analysis for factors associated with survival

Variables	Risk ratio (95% CI)	*P*
Tumor size (cm)		
> 3	1.0	
≤ 3	0.459 (0.179-1.174)	0.104
Serum PIVKA-Ⅱ level (ng/mL)		
≥ 300	1.0	
< 300	0.542 (0.191-1.535)	0.249
Serum albumin level (g/dL)		
> 3.5	1.0	
≤ 3.5	3.216 (1.407-7.353)	0.006
Initial treatment response		
Successful	1.0	
Unsuccessful	2.474 (1.076-5.692)	0.033

Abbreviations: PIVKA-Ⅱ, protein induced vitamin K absence or antagonist Ⅱ.

Factors for survival

In the univariate analysis, 5 variables were associated with survival (Table 2). Of the pre-treatment factors, Child-Pugh classification, tumor size, serum albumin level, and serum PIVKA-Ⅱ level were found to be significant predictors of survival. And of the treatment factors, initial treatment response was found to be a significant predictor of survival while the type of ablation therapy (RF ablation *vs* PEI) was not ($P = 0.9829$). Multivariate analysis disclosed two independent predictors: serum albumin level ≤ 3.5g/dL *vs* >3.5g/dL (risk ratio 3.216, 95%CI: 1.407-7.353, $P = 0.0056$) and successful initial treatment *vs* unsuccessful initial treatment (risk ratio 2.474, 95%CI: 1.076-5.692, $P = 0.0330$) (Table 3). When only pre-treatment factors were included in the multivariate analysis, serum albumin level (risk ratio 3.199, 95%CI: 1.405-7.281, $P = 0.0056$) was proved to be an independent predictor.

The sole predictive factor for survival in patients with a serum albumin level > 3.5g/dL proved to be the initial treatment response; therefore the survival was examined

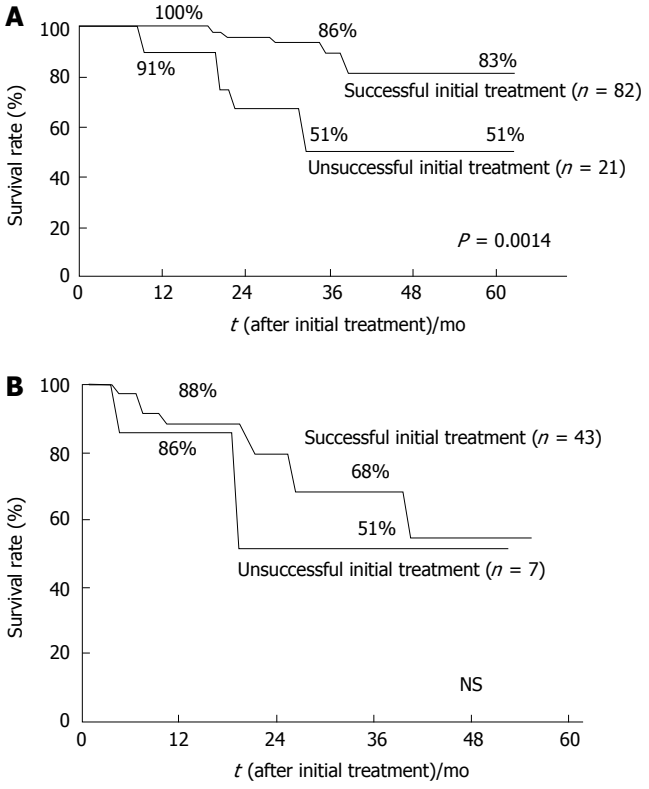

Figure 3 Overall probability of survival according to initial treatment response. **A**: In patients with a serum albumin level > 3.5 g/dL; **B**: In patients with a serum albumin level ≤ 3.5 g/dL.

in case groups with serum albumin levels > 3.5g/dL (n = 103) and ≤ 3.5g/dL (n = 50) according to the initial treatment response. In patients with a serum albumin level > 3.5g/dL, the 1-, 3-, and 5-year survival rates in patients who were judged as having had a successful initial treatment were 100%, 86%, and 83%, respectively (n = 82), and the survival rates in patients who were judged as having had an unsuccessful initial treatment were 91%, 51%, and 51% at 1-, 3-, and 5-year, respectively (n = 21) (P = 0.0014) (Figure 3A). On the other hand, in patients with a serum albumin level ≤ 3.5g/dL, the multivariate analysis proved no independent predictors for survival. The survival rates in 43 patients with a successful initial treatment were 88% and 68% at 1 and 3 years, and in 7 patients with an unsuccessful initial treatment, the survival rates were 86% and 51% at 1 and 3 years, respectively (P = 0.3813) (Figure 3B).

Initial treatment response was significantly associated with the tumor number (P = 0.0031), tumor size (P = 0.0441), serum alpha-fetoprotein level (P = 0.0156), and serum PIVKA-Ⅱ level (P = 0.0071), however it was not associated with the etiology of underlying cirrhosis, Child-Pugh class, and type of ablation therapy (Table 4).

Table 4 Comparison of clinical background between successful initial treatment group and unsuccessful initial treatment group

	Initial treatment	
	Successful (n = 125)	Unsuccessful (n = 28)
Sex		
Male/Female	75/50	18/10
Age (yr)		
< 70/≥ 70	67/58	12/16
Etiology		
HCV/HBV/Alcohol/Others	108/6/7/4	26/2/0/0
Child-Pugh class		
A/B	110/15	23/5
Serum albumin level (g/dL)		
≤ 3.5/> 3.5	43/82	7/21
Tumor size (cm)		
≤ 3/> 3	102/23	18/10[a]
Tumor number		
Single/Multiple	90/35	12/16[a]
Type of ablation therapy		
RF ablation/PEI	90/35	20/8
Serum alpha-fetoprotein level (ng/mL)		
< 400/≥ 400	119/6	23/5[a]
Serum PIVKA-Ⅱ level (ng/mL)		
< 300/≥ 300	113/12	20/8[a]

RF: radiofrequency; PEI: percutaneous ethanol injection; HCV: hepatitis C virus; HBV: hepatitis B virus; PIVKA-Ⅱ: protein induced vitamin K absence or antagonist Ⅱ. [a]P < 0.05 *vs* the successful initial treatment group.

DISCUSSION

In the current study, we examined a group of HCC patients whose tumors were percutaneously treated using RF ablation or PEI and analyzed the predictors that contributed to the prognosis. Multivariate analysis disclosed two independent predictors: serum albumin level and initial treatment response. In the cases with a serum albumin level > 3.5 g/dL, our data consistently showed that a successful initial treatment was the most predictive factor for long-term survival.

Examinations of the factor that could contribute to the long-term survival of patients undergoing percutaneous ablation therapy, have been reported previously; however, most of them were evaluations using PEI. Pompili *et al* evaluated the therapeutic efficacy of PEI for patients with Child-Pugh class A and tumors > 5 cm in diameter, and reported that alpha-fetoprotein level and liver function were factors which contributed to survival[21]. Ebara *et al* evaluated the therapeutic efficacy of PEI for patients with ≤ 3 lesions of small HCC, and found that alpha-fetoprotein level and liver function were factors contributed to the suvival[22]. Recently, Sala *et al*[14] and Xu *et al*[23] reported the prognostic predictors after percutaneous ablation therapies. However, most of the cases were treated with PEI in the former study[14], and in the latter study[23], 63% of treated cases were recurrent HCC and the selection for ablation procedures (microwave *vs* RF ablation) was not fully clarified. To establish an optimal therapeutic protocol after the introduction of RF ablation, we started this cohort study after 2000 when RF ablation was introduced in our institution. In this study, 72% of the patients were treated with RF ablation, and this may reflect the current state of the available percutaneous ablation procedures.

In our study, the serum albumin level was shown as the most important pre-treatment predictor for survival. Hepatic functional reserve as indicated by the serum albumin level has generally been identified to be a good

prognostic factor for survival. The serum albumin level has been shown to be one of the prognostic factors in HCC patients treated with hepatic resection[24] and PEI[25]. Ikeda *et al* reported that the serum albumin level was one of the independent factors associated with the carcinogens in HCV positive viral hepatitis[26]. In this study, 88% of patients had hepatitis C virus infection; therefore, the serum albumin level is selected as a significant factor that may provide for the recurrence of HCC after successful percutaneous local ablation therapy.

Furthermore, initial treatment response was shown as a second significant predictor for survival. Sala *et al* recently reported that initial treatment response was an outcome predictor of the survival after ablation therapy and initial complete tumor necrosis should be considered a relevant therapeutic target irrespective of tumor size and liver function[14]. In the present study, the impact of extensive tumor necrosis on survival has been observed in patients with good liver functional reserve (serum albumin level > 3.5 g/dL); however, it was not found in patients with poor liver functional reserve (serum albumin level ⩽ 3.5 g/dL). Therefore, in patients with poor liver function reserve, optimal selection of patients as candidates for ablation therapies and of the appropriate therapeutic schedule for each single patient to control the tumor growth, avoiding a clinically significant worsening of liver function, is essential to obtain an improvement in survival.

Treatment response was generally judged by CT at one month after the treatment based on the WHO criteria[15], however in this study, the initial treatment response was judged by CT at 6 mo after the initial treatment. This difference of the surveillance after the initial treatment may be explained as follows. First, 22% of our patients underwent TACE prior to ablation therapy, so it was difficult to achieve a detailed evaluation of treatment response with CT because of dense lipiodol accumulation in the treated area[27]. Second, 72% of the patients received RF ablation therapy, resulting in an inflammatory increased vascular flow rim of the outline of the ablated zone for about one month following treatment, which can disturb the evaluation of the local treatment by contrast-enhanced CT[28].

In this study, alpha-fetoprotein level, PIVKA-Ⅱ level, tumor size, and tumor number were significant factors for the initial treatment response by univariate analysis. Although there are few reports which have examined the factors for initial treatment response following percutaneous ablation therapy, there are several reports as to what contributes to local recurrence when RF ablation is selected. Lencioni *et al* showed that tumor size and type of ablation therapy were the factors for local recurrence-free survival in those cases treated with RF ablation and PEI[29]. Lin *et al* reported that tumor number, tumor size, histopathological (Edmondson's) grade, and type of ablation therapy were significant factors of local recurrence[30].

In summary, we demonstrated that the best candidates for percutaneous ablation therapy are those patients who have good hepatic functional reserve and can be expected to achieve successful initial treatment. Attempts to fully ablate large tumors (3-5 cm in diameter) are achieved successfully by the combined use of TACE, however, further studies are needed to clarify whether or not the combined use of TACE in RF ablation will be a therapeutic option to achieve complete tumor necrosis for the treatment of large HCC tumors.

REFERENCES

1 **Parkin DM**, Bray F, Ferlay J, Pisani P. Estimating the world cancer burden: Globocan 2000. *Int J Cancer* 2001; **94**: 153-156
2 **Bosch FX**, Ribes J, Borràs J. Epidemiology of primary liver cancer. *Semin Liver Dis* 1999; **19**: 271-285
3 **Primary liver cancer in Japan.** Clinicopathologic features and results of surgical treatment. *Ann Surg* 1990; **211**: 277-287
4 **Arii S**, Yamaoka Y, Futagawa S, Inoue K, Kobayashi K, Kojiro M, Makuuchi M, Nakamura Y, Okita K, Yamada R. Results of surgical and nonsurgical treatment for small-sized hepatocellular carcinomas: a retrospective and nationwide survey in Japan. The Liver Cancer Study Group of Japan. *Hepatology* 2000; **32**: 1224-1229
5 **Fong Y**, Sun RL, Jarnagin W, Blumgart LH. An analysis of 412 cases of hepatocellular carcinoma at a Western center. *Ann Surg* 1999; **229**: 790-799; discussion 799-800
6 **Ebara M**, Ohto M, Sugiura N, Kita K, Yoshikawa M, Okuda K, Kondo F, Kondo Y. Percutaneous ethanol injection for the treatment of small hepatocellular carcinoma. Study of 95 patients. *J Gastroenterol Hepatol* 1990; **5**: 616-626
7 **Castells A**, Bruix J, Bru C, Fuster J, Vilana R, Navasa M, Ayuso C, Boix L, Visa J, Rodés J. Treatment of small hepatocellular carcinoma in cirrhotic patients: a cohort study comparing surgical resection and percutaneous ethanol injection. *Hepatology* 1993; **18**: 1121-1126
8 **Rossi S**, Di Stasi M, Buscarini E, Quaretti P, Garbagnati F, Squassante L, Paties CT, Silverman DE, Buscarini L. Percutaneous RF interstitial thermal ablation in the treatment of hepatic cancer. *AJR Am J Roentgenol* 1996; **167**: 759-768
9 **Livraghi T**, Goldberg SN, Lazzaroni S, Meloni F, Solbiati L, Gazelle GS. Small hepatocellular carcinoma: treatment with radio-frequency ablation versus ethanol injection. *Radiology* 1999; **210**: 655-661
10 **Curley SA,** Izzo F, Delrio P, Ellis LM, Granchi J, Vallone P, Fiore F, Pignata S, Daniele B, Cremona F. Radiofrequency ablation of unresectable primary and metastatic hepatic malignancies: results in 123 patients. *Ann Surg* 1999; **230**: 1-8
11 **Suehiro T**, Sugimachi K, Matsumata T, Itasaka H, Taketomi A, Maeda T. Protein induced by vitamin K absence or antagonist II as a prognostic marker in hepatocellular carcinoma. Comparison with alpha-fetoprotein. *Cancer* 1994; **73**: 2464-2471
12 **Arii S**, Tanaka J, Yamazoe Y, Minematsu S, Morino T, Fujita K, Maetani S, Tobe T. Predictive factors for intrahepatic recurrence of hepatocellular carcinoma after partial hepatectomy. *Cancer* 1992; **69**: 913-919
13 **Nagao T,** Inoue S, Goto S, Mizuta T, Omori Y, Kawano N, Morioka Y. Hepatic resection for hepatocellular carcinoma. Clinical features and long-term prognosis. *Ann Surg* 1987; **205**: 33-40
14 **Sala M**, Llovet JM, Vilana R, Bianchi L, Solé M, Ayuso C, Brú C, Bruix J. Initial response to percutaneous ablation predicts survival in patients with hepatocellular carcinoma. *Hepatology* 2004; **40**: 1352-1360
15 **Bruix J**, Sherman M, Llovet JM, Beaugrand M, Lencioni R, Burroughs AK, Christensen E, Pagliaro L, Colombo M, Rodés J. Clinical management of hepatocellular carcinoma. Conclusions of the Barcelona-2000 EASL conference. European Association for the Study of the Liver. *J Hepatol* 2001; **35**: 421-430
16 **Llovet JM**, Vilana R, Brú C, Bianchi L, Salmeron JM, Boix L, Ganau S, Sala M, Pagès M, Ayuso C, Solé M, Rodés J, Bruix J. Increased risk of tumor seeding after percutaneous radiofrequency ablation for single hepatocellular carcinoma. *Hepatology* 2001; **33**: 1124-1129
17 **Livraghi T,** Solbiati L, Meloni MF, Gazelle GS, Halpern

EF, Goldberg SN. Treatment of focal liver tumors with percutaneous radio-frequency ablation: complications encountered in a multicenter study. *Radiology* 2003; **226**: 441-451

18 **Tanaka K,** Okazaki H, Nakamura S, Endo O, Inoue S, Takamura Y, Sugiyama M, Ohaki Y. Hepatocellular carcinoma: treatment with a combination therapy of transcatheter arterial embolization and percutaneous ethanol injection. *Radiology* 1991; **179**: 713-717

19 **Morimoto M,** Sugimori K, Shirato K, Kokawa A, Tomita N, Saito T, Tanaka N, Nozawa A, Hara M, Sekihara H, Shimada H, Imada T, Tanaka K. Treatment of hepatocellular carcinoma with radiofrequency ablation: radiologic-histologic correlation during follow-up periods. *Hepatology* 2002; **35**: 1467-1475

20 **Yamakado K,** Nakatsuka A, Ohmori S, Shiraki K, Nakano T, Ikoma J, Adachi Y, Takeda K. Radiofrequency ablation combined with chemoembolization in hepatocellular carcinoma: treatment response based on tumor size and morphology. *J Vasc Interv Radiol* 2002; **13**: 1225-1232

21 **Pompili M,** Rapaccini GL, Covino M, Pignataro G, Caturelli E, Siena DA, Villani MR, Cedrone A, Gasbarrini G. Prognostic factors for survival in patients with compensated cirrhosis and small hepatocellular carcinoma after percutaneous ethanol injection therapy. *Cancer* 2001; **92**: 126-135

22 **Ebara M,** Okabe S, Kita K, Sugiura N, Fukuda H, Yoshikawa M, Kondo F, Saisho H. Percutaneous ethanol injection for small hepatocellular carcinoma: therapeutic efficacy based on 20-year observation. *J Hepatol* 2005; **43**: 458-464

23 **Xu HX**, Lu MD, Xie XY, Yin XY, Kuang M, Chen JW, Xu ZF, Liu GJ. Prognostic factors for long-term outcome after percutaneous thermal ablation for hepatocellular carcinoma: a survival analysis of 137 consecutive patients. *Clin Radiol* 2005; **60**: 1018-1025

24 **Chen MF,** Tsai HP, Jeng LB, Lee WC, Yeh CN, Yu MC, Hung CM. Prognostic factors after resection for hepatocellular carcinoma in noncirrhotic livers: univariate and multivariate analysis. *World J Surg* 2003; **27**: 443-447

25 **Kuriyama H,** Okada S, Okusaka T, Ueno H, Ikeda M. Prognostic factors in patients with small hepatocellular carcinoma treated by percutaneous ethanol injection. *J Gastroenterol Hepatol* 2002; **17**: 1205-1210

26 **Ikeda K,** Saitoh S, Suzuki Y, Kobayashi M, Tsubota A, Koida I, Arase Y, Fukuda M, Chayama K, Murashima N, Kumada H. Disease progression and hepatocellular carcinogenesis in patients with chronic viral hepatitis: a prospective observation of 2215 patients. *J Hepatol* 1998; **28**: 930-938

27 **Nakamura H,** Hashimoto T, Oi H, Sawada S. Transcatheter oily chemoembolization of hepatocellular carcinoma. *Radiology* 1989; **170**: 783-786

28 **Goldberg SN,** Gazelle GS, Mueller PR. Thermal ablation therapy for focal malignancy: a unified approach to underlying principles, techniques, and diagnostic imaging guidance. *AJR Am J Roentgenol* 2000; **174**: 323-331

29 **Lencioni RA,** Allgaier HP, Cioni D, Olschewski M, Deibert P, Crocetti L, Frings H, Laubenberger J, Zuber I, Blum HE, Bartolozzi C. Small hepatocellular carcinoma in cirrhosis: randomized comparison of radio-frequency thermal ablation versus percutaneous ethanol injection. *Radiology* 2003; **228**: 235-240

30 **Lin SM**, Lin CJ, Lin CC, Hsu CW, Chen YC. Radiofrequency ablation improves prognosis compared with ethanol injection for hepatocellular carcinoma < or = 4 cm. *Gastroenterology* 2004; **127**: 1714-1723

S- Editor Liu Y **L- Editor** Ma JY **E- Editor** Ma WH

PO Box 2345, Beijing 100023, China
www.wjgnet.com
wjg@wjgnet.com

World J Gastroenterol 2007 February 21; 13(7): 1010-1017
World Journal of Gastroenterology ISSN 1007-9327

LIVER CANCER

Rab23 is a potential biological target for treating hepatocellular carcinoma

Yun-Jian Liu, Qian Wang, Wen Li, Xiao-Hui Huang, Mao-Chuan Zhen, Shu-Hong Huang, Lian-Zhou Chen, Ling Xue, Hong-Wei Zhang

Yun-Jian Liu, Qian Wang, Wen Li, Xiao-Hui Huang, Maochuan Zhen, Lian-Zhou Chen, Department of Hepatobiliary Surgery, First Affiliated Hospital of Sun Yat-Sen University, Guangzhou 510080, Guangdong Province, China
Ling Xue, Depatment of Pathology, First Affiliated Hospital of Sun Yat-Sen University, Guangzhou 510080, Guangdong Province, China
Shu-Hong Huang, Hong-Wei Zhang, Institute of Developmental Biology, School of Life Sciences, Shandong University, Jinan 250100, Shandong Province, China
Correspondence to: Qian Wang, PhD, Department of Hepatobiliary Surgery, First Affiliated Hospital of Sun Yat-Sen University, Guangzhou 510080, Guangdong Province, China. wangqian00@hotmail.com
Telephone: +86-13929572752
Received: 2006-12-11 Accepted: 2007-01-23

Abstract

AIM: To elucidate the role of Rab23 in hepatocellular carcinoma (HCC) by assessing the expression of Rab23 in HCC tissue and in HCC cell lines.

METHODS: Primary tumors (n = 100) were stained with Rab23 antibodies using immunohistochemistry and *in situ* hybridization in tissue microarrays. Relationships between gene expression and pathology parameters were analysed. The biological significance of Rab23 in Hep-3B cells was examined by knocking down Rab23 gene expression. We designed a pair of double-stranded RNAs against human rab23 and transfected siRNA into Hep-3B cells. Rab23 expression in these cells was examined using RT-PCR and Western blots. We investigated cell growth by MTT assays and fluorescence-activated cell sorting.

RESULTS: High cytoplasmic and nuclear expression of Rab23 was found in 38 of 71 (53.5%) and in 49 of 68 HCC patients (72%) respectively, which correlated with tumor size. HCC cell lines expressed Rab23. In Hep3B cells, siRNA for Rab23 decreased Rab23 mRNA by 4.5-fold and protein expression by 2-fold. Survival rates at 24 and 48 h for Hep-3B cells transfected with siRNA were lower and about 30% Hep-3B cells were apoptotic. Knocking down rab23 suppressed Hep3B cell growth, suggesting that rab23 could play an important role in Hep3B cell growth.

CONCLUSION: Rab23 is overexpressed and/or activated in HCC. Rab23 may be both a HCC predictor and a target for treating HCC.

Key words: Rab23; Sonic hedgehog; Hepatocellular carcinoma; Tissue microarray; siRNA

Liu YJ, Wang Q, Li W, Huang XH, Zhen MC, Huang SH, Chen LZ, Xue L, Zhang HW. Rab23 is a potential biological target for treating hepatocellular carcinoma. *World J Gastroenterol* 2007; 13(7): 1010-1017

http://www.wjgnet.com/1007-9327/13/1010.asp

INTRODUCTION

Hepatocellular carcinoma (HCC) is the most frequent primary malignant tumor of the liver. HCC is the third leading global cause of cancer-related death. Over 54% of HCC cases occur in China. Hepatitis B virus is a common causal agent of liver cancer, and other factors have also been found. However, the molecular mechanisms contributing to tumor progression to HCC remain unknown[1].

In recent years, targeted therapies for a variety of HCCs have achieved clinically significant response rates and have given oncologists the chance to develop individual-based strategies for patient therapy. One rationale for such therapeutic approaches is to detect target molecules in the tumor. There is a growing list of such target molecules, the levels of which are now routinely estimated by IHC staining in biopsy specimens or surgically removing tumor material. Such assays not only generate important data for therapeutic decisions, but also provide information relevant to the prognosis of patients[2].

An example is targeting of the hedgehog (Hh) pathway. Dysregulation of this pathway has been implicated in the genesis of cancers from multiple tissue types[3]. Moreover, from embryogenesis to adulthood, skin and gastrointestinal progenitors are regulated by Hh signaling[4-6]. This pathway is activated when sonic hedgehog (SHH) or Indian hedgehog (IHH) ligands bind to their receptor, patched (PTC). When unoccupied by ligand, PTC is a tumor suppressor that binds to and represses smoothened (SMO)[7], preventing the SMO proto-oncoprotein from

activating downstream transcription factors, such as GLi1. Conversely, when ligand binds to PTC, SMO is released and GLi1 is activated, resulting in the transcription of target genes including PTC and Gli1[7]. Hh signaling is now known to play a critical role in the gastrointestinal tract in both health and disease. Most recently, two research groups have simultaneously reported abnormal activation of the SHH pathway in HCC[8,9]. Although the investigators paid much attention to the relationships between hedgehog signaling and HCC, little is known about this pathway in carcinogenesis.

One regulator of SHH signaling is Rab23. In 1994, the full-length cDNA encoding Rab23, a novel Ras-related small GTPase, was isolated using the sequence of a previously described GTPases[10]. Northern analysis revealed that Rab23 mRNA is predominantly expressed in the brain, which places the protein together with Rab3a and Rab15, in the group of small GTPases characteristic of the nervous system[11]. Rab23, a new member of the RAB family expressed in retina, is composed of 7 exons spanning a 34 kb domain of genomic DNA. It is located in the pericentromeric region of chromosome 6 between microsatellite markers D6S257 and D6S1659, within the critical region of RP25[12] and localized at the plasma membrane and the endocytic pathway[12,13]. Rab23 is a negative regulator of SHH[13,14]. It acts on upstream of Gli transcription factors in patterning neural cell types in the spinal cord. The primary target of Rab23 is the Gli2 activator. Rab23 and Gli3 repressors have additive effects on patterning. Analysis of Gli3 protein suggests that Rab23 also has a role in promoting the production of Gli3 repressor. Although the patched and smoothened membrane proteins can change subcellular location in response to SHH, analysis demonstrates that Rab23 does not work through either patched or smoothened membrane protein. Instead, Rab23 appears to regulate subcellular localization of essential components of the hedgehog pathway that act both on downstream of smoothened and on upstream of Gli proteins[15].

Until now there have no reports about Rab23 expression in HCC or even in other human tumors. Since Rab23 is a negative regulator of SHH signaling which can induce malignant carcinoma, dysregulation of Rab23 also may result in HCC. If it is true, we may be able to find a new target for diagnosis and treatment of HCC. In the present study, we evaluated the hypothesis that increases in Rab23 signaling induce hepatocarcinogenesis by regulating Hh signaling in HCC tissues.

MATERIALS AND METHODS

Overall experimental design

We compared Rab23 expression in non-neoplastic and malignant human livers by IHC and *in situ* hybridization using tissue microarrays. Furthermore, since it has been confirmed that there is hedgehog signaling in Hep-3B cells[8,9], we examined the biological significance of the Rab23 gene in Hep-3B cells by knocking down Rab23 gene expression. To identify a possible role of Rab23 in HCC, we designed a pair of double-stranded RNAs (dsRNAs) against human Rab23, and transfected siRNAs into Hep-3B cells. We examined Rab23 expression in these cells using RT-PCR and Western blots. We investigated cell growth by MTT assays and fluorescence-activated cell sorting.

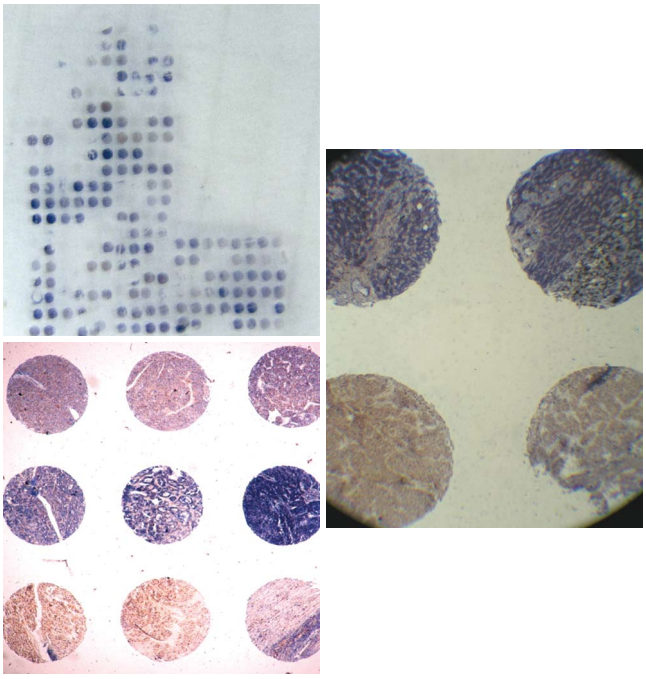

Figure 1 *In situ* hybridization using tissue microarrays.

Patient material

HCC samples from 100 patients were used in this study. All of them were from Sun Yat-Sen University (Guangzhou, China) and selected over a 4-year period (1993-1997). Twenty-five tumor adjacent liver tissue samples were also used. None of the patients received chemotherapy or radiation therapy. Each specimen was fixed in alcoholic formalin for 8-12 h and embedded in paraffin.

Construction of tissue microarray

A hundred archived formalin-fixed and paraffin-embedded anonymous, representative specimens of HCC were also assessed. Non-necrotic areas in tumor for coring into a tissue microarray (TMA) were marked using an indelible pen on a hematoxylin and eosin (HE) stained whole section from donor blocks. TMAs were assembled from formalin-fixed and paraffin-embedded tumor tissue samples as previously described[16] by using a precision instrument (Beecher Instruments, Silver Spring, MD). Cores (600 μm in diameter) were randomly arrayed in triplicate across the recipient block with asymmetrical placement for orientation. TMA coordinates and clinicopathological data were stored for reference. TMA slides were sectioned and mounted on Superfrost®/Plus microscope slides as 6-μm sections (Figure 1). Hematoxylin and eosin (H&E) stained TMA sections were used as morphological references.

Immunohistochemistry

Paraffin-embedded tissue sections were deparaffinized. Slides from each case were exposed to affinity purified rabbit anti-Rab23 primary antibody (BD Biosciences, San Jose, CA, USA) and diluted in PBS for 2 h at room temperature. Detection was carried out using Elivision TM Plus Polymer HRP (Mouse/Rabbit) immunohistochemistry kits (Maixin.Bio, Fuzhou,China). Location of peroxidase was visualized with diaminobenzidione(DAB). Hematoxylin was used for counterstaining. Sections were thoroughly washed with PBS between steps. Negative controls (absence of primary antibody) were run for each experiment. We defined a positive sample as one in which more than one third of one tissue chip was stained brown.

In situ hybridization

In situ hybridization was performed according to the manufacturer's instructions (Roche Molecular Biochemicals, Mannheim, Germany) and the published *in situ* hybridization protocol[17,18]. Sense and antisense probes were obtained by T3 or T7 *in vitro* transcription using a DIG RNA labeling kit from Roche (Mannheim, Germany). Rab23 (AY585189) was cloned into BamH1 of pBluescriptSK+. Tissue sections (8-μm thick) were mounted onto poly-L-lysine slides. Following deparaffinization, tissue sections were rehydrated in a series of ethanol dilutions. To enhance the signal and facilitate probe penetration, sections were immersed in 0.3% Triton X-100 solution for 15 min at room temperature and in proteinase K solution (20 μg/mL) for 20 min at 37℃, respectively. Sections were incubated with 4% (w/v) paraformaldehyde/phosphate-buffered saline (PBS) for 5 min at 4℃. After washed with PBS, slides were incubated with prehybridization solution (50% formamide, 50% 4 × SSC) for 2 h at 37℃. Probe was added to each tissue section at a concentration of 1 μg/mL and hybridized overnight at 42℃. After high stringency washing, the sections were incubated with an alkaline phosphatase-conjugated sheep anti-digoxigenin antibody, which catalyzes a color reaction with nitro-blue-tetrazolium (NBT)/5-bromo-4-chloro-3-indolyl phosphate (BCIP) substrate (Roche, Mannheim, Germany). A blue color indicated strong hybridization.

Culture of Hep-3B cell line

Hep-3B cells kindly donated by Professor Shi-Gang Xiong (Department of Pathology, Keck School of Medicine, University of Southern California, USA.), were cultured in Dulbecco's minimal essential medium (DMEM; Gibco BRL, Gaithersburg, MD, USA) supplemented with 10% fetal bovine serum (FBS; Bio-Whittaker, Walkersville, MD, USA), 100 IU/mL penicillin, and 100 μg/mL streptomycin. Cultures were incubated at 37℃ in a humidified atmosphere containing 50 mL/L CO_2, and the medium was changed twice a week. Cell viability was tested by trypan blue exclusion. All experiments were performed with Hep-3B cells from passages 6-15, which were exposed to serum-free culture medium containing 0.1% bovine serum albumin for 24 h.

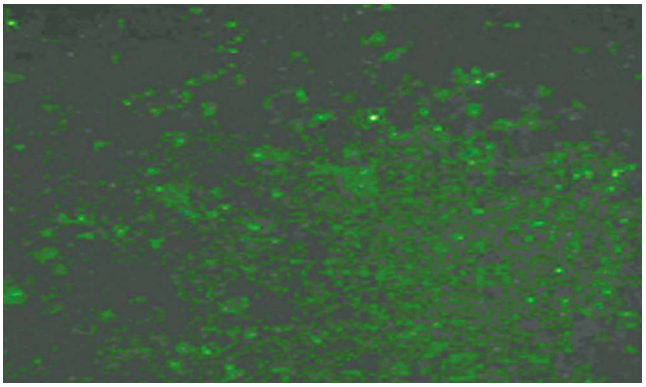

Figure 2 Rab23 gene silencing in Hep-3B cells. Green fluorescence could be detected in siRNA-transfected Hep-3B cells (negative control group).

Rab23 gene silencing in Hep-3B cells

Hep-3B cells were harvested by trypsinization and seeded 24 h prior to transfection, on 6-well plates at a density of 300 000 cells/well in 2 mL DMEM with 10% FBS. When the Hep-3B cells were at 90%-95% confluence, the culture medium was replaced with 1 mL of DMEM with or without 10% FBS. Following an overnight incubation, cells received 1 mL of complete medium and were incubated until 72 h post transfection.

According to the design principle of siRNA[19-21], short interfering RNA for Rab23 and negative control siRNA were designed. The target gene sequence of Rab23 is 5`-3` CCA GAA CTA ACG CAT TCA TCA A. The siRNA sequence (siRNA Duplex) is CCA GAA CUA ACG CAU UCA A dT dA dAdT GGU CUU GAU UGC GUA AGU U. The sequence of negative control siRNA is: sense 5`-UUC UCC GAA CGU GUC ACG UTT-3`, Anti-sense 5`-ACG UGA CAC GUU CGG AGA ATT-3`. Short interfering RNAs (siRNAs) for Rab23 were purchased from Guangzhou Ribobio CO., Ltd (Guangzhou, China) and negative control siRNAs were purchased from Shanghai GenePharma Co., Ltd (Shanghai, China). Double-strand RNA (final concentration of 50 and 100 nmol/L) in OPTI-MEM (80 μL) and oligofectamine (4 μL) in OPTI-MEM (15 μL) were mixed and allowed to stand at room temperature for 20 min according to the manufacturer's directions (Invitrogen, Carlsbad, USA). The mixture was added directly into a culture of Hep-3B cells (1×10^5/mL) in OPTI-MEM (0.4 mL). After 24 h, the consequences of transfection were watched through fluorescence of the cells (Figure 2). Transfection efficiency was normalized by monitoring luciferase activity from total cell lysates using the firefly luciferase (FLuc) assay kit (Promega, madison, USA). Cells were analyzed after 12 h by MTT assay. After 48 h they were analyzed by fluorescence-activated cell sorting, Western blots and RT-PCR . All experiments were performed in triplicate.

RNA isolation and two-step real-time RT-PCR

Two-step real-time RT-PCR was performed to compare the expression of Rab23 in normal liver tissue samples and Hep-3B cell lines. Total RNA was extracted using

TRIzol reagent (Sigma) according to the manufacturer's instructions. Reverse transcription with oligo (dT) priming was used to generate cDNAs from total RNA (2 μg) extracts. The synthesized cDNAs for Rab23 and β-actin were amplified using specific sets of primers. Optimal oligonucleotide primers were designed using Beacon Designer 2.0 software (MWG Biotech, High Point, NC). The primers used to amplify human Rab23 were synthesized according to the following sequences: forward primer: 5' GTA GTA GCC GAA GTG GGA 3', reverse primer: 5' CCT TTG TTT GTT GGGTCT C 3' according to ABO34244 in the gene bank. β-actin primer was designed based on published cDNA sequences: forward primer 5'TCA TCA CCA TTG GCA ATG AG3', reverse primer 5' CAC TGT GTT GGC GTA CAG GT 3'. Each PCR mixture contained the appropriate set of forward and reverse primers (0.2 μmol/L), each dNTP at 0.25 mmol/L, 1.25 U Taq polymerase, and 2.5 mmol/L $MgCl_2$ in a PCR buffer. The PCR procedure consisted of 28 cycles of denaturation at 95℃ for 1 min, annealing at 58℃ for 1 min, and extension at 72℃ for 1 min, with initial denaturation of sample cDNA at 95℃ for 3 min and an additional extension period of 10 min after the last cycle. The PCR products were subjected to 1.5% agarose gel electrophoresis stained with ethidium bromide and quantitated by densitometry using an Image Master VDS system and associated software (Pharmacia, USA).

Protein extraction and Western blotting

Cells were washed with cold PBS and lysed by the addition of a lysis buffer containing 1% Nonidet P-40, 50 mmol/L Tris (pH 7.5), 150 mmol/L NaCl, 0.1% SDS, and protease inhibitor cocktail (Boehringer Mannhein, Lewes, U.K.) for 20 min at 4℃. Insoluble materials were removed by centrifugation at 15000 r/min for 15 min at 4℃. The supernatant was saved and the protein concentration was determined using a Bio-Rad protein assay kit (Bio-Rad, Hercules, CA). Cell extracts (50 μg/lane) were separated *via* 10% gel electrophoresis and electroblotted onto PVDF membranes. Nonspecific binding sites were blocked by incubating nitrocellulose sheets for 1 h in phosphate-buffered saline containing 5% low-fat dry milk. Membranes were probed with primary antibodies overnight at 4℃, followed by a secondary horseradish peroxidase-conjugated second antibody. Blots were developed using an enhanced chemiluminescence detection system (ECL, Amersham Pharmacia Biotech) according to the manufacturer's instructions.

MTT assay

The cell proliferation and viability were determined by MTT assay as previously described[18]. Briefly, cells (5×10^3 cells per well) were seeded in 96-well microtiter plates (Nunc, Denmark). After different treatments for 12 , 24 , 48 h or 72 h, an aliquot (50 μL) of MTT (Sigma) solution (2 mg/mL in PBS) was added to each well and the plates were incubated for an additional 4 h at 37℃. MTT solution in medium was aspirated off. To achieve solubilization of the formazan crystal formed in viable cells, 150 μL DMSO was added to each well. The absorbance was read at 490 nm on a Dias automatic microwell plate reader with DMSO as the blank.

Fluorescence-activated cell sorting

After treatment for 48 h, cells were washed with cold sterile phosphate-buffered saline (PBS), and harvested in 70% cold alcohol solution for immediate analysis in a Becton Dickinson FACScan flow cytometer (Becton Dickinson, San Jose, CA). Data were acquired and analyzed using CellQuest software (BD Biosciences). The flow cytometer was calibrated daily with CaliBRITE 3 (BD biosciences) for fluorescence sensitivity and spectral overlap.

Statistical analysis

For immunohistochemistry and *in situ* hybridization results, Fisher's exact test or a binomial proportion analysis was used. $P < 0.05$ was considered statistically significant. Results of RT-PCR, Western blotting and MTT assays were expressed as mean ± SE of at least three separate experiments. Results were analyzed by one-way analysis of variance (ANOVA) followed by the Student-Neumann-Keuls test. Again, differences with P values of < 0.05 were considered statistically significant.

RESULTS

Expression of Rab23 in normal liver tissues and HCCs by immunohistochemistry

The expression of Rab23 in normal liver tissues has not been reported. Slight or no membranous staining of Rab23 in normal liver tissue was detected in our study. There was also no cytoplasmic or nuclear staining of Rab23 in normal liver tissues (Figure 3A). Conversely, expression of Rab23 was found in HCCs, and the expression rate was 53.5% (38 of 71 samples were positive, Table 1). Most samples expressed Rab23 in nuclei of HCC cells (Figure 3B and C). The results of expression of Rab23 correlated with tumor size ($P < 0.01$, Table 1), suggesting that Rab23 might be a useful prognostic indicator in HCC .

Expression of Rab23 in normal liver tissue and HCCs by in situ hybridization

No expression of Rab23 could be detected by *in situ* hybridization in five normal liver tissue samples (Figure 3D). To confirm this result, we also checked the transcripts by RT-PCR, and got the same result (data not shown).

To assess the frequency of Rab23 activation in HCC, we examined its expression in tissue samples derived from 100 different HCC cases (Table 1). We found positive staining for Rab23 in 38 of 71 (72%) HCC cases (Figure 3E and F). Further analyses again showed that activation of Rab23 correlated with tumor size ($P < 0.01$, Table 1).

Low expression of Rab23 in Hep-3B cell line when it was silenced by siRNA

Hep-3B cells were divided into three groups: a transfected group, a blank control group, and a negative control group. After 24 h of treatment with siRNA, Hep-3B cells were

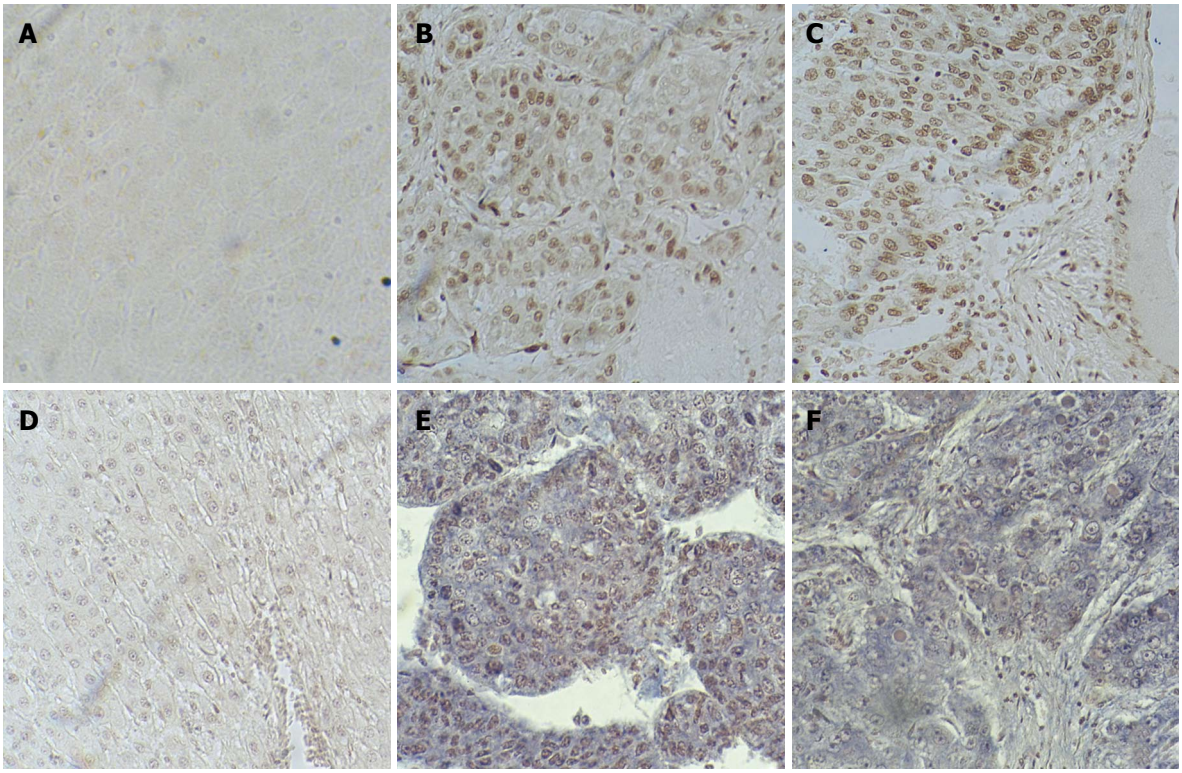

Figure 3 Expression of Rab23 in normal liver tissues and HCCs as seen by immunohistochemistry (**A-C**) and *in situ* hybridization (**D-F**).

Table 1 Expression of Rab23 in HCC (*in-situ* hybridization and immunohistochemistry)

	In-situ hybridization			limmunohistochemistry		
	Pos	Neg	*P*	Pos	Neg	*P*
Normal	0	5		0	5	
Paracarcinoma	0	18		0	18	
HCC	38	33		48	19	
Tumor Differentiation						
Well	4	3		6	1	
Mod and poor	34	30	0.3028	42	18	0.2681
Metastasis						
Yes	9	5		10	4	
No	29	28	0.2663	38	15	0.2591
Tumor size						
Small	3	11		4	13	
Large	35	22	0.0072	35	15	0.001
Age						
⩾ 50 yr	14	10		15	9	
< 50 yr	24	23	0.5613	33	10	0.2149
Sex						
Male	29	26		44	15	
Female	9	7	0.8036	4	4	0.1156
HBsAg						
Pos	34	31		46	17	
Neg	4	2	0.2721	2	2	0.2517
AFP						
⩾ 20 μg/L	26	24		35	12	
< 20 μg/L	12	9	0.6917	13	7	0.4314

Statistical analysis was performed by Fisher's exact test or Binomial proportions analysis. A *P* value < 0.05 was considered statistically significant. Pos: positive signal; Neg: Negative signal; Well: Well-differentiated tumors; Mod-poor: Moderately to poorly differentiated tumors.

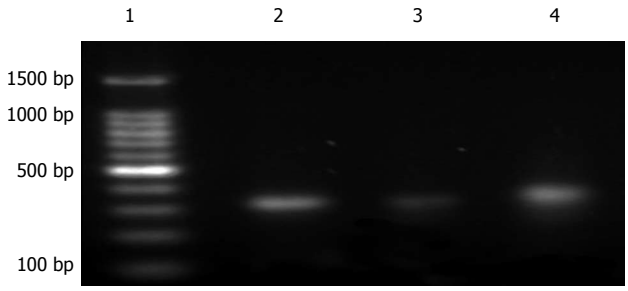

Figure 4 Electrophoresis of the RT-PCR products of Rab23 mRNA in Hep-3B cells after being silenced by siRNA. Lane 1: marker 1500; Lane 2: blank control group; Lane 3: transfection group; Lane 4: negative control group.

harvested and total RNA was extracted. RT-PCR was done as described previously[18]. The expression levels in the transfected group decreased almost 4.5 fold compared with the blank control group. There was no statistical significance between the blank control group and the negative control group (Figure 4,Figure 5, Figure 6).

Expression of Rab23 protein in Hep-3B cells decreased when it was silenced by siRNA

We used the same method for preparing Hep-3B cells for Western blots as for preparing cells for RT-PCR. After 24 h of treatment, Hep-3B cells were harvested and protein was extracted. Western blots were run according to a protocol described previously[22]. The expression levels in the transfected group decreased to almost half the level of the blank control group. There was no statistical

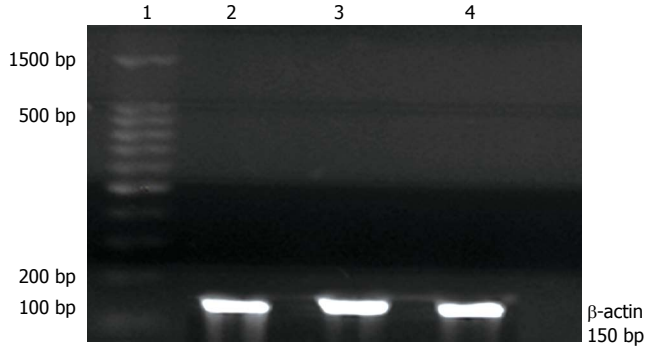

Figure 5 Electrophoresis of the RT-PCR products of β-actin mRNA in Hep-3B cells. Lane 1: marker 1500; Lane 2: blank control group; Lane 3: transfection group; Lane4: negative control group.

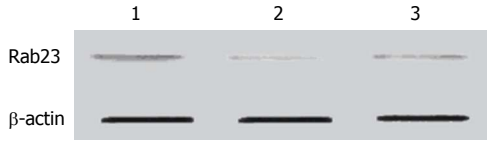

Figure 7 Western blot results for Rab23 in Hep-3B cells after being silenced by siRNA. Lane 1: blank control group; Lane 2: transfection group; Lane 3: negative control group.

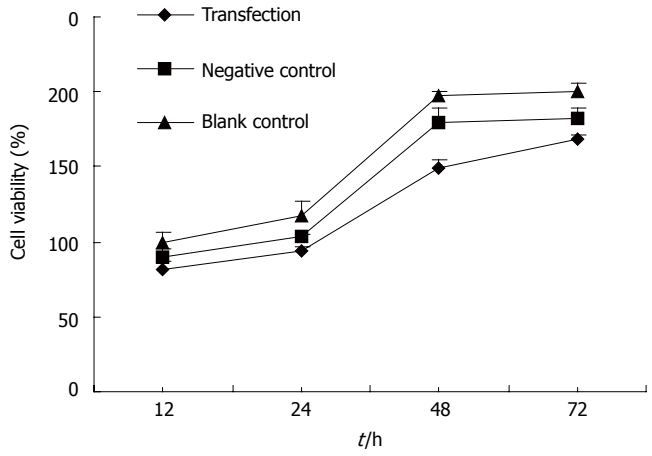

Figure 9 The results of MTT assays. At 48 h and 72 h, growth of Hep-3B cells was inhibited after being interferenced by siRNA against Rab23 gene. the survival rate of the transfection group decreased compared with controls. $P < 0.01$ *vs* control group. Again, there was no significant difference between blank and negative control groups, $P > 0.05$.

significance between the blank control group and the negative control group (Figure 7, Figure 8).

Viability of Hep-3B cells decreased after being transfected

Here we determined whether inhibition of the expression of Rab23 in Hep-3B cells also inhibits the proliferation of these cells by MTT assay. Forty-eight hours and 72 h after adding siRNA, the survival rate of the transfected group decreased compared with controls ($P < 0.05$, Figure 9). Again, there was no significant difference between the blank and negative control groups.

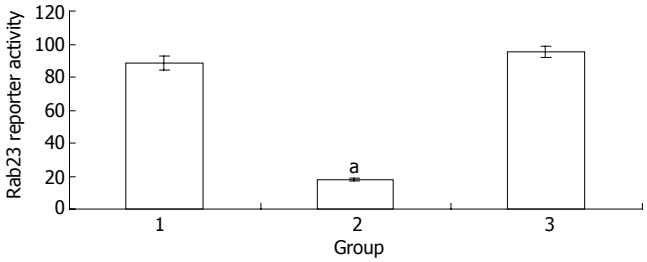

Figure 6 Electrophoresis of the RT-PCR products of Rab23 mRNA in Hep-3B cells after being silenced by siRNA. Lane 1: blank control group; Lane 2: transfection group; Lane 3: negative control group. [a]$P < 0.05$ *vs* control.

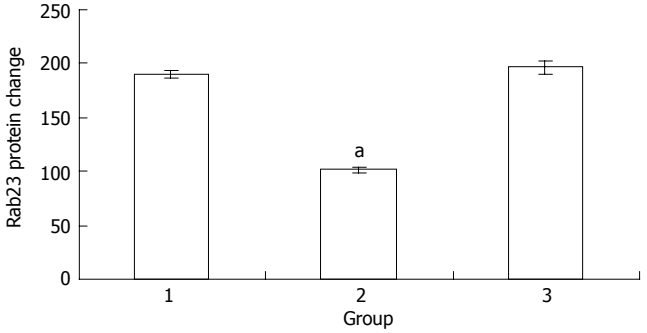

Figure 8 Western blot result for Rab23 in Hep-3B cells after being silenced by siRNA. Lane 1: blank control group; Lane 2: transfection group; Lane 3: negative control group. [a]$P < 0.05$ *vs* control.

Apoptosis rate of Hep-3B cells increased after the Rab23 gene was silenced by siRNA

Forty-eight hours after siRNA treatment, Hep-3B cells were tested by fluorescence- activated cell sorting. Apoptosis skewness was seen in the transfected group. The apoptotic rate of Hep-3B was 30% in the blank control group but 0% in the negative control groups (Figure 10).

DISCUSSION

The worldwide incidence of liver cancer is expected to rise over the next decade. This is serious because the prevalence and mortality rate of HCC are rather high at present[23]. Furthermore, the mechanisms underlying the initiation and progression of HCC remain elusive. One candidate mechanism involves the hedgehog (Hh) pathway. Dysregulation of this pathway has been implicated in the genesis of several kinds of cancer derived from multiple tissue types[3], including HCC[8,9]. One aspect of Hh signaling is negative regulation of this pathway by Rab23[13,15]. Rab23 acts on upstream of Gli transcription factors in patterning neural cell types in the spinal cord. The primary target of Rab23 is the Gli2 activator. Rab23 and Gli3 repressor have additive effects on pattering. Analysis of the Gli3 protein suggests that Rab23 also has a role in promoting the expression of Gli3 repressor. Although the membrane proteins patched and smoothened can change subcellular location in response to SHH, analysis demonstrates that Rab23 does not work through either patched or smoothened. Instead, Rab23 appears to

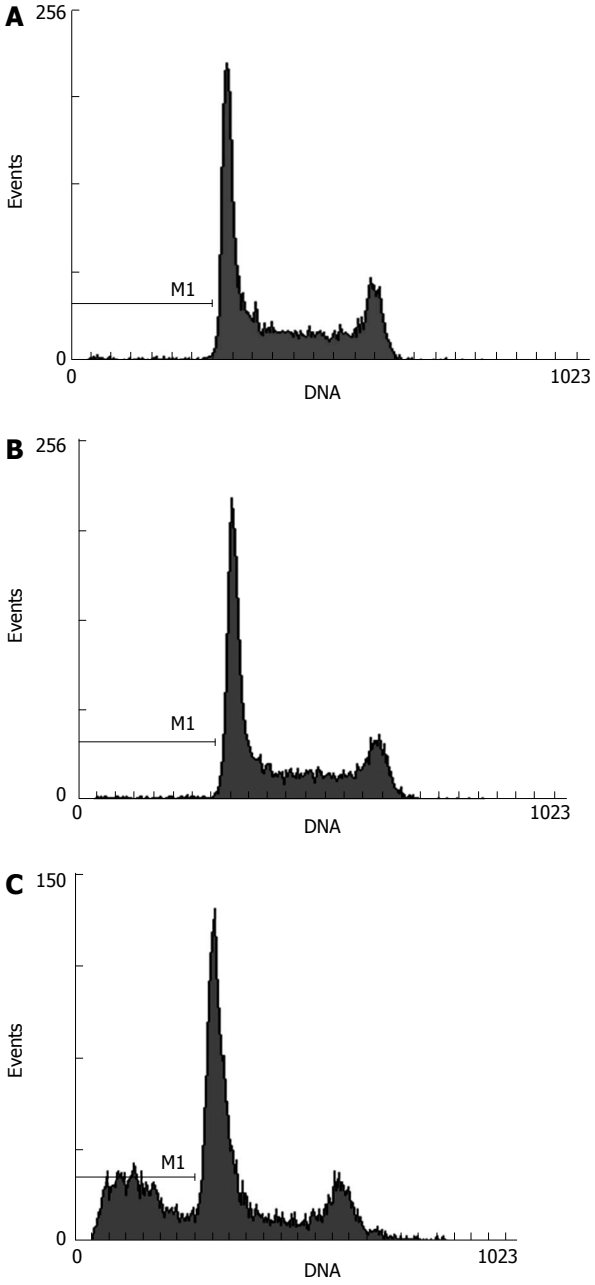

Figure 10 Apoptotic rate of Hep-3B cells measured by flow cytometry. in negative control (**A**), blank control (**B**) and transfected (**C**) groups.

regulate subcellular localization of essential components of the hedgehog pathway that act both on downstream of smoothened and on upstream of Gli proteins[14].

There are no reports about studies of Rab23 in HCC or even in any other human tumors. Since Rab23 is a negative regulator of SHH which can induce malignant carcinoma, Rab23 may also contribute to tumorigenesis in HCC.

Our results identify one potential mechanism underlying hepatocarcinogenesis, namely dysregulation of Rab23 and SHH signaling. In this study, we found that the aberrant expression of Rab23 was a general event during the development of HCC, and that the expression of the Rab23 gene correlated with tumor size. These findings are strongly supported by our studies of Hep3B cells in which Rab23 was silenced by siRNA, which inhibited cell proliferation and increased apoptosis. Further studies are now needed to identify the mechanisms by which Rab23 expression might contribute to dysregulation of SHH signaling and HCC tumorigenesis. Rab23 plays an important role in tumorigenesis of HCC and other human tumors. Also, Rab23 may be a new biological target for prognosis and treatment of HCC.

ACKNOWLEDGMENTS

The authors thank Dr. Ningning Wang, Department of Medical Statistics and Epidemics, School of Public Health, Sun Yat-Sen University, for her valuable advice on statistics.

REFERENCES

1 **Tien LT**, Ito M, Nakao M, Niino D, Serik M, Nakashima M, Wen CY, Yatsuhashi H, Ishibashi H. Expression of beta-catenin in hepatocellular carcinoma. *World J Gastroenterol* 2005; **11**: 2398-2401
2 **Iimuro Y**, Fujimoto J. Strategy of gene therapy for liver cirrohosis and hepatocellular carcinoma. *J Hepatobiliary Pancreat Surg* 2003; **10**: 45-47
3 **Beachy PA**, Karhadkar SS, Berman DM. Tissue repair and stem cell renewal in carcinogenesis. *Nature* 2004; **432**: 324-331
4 **Clatworthy JP**, Subramanian V. Stem cells and the regulation of proliferation, differentiation and patterning in the intestinal epithelium: emerging insights from gene expression patterns, transgenic and gene ablation studies. *Mech Dev* 2001; **101**: 3-9
5 **Ruiz i Altaba A**, Sánchez P, Dahmane N. Gli and hedgehog in cancer: tumours, embryos and stem cells. *Nat Rev Cancer* 2002; **2**: 361-372
6 **van den Brink GR**, Bleuming SA, Hardwick JC, Schepman BL, Offerhaus GJ, Keller JJ, Nielsen C, Gaffield W, van Deventer SJ, Roberts DJ, Peppelenbosch MP. Indian Hedgehog is an antagonist of Wnt signaling in colonic epithelial cell differentiation. *Nat Genet* 2004; **36**: 277-282
7 **Taipale J**, Beachy PA. The Hedgehog and Wnt signalling pathways in cancer. *Nature* 2001; **411**: 349-354
8 **Sicklick JK**, Li YX, Jayaraman A, Kannangai R, Qi Y, Vivekanandan P, Ludlow JW, Owzar K, Chen W, Torbenson MS, Diehl AM. Dysregulation of the Hedgehog pathway in human hepatocarcinogenesis. *Carcinogenesis* 2006; **27**: 748-757
9 **Huang S**, He J, Zhang X, Bian Y, Yang L, Xie G, Zhang K, Tang W, Stelter AA, Wang Q, Zhang H, Xie J. Activation of the hedgehog pathway in human hepatocellular carcinomas. *Carcinogenesis* 2006; **27**: 1334-1340
10 **Chavrier P**, Simons K, Zerial M. The complexity of the Rab and Rho GTP-binding protein subfamilies revealed by a PCR cloning approach. *Gene* 1992; **112**: 261-264
11 **Olkkonen VM**, Peterson JR, Dupree P, Lütcke A, Zerial M, Simons K. Isolation of a mouse cDNA encoding Rab23, a small novel GTPase expressed predominantly in the brain. *Gene* 1994; **138**: 207-211
12 **Marcos I**, Borrego S, Antiñolo G. Molecular cloning and characterization of human RAB23, a member of the group of Rab GTPases. *Int J Mol Med* 2003; **12**: 983-987
13 **Evans TM**, Ferguson C, Wainwright BJ, Parton RG, Wicking C. Rab23, a negative regulator of hedgehog signaling, localizes to the plasma membrane and the endocytic pathway. *Traffic* 2003; **4**: 869-884
14 **Eggenschwiler JT**, Espinoza E, Anderson KV. Rab23 is an essential negative regulator of the mouse Sonic hedgehog signalling pathway. *Nature* 2001; **412**: 194-198
15 **Eggenschwiler JT**, Bulgakov OV, Qin J, Li T, Anderson KV. Mouse Rab23 regulates hedgehog signaling from smoothened

to Gli proteins. *Dev Biol* 2006; **290**: 1-12
16 **Packeisen J**, Korsching E, Herbst H, Boecker W, Buerger H. Demystified...tissue microarray technology. *Mol Pathol* 2003; **56**: 198-204
17 **Ma X**, Sheng T, Zhang Y, Zhang X, He J, Huang S, Chen K, Sultz J, Adegboyega PA, Zhang H, Xie J. Hedgehog signaling is activated in subsets of esophageal cancers. *Int J Cancer* 2006; **118**: 139-148
18 **Ma X**, Chen K, Huang S, Zhang X, Adegboyega PA, Evers BM, Zhang H, Xie J. Frequent activation of the hedgehog pathway in advanced gastric adenocarcinomas. *Carcinogenesis* 2005; **26**: 1698-1705
19 **Amarzguioui M**, Prydz H. An algorithm for selection of functional siRNA sequences. *Biochem Biophys Res Commun* 2004; **316**: 1050-1058
20 **Reynolds A**, Leake D, Boese Q, Scaringe S, Marshall WS, Khvorova A. Rational siRNA design for RNA interference. *Nat Biotechnol* 2004; **22**: 326-330
21 **Ui-Tei K**, Naito Y, Takahashi F, Haraguchi T, Ohki-Hamazaki H, Juni A, Ueda R, Saigo K. Guidelines for the selection of highly effective siRNA sequences for mammalian and chick RNA interference. *Nucleic Acids Res* 2004; **32**: 936-948
22 **Li W**, Zhang J, Huang Q, Zhu H, Zhang X. Long-term administering low anticoagulant activity heparin can lessen rat hepatic fibrosis induced by either CCl(4) or porcine serum injection. *Hepatol Res* 2006; **36**: 115-123
23 **Marrero JA**. Hepatocellular carcinoma. *Curr Opin Gastroenterol* 2005; **21**: 308-312

S- Editor Liu Y **L- Editor** Wang XL **E- Editor** Ma WH

PO Box 2345, Beijing 100023, China
www.wjgnet.com
wjg@wjgnet.com

World J Gastroenterol 2007 February 21; 13(7): 1018-1026
World Journal of Gastroenterology ISSN 1007-9327

COLORECTAL CANCER

Decreased fragile histidine triad expression in colorectal cancer and its association with apoptosis inhibition

Jie Cao, Xiao-Ping Chen, Wang-Lin Li, Jie Xia, Hong Du, Wei-Biao Tang, Hui Wang, Xi-Wen Chen, Huan-Qing Xiao, Yu-Yuan Li

Jie Cao, Wang-Lin Li, Jie Xia, Wei-Biao Tang, Hui Wang, Xi-Wen Chen, Huan-Qing Xiao, Department of Gastrointestinal Surgery, Affiliated Guangzhou First People's Hospital, Guangzhou Medical College, Guangzhou 510180, Guangdong Province, China
Xiao-Ping Chen, Center of Hepatic Surgery, Tongji Hospital, Tongji Medical College, Huazhong University of Science and Technology, Wuhan 430030, Hubei Province, China
Hong Du, Department of Pathology, Affiliated Guangzhou First People's Hospital, Guangzhou Medical College, Guangzhou 510180, Guangdong Province, China
Yu-Yuan Li, Department of Gastroenterology, Affiliated Guangzhou First People's Hospital, Guangzhou Medical College, Guangzhou 510180, Guangdong Province, China
Supported by the Natural Science Foundation of Guangdong Province, No. 06020005
Correspondence to: Jie Cao, MD, Department of Gastrointestinal Surgery, Affiliated Guangzhou First People's Hospital, Guangzhou Medical College, 1# Pang Fu Road, Guangzhou 510180, Guangdong Province, China. czhongt@126.com
Telephone: +86-20-81048185 Fax: +86-20-81045937
Received: 2006-11-14 Accepted: 2007-01-18

Abstract

AIM: To detect the expression of fragile histidine triad (FHIT) in normal colorectal tissue, colorectal adenoma and colorectal cancer (CRC) tissue, and to analyze its relationship with the clinicopathological features of CRC, and apoptosis-associated proteins (Bcl-2, Bax, survivin) and apoptosis in colorectal cancer.

METHODS: FHIT mRNA analysis was performed by nested reverse transcription-polymerase chain reaction (RT-PCR) assay. Tissue microarray (TMA) was established to detect the expression of FHIT, Bcl-2, Bax and survivin genes in 80 CRC tissue specimens, 16 colorectal adenoma tissue specimens and 16 hemorrhoid (PPH) tissue specimens during the same period of time as the control. Citrate-microwave-SP was used as immunohistochemical method. The relationship between clinicopathological factors, such as differentiation grades and 5-year survival rate was observed. TUNEL assay was used to detect the apoptosis index in 80 CRC tissue specimens.

RESULTS: Ten out of 26 (38.5%) CRC tissue specimens expressed aberrant FHIT transcripts, none of the aberrant FHIT transcripts was observed in the matched normal tissue and colorectal adenoma tissue by nested RT-PCR assay. The positive rate of FHIT gene expression in normal colorectal tissue, colorectal adenoma and carcinoma tissue was 93.75%, 68.75% and 46.25%, respectively. Clinicopathological analysis of patients showed that the decreased FHIT gene expression was not associated with age, sex, serum CEA levels, tumor site and size, histological classification. However, the expression of FHIT was correlated with differentiation grades, pathological stages, lymph node metastases and 5-year survival rate after operation. The positive rate of apoptosis-associated proteins (Bax, Bcl-2 and survivin) in CRC tissue was 72.50%, 51.25% and 77.50%, respectively. The expression of these apoptosis-associated proteins in CRC tissue was correlated with the expression of FHIT. The mean apoptosis index in FHIT negative tumors was significantly lower than that in FHIT positive tumors (5.41 ± 0.23 *vs* 0.56 ± 0.10, $P < 0.01$).

CONCLUSION: The FHIT gene plays an important role in the regulation of apoptosis and decreased FHIT expression plays a key role in the initiation and progression of colorectal carcinoma.

Key words: Colorectal cancer; Fragile histidine triad; Expression; Apoptosis

Cao J, Chen XP, Li WL, Xia J, Du H, Tang WB, Wang H, Chen XW, Xiao HQ, Li YY. Decreased fragile histidine triad expression in colorectal cancer and its association with apoptosis inhibition. *World J Gastroenterol* 2007; 13(7): 1018-1026

http://www.wjgnet.com/1007-9327/13/1018.asp

INTRODUCTION

Colorectal cancer is the second leading cause of death in the United States, where the cumulative lifetime risk of developing colorectal cancer in both men and women is 6%[1]. In China, colorectal cancer is the fourth leading cause of death[2].

The fragile histidine triad (FHIT) gene, is a tumor suppressor gene located at the fragile site FRA3B on chromosome 3p14.2 that can be identified by positional

cloning, a region of the genome showing loss of heterozygosity (LOH) in a variety of cancers[3,4]. FHIT is involved in carcinogenesis of many human tissues, including digestive tract tissue. The FHIT gene contains an open reading frame (ORF) of 444 base pairs (bps) encoding a protein of 147 amino acids, which appears to be ubiquitously expressed in human tissues. Large deletions within FHIT transcripts occur frequently in multiple malignancies[5,6]. Most of the deletions described to date in the FHIT gene involve loss of one or more coding exons and lead to a truncated protein[6]. Loss of FHIT protein expression and abnormal FHIT transcripts, including deletions and insertions of exons, have been found in lung and breast cancers, as well as in head and neck cancers[7-11]. Ohta *et al*[3] reported that aberrant transcripts of the FHIT gene have been observed in 38% of CRC cases. It was also reported that the FHIT gene plays an important role in both oncogenesis and progression of CRC[12-14]. However, Thiagalingam *et al*[15] showed that there is no evidence that the FHIT gene is involved in CRC carcinogenesis. The clinicopathological significance of FHIT alterations in CRC still remains unclear.

The role of FHIT expression in the development of colorectal cancer (CRC) is poorly understood. Recently, tissue microarray (TMA) technique has been developed, which can significantly increase the throughput of immunohistochemistry (IHC) tumor analysis. TMA is composed of a large number of small tissue cores punched out from different tumors. These tissue core specimens obtained from tissue blocks, are then arranged into a single recipient paraffin block[16]. This approach allows analysis of a large number of different tumor samples in one IHC experiment. Arrays as large as 1000 samples have been reported[17]. TMA can be used to test the prognostic significance of antibodies against proteins encoded by differentially expressed genes using a large number of archival patient samples. Decreased p53 expression is correlated with lymph node metastasis in CRC[18]. In our present study, an expanded repertoire of TMA technique was used to demonstrate the novel relationship between FHIT expression and clinicopathological factors, such as differentiation, pathological stages, lymph node metastasis and 5-year survival rate.

The presence of FHIT gene mutations correlates significantly with decreased FHIT expression in human CRC. Several well integrated biochemical subroutines promote CRC cell growth and inhibit apoptosis, tipping the balance of colon epithelial cells towards an unrestricted proliferation and outliving the sequence of mutations required for carcinogenesis. Apoptosis is essential for successful embryonic development and maintenance of normal tissue homeostasis[19]. The present study was to test the hypothesis that decreased FHIT expression inhibits apoptosis and decreases apoptosis-associated protein expression, to characterize FHIT mRNA and protein expression in normal colorectal tissue, and adenoma and adenocarcinoma tissue, and to investigate the mechanism of FHIT gene inactivation and its association with apoptosis inhibition in the development and progression of human CRC.

MATERIALS AND METHODS

Colorectal carcinoma tissue samples

Human colorectal tissue specimens were obtained from patients at the Department of Gastrointestinal Surgery, Affiliated Guangzhou First People's Hospital, Guangzhou Medical College, China, from January 1997 to June 2000. All tissue specimens were snap- frozen and stored at -80℃. There were 48 male and 32 female patients with an average age of 62 years (range 32-81 years). Of the 80 specimens of human colorectal carcinoma we examined, 20, 22, 23 and 15 were classified as Dukes' stage A, B, C and D, respectively. Histologically, well-differentiated CRC was found in 16, moderately-differentiated CRC in 44, and poorly-differentiated in 22 specimens, respectively (Table 1). As a control, 16 normal colorectal tissue specimens and 16 colorectal adenoma specimens were also obtained. These tissue specimens were snap-frozen in liquid nitrogen, embedded in paraffin and stored at -80℃. Sections of each paraffin block were stained with hematoxylin and eosin.

RT-PCR assay

Total RNA was isolated from 26 colorectal cancer and 26 normal adjacent colonic tissue specimens, and 14 adenoma and 14 normal adjacent colonic tissue specimens with TRIzol™ reagent (Life Technologies). Nested RT-PCR was carried out as described previously[20]. A 24 μL mixture of total RNA (10 μg), 0.4 mmol/L oligo (dT) (New England Biolabs), and QH_2O was prepared. After incubation for 10 min at 70℃, the mixture was quickly cooled on ice, and 16 μL of RT-PCR mixture containing 8 μL of 5 × first strand buffer (Invitrogen) (250 mmol/L Tris–HCl pH 8.3, 375 mmol/L KCl, 15 mmol/L $MgCl_2$), 4 μL of 0.1 M DTT (Invitrogen), 2 μL 10 mmol/L deoxynucleotide mixture (dATP, dTTP, dCTP and dGTP, 10 mmol/L each) (Roche), 2 μL of RNase inhibitor (40 U/μL) (Roche) was added. The reaction proceeded in GeneAmp 2400 (Applied Biosystems) at 45℃ for 2 min. After 400 U of SuperScript™ RnaseH-reverse transcriptase (200 U/μL) (Invitrogen) was added and incubated for 45 min at 60℃, the reaction was inactivated at 70℃ for 15 min and at 94℃ for 3 min. cDNA was used as a template in the following RT-PCR.

Mutation analysis of FHIT mRNA transcripts and aberrant splicing in human CRC by sequencing

Mutation screening in aberrant RT-PCR products was performed using an ABI 377 automated sequencer with a pEGM-T vector as described previously[21]. Aberrant migrating bands were directly sequenced after isolation of bands from low melting agarose and purification on columns.

Analysis of FHIT, Bax, Bcl-2 and survivin protein expression by TMA-IHC

Construction of tissue microarray (TMA): Archival paraffin-embedded, formalin-fixed tissues from 80 Chinese CRC, 16 colonic adenoma and 16 noncancerous normal mucosa patients were collected. Two independent experienced pathologists selected representative areas from

Table 1 Expression of FHIT and clinical or pathological factors

	n	FHIT expression		χ^2	*P*
		Positive	Negative		
Age					
< 60	34	16	18	0.16	0.901
⩾ 60	46	21	25		
Sex					
M	42	19	23	0.04	0.849
F	38	18	20		
Differentiated					
Well	16	12	4	4.84	0.028
Moderately	44	20	24		
Poorly	20	5	15		
Dukes					
A, B	45	27	18	7.82	0.005
C, D	35	10	25		
Lymph node metastasis					
Positive	16	11	5	4.07	0.006
Negative	64	26	38		
Survival					
⩾ 5 yr	35	23	12	5.77	0.016
< 5 yr	18	5	13		

each donor tumor block, and then one 1-mm core was taken from a representative area of the tumor and inserted into a recipient paraffin block to create the TMA[6]. One TMA slide contained 112 samples. We employed the TMA technique to explore the expression of FHIT, Bax, Bcl-2 and survivin in colorectal tumor specimens and its correlation with apoptosis status by TMA-IHC and TMA-TUNEL. We investigated consecutively-cut serial sections and examined the same tumor region in three dimensions.

Immunohistochemical analysis of FHIT, Bax, Bcl-2 and survivin expression in human CRC by TMA-IHC: Immunohistochemical studies were performed using a citrate-microwave-streptavidin peroxydase technique. Immunohistochemical detection was done using anti-FHIT, anti-Bax, anti-Bcl-2 and anti-survivin antibodies, respectively. Endogenous peroxidase activity was quenched by methanol containing 3% hydrogen peroxide (Sigma, Taufkirchen, Germany). Nonspecific binding was blocked by applying normal rabbit serum in a humidity chamber at a dilution of 1:10 for 30 min. Primary antibodies were applied overnight at 4℃. The secondary antibody (goat to mouse immunoglobulins, DAKO, Denmark) was applied for 1 h at room temperature. Peroxidase–antiperoxidase (PAP rabbit, DAKO) conjugate diluted at 1:100 in phosphate-buffered saline (PBS) was applied for 45 min at room temperature. The sections were stained with diaminobenzidine tetrahydrochloride (DAB, Sigma) and then counterstained with hematoxylin. Negative control staining was performed by omitting the primary antibody. As a positive control for FHIT protein in immunohistochemical studies, we used paraffin sections of lung cancer positive for FHIT protein.

Quantitative measurements: Quantitative analysis of immune reactions related to the total tissue area was performed. We measured the percentage of positive immune reactivity with these antibodies in the tissue epithelium (normal and tumor). Histological images were captured with an OLYMPUS BX50 system microscope with an objective at magnification X 40, through a video camera, and digitized by appropriate software. In each section, 500 cells per core were calculated. The relative level of specific immunostaining and its localization were also judged. The relative intensity of cell immunostaining was evaluated semi-quantitatively. The data of tissue array were confirmed by a pathologist at the Department of Pathology of Affiliated Guangzhou First People's Hospital.

Hierarchical clustering and tree-view analysis: Hierarchical clustering was performed by the Cluster program (available at http://rana.lbl.gov/) as described previously in two dimensions: tumors were grouped together based on the relation of their immunostaining profiles, and antibodies were grouped based on tumors they stained. The clustered data were visualized with the Tree-view software tool programs originally developed for analyzing cDNA microarray data (Available at http://rana.lbl.gov/), which graphically displayed the results of the analysis as dendrograms and arrays, wherein the rows and columns corresponded to the raw staining data, presented in the order determined.

Detection of cell apoptosis state in human CRC by TUNEL assay

Cell apoptosis was detected in 80 CRC specimens by TMA-TUNEL assay (Apotag Peroxidase Kit, Oncor, Gaithersburg, MD) with the Apop-Tag™ peroxidase kit (Zhongshan Biotech, Beijing). For the evaluation of TUNEL index, the number of TUNEL-positive colonic epithelial cells was recorded using the × 40 objective lens. The case was considered positive for TUNEL if any colonic epithelial cells showed TUNEL staining. The TUNEL index was determined as the number of TUNEL-positive colonic epithelial cells expressed as a percentage of the total number of counted colonic epithelial cells. Necrotic areas were excluded.

Statistical analysis

Results were presented as mean ± SD. All statistical analyses were carried out using SPSS 11.0 for Windows statistical software (SPSS Inc, USA). The relationship between the clinicopathological variables and FHIT loci and protein alterations was examined by Fisher's exact test. The relationship between the expression of FHIT and prognosis of CRC was analyzed by Cox-Mantel test. $P < 0.05$ was considered statistically significant. All experiments were performed three times.

RESULTS

Analysis of aberrant splice of FHIT gene in human CRC

Expression of FHIT mRNA was detected by nested RT-PCR. According to the results, 34.6% samples with abnormal FHIT expression displayed two transcript categories: normal FHIT transcript (PCR products = 707 bp) and aberrant FHIT transcript (PCR products = 336 bp and 239 bp), respectively (Figure 1). However, the samples with normal FHIT expression only showed a normal FHIT transcript size.

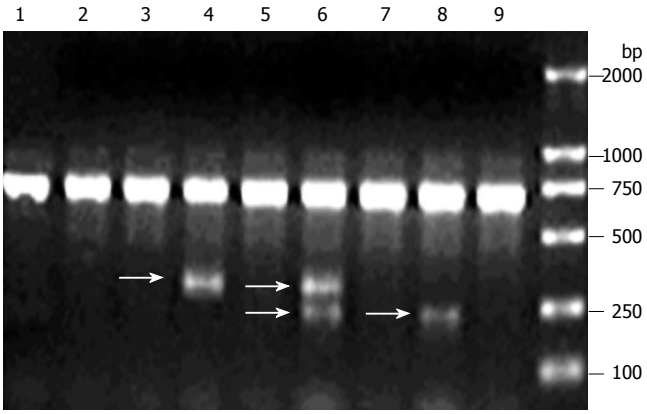

Figure 1 Frequency of intragenic deletions in FHIT transcripts in human CRC. Gel photo of FHIT RT-PCR products showing that the full length FHIT was the predominant transcript in samples 1-3, 5, 7 and 9. Both full length FHIT and shorter fragments representing transcripts containing deletions in FHIT could be seen in samples 4, 6 and 7. The arrow shows the gel position of splice variants.

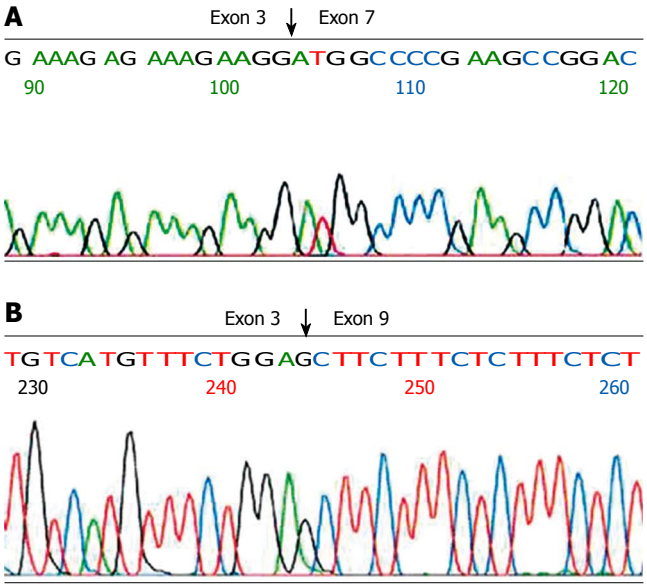

Figure 2 Sequencing analysis of aberrant FHIT transcripts. **A**: Deletion of exons 4-6 in the FHIT gene; **B**: Deletion of exons 4-8 in the FHIT gene.

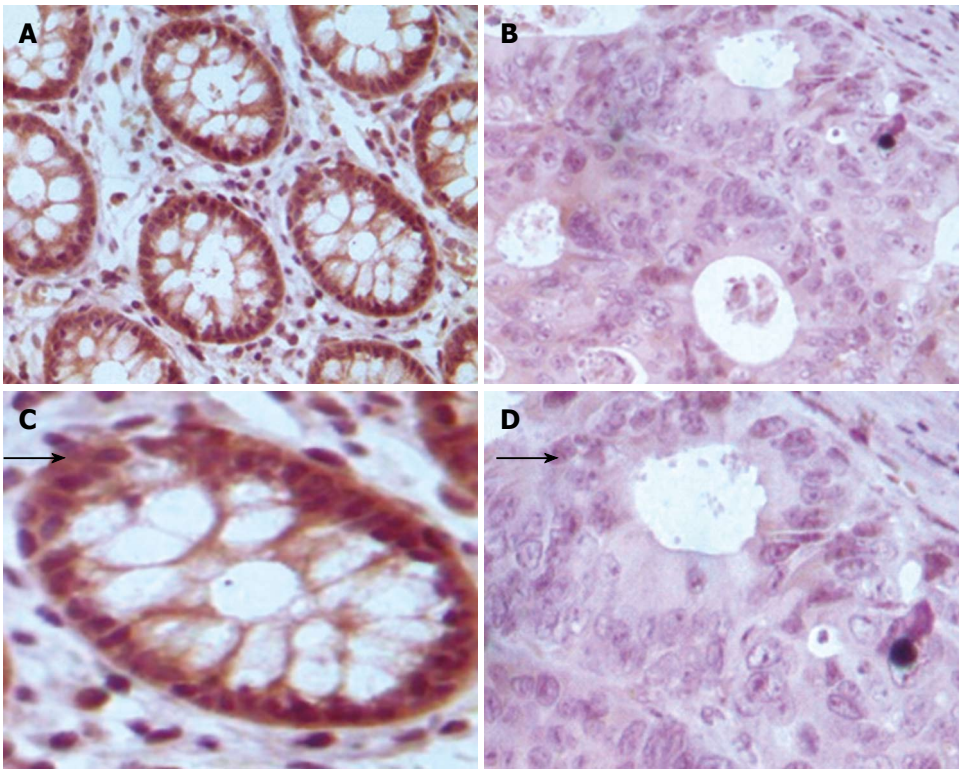

Figure 3 TMA-IHC assay showing significantly decreased FHIT expression in normal colonic mucosal samples (**A**), CRC tissue samples (**B**), and magnified views of the respective samples **A** and **B** (**C** and **D**).

Mutation analysis of FHIT gene in human CRC by sequencing

Aberrant RT-PCR products were sequenced after isolation of bands from low melting agarose and purification on columns. In the 336 bp fragment, Exon 3 was spliced to exon 7 (E3/E7), and thus the transcript lacked exons 4-6 (Figure 2A). In the 239 bp fragment, Exon 3 was spliced to exon 9 containing an E3/E9 aberrant transcript (Figure 2B).

Clinicopathological features and their relation to expression of FHIT in human CRC

The correlation between FHIT protein expression and clinicopathological data in the 80 carcinoma specimens is shown in Table 1, and a photograph of a representative specimen is provided in Figure 3. FHIT negative CRC was found in 43 and FHIT FHIT positive CRC was found in 37 specimens. Fifty-three percent (32 of 60) of specimens with well-differentiated CRC had positive

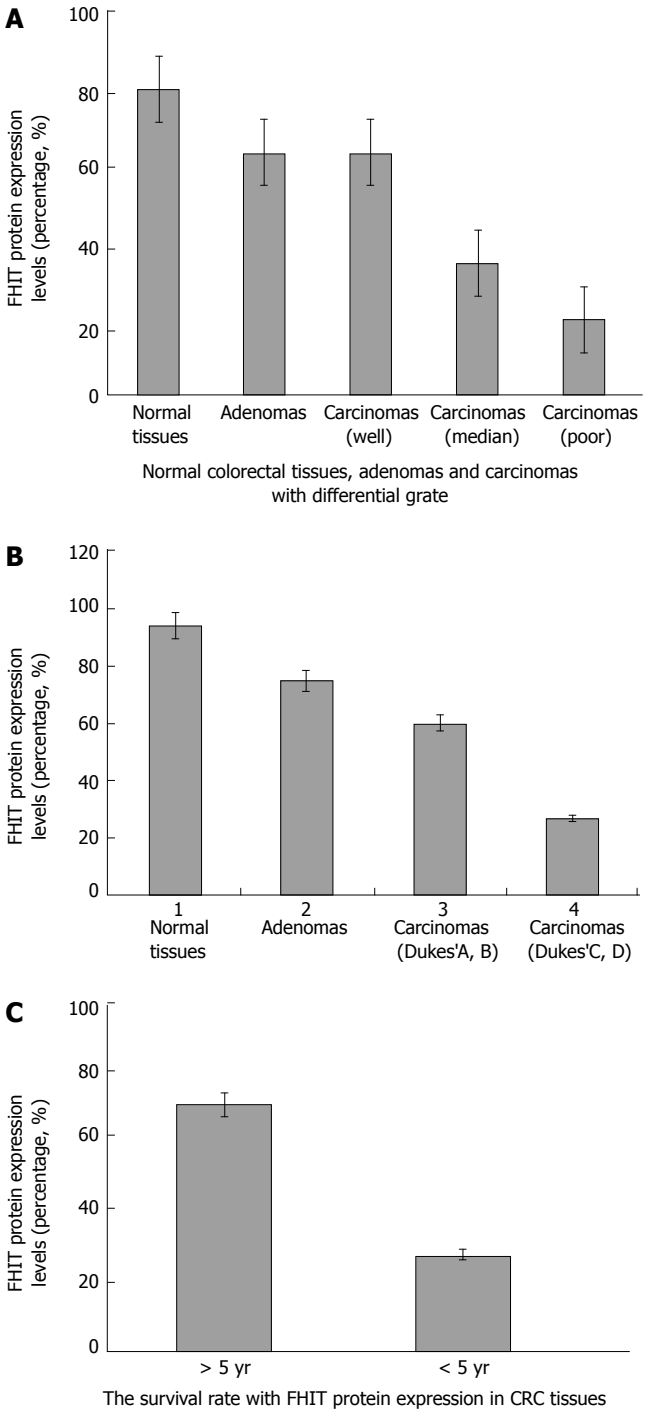

Figure 4 Relationships between FHIT expression and CRC differentiation grade (**A**) and stage (**B**), and survival rate (**C**) CRC patients.

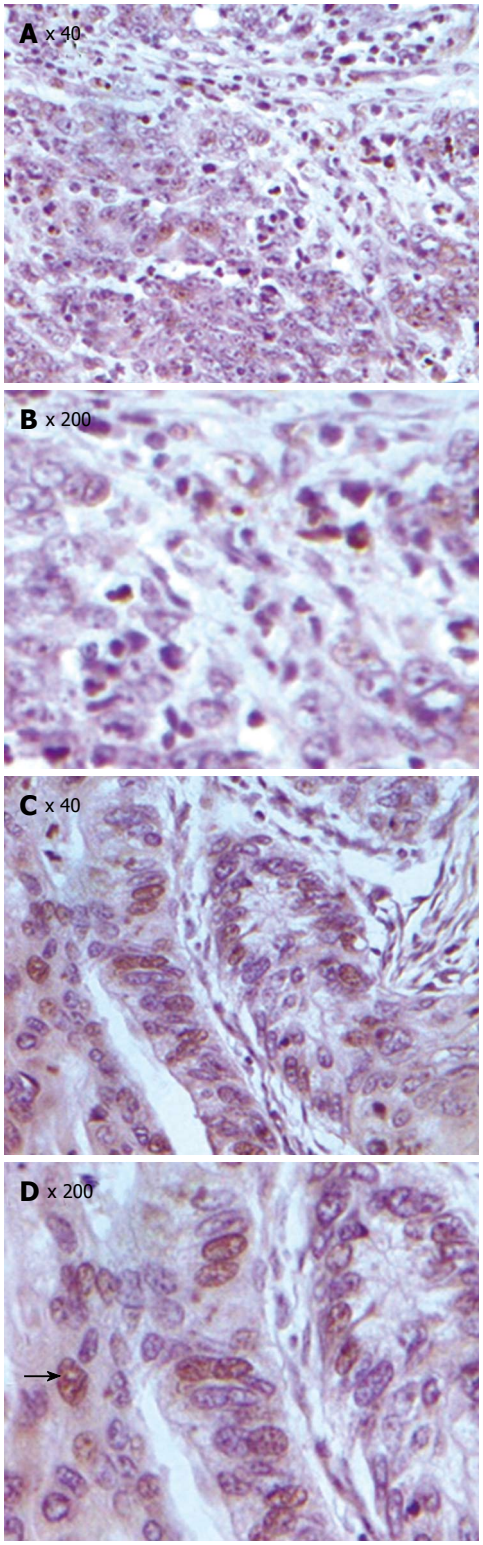

Figure 5 TUNEL assay showing significantly decreased apoptosis in FHIT-negative CRC cells (**A**), FHIT-positive CRC cells (**C**), and magnified views of the respective samples **A** and **C** (**B** and **D**).

FHIT expression, whereas 25% (5 of 20) of specimens with poorly-differentiated CRC had positive FHIT expression ($P < 0.05$), while 93.75% (15 of 16) and 75% (12 of 16) had positive FHIT expression in the normal colorectal tissue specimens and colorectal adenoma specimens, respectively (Figure 4A and Table 1). Sixty percent (27 of 45) of specimens with Dukes' A and B had positive FHITexpression, whereas only 28% (10 of 35) of specimens with Dukes' C and D had positive FHIT expression ($P < 0.005$) (Figure 4B and Table 1). Moreover, prognosis of the FHIT-negative cases was much poorer than the FHIT-positive cases (Figure 4C and Table 1). There was no significant correlation between other clinicopathological factors and FHIT expression.

Apoptosis status in human CRC as assessed by TUNEL

The role of FHIT protein in apoptosis as a proapoptic factor was detected by TUNEL assay. Aberrant expression of the FHIT gene was related to colonic epithelial cell apoptosis (Figures 5 and 6, Table 2). The apoptosis index was 5.41 ± 0.23 in colorectal cancer with normal FHIT

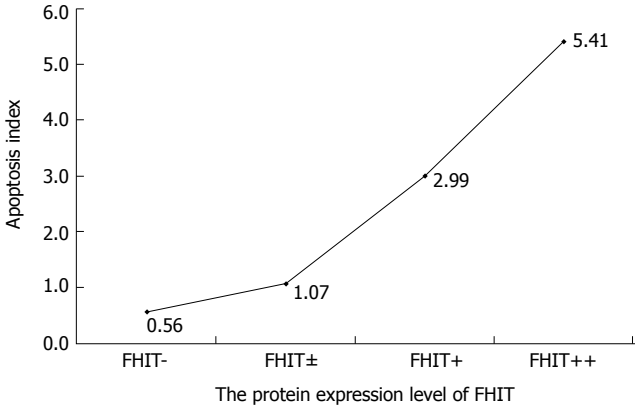

Figure 6 Decreased FHIT expression and apoptosis inhibition in human CRC. Reduced apoptosis index was detected in the same number of cells per field in CRC with FHIT-negative expression.

Table 2 Relationship between FHIT expression and apoptosis index (AI) in human CRC

FHIT	*n*	AI
-	11	0.56 ± 0.10
+/-	15	1.07 ± 0.16
+	17	2.99 ± 0.32
++	37	5.41 ± 0.23

expression and 0.56 ± 0.10 in tumors with absent FHIT expression. The rate of apoptosis was significantly lower in tumors with aberrant FHIT expression than in tumors with normal FHIT expression ($P < 0.05$).

Expression of Bax, Bcl-2 and survivin and its correlation with FHIT alteration

Since growth inhibitory effect of FHIT- expressing cells is related to apoptosis, we determined whether FHIT protein is related with other members in the apoptotic pathway. Of the CRC tissue specimens, 54% (43 of 80) had positive FHIT expression, whereas the remaining 46% (37 of 80) had no detectable FHIT expression by TMA-IHC assay (Figure 7, Figure 8, Figure 9 and Figure 10). Seventy-seven percent of FHIT protein-negative CRC specimens showed decreased Bax expression, whereas 75% and 60% FHIT protein-negative specimens displayed increased Bcl-2 and survivin expression (Figure 7, Figure 8, Figure 9 and Figure 10). The difference was statistically significant (Table 3).

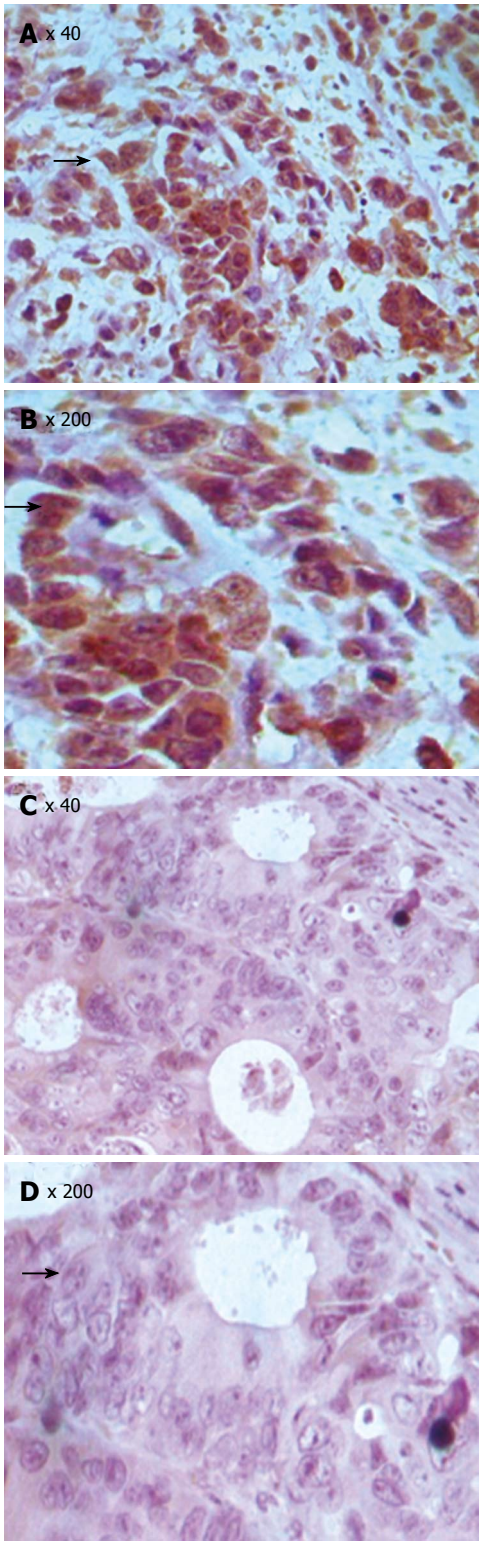

Figure 7 TMA-IHC showing significantly decreased Bax expression in FHIT positive CRC tissue samples (**A**), FHIT-negative CRC tissue samples (**C**), and magnified views of the respective samples **A** and **C** (**B** and **D**).

DISCUSSION

In the present study, frequent allelic loss was observed on chromosome 3p in lung cancer and preneoplastic bronchial lesions, indicating that inactivation of putative tumor suppressor genes on chromosome 3p may be involved in early steps of lung carcinogenesis. Ohta *et al*[3] have identified the FHIT gene on chromosome 3p14.2, spanning the FRA3B common fragile site and the t (3:8) break point associated with hereditary renal cell carcinomas. The FHIT gene is more than 1 Mb in size, encoding a 1.1-kb cDNA with 10 small exons and a cytoplasmic Mr 16 800 protein with diadenosine triphosphate (Ap3A) hydrolase activity [4]. In this study, truncated FHIT transcripts were observed frequently alongside full-length transcripts and sequence analysis of the truncated gene transcripts revealed mainly

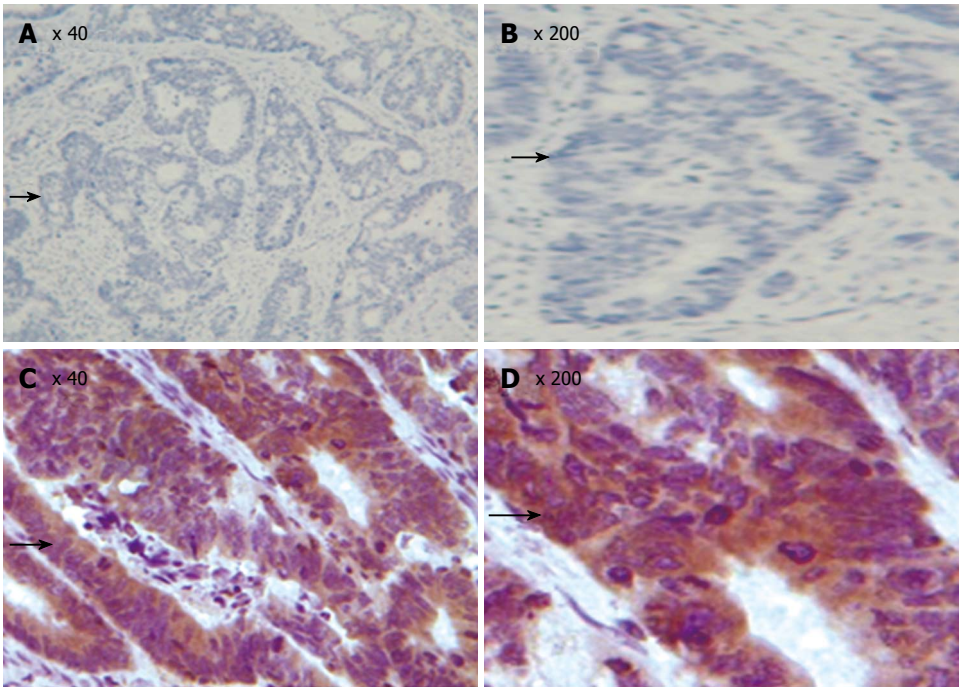

Figure 8 TMA-IHC showing significantly increased Bcl-2 expression FHIT positive CRC tissue samples (**A**), FHIT-negative CRC tissue samples (**C**), and magnified views of the respective samples **A** and **C** (**B** and **D**).

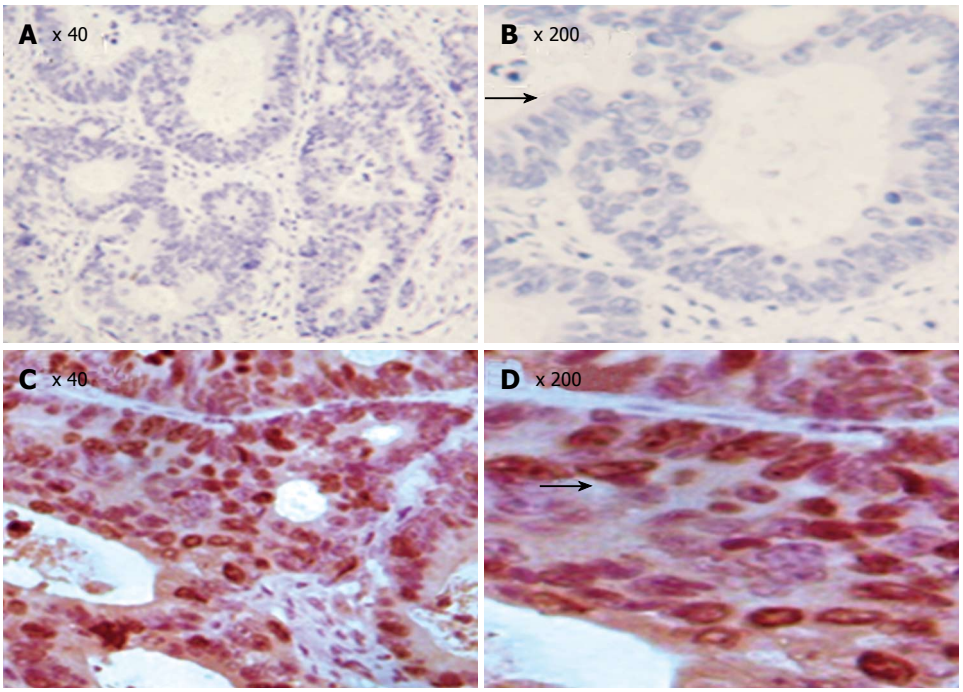

Figure 9 TMA-IHC showing significantly increased survivin expression in FHIT-positive CRC tissue samples (**A**), FHIT-negative CRC tissue samples (**C**), and magnified views of the respective samples **A** and **C** (**B** and **D**).

exon skipping and alternate RNA processing events. To elucidate the possible molecular mechanisms responsible for this loss of protein expression, we used RT-PCR for FHIT transcript analysis and cDNA sequencing for mutation detection. We found that 34.6% of the samples with decreased FHIT expression had an additional aberrant FHIT transcript product. However, aberrant FHIT was not identified in the samples with normal FHIT expression. These data suggest that loss and rearrangement of the FHIT gene derived from FRA3B breaks or gaps in the large FHIT intronic region may give rise to aberrant cDNA splicing and result in loss of FHIT protein, suggesting that the majority of aberrant FHIT transcripts lack exons 4-6 and 4-8. Our results indicate that higher incidence of aberrant processing of FHIT mRNA and mutation result in FHIT down-regulation in human CRC.

Loss of FHIT protein expression has been found in lung and breast cancers, as well as in head and neck cancers[7-10]. Ohta and colleagues[2] have reported significant loss or reduction of FHIT expression in 39% CRC patients. However, Thiagalingam *et al*[15] showed that the FHIT gene is not involved in CRC carcinogenesis. In this study, we demonstrated that loss of FHIT expression was associated with poorly- and well-differentiated CRC and frequent lymph node metastasis by TMA-IHC assay, indicating that FHIT plays a role in the progression of

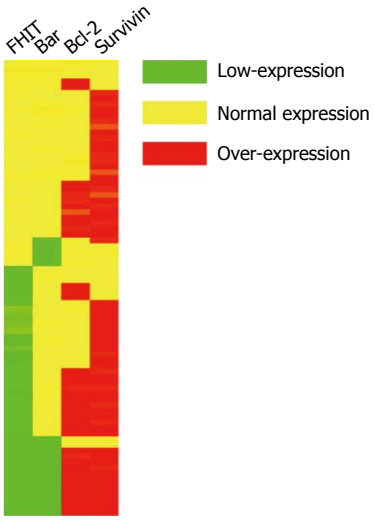

Figure 10 Tree-view of differential protein expression data from 80 CRC tissue samples. Tree-view demonstrated the FHIT protein expression related to Bax, Bcl-2 and survivin protein expression. Red indicates up-regulation, green indicates down-regulation, and yellow indicates no significant change.

Table 3 Expression of Bax, Bcl-2, survivin and correlation with FHIT alteration

		n	FHIT expression		χ^2	*P*
			Positive	Negative		
Bax	+	62	25	37	3.89	0.048
	-	18	12	6		
Bcl-2	+	58	32	26	6.75	0.009
	-	22	5	17		
Survivin	+	41	11	30	12.76	0
	-	39	26	13		

CRC because loss of FHIT protein is intimately associated with the development of CRC. Lack of FHIT gene expression and consequent protein expression can be due to deletions, mutations, or epigenetic modifications.

These results strongly indicate that aberrant expression of the FHIT gene is related to the development and progression of CRC. However, the relationship between FHIT expression and apoptosis has not been studied in human CRC, and the decreased apoptosis in FHIT deficient CRC has not been explained. We therefore designed this study to investigate the differential patterns of apoptosis-related protein expression associated with difference in FHIT expression, in order to identify specific changes that might reflect the pathway by which FHIT affects apoptosis. We performed TUNEL analysis in this study to assess apoptosis status and observed decreased apoptosis in FHIT negative CRC tissue samples compared to FHIT-positive CRC tissue samples. The apoptosis index was 5.41 ± 0.23 in tumors with normal FHIT expression and 0.56 ± 0.10 in tumors with aberrant expression. The rate of apoptosis in tumors with aberrant FHIT expression was significantly lower than that in tumors with normal FHIT expression ($P < 0.01$). Furthermore, we conducted tissue microarray analysis to identify differentially expressed proteins in relevant apoptosis pathways. For this initial pathway, we chose three key proteins belonging to the Bcl/Bax pathway (Bcl2 and Bax) and survivin-caspase pathway (survivin). In this study, the FHIT-negative CRC tissue samples were associated with down-regulation of Bax and up-regulation of Bcl-2. It is known that the Bax gene is an apoptosis-promoting member of the BCL-2 gene family, and apoptosis is known to be accelerated when the Bax function is predominant[22]. On the other hand, over-expression of Bcl-2 seems to be associated with the blocking of apoptosis. The ability of Bcl-2 to inhibit apoptosis is dependent on the expression of Bcl-2 and formation of hetero- and homo-dimers between members of the Bcl-2 family[23]. We observed a significant correlation between FHIT protein expression and members of the Bcl/Bax pathway in human CRC ($P < 0.05$). Survivin is minimally expressed in normal adult tissues but over-expressed in a wide range of human cancers, including cancer of the breast, lung, esophagus and urinary bladder. Survivin is one member of inhibitors of apoptosis and appears to block apoptosis by interfering with the caspase activation pathway[24]. In the present study, we demonstrated that survivin, an inhibitor of apoptosis protein family, was significantly increased in FHIT-negative CRC, indicating that FHIT plays a critical role in FHIT-induced apoptosis, occurring through inactivation of the survivin-caspase signal pathway. Accordingly, future investigations must address protein-protein interactions that lead to these changes in expression and apoptosis, thus allowing us to place FHIT at its correct position within the pathways, ultimately helping to elucidate the precise mechanism by which its expression modulates apoptosis in human CRC.

In conclusion, decreased FHIT expression is caused by mutations of the FHIT gene in human CRC. Down-regulation of FHIT is associated with down-regulation of Bax and up-regulation of Bcl-2 and survivin, which results in alterations in apoptosis status. Differential FHIT expression in human CRC plays a role in control of cell growth and apoptosis. FHIT is a potentially important growth suppressor gene that plays a role in the development and progression of human CRC. FHIT may be a candidate for therapeutic modulation of apoptosis in human CRC.

ACKNOWLEDGMENTS

We thank Dr. Ziqiang Yuan at Department of Molecular Genetics, Albert Einstein College of Medicine, NY, USA for revising the manuscript.

REFERENCES

1 **Hawk ET**, Levin B. Colorectal cancer prevention. *J Clin Oncol* 2005; **23**: 378-391
2 **Li M**, Gu J. Changing patterns of colorectal cancer in China over a period of 20 years. *World J Gastroenterol* 2005; **11**: 4685-4688
3 **Ohta M**, Inoue H, Cotticelli MG, Kastury K, Baffa R, Palazzo J, Siprashvili Z, Mori M, McCue P, Druck T, Croce CM, Huebner K. The FHIT gene, spanning the chromosome 3p14.2 fragile site and renal carcinoma-associated t(3;8) breakpoint, is abnormal in digestive tract cancers. *Cell* 1996; **84**: 587-597
4 **Boldog F**, Gemmill RM, West J, Robinson M, Robinson L, Li E, Roche J, Todd S, Waggoner B, Lundstrom R, Jacobson J, Mullokandov MR, Klinger H, Drabkin HA. Chromosome 3p14 homozygous deletions and sequence analysis of FRA3B. *Hum Mol Genet* 1997; **6**: 193-203

5 **Hayashi S**, Tanimoto K, Hajiro-Nakanishi K, Tsuchiya E, Kurosumi M, Higashi Y, Imai K, Suga K, Nakachi K. Abnormal FHIT transcripts in human breast carcinomas: a clinicopathological and epidemiological analysis of 61 Japanese cases. *Cancer Res* 1997; **57**: 1981-1985

6 **Huebner K**, Hadaczek P, Siprashvili Z, Druck T, Croce CM. The FHIT gene, a multiple tumor suppressor gene encompassing the carcinogen sensitive chromosome fragile site, FRA3B. *Biochim Biophys Acta* 1997; **1332**: M65-M70

7 **Siprashvili Z**, Sozzi G, Barnes LD, McCue P, Robinson AK, Eryomin V, Sard L, Tagliabue E, Greco A, Fusetti L, Schwartz G, Pierotti MA, Croce CM, Huebner K. Replacement of Fhit in cancer cells suppresses tumorigenicity. *Proc Natl Acad Sci USA* 1997; **94**: 13771-13776

8 **Wistuba II**, Behrens C, Virmani AK, Mele G, Milchgrub S, Girard L, Fondon JW, Garner HR, McKay B, Latif F, Lerman MI, Lam S, Gazdar AF, Minna JD. High resolution chromosome 3p allelotyping of human lung cancer and preneoplastic/preinvasive bronchial epithelium reveals multiple, discontinuous sites of 3p allele loss and three regions of frequent breakpoints. *Cancer Res* 2000; **60**: 1949-1960

9 **Sozzi G**, Sard L, De Gregorio L, Marchetti A, Musso K, Buttitta F, Tornielli S, Pellegrini S, Veronese ML, Manenti G, Incarbone M, Chella A, Angeletti CA, Pastorino U, Huebner K, Bevilaqua G, Pilotti S, Croce CM, Pierotti MA. Association between cigarette smoking and FHIT gene alterations in lung cancer. *Cancer Res* 1997; **57**: 2121-2123

10 **Campiglio M**, Pekarsky Y, Menard S, Tagliabue E, Pilotti S, Croce CM. FHIT loss of function in human primary breast cancer correlates with advanced stage of the disease. *Cancer Res* 1999; **59**: 3866-3869

11 **Pavelić K**, Krizanac S, Cacev T, Hadzija MP, Radosević S, Crnić I, Levanat S, Kapitanović S. Aberration of FHIT gene is associated with increased tumor proliferation and decreased apoptosis-clinical evidence in lung and head and neck carcinomas. *Mol Med* 2001; **7**: 442-453

12 **Hibi K**, Taguchi M, Nakamura H, Hirai A, Fujikake Y, Matsui T, Kasai Y, Akiyama S, Ito K, Takagi H. Alternative splicing of the FHIT gene in colorectal cancers. *Jpn J Cancer Res* 1997; **88**: 385-388

13 **Luceri C**, Guglielmi F, De Filippo C, Caderni G, Mini E, Biggeri A, Napoli C, Tonelli F, Cianchi F, Dolara P. Clinicopathologic features and FHIT gene expression in sporadic colorectal adenocarcinomas. *Scand J Gastroenterol* 2000; **35**: 637-641

14 **Hao XP**, Willis JE, Pretlow TG, Rao JS, MacLennan GT, Talbot IC, Pretlow TP. Loss of fragile histidine triad expression in colorectal carcinomas and premalignant lesions. *Cancer Res* 2000; **60**: 18-21

15 **Thiagalingam S**, Lisitsyn NA, Hamaguchi M, Wigler MH, Willson JK, Markowitz SD, Leach FS, Kinzler KW, Vogelstein B. Evaluation of the FHIT gene in colorectal cancers. *Cancer Res* 1996; **56**: 2936-2939

16 **Kononen J**, Bubendorf L, Kallioniemi A, Bärlund M, Schraml P, Leighton S, Torhorst J, Mihatsch MJ, Sauter G, Kallioniemi OP. Tissue microarrays for high-throughput molecular profiling of tumor specimens. *Nat Med* 1998; **4**: 844-847

17 **Knösel T**, Emde A, Schlüns K, Chen Y, Jürchott K, Krause M, Dietel M, Petersen I. Immunoprofiles of 11 biomarkers using tissue microarrays identify prognostic subgroups in colorectal cancer. *Neoplasia* 2005; **7**: 741-747

18 **Cao J**, Li WL, Du H, Tang WB, Wang H.FHIT and p53 expression in human colonic carcinoma. *Chin J Exp Surg* 2006; **23**: 787-789

19 **Vaux DL**, Korsmeyer SJ. Cell death in development. *Cell* 1999; **96**: 245-254

20 **Druck T**, Hadaczek P, Fu TB, Ohta M, Siprashvili Z, Baffa R, Negrini M, Kastury K, Veronese ML, Rosen D, Rothstein J, McCue P, Cotticelli MG, Inoue H, Croce CM, Huebner K. Structure and expression of the human FHIT gene in normal and tumor cells. *Cancer Res* 1997; **57**: 504-512

21 **Virgilio L**, Shuster M, Gollin SM, Veronese ML, Ohta M, Huebner K, Croce CM. FHIT gene alterations in head and neck squamous cell carcinomas. *Proc Natl Acad Sci USA* 1996; **93**: 9770-9775

22 **Yang E**, Zha J, Jockel J, Boise LH, Thompson CB, Korsmeyer SJ. Bad, a heterodimeric partner for Bcl-XL and Bcl-2, displaces Bax and promotes cell death. *Cell* 1995; **80**: 285-291

23 **Reed JC**. Bcl-2 and the regulation of programmed cell death. *J Cell Biol* 1994; **124**: 1-6

24 **Altieri DC**. Survivin, versatile modulation of cell division and apoptosis in cancer. *Oncogene* 2003; **22**: 8581-8589

S- Editor Liu Y **L- Editor** Wang XL **E- Editor** Ma WH

PO Box 2345, Beijing 100023, China
www.wjgnet.com
wjg@wjgnet.com

World J Gastroenterol 2007 February 21; 13(7): 1027-1031
World Journal of Gastroenterology ISSN 1007-9327

Hepatitis B virus infection and replication in primarily cultured human fetal hepatocytes

Min Lin, Qun Chen, Li-Ye Yang, Wen-Yu Li, Xi-Biao Cao, Jiao-Ren Wu, You-Peng Peng, Mo-Rui Chen

Min Lin, Li-Ye Yang, Wen-Yu Li, Xi-Biao Cao, Jiao-Ren Wu, You-Peng Peng, Mo-Rui Chen, Chaozhou Central Hospital, Chaozhou 521000, Guangdong Province, China
Qun Chen, Guangdong Medical College, Zhanjiang 524023, Guangdong Province, China
Supported by the Social Development Plan, Guangdong Province, No. 20051010057
Correspondence to: Dr. Li-Ye Yang, Chaozhou Central Hospital, Chaozhou 521021, Guangdong Province, China. yangleeyee@sina.com
Telephone: +86-768-2224092-2210 Fax: +86-768-2229563
Received: 2006-12-18 Accepted: 2007-01-26

Abstract

AIM: To investigate the infection and replication of hepatitis B virus (HBV) in primarily cultured human fetal hepatocytes (HFHs).

METHODS: The human fetal hepatocytes were cultured in serum-free medium, HBV-positive serum was added into the medium to study the susceptibility of hepatocytes to HBV infection. The supernatant was collected for ELISA assay of HBsAg and HBeAg, and quantitative fluorescence PCR for HBV-DNA assay daily. Albumin and HBcAg, CK8 and CK18 expressions were detected by immunohistochemistry in cultured hepatocytes. Content of lactate dehydrogenate (LDH) was measured to find out the integrity of the cell membrane.

RESULTS: A stable hepatocyte culture system was established. HBV could infect the hepatocytes and replicate, and HBcAg expression could be detected by immunohistochemistry in hepatocyte-like cells. HBV-DNA in the supernatant could be detected from d 2 to d 18 and HBsAg and HBeAg were positive on d 3-d 18 after HBV infection. HBV in medium increased from d 0 to d 6 and subsequently decreased as the cells were progressively loosing their hepatocyte phenotypes.

CONCLUSION: HBV could infect human fetal hepatocytes and replicate. This *in vitro* model allowed a detailed study on early events associated with human HBV entry into cells and subsequent replication.

Key words: Hepatitis B virus; Infection; Human fetal hepatocytes; Culture

Lin M, Chen Q, Yang LY, Li WY, Cao XB, Wu JR, Peng YP, Chen MR. Hepatitis B virus infection and replication in primarily cultured human fetal hepatocytes. *World J Gastroenterol* 2007; 13(7): 1027-1031

http://www.wjgnet.com/1007-9327/13/1027.asp

INTRODUCTION

Hepatitis B virus (HBV) infection is one of the commonest infections in the world. According to some reports, about 400 million people have been infected with HBV, and about 5% are chronically infected[1]. Chronic hepatitis B can cause cirrhosis and liver cancer[2-4]. It is estimated that there are more than one million deaths of this infection and 320 thousand deaths from liver cancer associated with HBV each year in the world[5]. There are about 400 million people with chronic hepatitis B worldwide[6]. HBV exhibits a very narrow host range and shows a strong tropism for liver parenchyma cells. It has therefore, been assumed that the susceptibility to HBV infection is restricted to differentiated cells. It was found by some authors that human primarily cultured hepatocytes were more susceptible than other kinds of cells to HBV infection[7,8]. Here we describe a system of experimental infection by HBV virus using primary human fetal hepatocytes. Infection was obtained by co-cultivation of human fetal hepatocytes with HBV-positive serum. The infected fetal hepatocytes *in vitro* were found to initiate viral DNA replication, and they produced infectious viral particles into medium.

MATERIALS AND METHODS

Primary culture of human fetal hepatocytes

Hepatocytes were prepared from 6 wk old human fetal liver. Embryos procurement was approved by the Ethics Committee of Chaozhou Central Hospital. The sera from the mothers were negative for hepatitis C virus (HCV), HBV and human immunodeficiency virus (HIV) by ELISA (Shanghai SIIC Ke-Hua Biotechnology). Firstly, we used Hank's liquid to wash the aborted fetus 3 times, and liver tissues were taken out. Secondly, the liver tissues were cut with scissors into 0.1-0.5 mm^3 pieces. At last, the little pieces were shattered with 5 mL syringe to single cells or cell aggregates. Viability, assessed by the trypan blue exclusion test, was between 70% and 90%. The cells

were seeded into 12-well culture dishes (Orange Scientific) at about 2×10^5 cells per well and incubated with 1 mL of 10% FBS (Gibco) in DMEM (Dulbecco's Modified Eagle's Medium)/F12 (Nutrient Mixture F-12 HAM) (1:1) (Sigma-Aldrich) supplemented with 0.1 U/L penicillin, 0.1 ng/L streptomycin, and 0.1 ng/L fluconazole at 37℃ under 5% CO_2 in air. The medium was changed after the first 48 h with serum-free medium. The serum-free medium was composed of DMEM/F12 (1:1) and 0.01 nmol/L nicotinamide, 0.02 ng/L epidermal growth factor (EGF), 0.02 ng/L basic fibroblast growth factor (bFGF), 0.365 ng/L glutamate, B27 (1:50) (Sigma), 0.1 U/L penicillin, 0.1 ng/L streptomycin, and 0.1 ng/L fluconazole.

Viral sources

A serum sample for infection test from HBV carriers was analyzed. The patient was anti-HbsAb positive as detected by the ELISA (Shanghai SIIC Ke-Hua Biotechnology), and HBV-DNA in the serum sample was quantified with fluorescence quantitative polymerase chain reaction (FQ-PCR) assay (Da-An Gene Corp). The patient had received no antiviral therapy prior to the study, and not infected with HCV or HIV. The sera were stored at -80℃ until use. The number of serum HBV was 7.6×10^7 copy/mL as quantified by FQ-PCR.

In vitro infection

After 24 h culture in serum-free medium as mentioned above, infection was obtained by incubation 1 mL serum-free culture medium with 5% dimethyl sulphoxide (DMSO) and 100 μL HBV serum. Following 24 h exposure, cells were washed 6 times with 3 mL Hank's liquid and incubated in 1 mL fresh serum-free medium as described above. The medium was changed every day, and the supernatant was collected at various times during the culture period and stored at -80℃. We used one-well cells without HBV serum sample as negative control.

Detection of HBV-DNA by FQ-PCR

To qualify these DNA molecules, virus DNA was extracted from the culture medium using an alkaline lysis method for FQ-PCR analyses[9]. For detection of HBV-DNA in cultured cells, all of the cells were digested by trypsin-EDTA (0.25%-0.01 mmol/L) solution and centrifugated, then were washed six times with PBS. Cells were lysed with 0.05 mol/L Tris-HCl (pH 7.4)-1% sodium dodecyl sulfate (SDS)-0.02 mol/L NaCl-0.02 mol/L EDTA and incubated with 0.5 g/L of proteinase K at 37℃ overnight[9]. Total DNA was extracted by an alkaline lysis method.

HBV-DNA was measured by FQ-PCR diagnostic kit from Da-An Gene Corp. with Lightcycler™ Roche. In this reaction, the nucleotide sequences of the primers were as follows: P1: 5'ATCCTGCTGCTATGCCTCATC TT3' (23 bp), P2: 5'ACAGTGGGGGAAAGCCCTACG AA3' (23 bp), FISH: 5'TGGCTAGTTTACTAGTGCCA TTTG3' (25 bp)[10].

QT-PCR amplification was performed using Roche QT-PCR system with 2 min initial denaturation at 93℃ for 40 cycles of 5 s at 93℃ and 45 s at 57℃, followed by 1 s of extension at 37℃.

Detection of HBsAg and HbeAg by ELISA

HBsAg and HBeAg levels in the supernatant were detected using the monoclonal Ⅱ enzyme-linked immunosorbent assay. ELISA kits were obtained from Shanghai SIIC Ke-Hua Biotechnology. Titers were expressed as the ratios against cut-off values (A450 of negative control + 0.05 for HBsAg and + 0.05 for HBeAg).

Periodic acid- Schiff's staining

To discriminate liver cells from stromal cells for general observation of morphology, cells were stained with periodic acid-Schiff's reagent (PAS) by standard methods[12]. The reagents were from Shanghai Zhu-Chun Biotechnology.

Detection of albumin and HBcAg by immunohistochemical staining

The cells were fixed in 0.4% formaldehyde in PBS at room temperature for 15 min, and washed 3 times by PBS. After that, they were incubated for 15 min with 0.25% Triton-X100 and washed 3 times by PBS. Cells were then incubated with the following dilutions of primary antibodies for 1 h at room temperature: antibody to cytokeratin-8 (CK-8) and cytokeratin-18 (CK-18) (Beijing Zhong-Shan Biotechnology), which were diluted at 1:100 in PBS; antibody to HBcAg (1:1) (Fuzhou Maxim Biotechnology); and antibody to human albumin diluted at 1:1000 in PBS (Sigma). Other steps were performed according to manufacturer's instruction of SP-9000 kits, and AEC served as chromagens.

Determination of integrity of cell membranes

Content of LDH was measured using automatic blood biochemistry analysis (HITACHI 7060) with Roche reagents. LDH was expressed as U/L released into the medium to find out the integrity of the cell membrane every 24 h.

Statistical analysis

The statistical analysis was performed with SPSS 13.0 statistic software.

RESULTS

Properties and phenotypes of cultured hepatocytes

Single cells or cell aggregates were isolated from fetal human livers. The initial cell population was an obvious mixture of hematopoietic and epithelial cells. For instance, red blood cells were copious, although these were rapidly removed at the first medium change. They were plated onto plastic dishes with serum containing medium. After 12 h, the hepatocytes started to attach to the dishes but did not proliferate. After 48 h, the media became serum free, and the HFHs began to show two kinds of state, including cell aggregates or spheroid and scattered cells. The spheroid was made up of many epithelial cells, and fibroblast-like cells migrated from them (Figure 1A). With the elongation of culture time, the percentage of fibroblast-like cells gradually increased and the percentage of flat epithelial cells gradually decreased. After 3-5 wk, fibroblast-like cells proliferated to form a monolayer (Figure 1C).

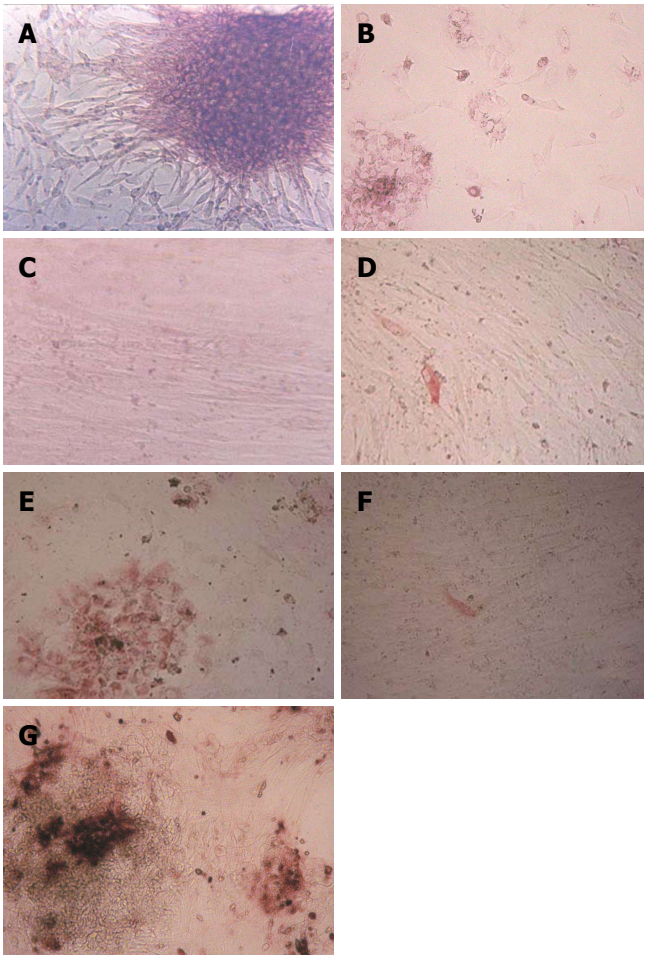

Figure 1 Morphology, PAS and S-P staining of the HFHs under light microscope. **A:** Isolated HFHs formed epithelial-like spheroid and they were surrounded by fibroblast-like cells in culture after 48 h; **B:** HFHs were stained by PAS, the majorities of cultured cells were positive; **C:** HFHs state *in vitro* for 50 d; **D:** HFHs were positive for CK8 in hepatocytes *in vitro* for 50 d (S-P); **E:** HFHs expressed liver marker CK18 *in vitro* for 14 d (S-P); **F:** Only a few of hepatocytes were positive for CK18 *in vitro* for 50 d (S-P); **G:** HFHs expressed ALB *in vitro* for 14 d (S-P). (Original magnification, × 40).

To confirm the phenotypes of HFHs after 2 wk, cells were analyzed by PAS staining. The majority of cells were stained, and these cells were multiangular and flat, their morphology were similar to that of hepatocytes (Figure 1B), Furthermore, we performed S-P staining using primary antibodies against ALB, CK8 and CK18, the results showed clearly that these proteins were expressed in about 90% cells, confirming that the cells expressed hepatocyte phenotypes (Figure 1E and 1G). After 50 d, only less than 1% cells expressed CK8 and CK18 (Figure 1F). The above-mentioned results were also reported by HU *et al*[11]. CK8 and CK18 are cytoskeletal proteins characteristic of hepatocytes, they play a very important role in maintaining the structure of hepatocytes, and are expressed in the hepatocyte cytoplasm of the fetal hepatocytes *in vivo*. Thus, they are good markers for hepatocytes. As culture time extending, the cells that expressed hepatocyte phenotypes gradually decreased, while those cells that expressed fibroblast phenotypes gradually increased. In our opinion, there were two factors to explain this situation: (1) the fibroblast-like cells

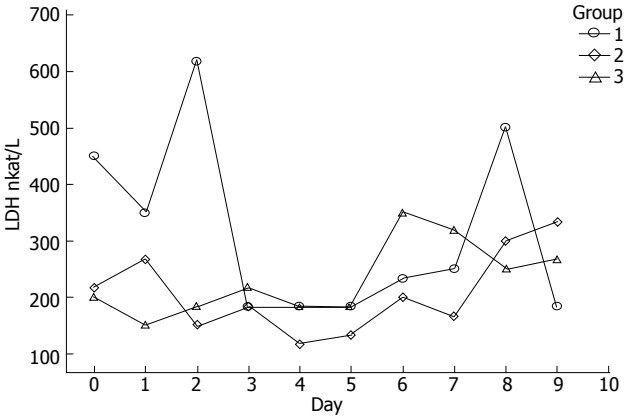

Figure 2 Lactate dehydrogenase (LDH) released in primary human hepatocytes.

proliferated faster than hepatocyte-like cells. Therefore, after several weeks culture, fibroblast-like cells proliferated to form a monolayer and few hepatocyte-like cells could be observed; (2) HFHs could change their phenotypes from hepatocytes to mesenchymal cells, this phenomenon has also been reported by other studies[9].

In the course of this study, it was visually apparent that the tendency of LDH increased with culture time in serum-free medium (Figure 2). The amount of LDH in the supernatant ranged from 620 nkat/L to 130 nkat/L.

Production of viral antigens in fetal liver cells

The serum-free culture medium was collected periodically and the levels of HBsAg and HBeAg were analyzed. As shown in Figures 3A and 3B, the HBsAg and HBeAg were first detected at d 3 after the infection and continued to appear positive during the following 16 d. They must have been synthesized in liver cells because the wash liquid (time zero) and medium from d 1 to d 2 were negative for HBsAg and HBeAg. Thus, the human fetal hepatocytes should be infected by wild virus and replicated HBV.

Human fetal hepatocytes were cultured for 24 h with HBV serum, washed, and incubated with serum-free medium. The supernatant was taken every day and assayed for HBsAg and HBeAg.

Detection of HBV-DNA in media and cultured cells

The culture media were collected from d 0 to d 18 (the day of human HBV serum deprivation was indicated as d 0), and were measured by FQ-PCR. HBV-DNA appeared at d 2, and reached a secretion peak from d 3 to d 6. The tendency began to decrease on d 6. Because there was no HBV-DNA in the medium at d 0-2 after infection, HBV-DNA was detected in the serum-free medium from d 3 to d 18 (Figure 4). Therefore, they must have been released from the infected hepatocytes, and the hepatocytes must release and replicate virus DNA. The results of HBV-DNA in liver cells are shown in Table 1.

Detection of HBcAg by immunohistochemical staining

To estimate the population of infected cells, immunohistochemical staining was used to assay HBcAg. HBcAg was detected in about 10% of hepatocyte-like cells 3 d after infection (Figure 5A), whereas no HBcAg was found

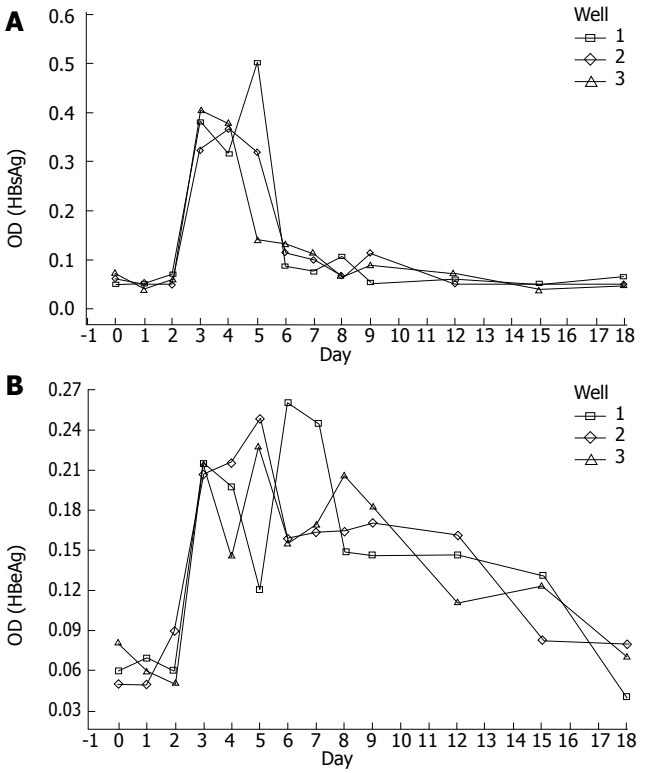

Figure 3 HBsAg (**A**) and HBeAg (**B**) in supernatant detected by ELISA (OD: optical denisity).

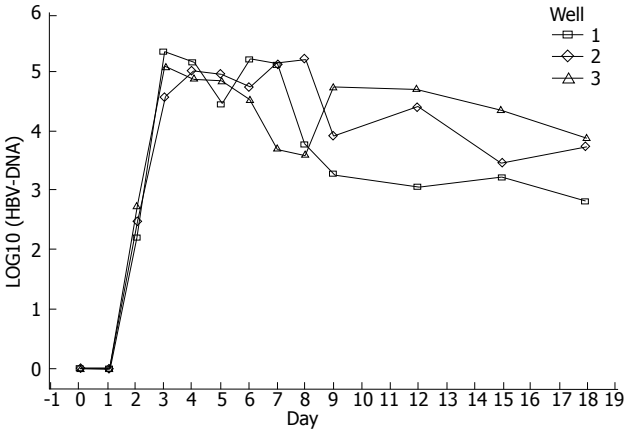

Figure 4 HBV-DNA in media detected by FQ-PCR.

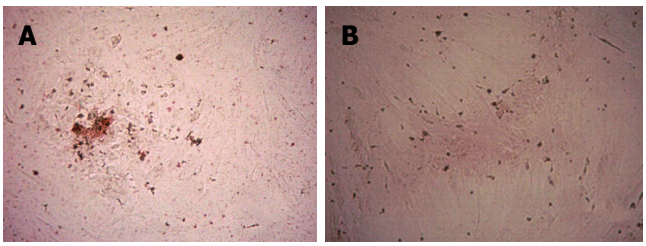

Figure 5 Detection of HBcAg by immunohistochemistry staining (S-P). **A:** The HBcAg positive in hepatocytes; **B:** Negative control for HBcAg. Original magnification, × 40.

Table 1 Cells quantified by FQ-PCR on d 18

Well	Cell number	HBV-DNA (copy/L)
1	1.0×10^4	2.092×10^9
2	1.5×10^4	8.506×10^9
3	1.1×10^5	1.371×10^{10}

in the negative control (Figure 5 B).

DISCUSSION

Replication of HBV has been achieved in human hepatoma cell lines using integrated or transfected HBV genomes as templates[13-16]. Duck cells and adult human liver cells were also successfully infected by HBV[17,18]. However, no signs of viral penetration, replication, or particle production have been observed except for a transient expression of some viral markers in hepatoma cell lines[14-15]. Duck cells and adult human liver cells could not perfectly analogue the process of the HBV infection in human fetal hepatocytes[17,18], and human fetal hepatocytes were used in a few experiments for HBV infection[19,20]. We demonstrated in this study that primary cultures of fetal human hepatocytes could maintain HBV infection *in vitro* and support the replication of HBV DNA.

In this study, an evidence of virus DNA replication in primary human fetal hepatocytes was testified from d 2 to d 18 after infection by FQ-PCR, another evidence was that HBsAg and HBeAg appeared positive from d 3 to d 18 by ELISA. The process of HBV replication and release continued for 16 d. The results were similar to other experiments with DMSO supplement[18]. But the HBV secretion time in our experiment was longer than the experiments without DMSO[19-21]. The data demonstrated that viral replication *in vitro* might be strongly enhanced by DMSO.

Previous studies of primary hepatocytes provided very little information about the quantity of HBV-DNA in the culture medium[21-23]. In their reports, DNA or RNA used to be detected by Southern blot or Northern blot[14,18,23]. The procedures of these methods were complicated, and the results were not stable. In our experiment, we used FQ-PCR to measure the HBV-DNA in the supernatant and cultured cells. FQ-PCR combines gene amplification and molecule hybridization with fluorescence physics, conducts the whole process of DNA amplification and PCR products analysis in an enclosed tube, and real-time detection as well as auto-analysis under computer control[10]. As a result, the cross-contamination of conventional PCR products and incapacity of quantification can be eliminated fundamentally[10]. Furthermore, the specificity and sensitivity increased remarkably. This method could provide reliable and precise data for HBV quantification.

The quantity of HBV in medium increased from d 0 to d 6 and decreased from d 7 to d 18 in the infection process. From d 0 to d 6, HBV replicated in infected cells and released to the medium, and then the free HBV infected other hepatocytes. With the increasing number of hepatocytes, it formed one infected cycle in cells and

the quantity of HBV increased in the medium. From d 7 to d 18, a part of cells gradually lost their hepatocyte phenotypes and HBV infection susceptibility, and the cycle was broken. Meanwhile, a part of floating cells and cell spheroid died gradually, subsequently, the quantity of HBV decreased.

In this study, we found that the presence of HbeAg was more correlated with HBV-DNA in the medium than that of HBsAg. According to our knowledge, HBeAg was a marker of extensive viral replication in HBsAg-positive sera of patients with hepatitis B virus infection[24]. The presence of HBeAg in the serum correlated well with hepatitis B-DNA[24]. Therefore, our results were similar to the status in human body.

By immunohistochemical analysis, we were able to observe a part of infection of the hepatocytes in the cultures. Similar results have previously been reported[23]. Recently, Tuttleman *et al*[17] used primary duck hepatocytes to infect HBV and only 10% of the primary duck hepatocytes displayed HBcAg[25]. The events could be observed in duck hepatocytes and human fetal liver cells. According to some reports, the procedure of liver cell isolation could destroy the capacity for infection of all but some cells. As it is well known, human hepatocytes were hard to maintain in cultures, such as albumin expression. Such phenotypes are easily lost within one week culture when the cells are inoculated in serum-containing medium. In our observation, the shape of the hepatocytes was polygonal at 48 h. With elongation of culture time, some hepatocytes gradually changed and extended in shape and became fibroblast-like, meanwhile they lost hepatocyte phenotypes such as ALB, CK18 and CK8 expressions. So it is likely that some flat cells may lessen the susceptibility to HBV infection.

HBV infection in primary fetal hepatocyte cultures is suitable for cloning virus because of the limited infectivity of the cells. However, our system *in vitro* has been found very useful for studying the early events in viral entry into cells as well as viral replication.

REFERENCES

1 **Lee WM**. Hepatitis B virus infection. *N Engl J Med* 1997; **337**: 1733-1745
2 **Liu CJ**, Chen BF, Chen PJ, Lai MY, Huang WL, Kao JH, Chen DS. Role of hepatitis B virus precore/core promoter mutations and serum viral load on noncirrhotic hepatocellular carcinoma: a case-control study. *J Infect Dis* 2006; **194**: 594-599
3 **Whitworth A**. Ten years later: liver cancer treatment reevaluated. *J Natl Cancer Inst* 2006; **98**: 958-959
4 **Kremsdorf D**, Soussan P, Paterlini-Brechot P, Brechot C. Hepatitis B virus-related hepatocellular carcinoma: paradigms for viral-related human carcinogenesis. *Oncogene* 2006; **25**: 3823-3833
5 **Di Bisceglie AM**, Rustgi VK, Hoofnagle JH, Dusheiko GM, Lotze MT. NIH conference. Hepatocellular carcinoma. *Ann Intern Med* 1988; **108**: 390-401
6 **Yan JC**, Ma JY, Pan BR, Ma LS. The study of chronic hepatitis B in China. *Shijie Huaren Xiaohua Zazhi* 2001; **9**: 611-616
7 **Guha C**, Mohan S, Roy-Chowdhury N, Roy-Chowdhury J. Cell culture and animal models of viral hepatitis. Part I: hepatitis B. *Lab Anim (NY)* 2004; **33**: 37-46
8 **Walter E**, Keist R, Niederöst B, Pult I, Blum HE. Hepatitis B virus infection of tupaia hepatocytes in vitro and in vivo. *Hepatology* 1996; **24**: 1-5
9 **Klintschar M**, Neuhuber F. Evaluation of an alkaline lysis method for the extraction of DNA from whole blood and forensic stains for STR analysis. *J Forensic Sci* 2000; **45**: 669-673
10 **Cheng G**, He YS, Zhou XY. Fluorescence quantitative PCR and its application in detection of hepatitis B virus. *Zhonghua Jianyan Yixue Zazhi* 1999; **22**: 135-136
11 **Roberts GP**. Histochemical detection of sialic acid residues using periodate oxidation. *Histochem J* 1977; **9**: 97-102
12 **Hu A**, Cai J, Zheng Q, He X, Pan Y, Li L. Hepatic differentiation from embryonic stem cells in vitro. *Chin Med J (Engl)* 2003; **116**: 1893-1897
13 **Lu X**, Block TM, Gerlich WH. Protease-induced infectivity of hepatitis B virus for a human hepatoblastoma cell line. *J Virol* 1996; **70**: 2277-2285
14 **Tsurimoto T**, Fujiyama A, Matsubara K. Stable expression and replication of hepatitis B virus genome in an integrated state in a human hepatoma cell line transfected with the cloned viral DNA. *Proc Natl Acad Sci USA* 1987; **84**: 444-448
15 **Sells MA**, Chen ML, Acs G. Production of hepatitis B virus particles in Hep G2 cells transfected with cloned hepatitis B virus DNA. *Proc Natl Acad Sci USA* 1987; **84**: 1005-1009
16 **Sureau C**, Romet-Lemonne JL, Mullins JI, Essex M. Production of hepatitis B virus by a differentiated human hepatoma cell line after transfection with cloned circular HBV DNA. *Cell* 1986; **47**: 37-47
17 **Tuttleman JS**, Pugh JC, Summers JW. In vitro experimental infection of primary duck hepatocyte cultures with duck hepatitis B virus. *J Virol* 1986; **58**: 17-25
18 **Gripon P**, Diot C, Thézé N, Fourel I, Loreal O, Brechot C, Guguen-Guillouzo C. Hepatitis B virus infection of adult human hepatocytes cultured in the presence of dimethyl sulfoxide. *J Virol* 1988; **62**: 4136-4143
19 **Jiang YG**, Li QF, Qing M, Wang YM, Primary human fetal hepatocytes with HBV infection in vitro. *Shijie Huaren Xiaohua Zazhi* 2000; **8**: 403-405
20 **Wang F**, Wang YM, Tang B, Liu J, Liu GD, Wang XH. Assays for HBV infection in primary human fetal hepatocytes cultured in vitro, *Disan Junyidaxue Xuebao* 2004; **26**: 74-77
21 **Tang B**, Wang YM, Wang F, Liu J, Zhang R. Susceptibility change to HBV in primary culture of first trimester human fetal hepatocytes. *Zhonghua Ganzangbing Zazhi* 2004; **12**: 21-24
22 **Galle PR**, Hagelstein J, Kommerell B, Volkmann M, Schranz P, Zentgraf H. In vitro experimental infection of primary human hepatocytes with hepatitis B virus. *Gastroenterology* 1994; **106**: 664-673
23 **Ochiya T**, Tsurimoto T, Ueda K, Okubo K, Shiozawa M, Matsubara K. An in vitro system for infection with hepatitis B virus that uses primary human fetal hepatocytes. *Proc Natl Acad Sci USA* 1989; **86**: 1875-1879
24 **Lu ZR**, Lei H. Textbook of Diagnostics (Engl). 1st ed. Oxford: Chin Sci Pub, 2006: 301
25 **Zhou GY**, Jiang XC, Textbook of Pathology (Engl). 1st ed. Oxford: Chin Sci Pub, 2006: 243

S- Editor Liu Y **L- Editor** Ma JY **E- Editor** Lu W

PO Box 2345, Beijing 100023, China
www.wjgnet.com
wjg@wjgnet.com

World J Gastroenterol 2007 February 21; 13(7): 1032-1041
World Journal of Gastroenterology ISSN 1007-9327

BASIC RESEARCH

Role of soluble factors and three-dimensional culture in *in vitro* differentiation of intestinal macrophages

Tanja Spoettl, Martin Hausmann, Katrin Menzel, Heidi Piberger, Hans Herfarth, Juergen Schoelmerich, Frauke Bataille, Gerhard Rogler

Tanja Spoettl, Martin Hausmann, Katrin Menzel, Heidi Piberger, Hans Herfarth, Juergen Schoelmerich, Frauke Bataille, Gerhard Rogler, Department of Internal Medicine I, and Institute of Pathology, University of Regensburg, Regensburg 93042, Germany
Supported by the Deutsche Forschungsgemeinschaft (SFB585, Ro 1236/3-2) and the BMBF Kompetenznetz-CED
Correspondence to: Gerhard Rogler, MD, PhD, Department of Internal Medicine I, University Hospital of Zuerich, Raemistrasse 100, 8091 Zuerich, Switzerland. gerhard.rogler@usz.ch
Telephone: +49-941-9447180 Fax: +49-941-9447179
Received: 2006-05-16 Accepted: 2006-09-20

Abstract

AIM: To examine the factor(s) involved in differentiation of intestinal macrophages (IMACs) using a recently established *in vitro* model.

METHODS: To test whether soluble or membrane bound factors induce IMAC-differentiation, freshly elutriated monocytes (MO) were incubated with conditioned media or cell membranes of intestinal epithelial cells (IEC) or cultured with IEC in transwell systems. To determine the importance of an active migration of MO, three-dimensional aggregates from a 1:1-mixture of MO and IEC were examined by immunohistochemistry and flow cytometry. Apoptosis was examined by caspase-3 Western blots. Extracellular matrix production in differentiation models was compared by immunohistochemistry.

RESULTS: IMAC differentiation was observed in a complex three-dimensional co-culture model (multicellular spheroid, MCS) with IEC after migration of MO into the spheroids. By co-culture of MO with conditioned media or membrane preparations of IEC no IMAC differentiation was induced. Co-culture of MO with IEC in transwell-cultures, with the two cell populations separated by a membrane also did not result in intestinal-like differentiation of MO. In contrast to IEC-spheroids with immigrating MO in mixed MCS of IEC and MO only a small subpopulation of MO was able to survive the seven day culture period.

CONCLUSION: Intestinal-like differentiation of MO *in vitro* is only induced in the complex three-dimensional MCS model after immigration of MO indicating a role of cell-matrix and/or cell-cell interactions during the differentiation of IMACs.

Key words: Intestinal macrophages; Intestinal epithelial cells; Multicellular spheroids; Inflammatory bowel disease; Tolerance differentiation

Spoettl T, Hausmann M, Menzel K, Piberger H, Herfarth H, Schoelmerich J, Bataille F, Rogler G. Role of soluble factors and three-dimensional culture in *in vitro* differentiation of intestinal macrophages. *World J Gastroenterol* 2007; 13(7): 1032-1041

http://www.wjgnet.com/1007-9327/13/1032.asp

INTRODUCTION

Macrophages represent a component of the innate immune system which is of central importance. One of the largest populations of macrophages in the body is intestinal macrophages (IMACs)[1]. They are localized directly underneath the epithelial barrier at the sites of antigen entry, in particular in the sub-epithelial region of the small and large intestine and in the subepithelial domes of Peyer's patches[2-4]. IMACs constitute 10%-20% of mononuclear cells in the human lamina propria[2,5-8]. They undergo a specific process of differentiation. This specific differentiation is believed to be essential for the specific functions of IMACs in the mucosal innate but also adaptive immune system. As IMACs are central players of both systems, a better understanding of the factors determining their differentiation may allow the definition of new targets for therapeutic interventions during acute and chronic mucosal inflammation. The importance of IMACs is supported by the finding that NOD2/CARD15, the first gene identified to increase susceptibility to Crohn's disease, is mainly expressed in macrophages in the colonic mucosa[9,10].

The phenotype of IMACs is remarkable: Less than 10% of the macrophages (MACs) isolated from normal colonic mucosa express the typical MO/MAC-specific surface markers CD14, CD16, CD11b, CD11c[11-13]. Furthermore, the expression of co-stimulatory molecules B7-1 (CD80) and B7-2 (CD86) on IMACs is low[14,15]. In

addition, the expression of pattern recognition receptor (PRR) toll like receptor (TLR) 2 and TLR 4 is also down-regulated in IMACs on transcriptional and translational levels[16]. The prototypic MO/MAC functions such as generation of superoxide radicals (oxidative burst reaction) are absent in normal mucosal IMACs due to a lack of NADPH-oxidase subunit expression[17], indicating that normal IMACs constitute a non-reactive cell population, which might be important for the induction of tolerance in the intestinal mucosa. A disturbance of the differentiation process followed by a reactive cell type retaining PRRs and activation functions could be followed by chronic inflammation.

Recently we used a three-dimensional co-culture model (multicellular spheroid model, MCS-model) of intestinal epithelial cells (IEC) and monocytes (MO) to induce the *in vitro* differentiation of intestinal-like macrophages[18]. We demonstrated that IEC clearly play an important role in the differentiation of IMACs. Freshly elutriated MO, which adhered and infiltrated IEC-MCS, changed their phenotype during a seven-day co-culture period[18]. Typical MO/MAC specific surface antigens such as CD14, CD16, CD11b and CD11c, which were detectable on invading cells after 24 h, were down-regulated after seven days. This differentiation was of functional relevance as seen by the loss of LPS-induced IL-1β transcription in IEC-MCS/MO co-cultures compared to control experiments[18]. As the gut specific differentiation of IMACs is of great functional importance and the MCS-model resembled the differentiation process *in vitro*, we addressed the question of which factor(s) induce the specific IMAC-differentiation.

Little is known about the direct interaction between IEC and MO/MAC. In normal intestinal mucosa tissue IMAC are separated from IEC by the basement membrane[2,4]. Doe and co-workers[19] have localized IMACs beneath the luminal epithelium[19]. It has been shown that IMACs or dendritic cells can transmigrate and return again across the basement membrane[20] and that the basement membrane is as easily permeable for large molecules as complement factors[21]. Martin and co-workers[22] found that murine MO/MAC and IEC are coupled by gap junctions and that gap junctional communication may provide a tool by which inflammatory cells regulate IEC function and vice versa.

In the present study, we aimed to study whether the induction of intestinal like differentiation of MAC is induced by soluble or secreted proteins, whether direct cell-cell interactions are necessary, whether cell-matrix interactions play a major role and whether all MO or just a subpopulation of MO is capable of differentiating into IMACs.

MATERIALS AND METHODS

Monocyte isolation and cell culture

Primary blood MO were obtained by leukapheresis of healthy donors, followed by density gradient centrifugation over Ficoll/Hypaque as described previously[18]. Two intestinal epithelial cell lines (HT-29 and WiDr) and a control cell line of non-intestinal origin (urothelial carcinoma, J82) were used. All cell lines were cultured under standard tissue-culture conditions[23,24]. The isolation of monocytes was approved by the local institutional review board.

Conditioned medium

Confluent monolayers of IEC lines or the control cell line were incubated with cell culture medium with or without fetal calf serum (FCS). After 48 h the medium was removed, centrifuged and stored at -20℃. Freshly elutriated MO were incubated in conditioned medium for up to seven days.

Immunohistochemistry

Immunohistochemical staining was carried out according to the standard alkaline phosphatase anti-alkaline phosphatase (APAAP) or diaminobenzidine (DAB) technique[25]. The following monoclonal antibodies against MO/MAC-antigens were used: anti-CD68 (clone: KP1, Dako, Hamburg, Germany), anti-CD11b (clone: BEAR1, Immunotech, Hamburg, Germany), anti-CD11c (clone: BU15, Immunotech, Hamburg, Germany), anti-CD14 (clone: RMO52, Immunotech, Hamburg, Germany) and anti-CD16 (clone: 3G8, Immunotech, Hamburg, Germany). For detection of extracellular matrix antibodies against fibronectin (clone: 568, Progen, Heidelberg, Germany), laminin (clone: 4C7, Dako, Hamburg, Germany) and collagen Ⅳ (clone: CIV 22.(1), Dako, Hamburg, Germany) were used.

Cell ELISA

Fixed MO were washed with NKH buffer (0.14 mol/L NaCl, 5 mmol/L KCl and 2 mmol/L HEPES, all Merck, Darmstadt, Germany) and unspecific binding was blocked with 10% FCS in NAG buffer (0.1% NaN_3, 2 mmol/L HEPES, 0.2% gelatine, all Merck, Darmstadt, Germany and 0.2% BSA, Sigma-Aldrich, Deisenhofen, Germany). Antibodies against CD68, CD14, CD16 and β_2-microglobuline (anti-β_2M, Dianova, Hamburg, Germany) as a positive control were applied. After rinsing, rabbit anti-mouse IgG (Dako, Hamburg, Germany) was added and incubated with peroxidase-conjugated goat-anti-rabbit antibody (Immunotech, Hamburg, Germany). Subsequent incubation with 1.2-phenylendiamine-dihydrochloride substrate (OPD, Fluka, Deisenhofen, Germany) for exact 12 min resulted in a yellow color. The reaction was stopped with 1 mol/L H_2SO_4 (Merck, Darmstadt, Germany) and the extinction was determined photometrically. As a reference value the extinction of ß$_2$M was set 1. All measured values were standardized on the β_2M-extinction.

Proliferation and cell viability assay (MTS-test)

A total of 100 000 MO per well were grown either in conditioned media of IEC or in control media in 96-well plates for seven days. A colorimetric assay (MTS, Endogen, Woburn, Germany) for quantification of cell proliferation and cell viability was performed according to the manufacturer's protocol. The absorption was measured 8 h after addition of the MTS-labeling mixture.

Cell membranes

IEC or control cells were washed with PBS, resuspended in homogenization buffer (Tris 50 mmol/L, EDTA 1 mmol/L, PMSF 1 mmol/L, benzamidine 1 mmol/L, saccharose 0.25 mmol/L) and lyzed by sonification. Cell membranes were isolated in three subsequent centrifugation steps (400 × *g* for 10 min, 8500 × *g* for 10 min, 25000 × *g* for 30 min). During the third centrifugation step, the cell membranes were sedimented, re-suspended in PBS and incubated in 96-well plates to allow adherence to the plastic surface. After 30 min the supernatants were removed and replaced by a suspension of freshly elutriated MO.

Transwell co-cultures

IEC were seeded onto filter inserts with a pore size of 12 μm or 3 μm (preventing IEC from transmigration through the membranes). After formation of an IEC-monolayer the supernatant was removed and freshly elutriated MO in medium supplemented with 2% of human AB-serum were added to each filter insert. After seven days of incubation migrated cells were fixed for immunohistochemistry. Cells in suspension were collected separately and subjected to flow cytometrical analysis.

Generation of MCS

MCS from only IEC or from a 1:1 mixture of IEC and MO were generated according to the liquid overlay culture technique[18]. Mixed spheroids were also generated with addition of a blocking anti-Fas antibody (Upstate Biotechnology, Lake Placid, USA) to the cell suspension 30 min before seeding.

Flow cytometry

Flow cytometry was performed using a Coulter EPICS® XL-MCL (Coulter, Krefeld, Germany). Cells were double stained with a FITC-conjugated anti-CD14 antibody (clone Tük4, Coulter, Krefeld, Germany) and a PE-conjugated anti-CD33 antibody (clone MY9, Coulter, Krefeld, Germany) as described previously.

Data acquisition and analysis were performed using WIN-MDI software (http://facs.scripps.edu/help/html/).

Immunoblotting

Cells were resuspended in RIPA buffer (1% Nonidet P-40, 0.5% sodium deoxycholate, 0.1% SDS, 1 mmol/L Na_3VO_4, 50 mmol/L NaF and 1 tablet of complete proteinase inhibitor cocktail [Boehringer, Mannheim, Germany] per 50 mL PBS) for 10 min on ice and centrifuged (12000 ×*g* for 15 min at 4℃). The protein concentration of the supernatant (protein fraction) was determined by BCA protein assay (Sigma-Aldrich Chemie, Deisenhofen, Germany). Thirty μg of protein was mixed with an equivalent volume of 2 × protein loading buffer containing 2-β-mercaptoethanol and boiled for 5 min before it was loaded onto SDS polyacrylamide gels. After electrophoresis, proteins were transferred onto nitro-cellulose membranes using the Xcell blot module (Invitrogen BV/NOVEX; Gronigen, Netherlands) and blocked in TBST (50 mmol/L Tris-HCl, pH 7.5, 150 mmol/L NaCl, 0.05% Tween 20) containing 5% non-fat dry milk powder. Protein immunoblots were performed using specific antibodies to caspase-3 (clone 19, Transduction Laboratories, Lexington, USA) and β-actin (clone JLA20, Calbiochem, Cambridge, USA). The membranes were further incubated with peroxidase-conjugated secondary antibodies and protein bands were visualized using a chemoluminescence kit (ECL Plus ™, Amersham, Buckinghamshire, UK) according to the manufacturer's protocol.

RESULTS

Recently we demonstrated *in vitro* differentiation of MO into IMACs in complex three- dimensional co-culture models (MCS model) with IEC after migration of MO into the IEC complexes. Here we further studied whether soluble factors or cell-cell interactions might be more relevant to this differentiation.

IEC-conditioned media did not induce differentiation of IMACs

To test whether soluble factors secreted by IEC induce the intestinal-like differentiation of MO, freshly elutriated MO were incubated with IEC-conditioned medium for seven days. Immunohistochemical analysis of MO showed no intestinal-like differentiation. CD14, CD16, CD11b and CD11c, which are down-regulated during differentiation of IMACs and therefore absent on MAC from normal non-inflamed mucosa, were all detectable. CD14 was expressed by 70%-80%, CD16 by 50%-60%, CD11b by 80%-90% and CD11c by 90%-100% of the MO/MAC incubated in HT-29-conditioned medium for seven days. Same results obtained with conditioned medium of the second tested IEC line WiDr were not significantly different from the values obtained with the MO/MAC incubated in control media (Figure 1). When cells were analysed by flow cytometry these findings were confirmed as no down-regulation of CD14, CD16, CD11b and CD80 expression could be observed in MO after seven-day co-culture with IEC-conditioned media (CD14 expression shown in Figure 2).

The results were further confirmed and quantified using the cell-ELISA technique able to detect minor changes in antigen expression. As a positive control and for reference values we determined the expression of the MAC housekeeping gene β_2M (Figure 3A). All other values were standardized in relation to $ß_2$M-expression. The antigen expression of MO/MAC, incubated in IEC-conditioned medium did not differ significantly from that of cells, incubated in control medium. The expression of CD16 was always slightly decreased, but could also be observed in control experiments and was not specific for IEC-conditioned media (Figure 3B).

IMAC differentiation was not induced by IEC-membrane bound factors

To determine whether membrane-bound factors of IEC induce the intestinal-like differentiation of MO, freshly elutriated blood MO were co-cultured with membrane preparations of IEC as described in Materials and

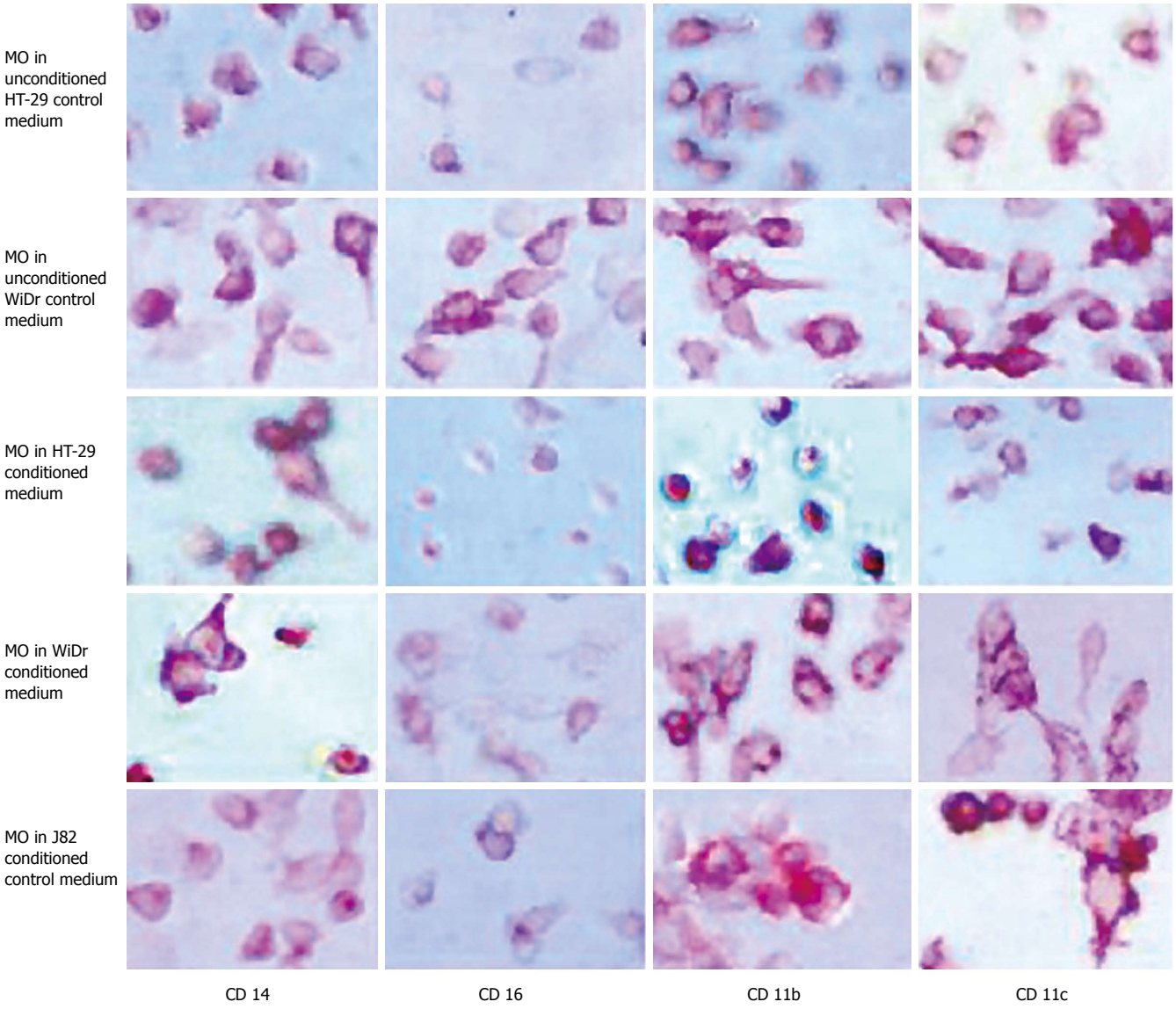

Figure 1 Immunohistochemical detection of MO/MAC antigen expression after 7 d of culture in IEC conditioned medium. Freshly elutriated MO were incubated in unconditioned control media, conditioned media of the IEC lines HT-29 and WiDr and conditioned medium of the control cell line J82 of non-intestinal origin for seven days. Antigen expression was determined by immunohistochemistry (APAAP-method). Expression of the MO/MAC specific antigens CD14, CD16, CD11b and CD11c was determined. All tested antigens were detectable on the cells after the seven-day culture period. Incubation in IEC-conditioned medium had no influence on antigen expression.

Methods. After an incubation period of seven days MO co-cultured with IEC-membranes showed no differentiation into intestinal-like MAC. The tested antigens CD14, CD16, CD11b and CD11c were still detectable after seven days of culture of MO/MAC together with membrane preparations of the IEC line HT-29. MO/MAC incubated for seven days without membrane preparations showed the same pattern of antigen expression (Figure 4).

Same results were obtained with membranes of a second intestinal epithelial cell line (WiDr) and the control cell line J82 (data not shown).

IMAC differentiation was not observed in transwell culture

To test whether a short direct contact between MO and IEC is able to induce intestinal-like differentiation of MO, we incubated MO and IEC in so called "transwell-cultures". MO were added to IEC grown in filter inserts. When filters with a pore size of three μm were used, only MO were able to migrate through the membrane as confirmed by negative staining for the epithelial cell marker EP-4 and positive staining for the MO/MAC-marker CD33 (Figure 5A). Twelve-μm long filters allowed also IEC to migrate through the membranes. IEC could be easily distinguished from MO/MAC by morphology and showed no expression of the tested MO/MAC-specific antigens. MO either migrated through the IEC layer or stayed in the upper compartment of transwell-culture. Antigen expression of cells adherent to the plastic dishes after transmigration was examined by immunohistochemistry. MO/MAC were all positive for the intracellular MO/MAC marker CD68 and showed a high expression of CD14, CD16, CD11b and CD11c after the seven day culture period (Figure 5B). Non adherent cells from the upper or lower compartment of the filter insert were analysed by

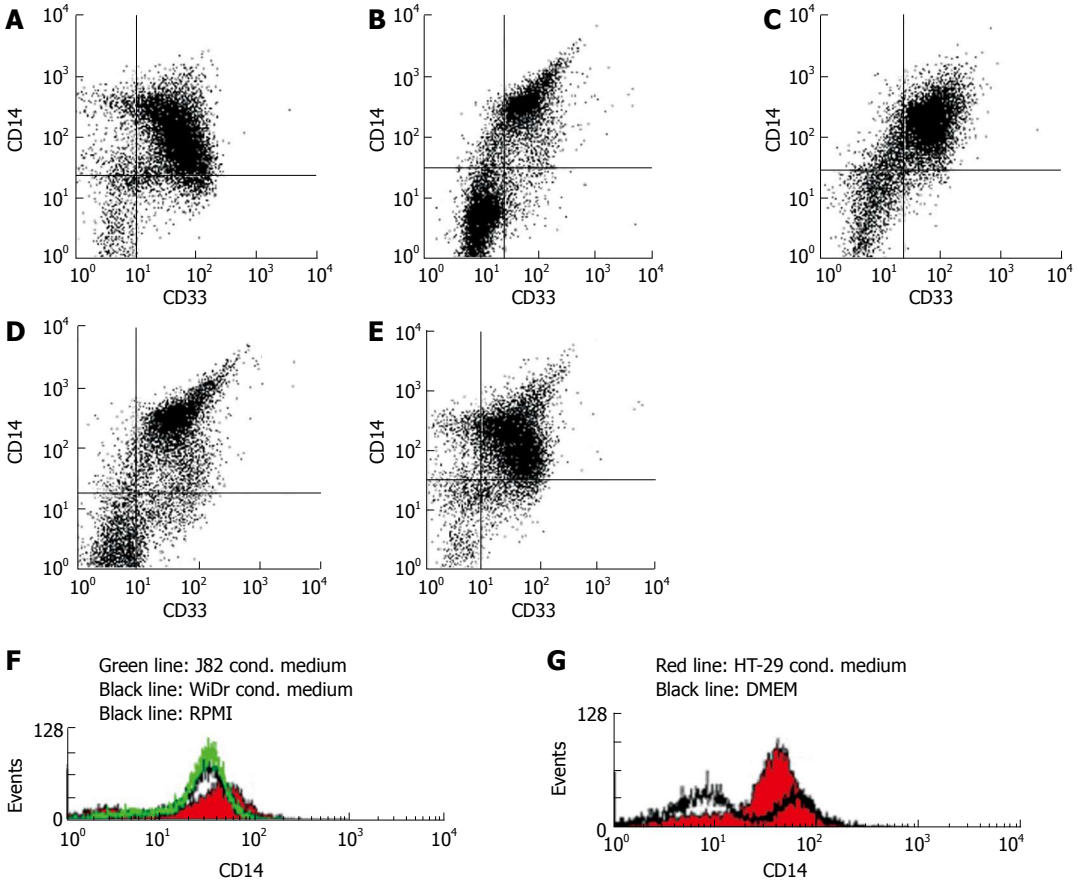

Figure 2 Flow cytometrical quantification of MO/MAC antigen expression after seven days of culture in IEC conditioned medium. **A**: Ninety-two percent of CD33+ cells (MO/MAC) showed expression of CD14 in MO cultured in unconditioned control medium (RPMI) without FCS supplemented with 2% human AB serum for seven days; **B**: Ninety-five percent of CD33+ cells (MO/MAC) were CD14-positiv in MO cultured in WiDr conditioned medium without FCS supplemented with 2% human AB serum for seven days; **C**: Ninety-two percent of CD33+ cells (MO/MAC) were CD14-positive in MO cultured in J82 conditioned medium (control cell line of non-intestinal origin) without FCS supplemented with 2% human AB serum for seven days; **D**: Ninety-four percent of CD33+ cells (MO/MAC) showed expression of CD14 in MO cultured in unconditioned control medium (DMEM) without FCS supplemented with 2% human AB serum for seven days; **E**: Ninety-eight percent of CD33+ cells (MO/MAC) were CD14-positive in MO cultured in HT-29 conditioned medium without FCS supplemented with 2% human AB serum for seven days; **F**: No down-regulation of CD14 expression was observed on histogram of CD14 expressing mononuclear cells after seven days of culture in RPMI (control medium), J82 (control cell line) or WiDR conditioned medium; **G**: Histogram of CD14 expressing mononuclear cells after seven days of culture in DMEM (control medium) and HT-29 conditioned medium.

flow cytometry and showed a similar antigen pattern with high CD14, CD16 and CD11b expressions (Figure 5C and D).

Immigration of MO into MCS was relevant to IMAC differentiation

To test whether the process of invading the three-dimensional IEC-spheroids is necessary for the differentiation of MO into IMACs, we generated "mixed spheroids" from a 1:1-mixture of IEC and MO. In these experiments MO were added during the generation of MCS and did not invade the three-dimensional aggregates.

Flow cytometrical analysis showed 15.2% MO/MAC inside spheroids of the control cell line J82 after 24 h of co-culture. This percentage was nearly constant during a seven-day culture period (13.2%, d 7, n = 5). In spheroids with the IEC line HT-29 a different effect could be observed. After 24 h 21.7% MO/MAC inside the spheroids could be detected. On day seven of co-culture the percentage of MO/MAC inside the spheroids decreased to 1.4% (n = 4). Similar results could be obtained with spheroids of the IEC line WiDr. The percentage of MO/MAC inside the spheroids decreased from 14.6% (24 h) to 2.4% (d 7, n = 4) (Figure 6A). Remaining MO/MAC inside the aggregates showed no differentiation into IMACs. The results showed that active invasion of the aggregates by MO was an essential step in the process of IMAC differentiation.

To test whether the observed decrease in the relative amount of MO in "mixed spheroids" is due to Fas-induced apoptosis, we added a blocking anti-Fas antibody to the cell suspensions before generating "mixed spheroids". Addition of the anti-Fas antibody did not change the results significantly. The number of MO/MAC decreased from 14.2% (24 h) to 0.8% (7d) in HT-29 MCS and from 20% (24 h) to 2.3% (7d) in WiDr spheroids. In control experiments with J82 spheroids the number of MO/MAC was almost constant with 13.9% at 24 h and 12% on day seven (n = 3) (Figure 6B).

In addition, Western-blots for caspase-3 were

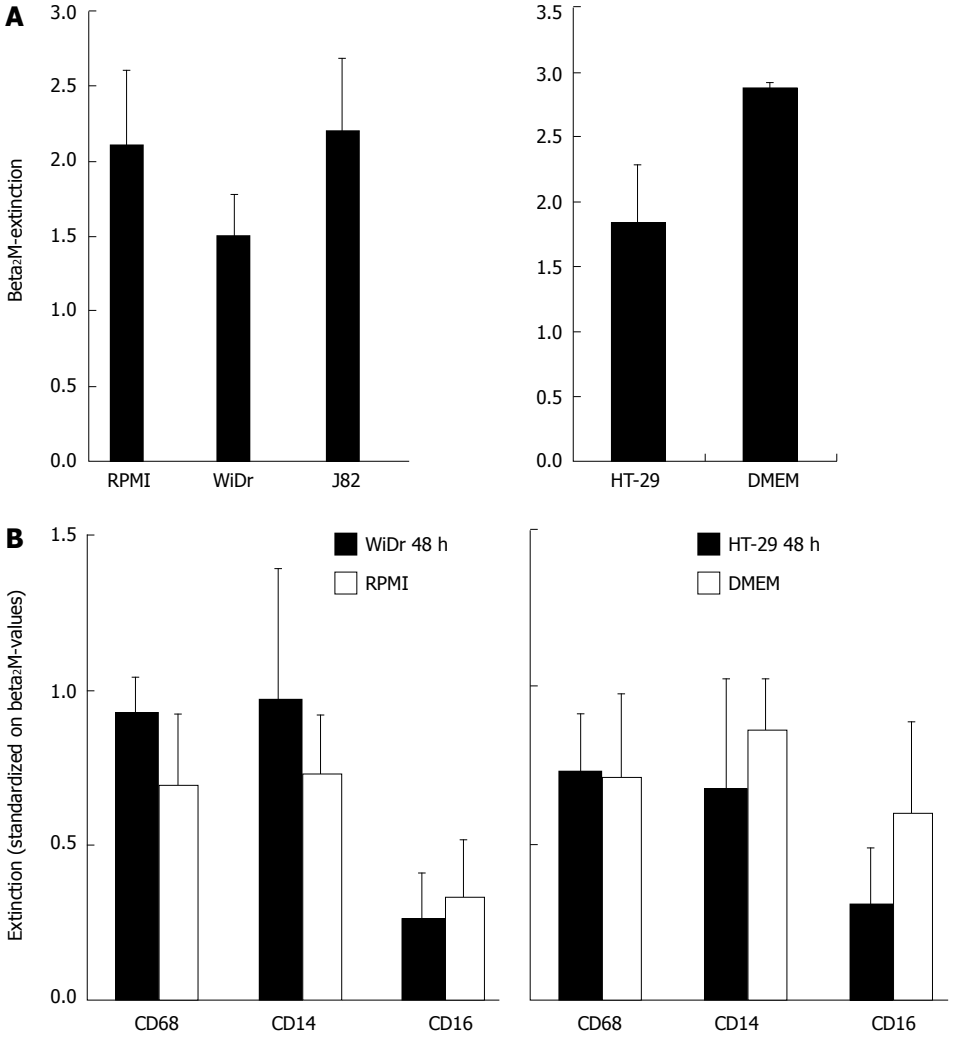

Figure 3 Cell ELISA of MO/MAC antigen expression after seven days of co-culture with IEC conditioned media. **A**: Freshly elutriated MO were incubated in conditioned medium of the IEC line WiDr or control media (left graph) of HT-29 and control media (right graph) for seven days. Expression of the housekeeping antigen β2M was determined an extinction is given as absolute value; **B**: CD68, CD14 and CD16 antigen expression of MO incubated in conditioned medium of the IEC line WiDr or non-conditioned control medium (left graph) or HT-29 and control medium (right graph) after seven days was also determined by cell ELISA. Values are standardized on β_2M-extinction.

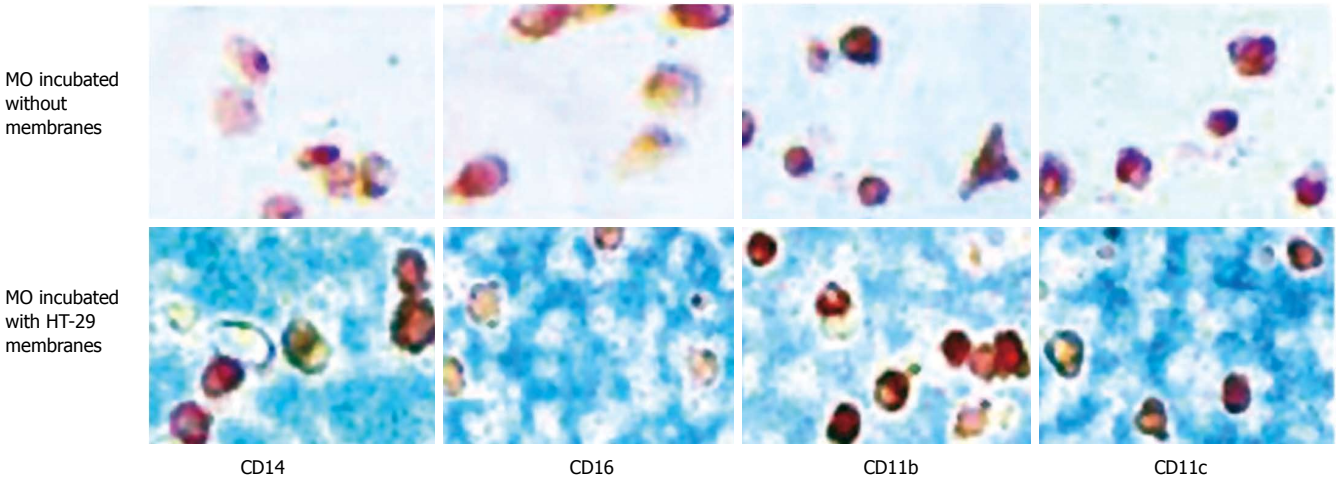

Figure 4 MO/MAC antigen expression after seven days of culture with IEC membranes. Freshly elutriated MO were incubated for seven days with membrane preparations of the IEC line HT-29 or without membranes. Antigen expression was determined by immunohistochemistry (APAAP-method). There was no difference in expression of CD14, CD16, CD11b and CD11c in cells incubated with or without IEC membranes.

performed. After 24 h and three days no activated caspase-3 was detected in "mixed MCS" of IEC and MO or in control cells and MO (Figure 7).

Potential role of extracellular matrix in IMAC differentation

The expression of extracellular matrix (ECM) proteins (fibronectin, laminin and collagen IV) in the "normal" and mixed spheroids was determined by immunohistochemistry. Laminin and collagen IV were not detectable in both mixed spheroids and spheroids invaded by MO. In contrast, a strong expression of fibronectin could be detected in spheroids invaded by MO, which was

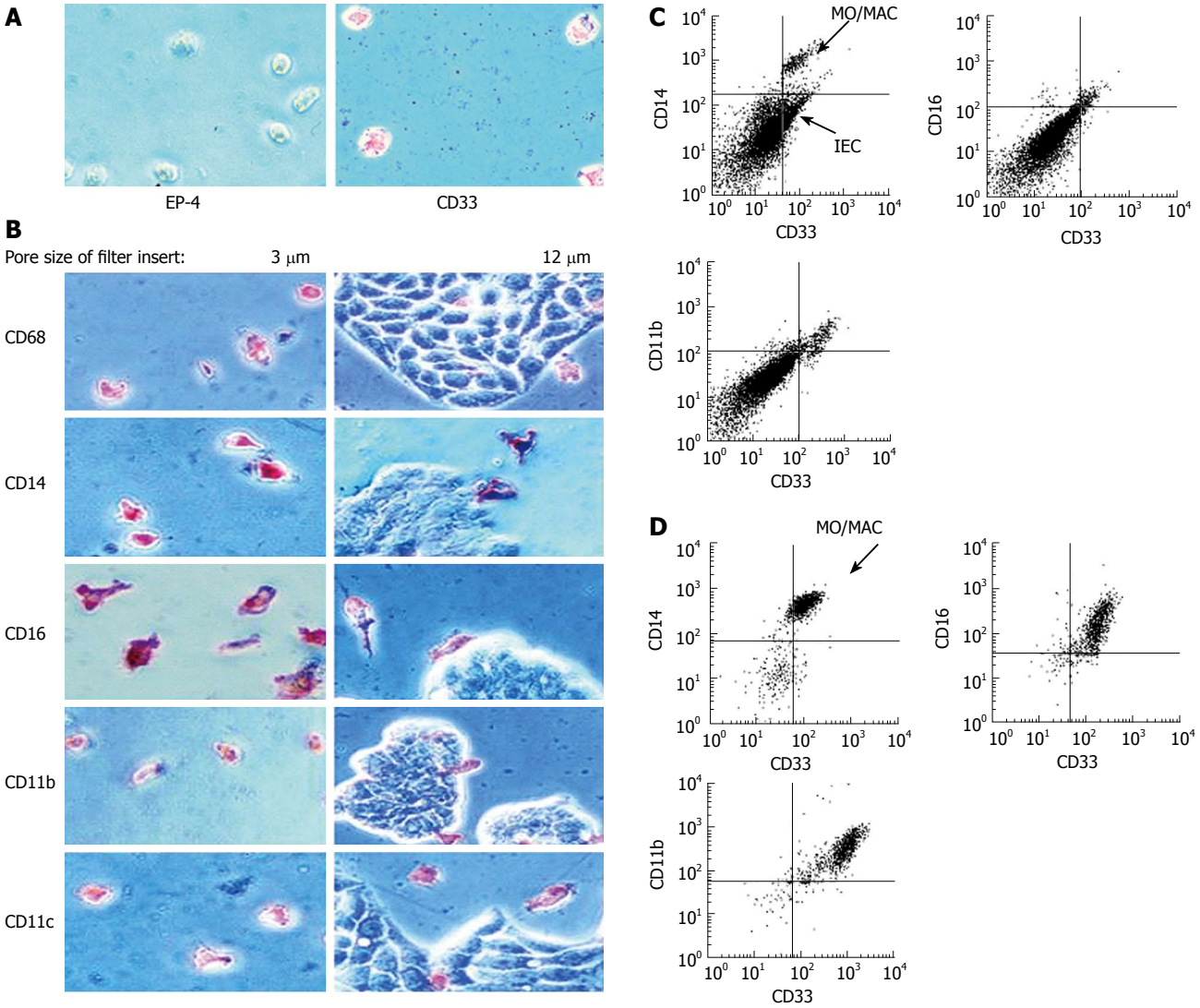

Figure 5 Antigen expression of MO/MAC incubated with IEC in trans-well cultures. Freshly elutriated MO were incubated with the IEC line HT-29 seeded on filter inlays for seven days. Depending on pore size of the inlays only MO or MO and IEC could migrate through the filter. Antigen expression of migrating and non-migrating cells was examined by immunohistochemistry (APAAP-method) and flow cytometry. **A**: Migrating cells adhered to the plastic surface of the cell culture plate. When filters with a pore size of 3 μm were used, only MO were able to migrate through the membrane. Migrating cells were all negative for the epithelial cell specific marker EP-4 and positive for the MO/MAC-marker CD33; **B**: Migrating cells showed expression of CD68, CD14, CD16, CD11b and CD11c (left column). Twelve μm pores allowed migration of MO and IEC. None of the tested antigens was expressed by IEC (right column); **C**: Non migrating cells which remained in the upper compartment of the filter insert were examined by flow cytometry. The CD33-positive cell population (MO/MAC) showed also expression of CD14, CD16 and CD11b; **D**: Migrating cells which did not adhere to the plastic dish were examined by flow cytometry. Cells showed CD33-expression and were positive for CD14, CD16 and CD11b.

up-regulated from three to seven days of culture and was absent in mixed spheroids incubated for the same time. The expression of fibronectin was localized in the inner region of aggregates (Figure 8).

DISCUSSION

As IMACs are essential players in local immune responses and the innate immune system of intestinal barrier, their specific phenotype must be of importance. Compared to IMACs from inflammatory bowel disease (IBD) patients, IMACs from normal intestinal mucosa show a down-regulation of several surface markers, co-stimulatory molecules and proteins necessary for LPS-induced signal transduction[11-13,16], which may be responsible for the induction of tolerance.

Recently we have shown that MO differentiate into IMACs after immigration into the MCS co-culture with IEC *in vitro*[18]. In this study, factor(s) inducing IMAC differentiation *in vitro* were analysed. We showed that the specific IMAC differentiation was not mediated by soluble or membrane bound factors of IEC alone, as no intestinal-like differentiation was observed in freshly elutriated MO cultured together with IEC-conditioned medium or IEC-membranes. Also "weak interactions" between MO and IEC in trans-well cultures, in which MO and IEC (monolayers) were only separated by filter membranes, were not sufficient for differentiation. IMAC differentiation could only be induced in the complex three-dimensional MCS model with close contact between MO, IEC and ECM[18]. Loss of MO observed in 1:1 "mixed spheroids" of the IEC lines HT-29 and WiDr was obviously not due to apoptosis, as we could neither block this effect by adding an anti-Fas antibody nor detect

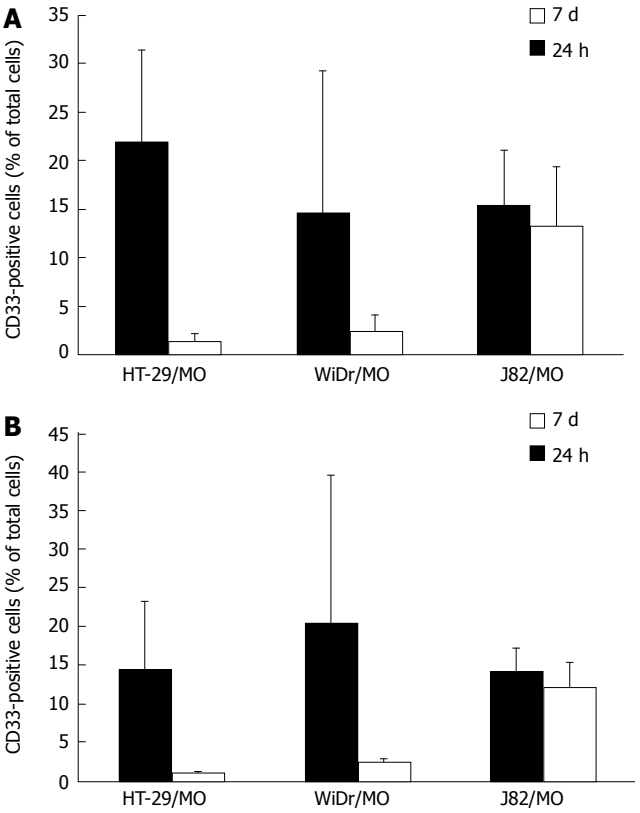

Figure 6 Mixed spheroids of MO and IEC or the control cell line. Mixed spheroids of the IEC lines HT-29 and WiDr or the control cell line J82 and MO were generated and cultured for seven days, disaggregated and examined by flow cytometry. **A**: There was a strong decrease of surviving MO/MAC (CD33+ cells) inside IEC spheroids compared to control spheroids over the seven-day culture period. In HT-29 spheroids the percentage decreased from 21.7% (24 h) to 1.4% (7 d). In WiDr spheroids a slighter decrease was observed with 14.6% MO/MAC after 24 h and 2.4% after seven days. In spheroids of the control cell line J82 no selection of a MO/MAC subpopulation could be observed. The number of MO/MAC inside the aggregates was nearly constant with 15.2% (24 h) and 13.2 (7 d); **B**: Addition of a blocking anti-Fas antibody 30 min before generation of the mixed spheroids did not change the results. In IEC-MCS a strong decrease of MO/MAC was observed (HT-29: 14.2% 24 h, 0.8% 7 d, WiDr: 20.1% 24 h, 2.3% 7 d). The MO/MAC number in control cell MCS was nearly constant with 13.9% (24 h) and 12.0% (7 d).

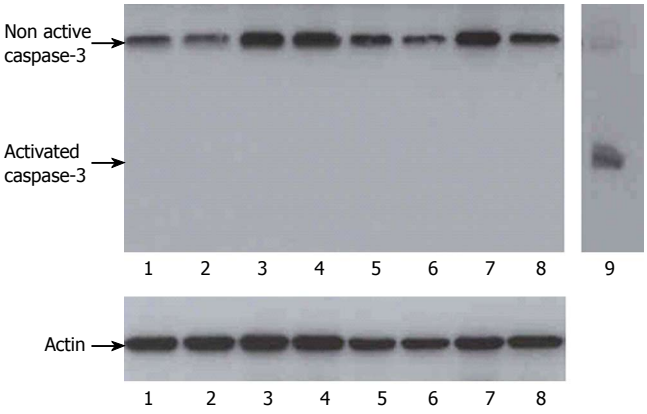

Figure 7 Western-blot for caspase-3 of mixed spheroids after 24 h and three days. Mixed spheroids of IEC and MO, control cells and MO or control spheroids generated only from IEC or control cells were disaggregated after 24 h and three days of culture. Western-blots for activated caspase-3 were performed. Lane 1: HT-29 without MO 24 h; lane 2: HT-29/MO (1:1) 24 h; lane 3: J82 without MO 24 h; lane 4: J82/MO (1:1) 24 h; lane 5: HT-29 without MO 3 d; lane 6: HT-29/MO (1:1) 3 d; lane 7: J82 without MO 3 d; lane 8: J82/MO (1:1) 3 d; lane 9: positive control for activated caspase-3. No activated caspase-3 could be detected in co-cultures of MO and IEC or in spheroids generated only from IEC.

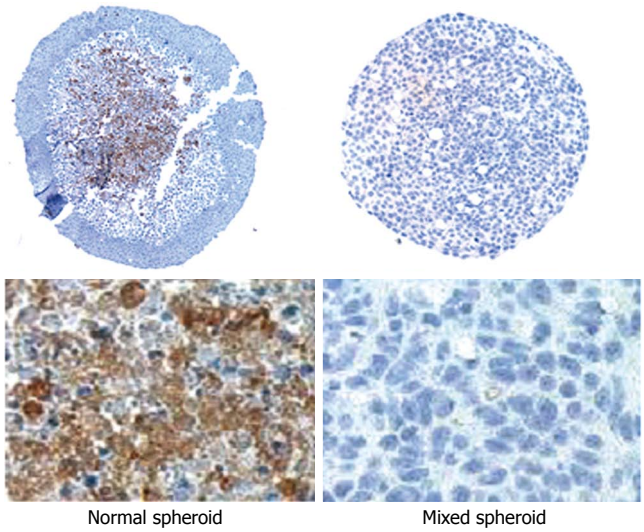

Figure 8 Immunohistochemical staining for the ECM-protein fibronectin in "normal" and mixed spheroids of the IEC line HT-29 after seven days. Fibronectin could be detected in spheroids invaded by MO and cultured for seven days. Expression was preferentially localized in the center of aggregates. In mixed spheroids cultured for seven days no fibronectin expression was observed.

activated caspase-3 during the incubation period.

Although MCS do not resemble the *in vivo* situation where IMACs are separated from the IEC by the basement membrane, many conditions such as O_2-gradient, pH or ECM production are similar to those in the body[26-28]. In MCS, cells are also able to form cell-cell and cell-matrix contacts which are found *in vivo*[29-31] and may therefore be regarded as a useful model to study the important aspects of IMAC differentiation.

In general, interactions between different cell types, special cytokine milieus and contact with components of the ECM can trigger cells to develop a special phenotype. Hohn and co-workers[32] showed that components of the basement membrane and ECM are involved in choriocarcinoma cell differentiation. Hanspal *et al*[33] have demonstrated the importance of cell-cell interactions during the regulation of erythropoiesis. The ECM protein, vitronectin, controls the differentiation of cerebellar granular cells[34]. It was reported that ECM also plays a role in the differentiation of embryonic stem cells[35] and skeletal muscle cells[36]. Armstrong *et al*[37] have shown that ECM proteins have effects on MAC differentiation, growth and function.

Jacob *et al*[38] induced differentiation of MO to MAC *in vitro* by culturing MO on different ECM protein substrates, and found that specific markers associated with differentiation are changes in the expression of cell surface antigens. FACS analysis showed a down-regulation of CD14 occurring in a substrate dependent manner, which was the highest in MO maintained on fibronectin in their study[38].

In our experiments, MCS invaded by MO and cultured

for seven days contained a large amount of ECM protein fibronectin. In addition, the expression of fibronectin was up-regulated during the culture period, which is correlated with the previously described down-regulation of CD14 and other MO-specific surface markers[18]. In mixed spheroids no fibronectin expression could be detected, which could be due to a stronger degradation of ECM proteins by the larger amount of MO added or a lack of synthesis induction. Fibronectin present in the described co-culture model seems to be an important factor contributing to the *in vitro* differentiation of IMACs as well as the active invasion of MO into the three-dimensional aggregates, indicating that only a subpopulation of blood MO is able to differentiate into IMACs.

The loss of MO in the "mixed spheroids" could have several reasons. First, differentiation into the intestinal phenotype is necessary for survival in the epithelial cell environment. Second, the higher number of mononuclear cells in the mixed spheroids compared to the model with MO invasion induces factors that lead to cell death or prevent the synthesis of survival factors. Third, we cannot exclude that this is a self protection effect of the tumor cell lines used and that MO only enter the MCS in the MCS model.

We cannot exclude that there is a pre-primed subpopulation of MO in the peripheral blood that is especially suited to get in contact with IEC. According to such a hypothesis only this pre-primed subpopulation would enter the MCS model or the mucosa and further differentiate into IMACs. This natural selection would not be observed in co-cultures of all elutriated peripheral MO with conditioned media, membrane preparations or in mixed spheroids. The number of differentiating cells would be too low to reach a significant difference. In the present study, we investigated this possibility of a pre-primed subpopulation of MO suited for IMAC differentiation.

To understand the differentiation process of IMACs in healthy individuals may further help to find an approach for the therapy of IBD. Local induction of a tolerogenic and anergic IMAC cell type could down-regulate or stop mucosal inflammation. A therapeutic approach inducing differentiation of this cell type would be one step up the inflammatory cascade not aimed at T-cells but at the site of the first contact with antigen entry in the mucosa.

REFERENCES

1 **Lee SH**, Starkey PM, Gordon S. Quantitative analysis of total macrophage content in adult mouse tissues. Immunochemical studies with monoclonal antibody F4/80. *J Exp Med* 1985; **161**: 475-489

2 **Pavli P**, Doe WF. Intestinal macrophages. In: Mac Dermott RP, Stenson WF, editors. Inflammatory bowel disease. New York: Elsevier, 1992: 177-188

3 **LeFevre ME**, Hammer R, Joel DD. Macrophages of the mammalian small intestine: a review. *J Reticuloendothel Soc* 1979; **26**: 553-573

4 **Bockman DE**, Boydston WR, Beezhold DH. The role of epithelial cells in gut-associated immune reactivity. *Ann N Y Acad Sci* 1983; **409**: 129-144

5 **Bull DM**, Bookman MA. Isolation and functional characterization of human intestinal mucosal lymphoid cells. *J Clin Invest* 1977; **59**: 966-974

6 **Donnellan WL**. The structure of the colonic mucosa. The epithelium and subepithelial reticulohistiocytic complex. *Gastroenterology* 1965; **49**: 496-514

7 **Golder JP**, Doe WF. Isolation and preliminary characterization of human intestinal macrophages. *Gastroenterology* 1983; **84**: 795-802

8 **Pavli P**, Woodhams CE, Doe WF, Hume DA. Isolation and characterization of antigen-presenting dendritic cells from the mouse intestinal lamina propria. *Immunology* 1990; **70**: 40-47

9 **Hugot JP**, Chamaillard M, Zouali H, Lesage S, Cézard JP, Belaiche J, Almer S, Tysk C, O'Morain CA, Gassull M, Binder V, Finkel Y, Cortot A, Modigliani R, Laurent-Puig P, Gower-Rousseau C, Macry J, Colombel JF, Sahbatou M, Thomas G. Association of NOD2 leucine-rich repeat variants with susceptibility to Crohn's disease. *Nature* 2001; **411**: 599-603

10 **Ogura Y**, Bonen DK, Inohara N, Nicolae DL, Chen FF, Ramos R, Britton H, Moran T, Karaliuskas R, Duerr RH, Achkar JP, Brant SR, Bayless TM, Kirschner BS, Hanauer SB, Nuñez G, Cho JH. A frameshift mutation in NOD2 associated with susceptibility to Crohn's disease. *Nature* 2001; **411**: 603-606

11 **Andus T**, Rogler G, Daig R, Falk W, Schölmerich J, Gross V. The role of macrophages. In: Tygat GNJ, Bartelsman JFWM, van Deventer SJH, editors. Inflammatory bowel disease. The Netherlands: Kluwer Dordrecht, 1995: 281-297

12 **Rogler G**, Hausmann M, Vogl D, Aschenbrenner E, Andus T, Falk W, Andreesen R, Schölmerich J, Gross V. Isolation and phenotypic characterization of colonic macrophages. *Clin Exp Immunol* 1998; **112**: 205-215

13 **Rogler G**, Andus T, Aschenbrenner E, Vogl D, Falk W, Schölmerich J, Gross V. Alterations of the phenotype of colonic macrophages in inflammatory bowel disease. *Eur J Gastroenterol Hepatol* 1997; **9**: 893-899

14 **Rugtveit J**, Bakka A, Brandtzaeg P. Differential distribution of B7.1 (CD80) and B7.2 (CD86) costimulatory molecules on mucosal macrophage subsets in human inflammatory bowel disease (IBD). *Clin Exp Immunol* 1997; **110**: 104-113

15 **Barbosa IL**, Gant VA, Hamblin AS. Alveolar macrophages from patients with bronchogenic carcinoma and sarcoidosis similarly express monocyte antigens. *Clin Exp Immunol* 1991; **86**: 173-178

16 **Hausmann M**, Kiessling S, Mestermann S, Webb G, Spöttl T, Andus T, Schölmerich J, Herfarth H, Ray K, Falk W, Rogler G. Toll-like receptors 2 and 4 are up-regulated during intestinal inflammation. *Gastroenterology* 2002; **122**: 1987-2000

17 **Hausmann M**, Spöttl T, Andus T, Rothe G, Falk W, Schölmerich J, Herfarth H, Rogler G. Subtractive screening reveals up-regulation of NADPH oxidase expression in Crohn's disease intestinal macrophages. *Clin Exp Immunol* 2001; **125**: 48-55

18 **Spöttl T**, Hausmann M, Kreutz M, Peuker A, Vogl D, Schölmerich J, Falk W, Andreesen R, Andus T, Herfarth H, Rogler G. Monocyte differentiation in intestine-like macrophage phenotype induced by epithelial cells. *J Leukoc Biol* 2001; **70**: 241-251

19 **Pavli P**, Maxwell L, Van de Pol E, Doe F. Distribution of human colonic dendritic cells and macrophages. *Clin Exp Immunol* 1996; **104**: 124-132

20 **D'Amico G**, Bianchi G, Bernasconi S, Bersani L, Piemonti L, Sozzani S, Mantovani A, Allavena P. Adhesion, transendothelial migration, and reverse transmigration of in vitro cultured dendritic cells. *Blood* 1998; **92**: 207-214

21 **Fujigaki Y**, Nagase M, Kojima K, Yamamoto T, Hishida A. Glomerular handling of immune complex in the acute phase of active in situ immune complex glomerulonephritis employing cationized ferritin in rats. Ultrastructural localization of immune complex, complements and inflammatory cells. *Virchows Arch* 1997; **431**: 53-61

22 **Martin CA**, Homaidan FR, Palaia T, Burakoff R, el-Sabban ME. Gap junctional communication between murine macrophages and intestinal epithelial cell lines. *Cell Adhes Commun* 1998; **5**: 437-449

23 **Marshall CJ**, Franks LM, Carbonell AW. Markers of neoplastic

transformation in epithelial cell lines derived from human carcinomas. *J Natl Cancer Inst* 1977; **58**: 1743-1751
24 **Noguchi P**, Wallace R, Johnson J, Earley EM, O'Brien S, Ferrone S, Pellegrino MA, Milstien J, Needy C, Browne W, Petricciani J. Characterization of the WIDR: a human colon carcinoma cell line. *In Vitro* 1979; **15**: 401-408
25 **Aigner A**, Neumann S. Immunchemie: Grundlagen, Anwendungen, Perspektiven. Jena: Gustav Fischer**,** 1997
26 **Inch WR**, McCredie JA, Sutherland RM. Growth of nodular carcinomas in rodents compared with multi-cell spheroids in tissue culture. *Growth* 1970; **34**: 271-282
27 **Mueller-Klieser W**. Multicellular spheroids. A review on cellular aggregates in cancer research. *J Cancer Res Clin Oncol* 1987; **113**: 101-122
28 **Konur A**, Kreutz M, Knüchel R, Krause SW, Andreesen R. Cytokine repertoire during maturation of monocytes to macrophages within spheroids of malignant and non-malignant urothelial cell lines. *Int J Cancer* 1998; **78**: 648-653
29 **Sutherland RM**. Cell and environment interactions in tumor microregions: the multicell spheroid model. *Science* 1988; **240**: 177-184
30 **Olive PL**, Durand RE. Drug and radiation resistance in spheroids: cell contact and kinetics. *Cancer Metastasis Rev* 1994; **13**: 121-138
31 **Davies CD**, Müller H, Hagen I, Gårseth M, Hjelstuen MH. Comparison of extracellular matrix in human osteosarcomas and melanomas growing as xenografts, multicellular spheroids, and monolayer cultures. *Anticancer Res* 1997; **17**: 4317-4326
32 **Hohn HP**, Grümmer R, Bosserhoff S, Graf-Lingnau S, Reuss B, Bäcker C, Denker HW. The role of matrix contact and of cell-cell interactions in choriocarcinoma cell differentiation. *Eur J Cell Biol* 1996; **69**: 76-85
33 **Hanspal M**. Importance of cell-cell interactions in regulation of erythropoiesis. *Curr Opin Hematol* 1997; **4**: 142-147
34 **Wechsler-Reya RJ**. Caught in the matrix: how vitronectin controls neuronal differentiation. *Trends Neurosci* 2001; **24**: 680-682
35 **Czyz J**, Wobus A. Embryonic stem cell differentiation: the role of extracellular factors. *Differentiation* 2001; **68**: 167-174
36 **Osses N**, Brandan E. ECM is required for skeletal muscle differentiation independently of muscle regulatory factor expression. *Am J Physiol Cell Physiol* 2002; **282**: C383-C394
37 **Armstrong JW**, Chapes SK. Effects of extracellular matrix proteins on macrophage differentiation, growth, and function: comparison of liquid and agar culture systems. *J Exp Zool* 1994; **269**: 178-187
38 **Jacob SS**, Shastry P, Sudhakaran PR. Monocyte-macrophage differentiation in vitro: modulation by extracellular matrix protein substratum. *Mol Cell Biochem* 2002**; 233:** 9-17

S- Editor Liu Y **L- Editor** Wang XL **E- Editor** Ma WH

PO Box 2345, Beijing 100023, China
www.wjgnet.com
wjg@wjgnet.com

World J Gastroenterol 2007 February 21; 13(7): 1042-1052
World Journal of Gastroenterology ISSN 1007-9327

BASIC RESEARCH

Evidence for a sequential transfer of iron amongst ferritin, transferrin and transferrin receptor during duodenal absorption of iron in rat and human

Vasantha L Kolachala, B Sesikeran, K Madhavan Nair

Vasantha L Kolachala, Division of Digestive Diseases, Department of Medicine, Emory University, Atlanta, GA, United States
B Sesikeran, K Madhavan Nair, National Institute of Nutrition, Indian Council of Medical Research, Jamai-Osmania PO, Hyderabad 500007, India
Supported by Council of Scientific and Industrial research, India: schemes no (812) 93-EMR-11 to KMN
Correspondence to: K Madhavan Nair, National Institute of Nutrition, Indian Council of Medical Research, Jamai-Osmania PO, Hyderabad 500007, India. nairthayil@gmail.com
Telephone: +91-40-27008921 Fax: +91-40-27019074
Received: 2006-10-31 Accepted: 2007-01-04

Abstract

AIM: To elucidate the sequential transfer of iron amongst ferritin, transferrin and transferrin receptor under various iron status conditions.

METHODS: Incorporation of ^{59}Fe into mucosal and luminal proteins was carried out in control WKY rats. The sequential transfer of iron amongst ferritin, transferrin and transferrin receptor was carried out in iron deficient, control and iron overloaded rats. The duodenal proteins were subjected to immunoprecipitation and quantitation by specific ELISA and *in situ* localization by microautoradiography and immunohistochemistry in tandem duodenal sections. Human duodenal biopsy (n = 36) collected from subjects with differing iron status were also stained for these proteins.

RESULTS: Ferritin was identified as the major protein that incorporated iron in a time-dependent manner in the duodenal mucosa. The concentration of mucosal ferritin was significantly higher in the iron excess group compared to control, iron deficient groups (731.5 ± 191.96 *vs* 308.3 ± 123.36, 731.5 ± 191.96 *vs* 256.0 ± 1.19, $P < 0.005$), while that of luminal transferrin which was significantly higher than the mucosal did not differ among the groups (10.9 ± 7.6 *vs* 0.87 ± 0.79, 11.1 ± 10.3 *vs* 0.80 ± 1.20, 6.8 ± 4.7 *vs* 0.61 ± 0.63, $P < 0.001$). *In situ* grading of proteins and iron, and their superimposition, suggested the occurrence of a sequential transfer of iron. This was demonstrated to occur through the initial binding of iron to luminal transferrin then to absorptive cell surface transferrin receptors. The staining intensity of these proteins varied according to the iron nutrition in humans, with intense staining of transferrin receptor observed in iron deficient subjects.

CONCLUSION: It is concluded that the intestine takes up iron through a sequential transfer involving interaction of luminal transferrin, transferrin-transferrin receptor and ferritin.

Key words: Mucosa; Lumen; Iron-binding proteins

Kolachala VL, Sesikeran B, Nair KM. Evidence for a sequential transfer of iron amongst ferritin, transferrin and transferrin receptor during duodenal absorption of iron in rat and human. *World J Gastroenterol* 2007; 13(7): 1042-1052

http://www.wjgnet.com/1007-9327/13/1042.asp

INTRODUCTION

Iron homeostasis is accomplished by regulating absorption in the proximal small intestine and is regulated according to the body's needs. Failure to maintain this equilibrium leads to pathological conditions resulting in either iron deficiency or iron overload. Iron deficiency anemia remains the most important micronutrient deficiency world wide. Iron is essential because of its unique ability to serve as both an electron donor and acceptor. Because of iron's virtual insolubility and potential toxicity under physiological conditions, special molecules have evolved for its acquisition, transport and storage in soluble, nontoxic form. In humans, heme iron is absorbed more efficiently than non-heme iron[1]. Recent studies demonstrate that non-heme iron is transported into the cell in the ferrous [Fe (Ⅱ)] form, mainly by carrier divalent metal transporter 1 (DMT1)-also known as natural resistance associated macrophage protein 2 (Nramp2) or divalent cation transporter 1 (DCT1)[2] . However, iron absorption is not impaired by mutation of DMT-1, suggesting that DMT-1 is not the only transporter operating within the endosomes of crypt cells. Studies of Conrad *et al*[3], showed that ferric iron is absorbed by β3 integrin and mobilferrin pathway which is shared with other nutritional metals .

In last few decades, several candidate proteins involved

in the transmembrane transport of iron have been identified[4] . Several years ago, Granick *et al* demonstrated that ferritin sequesters iron and provides the block to iron uptake. Although this model remains unproven, the hypothesis that the amount of mucosal ferritin dictates the extent of iron absorbed by the enterocytes is still intriguing. It has been postulated that iron absorption was the primary method of maintaining body iron homeostasis and was regulated by a mucosal receptor that blocked iron absorption when it became satiated with iron. For two decades, it was believed that ferritin was the receptor that regulates iron absorption, and that apoferritin enhances iron absorption while holoferritin blocks iron uptake. This hypothesis was disproved by immunological studies showing that there was little or no apoferritin in the absorptive cells of iron deficient animals[5]. Despite the close relationship between ferritin levels and intestinal iron absorption[6] it is not clear whether this protein plays a passive or active role in transport regulation.

There are studies to argue for[7-11] and against[12-14] the view that transferrin (Tf) is an important mediator of iron absorption. The proposal that mucosal Tf acts as a shuttle protein for iron absorption was suggested by Huebers *et al*[15]. Selective localization of transferrin in the duodenal epithelium in rat[16,17] and in human[17] , and the co-localization of transferrin receptor (TfR) and transferrin in coated pits on the basal and lateral membranes of crypt cells in mouse have been demonstrated[18]. However, an ultrastructural study of Parmley *et al*[19] failed to identify TfR on the surface of enterocyte microvilli. Thus, the role of transferrin and transferrin receptor in the duodenal uptake was not identified with certainty. In 1983, it was postulated that transferrin was secreted into the intestinal lumen to bind iron and enter the absorptive cell as a transferrin iron complex in a manner similar to non-intestinal cells[15]. Recent studies of transferrin receptor knockout mice ($TfR^{-/-}$) provide new insights regarding the physiologic role of the transferrin/transferrin receptor cycle. Homozygous $TfR^{-/-}$ animals die *in utero* with impaired erythropoiesis and defective neurological development. Thus, the $TfR^{-/-}$ mice provide a convincing demonstration that the transferrin/transferrin receptor cycle plays a central role in the maintenance of normal iron metabolism. Whether transferrin is associated with receptor and whether it plays any role in iron absorption at this site is yet to be determined. A protein called hereditary hemochromatosis (HFE) has been shown to interact with transferrin receptor 1 (TfR1)[20] to influence the rate of receptor mediated uptake of transferrin-bound iron[21-24] . Thus, these investigations of exact localization of mucosal transferrin and transferrin receptor, inside or outside the enterocytes, are conflicting. Therefore, an attempt was made to describe the sequential movement of iron across intestine. The events were sequenced by *in situ* localization of iron by microautoradiography and immunohistochemistry of ferritin, transferrin and transferrin receptor in serial sections of intestine.

MATERIALS AND METHODS

Radioactive $^{59}FeCl_3$ (sp.act 4.0 Ci/g iron in 0.01 mol/L HCl) was obtained from BRIT (Mumbai, India). Photographic emulsion LM-1 was obtained from Amersham (Amersham International plc, UK). SIH universal anti-rabbit kit, human and rat serotransferrin was obtained from Sigma Aldrich Co (St. Louis, USA). Ferritin, transferrin antisera against purified proteins were produced in New Zealand white rabbits. Polyclonal antiserum against rat placental transferrin receptor was a gift from James D. Cook, M.D (University of Kansas Medical Center, Kansas City, USA). All other chemicals used were of analytic grade and procured locally.

Studies in rats

Rats from National Centre for Laboratory Animal Sciences (National Institute of Nutrition, Hyderabad) were used for the study. All animal experiments were approved by the institutional animal ethics committee.

Incorporation of radioactive iron into various iron binding protein was carried out in *Wistar/Kyoto* (*WKY*) adult male normal rats (body weight 200 g). Food was withheld for 16-18 h before administering 1 mL of 7-10 μci of $^{59}FeCl_3$ in 0.01N HCl by gavage. Rats were sacrificed at various time intervals starting at 15, 30 min, 1, 2, 4 and 12 h to study the time-dependent incorporation of iron into luminal and mucosal proteins of various segments. All the subsequent operations were carried out on ice. The luminal content was collected by flushing with 5-10 mL of saline containing protease inhibitors. The mucosal scrapings were obtained by scrapping off the everted segments with a glass slide. The intestinal contents obtained from three rats from each group were pooled together for each time point. The contents were homogenized in 1:4 v/v of saline containing a cocktail of protease inhibitors (PMSF 75 μg/mL, leupeptin 1 μg/mL and iodoacetate186 μg/mL), and subjected to 60% ammonium sulphate fractionation. A clear supernatant was prepared for subsequent analysis.

Further to explore the specific role of duodenal transferrin and ferritin during iron absorption, time-dependent (5 min-4 h) incorporation of radioactive iron into these proteins, along with quantitation by specific ELISA and immunoprecipitation techniques for ferritin and transferrin, was carried out in control, iron-deficient, and excess iron fed rats. For this, 74 *WKY* male weanling rats (body weight 37.5 ± 7.63) were randomly selected and housed individually into iron deficient (n = 30), control (n = 24) and iron excess (n = 24) groups. They were allowed to have free access to food and water for 7 weeks. The rats were placed on one of the three diets each containing identical protein, fat, carbohydrate, and complete vitamin and fiber supplements. The diets were produced in accordance with the recommendations of American Institute of Nutrition (AIN93)[25]. The diet also contained a balanced mineral mix, differing only in the iron content. The deficient group received iron deficient semi-synthetic diet containing < 10 mg iron/kg diet, while the iron adequate and excess groups received diet containing 35 and 250 mg/kg diet, respectively. At the end of this period rats were administered 7-10 μCi of radioactive iron and sacrificed at different time points. Duodenal segments

of intestine were collected at 5, 15, 30 min, 1, 2, 4 h and processed. Homogenates of luminal and mucosal contents were analyzed for ferritin and transferrin by specific sandwich ELISA. Incorporation of radiolabelled iron into these proteins was studied by imunoprecipitation with specific antibodies.

Finally, studies were carried out to understand the sequential movement of iron across intestine under various iron status conditions. *WKY* male weanling rats (body weight 36.8 ± 6.56) were equally (n = 8) distributed into iron deficient, control and iron overload groups. For iron overloading, in addition to iron excess diet as mentioned above, we gave 4 intra-peritonial injections of 1 mL of imferon, an iron sorbitol citric acid complex in water (50 mg of iron/mL, Rallies India Ltd, Mumbai, India) at weekly intervals. After 7 wk, rats were fasted overnight and given 100 μCi of $^{59}FeCl_3$ with 0.25 mg of carrier iron as ferrous sulphate by gavage. Duodenal segment of intestine were collected at 5, 15, 30 min, 1, 2, 4, 16 h. The segments were flushed with formalin, cut opened longitudinally and fixed in 10% neutral formalin for 12 h. These intestinal segments were rolled longitudinally (Swiss-roll), and further processed for microautoradiography and immunohistochemistry.

Western blotting and autoradiography

The protein content was estimated by the method of Bradford[26]. Both luminal and mucosal proteins (100 μg) were subjected to 4%-20% PAGE along with rat liver ferritin as a marker. The separated protein bands were visualized by autoradiography and probed with ferritin antibody.

ELISA of ferritin and transferrin

Ferritin and transferrin proteins in the luminal and mucosal contents were quantified using a specific sandwich ELISA system developed by us.

Immunoprecipitation

In order to understand the role of different iron binding proteins during absorption, luminal contents and mucosal proteins were lyophilized. Duodenal mucosal and luminal proteins obtained at initial time points (5, 15, 30 min) were reconstituted and subjected to immunoprecipitation with ferritin and transferrin antisera. Equal volumes (1 mL) of duodenal mucosal and luminal proteins (2-4 mg) and 1:32 diluted ferritin and transferrin antisera were incubated at 37℃ for 1 h and at 4℃ overnight. The specificity of ferritin and transferrin antisera was demonstrated by replacing immune serum with non-immune serum in the immunoprecipitation protocol. The immunoprecipitate was collected and washed three times with PBS. ^{59}Fe radioactivity in the fraction was counted in a gamma counter (Packard Autogamma, Cobra Ⅱ). A known activity of $^{59}FeCl_3$ was run with samples to correct for decay and counting efficiency of the gamma counter.

Preparation of intestinal sections for microautoradiography and immunohistochemistry

An automatic tissue processor (Shandon, Processor 2LE) using ascending grades of isopropyl alcohol and chloroform was used. The processed tissue samples were embedded in paraffin (58-60℃) using a Leica tissue-embedding unit. A set of 10 serial sections of 4 μ thickness were taken from each block using Reichert-Jung 2030 rotary manual microtome. The sections were mounted on chromalum-gelatin coated glass slides and further processed for immunohistochemistry and microautoradiography according to standard procedures.

Microautoradiography

In situ localization of radiolabelled iron was carried out in dehydrated sections. The sections were processed with photographic emulsion according to the manufacturer's guidelines (Amersham LM-1, Amersham UK). These sections were stained with hematoxylin, dehydrated and mounted with DPX mounting medium. For signals, the sections were viewed under light microscope (Leitz Ortholux) and photographed.

Immunohistochemistry

Serial sections were used for immunohistochemical localization of transferrin, transferrin receptor and ferritin, using respective antisera. The binding of each antiserum to their respective proteins was done using Sigma SIH kit. Counter-staining was done with Mayer's hematoxylin. Control slides were layered with non-immune serum instead of primary antiserum. The localization of the antigen was done using goat anti-rabbit HRPO conjugate. The comparison of staining intensity and the quantification of positively stained cells was carried out under light microscope with the magnification set at 10 ×, 25 × or 40 ×. In addition, the distribution of intestinal mucosal ferritin, transferrin and transferrin receptor in relation to iron status was evaluated in human biopsy specimens.

Human duodenal mucosal biopsy

Endoscopic intestinal (duodenal) biopsy specimens were collected by a gastroenterologist from 30 males and 6 females attending the Gastroenterology Department of Gandhi Hospital (Secunderabad, India) for various upper GI tract related ailments. Informed oral consent was obtained from all the subjects. All the subjects were classified based on their hematological and iron status parameters. Accordingly, a cut off value of hemoglobin < 13 g/dL for male and < 12 g/dL for female was classified as anemia, while anemia with serum ferritin < 12 μg/L as iron deficiency anemia. Biopsy specimens of 3-4 mm were collected and immediately spread on a wire mesh. These specimens were then immersed in 10% neutral buffered formalin solution and processed for immunohistochemistry of ferritin, transferrin and transferrin receptor, as described earlier.

Haematological and iron status indicators

Fasting blood samples were collected from rats and human subjects to estimate haemoglobin and iron status parameters. Hemoglobin was estimated by an automated hematology counter (Serono system 9000 Rx). Quantitation

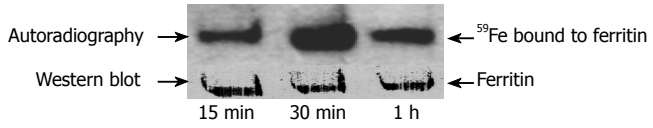

Figure 1 Ferritin takes up radiolabelled iron in a time dependent manner and has a direct role in iron absorption: Upper panel: Autoradiogram of duodenal proteins. Duodenal mucosal proteins (100 μg) obtained after 15 min, 30 min, 1 h after an oral dose of 7-10 μCi of $^{59}FeCl_3$ were subjected to 4%-20% PAGE and dehydrated. The radioactive bands were developed on X-ray film. As shown in the figure, one radioactive band corresponding to ferritin whose intensity was maximal at 30 min and then decreased with time. Lower panel: These proteins were subjected to western blot with ferritin antibody.

of human and rat serum ferritin, rat mucosal, and luminal ferritin and transferrin was estimated by homologous sandwich ELISA systems developed by us. Liver iron was estimated by dry ashing followed by an estimation of iron in the mineral solution by bathophenathroline method[1].

RESULTS

Initially, a kinetic study was carried out to understand the *in vivo* time course of iron absorption of ^{59}Fe given by oral gavage to rats with normal iron status condition. Specific activity of duodenal mucosa was found to be highest, followed by jejunum, ileum and stomach at all time points studied. The specific activity of ^{59}Fe was found to increase with time and attained a peak at 30 min in duodenal mucosa (data not shown).

Ferritin takes up radio-labelled iron in a time dependent manner and has a direct role in iron absorption

In order to understand the role of ferritin in iron absorption, an autoradiogram was performed with proteins obtained from 60% ammonium sulphate precipitation of luminal and mucosal fractions after oral administration of ^{59}Fe. As shown in Figure 1, upper panel, rats with normal iron status showed a single radioactive protein band identical to purified rat liver ferritin. The intensity of the radioactive band associated with ferritin increased with time and showed maximal band intensity at 30 min and decreased subsequently with no change in the ferritin protein band intensity (Figure 1, lower panel). These results suggested that intestinal ferritin is an important component of the intestinal iron transport system and seems to take up iron and facilitate its transfer across the mucosal cells. Thus these results demonstrate that ferritin is not just a sink but takes up iron and releases it in a time-dependent manner during the absorptive process.

To determine the specific role of iron binding proteins like ferritin, transferrin and transferrin receptor, rats were given different amounts of iron. Haematological and iron status parameters indicated the induction of iron deficiency and iron overloading in respective groups (data not shown). Table 1 shows the ferritin and transferrin concentrations in the intestinal luminal and mucosal contents of rats with various iron status parameters. The concentration of ferritin was higher in mucosa than in the lumen of duodenum in all the groups. In iron excess group, there was a significantly higher concentration of ferritin, both in lumen and mucosa, compared to deficient and control groups. In contrast, the transferrin concentration was significantly higher in lumen than in mucosa within the group and was similar between the groups.

Table 1 Ferritin and transferrin concentrations in rat duodenum under various iron status conditions

Parameter	Control	Iron deficient	Iron excess
Ferritin (ng/mg protein)			
Lumen	126.0^{a} ± 61.42	105.8^{a} ± 35.81	228.8^{c} ± 73.54
Mucosa	308.3^{c} ± 123.36	256.0^{c} ± 1.19	731.5^{e} ± 191.96
Transferrin (μg/mg protein)			
Lumen	10.9^{b} ± 7.6	11.1^{b} ± 10.3	6.8^{b} ± 4.7
Mucosa	0.87^{d} ± 0.79	0.80^{d} ± 1.20	0.61^{d} ± 0.63

Values with different superscript letters within each column and row are significantly different at $^{a,c,e}P < 0.005$ for ferritin and $^{b,d}P < 0.001$ for transferrin by one way ANOVA ($n = 5$).

Reciprocal relationship between luminal transferrin and mucosal ferritin iron

To understand the interaction between luminal transferrin and mucosal ferritin after oral administration of ^{59}Fe, rats were sacrificed at 5, 15 and 30 min. As shown in Figure 2A the percentage of radioactive iron in duodenal lumen was found to decrease with time. The highest luminal specific activity was seen in iron-deficient rats followed by control and iron excess fed rats. In deficient and control rats, there was a progressive increase in specific activity while in the excess iron fed group, the radioactivity was retained at the site of absorption (Figure 2B). This was supported by the findings on luminal and mucosal radioactivity, which showed a faster transit of iron from lumen to mucosa in iron-deficient and control rats. On the other hand, in the iron excess fed rats luminal radioactivity showed slower transit as indicated by increase in the radioactivity from 30 min onwards. The plasma radioactivity during the same time periods reflected the slower transit of duodenal iron in iron excess fed rats (plasma specific activity of 150 ± 20 dpm/mL during 15-60 min) which showed no peak in plasma iron as compared to the iron-deficient and control groups (plasma specific activity of 700 ± 50 and 400 ± 50 dpm/mL, respectively). The luminal transferrin iron declined with time in all the groups while that of mucosal ferritin increased only in deficient and sufficient groups during the 5-30 min of iron uptake (Figure 2). As shown in Figure 2B percentage of ferritin bound iron reached a peak and showed a decline confirming the release of iron from ferritin in deficient and control groups. In the iron excess group the percentage ferritin-bound iron did not change with time, confirming the blockage of iron in this group.

Microautradiography demonstrate the sequential transfer of radiolabelled iron

In order to study the *in vivo* translocation of iron after oral administration of radiolabelled iron, duodenal

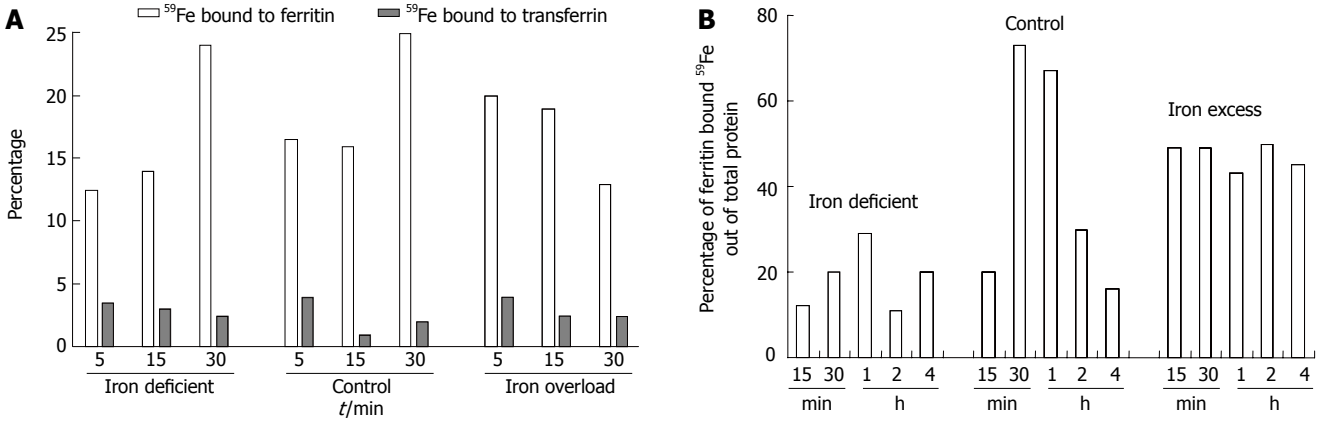

Figure 2 Reciprocal relationship between luminal transferrin and mucosal ferritin. **A**: Luminal and mucosal proteins collected after oral administration of ^{59}Fe after various time intervals were subjected to immunoprecipitation with ferritin and transferrin antibodies. The bar graph represents percentage incorporation of ^{59}Fe in luminal transferrin (crossed bars) and mucosal ferritin (open bars) of duodenum; **B**: Percentage of ferritin bound iron out of total protein bound iron with time, in various iron status conditions.

Table 2 Summary of *in situ* grading of sequential autoradiographic and immunohistochemical staining signals

Radioactive iron/protein	Iron status	Basal	5 min	15 min	30 min	2h
^{59}Fe	ID	-	SUR+	IE+++	IE+++	-
	OL	-	SUR+++	IE±	IE±	-
Tf	ID	IV±	IV++	IE+++ IV++		IE+ IV++
	OL	IV±	IE± IV±	IE± IV±		
TfR	ID	SUR±	SUR++	IE++	IE+	SUR±
	OL	SUR±	SUR++	SUR+	-	-
Fe	ID	IE± IV±	-	-		IE±
	OL	IE±	-		IE±	IE± IV+++

Tf: transfferin; TfR: Transferrin receptor; Fe: Ferritin; ID: Iron deficient; OL: Iron overload; IE: Intra epithelial; IV: Intra vascular; SUR: Surface; Grading +: minimal staining; ++: good; +++: intense; –: nil.

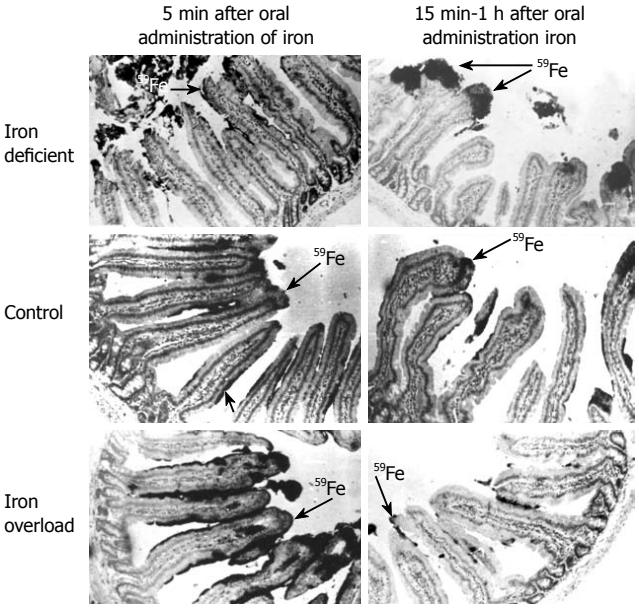

Figure 3 Microautoradiography demonstrated the sequential transfer of iron: Microautoradiography of duodenal sections of intestine obtained after oral administration of 100 μCi of $^{59}FeCl_3$ and 250 g of carrier iron in iron deficient top panel (ID), control middle panel (C) and iron overload bottom panel (OL) rats. These photographs illustrate the progressive transfer of iron into the villi (25 x).

segments were processed for microautoradiography under various iron status conditions. Table 2 shows the grading of staining intensities of radiolabelled iron, ferritin, transferrin/transferrin receptor in the iron deficient and iron excess groups. The radioactivity at 5 min was localized on the surface of the villi in the iron deficient group (top left panel ID, 5 min) (Figure 3). Subsequently, the radioactivity was present in the columnar epithelial cells (absorptive cells) at the tip of the villi between 15 min to 1 h in iron deficient (top right, panel ID, 15, 30 min, 1 h, and Table 2). At 2 and 4 h most of the radioactive iron was seen inside the villi in the lamina propria. A similar trend was observed in the control group (middle, panel C, 5 min and 15, 30 min, 1 h). However, in iron-overloaded intestine, high intensity radioactivity was noticed at 5 min on the surface (bottom left, panel OL, 5 min) but was minimal signals at 15 and 30 min (bottom right panel OL, 15 min and Table 2). The radioactive signals at 15 and 30 min associated with iron were maximal intraepithelially in iron-deficient rats and plasma radioactivity indicated maximum absorption. In iron-overloaded rats the signal was maximal at 5 min and seen only at the absorptive surface and retained at the site of absorption (Table 2).

Ferritin appears in the epithelial cells after oral administration of iron

Immunohistochemistry with ferritin antibody demonstrated that at 5 min, ferritin staining was maximal intraepithelially in iron-deficient intestine (Figure 4), while intense staining was seen both intraepithelially and intravascularly, in iron-overloaded intestine (Figure 4 top right, panel OL, 5 min Fe). The intensity of staining within the villi at 1 h (bottom left panel ID-1 h, Fe) was minimal and similar to that seen at basal status in iron deficient intestine. On the other hand, the staining intensity was

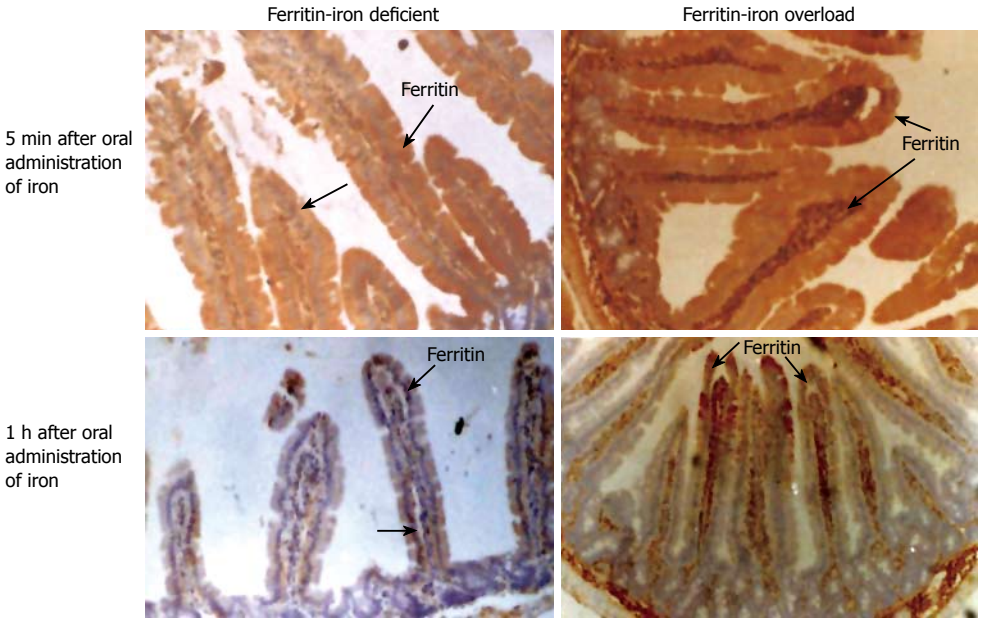

Figure 4 Ferritin appears in the epithelial cells after oral administration of ^{59}Fe: Immunohistochemical localization of ferritin (Fe) in the duodenal sections of intestine of iron deficient left panel (ID) and iron overload right panel (OL) rats at various time points after oral administration of radioactive iron (25 X).

lower in iron-loaded intestine after 15 min indicating the presence of holoferritin and blocking of iron absorption (Table 2).

Microautoradiography and immunohistocheminstry with transferrin and transferrin receptor demonstrates the in vivo uptake of iron through transferrin receptor

The *in situ* localization of radioactive iron in the iron deficient group indicated its presence on the cell surface (5 min) and then intraepithelially (15, 30 min) in the villi (Table 2). The intensity of transferrin staining was found to be maximal at the tip of the epithelial cells at 15 min (Figure 5, left panel ID 15 min Tf) and subsequently decreased to basal status. Staining of the blood vessels for transferrin started to appear from 2 h onwards in ID (bottom left panel ID, 2 h Tf). The staining for transferrin at 15 min within the epithelial cells was not observed in iron-overload group (Table 2). In the iron-overload group, staining due to transferrin was minimal at 5-30 min (Figure 5B, top left panel Tf, OL 30 min). In both groups, the transferrin receptor was localized mainly on the surface of the duodenal villi, thus demonstrating margination of transferrin receptor after oral administration of iron (right top panel Figure 5A, TfR, Basal). This, however, at 15 min was internalized at the tip of the epithelial cells along with iron and transferrin (Figure 5A). After 2hr TfR reappeared on the surface of the villi in the iron deficient (Figure 5A, middle right panel, TfR, ID, 15 min, 2 h) demonstrating the *in vivo* receptor recycling. In contrast, in the iron-overload group TfR was seen only at the surface even at 30 min and 1 h (Figure 5B, bottom panel, TfR, OL, 15 min, 1h) showing no internalization of receptor.

The radioactive signals at 15 min were maximal intraepithelially in the iron deficient group. During this time period, transferrin and its receptor were also co-localized maximally within the epithelial cells (Figure 5C). The intensities of both these proteins subsequently diminished and minimal staining was seen at the margin of the absorptive surface. The intensity of transferrin receptor staining was maximal along the entire margin during different time points in the iron-overloaded intestine. This was a striking difference between the two extreme conditions. Microautoradiography along with the immunohistochemistry of ferritin and the transferrin/transferrin receptor demonstrated the *in vivo* internalization of transferrin and its receptor along with radiolabelled iron and recycling of the receptor to the surface. This clearly shows a transferrin-mediated iron uptake at the absorptive surface of the rat intestine.

Staining intensity of ferritin, transferrin/ transferrin receptor in human duodenal biopsy under different iron nutritional status

In addition, we have performed immonohistochemistry of ferritin, transferrin/transferrin receptor in human duodenal biopsy specimens collected from various iron status conditions. All the subjects were classified according to their indicators of iron status such as haemoglobin, serum ferritin (Table 3). According to these parameters, 13 of them belonged to normal group, 6 had iron-deficient anemia, 14 anemia, one each had blood transfused, iron injected and iron given orally as supplement. Representative immunohistochemical images for ferritin, transferrin and transferrin receptor of duodenal biopsy from normal, iron deficient anemia and blood transfused are given in Figure 6. The staining intensity for ferritin varied according to iron status and thus staining was +++ normal (top left), ± iron deficient (middle left panel Fe ID) and ++ in blood transfused (Figure 6 bottom left panel Fe BT) subjects. The intensity of transferrin staining was also similar to that of ferritin staining in normal, iron-deficient and in blood transfused subjects (center top, middle and bottom panels respectively). The transferrin receptor on the other hand, stained more intensely with a grading score of (+++) in

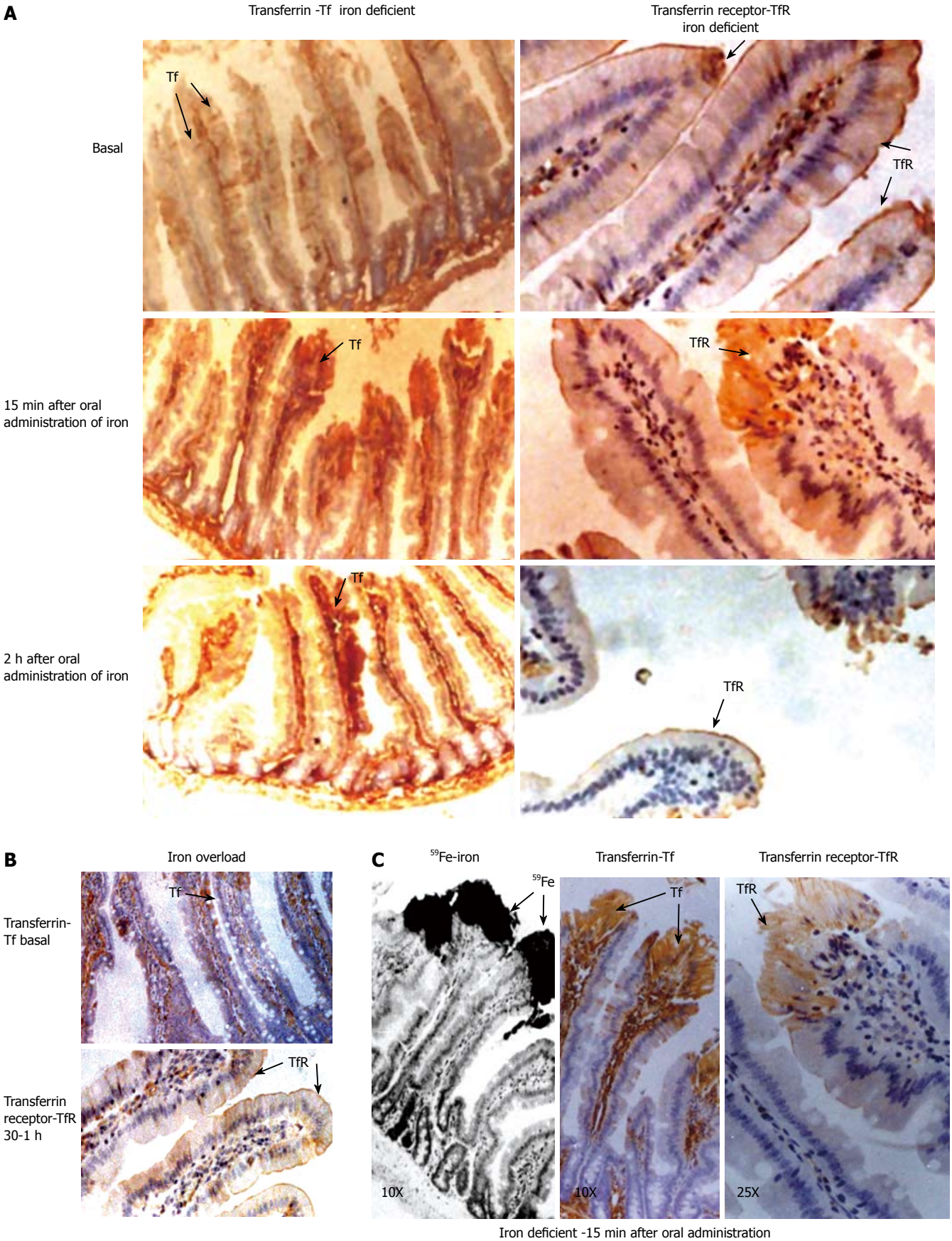

Figure 5 Microautoradiography and immunohistocheminstry with transferrin and transferrin receptor demonstrates the in vivo uptake of iron through transferrin receptor. **A**: Immunohistochemical localization of transferrin left panel (Tf) and transferrin receptor right panel (TfR) in the duodenal sections of intestine of iron deficient rat (ID); **B**: transferrin stain in iron over loaded rat (top panel) (OL)at basal status and tranferrin receptor on the surface of the epithelial cells showing no internalization(bottom panel) in iron overloaded condition after oral administration of radioactive iron (10X); **C**: Co-localization of iron, transferrin and transferrin receptors in the duodenal sections of intestines of iron deficient rats obtained 15 min after oral administration of radioactive iron. Microautoradiographic localization of iron immunohistochemical localization of transferrin transferring receptor.

Table 3 Classification of human subjects according to iron status indicators

	Sex	No	Age (yr)	Hb (g/dL)	PCV	RBC M/cu mm	Serum ferritin (μg/L)
Normal	M	12	36.5 ± 10.6	14.8 ± 0.9	44.5 ± 3.3	5.8 ± 0.7	43 ± 22.1
	F	1	7.2	12.4	36	4.5	71.7
Iron deficient anemia	M	4	24.5 ± 20.9	7.4 ± 2.6	23.3 ± 9.0	4.1 ± 1.7	7.2 ± 4.0
	F	2	20.5	7.3	26.5	3.5	6.5
	M	10	44.3 ± 16.5	11.1 ± 1.64	33.6 ± 5.2	4.5 ± 1.4	75.3 ± 32.2
Anemia	F	4	21 ± 6.6	6.8 ± 3.0	20.8 ± 9.0	2.1 ± 1.2	57.4 ± 13.4
Iron supplements	F						
Blood transfusion	M	1	32	9.5	29	4.7	28.6
Iron injection	F	1	32	8.4	27	4.3	101
Oral iron	F	1	20	9.7	30	3	38

Values are mean ± SD. Cut off values for defining deficiency, Hb: Male < 13 g/dL, Female < 12 g/dL, serum ferritin < 12 μg/L.

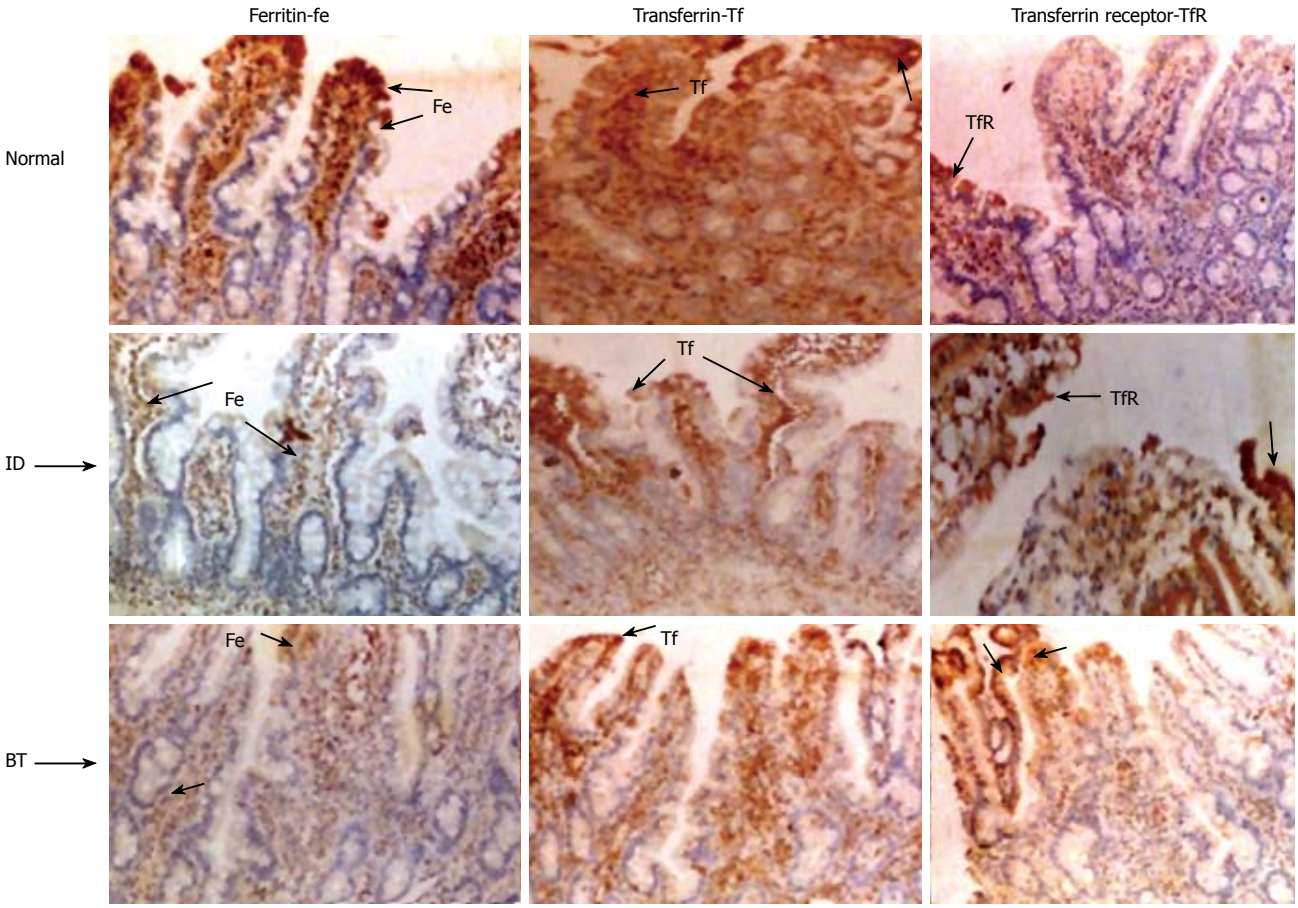

Figure 6 Staining intensity of ferritin, transferrin and transferrin receptor in human duodenal biopsy under different iron nutritional status: Immunohistochemical localization of ferritin (Fe), transferrin (Tf) and transferrin receptor (TfR) in the duodenal biopsy sections of normal (top panel, N), iron deficient (middle panel, ID) and blood transfused (bottom panel, BT) human subjects. Staining intensity; ± represents Light, + normal, ++ good, +++ intense.

the iron-deficient subjects (Figure 6 middle right panel ID TfR) compared to + in normal (top right panel, TfR) and blood transfused subjects (bottom right panel BT TfR).

DISCUSSION

Ferritin, transferrin and transferrin receptor are the important proteins that regulate iron homeostasis in almost all the cells. However, the actions of these proteins in the absorptive cells remain unclear. Data on the role of these proteins were obtained mainly by studying one protein at a time. By attempting to sequence serially the role of these proteins together, during intestinal uptake, we were able to provide evidence for *in vivo* receptor mediated uptake of iron.

The radioactive signals at 15 to 30 min associated with iron were maximal intraepithelially in iron deficient rats. Along with iron, both transferrin and transferrin receptor

were co-localized at this time. The intensities of both these proteins were subsequently decreased and minimal amounts were seen at the margin of absorptive surface in iron deficient intestine. In addition, ferritin appeared intraepithelial in iron deficient and control groups, suggesting its modulation during the absorptive phase. Presence of most of the radiolabelled signal only on absorptive surface at 5 min and beyond in iron-overloaded rats suggest its restricted entry into the duodenum due to the presence of mucosal holo ferritin. This is supported by the intense ferritin staining seen both intraepithelial and intravascular in iron overloaded intestine, especially during absorptive phase and beyond. Further, the presence of transferrin receptor along the entire margin during different phases of iron uptake suggests no internalization of transferrin receptor in iron excess condition.

It is interesting to note that the concentration of mucosal ferritin and the iron associated with it was similar in control and iron deficient groups, and was significantly lower than that seen in the excess iron fed group. This could be due to the regulatory role of mucosal ferritin at the site of adsorption in the case of iron excess, while in the case of normal and iron deficient duodenum it could release the incorporated iron.

A positive relationship between *in situ* localization of ferritin and better iron status was demonstrated in rats and humans. The results on autoradiography of rat duodenal mucosal and luminal preparations suggests that intestinal ferritin takes up iron and releases it in a time dependent manner during the absorptive process. This is supported by the findings on localization of iron in the duodenal mucosa during absorption which showed a positive relationship, with better iron status at 5 min and a negative relationship at 15 min-1h. Similarly in human subjects, the intensity of ferritin staining was lowest in iron deficient subjects, highest in normal subjects and in between in the case of the blood transfused subjects. These observations suggest that mucosal ferritin is an important component of the intestinal iron transport system which takes up iron and facilitates its transfer across the mucosal cells

The studies of Miyoshi *et al*[27] support the presence of ferritin in duodenum. Their studies showed accumulation of iron in the apical area of duodenal villous cells with in ferritin. The presence of maximal ^{55}Fe radioactivity at 5 min over the brush border and terminal web was demonstrated by Bedard *et al*[28]. They observed that during the next 3 h, radioactivity was present almost exclusively in absorptive cells and in lamina propria. In contrast, Conrad and Crosby[29] observed very little radioactivity in the small intestinal mucosa of iron-depleted and iron overload rats from 2-48 h after gastric administration of ^{59}Fe. This discrepancy may be due to the fact that they did not included time points earlier than 2 h. Because it is an inducible protein, it is possible that ferritin expression at the sites of absorption may be related to the iron status. This suggests that iron absorption is probably dependent on the relative concentrations of mucosal apo and holo ferritins, and is inhibited in conditions of iron overload and enhanced in iron deficiency.

Quantitatively, the amount of transferrin in the lumen is 10 times higher than that of mucosa and is not dependent on iron nutritional status (Table 1). The observation on identical amounts of luminal transferrin, irrespective of iron nutritional status, implies that this protein may be presenting equal amount of iron for absorption. The net amount of iron, which is taken up by the mucosa, thus depends on mucosal transferrin receptors. Duodenal mucosal transferrin receptor showed reciprocal relationship with iron status. The significance of this may be to present equal amounts of iron for absorption through binding to luminal transferrin. Consequently, the amount of iron absorbed by the mucosa may depend only on the mucosal transferrin receptor which has inverse relationship with better iron status.

Huebers *et al*[8,15] suggest that luminal transferrin acts as a shuttle protein for iron uptake. Autoradiographic studies by Conrad and Crosby[30] and Bedard *et al*[28] also suggest that intestinal crypt cells are able to take up transferrin-bound iron from circulation. According to some other investigators, however, transferrin is unlikely to be a major transporter of iron from lumen to the baso-lateral membrane[31-33]. According to Idzerda[34], the transferrin gene is not expressed in the intestine and, therefore, cannot be synthesized. Thus, it is possible that the luminal transferrin may be imported from plasma, as hypothesized by Parmley *et al*[19].

Although the receptor mediated cellular uptake of iron is well known and takes place in all dividing cells, such a mechanism operating in the intestine has not been documented earlier. The results of this study, in conjunction with earlier observations[5,35-37], allow us to propose a model for intestinal iron absorption whereby., the recycling of transferrin and transferrin receptors enables luminal transferrin bound iron to enter the enterocytes. The receptor density at the absorptive surface, which is inversely proportional to better iron nutritional status, might regulate this iron uptake process.

The presence of transferrin and its receptor on the margin during basal condition, and the appearance of both the receptor and the ligand at 15 min intraepithelially along with the radiolabelled iron in iron depleted rat intestine, support the above model. The appearance of TfR after 2 h on the margin of villi suggests that the receptor protein returned to the surface after releasing iron. In contrast, there was no evidence of intraepithelial transferrin and transferrin receptor in iron overloaded intestine, as evidenced by the presence of receptor on the margin even at 30 min.

Though the staining intensity of transferrin in duodenal section was high in control subjects, there was no obvious difference between iron deficient subject and blood transfused subjects. Staining for transferrin was intense in the apical portion and blood vessels, while that of transferrin receptor was more concentrated at the epithelial lining of duodenum (Figure 6). The higher intensity of transferrin receptor in iron deficient subjects and minimal in control and blood transfused subjects suggests a role for it in iron absorption. This is supported

by the reciprocal relationship observed between transferrin receptor and ferritin staining. Similar finding on TfR staining at the margin of the villi was observed by Banerjee *et al*[36] . The ultrastructural studies of Levine *et al*[31] have shown that transferrin receptor and transferrin are co-localized in coated pits on the basal and lateral membranes of crypt cells. Further, Anderson *et al*[35] confirmed that the TfR is a prominent protein on the basal and lateral membranes of intestinal epithelial cells.

The above findings, along with earlier observation, suggest that luminal transferrin must be presenting equal amount of iron for absorption since this protein does not respond to iron status. The net amount of iron taken up by mucosa depends on mucosal transferrin receptors, which respond reciprocally with better iron status. These results suggest that mucosal ferritin, luminal transferrin and mucosal cell surface transferrin receptors are closely related to iron status and interact with each other in carrying iron across the intestinal mucosa.

ACKNOWLEDGMENTS

Vasantha L Kolachala was the recipient of an Indian Council of Medical Research Fellowship. Grateful acknowledgement also to Dr. Rupender Prasad (Mahavir Hospital, Hyderbad, India), and Dr. A Vidyasagar and Dr. B Prahlad (Gandhi Hospital, Hyderabad, India) for their help in providing human biopsy specimens.

REFERENCES

1 **Bothwell TH**, Charlton RW. Current problems of iron overload. *Recent Results Cancer Res* 1979; **69**: 87-95
2 **Touret N**, Furuya W, Forbes J, Gros P, Grinstein S. Dynamic traffic through the recycling compartment couples the metal transporter Nramp2 (DMT1) with the transferrin receptor. *J Biol Chem* 2003; **278**: 25548-25557
3 **Conrad ME**, Umbreit JN, Moore EG, Hainsworth LN, Porubcin M, Simovich MJ, Nakada MT, Dolan K, Garrick MD. Separate pathways for cellular uptake of ferric and ferrous iron. *Am J Physiol Gastrointest Liver Physiol* 2000; **279**: G767-G774
4 **Conrad ME**, Umbreit JN. Pathways of iron absorption. *Blood Cells Mol Dis* 2002; **29**: 336-355
5 **Brittin GM**, Raval D. Duodenal ferritin synthesis during iron absorption in the iron-deficient rat. *J Lab Clin Med* 1970; **75**: 811-817
6 **Whittaker P**, Skikne BS, Covell AM, Flowers C, Cooke A, Lynch SR, Cook JD. Duodenal iron proteins in idiopathic hemochromatosis. *J Clin Invest* 1989; **83**: 261-267
7 **Pollack S**, Lasky FD. A new iron-binding protein isolated from intestinal mucosa. *J Lab Clin Med* 1976; **87**: 670-679
8 **Huebers H**, Huebers E, Rummel W, Crichton RR. Isolation and characterization of iron-binding proteins from rat intestinal mucosa. *Eur J Biochem* 1976; **66**: 447-455
9 **Savin MA**, Cook JD. Mucosal iron transport by rat intestine. *Blood* 1980; **56**: 1029-1035
10 **Osterloh K**, Forth W. Determination of transferrin-like immunoreactivity in the mucosal homogenate of the duodenum, jejunum, and ileum of normal and iron deficient rats. *Blut* 1981; **43**: 227-235
11 **Johnson G**, Jacobs P, Purves LR. Iron binding proteins of iron-absorbing rat intestinal mucosa. *J Clin Invest* 1983; **71**: 1467-1476
12 **Cox TM**, Mazurier J, Spik G, Montreuil J, Peters TJ. Iron binding proteins and influx of iron across the duodenal brush border. Evidence for specific lactotransferrin receptors in the human intestine. *Biochim Biophys Acta* 1979; **588**: 120-128
13 **Simpson RJ**, Osterloh KR, Raja KB, Snape SD, Peters TJ. Studies on the role of transferrin and endocytosis in the uptake of Fe3+ from Fe-nitrilotriacetate by mouse duodenum. *Biochim Biophys Acta* 1986; **884**: 166-171
14 **Worwood M**, Edwards A, Jacobs A. Non-ferritin iron compound in rat small intestinal mucosa during iron absorption. *Nature* 1971; **229**: 409-410
15 **Huebers HA**, Huebers E, Csiba E, Rummel W, Finch CA. The significance of transferrin for intestinal iron absorption. *Blood* 1983; **61**: 283-290
16 **Isobe K**, Isobe Y. Localization of transferrin in rat duodenal mucosa by immunoperoxidase technique. *Nihon Ketsueki Gakkai Zasshi* 1983; **46**: 797-807
17 **Mason DY**, Taylor CR. Distribution of transferrin, ferritin, and lactoferrin in human tissues. *J Clin Pathol* 1978; **31**: 316-327
18 **Levine DS**, Woods JW. Immunolocalization of transferrin and transferrin receptor in mouse small intestinal absorptive cells. *J Histochem Cytochem* 1990; **38**: 851-858
19 **Parmley RT**, Barton JC, Conrad ME. Ultrastructural localization of transferrin, transferrin receptor, and iron-binding sites on human placental and duodenal microvilli. *Br J Haematol* 1985; **60**: 81-89
20 **Parkkila S**, Waheed A, Britton RS, Bacon BR, Zhou XY, Tomatsu S, Fleming RE, Sly WS. Association of the transferrin receptor in human placenta with HFE, the protein defective in hereditary hemochromatosis. *Proc Natl Acad Sci USA* 1997; **94**: 13198-13202
21 **Gross CN**, Irrinki A, Feder JN, Enns CA. Co-trafficking of HFE, a nonclassical major histocompatibility complex class I protein, with the transferrin receptor implies a role in intracellular iron regulation. *J Biol Chem* 1998; **273**: 22068-22074
22 **Roy CN**, Blemings KP, Deck KM, Davies PS, Anderson EL, Eisenstein RS, Enns CA. Increased IRP1 and IRP2 RNA binding activity accompanies a reduction of the labile iron pool in HFE-expressing cells. *J Cell Physiol* 2002; **190**: 218-226
23 **Salter-Cid L**, Brunmark A, Li Y, Leturcq D, Peterson PA, Jackson MR, Yang Y. Transferrin receptor is negatively modulated by the hemochromatosis protein HFE: implications for cellular iron homeostasis. *Proc Natl Acad Sci USA* 1999; **96**: 5434-5439
24 **Waheed A**, Grubb JH, Zhou XY, Tomatsu S, Fleming RE, Costaldi ME, Britton RS, Bacon BR, Sly WS. Regulation of transferrin-mediated iron uptake by HFE, the protein defective in hereditary hemochromatosis. *Proc Natl Acad Sci USA* 2002; **99**: 3117-3122
25 **Reeves PG**, Nielsen FH, Fahey GC. AIN-93 purified diets for laboratory rodents: final report of the American Institute of Nutrition ad hoc writing committee on the reformulation of the AIN-76A rodent diet. *J Nutr* 1993; **123**: 1939-1951
26 **Bradford MM**. A rapid and sensitive method for the quantitation of microgram quantities of protein utilizing the principle of protein-dye binding. *Anal Biochem* 1976; **72**: 248-254
27 **Miyoshi H**, Ashida K, Hirata I, Ohshiba S, Naitoh T. Transferrin is not involved in initial uptake process of iron in rat duodenal mucosa. Ultrastructural study by x-ray energy spectrometry. *Dig Dis Sci* 1995; **40**: 1484-1490
28 **Bédard YC**, Pinkerton PH, Simon GT. [Iron absorption by the duodenal mucosa (author's transl)]. *Nouv Rev Fr Hematol* 1973; **13**: 727-743
29 **Crosby WH**, Conrad ME, Wheby MS. The rate of iron accumulation in iron storage disease. *Blood* 1963; **22**: 429-440
30 **Bédard YC**, Pinkerton PH, Simon GT. Uptake of circulating iron by the duodenum of normal mice and mice with altered iron stores, including sex-linked anemia: high resolution radioautographic study. *Lab Invest* 1976; **34**: 611-615
31 **Levine PH**, Levine AJ, Weintraub LR. The role of transferrin

in the control of iron absorption: studies on a cellular level. *J Lab Clin Med* 1972; **80**: 333-341
32 **Schümann K**, Osterloh K, Forth W. Independence of in vitro iron absorption from mucosal transferrin content in rat jejunal and ileal segments. *Blut* 1986; **53**: 391-400
33 **Mazurier J**, Montreuil J, Spik G. Visualization of lactotransferrin brush-border receptors by ligand-blotting. *Biochim Biophys Acta* 1985; **821**: 453-460
34 **Idzerda RL**, Huebers H, Finch CA, McKnight GS. Rat transferrin gene expression: tissue-specific regulation by iron deficiency. *Proc Natl Acad Sci USA* 1986; **83**: 3723-3727
35 **Anderson GJ**, Powell LW, Halliday JW. The endocytosis of transferrin by rat intestinal epithelial cells. *Gastroenterology* 1994; **106**: 414-422
36 **Banerjee D**, Flanagan PR, Cluett J, Valberg LS. Transferrin receptors in the human gastrointestinal tract. Relationship to body iron stores. *Gastroenterology* 1986; **91**: 861-869
37 **El-Shobaki FA**, Rummel W. Mucosal transferrin and ferritin factors in the regulation of iron absorption. *Res Exp Med* (Berl) 1977; **171**: 243-253

S- Editor Liu Y **L- Editor** Banati RB **E- Editor** Ma WH

PO Box 2345, Beijing 100023, China
www.wjgnet.com
wjg@wjgnet.com

World J Gastroenterol 2007 February 21; 13(7): 1053-1059
World Journal of Gastroenterology ISSN 1007-9327

BASIC RESEARCH

Influence of heme oxygenase-1 gene transfer on the viability and function of rat islets in *in vitro* culture

Xiao-Bo Chen, Yong-Xiang Li, Yang Jiao, Wei-Ping Dong, Ge Li, Jing Chen, Jian-Ming Tan

Xiao-Bo Chen, Yong-Xiang Li, Yang Jiao, Wei-Ping Dong, Jian-Ming Tan, Department of Renal Transplantation and Urology, the First People's Hospital, Shanghai Jiao Tong University; Shanghai Clinical Medical Center of Organ Transplantation , Shanghai 200080, China
Ge Li, Jing Chen, State Key Laboratory of Genetic Engineering, Institute of Genetics, School of Life Sciences, Fudan University, Shanghai 200433, China
Supported by the National Natural Science Foundation of China, No. 30571759 and Social Development Foundation of Shanghai, No. 2002-53
Correspondence to: Dr Jian-Ming Tan, Department of Renal Transplantation and Urology, the First People's Hospital, Shanghai Jiao Tong University; Shanghai Clinical Medical Center of Organ Transplantation, Shanghai 200080, China. jmtan156@yahoo.com.cn
Telephone: +86-21-63069482 Fax: +86-21-63069482
Received: 2006-10-14 Accepted: 2006-11-14

Abstract

AIM: To investigate the influence of heme oxygenase-1 (HO-1) gene transfer on the viability and function of cultured rat islets *in vitro.*

METHODS: Islets were isolated from the pancreata of Sprague-Dawley rats by intraductal collagenase digestion, and purified by discontinuous Ficoll density gradient centrifugation. Purified rat islets were transfected with adenoviral vectors containing human HO-1 gene (Ad-HO-1) or enhanced green fluorescent protein gene (Ad-EGFP), and then cultured for seven days. Transfection was confirmed by fluorescence microscopy and Western blot. Islet viability was evaluated by acridine orange/propidium iodide fluorescent staining. Glucose-stimulated insulin release was detected using insulin radioimmunoassay kits and was used to assess the function of islets. Stimulation index (SI) was calculated by dividing the insulin release upon high glucose stimulation by the insulin release upon low glucose stimulation.

RESULTS: After seven days culture, the viability of cultured rat islets decreased significantly (92% ± 6% *vs* 52% ± 13%, $P < 0.05$), and glucose-stimulated insulin release also decreased significantly (6.47 ± 0.55 mIU/L/30IEQ *vs* 4.57 ± 0.40 mIU/L/30IEQ, 14.93 ± 1.17 mIU/L/30IEQ *vs* 9.63 ± 0.71 mIU/L/30IEQ, $P < 0.05$). Transfection of rat islets with adenoviral vectors at an MOI of 20 was efficient, and did not impair islet function. At 7 d post-transfection, the viability of Ad-HO-1 transfected islets was higher than that of control islets (71% ± 15% *vs* 52% ± 13%, $P < 0.05$). There was no significant difference in insulin release upon low glucose stimulation (2.8 mmol/L) among Ad-HO-1 transfected group, Ad-EGFP transfected group, and control group ($P > 0.05$), while when stimulated by high glucose (16.7 mmol/L) solution, insulin release in Ad-HO-1 transfected group was significantly higher than that in Ad-EGFP transfected group and control group, respectively (12.50 ± 2.17 mIU/L/30IEQ *vs* 8.87 ± 0.65 mIU/L/30IEQ; 12.50 ± 2.17 mIU/L/30IEQ *vs* 9.63 ± 0.71 mIU/L/30IEQ, $P < 0.05$). The SI of Ad-HO-1 transfected group was also significantly higher than that of Ad-EGFP transfected group and control group, respectively (2.21 ± 0.02 *vs* 2.08 ± 0.05; 2.21 ± 0.02 *vs* 2.11 ± 0.03, $P < 0.05$).

CONCLUSION: The viability and function of rat islets decrease over time in *in vitro* culture, and heme oxygenase-1 gene transfer could improve the viability and function of cultured rat islets.

Key words: Islet viability; Islet function; Heme oxygenase-1; Gene transfer; Adenoviral vectors

Chen XB, Li YX, Jiao Y, Dong WP, Li G, Chen J, Tan JM. Influence of heme oxygenase-1 gene transfer on the viability and function of rat islets in *in vitro* culture. *World J Gastroenterol* 2007; 13(7): 1053-1059

http://www.wjgnet.com/1007-9327/13/1053.asp

INTRODUCTION

Diabetes affects more than 200 million people worldwide[1]. The mainstay treatment for type Ⅰ diabetic patients is chronic insulin injection. While exogenous insulin therapy has dramatically reduced mortality in diabetes, patients often succumb to the long-term sequelae of diabetic angiopathy, either in the form of nephropathy, neuropathy or retinopathy. Vascularized pancreas transplantation reliably restores normoglycemia and maintains long-term glucose homeostasis, but it has significant surgical morbidity and mortality[2]. In 2000, with the success of the 'Edmonton protocol', which had produced insulin independence in 85% of type Ⅰ diabetic patients one year after allogeneic islets transplantation combined with a non-steroid immunosuppressive regimen, islet transplantation has progressed from research to clinical reality[3].

The technique to maintain isolated islet preparations in tissue culture has been adopted by most islet transplant centers. Islet culture for a brief period (24 to 72 h) has emerged as the current standard procedure prior to clinical transplantation[4,5]. It offers advantages over immediate infusion post-isolation, enabling assessment of islet quality and safety, and reducing islet immunogenicity as well as recipient travel to the transplantation site and immunosuppression before transplantation[6]. But *in vitro* culture of islets has been shown to result in loss of viable tissue over time, and a decrease in glucose responsiveness has been observed in those islets which survive[7,8].

Several phenomena, including activation of free radicals, apoptosis and necrosis, may be responsible for these effects. Therefore, approaches towards enhancing islets resistance to these insults would facilitate both clinical and investigative trials. As a cellular graft, islets are especially suited for gene therapy. An attractive strategy for protecting islets in *in vitro* culture is to use gene therapy to transduce islets with cytoprotective genes that can make islets more resistant to injury.

Heme oxygenase-1 (HO-1) is the rate-limiting enzyme in the heme degradative pathway that catalyzes the oxidation of heme into biliverdin, carbon monoxide (CO), and free iron[9,10], and it has been described as a ubiquitous inducible stress protein capable of cytoprotection *via* radical scavenging and apoptosis prevention. Overexpression of HO-1 by chemical induction or gene therapy has been used to reduce the deleterious effects of oxidative stress and apoptosis in various cell types and animal models[11-14].

Compared with chemical induction, gene transfer can provide effective, targeted, and relatively persistent expression of HO-1. The aim of the present study was to investigate the influence of HO-1 gene transfer on the viability and function of cultured rat islets, and to explore the potential value of HO-1 gene transfer in islet transplantation.

MATERIALS AND METHODS

Animals

Twenty male Sprague-Dawley rats weighing 250 to 300 g were purchased from Shanghai Experimental Animal Center of Chinese Academy of Sciences.

Rat islet isolation and culture

Rat islets were isolated from the pancreata of the outbred male Sprague-Dawley rats by a collagenase digestion technique and discontinuous Ficoll density gradient centrifugation[15]. The main bile duct was located and clamped at both ends. Ten milliliters of collagenase *P* (Roche Applied Science, Indianapolis, Ind, USA) solution (1 g/L, pH 7.8) was injected into the duct and then the distended pancreas was surgically resected, and incubated at 38℃ for 15 min. The digested gland was vigorously shaken for 10 s and the digestion was stopped by Hank's solution (4℃) with 100 mL/L fetal calf serum (Gibco, BRL, USA). The tissue was filtered through a 600 μm screen, and then washed by Hank's solution twice. Islets were purified by centrifugation at 3000 r/min for 20 min on discontinuous Ficoll (Pharmacia Fine Chemicals, Uppsala, Sweden) gradients. After several washes with Hank's solution, islets were suspended in RPMI-1640 medium (Gibco, BRL, USA) containing 100 mL/L fetal calf serum (Gibco, BRL, USA), 20 mmol/L HEPES (Sigma-Aldrich Chemicals, Louis Mo, USA), 100 kU/L of penicillin and 100 g/L of streptomycin at 37℃ in a humidified atmosphere of 50 mL/L CO_2. Islets purity was assessed by dithizone (Sigma-Aldrich Chemicals, Louis Mo, USA) staining, and islets were counted and scored in size. An algorithm was used for the calculation of 150 μm-diameter islet equivalent number (IEQ).

Adenoviral vectors

Adenoviral vectors were prepared by use of the AdEasy system (Stratagene, Baltimore, USA). Human HO-1 cDNA was cloned into pAdTrack-CMV. Once constructed, the shuttle vector was linearized with *Pme* I and co-transformed into *E. coli* BJ5183 together with pAdEasy-1, the supercoiled viral DNA plasmid. Transformants were selected on kanamycin and the recombinants were subsequently identified by restriction digestion. Once a recombinant was identified, it was produced in bulk using the recombination-deficient XL10-Gold® strain. Purified recombinant adenoviral plasmid DNA was then linearized by *Pac* I to expose its inverted terminal repeats (ITR) and transfected into HEK293 cells where deleted viral genes necessary for virus assembly were complemented *in vivo*. The pAdEasy-1 vector will not replicate in cells other than complementing cells (293 cells). This vector has been developed to infect but not replicate in non-permissive target cells. Ad-EGFP was generated using the same system and supplied by the Institute of Genetics of Fudan University. Viral titers were determined by plaque assay and expressed as plaque forming units per mL (pfu/mL). Viral titers of Ad-HO-1 and Ad-EGFP were 1.96×10^9 and 1.99×10^9 pfu/mL, respectively.

Adenovirus infection

Aliquots of 30 IEQ were resuspended in 0.5 mL serum-free culture medium and placed in a 24-well culture plate and incubated with Ad-HO-1 and Ad-EGFP vectors at a multiplicity of infection (MOI) of 20 at 37℃ for 4 h with agitation every 1 h. MOI was calculated using the assumption that islets contain on average 1000 cells. After infection, islets were washed twice with culture medium and incubated for at least 48 h before further analysis to allow for transgene expression. Control islets were mock infected. Mock infected islets underwent a similar procedure, but were not exposed to viruses during the incubation period and were not incubated with any vectors.

Western blot analysis

Islet cells (48 h post-transfection) were washed with cold phosphate buffered saline (PBS) and lysed in 2% SDS, Tris-HCl 60 mmol/L (pH 6.8) buffer, incubated at 95℃, sonicated in a water bath at 37℃ and centrifuged at 12 000 r/min for 15 min. Assessment of the total protein content was carried out with the BCA detection kit (Pierce Biotechnology, Rockford, IL, USA). Aliquots corresponding to 100 μg of protein were subjected to electrophoresis on a 15% SDS-PAGE pre-cast gel

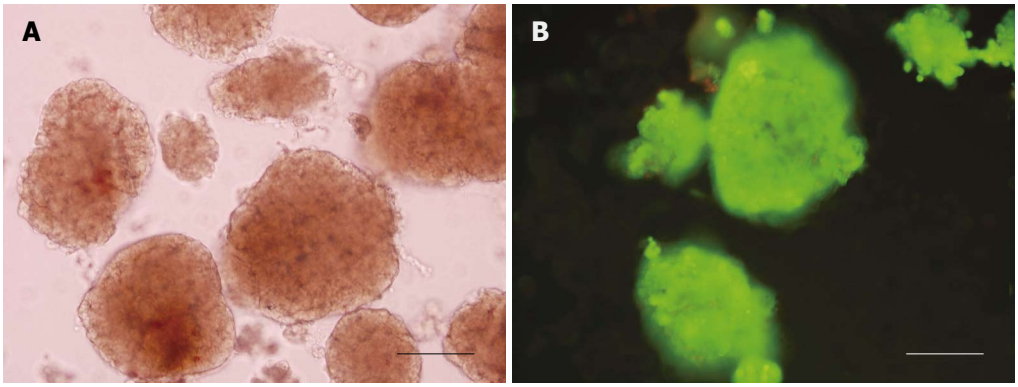

Figure 1 Purity and viability of freshly isolated rat islets. **A**: Islets stained with DTZ (red staining indicates islets; islet purity was above 90%); **B**: Islets stained with AO/PI (green staining indicated live cells, red staining indicated dead cells; islet via bility was above 90%). Bar = 150 μm, × 200 magnification.

and transferred electrophoretically to a nitrocellulose membrane. The membranes were incubated with 50 g/L non-fat dry milk in TBS (20 mmol/L Tris, 500 mmol/L NaCl, pH 7.5) overnight at 4℃ to block non-specific binding. The blots are then incubated with the murine antihuman HO-1 monoclonal antibodies (StressGen, Victoria, BC, Canada) at a dilution of 1:200 for 2 h at room temperature; this was followed by a 1 h incubation with the AP-conjugated rabbit antimouse polyclonal antibody (Promega, USA) at a dilution of 1:1000. The protein bands were visualized by the NBT + BCIP staining system (Haoyang Biological Manufacture Co, Ltd, Tianjin, China).

Islet viability

Islet viability was evaluated by acridine orange (AO)/propidium iodide (PI) (Sigma-Aldrich Chemicals, Louis Mo, USA) fluorescent staining. The fluorescent dye, containing 10 μL AO (670 μmol/L) and 1mL PI (750 μmol/L), was used at a 1:10 dilution. After the islets were washed twice with Hank's solution, the fluorescent dye was added to each well. Ten minutes later, islets were analyzed under a fluorescence microscope. Living cells were identified by green staining (AO), whereas dead cells showed a brown-red staining (PI).

Islet function

In vitro function of freshly isolated islets and cultured islets was assessed by glucose-stimulated insulin release. Islets of different groups were washed with PBS twice, and incubated first in low (2.8 mmol/L) and then in high (16.7 mmol/L) concentrations of glucose in culture medium. The static incubation assay was performed in a 24-well flat-bottomed culture plate with 30 IEQ/well and 3 duplicate wells for each islet group. Supernatant from each well was collected after each 1 h incubation, and the concentration was measured using an insulin radioimmunoassay kit (Jiuding Biotech Co, Ltd, Tianjin, China). Stimulation index (SI) was calculated by dividing the insulin release upon high glucose by the insulin release upon low glucose stimulation.

Statistical analysis

Data are expressed as mean ± SD. Statistical and graphical analysis was performed with software of SPSS10.0. Analyses were performed using the two-tailed Student's t-test where appropriate.

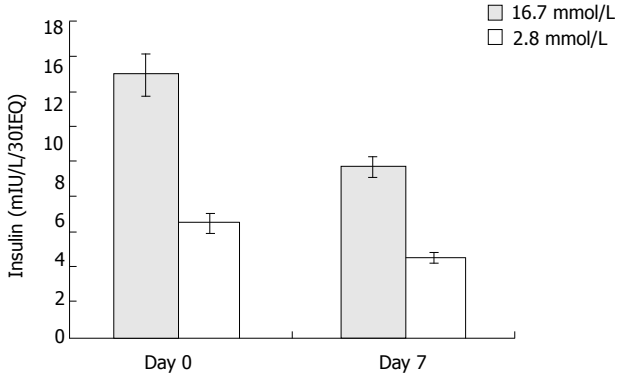

Figure 2 Effect of culture on glucose-stimulated insulin release. The insulin release upon either high or low glucose stimulation decreased conspicuously after seven days culture, $P < 0.05$

RESULTS

Purity and viability of freshly isolated rat islets

The purity of freshly isolated islets was above 90% calculated from the ratio of dithizone stained cells to dithizone nonstained cells as a percentage of the total cell number (Figure 1A). The viability of freshly isolated islets was above 90% calculated from the ratio of AO staining cells (living cells) to PI staining cells (dead cells) as a percentage of the total cell number (Figure 1B).

Effect of in vitro culture on insulin release

The glucose-stimulated insulin release was used to assess the function of cultured rat islets. As shown in Figure 2, after 7 d culture, the insulin release upon low and high glucose stimulation decreased from 6.47 ± 0.55 to 4.57 ± 0.40 mIU/L/30IEQ, and from 14.93 ± 1.17 to 9.63 ± 0.71 mIU/L/30IEQ, respectively. In other words, islet function decreased conspicuously over time in *in vitro* culture.

Exogenous gene expression in adenovirus-transduced rat islets

Typical fluorescence micro-photographs of rat islets transfected with Ad-EGFP at an MOI of 20 were taken at 48 h post-transfection. As shown in Figure 3A and B, the fluorescence in Ad-EGFP transfected islets was intense. Western blot was used to detect the expression of human HO-1 protein in three groups of islets. Figure 4 shows that human HO-1 protein was detected in Ad-HO-1 transfected islets but not in uninfected or Ad-

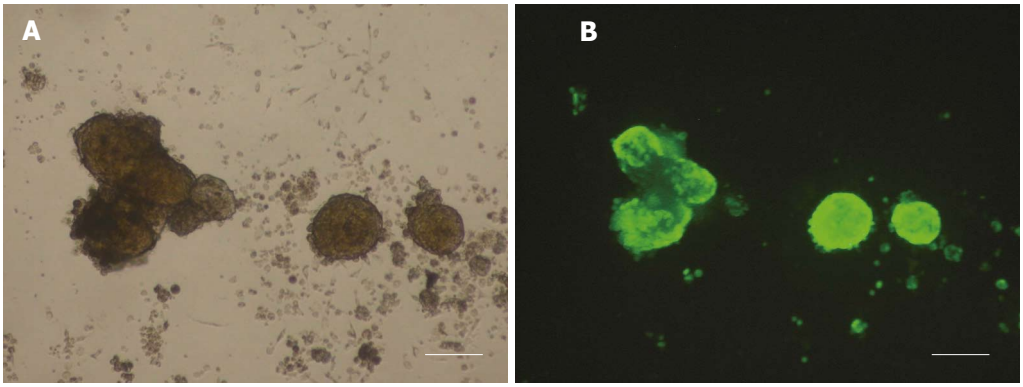

Figure 3 Ad-EGFP transduced islets. Microphotographs were taken at 48 h post-transfection (**A**, **B**). Fluorescence was intense at an MOI of 20 (**B**). Bar = 200 μm, × 100 magnification.

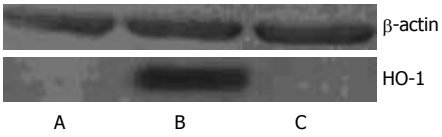

Figure 4 Western blot for hHO-1. Islets infected with Ad-HO-1, Ad-EGFP, or mock infected for 48 h were examined by Western blot. HO-1 expression was only detected in Ad-HO-1 group. A: control group; B: Ad-HO-1 group; C: Ad-EGFP group.

EGFP transfected islets. Therefore, adenovirus mediated exogenous gene transfer into rat islets was successful.

Effect of HO-1 gene transfer on the viability of cultured rat islets

The viability of islets was assessed by AO/PI fluorescent staining.

Representative pictures are shown in Figure 5. The viability of control islets was greatly reduced as shown by the large number of dead cells within the islets (Figure 5A). Nevertheless, the number of dead cells was reduced when islets were transfected with HO-1 gene (Figure 5B). Quantitative analysis of islet viability was performed by using fluorescence microscopy to determine the proportion of living cells within islets. As shown in Figure 5C, islet viability decreased greatly after 7 d culture (92% ± 6% *vs* 52% ± 13%, $P < 0.05$), but HO-1 gene transfer could reverse the viability reduction (71% ± 15% *vs* 52% ± 13%, $P < 0.05$).

Influence of adenoviral transfection on insulin release

Since adenoviral transfection at a high transfecting dose may damage islets and interfere with their biologic function[16], glucose-stimulated insulin release was employed to evaluate the influence of adenoviral transfection at an MOI of 20 on insulin release. As shown in Figure 6, there was no significant difference in glucose-stimulated insulin release between Ad-EGFP transfected islets and control islets at 7 d post-transfection (4.30 ± 0.40 *vs* 4.57 ± 0.40 mIU/L/30IEQ, 8.87 ± 0.65 *vs* 9.63 ± 0.71 mIU/L/30IEQ, respectively). It demonstrated that adenoviral transfection at an MOI of 20 was safe for islets.

Effect of HO-1 gene transfer on the function of cultured rat islets

After 7 d culture post transfection, the insulin release upon low and high glucose of uninfected (control islets), Ad-EGFP transfected, and Ad-HO-1 transfected islets were 4.57 ± 0.40 *vs* 9.63 ± 0.71 mIU/L/30IEQ, 4.30 ± 0.40 *vs* 8.87 ± 0.65 mIU/L/30IEQ, 5.67 ± 0.99 *vs* 12.50 ± 2.17 mIU/L/30IEQ, respectively. SI of control group, Ad-EGFP group, and Ad-HO-1 group were 2.11 ± 0.03, 2.08 ± 0.05, 2.21 ± 0.02, respectively. As shown in Figures 6 and 7, the insulin release upon high level glucose stimulation and SI of Ad-HO-1 transfected islets were significantly higher than those of Ad-EGFP transfected islets and control islets ($P < 0.05$). Therefore, HO-1 gene transfer can improve the function of cultured islets.

DISCUSSION

With recent advances in techniques of islet isolation and the introduction of more potent and less diabetogenic immunosuppressive therapies, islet transplantation has progressed from research to clinical reality, and it has been regarded as a safe and viable route to achieve insulin independence in a population of patients with type Ⅰ diabetes[3]. Many transplant protocols incorporate a period of short-term (24 to 72 h) islet culture before transplantation for the recipient to be treated with immunodepleting agents[4,5,17,18], and to provide time for *in vitro* assessment of islet quality. Short-term islet culture indeed has some benefits, such as purification of the islet preparation, immunomodulation[6], and possibly improved allograft survival. However, cultured islets are known to degrade rapidly[19,20], and lose viability and functional responsiveness to glucose stimulation with the extension of culturing time[7,8]. Islet loss as high as 30% to 50% has been reported after 48 hours of culture[21].

The islet, once removed from its natural surroundings within the pancreas and placed within the alien environment of the culture plate, becomes deprived of normal physiological organization and exposed to a number of hostile factors, such as hypoxia, activation of free radicals, apoptosis and necrosis that cause its premature demise. The quality of the transplanted islets is of the utmost importance to successfully achieve normal levels of glucose in transplant recipients, therefore, preservation of viability and function of islets post-isolation is a pre-requisite in islet transplantation. Pancreatic islets, as a cellular graft, are especially suited for gene therapy, as they can be infected efficiently *ex vivo* and then transplanted with minimal systemic exposure of the recipient to the vector.

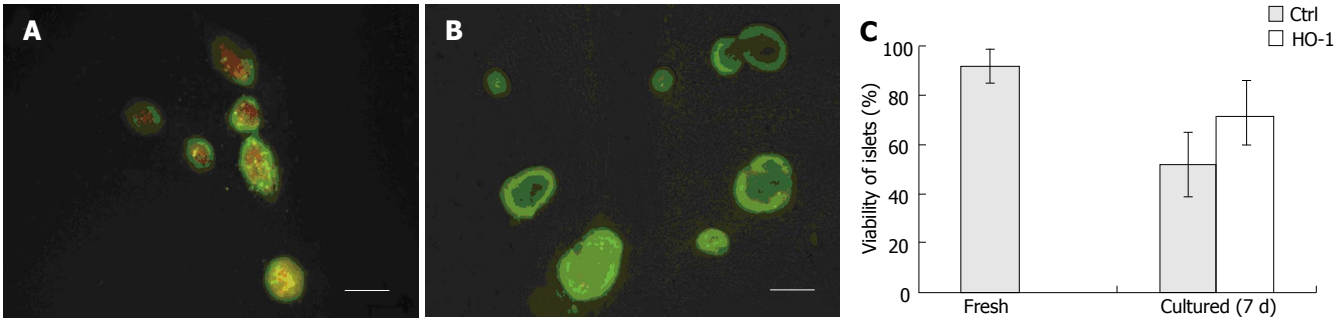

Figure 5 Effect of HO-1 gene transfer on the viability of cultured rat islets. At 7 d post-transfection, the control group showed the presence of numerous dead cells (red) at the center of the islets (**A**), while the Ad-HO-1 group showed more living cells (**B**). Bar = 200 Um, × 100 magnification. The islet viability was decreased greatly after 7 d culture ($P < 0.05$), whereas HO-1 gene transfer could reduce the loss of islet viability ($P < 0.05$).

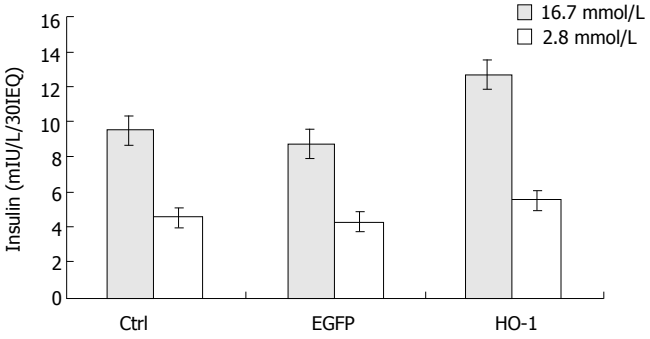

Figure 6 Effect of HO-1 gene transfer on insulin release of cultured rat islets. At 7 d post-transfection, no significant difference in glucose-stimulated insulin release was detected between Ad-EGFP transfected islets and control islets, however, the insulin release upon high glucose stimulation of Ad-HO-1 transfected islets was significantly higher than that of Ad-EGFP transfected islets and control islets, $P < 0.05$.

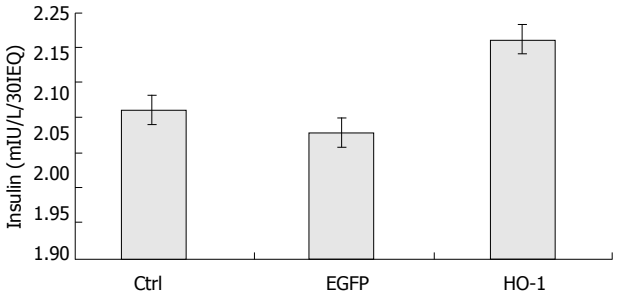

Figure 7 Effect of HO-1 gene transfer on stimulation index of cultured rat islets. The SI of Ad-HO-1 transfected islets was significantly higher than that of Ad-EGFP transfected islets and control islets, $P < 0.05$.

HO-1 has been identified as a ubiquitous stress protein induced in many cell types by various stimulants, such as hemolysis, inflammatory cytokines, oxidative stress, heat shock, heavy metals, and endotoxin[22]. HO-1 is the rate-limiting enzyme of heme degradation into its byproducts biliverdin, CO, and iron[9,10]. Biliverdin is subsequently reduced into bilirubin, a powerful anti-oxidant, and it may inhibit the generation of reactive oxygen species[23].

CO has a cytoprotective role in different systems[24-26], including pancreatic β-cells[27]. Heme catabolism by HO-1 also releases free iron, which has the potential to exacerbate the cytotoxic effects of reactive oxygen species[28,29].

However, generation of intracellular free iron upregulates the expression of ferritin[28,29], which has a high capacity to store free iron[29]. Ferritin has been shown to protect endothelial cells against activated neutrophils as well as H_2O_2-mediated cytotoxicity[29], suggesting that some of the effects of HO-1 may be mediated by ferritin[28,29]. As HO-1 is not expressed constitutively, it has been demonstrated that overexpression of HO-1 by chemical induction can protect islet cells from apoptosis and improve *in vivo* function after transplantation[22]. Compared with chemical induction, gene transfer can provide effective, targeted, and relatively persistent expression of HO-1.

Adenoviral vectors are useful for efficient gene delivery to differentiated and non-proliferating cells, such as isolated pancreatic islets[30]. In addition, adenoviral vectors can be produced in high titers and there is no risk of insertional mutagenesis as their genomes are not integrated into chromosomes. In the present study, recombinant adenoviral vectors were generated by use of the AdEasy system, and employed to transfect rat islets at an MOI of 20. According to fluorescence photographs taken at 48 h post-transfection, the expression of EGFP was intense. Furthermore, human HO-1 protein was detected by Western blot in Ad-HO-1 transfected islets at the same time. This demonstrated that recombinant adenoviral vectors were efficient to deliver exogenous genes into rat islets *in vitro*. Insulin release upon glucose stimulation was a measure of islet function, which was a prerequisite to any gene therapy program for diabetes treatment by islet transplantation[31]. In our experiments, no significant difference in glucose-stimulated insulin release was detected between Ad-EGFP transfected islets and control islets at 7 d post-transfection. This is consistent with the results reported by others showing that adenoviral vectors at a low transfecting dose (MOI 20) provided effective transfer of a marker gene into islet cells without impairing cell function[16].

Even though many clinical islet transplant protocols culture islets for only 24 to 72 h, islets were cultured for seven days in our study. This culture period was selected to minimize the effects of isolation factors on islet function, while maximizing the effect of culture. After

seven days culturing, the insulin release upon either low or high concentration glucose stimulation was significantly lower than that of freshly isolated islets ($P < 0.05$). This is consistent with previous reports showing that islet function degrades in *in vitro* culture over time. Nevertheless, the insulin release upon high concentration glucose stimulation and stimulation index (SI) of Ad-HO-1 transfected islets were significantly higher than those of Ad-EGFP transfected islets and control islets ($P < 0.05$). As glucose-stimulated insulin release was a favourable marker of the function of islets, our study demonstrated that HO-1 gene transfer conferred cytoprotection and improved islet function in *in vitro* culture. This was probably related to the effect of CO, which was not only a stimulator of insulin release but also a trigger of the transients of $[Ca^{2+}]$ i assumed to coordinate the secretory activity of the β-cells[32]. Furthermore, results of fluorescence microscopy studies with AO/PI staining indicated that HO-1 gene transfection significantly improved islet viability and survival during *in vitro* culture.

Despite the efficient transfection capacity of adenoviral vectors, the transgene cannot integrate into the host cell genome, leading to transient transgenic expression. In our study, we found that the EGFP expression time in cultured islets was more than 3 wk (data not shown). However, for some therapeutic strategies, such as islet cytoprotection in *in vitro* culture or early after transplantation, temporal expression of the cytoprotective transgene mediated by adenoviral vectors is still recommended because the factors related to early islet injury usually play a major role in the outcome of islet transplantation.

In summary, we demonstrated that adenoviral vectors could successfully transfer exogenous HO-1 gene into rat islet cells, and HO-1 gene transfer could improve rat islet viability and function in *in vitro* culture. Strategies using HO-1 gene transfer to islets might lead to better outcome in islet transplantation.

ACKNOWLEDGMENTS

We thank the staff of the Diabetes Research Laboratory, the First Affiliated Hospital of Shanghai Jiao Tong University, for helping us to isolate rat islets.

COMMENTS

Background

With recent advances in methods of islet isolation and the introduction of more potent and less diabetogenic immunosuppressive therapies, islet transplantation has progressed from research to clinical reality. Islet culture for a brief period (24 to 72 h) has emerged as the current standard procedure prior to clinical transplantation. Short-term islet culture indeed have some benefits, such as purification of the islet preparation, immunomodulation, assessment of islet quality, and possibly improved allograft survival. But *in vitro* culture of islets has been shown to result in a loss of viability over time, and a decrease in glucose responsiveness has been observed for those islets which survive.

As a cellular graft, islets are especially suited for gene therapy applications. HO-1 has been described as a ubiquitous inducible stress protein capable of cytoprotection via radical scavenging and apoptosis prevention. Overexpression of HO-1 can be chemically induced, but compared with chemical induction, gene transfer can provide effective, targeted, and relatively persistent expression of HO-1. It's an attractive strategy to protect islets *in vitro* culture by using gene therapy to transduce islets with cytoprotective gene that can make islets more resistant to injury.

Research frontiers

Although advances in islet isolation and less diabetogenic immunosuppression have moved islet transplantation forward from research to clinical reality, many challenges have to be faced with, such as keeping islet viable, single donor grafts, limited donor supply, tolerance induction.

Innovations and breakthroughs

Overexpression of HO-1 by chemical induction can protect islet cells from apoptosis and improve islet function. We used gene technique to modify rat islets *in vitro*, and found that HO-1 gene transfer could protect islet viability and function after seven days culture. Compared with chemical induction, gene transfer can provide effective, targeted, and relatively persistent expression of HO-1.

Applications

HO-1 gene transfer can improve islet viability and function. It suggests a potential therapeutic application for HO-1 gene in improving islet survival/function in islet transplantation.

Terminology

Islet equivalent (IEQ): islets with an average diameter of 150 μm.

Peer review

In this manuscript, Chen *et al.* have analyzed whether adenovirus-mediated gene transfer of heme oxygenase-1 into rat isolated pancreatic islets, affect the long term viability of the cells. This manuscript is well written, experiments and analyses of data are adequately performed.

REFERENCES

1 **Boyle JP**, Honeycutt AA, Narayan KM, Hoerger TJ, Geiss LS, Chen H, Thompson TJ. Projection of diabetes burden through 2050: impact of changing demography and disease prevalence in the U.S. *Diabetes Care* 2001; **24**: 1936-1940
2 **Stratta RJ**. Mortality after vascularized pancreas transplantation. *Surgery* 1998; **124**: 823-830
3 **Shapiro AM**, Lakey JR, Ryan EA, Korbutt GS, Toth E, Warnock GL, Kneteman NM, Rajotte RV. Islet transplantation in seven patients with type 1 diabetes mellitus using a glucocorticoid-free immunosuppressive regimen. *N Engl J Med* 2000; **343**: 230-238
4 **Hering BJ**, Kandaswamy R, Harmon JV, Ansite JD, Clemmings SM, Sakai T, Paraskevas S, Eckman PM, Sageshima J, Nakano M, Sawada T, Matsumoto I, Zhang HJ, Sutherland DE, Bluestone JA. Transplantation of cultured islets from two-layer preserved pancreases in type 1 diabetes with anti-CD3 antibody. *Am J Transplant* 2004; **4**: 390-401
5 **Hering BJ**, Kandaswamy R, Ansite JD, Eckman PM, Nakano M, Sawada T, Matsumoto I, Ihm SH, Zhang HJ, Parkey J, Hunter DW, Sutherland DE. Single-donor, marginal-dose islet transplantation in patients with type 1 diabetes. *JAMA* 2005; **293**: 830-835
6 **Kim SC**, Han DJ, Kim IH, Woo KO, We YM, Kang SY, Back JH, Kim YH, Kim JH, Lim DG. Comparative study on biologic and immunologic characteristics of the pancreas islet cell between 24 degrees C and 37 degrees C culture in the rat. *Transplant Proc* 2005; **37**: 3472-3475
7 **Schmied BM**, Ulrich A, Matsuzaki H, Ding X, Ricordi C, Moyer MP, Batra SK, Adrian TE, Pour PM. Maintenance of human islets in long-term culture. *Differentiation* 2000; **66**: 173-180
8 **Cui YF**, Ma M, Wang GY, Han DE, Vollmar B, Menger MD. Prevention of core cell damage in isolated islets of Langerhans by low temperature preconditioning. *World J Gastroenterol* 2005; **11**: 545-550
9 **Maines MD**. The heme oxygenase system: a regulator of second messenger gases. *Annu Rev Pharmacol Toxicol* 1997; **37**: 517-554
10 **Katori M**, Busuttil RW, Kupiec-Weglinski JW. Heme oxygenase-1 system in organ transplantation. *Transplantation* 2002; **74**: 905-912

11 **Tobiasch E**, Günther L, Bach FH. Heme oxygenase-1 protects pancreatic beta cells from apoptosis caused by various stimuli. *J Investig Med* 2001; **49**: 566-571

12 **Tsuburai T**, Suzuki M, Nagashima Y, Suzuki S, Inoue S, Hasiba T, Ueda A, Ikehara K, Matsuse T, Ishigatsubo Y. Adenovirus-mediated transfer and overexpression of heme oxygenase 1 cDNA in lung prevents bleomycin-induced pulmonary fibrosis via a Fas-Fas ligand-independent pathway. *Hum Gene Ther* 2002; **13**: 1945-1960

13 **McCarter SD**, Akyea TG, Lu X, Bihari A, Scott JR, Badhwar A, Dungey AA, Harris KA, Feng Q, Potter RF. Endogenous heme oxygenase induction is a critical mechanism attenuating apoptosis and restoring microvascular perfusion following limb ischemia/reperfusion. *Surgery* 2004; **136**: 67-75

14 **Wang XH**, Wang K, Zhang F, Li XC, Li J, De W, Guo J, Qian XF, Fan Y. Heme oxygenase-1 alleviates ischemia/reperfusion injury in aged liver. *World J Gastroenterol* 2005; **11**: 690-694

15 **Sutton R**, Peters M, McShane P, Gray DW, Morris PJ. Isolation of rat pancreatic islets by ductal injection of collagenase. *Transplantation* 1986; **42**: 689-691

16 **Weber M**, Deng S, Kucher T, Shaked A, Ketchum RJ, Brayman KL. Adenoviral transfection of isolated pancreatic islets: a study of programmed cell death (apoptosis) and islet function. *J Surg Res* 1997; **69**: 23-32

17 **Stock PG**, Bluestone JA. Beta-cell replacement for type I diabetes. *Annu Rev Med* 2004; **55**: 133-156

18 **Markmann JF**, Deng S, Huang X, Desai NM, Velidedeoglu EH, Lui C, Frank A, Markmann E, Palanjian M, Brayman K, Wolf B, Bell E, Vitamaniuk M, Doliba N, Matschinsky F, Barker CF, Naji A. Insulin independence following isolated islet transplantation and single islet infusions. *Ann Surg* 2003; **237**: 741-749; discussion 749-750

19 **Brendel MD**, Kong SS, Alejandro R, Mintz DH. Improved functional survival of human islets of Langerhans in three-dimensional matrix culture. *Cell Transplant* 1994; **3**: 427-435

20 **Korbutt GS**, Pipeleers DG. Cold-preservation of pancreatic beta cells. *Cell Transplant* 1994; **3**: 291-297

21 **London NJ**, Swift SM, Clayton HA. Isolation, culture and functional evaluation of islets of Langerhans. *Diabetes Metab* 1998; **24**: 200-207

22 **Pileggi A**, Molano RD, Berney T, Cattan P, Vizzardelli C, Oliver R, Fraker C, Ricordi C, Pastori RL, Bach FH, Inverardi L. Heme oxygenase-1 induction in islet cells results in protection from apoptosis and improved in vivo function after transplantation. *Diabetes* 2001; **50**: 1983-1991

23 **Stocker R**, Yamamoto Y, McDonagh AF, Glazer AN, Ames BN. Bilirubin is an antioxidant of possible physiological importance. *Science* 1987; **235**: 1043-1046

24 **Brouard S**, Otterbein LE, Anrather J, Tobiasch E, Bach FH, Choi AM, Soares MP. Carbon monoxide generated by heme oxygenase 1 suppresses endothelial cell apoptosis. *J Exp Med* 2000; **192**: 1015-1026

25 **Peyton KJ**, Reyna SV, Chapman GB, Ensenat D, Liu XM, Wang H, Schafer AI, Durante W. Heme oxygenase-1-derived carbon monoxide is an autocrine inhibitor of vascular smooth muscle cell growth. *Blood* 2002; **99**: 4443-4448

26 **Maines MD**. Heme oxygenase 1 transgenic mice as a model to study neuroprotection. *Methods Enzymol* 2002; **353**: 374-388

27 **Günther L**, Berberat PO, Haga M, Brouard S, Smith RN, Soares MP, Bach FH, Tobiasch E. Carbon monoxide protects pancreatic beta-cells from apoptosis and improves islet function/survival after transplantation. *Diabetes* 2002; **51**: 994-999

28 **Ferris CD**, Jaffrey SR, Sawa A, Takahashi M, Brady SD, Barrow RK, Tysoe SA, Wolosker H, Barañano DE, Doré S, Poss KD, Snyder SH. Haem oxygenase-1 prevents cell death by regulating cellular iron. *Nat Cell Biol* 1999; **1**: 152-157

29 **Balla G**, Jacob HS, Balla J, Rosenberg M, Nath K, Apple F, Eaton JW, Vercellotti GM. Ferritin: a cytoprotective antioxidant strategem of endothelium. *J Biol Chem* 1992; **267**: 18148-18153

30 **Wilson JM**. Adenoviruses as gene-delivery vehicles. *N Engl J Med* 1996; **334**: 1185-1187

31 **Fernandes JR**, Duvivier-Kali VF, Keegan M, Hollister-Lock J, Omer A, Su S, Bonner-Weir S, Feng S, Lee JS, Mulligan RC, Weir GC. Transplantation of islets transduced with CTLA4-Ig and TGFbeta using adenovirus and lentivirus vectors. *Transpl Immunol* 2004; **13**: 191-200

32 **Lundquist I**, Alm P, Salehi A, Henningsson R, Grapengiesser E, Hellman B. Carbon monoxide stimulates insulin release and propagates Ca^{2+} signals between pancreatic beta-cells. *Am J Physiol Endocrinol* Metab 2003; **285**: E1055-E1063

S- Editor Wang J **L- Editor** Zhu LH **E- Editor** Lu W

PO Box 2345, Beijing 100023, China
www.wjgnet.com
wjg@wjgnet.com

World J Gastroenterol 2007 February 21; 13(7): 1060-1066
World Journal of Gastroenterology ISSN 1007-9327

BASIC RESEARCH

Uric acid enhances T cell immune responses to hepatitis B surface antigen-pulsed-dendritic cells in mice

Xiao-Jun Ma, De-Ying Tian, Dong Xu, Dao-Feng Yang, Hui-Fen Zhu, Zhi-Hui Liang, Zheng-Gang Zhang

Xiao-Jun Ma, De-Ying Tian, Dong Xu, Dao-Feng Yang, Zheng-Gang Zhang, Department of Infectious Diseases, Tongji Hospital, Tongji Medical College, Huazhong University of Science and Technology, Wuhan 430030, Hubei Province, China
Hui-Fen Zhu, Zhi-Hui Liang, Department of Immunology, Tongji Medical College, Huazhong University of Science and Technology, Wuhan 430030, Hubei Province, China
Supported by the National Natural Science Foundation of China, No. 30471533
Correspondence to: Dr. De-Ying Tian, Department of Infectious Diseases, Tongji Hospital, Tongji Medical College, Huazhong University of Science and Technology, Jiefang Avenue 1095,Wuhan 430030, Hubei Province, China. langz2004@126.com
Telephone: +86-27-69807982 Fax: +86-27-83613408
Received: 2006-11-12 Accepted: 2006-12-25

Abstract

AIM: To study the induction of T cellular immune responses in BALB/c mice immunized with uric acid and dendritic cells (DCs) pulsed with hepatitis B virus surface antigen (HBsAg).

METHODS: DCs were generated from bone-marrow cells of BABL/c mice, and then pulsed or unpulsed with HBsAg protein (HBsAg-pulsed-DCs or unpulsed-DCs) in vitro. BABL/c mice were immunized with HBsAg-pulsed-DCs (1×10^6) and uric acid, injected through the tail vein of each mouse. The mice in control groups were immunized with HBsAg-pulsed-DCs alone, unpulsed-DCs alone or 200 μg uric acid alone or PBS alone. The immunization was repeated 7 d later. Cytotoxic T lymphocytes (CTLs) *in vivo* were determined by the CFSE labeled spleen lysis assay. Spleen cells or spleen T cells were isolated, and re-stimulated *in vitro* with HBsAg for 120 h or 72 h. Production of IFN-γ and IL-4 secreted by spleen cells were determined by ELISA method; proliferation of spleen T cells were detected by flow cytometry.

RESULTS: The cytotoxicities of HBsAg-specific-CTLs, generated after immunization of HBsAg-pulsed-DCs and uric acid, were 68.63% ± 11.32% and significantly stronger than that in the control groups ($P < 0.01$). Compared with control groups, in mice treated with uric acid and HBsAg-pulsed-DCs, the spleen T cell proliferation to HBsAg re-stimulation was stronger (1.34 ± 0.093 *vs* 1.081 ± 0.028, $P < 0.01$), the level of IFN-γ secreted by splenocytes was higher (266.575 ± 51.323 *vs* 135.223 ± 32.563, $P < 0.01$) , and IL-4 level was lower (22.385 ± 2.252 *vs* 40.598 ± 4.218, $P < 0.01$).

CONCLUSION: Uric acid can strongly enhance T cell immune responses induced by HBsAg-pulsed-DCs vaccine. Uric acid may serve as an effective adjuvant of DC vaccine against HBV infection.

Key words: Uric acid; Dendritic cells; Hepatitis B virus surface antigen; Cytotoxic T lymphocytes; Mouse

Ma XJ, Tian DY, Xu D, Yang DF, Zhu HF, Liang ZH, Zhang ZG. Uric acid enhances T cell immune responses to hepatitis B surface antigen-pulsed-dendritic cells in mice. *World J Gastroenterol* 2007; 13(7): 1060-1066

http://www.wjgnet.com/1007-9327/13/1060.asp

INTRODUCTION

It is generally accepted that dendritic cells (DCs) are the most efficient and powerful antigen presenting cells and play a center role in exciting T cell immune reactions. T-cell mediated immune responses, especially Hepatitis B virus (HBV) specific- cytotoxic T lymphocyte (CTL) response, may play an important role in resolving HBV infection[1,2]. hepatitis B surface antigen (HBsAg) pulsed DCs can activate lymphocytes to become HBsAg-specific CTLs or specific $CD4^+$ T cells *in vivo*[3]. Shimizu *et al*[4] immunized HBV transgenic mice with DCs loading HBsAg, and found that DC vaccine could break tolerance to HBV and induce an effective anti-viral immune response. Chen *et al*[5] reported that HBsAg-pulsed DCs from the peripheral blood could effectively suppress HBV replication in chronic hepatitis B patients. However, anti-HBV immune effects of DC vaccine are varied and instable. This may be due to the diversity of DC vaccine preparations; however, the main cause may be the insufficiency of DC vaccines. For example, some researchers carried out similar immune therapy in volunteers, but no evident immune response was shown[3,6-8]. Therefore, the basic research of DC vaccine as well as how to improve the immune response to DC vaccine is still a significant challenge.

Recently, it was reported that uric acid (UA) could stimulate DCs to mature, promote DCs to present foreign antigens and stimulate T lymphocytes[9,10]. These findings demonstrate the adjuvant effects of uric acid and encourage the potential application of uric acid in

vaccination.

This study aimed to observe the T cell immune response after immunization with HBsAg pulsed DCs (HBsAg-pulsed-DCs) and uric acid in mice. The results demonstrated that administration of uric acid could enhance the T cell immune response to HBsAg-pulsed-DCs.

MATERIALS AND METHODS

Mice

Male or female BALB/c (H-2^d) mice aged 8 to 10 wk were obtained from the Department of Experimental Animals, Tongji Medical College, Huazhong University of Science and Technology, Wuhan, China. All animal experiments followed the guidelines for the care and use of animals established by Tongji Medical College, Huazhong University of Science and Technology, and were approved by the Ethics Committee of Tongji Medical College.

Agents

Uric acid (UA, Sigma-aldrich) was dissolved at a concentration of 5 mg/mL in 0.1 mol/L sodium borate buffer (pH 8.5) for more than 72 h[9,11]. The HBsAg protein was synthesized by Shanghai SanGon Company, China. The purity (> 99%) of the protein was confirmed by high performance liquid chromatography (HPLC) and mass spectrometry. Carboxy-fluorescein diacetate, succinimidyl ester (CFSE, Molecular Probes, USA) was dissolved in dimethyl sulfoxide (DMSO) at a concentration of 10 mmol/L.

Preparation and culture of bone marrow DCs

DCs were prepared as described previously[12]. Briefly, bone marrow cells were collected from the femur and tibiae of BALB/c mice, and DCs were grown from precursors at a starting concentration of 2×10^6 cells per ml in complete RPMI 1640 (RPMI 1640 supplemented with 10% inactivated fetal calf serum, 2 mmol/L L-glutamine, 100 U/mL penicillin G and 100 μg/mL streptomycin), and cultured in six-well flat bottom plates (Falcon) at 37℃, 5% CO_2 for 3 h and then non-adherent cells were washed out. rmGM-CSF at 10 ng/mL (PeproTech, Rocky Hill, NJ) and rmIL-4 at 10 ng/mL (PeproTech, Rocky Hill, NJ) were added to the culture. On days 3, 5 and 7, half of the medium was replaced with a fresh medium. On day 7, cells were incubated with uric acid (100, 200 and 400 μg/mL) or 1 μg/mL lipopolysaccharide (LPS, Sigma), respectively. Serum-free RPMI 1640 was used as control. On day 9, cells and culture supernatants were collected for further experiments and analysis.

Analysis of cell surface markers on DCs by flow cytometry

Expression of DC cell surface molecules (CD11c, CD83, IA/IE, CD86) were determined by flow cytometric analysis. Cells were washed twice with an ice cold FACScan buffer (PBS containing 2% FCS and 0.1% sodium azide). The same buffer was used for the incubation with antibodies as well as for all washes. Twenty percent of mixed sera of mice and rats were used to prevent nonspecific antibody binding. FITC-conjugated anti-mouse CD1lc (Clone: N418, eBioscience) and IA/IE(Clone: M5/114.15.2, eBioscience) or PE-conjugated anti-mouse CD83 (Clone:Michel-17, eBioscience) and CD86 (Clone: RMMP-2, Caltag Laboratories) were added, respectively, to the cells and the samples were left on ice for 45 min in the dark. Fluorescence profiles were generated on an FACScan flow cytometer (Becton Dickinson). Histogram was produced with the CellQuest software package.

Measurement of IL-12P70 concentrations

The concentration of IL-12P70 in DC culture supernatants was determined by using an enzyme-linked immunosorbent assay (ELISA) kit (R&D Systems) according to the manufacturer's instructions.

Preparation of HBsAg-pulsed-DCs

Mature DCs stimulated by 1 μg/mL LPS were collected and used to pulse with HBsAg. The procedure for pulsing DCs was the same as previously described[13]. Briefly, 1×10^6 mature DCs were incubated with 10 μg/mL HBsAg for 6 h. DCs were washed three times and resuspended in PBS.

Immunization of mice

Totally 1×10^6 HBsAg-pulsed-DCs (total volume 200 μL) were injected through the tail vein of each mouse, together with 200 μg uric acid. The mice immunized with HBsAg-pulsed-DCs (1×10^6) or unpulsed-DCs (1×10^6) alone were used as controls. The mice treated with 200 μg uric acid or 200 μL PBS alone were used as controls as well. Ten mice were in each group. The immunization was repeated 7 d later.

Assay of CTL cytotoxic activity in vivo

Seven days after immunization with DCs for the second and last time, each mouse received spleen cells labeled with CFSE. To prepare target cells to detect in vivo cytotoxic activity[14,15], erythrocytes were removed from naive BALB/c spleen cell suspensions by lysis in ammonium chloride solution. The cells were then washed and split into two populations. One population was pulsed with 10 μg/mL HBsAg, incubated at 37℃ for 4 h, and labeled with a high concentration of CFSE (5.0 μmol/L) (CFSE^{high} cells). Another population as control target cells was left without HBsAg and was labeled with a low concentration of CFSE (0.5 μmol/L) (CFSE^{low} cells)[16]. An equal number of cells from each population were mixed together, and each mouse received a total of 2×10^7 mixed cells in 400 μL of PBS. Cells were intravenously injected into all mice as above. And 10 h later, the mice were sacrificed and their spleen cells were obtained. Cell suspensions were analyzed by flow cytometry, and each population was detected for their differential CFSE fluorescence intensities. Up to 1×10^4 CFSE-positive cells were collected for analysis. To calculate specific lysis, the following formula was used: Ratio = (percentage CFSE^{low}/percentage CFSE^{high}). Percentage specific lysis = [1- (ratio unprimed/ratio primed) × 100][14,15].

Cytokine production by spleen cells

Spleen cells from the immunized mice were depleted

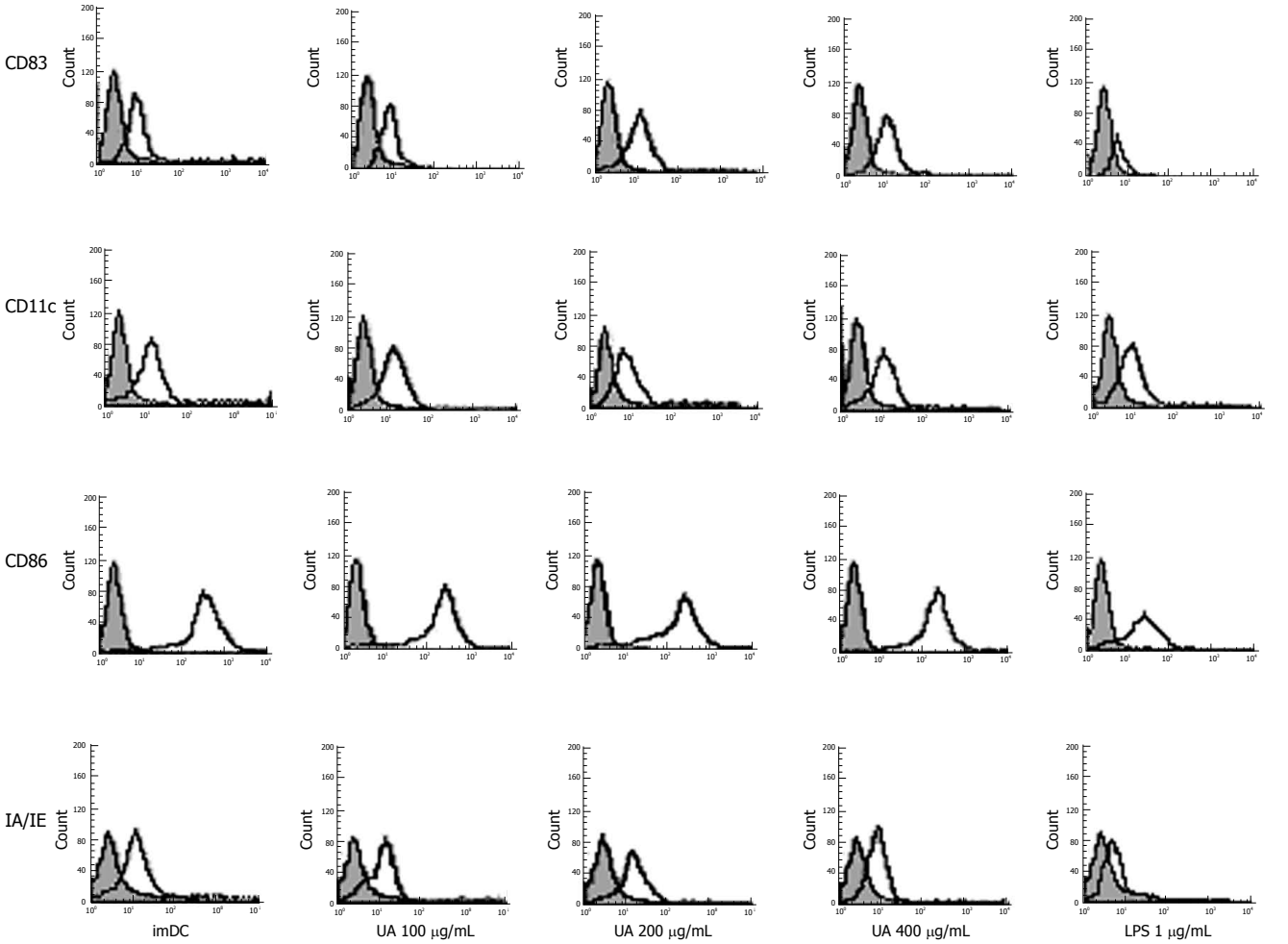

Figure 1 The cell surface markers analysis on dendritic cells by flow cytometry after exposure to uric acid or LPS. Bone marrow-derived DCs were stimulated with 100, 200 and 400 μg/mL uric acid or 1 μg/mL LPS or Serum-free RPMI media 1640 for 48 h and immunostained with mAbs against CD11c, CD83, CD86 and IA/IE molecules (open histograms). Shade histograms represent the isotype control mAb staining of the cells. The histograms (Figure 1) and data (Table 1) are representative of five independent experiments.

of erythrocytes and washed twice with PBS. The cells obtained were resuspended with complete RPMI 1640, and seeded in duplicate into flat-bottomed 24-well microtitration plates(Costar, Brumath, France) at 2×10^6 cells per well in 1 mL of culture medium containing 10 μg/mL HBsAg. The cell-free culture supernatants were harvested after 72 h and assayed for IFN-γ and IL-4 activity. The cytokine concentrations were determined by using a commercial ELISA kit (eBioscience Inc.) according to the manufacturer's instructions, and the standard curves corresponding to known amounts of mouse recombinant IFN-γ, IL-4. The sensitivity limits for the assays are 15 pg/mL for IFN-γ, and 4 pg/mL for IL-4.

Cell proliferative response of spleen T cells

Erythrocytes were removed from the spleen cells of mice 14 d after immunization as above. The cells were resuspended with complete RPMI 1640, and then T cells were separated by a nylon wool column method[17]. In brief, 1×10^8 cells were drained through a nylon wool column (Polysciences. Inc., Warrington, PA) for 45 min at 37℃, and then nonadherent T cells were collected after two washes. T cells were labeled with 2.5 μmol/L CFSE and washed three times in the medium as described above, counted, and resuspended at a concentration of 1×10^6 cells/mL. The samples were seeded in triplicate into 24-well microtitration plates (Costar, Brumath, France) at 2×10^6 cells per well in 2 mL of culture medium containing 10 μg/mL HBsAg or PBS. T cells from the untreated mice were used as the negative control; and T cells from the untreated mice stimulated with 10 μg/mL concanavalin A (ConA) and 10 μg/mL HBsAg or PBS was served as the positive controls. The plates were incubated for 72 h in 5% CO_2 at 37℃. Cell proliferation was estimated by flow cytometry[16]. Histogram was produced with the Motif 3.0 software package.

Statistical analysis

All data were presented as mean ± SD and analyzed using the Student-Newman-Keuls test and LSD multiple comparisons with SPSS11.5 software in the experiments. $P < 0.05$ was regarded as statistically significant.

RESULTS

Cell surface markers on DCs

We demonstrated an increase in CD83, IA/IE, and CD86 expression by DCs, stimulated with uric acid previously (Figure 1, Table 1). The effect of uric acid was dose-dependent and was still observed when the uric acid was

Table 1 Surface molecular expression of DCs (%, mean ± SD)

Group	*n*	CD11C	CD83	CD86	MHC
RMPI-1640	5	72.85 ± 1.64	21.66 ± 5.34[f]	37.77 ± 1.62[f]	27.34 ± 1.81[f]
UA100	5	73.16 ± 1.05	47.71 ± 4.75[b,d]	78.48 ± 2.98[b,f]	75.83 ± 2.49[b,f]
UA200	5	73.18 ± 0.95	52.23 ± 0.83[b]	80.14 ± 1.01[b]	79.47 ± 0.92[b]
UA400	5	73.36 ± 1.46	52.33 ± 0.94[b]	81.08 ± 1.25[b]	80.36 ± 1.22[b]
LPS	5	73.44 ± 1.33	53.28 ± 1.12[b]	82.50 ± 2.29[bb]	81.42 ± 2.21[b]

[b]$P < 0.001$ *vs* RMPI-1640; [d]$P < 0.01$ *vs* LPS; [f]$P < 0.001$ *vs* LPS.

Table 2 IL-12 p70 production in DC supernatants (mean ± SD, *n* = 5, ng/mL)

Group	imDC	UA100	UA200	UA400	LPS
IL-12P70	2.53 ± 0.27	3.52 ± 0.22[b]	3.99 ± 0.28[b]	4.37 ± 0.19[b]	4.38 ± 0.17[b]

[b]$P < 0.001$ *vs* imDC.

Table 3 IFN-γ production of spleen cells (mean ± SD, *n* = 10, pg/mL)

Group	IL-4	γ-IFN
PBS	40.598 ± 4.218	135.223 ± 32.563
UA	39.387 ± 3.657	141.500 ± 32.654
Unpulsed-DC	37.352 ± 3.238	149.32 ± 37.354
HBsAg-pulsed-DC	22.385 ± 2.252[b]	266.575 ± 51.323[b]
UA-DC	15.123 ± 1.353[d]	429.216 ± 59.232[d]

[b]$P < 0.01$, [d]$P < 0.001$ *vs* PBS group.

administered at 100 μg/mL. After stimulation with uric acid (100-400 μg/mL), the percentage of various markers increased from 2.0- fold to 3.0-fold. The stimulatory effect elicited by uric acid at a concentration of 200-400 μg/mL was similar to that induced by LPS (1 μg/mL). After stimulation with uric acid or LPS, the CD11c expression in each group was high and similar, including the imDC group.

IL-12 p70 production in DC supernatants

Using the ELISA technique, the IL-12 p70 secretion by DCs was detected 48h after stimulation with uric acid or LPS. IL-12p70 production was markedly increased in response to uric acid stimulation in a dose-dependent manner. The IL-12p70 production stimulated by 200-400 μg/mL uric acid was similar to LPS treatment (Table 2).

Cytokine production by spleen cells

The supernatants of cultured immune spleen cells were evaluated for the production of IL-4 (Th2 cytokine) or IFN-γ (Th1 cytokine) in response to HBsAg re-stimulation on day 14 (Figure 2, Table 3).

The production of IL-4 in mice immunized with HBsAg-pulsed-DCs and uric acid was lower than that of mice immunized with HBsAg-pulsed-DCs alone or unpulsed-DCs alone or PBS alone($P < 0.001$ for all) (Figure 2A).

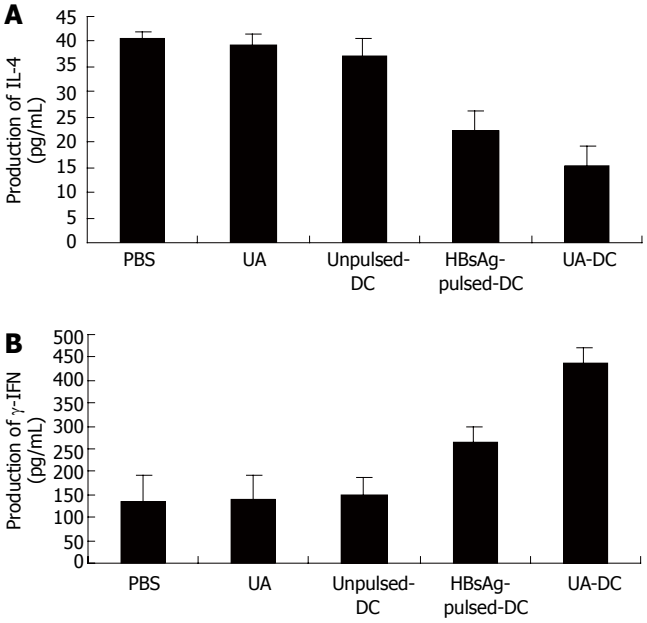

Figure 2 Cytokine production by splenocytes. Fourteen days after immunization, spleen cells were isolated, then stimulated with HBsAg (10 μg/mL) *in vitro*. Values were measured at 72 h for IL-4 (**A**), IFN-γ (**B**) by ELISA. The results are representative of ten samples from each group. The data show the mean ± SD.

The production of IFN-γ (Figure 2B) in mice immunized with HBsAg-pulsed-DCs and uric acid was significantly greater ($P < 0.001$ for all) than that in mice immunized with HBsAg-pulsed-DCs alone. Spleen cells from mice immunized with unpulsed-DCs alone or PBS alone produced a few IFN-γ.

Spleen cells from mice immunized with uric acid alone failed to enhance the secretion of IFN-γ or inhibit the secretion of the IL-4 (Figure 2).

Cell proliferative response in spleen T cells

Fourteen days after immunization, CFSE-labeled-T cells from each mouse were re-stimulated with 10 μg/mL HBsAg or PBS for 72 h *in vitro*, and cellular proliferations were assayed by flow cytometry (Figure 3, Table 4).

A strong proliferative response to HBsAg re-stimulation was observed in T cells of mice immunized with HBsAg-pulsed-DCs and uric acid (Figure 3).

Proliferative response to HBsAg re-stimulation was also observed in T cells of mice treated with HBsAg-pulsed-DCs. Insignificant proliferation was observed in T cells of mice treated with unpulsed-DCs. No proliferation to HBsAg re-stimulation was observed in T cells of mice treated with uric acid alone or PBS (Figure 3).

PBS re-stimulation *in vitro* failed to stimulate T cell proliferation in each mouse (Table 4).

Determination of HBsAg-specific-CTL cytotoxicity

We directly determined the activity of HBsAg-specific-CTLs with an in vivo cytotoxicity assay. The extent of lysis of HBsAg-pulsed spleen cells was expressed as R-values (Figure 4) and the cytotoxicity activity of HBsAg-specific-CTLs were calculated (Table 5).

A significant strong cytotoxicity of HBsAg-specific CTLs was observed in the mice immunized with HBsAg-pulsed-DCs and uric acid; whereas immunization with

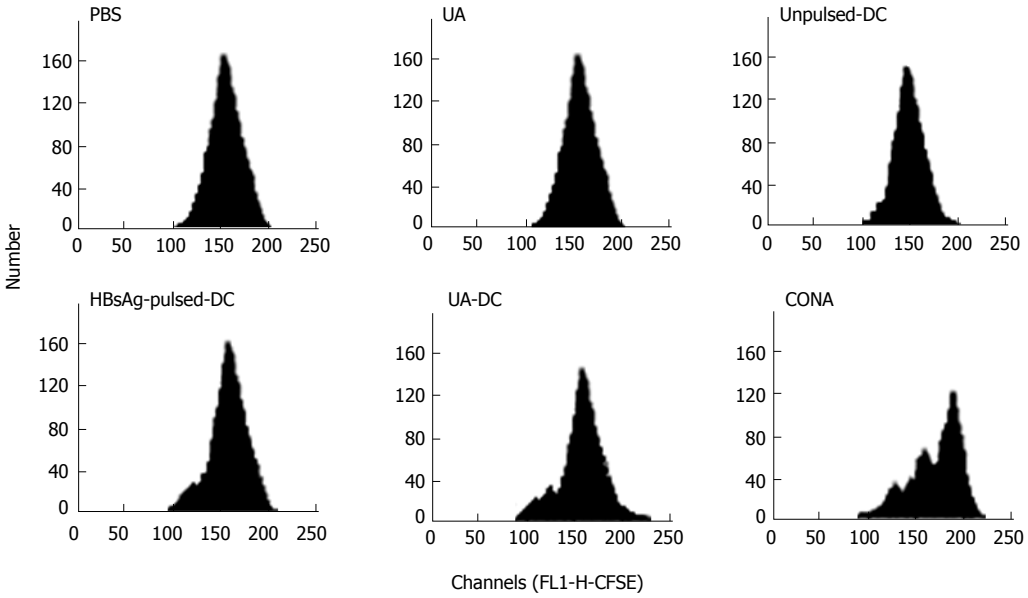

Figure 3 Celluar proliferative response in spleen T cells after stimulation with HBsAg or PBS for 72 h *in vitro*. Celluar proliferative response was estimated by flow cytometry. Spleen T cells of PBS group mice were cultured with HBsAg or PBS and ConA, used as ConA group. Histogram was produced by the modfit 3.0 software packages. These results showed were from individual mice that were representative of per experiment group.

Table 4 T cell proliferative response

Group	*n*	SI (HBsAg)	SI (PBS)
PBS	10	1.09 ± 0.028	1.062 ± 0.027
UA	10	1.17 ± 0.035	1.067 ± 0.031
Unpulsed-DC	10	1.19 ± 0.055	1.076 ± 0.035
HBsAg-pulsed-DC	10	1.34 ± 0.093[b]	1.081 ± 0.028
UA-DC	10	1.59 ± 0.156[d]	1.081 ± 0.029
ConA	10	2.53 ± 0.179[d]	2.487 ± 0.146

[b]$P \leqslant 0.01$, [d]$P \leqslant 0.001$, *vs* PBS group.

Table 5 HBsAg-specific CTL cytotoxicity (%, mean ± SD, *n* = 10)

Group	PBS	UA	Unpulsed-DC	HBsAg-pulsed-DC	UA-DC
Cytotoxicity	3.51 ± 1.14	3.52 ± 1.15	6.32 ± 2.18	27.32 ± 7.32[b]	68.63 ± 11.32[d]

[b]$P \leqslant 0.01$, [d]$P \leqslant 0.001$, *vs* PBS group.

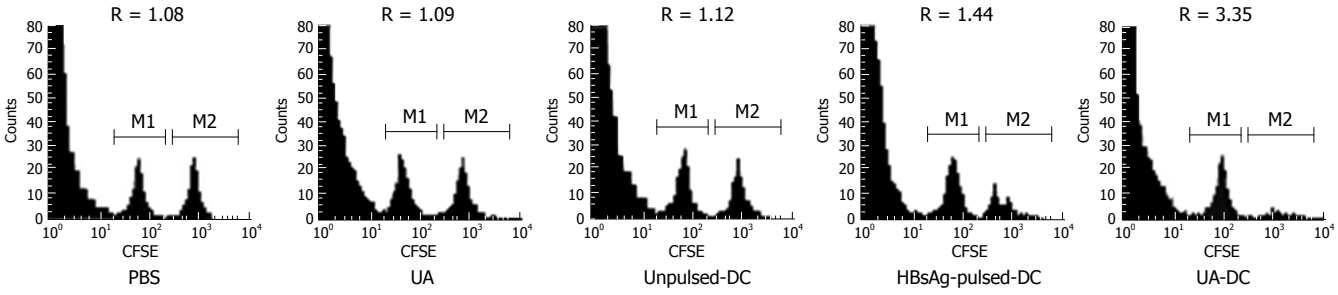

Figure 4 Analyze CTL activity against HBsAg of immunization mice by flow cytometry in vivo at 2 wk. Flow cytometric analysis of each mouse was adoptively transferred with a 1:1 mixture of Protein-pulsed ($CFSE^{high}$) and unpulsed ($CFSE^{low}$) naive mouse splenocytes 10 h previously. Then ratio between percentage of $CFSE^{low}$ cells and $CFSE^{high}$ cells were calculated. HBsAg-specific CTL cytotocity was determined (Table 5). These histogram results were from individual mice that were representative of ten experiments.

HBsAg-pulsed-DCs alone or unpulsed-DCs induced low cytotoxicities of HBsAg-specific CTLs (Table 5).

In mice immunized with uric acid 200 μg alone or PBS, R values or CTL cytotoxicity were similar ($P > 0.05$) (Figure 4). It demonstrated that no significant specific lysis was observed and immunization with uric acid 200 μg alone failed to induce HBsAg-specific CTLs.

DISCUSSION

It has been shown that T-cell mediated immune responses are very important in overcoming HBV infection[1,2] and DCs can efficiently prime T-cell response, so the development of a vaccine of DCs has attracted considerable interest[18,19].

Several studies indicated that uric acid had excellent immune adjuvant activity, which could promote the specific immune response to vaccines efficiently[9,11]. Shi and colleagues have shown that the generation of responses from specific CTL activity was significantly enhanced, when uric acid was injected into mice along with the gp120 protein of the human immunodeficiency virus (HIV)[9]. Hu and colleagues showed that eliminating uric acid, by administration of allopurinol or uricase, delayed tumor

immune rejection, whereas subcutaneous administration of uric acid enhanced the rejection process[11].

Uric acid crystals might be the biologically active form. It was shown that preformed crystals were highly stimulatory, whereas soluble uric acid was not[9-11]. The concentrations of uric acid that stimulated DCs corresponded to one at which uric acid crystals were precipitated. Injection of purified uric acid (> 70 μg /mL) was shown to boost CTL responses in spleen cells isolated from mice, which had been primed with particulate antigens, by triggering increased DC expression of the costimulatory molecules CD86 and CD80[9,11]. Allopurinol and uricase treatment, which substantially reduced plasma uric acid concentrations, was shown to markedly inhibit this T-cell priming. Uric acid crystals are known to stimulate monocytes to produce inflammatory mediators[20], and it seems likely that DCs are stimulated in a similar way.

As highly specialized antigen presenting cells (APC), DCs play a central role in antigen presentation to $CD4^+$ or $CD8^+$ T cells and allogeneic T cell proliferation[8]. It has been known that phenotypic and functional maturation was critical for DCs to activate immune responses effectively[21]. In a previous study, it was reported that uric acid could promote expression of co-stimulatory molecules (CD86, CD80) on DC surfaces[9]. Our data showed that uric acid promoted maturation of DCs ($CD83^{high}$) and up-regulated the expression of co-stimulatory molecules CD86, and IA/IE (MHC-I molecule).

DCs have a crucial role in determining the type of T cell mediated response[22,23]. IL-12 is an important immune modulatory molecule, which specifically promotes Th1 cell differentiation and suppresses Th2 cell function, and induces a Th1 cell immune response[24]. In this study, uric acid could promote DCs to secrete IL-12p70 in vitro; after combination of immunization with uric acid, in spleen cells of mice, production of IFN-γ was significantly up-regulated, and IL-4 production was down-regulated. This indicated that uric acid might enhance Th1 cell immune responses by promoting DC to secrete IL-12. And then Th1 cells can induce the proliferation of CTLs and amplification of $CD8^+$ T cell responses[25].

In addition, we showed that combination immunization of uric acid and HBsAg-pulsed-DCs could elicit a strong T cell-mediated immune response. Compared with HBsAg-pulsed-DCs vaccine alone, combination immunization elicited significantly greater T cell immune responses as evidenced by T cell proliferation to HBsAg re-stimulation, Th1 cytokine secretion and HBsAg-specific CTL responses. Uric acid may enhance the T cell immune responses by stimulating DC maturation and enhance its functions.

In hyperuricemia, it is well-known that uric acid can precipitate in the joints, where they cause gout, and/or in other tissues causing inflammation[26]. Therefore, the dose of uric acid administration is of crucial importance. In our study, the dose of uric acid was 200 μg. According to Shi and Hu *et al*[9,11], this dose of uric acid was safe and had an adjuvant effect.

We immunized both treated and control mice with 200 μg uric acid alone for two weeks. As expected, the T cell mediated immune responses were not enhanced. It demonstrated that uric acid has no adjuvant activity in the absence of exogenous antigens. It is important that no autoimmunity is induced, using uric acid as an adjuvant of vaccine.

In the murine model, combination of uric acid and HBsAg-pulsed-DCs seemed to be very effective. However, the anti-HBV effect of this vaccine strategy must be tested further in the HBV animal model.

In summary, we have demonstrated that uric acid can strongly enhance T cell immune responses to HBsAg-pulsed-DCs. We conclude that uric acid might serve as an effective adjuvant for DC vaccine against HBV infection. This strategy provides a model to develop therapeutic vaccines against HBV infection.

ACKNOWLEDGMENTS

We are grateful to Professor Zuo-Ya Li, and Guan-Xin Shen for valuable advice on ELISA.

REFERENCES

1 **Meyer zum Büschenfelde KH.** Immunopathology of chronic liver diseases. *Verh Dtsch Ges Pathol* 1995; **79**: 186-197
2 **Bertoletti A**, Gehring AJ. The immune response during hepatitis B virus infection. *J Gen Virol* 2006; **87**: 1439-1449
3 **Akbar SM**, Horiike N, Onji M. Immune therapy including dendritic cell based therapy in chronic hepatitis B virus infection. *World J Gastroenterol* 2006; **12**: 2876-2883
4 **Shimizu Y**, Guidotti LG, Fowler P, Chisari FV. Dendritic cell immunization breaks cytotoxic T lymphocyte tolerance in hepatitis B virus transgenic mice. *J Immunol* 1998; **161**: 4520-4529
5 **Chen M**, Li YG, Zhang DZ, Wang ZY, Zeng WQ, Shi XF, Guo Y, Guo SH, Ren H. Therapeutic effect of autologous dendritic cell vaccine on patients with chronic hepatitis B: a clinical study. *World J Gastroenterol* 2005; **11**: 1806-1808
6 **Santini SM**, Belardelli F. Advances in the use of dendritic cells and new adjuvants for the development of therapeutic vaccines. *Stem Cells* 2003; **21**: 495-505
7 **Sallusto F**, Lanzavecchia A. Efficient presentation of soluble antigen by cultured human dendritic cells is maintained by granulocyte/macrophage colony-stimulating factor plus interleukin 4 and downregulated by tumor necrosis factor alpha. *J Exp Med* 1994; **179**: 1109-1118
8 **Banchereau J**, Steinman RM. Dendritic cells and the control of immunity. *Nature* 1998; **392**: 245-252
9 **Shi Y**, Evans JE, Rock KL. Molecular identification of a danger signal that alerts the immune system to dying cells. *Nature* 2003; **425**: 516-521
10 **Jerome KR**, Corey L. The danger within. *N Engl J Med* 2004; **350**: 411-412
11 **Hu DE**, Moore AM, Thomsen LL, Brindle KM. Uric acid promotes tumor immune rejection. *Cancer Res* 2004; **64**: 5059-5062
12 **Inaba K**, Inaba M, Romani N, Aya H, Deguchi M, Ikehara S, Muramatsu S, Steinman RM. Generation of large numbers of dendritic cells from mouse bone marrow cultures supplemented with granulocyte/macrophage colony-stimulating factor. *J Exp Med* 1992; **176**: 1693-1702
13 **Overwijk WW**, Surman DR, Tsung K, Restifo NP. Identification of a Kb-restricted CTL epitope of beta-galactosidase: potential use in development of immunization protocols for "self" antigens. *Methods* 1997; **12**: 117-123
14 **Coles RM**, Mueller SN, Heath WR, Carbone FR, Brooks AG. Progression of armed CTL from draining lymph node to

spleen shortly after localized infection with herpes simplex virus 1. *J Immunol* 2002; **168**: 834-838
15 **Salio M**, Palmowski MJ, Atzberger A, Hermans IF, Cerundolo V. CpG-matured murine plasmacytoid dendritic cells are capable of in vivo priming of functional CD8 T cell responses to endogenous but not exogenous antigens. *J Exp Med* 2004; **199**: 567-579
16 **Lyons AB**. Analysing cell division in vivo and in vitro using flow cytometric measurement of CFSE dye dilution. *J Immunol Methods* 2000; **243**: 147-154
17 **Dixon DM**, Misfeldt ML. Proliferation of immature T cells within the splenocytes of athymic mice by Pseudomonas exotoxin A. *Cell Immunol* 1994; **158**: 71-82
18 **Böcher WO**, Dekel B, Schwerin W, Geissler M, Hoffmann S, Rohwer A, Arditti F, Cooper A, Bernhard H, Berrebi A, Rose-John S, Shaul Y, Galle PR, Löhr HF, Reisner Y. Induction of strong hepatitis B virus (HBV) specific T helper cell and cytotoxic T lymphocyte responses by therapeutic vaccination in the trimera mouse model of chronic HBV infection. *Eur J Immunol* 2001; **31**: 2071-2079
19 **Akbar SM**, Furukawa S, Hasebe A, Horiike N, Michitaka K, Onji M. Production and efficacy of a dendritic cell-based therapeutic vaccine for murine chronic hepatitis B virus carrierer. *Int J Mol Med* 2004; **14**: 295-299
20 **Landis RC**, Yagnik DR, Florey O, Philippidis P, Emons V, Mason JC, Haskard DO. Safe disposal of inflammatory monosodium urate monohydrate crystals by differentiated macrophages. *Arthritis Rheum* 2002; **46**: 3026-3033
21 **Cella M**, Sallusto F, Lanzavecchia A. Origin, maturation and antigen presenting function of dendritic cells. *Curr Opin Immunol* 1997; **9**: 10-16
22 **Santana MA**, Esquivel-Guadarrama F. Cell biology of T cell activation and differentiation. *Int Rev Cytol* 2006; **250**: 217-274
23 **Tan P**, Anasetti C, Hansen JA, Melrose J, Brunvand M, Bradshaw J, Ledbetter JA, Linsley PS. Induction of alloantigen-specific hyporesponsiveness in human T lymphocytes by blocking interaction of CD28 with its natural ligand B7/BB1. *J Exp Med* 1993; **177**: 165-173
24 **Kourilsky P**, Truffa-Bachi P. Cytokine fields and the polarization of the immune response. *Trends Immunol* 2001; **22**: 502-509
25 **Gately MK**, Wolitzky AG, Quinn PM, Chizzonite R. Regulation of human cytolytic lymphocyte responses by interleukin-12. *Cell Immunol* 1992; **143**: 127-142
26 **Gentili A**. The advanced imaging of gouty tophi. *Curr Rheumatol Rep* 2006; **8**: 231-235

S- Editor Liu Y **L- Editor** Zhu LH **E- Editor** Ma WH

PO Box 2345, Beijing 100023, China
www.wjgnet.com
wjg@wjgnet.com

World J Gastroenterol 2007 February 21; 13(7): 1067-1073
World Journal of Gastroenterology ISSN 1007-9327

CLINICAL RESEARCH

Feasibility and safety of autologous bone marrow mononuclear cell transplantation in patients with advanced chronic liver disease

Andre Castro Lyra, Milena Botelho Pereira Soares, Luiz Flavio Maia da Silva, Marcos Fraga Fortes, André Goyanna Pinheiro Silva, Augusto César de Andrade Mota, Sheilla A Oliveira, Eduardo Lorens Braga, Wilson Andrade de Carvalho, Bernd Genser, Ricardo Ribeiro dos Santos, Luiz Guilherme Costa Lyra

Andre Castro Lyra, Milena Botelho Pereira Soares, Luiz Flavio Maia da Silva, Marcos Fraga Fortes, André Goyanna Pinheiro Silva, Eduardo Lorens Braga, Wilson Andrade de Carvalho, Ricardo Ribeiro dos Santos, Luiz Guilherme Costa Lyra, Hospital Sao Rafael, Salvador, Bahia, Brazil
Andre Castro Lyra, Eduardo Lorens Braga, Luiz Guilherme Costa Lyra, Gastro-Hepatology Unit, Federal University of Bahia, Salvador, Bahia, Brazil
Milena Botelho Pereira Soares, Augusto César de Andrade Mota, Sheilla A Oliveira, Ricardo Ribeiro dos Santos, Centro de Pesquisas Goncalo Moniz, Fundacao Oswaldo Cruz, Salvador, Bahia, Brazil
Sheilla A Oliveira, Centro de Pesquisas Aggeu Magalhaes, Fundaçao Oswaldo Cruz, Recife, Pernambuco, Brazil
Bernd Genser, BGStats Consulting, Graz, Austria
Supported by IMBT-MCT/CNPq and Monte Tabor/Hospital Sao Rafael
Correspondence to: André Castro Lyra, Gastro-Hepatology Unit, Federal University of Bahia, R Socrates Guanaes Gomes 84/401, Salvador, Bahia 40296720, Brazil. aclyra@atarde.com.br
Telephone: +55-71-32357048 Fax: +55-71-32357048
Received: 2006-10-14 Accepted: 2006-11-14

Abstract

AIM: To evaluate the safety and feasibility of bone marrow cell (BMC) transplantation in patients with chronic liver disease on the waiting list for liver transplantation.

METHODS: Ten patients (eight males) with chronic liver disease were enrolled to receive infusion of autologous bone marrow-derived cells. Seven patients were classified as Child-Pugh B and three as Child-Pugh C. Baseline assessment included complete clinical and laboratory evaluation and abdominal MRI. Approximately 50 mL of bone marrow aspirate was prepared by centrifugation in a ficoll-hypaque gradient. At least of 100 millions of mononuclear-enriched BMCs were infused into the hepatic artery using the routine technique for arterial chemoembolization for liver tumors. Patients were followed up for adverse events up to 4 mo.

RESULTS: The median age of the patients was 52 years (range 24-70 years). All patients were discharged 48 h after BMC infusion. Two patients complained of mild pain at the bone marrow needle puncture site. No other complications or specific side effects related to the procedure were observed. Bilirubin levels were lower at 1 (2.19 ± 0.9) and 4 mo (2.10 ± 1.0) after cell transplantation that baseline levels (2.78 ± 1.2). Albumin levels 4 mo after BMC infusion (3.73 ± 0.5) were higher than baseline levels (3.47 ± 0.5). International normalized ratio (INR) decreased from 1.48 (SD = 0.23) to 1.43 (SD = 0.23) one month after cell transplantation.

CONCLUSION: BMC infusion into hepatic artery of patients with advanced chronic liver disease is safe and feasible. In addition, a decrease in mean serum bilirubin and INR levels and an increase in albumin levels are observed. Our data warrant further studies in order to evaluate the effect of BMC transplantation in patients with advanced chronic liver disease.

Key words: Bone marrow; Cell transplantation; Liver failure; Stem cell; Cirrhosis

Lyra AC, Soares MBP, da Silva LFM, Fortes MF, Silva AGP, Mota ACA, Oliveira SA, Braga EL, de Carvalho WA, Genser B, dos Santos RR, Lyra LGC. Feasibility and safety of autologous bone marrow mononuclear cell transplantation in patients with advanced chronic liver disease. *World J Gastroenterol* 2007; 13(7): 1067-1073

http://www.wjgnet.com/1007-9327/13/1067.asp

INTRODUCTION

Chronic liver disease may progress to end-stage liver disease (ESLD), liver failure and death. Patients with ESLD may experience serious complications such as encephalopathy, ascites and esophagogastric variceal hemorrhage. Liver transplantation is the only available therapy for patients with chronic liver failure. Because of the shortage of donated organs, up to 10%-15% of these patients die without receiving an organ in developed countries[1]. In some undeveloped countries the number of deaths on the waiting list might be greater. In some regions

of Brazil it takes an average of more than two years until liver transplantation. Therefore, alternative methods such as cell therapy are necessary to increase patient survival on the liver transplant waiting list. Several sources of stem cells have been proposed for cell therapy. Embryonic stem cells are the most potent in terms of their differentiation potential but may be oncogenic when transplanted *in vivo* and their use has been a matter of controversy because of ethical issues[2]. A number of studies during the last decade have identified cells both within and outside the liver that have properties of hepatic stem cells and might differentiate into hepatocytes or bile duct epithelial cells[3-5]. Hematopoietic tissue is most accessible and of special interest , and it has been demonstrated that bone marrow contains multipotent adult progenitor cells that can generate a variety of cell types found in other tissues[6-8].

Studies in animal models of liver diseases have demonstrated that bone marrow cell (BMC) transplantation may accelerate the liver regeneration process, reduce hepatic fibrosis and improve liver function and survival rate[9-11]. However, its mechanism is still controversial. Several studies have suggested that hematopoietic cells may generate hepatocyte-like cells, while others hypothesized that they should act mainly by fusion with hepatocytes or by paracrine effect[12-15]. Fusion between hepatocytes and hematopoietic cells produces heterokaryotic hybrid cells that initially contain the genetic elements and organelles of both cell types and may then express the hepatocyte phenotype. Several studies suggest that cytokines and growth factors produced by infused hematopoietic cells may support liver function and repair in adult animals without forming new hepatocytes from the infused cells[15]. Based on the findings from other studies that suggest improvement of liver fibrosis in experimental models of liver disease and because bone marrow cell transplantation itself is already an established treatment for hematological and oncological diseases, we conducted a clinical trial to evaluate the safety and feasibility of autologous BMC therapy in patients with chronic liver disease on the waiting list for liver transplantation.

MATERIALS AND METHODS

Subjects

The study group comprised 10 patients with chronic liver disease (8 males, 2 females, age: 24 to 70 years) on the waiting list for liver transplantation. They were enrolled to receive infusion of autologous BMC from September 2005 to January 2006. Informed written consent was obtained from all subjects. The study protocol conformed to the ethical guidelines of the 1975 Declaration of Helsinki and was approved by the Ethics Committee of Hospital São Rafael, Salvador, Brazil and by the Brazilian National Ethics Committee (CONEP). Eligible patients had all the following inclusion criteria: age range between 18-75 years, advanced chronic liver disease of different etiologies classified as Child Pugh B or C, absence of liver tumors and appropriate use of contraception method for women of child-bearing potential. Patients were excluded from the study if they had one or more of the following exclusion criteria: risk for bone marrow aspiration, sepsis, human immunodeficiency virus infection, active hepatic encephalopathy, liver tumor, history of malignant neoplasm except for non-melanoma skin cancer, decompensated heart failure, platelet count < 30000/mm^3, international normalized ratio (INR) > 2.2, renal failure (creatinine > 2.5 mg/dL), participation in other clinical trials, pregnancy or lactation.

Baseline assessment included complete clinical and laboratorial evaluation as well as abdominal magnetic resonance imaging to exclude liver tumor. Laboratory tests consisted of complete blood count, serum bilirubin levels, prothrombin time, serum blood glucose, urea, creatinine, alpha-fetoprotein, total proteins and albumin levels, serum aminotransferase concentrations, alkaline phosphatase and gamma-glutamyl transferase levels, thyroid stimulating hormone (TSH) concentrations. Patients were followed up for adverse events with clinical and laboratory evaluations on d 1, 2, 3, 7, 15, 30, 45, 60, 90, 120 after BMC transplantation.

Bone marrow cell therapy

Approximately 50 mL of bone marrow was aspirated from the iliac crest. An enriched fraction of bone marrow mononuclear cells was prepared by centrifugation of total bone marrow in a ficoll-hypaque gradient. At least 100 millions of mononuclear-enriched BMC suspended in 20 mL of saline was infused into the hepatic artery of included patients by a catheter, using the routine technique for arterial chemoembolization of liver tumors[16].

Statistical analysis

Exploratory data analysis was conducted to calculate means, standard deviations and 95% confidence intervals of measurements (laboratory tests, Child Pugh score at baseline at 1 and 4 mo). Relative mean changes at 1 and 4 mo with respect to the baseline level were calculated. To examine the development of laboratory parameters after BMC infusion individual response profiles were plotted as a function of weeks after intervention. In addition, estimates of the mean response profiles and 95% confidence intervals were obtained by calculating moving averages of patients' measurements over a period of 4 weeks and by applying linear interpolation. All statistical analyses were conducted by the statistical software package STATA (StataCorp. 2005. Stata Statistical Software: Release 8. College Station, TX: StataCorp LP).

RESULTS

The median age of the study population was 52 years (range 24-70 years). Four patients had alcoholic liver disease, 4 had chronic hepatitis C, one had chronic cholestatic liver disease and one cryptogenic cirrhosis (Table 1). Seven patients were classified as Child-Pugh B and 3 patients as Child-Pugh C. None had a liver tumor.

The number of BMCs infused in each patient is shown in Table 1. All patients were discharged 48 h after BMC infusion. Two patients complained of mild pain at the bone marrow needle puncture site. No other complications

Table 1 Clinical characteristics of studied patients and the number of transplanted autologous BMCs

Patient ID	Age (yr)	Sex	Etiology of cirrhosis	BMCs transplanted (*n*)
JWOR	49	Male	Alcohol + HCV	2.8×10^8
FMB	60	Male	Alcohol	5.2×10^8
EAS	63	Female	HCV	3.2×10^8
RNR	24	Male	Cholestatic	13.1×10^8
IAN	49	Male	Alcohol + HCV	2.6×10^8
NPA	55	Female	Cryptogenic	3.5×10^8
RBC	49	Male	Alcohol	4.8×10^8
RMV	66	Male	HCV	3.4×10^8
GAFL	70	Male	Alcohol	1.6×10^8
ABSF	40	Male	HCV	2.4×10^8

Table 2 Characteristics of the distribution of serum bilirubin, albumin and INR levels in 10 patients with chronic liver failure at baseline, 1 and 4 mo after transplantation of autologous BMCs

Bilirubin (mg/dL)	Minimum	Maximum	Mean	Median	Standard deviation	Relative mean change from baseline (%)
Baseline	1.2	4.83	2.78	2.45	1.16	
1 mo	0.5	3.56	2.19	2.28	0.91	-21
4 mo	0.72	4.16	2.1	1.87	1.04	-24
Albumin (unit)						
Baseline	2.5	4.4	3.47	3.5	0.51	
1 mo	2.9	4.5	3.44	3.25	0.52	-1
4 mo	3.1	4.8	3.73	3.6	0.51	7
INR (unit)						
Baseline	1.08	1.89	1.46	1.48	0.23	
1 mo	1.1	1.94	1.44	1.43	0.23	-1
4 mo	1.16	1.75	1.42	1.43	0.18	-3

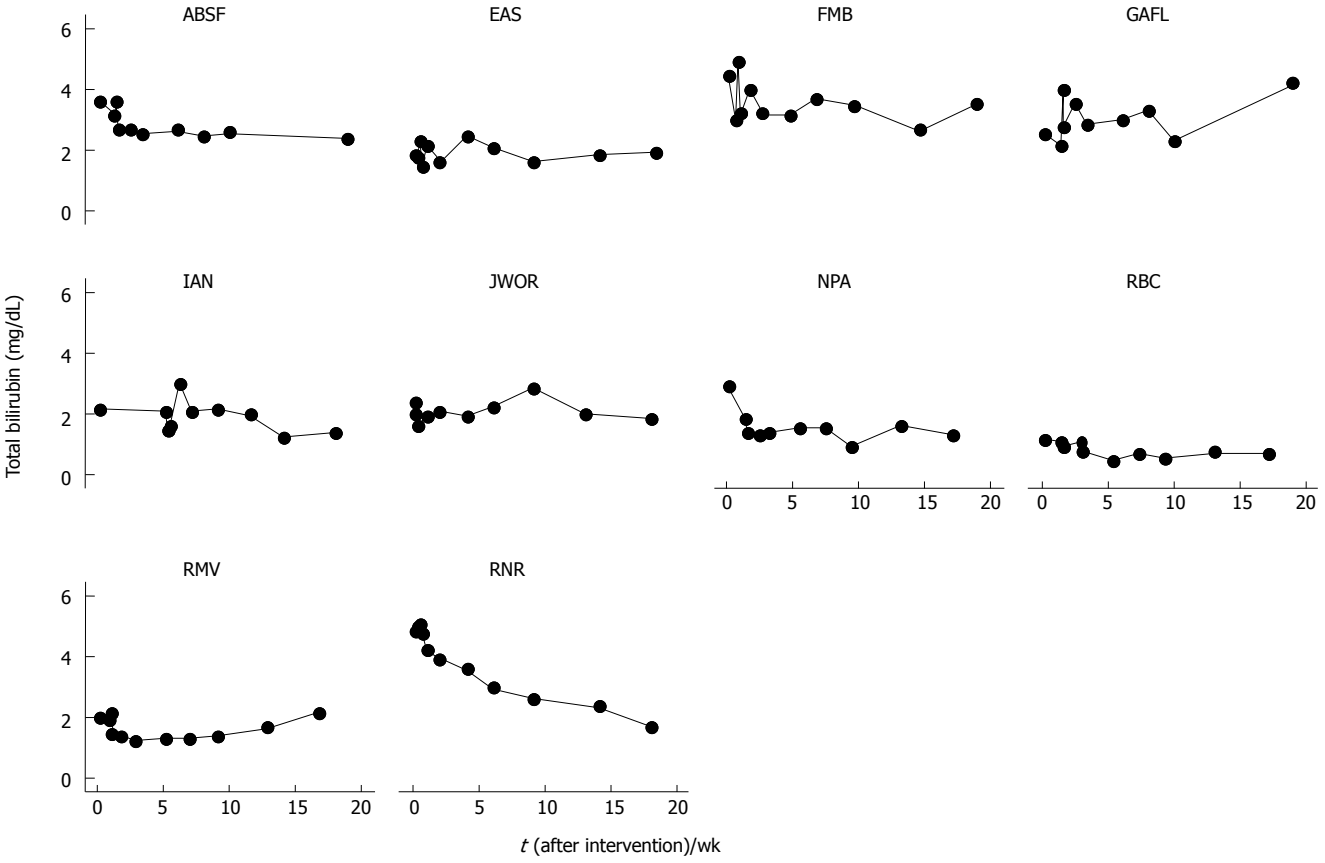

Figure 1 Serum bilirubin levels in 10 patients with chronic liver disease as a function of weeks after transplantation of autologous BMCs.

or specific side effects related to the infusion procedure were reported. A 70-year old patient with a history of previous episodes of hepatic encephalopathy developed reversible grade I encephalopathy 33 d after BMC infusion. The episode was controlled without requirement of hospitalization and was not considered an adverse event since 3 identical episodes were documented for this patient in the last year before his inclusion in the study.

Total bilirubin levels were 21% lower at 1 mo (2.19 ± 0.91) and 24% lower at 4 mo (2.10 ± 1.04) after BMC transplantation that baseline levels (2.78 ± 1.16) (Table 2). When individual response profiles were evaluated, a decrease in total bilirubin levels was observed in 7 of 10 patients after BMC transplantation (Figure 1). The mean profile of bilirubin levels after BMC infusion is shown in Figure 2.

Albumin levels were 1% lower at 1 mo (3.44 ± 0.52) and 7% higher at 4 mo after BMC infusion (3.73 ± 0.51) that baseline levels (3.47 ± 0.51) (Table 2). The analysis of individual levels showed an increase in albumin levels

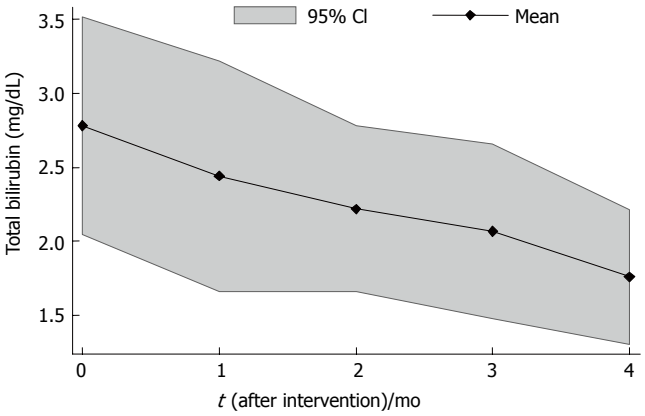

Figure 2 Mean profile of serum total bilirubin levels including a 95% confidence band in 10 patients with chronic liver disease as a function of weeks after transplantation of autologous BMCs.

in 6 patients and a reduction in 1 patient 4 mo after BMC transplantation (Figure 3). The mean profile of serum albumin levels is shown in Figure 4.

INR levels were 1% lower at 1 mo (1.44 ± 0.23) and 4% lower at 4 mo (1.42 ± 0.18) after BMC transplantation that baseline levels (1.46 ± 0.23) (Table 2). INR levels reduced in 7 patients and increased in 1 patient after BMC transplantation (Figure 5). The mean profiles of INR levels are shown in Figure 6.

The data about other relevant laboratory parameters (WBC, hemoglobin, ALT, AST, GGT, creatinine) before and after the intervention are shown in Table 3.

Table 3 Characteristics of the distribution of laboratory parameters in 10 patients with chronic liver failure at baseline, 1 and 4 mo after BMC transplantation

	Minimum	Maximum	Mean	Median	Standard deviation	Relative mean change from baseline (%)
Hemoglobin (g/dL)						
Baseline	11.30	16.90	13.16	12.2	1.90	
1 mo	9.50	16.00	12.26	11.95	1.81	-8
4 m	10.30	15.10	12.80	12.7	1.47	-3
WBC (x 10^3/mm^3)						
Baseline	2.60	5.40	3.94	4	0.97	
1 mo	2.30	5.10	3.35	2.85	1.04	-15
4 mo	2.30	6.00	3.60	3.25	1.14	-9
GGT (U/L)						
Baseline	50.00	543.00	172.20	139	147.50	
1 mo	48.00	474.20	157.20	134.5	129.00	-9
4 mo	47.00	489.67	163.50	132.5	133.25	-5
AST (U/L)						
Baseline	29.00	192.00	100.60	92.5	56.24	
1 mo	26.00	173.00	86.90	79	47.58	-14
4 mo	29.00	180.00	85.80	64	46.87	-15
ALT(U/L)						
Baseline	11.00	120.00	56.00	43	35.54	
1 mo	22.00	115.00	54.80	42.5	32.71	-2
4 mo	17.00	131.00	53.50	41	34.97	-4
Creatinine (mg/dL)						
Baseline	0.60	1.50	0.86	0.8	0.26	
1 mo	0.70	1.30	0.90	0.85	0.20	5
4 mo	0.60	1.20	0.87	0.85	0.19	1

DISCUSSION

There is an urgent need to search for alternatives to whole organ transplantation. Based on the ability of stem cells to differentiate into specific cell types according to their environment, cell transplantation has become an attractive therapeutic method for the treatment of patients with liver disease aiming, at least, at a temporary support of hepatic function until a liver becomes available for organ transplantation.

This phase I study aimed to evaluate the feasibility and safety of autologous bone marrow cell transplantation into the hepatic artery of patients with advanced chronic liver disease. In the present study, we infused BMCs into the hepatic artery using the same routine technique for arterial chemoembolization of liver tumors which is feasible and not associated with serious local side effects[16], and used the hepatic artery for cell infusion since the blood inflow to the liver could be mostly secured. Our results confirmed the feasibility and safety of BMC infusion into hepatic artery in such patients. BMC transplantation was well tolerated to all patients and only two patients complained of mild pain at the bone marrow needle puncture site. We did not detect any other side effects. The episode of reversible hepatic encephalopathy 33 d after BMC infusion in a 70-year old man with alcoholic cirrhosis was not interpreted as an adverse event related to the procedure because identical episodes were observed in the previous year.

In addition to the evaluation of safety and feasibility, our results indicated that there were alterations of liver function parameters after transplantation of autologous BMCs in patients with advanced chronic liver disease. Four months after BMC transplantation the mean serum bilirubin and INR levels decreased while the mean albumin levels increased. Of note, 7 patients had their bilirubin levels reduced while 6 patients had their albumin levels increased. The greatest reduction in the bilirubin levels was observed in a 24-year old patient (R.N.R.) with chronic cholestatic liver disease who had the highest amount of transplanted BMCs (13.1×10^8) compared to the others (Table 1). The number of transplanted BMCs was lower in patients with cirrhosis caused by HCV and in the 70-year old patient.

Recently, two phase I studies using granulocyte-colony stimulating factor (G-CSF) to mobilize BMCs in patients with chronic liver disease were conducted[17,18]. Gaia *et al*[17] evaluated the feasibility and safety of BMC mobilization in 8 patients with end stage liver cirrhosis following G-CSF administration. Mobilization (monitored by the number of CD34 + ve cells) was observed in all patients after G-CSF administration, which was well tolerated and free of adverse events. Child-Pugh score decreased by 2 or more points in four patients, increased in one patient, while it was unchanged (or decreased by less than 2 points) in three patients. Overall, the MELD score decreased from a median pre-treatment value of 17.5 (range 11-20) to 14.5

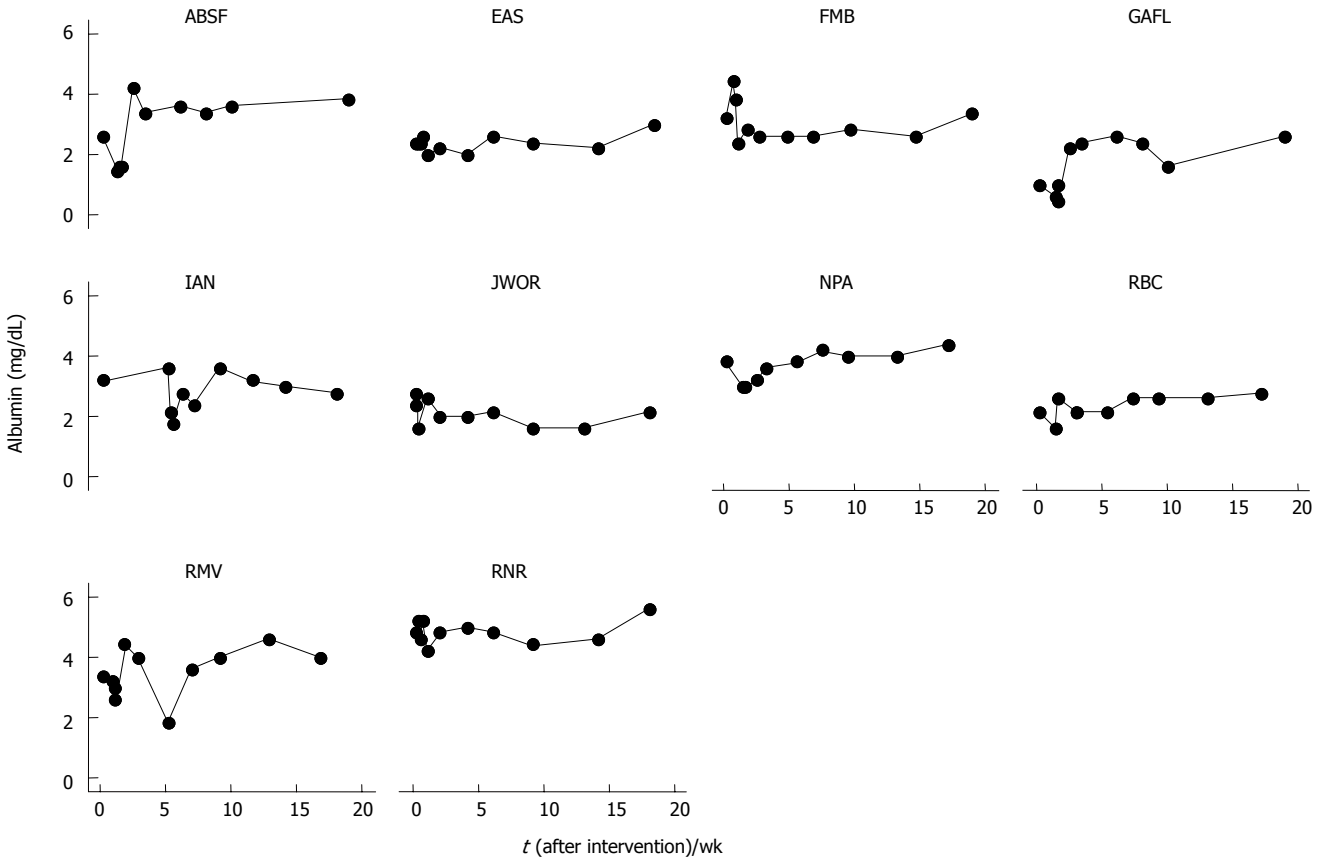

Figure 3 Serum albumin levels in 10 patients with chronic liver disease as a function of weeks after transplantation of autologous BMCs.

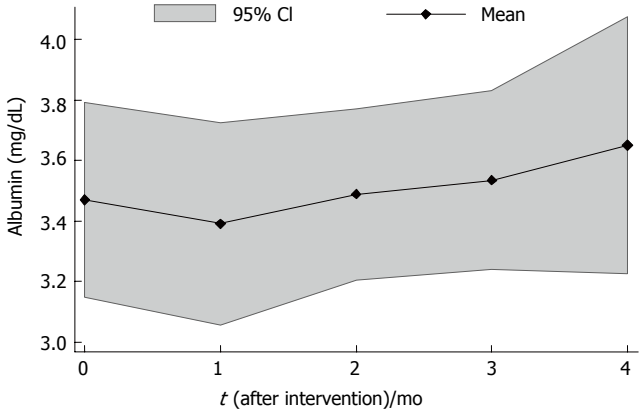

Figure 4 Mean profile of serum albumin levels including a 95% confidence band in 10 patients with chronic liver failure as a function of weeks after transplantation of autologous BMCs.

(range 9-20) at end of follow-up. In another study Gordon *et al*[18] evaluated the safety and tolerability of autologous CD34+ cell injection into five patients with liver insufficiency. Included patients were given subcutaneously 520 μg G-CSF and CD34+ cells were collected and then returned to the patients via the hepatic artery or the portal vein. No major complications or specific side effects related to the procedure were observed. Three of the five patients showed a reduction in serum bilirubin and four of five showed an increase in serum albumin. The results of these two studies appear to be in agreement with ours. The choice of utilizing purified stem cells instead of mononuclear cell fraction depends on a future comparison of the efficacy in the two cell populations. In addition, purification procedures to obtain a specific cell population increase the costs of the therapy.

Studies in animal models of liver diseases have demonstrated that bone marrow cell transplantation decreases hepatic fibrosis and improves survival rate. Sakaida *et al*[11] investigated the effect of BMC transplantation on mice with established liver fibrosis induced by carbon tetrachloride (CCl_4) administration. Four weeks after BMC transplantation, the mice had significantly reduced liver fibrosis, as assessed by hydroxyproline content in the livers, compared to mice treated with CCl_4 alone. Similar results have been observed in other studies[9,19,20]. In addition, improvement in several parameters of liver function, such as albumin and bilirubin levels and prothrombin time has been reported[8,12,21]. These experimental studies suggest that BMC infusion may be responsible for the potential beneficial effects on liver function as observed in our clinical study.

Our study was not able to evaluate the efficacy of BMC infusion in patients with liver disease due to its design. Controlled studies would be required to address this issue. Further studies are also necessary to determine the number of BMCs required for achievement of therapeutic effect, which may vary with the patient's age and the etiology of liver disease.

In summary, BMC infusion into the hepatic artery of patients with advanced chronic liver disease is safe and

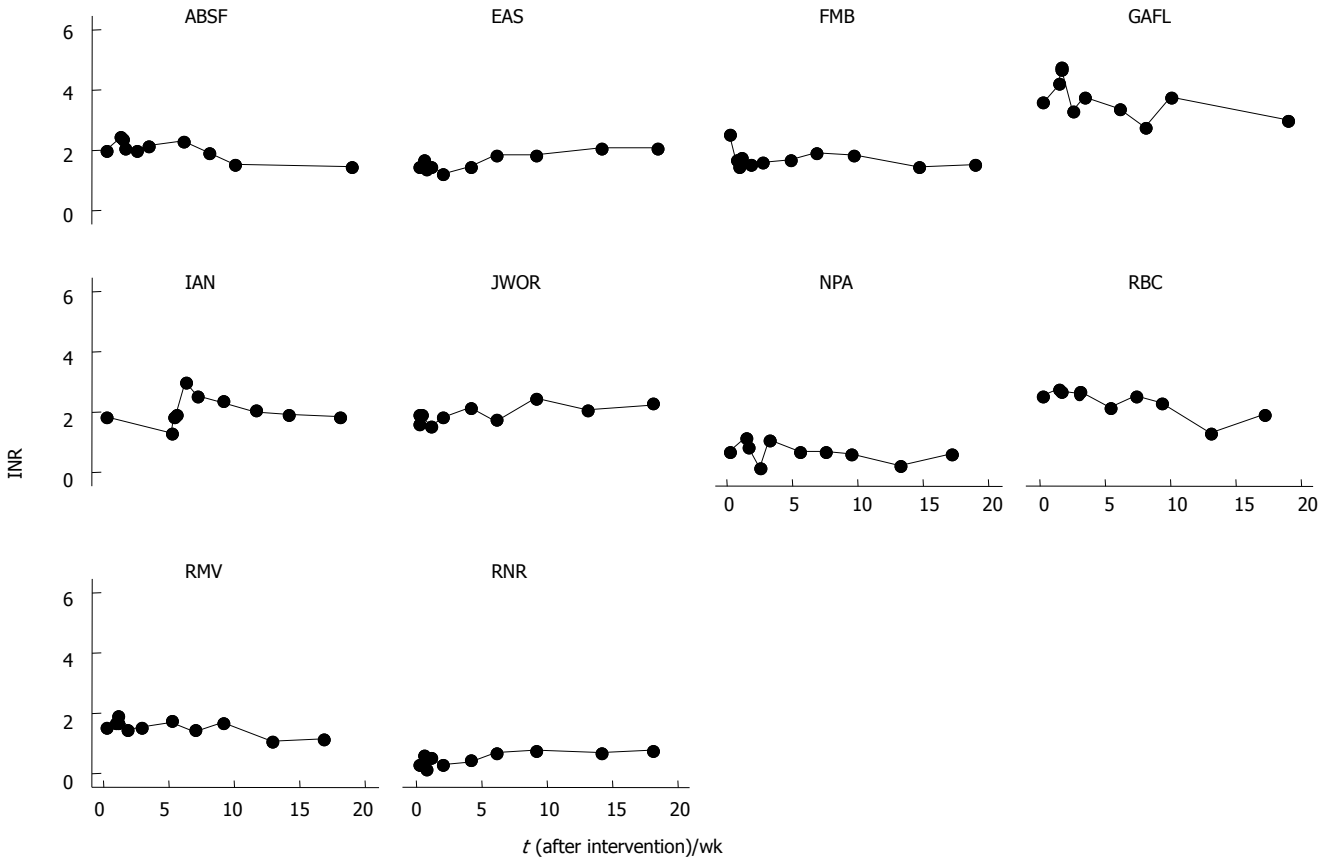

Figure 5 INR levels in 10 patients with chronic liver failure as a function of weeks after transplantation of autologous BMCs.

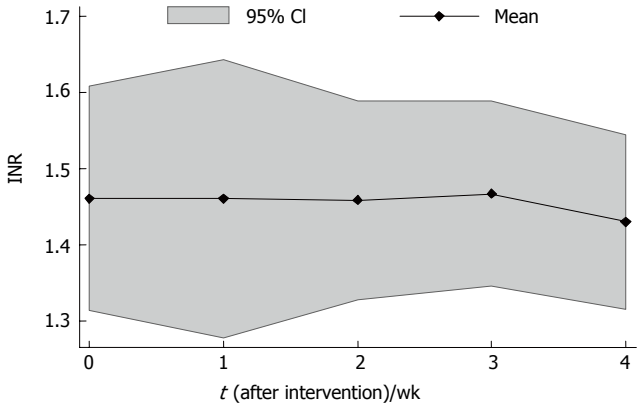

Figure 6 Mean profile of INR levels including a 95% confidence band in 10 patients with chronic liver failure as a function of weeks after transplantation of autologous bone marrow cells.

feasible. In addition, in most patients there is a decrease in mean serum bilirubin and INR levels, and an elevation of serum albumin. Our results warrant further studies in order to evaluate the effects of BMC transplantation in patients with advanced chronic liver disease.

ACKNOWLEDGMENTS

We thank Dr Patricia Seixas A Brandrao, Heleni F de Carvalho, Andrea da S Sant'Ana, Dr. Paulo Engracio M de Souza, Dr Sonia M Duarte Cathala and Dr. Gabriela Fortes for their invaluable assistance in the care of the patients and Carol O Ramos, Luciano Coelho, Amanda A. Mascarenhas and Carlos Daniel VB de Carvalho for their support in the organization of the clinical data.

REFERENCES

1 **Allen KJ**, Buck NE, Williamson R. Stem cells for the treatment of liver disease. *Transpl Immunol* 2005; **15**: 99-112
2 **Teramoto K**, Hara Y, Kumashiro Y, Chinzei R, Tanaka Y, Shimizu-Saito K, Asahina K, Teraoka H, Arii S. Teratoma formation and hepatocyte differentiation in mouse liver transplanted with mouse embryonic stem cell-derived embryoid bodies. *Transplant Proc* 2005; **37**: 285-286
3 **Haque S**, Haruna Y, Saito K, Nalesnik MA, Atillasoy E, Thung SN, Gerber MA. Identification of bipotential progenitor cells in human liver regeneration. *Lab Invest* 1996; **75**: 699-705
4 **Theise ND**, Saxena R, Portmann BC, Thung SN, Yee H, Chiriboga L, Kumar A, Crawford JM. The canals of Hering and hepatic stem cells in humans. *Hepatology* 1999; **30**: 1425-1433
5 **Yasui O**, Miura N, Terada K, Kawarada Y, Koyama K, Sugiyama T. Isolation of oval cells from Long-Evans Cinnamon rats and their transformation into hepatocytes in vivo in the rat liver. *Hepatology* 1997; **25**: 329-334
6 **Alison MR**, Poulsom R, Jeffery R, Dhillon AP, Quaglia A, Jacob J, Novelli M, Prentice G, Williamson J, Wright NA. Hepatocytes from non-hepatic adult stem cells. *Nature* 2000; **406**: 257
7 **Braun KM**, Sandgren EP. Cellular origin of regenerating parenchyma in a mouse model of severe hepatic injury. *Am J Pathol* 2000; **157**: 561-569
8 **Lagasse E**, Connors H, Al-Dhalimy M, Reitsma M, Dohse M, Osborne L, Wang X, Finegold M, Weissman IL, Grompe M. Purified hematopoietic stem cells can differentiate into hepa-

tocytes *in vivo*. *Nat Med* 2000; **6**: 1229-1234
9 **Fang B**, Shi M, Liao L, Yang S, Liu Y, Zhao RC. Systemic infusion of FLK1(+) mesenchymal stem cells ameliorate carbon tetrachloride-induced liver fibrosis in mice. *Transplantation* 2004; **78**: 83-88
10 **Sakaida I**, Terai S, Nishina H, Okita K. Development of cell therapy using autologous bone marrow cells for liver cirrhosis. *Med Mol Morphol* 2005; **38**: 197-202
11 **Sakaida I**, Terai S, Yamamoto N, Aoyama K, Ishikawa T, Nishina H, Okita K. Transplantation of bone marrow cells reduces CCl4-induced liver fibrosis in mice. *Hepatology* 2004; **40**: 1304-1311
12 **Vassilopoulos G**, Wang PR, Russell DW. Transplanted bone marrow regenerates liver by cell fusion. *Nature* 2003; **422**: 901-904
13 **Wang X**, Willenbring H, Akkari Y, Torimaru Y, Foster M, Al-Dhalimy M, Lagasse E, Finegold M, Olson S, Grompe M. Cell fusion is the principal source of bone-marrow-derived hepatocytes. *Nature* 2003; **422**: 897-901
14 **Quintana-Bustamante O**, Alvarez-Barrientos A, Kofman AV, Fabregat I, Bueren JA, Theise ND, Segovia JC. Hematopoietic mobilization in mice increases the presence of bone marrow-derived hepatocytes *via in vivo* cell fusion. *Hepatology* 2006; **43**: 108-116
15 **Thorgeirsson SS**, Grisham JW. Hematopoietic cells as hepatocyte stem cells: a critical review of the evidence. *Hepatology* 2006; **43**: 2-8
16 **Ahrar K**, Gupta S. Hepatic artery embolization for hepatocellular carcinoma: technique, patient selection, and outcomes. *Surg Oncol Clin N Am* 2003; **12**: 105-126
17 **Gaia S**, Smedile A, Omedè P, Olivero A, Sanavio F, Balzola F, Ottobrelli A, Abate ML, Marzano A, Rizzetto M, Tarella C. Feasibility and safety of G-CSF administration to induce bone marrow-derived cells mobilization in patients with end stage liver disease. *J Hepatol* 2006; **45**: 13-19
18 **Gordon MY**, Levicar N, Pai M, Bachellier P, Dimarakis I, Al-Allaf F, M'Hamdi H, Thalji T, Welsh JP, Marley SB, Davies J, Dazzi F, Marelli-Berg F, Tait P, Playford R, Jiao L, Jensen S, Nicholls JP, Ayav A, Nohandani M, Farzaneh F, Gaken J, Dodge R, Alison M, Apperley JF, Lechler R, Habib NA. Characterization and clinical application of human CD34+ stem/progenitor cell populations mobilized into the blood by granulocyte colony-stimulating factor. *Stem Cells* 2006; **24**: 1822-1830
19 **Zhao DC**, Lei JX, Chen R, Yu WH, Zhang XM, Li SN, Xiang P. Bone marrow-derived mesenchymal stem cells protect against experimental liver fibrosis in rats. *World J Gastroenterol* 2005; **11**: 3431-3440
20 **Oyagi S**, Hirose M, Kojima M, Okuyama M, Kawase M, Nakamura T, Ohgushi H, Yagi K. Therapeutic effect of transplanting HGF-treated bone marrow mesenchymal cells into CCl4-injured rats. *J Hepatol* 2006; **44**: 742-748
21 **Jang YY**, Collector MI, Baylin SB, Diehl AM, Sharkis SJ. Hematopoietic stem cells convert into liver cells within days without fusion. *Nat Cell Biol* 2004; **6**: 532-539

S- Editor Wang J **L- Editor** Wang XL **E- Editor** Ma WH

PO Box 2345, Beijing 100023, China
www.wjgnet.com
wjg@wjgnet.com

World J Gastroenterol 2007 February 21; 13(7): 1074-1078
World Journal of Gastroenterology ISSN 1007-9327

RAPID COMMUNICATION

Hepatitis C risk assessment, testing and referral for treatment in urban primary care: Role of race and ethnicity

Stacey B Trooskin, Victor J Navarro, Robert J Winn, David J Axelrod, A Scott McNeal, Maricruz Velez, Steven K Herrine, Simona Rossi

Stacey B Trooskin, Victor J Navarro, Maricruz Velez, Steven K Herrine, Simona Rossi, Division of Gastroenterology and Hepatology, Thomas Jefferson University, Philadelphia, PA 19107, United States
Robert J Winn, Department of Family Medicine, Thomas Jefferson University, Philadelphia, PA 19107, United States
David J Axelrod, Division of Internal Medicine, Thomas Jefferson University, Philadelphia, PA 19107, United States
A Scott McNeal, Delaware Valley Community Health Inc., Philadelphia, PA 19107, United States
Supported by an educational grant from Roche
Correspondence to: Dr. Victor Navarro, Thomas Jefferson University, Division of Gastroenterology and Hepatology, 132 South 10th Street, Suite 480 Main Building, Philadelphia, PA 19107, United States. victor.navarro@jefferson.edu
Telephone: +1-215-9555271
Received: 2006-11-15 Accepted: 2007-01-26

Abstract

AIM: To determine rates of hepatitis C (HCV) risk factor ascertainment, testing, and referral in urban primary care practices, with particular attention to the effect of race and ethnicity.

METHODS: Retrospective chart review from four primary care sites in Philadelphia; two academic primary care practices and two community clinics was performed. Demographics, HCV risk factors, and other risk exposure information were collected.

RESULTS: Four thousand four hundred and seven charts were reviewed. Providers documented histories of injection drug use (IDU) and transfusion for less than 20% and 5% of patients, respectively. Only 55% of patients who admitted IDU were tested for HCV. Overall, minorities were more likely to have information regarding a risk factor documented than their white counterparts (79% *vs* 68%, $P < 0.0001$). Hispanics were less likely to have a risk factor history documented, compared to blacks and whites ($P < 0.0001$). Overall, minorities were less likely to be tested for HCV than whites in the presence of a known risk factor (23% *vs* 35%, $P = 0.004$). Among patients without documentation of risk factors, blacks and Hispanics were more likely to be tested than whites (20% and 24%, *vs* 13%, $P < 0.005$, respectively).

CONCLUSION: (1) Documentation of an HCV risk factor history in urban primary care is uncommon, (2) Racial differences exist with respect to HCV risk factor ascertainment and testing, (3) Minority patients, positive for HCV, are less likely to be referred for subspecialty care and treatment. Overall, minorities are less likely to be tested for HCV than whites in the presence of a known risk factor.

Key words: Hepatitis C; Minority groups; Urban health; Primary health care; Risk assessment

Trooskin SB, Navarro VJ, Winn RJ, Axelrod DJ, McNeal AS, Velez M, Herrine SK, Rossi S. Hepatitis C risk assessment, testing and referral for treatment in urban primary care: Role of race and ethnicity. *World J Gastroenterol* 2007; 13(7): 1074-1078

http://www.wjgnet.com/1007-9327/13/1074.asp

INTRODUCTION

Several studies have suggested that hepatitis C (HBV) manage-ment is suboptimal in primary care settings[1-5]. In fact, only 59% of primary care physicians (PCPs) reported asking patients about HCV risk factors[3]. A similar conclusion was made by another study which found that 46% and 62% of physicians reported that they routinely asked patients about a history of blood transfusion and injection drug use, respectively[4]. Shehab reported that HCV testing is rarely initiated in primary care clinics based on physician identified risk factors such as transfusion prior to 1992 or a history of injection drug use[1]. Similar studies among urban primary care practices, comprising patients at highest risk for exposure to HCV risk factors, have not been reported. Such a study would be important to better assess the feasibility of implementing wide scale risk assessment, testing, and treatment strategies.

The purpose of this retrospective cohort study is to assess the rates of HCV risk factor ascertainment, testing and referral for treatment in urban primary care practices, with particular attention to the effect of race and ethnicity as determined by systematic review of the medical records.

MATERIALS AND METHODS

A retrospective chart review was conducted in four

Table 1 Population demographics

Primary care practice	Total	Mean age	Gender (% male)	Insured (%)	Race				
					White (%)	Black (%)	Hisp (%)	OTH (%)	Unknown (%)
Clinic #1	1182	40	34	62	1	4	84	< 0.5	11
Clinic #2	948	41	62	57	4	65	7	1	24
Clinic #3	1089	42	34	95	26	37	2	5	31
Clinic #4	1188	48	43	98	45	22	2	6	26

urban primary care clinic sites in Philadelphia. These sites included two federally qualified health clinics serving predominantly minority populations and two university-based primary care practices; a family medicine practice and an internal medicine practice. Each of the four study sites is unique in the population that it serves. Clinic #1 is a community clinic which serves a predominantly Hispanic population (84%), comprised of mostly female patients (66%); in 2005 this clinic served approximately 15 000 patients. Clinic #2 is a community clinic which serves a predominantly black population (65%-70%); this clinic served approximately 7000 patients in 2005. The majority of the patients attending the two community clinics are either uninsured, or covered by a Medicaid HMO. The two university-based practices serve racially diverse populations. Approximately 60% of the patients attending the Family Medicine university-based practice (clinic #3, patient population served in 2005, 23 000) are black. The majority of the patients attending the practice have traditional insurance. Those with Medicare coverage and the uninsured make up a small percentage of the patient population, 6% and 5% respectively. Approximately 45% of the patients attending the Internal Medicine university-based practice (patients served in 2005, 21 000) are black (clinic #4), and the majority of the patients attending the practice have traditional insurance.

Random charts were selected at systematic intervals, based upon practice size, so that a total of approximately 1000 charts were reviewed from each practice. The number of charts required was calculated by taking into account the prevalence of risk factors among minority and non-minority subjects, the rate of risk factors recognized, the proportion of persons at risk screened for HCV and of those who tested positive. All these assumptions were derived from previous studies and from the authors' experience.

All patient visits in each selected chart were reviewed by a team of trained chart reviewers. No identifying information was collected. Data were available dating back to the patients' first visit, with a mean of 3.6 years (standard deviation 4.9 years) prior to the patients' most recent documented visit. Specific data collected included sex, age, race/ethnicity, as well as documentation of HCV risk factors. An HCV risk factor was broadly defined as any potential exposure to HCV; these included injection drug use, blood transfusion prior to 1992, percutaneous exposure as in the case of an exposed health care worker), non-injection drug use, tattoos, body piercing, history of sexually transmitted diseases, incarceration, and unprotected sex[9]. When documentation of an HCV risk factor was identified, it was determined if HCV testing was ordered and if the patient was referred for subspecialty care.

Statistical analysis

Data were collected using a standardized data collection instrument. All chart reviewers were trained and accompanied by an investigator. An investigator (SBT, VJN) re-reviewed at least 10% of all charts at random to check for accuracy. Trained data entry personnel entered the data into data management software (Microsoft Access). All data were analyzed using SAS v 9.14. Descriptive statistics and frequency tables were generated. Chi-square tests and logistic regression were used to assess statistical differences.

RESULTS

Study cohort

The total number of charts reviewed was 4407. One thousand one hundred eighty two charts were sampled from clinic #1; 948 charts from clinic #2; and 1089 from clinic #3 and 1 188 charts were reviewed from clinic #4 (Table 1). In order to facilitate a comparison of HCV management practices between races, we included only those charts in which race information was recorded. Approximately 23% of the charts reviewed did not include the race or ethnicity of the patient with clinic #1 having the lowest percentage of undocumented race/ethnicity (11%). Clinic #2 was missing approximately 24% of race/ethnicity documentation as compared to 26% for the Internal Medicine university-based practice and 31% for the Family Medicine university-based practice. Of the 3 413 charts with documented race/ethnicity which were included in the analysis, 1333, 1103, and 846 were reported as black, Hispanic, and white patients, respectively. Racial/ethnic groups were similar with respect to the average age of patients at the time of review (mean age 43). Forty-four percent of blacks were male, as compared to 34% of Hispanics and 45% of whites.

Documentation rate of HCV risk factors and the effect of race/ethnicity

Primary care providers documented a history (positive or negative) of IDU and/ or transfusion, arguably the most important risk factors for HCV acquisition, for 12% and 2% of patients, respectively. Only 0.48% (n = 21) of the total study population (n = 4407) were documented as having a positive history of transfusion prior to 1992. A history of percutaneous exposure as a health care

Table 2 Prevalence of HCV risk factors documented in patient charts by race/ethnicity

HCV risk factor	Black *n* = 1333		Hispanic *n* = 1103		White *n* = 846	
	Info available *n* (%)	With risk factor *n* (%)	Info available *n* (%)	With risk factor *n* (%)	Info available *n* (%)	With risk factor *n* (%)
IDU	241 (18)	54 (22)	48 (4.4)[e]	19 (40)	134 (16)	11 (8.2)
Transfusion	22 (1.7)	7 (32)	11 (1.0)	2 (18)	29 (3.4)	9 (31)
HCV needle stick	1 (0.1)	1 (100)	2 (0.2)	2 (100)	1 (0.1)	1 (100)
History of drug use	957 (72)[a]	359 (38)[b,c]	820 (74)[a]	94 (11)	535 (63)	53 (10)
History of STD	517 (39)[b]	350 (68)[b,c]	550 (50)[b]	185 (34)	164 (19)	53 (32)
History of HIV testing	452 (34)[b]	390 (86)	396 (36)[b]	305 (77)[a]	119 (14)	108 (91)
Tattoos	15 (1.1)	11 (73)	2 (0.2)	1 (50)	21 (2.5)	17 (80)
Piercing	2 (0.2)	0 (0)	1 (0.1)	0 (0)	1 (0.1)	1 (100)
Prostitution	9 (0.7)	6 (67)	3 (0.3)	2 (67)	1 (0.12)	1 (100)
Incarceration	38 (2.8)	36 (95)	12 (1.1)	12 (100)	4 (0.5)	3 (75)

[a]$P < 0.05$ *vs* whites; [c]$P < 0.05$ *vs* Hispanics; [b]$P < 0.001$ *vs* whites; [e]$P < 0.05$ *vs* blacks and whites.

worker was rarely specified ($n = 4$). Patients' histories of prostitution, incarceration, tattoos or body piercing were recorded for less than 2% of patients. Ascertainment of a history of non-injection drug use and sexually transmitted diseases occurred for 67% and 34% of patients, respectively (Table 2).

When documentation of HCV risk factor ascertainment was compared between different races/ethnicities, overall, minorities were more likely to have information regarding a risk factor documented than their white counterparts (79% *vs* 68%, $P < 0.0001$). Hispanics were much less likely to have had a history of IDU (positive or negative) documented than other groups; (4.4% ascertainment rate compared with 18% and 16% for blacks and whites, respectively) ($P < 0.0001$). Blacks and Hispanics were more likely to have had a documented history of non-IDU (72% and 74%, respectively) as compared to whites (63%, $P < 0.05$). Hispanics were more likely to have a chart entry regarding sexually transmitted diseases than were blacks (50% *vs* 39%) and blacks were more likely to have this history documented than whites (39% *vs* 19%, $P < 0.001$). Statistical comparisons were not used to assess differences between racial/ethnic groups for prostitution, incarceration, tattoos or body piercing due to the low rate of ascertainment.

Among patients who denied IDU, higher rates of other risk factors were reported among minorities. For example, 64% (29/45) of the minorities who denied IDU admitted non-injection drug use as compared to 31% (5/16) of the whites ($P < 0.05$). In addition, 25% of minorities (55/216) who denied IDU had a history of an STD documented as compared to 5% (7/123) of whites ($P < 0.05$).

Overall, females (74%, $n = 2\ 469$) were more likely than males (71%, $n = 1\ 818$) to have information regarding a risk factor history (positive or negative history) documented in the chart ($P = 0.0091$). However, among those individuals who had risk factor information documented, males (54%) were more likely to have a positive risk factor history than females (30%) ($P < 0.0001$). Among individuals with a documented positive HCV risk factor, there was no difference in the percentage of males and females tested for HCV ($P = 0.176$).

The odds of having documented information regarding HCV risk factors decreased by 1.4% with each additional year of age ($P < 0.0001$). Among those individuals who had risk factor information documented ($n = 3113$), the odds of having a positive risk factor history decreased by 1.7% with each additional year of age ($P < 0.0001$). Among individuals with a documented positive HCV risk factor ($n = 1158$), the odds of being tested increased by 1.3% with each additional year of age ($P = 0.025$).

HCV testing

Overall, minorities were less likely to be tested for HCV than whites in the presence of a known risk factor (23% *vs* 35%, $P = 0.004$). Of the 12% of patients for whom information regarding IDU was recorded ($n = 531$), 19% admitted this behavior. Of this group (blacks $n = 54$, Hispanics $n = 19$, whites $n = 11$), 55%-58% were tested for HCV, with no differences among the race or ethnic groups. Of the 21 patients documented as having a history of blood transfusion prior to 1992, approximately 67% were tested for HCV. Because the rate of documentation was so low for a history of transfusion, comparisons between racial/ethnic groups could not be made with respect to the rate of testing in the presence of this risk factor. Thirty-six percent of patients with tattoos and 50% of individuals with body piercing and with no identified other risk factor were tested for HCV (Table 3). Of those patients with a history of incarceration, 30% were tested. In the absence of IDU or prior blood transfusion, a history of sexually transmitted disease, non-injection drug use, engaging in sexual activity with or as a commercial sex worker, or a history of HIV testing were associated with testing rates of 19%, 22%, 33% and 24%, respectively. Due to the low rate of documentation of risk factors by the physicians, it was not possible to compare rates of testing between racial groups for piercing, incarceration, prostitution, and tattoos.

Among patients who denied risk factors when asked,

Table 3 Rates of testing among individuals with a documented non conventional HCV risk factor but no conventional risk factors

	Number with only non-conventional risk factors[1]	Tested (%)
Tattoos	33	36.4
Piercing	4	50.0
History of drug use	513	21.6
Prostitution	6	33.3
Incarceration	60	30.0
History of STD	706	19.4
History of HIV testing	903	24.1

[1]Patient may be included in more than one category.

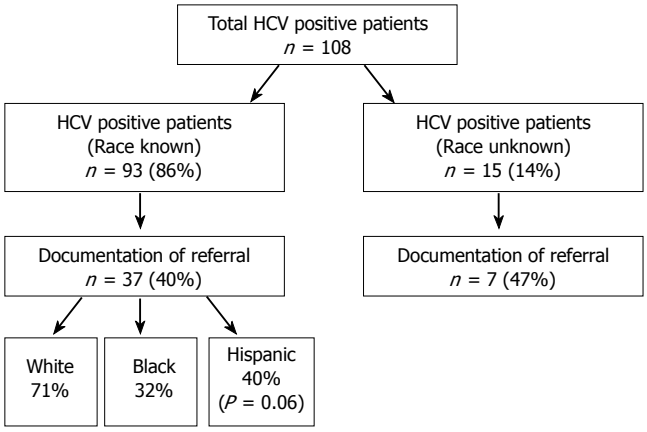

Figure 1 HCV referral practices.

the proportion tested for HCV was higher for blacks (20%, $n = 187$) and Hispanics (24%, $n = 29$) than for whites (13%, $n = 123$) ($P < 0.05$).

Overall, seven percent of patients in whom no risk factors were documented ($n = 3212$) were still tested for HCV. Hispanics (9.9%, $n = 848$) were more likely to be tested than both blacks (5.4%, $n = 737$) and whites (6.4%, $n = 733$) in the absence of any documented risk factor.

HCV referral practices

Of the 93 patients who were identified as being HCV positive (and for whom race/ethnicity was known), 37 (40%) had chart documentation of referral to a specialist. Of this group, 71% of white patients were referred, as compared to 40% of Hispanics ($P = 0.06$), and 32% of blacks (Figure 1). Among HCV positive patients whose race was not known ($n = 15$), 47% were referred to a specialist. Of these, 10 patients were from clinic #2, which serves a predominantly black population.

DISCUSSION

Overall, minorities were more likely to have information regarding HCV risk factors documented than their white counterparts. However, the ascertainment of IDU and blood transfusion prior to 1992, arguably the most important risk factors for HCV acquisition, was low, 12% and 1.8% respectively. Perhaps the greatest significance of these findings is that even in populations with expected high rates of risk factors, recommended management practices for risk factor ascertainment are infrequently followed[9].

Overall, minorities were less likely to be tested for HCV than whites in the presence of a known risk factor. The underlying reason for this is unknown but deserves further study. Rates of testing among patients who had a documented history of IDU or blood transfusion prior to 1992 were low, regardless of race. This finding demonstrates that recommendations regarding HCV testing practices are infrequently followed[9-12]. The reason for low rates of testing among minorities in the presence of a risk factor is likely to be multifactorial. Practitioners may be more likely to ask minority patients about risk behaviors, given an implicit understanding of the surrounding urban community and the epidemiology of HCV, but less likely to test if the provider feels that the patient would not be a candidate for treatment or if the patient would not opt for treatment.

Minorities were more likely than non-minorities to be tested for HCV in the absence of a recorded risk factor, or if such a history was denied. This finding could be explained by undocumented factors which might have led to testing, or the more frequent documentation of non-intravenous drug use in this population, which might be, in turn, interpreted as a risk for the acquisition of HCV. Unfortunately, medical record information did not allow us to more carefully assess these factors.

The rate of referral among patients who tested positive for HCV differed among the race groups. Specifically, minorities were less likely than whites to be referred for subspecialty evaluation. Although of potential significance, this finding may have been affected by missing referral information, local resources, as well as patient and provider perception of the need for and benefit of treatment.

Our study is limited in scope due to several factors. We performed the study in a relatively small number of practices which may reflect idiosyncrasies of a few treating physicians or have been affected by patient demographics which were unique to the local area. Moreover, we could not assess whether cultural, educational, or economic factors affected risk assessment and testing practices. Despite these limitations, the low rate of testing in a potentially high-risk population has serious implications; any strategy to test patients at risk for acquisition of HCV must be preceded by a plan that increases the rate of risk factor ascertainment in primary care.

Therefore, recommendations must be developed for physicians to increase the rate of identification of individuals who may have been exposed to HCV in the past as well as appropriate testing. Although primary care physicians are responsible for screening for multiple health problems during a routine health care visit, the benefits of identifying HCV risk factors and infection must not be overlooked. Risk factor screening and identification allows for patients to be educated regarding the risks of injection drug use and needle sharing. Appropriate testing and diagnosis of HCV allows for the patient to be evaluated

for treatment and receive counseling regarding alcohol cessation. In addition to physician education, patient education campaigns must also be developed to increase patient compliance with testing recommendations made by their physicians.

ACKNOWLEDGMENTS

The authors thank Sidney Cohen, MD for his assistance in preparation of the manuscript.

COMMENTS

Background

The increasing prevalence of hepatitis C virus (HCV) infection in the United States makes it an important challenge for primary care physicians (PCPs) and subspecialists. There are several potential benefits to diagnosing hepatitis C in a primary care setting.Diagnosis provides the patient with the opportunity to be counseled regarding behaviors that may transmit the infection to others such as sharing needles in the context of IDU. Diagnosis also allows the health care provider to educate the patient regarding behaviors that may hasten the progression of liver disease such as alcohol intake. Furthermore, early diagnosis allows the patient to be provided with appropriate preventive services such as hepatitis A and B vaccines. Lastly, early diagnosis allows the patient to be evaluated for hepatitis C therapy at a time when treatment may be more effective; prior to progression to fibrotic liver disease.

Research frontiers

Several studies have suggested that hepatitis C management is suboptimal in primary care settings. The purpose of this retrospective cohort study is to assess the rates of HCV risk factor ascertainment, testing and referral for treatment in urban primary care practices, with particular attention to the effect of race and ethnicity as determined by systematic review of the medical records.

Related publications

This publication is the first to result from our studies related to HCV management in primary care settings. Three additional manuscripts are in preparation. However, there are several articles, cited throughout this manuscript, from other investigators, that can provide additional information related to HCV management in primary care.

Innovations and breakthroughs

Very few studies have examined hepatitis C risk assessment, testing and referral for treatment in urban primary care settings. Moreover, no studies have examined racial differences within these practices. The findings indicate that (1) Documentation of an HCV risk factor history in urban primary care is uncommon, (2) Racial differences exist with respect to HCV risk factor ascertainment and testing, and (3) Minority patients, positive for HCV, were less likely to be referred for subspecialty care and treatment. Overall, minorities were less likely to be tested for HCV than whites in the presence of a known risk factor.

Applications

The findings presented may be applied in a number of settings where advances in the identification, testing and referral of primary care patients, specifically racial and ethnic minorities are sought. The results of this study may be of interest to epidemiologists and other public health professionals. The findings of this study address a deficit in the literature related to HCV in minorities and provide the background for future studies and intervention endeavors aimed at improving HCV identification and management in primary care settings.

Peer review

The results show that risk factors are often missed and minority patients are less likely to be tested for HCV and to be referred for treatment. The authors conclude that, although their investigation has some selection biases, the results indicate the existence of a consistent reservoir of infection in subgroups of patients, [specifically] black and Hispanic. Although "expected" given the characteristics of the population selected, the results are interesting.

REFERENCES

1 **Shehab TM**, Orrego M, Chunduri R, Lok AS. Identification and management of hepatitis C patients in primary care clinics. *Am J Gastroenterol* 2003; **98**: 639-644
2 **Shehab TM**, Sonnad SS, Jeffries M, Gunaratnum N, Lok AS. Current practice patterns of primary care physicians in the management of patients with hepatitis C. *Hepatology* 1999; **30**: 794-800
3 **Shehab TM**, Sonnad SS, Lok AS. Management of hepatitis C patients by primary care physicians in the USA: results of a national survey. *J Viral Hepat* 2001; **8**: 377-383
4 **Navarro VJ**, St Louis TE, Bell BP. Identification of patients with hepatitis C virus infection in New Haven County primary care practices. *J Clin Gastroenterol* 2003; **36**: 431-435
5 **Nicklin DE**, Schultz C, Brensinger CM, Wilson JP. Current care of hepatitis C-positive patients by primary care physicians in an integrated delivery system. *J Am Board Fam Pract* 1999; **12**: 427-435
6 **Frischer M**, Leyland A, Cormack R, Goldberg DJ, Bloor M, Green ST, Taylor A, Covell R, McKeganey N, Platt S. Estimating the population prevalence of injection drug use and infection with human immunodeficiency virus among injection drug users in Glasgow, Scotland. *Am J Epidemiol* 1993; **138**: 170-181
7 **Wolf RC**, Case P, Pagano M. Estimation of the prevalence of injection drug use in greater Boston in 1993. *J Psychoactive Drugs* 1998; **30**: 21-24
8 **Shehab TM**, Sonnad S, Gebremariam A, Schoenfeld P. Knowledge of hepatitis C screening and management by internal medicine residents: trends over 2 years. *Am J Gastroenterol* 2002; **97**: 1216-1222
9 **Recommendations for prevention and control of hepatitis C virus (HCV) infection and HCV-related chronic disease.** Centers for Disease Control and Prevention. *MMWR Recomm Rep* 1998; **47**: 1-39
10 **Management of hepatitis C.** *NIH Consens Statement* 1997; **15**: 1-41
11 **Screening for hepatitis C virus infection in adults: recommendation statement.** *Ann Intern Med* 2004; **140**: 462-464
12 **Strader DB**, Wright T, Thomas DL, Seeff LB. Diagnosis, management, and treatment of hepatitis C. *Hepatology* 2004; **39**: 1147-1171

S- Editor Liu Y **L- Editor** Zhu LH **E- Editor** Ma WH

PO Box 2345, Beijing 100023, China
www.wjgnet.com
wjg@wjgnet.com

World J Gastroenterol 2007 February 21; 13(7): 1079-1084
World Journal of Gastroenterology ISSN 1007-9327

RAPID COMMUNICATION

A new oral formulation for the release of sodium butyrate in the ileo-cecal region and colon

Aldo Roda, Patrizia Simoni, Maria Magliulo, Paolo Nanni, Mario Baraldini, Giulia Roda, Enrico Roda

Aldo Roda, Maria Magliulo, Paolo Nanni, Department of Pharmaceutical Sciences, University of Bologna, Via Belmeloro 6, Bologna 40126, Italy
Patrizia Simoni, Mario Baraldini, Giulia Roda, Enrico Roda, Department of Internal Medicine and Gastroenterology, University of Bologna, via Massarenti 9, Bologna 40126, Italy
Correspondence to: Professor Aldo Roda, Department of Pharmaceutical Sciences, University of Bologna, Via Belmeloro 6, Bologna 40126, Italy. aldo.roda@unibo.it
Telephone: +39-51-343398 Fax: +39-51-343398
Received: 2006-11-10 Accepted: 2007-01-22

Abstract

AIM: To develop a new formulation with hydroxy propyl methyl cellulose and Shellac coating for extended and selective delivery of butyrate in the ileo-caecal region and colon.

METHODS: One-gram sodium butyrate coated tablets containing ^{13}C-butyrate were orally administered to 12 healthy subjects and 12 Crohn's disease patients and the rate of ^{13}C-butyrate absorption was evaluated by $^{13}CO_2$ breath test analysis for eight hours. Tauroursodeoxycholic acid (500 mg) was co-administered as a biomarker of oro-ileal transit time to determine also the site of release and absorption of butyrate by the time of its serum maximum concentration.

RESULTS: The coated formulation delayed the ^{13}C-butyrate release by 2-3 h with respect to the uncoated tablets. Sodium butyrate was delivered in the intestine of all subjects and a more variable transit time was found in Crohn's disease patients than in healthy subjects. The variability of the peak $^{13}CO_2$ in the kinetic release of butyrate was explained by the inter-subject variability in transit time. However, the coating chosen ensured an efficient release of the active compound even in patients with a short transit time.

CONCLUSION: Simultaneous evaluation of breath $^{13}CO_2$ and tauroursodeoxycholic acid concentration-time curves has shown that the new oral formulation consistently releases sodium butyrate in the ileo-cecal region and colon both in healthy subjects and Crohn's disease patients with variable intestinal transit time. This formulation may be of therapeutic value in inflammatory bowel disease patients due to the appropriate release of the active compound.

Key words: Sodium butyrate; Inflammatory bowel diseases; Ulcerative colitis; Crohn's disease; Controlled release formulation; Pharmacokinetics; Stable isotope; Breath test

Roda A, Simoni P, Magliulo M, Nanni P, Baraldini M, Roda G, Roda E. A new oral formulation for the release of sodium butyrate in the ileo-cecal region and colon. *World J Gastroenterol* 2007; 13(7): 1079-1084

http://www.wjgnet.com/1007-9327/13/1079.asp

INTRODUCTION

Butyric acid, a short chain fatty acid, is the main colonic bacterial product of non-starch polysaccharides[1]. Impaired butyric acid metabolism (usually as butyrate species) has been implicated in the development of ulcerative colitis (UC)[2] but there are conflicting data regarding its role in the pathogenesis of UC[3-11]. Large bowel mucosa biopsy specimens from quiescent UC patients have also shown reduced oxidation of butyrate but not of glucose and glutamine, the two other major fuel sources for colonic epithelium[3]. *In vitro* studies conducted in terminal ileal mucosa biopsy specimens from UC patients support this concept[4]. A study on colonic sodium butyrate (NaB) metabolism using ^{14}C-butyrate rectal instillation and $^{14}CO_2$-breath test in patients affected by extensive UC showed a reduction in NaB oxidation, which returned to normal on remission[10]. The authors concluded that while impaired NaB metabolism is unlikely to be a primary cause of UC, impairment of short chain fatty acid metabolism by coloncytes may be a pathogenic factor. Another study indicated that in quiescent UC patients, the rate of NaB metabolism is not impaired[11].

It has recently been demonstrated that NaB exhibits anti-inflammatory properties as documented by a strong inhibition of interleukin (IL)-12 production by suppressing both IL-12p35 and IL-12p40 mRNA accumulation, and enhances IL-10 secretion in Staphylococcus aureus cell-stimulated human monocytes[12]. Investigation of the effects of NaB on some G1 phase-related proteins in a colon carcinoma cell line (HT29) has revealed another potential pharmacological property, since NaB is able to reduce cyclin D1 and p53 level in a dose-dependent

fashion and to suppress cell growth[13]. Thus, the lack of NaB in diets poor in carbohydrates could lead to clinically relevant functional alterations. In vivo, the growth inhibitory effects of NaB on colon cancer cells appear to be somewhat less marked[14,15].

Some clinical applications of NaB treatment have already been successfully evaluated. NaB enemas seem to provide an effective treatment for acute radiation proctitis, accelerating the healing process[16,17]. Oral co-administration of NaB and mesalazine in patients with active UC seems to improve the efficacy of mesalazine monotherapy[18,19].

These considerations prompted us to develop a new oral formulation in which NaB is released in the terminal ileum and colon, the target of its potential pharmacological activity[19].

The main problem in the development of controlled release formulation is to extrapolate *in vitro* release data to those achieved during *in vivo* studies. This is particularly crucial for drugs used in patients with gastrointestinal diseases in which the intestinal transit time shows a high variability.

The colonic target release of enteric coated butyrate requires an optimized coating able to prevent an early release (duodenum-jejunum-ileum) resulting in an absorption and metabolism of butyrate before reaching the colon. The coating is expected to release NaB from the ileo-caecal region as a result of a variation of intestinal pH but a delayed release delivery kinetic would result in a loss of a relatively high amount of butyrate in the stools.

Tuleu *et al*[20] have developed pellets for colonic delivery of NaB *via* oral route. When they are administered to rats a large amount is lost in the caecum for coating dissolution problems.

Optimization of the tablets is therefore crucial to determine in the healthy subjects and patients with Inflammatory bowel disease (IBD) the exact delivery site of butyrate in the intestine thus reducing false negative data in term of efficacy due to a poor delivery of the active compound in the target area.

Sodium butyrate tablets (1 g) coated with hydroxyl propyl methylcellulose (HPMC) and natural polymer Shellac have been developed and optimized by conventional *in vitro* studies. In the present study the optimal coating thickness was optimized *in vivo* by evaluating the release of the active ingredient by the kinetics of $^{13}CO_2$ excretion in the breath of healthy subjects and Crohn's disease patients after oral administration of ^{13}C-labeled NaB included in the 1 g tablets. The rate of $^{13}CO_2$ production is the result of ^{13}C-NaB intestinal absorption and metabolism that was evaluated by the rate of production of $^{13}CO_2$ in exhaled breath over 8 h. The $^{13}C/^{12}C$ isotope ratio was measured by isotope ratio mass spectrometry (IRMS). The intestinal transit time was evaluated by simultaneous co-administration of tauroursodeoxycholic acid (TUDCA).

TUDCA was selected as a biomarker of oro-ileal transit time since it is absorbed actively only in the ileum, the time of its peak serum level reflects the oro-ileal transit time. A sensitive and specific enzyme immunoassay was performed to evaluate serum TUDCA concentration at various time intervals after administration as previously described[21].

To evaluate the kinetics of the release of NaB from the tablets, we compared the time of maximum $^{13}CO_2$ excretion with that of peak serum TUDCA concentration within individual subjects in order to overcome the high variability in intestinal transit time.

MATERIALS AND METHODS

Oral NaB formulation

Plain and coated tablets containing hydroxyl propyl methylcellulose and shellac with a pH dependent extended release coating were used in the study. Both formulations contained 1 g of NaB and three batches of tablets containg 5%, 10% and 20% w/w of ^{13}C-NaB (CIL, Andover MA, USA) were prepared.

The difference between the two tablets was the internal pre-coating of HPMC and external coating of shellac, which is resistant to desgregation up to pH 7. All other excipients of the formulations were identical. The pre-coating of HPMC was made to avoid that basic characteristics of the active ingredient in the tablet nucleus would induce an early dissolution of shellac which is resistant to acid pH and soluble to basic pH. In order to optimize the release of NaB in the colon, different thickness films of shellac (50, 80 and 120 μm) were studied. Coated tablets (Sobutir) were supplied by Promefarm srl, Milan, Italy. The different formulations were then administered to the same subjects in order to verify simultaneously the kinetic of NaB release in relation to the oro-ileal transit time evaluated by the time of the serum TUDCA peak and select the formulation that would be admitted to the complete study.

Subjects studied

The study was carried out in 12 healthy subjects (6 males and 6 females, median age 42 years, range 18-60 years) and 12 Crohn's disease patients (9 females and 4 males, median age 40 years, range 18-65 years) with a relatively mild activity index ranging from $320 \geqslant$ C.D.A.I. $\geqslant 220$[22]. To avoid any difference in the transit time, we studied only patients with the same level of activity index. In addition, the patients studied had no pure ileal or ileo-colonic involvement and they did not receive steroid or immunosuppressive treatment. All patients during the study presented diarrhoea. Before this final controlled study volunteers received the different formulations under development and between the different studies a washout period of one week was used. Thirty minutes before the study, 2 mL of blood was collected for the baseline values, as were two separate samples of breath in a 10 mL capped glass tube. After administration of the 1 g ^{13}C-NaB tablet and of 500 mg TUDCA as gelatine capsules (Tudcabil®, Pharmacia Upjohn, Milan, Italy), the subjects received a standard liquid test meal of 375 Kcal, containing 17 g of fat, 10.4 g of protein and 10 g of carbohydrates. Breath and blood samples were collected at 30 min intervals over an 8-h period (unless otherwise specified). The oro-ileal transit time was defined as the time interval between administration of TUDCA and the peak serum TUDCA (C_{max}) time[21]. The time of the maximum $^{13}CO_2$ breath excretion was used to represent the time of release and absorption of sodium butyrate. The study approved by

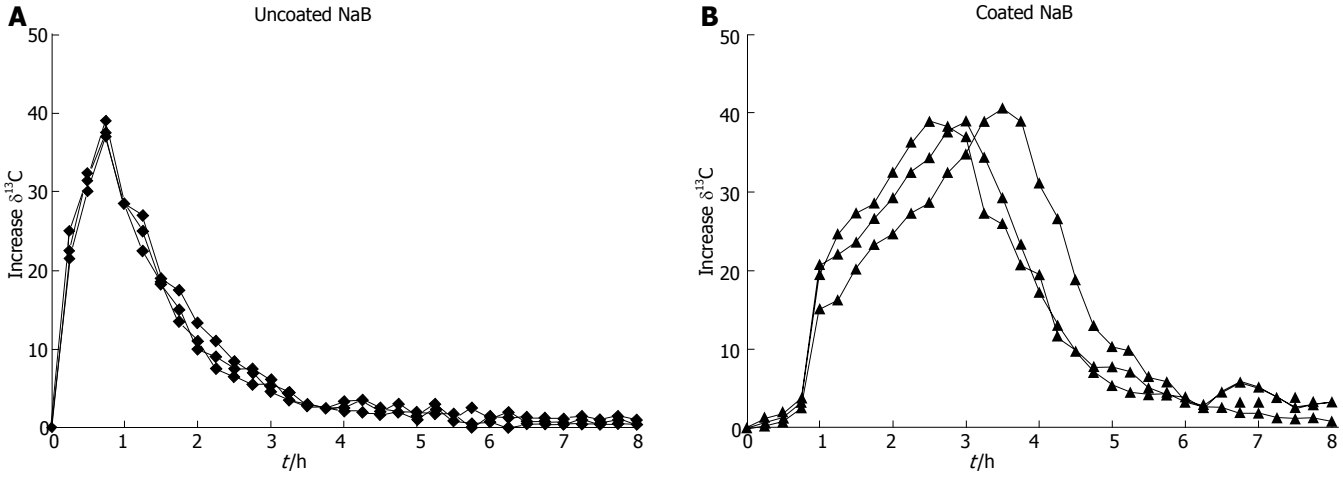

Figure 1 Excretion of breath $^{13}CO_2$ after oral administration of uncoated (**A**) and shellac-coated (**B**) 1 g NaB tablets containing 10% w/w of ^{13}C-NaB in 12 healthy subjects. The experiment of each formulation was repeated three times in the same subject for different weeks.

the Ethical Committee of University of Bologna was conducted according to the institutional guidelines.

Analytical methods

$^{13}CO_2$ breath test: $^{13}CO_2$ in each of the duplicate breath samples was analyzed by continuous flow isotope ratio mass spectrometry (IRMS; ANCA, PDZ Europa Ltd, Cheshire U.K.). The results were expressed as δ^{13}C that was calculated from:

$$\delta^{13}C = \left(\frac{^{13}C/^{12}C\ (sample)}{^{13}C/^{12}C\ (std)} - 1 \right) \times 1000$$

where $^{13}C/^{12}C$ (std) is the Pee Dee Belemnite (PDB) reference standard $^{13}C/^{12}C$ ratio, the final value was expressed as a milli percentage (δ^{13}C‰).

Serum TUDCA enzyme immunoassay

Serum TUDCA levels were determined by a specific chemiluminescent enzyme immunoassay previously developed and optimized in our laboratory[21]. The method is a solid-phase competitive format with a TUDCA-specific polyclonal antibody immobilized on 96 wells black polystyrene microtiter plates. A horseradish peroxidase (HRP)-UDCA conjugate was synthesized, purified, properly characterized, and used as enzymatic tracer.

For the TUDCA assay 100 μL of the sample (serum diluted 1/50, v/v with assay buffer: 0.05 mol/L phosphate/EDTA buffer, pH 7.4, containing 1 g/L bovine serum albumin) or of six standard TUDCA solutions with a concentration ranging from 0.01 to 1000 nmol/L was incubated in the 96-well microtiter plates coated with the antibody for 1 h at 37℃ with 100 μL of the properly diluted HRP-UDCA tracer. After washed with assay buffer, 100 μL of the chemiluminescent substrate (H_2O_2/luminol/enhancer SuperSignal ELISA Pico, Pierce, Ⅱ, USA) was added and the light signal was measured using a PMT based luminometer microtiter reader (Luminoskan Ascent, Thermo Electron Corporation MA, USA) .

TUDCA concentrations were determined by a plot of chemiluminescent (CL) signal *vs* the log of concentration and the best data fit was obtained by linear regression of the six point standards. Serum TUDCA was expressed as nmol/L of serum.

RESULTS

Optimization of NaB oral formulation

The ^{13}C-NaB dose to include in the 1 g NaB tablet was standardized by quantifying the amount of label to produce a breath CO_2 enrichment of the ^{13}C-isotope that could be accurately evaluated with respect to the baseline value representing its natural abundance.

During the course of three separate weeks, three 1-g NaB tablets containing 5%, 10% and 20% w/w of ^{13}C-NaB respectively, were administered to six healthy subjects. The excretion rate of $^{13}CO_2$ in breath was measured and the maximum value was calculated. The dose of 100 mg of the label was chosen giving a δ^{13}C‰ of 15.3 that was much higher than the baseline value of -28%. This wide cut off could allow the accurate evaluation of not only the maximum excretion of $^{13}CO_2$ but also small variations during the 8-h study period and eventually low $^{13}CO_2$ excretion resulting in patients with impaired metabolism of NaB. The coating thickness was optimized according to the kinetics of the $^{13}CO_2$ excretion accounting for the release and absorption of butyrate from the tablet. The results obtained with 50, 80 and 120 μm thickness coating suggested that the coating size of 80 μm was the most adequate to prevent a too early release and absorption of NaB as occurred with the 50 μm thickness and to ensure complete release of the active ingredient in a time comparable with the oro-ileal transit time.

The NaB tablet containing 10% w/w of ^{13}C-NaB and 80 μm-thick coating was used to evaluate the final performance of the formulation. The intra-subject variability was evaluated by administering either coated or uncoated NaB formulations three times to the same subject in separate experiments and monitoring the excretion of $^{13}CO_2$ at 15 min time intervals (Figure 1). In the uncoated tablet, the intra-subject variability was very low and the curves were almost super impossible.

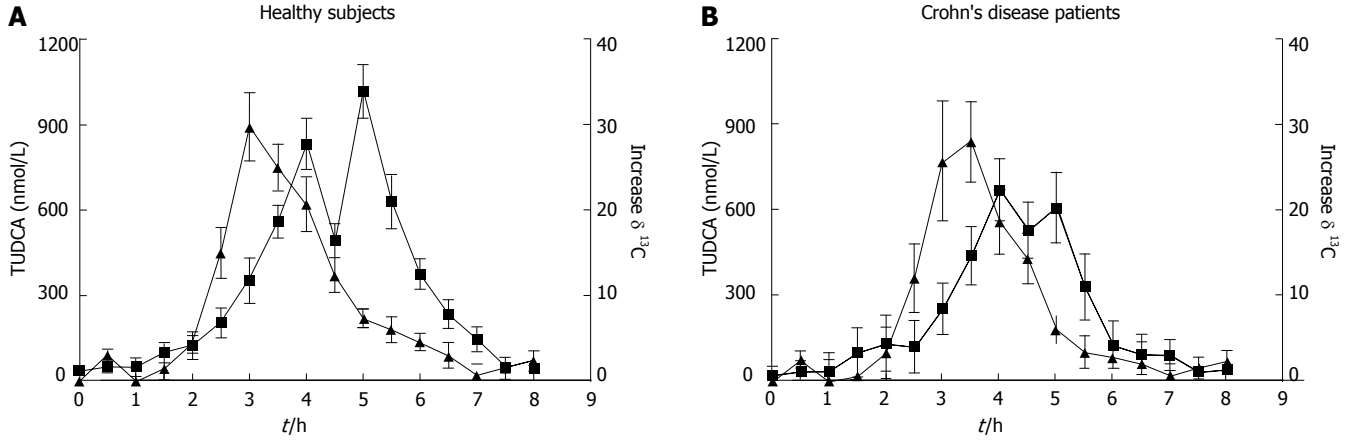

Figure 2 Profiles of the mean $^{13}CO_2$ breath excretion (▲) and serum TUDCA concentrations (■) plotted against time. Data were collected after administration of the Shellac-coated tablet containing 10% w/w of ^{13}C-butyrate and two gelatine capsules containing 250 mg each of TUDCA. Data are expressed as mean ± SD in 12 healthy subjects (**A**) and 12 Crohn's disease patients (**B**).

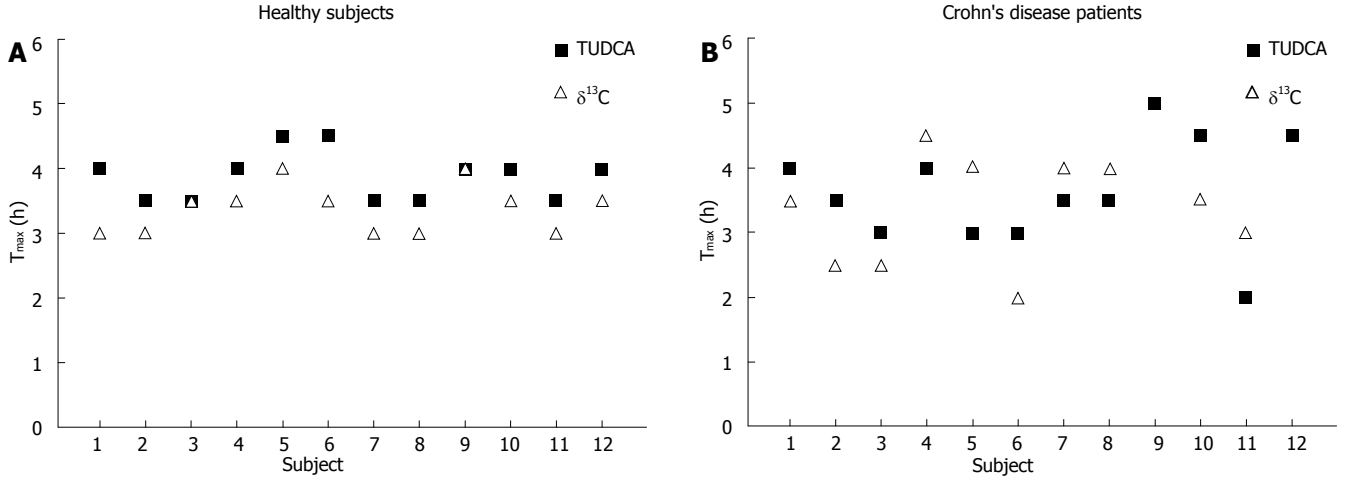

Figure 3 Tmax obtained in control subjects (**A**) and Crohn's disease patients (**B**) using serum TUDCA and $^{13}CO_2$ breath tests.

The maximum excretion was achieved 45 min after administration of the dose and the absorption started just in the first 15 min. A slightly higher variability was observed when the coated formulation was administered as a result of an intra-subject variability in gastric emptying and overall gastrointestinal transit. The mean peak $^{13}CO_2$ excretion time of the coated tablets was 180 min (range 150-225 min), showing the extended release of NaB caused by the shellac coating.

Serum TUDCA chemiluminescent enzyme immunoassay

Chemiluminescent enzyme immunoassay fulfilling all the standard requirements of accuracy and precision was used. The intra and inter studies showed that the coefficient of variation was always below 9%. The limit of quantification of 10 nmol/L allowed direct analysis of TUDCA in a 20-fold diluted serum sample.

The mean serum TUDCA profiles together with the kinetics of $^{13}CO_2$ excretion obtained in the healthy subjects and Crohn's disease patients are shown in Figure 2. The serum TUDCA profile was characterized by two peaks. The first peak was reached 180-200 min after TUDCA administration and represented the oro-ileal transit time, the second peak was observed after 300-400 min as a result of the enterohepatic circulation of the absorbed TUDCA.

In the healthy subjects peak of serum TUDCA concentration was achieved at a median of 4 h (range 3-5 h) after NaB administration. The mean peak $^{13}CO_2$ excretion time occurred slightly earlier at 3.5 h and the range of variability was similar to that of TUDCA. A similar behavior was observed in Crohn's disease patients with a higher variability due to variation in the intestinal transit time.

Top panel and bottom panel are shown in Figure 3. The Tmax was obtained in control subjects and Crohn's disease patients using the serum TUDCA and $^{13}CO_2$ breath tests. No subject and Crohn's disease patient had an earlier release of $^{13}CO_2$ after administration of the coated tablets with respect to the Tmax of TUDCA. Similarly no subject and patient missed to give a peak of $^{13}CO_2$ excretion or reported the loss of intact tablets in stools.

The ileal release was defined (a priori) as the $^{13}CO_2$ peak occurring within 30 min from the time of TUDCA peak whereas colonic release was considered as the $^{13}CO_2$

peak occurring after this interval.

The temporal correspondence between the maximum $^{13}CO_2$ excretion times, with the TUDCA time at the Cmax representing the biomarker oro-ileal transit time even if occurring at different times, usually slightly earlier suggested that the active ingredient was still delivered in the colon in high concentration and therefore we expected that it would exert its activity in IBD patients.

In all the studied subjects, NaB was efficiently released by the coated tablet, suggesting that the formulation developed could be used in these subjects to prevent an early absorption and deliver a large amount of NaB in the colon just starting from the terminal ileum as shown by the kinetic profile of $^{13}CO_2$ and serum TUDCA.

DISCUSSION

The present study was designed to evaluate a new NaB formulation able to deliver the active ingredients of 1 g tablets coated with shellac into the colon by oral administration. The coating delayed the release of the active ingredients by two-three hours with respect to the uncoated formulation, thus a large amount of NaB could reach the colon, as demonstrated by the temporal similarity between the profiles of $^{13}CO_2$ breath test and serum TUDCA concentration. In fact, TUDCA is absorbed by an active carrier-mediated mechanism only in the ileum[23, 24], and previous studies comparing the TUDCA serum levels after its oral administration with other markers of intestinal transit-time such as sulfasalazine showed that this method provides a valid and practical means of assessment of the oro-ileal transit-time[21]. Comparison of the peak times of $^{13}CO_2$ excretion and serum TUDCA concentration could confirm the efficacy of shellac coating in delivering NaB to the colon independently of intestinal transit-time variability. The dissolution of Shellac coating at pH 7 and its thickness driving the kinetics of the dissolution process has been well optimized and a large amount of NaB which starts to be delivered after two hours reaches the intact ileo-cecal region as shown by the kinetics of TUDCA intestinal absorption.

It was recently reported that topical butyrate improves the efficacy of 5-ASA in refractory distal ulcerative colitis[17], due to the presence of NaB in the colon administered topically *in situ*. Vernia *et al*[16] demonstrated in a pilot study that oral butyrate may improve the efficacy of oral mesalazine in active ulcerative colitis but a large scale investigation to confirm the present findings is still required. In this case the NaB was administered as tablets coated with a pH-dependent soluble polymer. More recently it has been reported that chronic feeding (tablets, 4 g a day for 8 wk) of this enteric coated NaB formulation (tablets, 4 g a day for 8 wk) (tablets, 4 g a day for 8 wk) can effectively induce clinical improvement/remission in mild Crohn's disease[25].

An adequate enteric coating is needed for therapy of ileo-colonic disorders since when uncoated uncoated oral formulation of NaB is administered in an uncoated oral formulation, the compound is promptly dissolved and rapidly metabolized before reaching the colon as shown by the time of the maximum $^{13}CO_2$ excretion occurring within 30-45 min after the ^{13}C butyrate oral administration. A specific enteric coated formulation has been therefore designed to deliver the drug in that portion of the intestine keeping into account the high variability of the intestinal transit time observed in IBD patients.

The amount of $^{13}CO_2$ excreted in breath was similar among the Crohn's disease patients, showing that the rate and efficiency of NaB metabolism are similar in the healthy subjects. The patients were characterized by a mild active disease accounting for the efficient metabolism of butyrate and the oral formulation was expected to deliver NaB into the colon in a similar extent as to enema administration.

Furthermore the new coated ^{13}C-NaB oral formulation containing ^{13}C-labeled butyrate can also be used to evaluate the rate of colocyte-metabolized NaB by performing $^{13}CO_2$ breath test before and after chronic administration of NaB. The impairment of NaB utilization by colonocytes that has been observed in previous studies[2-4] can then readily be evaluated by measuring the reduction in cumulative $^{13}CO_2$ excretion in the 8-h period following oral administration of colon-targeted NaB tablets. A similar approach could also be used to evaluate the effectiveness of therapies for IBD patients with mesalazine (either alone or in combination with NaB) and new formulations designed to improve NaB absorption and metabolism. The reported NaB formulation can effectively improve oral administration of NaB ensuring the release of the active compound in the lower intestine portion which is the target for its pharmacological activity.

REFERENCES

1 **Cummings JH**. Short chain fatty acids in the human colon. *Gut* 1981; **22**: 763-779
2 **Roediger WE**, Nance S. Metabolic induction of experimental ulcerative colitis by inhibition of fatty acid oxidation. *Br J Exp Pathol* 1986; **67**: 773-782
3 **Chapman MA**, Grahn MF, Boyle MA, Hutton M, Rogers J, Williams NS. Butyrate oxidation is impaired in the colonic mucosa of sufferers of quiescent ulcerative colitis. *Gut* 1994; **35**: 73-76
4 **Chapman MA**, Grahn MF, Hutton M, Williams NS. Butyrate metabolism in the terminal ileal mucosa of patients with ulcerative colitis. *Br J Surg* 1995; **82**: 36-38
5 **Finnie IA**, Taylor BA, Rhodes JM. Ileal and colonic epithelial metabolism in quiescent ulcerative colitis: increased glutamine metabolism in distal colon but no defect in butyrate metabolism. *Gut* 1993; **34**: 1552-1558
6 **Scheppach W**, Sommer H, Kirchner T, Paganelli GM, Bartram P, Christl S, Richter F, Dusel G, Kasper H. Effect of butyrate enemas on the colonic mucosa in distal ulcerative colitis. *Gastroenterology* 1992; **103**: 51-56
7 **Steinhart AH**, Hiruki T, Brzezinski A, Baker JP. Treatment of left-sided ulcerative colitis with butyrate enemas: a controlled trial. *Aliment Pharmacol Ther* 1996; **10**: 729-736
8 **Patz J**, Jacobsohn WZ, Gottschalk-Sabag S, Zeides S, Braverman DZ. Treatment of refractory distal ulcerative colitis with short chain fatty acid enemas. *Am J Gastroenterol* 1996; **91**: 731-734
9 **Scheppach W**. Treatment of distal ulcerative colitis with short-chain fatty acid enemas. A placebo-controlled trial. German-Austrian SCFA Study Group. *Dig Dis Sci* 1996; **41**: 2254-2259
10 **Den Hond E**, Hiele M, Evenepoel P, Peeters M, Ghoos Y, Rutgeerts P. In vivo butyrate metabolism and colonic permeability in extensive ulcerative colitis. *Gastroenterology*

1998; **115**: 584-590
11 **Simpson EJ**, Chapman MA, Dawson J, Berry D, Macdonald IA, Cole A. In vivo measurement of colonic butyrate metabolism in patients with quiescent ulcerative colitis. *Gut* 2000; **46**: 73-77
12 **Säemann MD**, Böhmig GA, Osterreicher CH, Burtscher H, Parolini O, Diakos C, Stöckl J, Hörl WH, Zlabinger GJ. Anti-inflammatory effects of sodium butyrate on human monocytes: potent inhibition of IL-12 and up-regulation of IL-10 production. *FASEB J* 2000; **14**: 2380-2382
13 **Coradini D**, Pellizzaro C, Marimpietri D, Abolafio G, Daidone MG. Sodium butyrate modulates cell cycle-related proteins in HT29 human colonic adenocarcinoma cells. *Cell Prolif* 2000; **33**: 139-146
14 **Otaka M**, Singhal A, Hakomori S. Antibody-mediated targeting of differentiation inducers to tumor cells: inhibition of colonic cancer cell growth in vitro and in vivo. A preliminary note. *Biochem Biophys Res Commun* 1989; **158**: 202-208
15 **Avivi-Green C**, Polak-Charcon S, Madar Z, Schwartz B. Apoptosis cascade proteins are regulated in vivo by high intracolonic butyrate concentration: correlation with colon cancer inhibition. *Oncol Res* 2000; **12**: 83-95
16 **Vernia P**, Monteleone G, Grandinetti G, Villotti G, Di Giulio E, Frieri G, Marcheggiano A, Pallone F, Caprilli R, Torsoli A. Combined oral sodium butyrate and mesalazine treatment compared to oral mesalazine alone in ulcerative colitis: randomized, double-blind, placebo-controlled pilot study. *Dig Dis Sci* 2000; **45**: 976-981
17 **Vernia P**, Annese V, Bresci G, d'Albasio G, D'Incà R, Giaccari S, Ingrosso M, Mansi C, Riegler G, Valpiani D, Caprilli R. Topical butyrate improves efficacy of 5-ASA in refractory distal ulcerative colitis: results of a multicentre trial. *Eur J Clin Invest* 2003; **33**: 244-248
18 **Pinto A**, Fidalgo P, Cravo M, Midões J, Chaves P, Rosa J, dos Anjos Brito M, Leitão CN. Short chain fatty acids are effective in short-term treatment of chronic radiation proctitis: randomized, double-blind, controlled trial. *Dis Colon Rectum* 1999; **42**: 788-795; discussion 795-796
19 **Høverstad T**, Bøhmer T, Fausa O. Absorption of short-chain fatty acids from the human colon measured by the $14CO_2$ breath test. *Scand J Gastroenterol* 1982; **17**: 373-378
20 **Tuleu C**, Andrieux C, Cherbuy C, Darcy-Vrillon B, Duée PH, Chaumeil JC. Colonic delivery of sodium butyrate via oral route: acrylic coating design of pellets and in vivo evaluation in rats. *Methods Find Exp Clin Pharmacol* 2001; **23**: 245-253
21 **Azzaroli F**, Mazzella G, Mazzeo C, Simoni P, Festi D, Colecchia A, Montagnani M, Martino C, Villanova N, Roda A, Roda E. Sluggish small bowel motility is involved in determining increased biliary deoxycholic acid in cholesterol gallstone patients. *Am J Gastroenterol* 1999; **94**: 2453-2459
22 **Best WR**, Becktel JM, Singleton JW, Kern F. Development of a Crohn's disease activity index. National Cooperative Crohn's Disease Study. *Gastroenterology* 1976; **70**: 439-444
23 **Wilson FA**. Intestinal transport of bile acids. In: Schultz SG, Field M, Frizzell RA, editors. Handbook of physiology. The gastrointestinal system. Intestinal absorption and secretion. Bethesda: Am Physiol Soc, 1991: 389-404
24 **Aldini R**, Montagnani M, Roda A, Hrelia S, Biagi PL, Roda E. Intestinal absorption of bile acids in the rabbit: different transport rates in jejunum and ileum. *Gastroenterology* 1996; **110**: 459-468
25 **Di Sabatino A**, Morera R, Ciccocioppo R, Cazzola P, Gotti S, Tinozzi FP, Tinozzi S, Corazza GR. Oral butyrate for mildly to moderately active Crohn's disease. *Aliment Pharmacol Ther* 2005; **22**: 789-794

S- Editor Liu Y L- Editor Wang XL E- Editor Lu W

PO Box 2345, Beijing 100023, China
www.wjgnet.com
wjg@wjgnet.com

World J Gastroenterol 2007 February 21; 13(7): 1085-1089
World Journal of Gastroenterology ISSN 1007-9327

RAPID COMMUNICATION

Possible role of human cytomegalovirus in pouchitis after proctocolectomy with ileal pouch-anal anastomosis in patients with ulcerative colitis

Damian Casadesus, Tatsuo Tani, Toshifumi Wakai, Satoshi Maruyama, Tsuneo Iiai, Haruhiko Okamoto, Katsuyoshi Hatakeyama

Damian Casadesus, Tatsuo Tani, Toshifumi Wakai, Satoshi Maruyama, Tsuneo Iiai, Haruhiko Okamoto, Katsuyoshi Hatakeyama, Division of Digestive and General Surgery, Niigata University Graduate School of Medical and Dental Sciences, Niigata, Japan
Correspondence to: Tatsuo Tani, MD, PhD, Division of Digestive and General Surgery, Niigata University Graduate School of Medical and Dental Sciences, 1-757 Asahimachi-dori, Niigata City 951-8510, Japan. ttani@med.niigata-u.ac.jp
Telephone: +81-25-2272228 Fax: +81-25-2270779
Received: 2006-10-24 Accepted: 2006-11-11

Abstract

AIM: To detect the presence of human cytomegalovirus (HCMV) proteins and genes on the ileal pouch of patients with ulcerative colitis who have undergone proctocolectomy with ileal pouch-anal anastomosis (IPAA).

METHODS: Immunohistochemistry, polymerase chain reaction (PCR) and PCR sequencing methods were utilized to test the presence of HCMV in pouch specimens taken from 34 patients in 86 endoscopies.

RESULTS: HCMV genes and proteins were detected in samples from 12 (35.2%) patients. The rate of detection was significant in the endoscopies from patients diagnosed with pouchitis (5 of 12, 41.6%), according to the Japanese classification of pouchitis, in comparison to patients with normal pouch (7 of 62, 11.2%; P = 0.021). In all patients with pouchitis in which the HCMV was detected, it was the first episode of pouchitis. The virus was not detected in previous biopsies taken in normal endoscopies of these patients. During the follow-up, HCMV was detected in one patient with recurrent pouchitis and in 3 patients whose pouchitis episodes improved but whose positive endoscopic findings persisted.

CONCLUSION: HCMV can take part in the inflammatory process of the pouch in some patients with ulcerative colitis who have undergone proctocolectomy with IPAA.

Key words: Human cytomegalovirus; Pouchitis; Inflammatory bowel disease; Ileal pouch-anal anastomosis

Casadesus D, Tani T, Wakai T, Maruyama S, Iiai T, Okamoto H, Hatakeyama K. Possible role of human cytomegalovirus in pouchitis after proctocolectomy with ileal pouch-anal anastomosis in patients with ulcerative colitis. *World J Gastroenterol* 2007; 13(7): 1085-1089

http://www.wjgnet.com/1007-9327/13/1085.asp

INTRODUCTION

Human cytomegalovirus (HCMV) is a ubiquitous, species-specific beta-herpes virus that can establish lifelong latency in the host after the primary infection. HCMV infection is endemic within the human population, and its role as a pathogen in the colon and ileum is still unclear. Early studies suggested that HCMV infection initiates some cases of ulcerative colitis (UC)[1,2], plays a role in UC exacerbation[3], causes self-limited colitis[4], and increases the incidence of complications, emergency surgery or death in patients with UC[3,5,6].

Pouchitis is a frequent complication in patients with UC who have undergone colectomy with ileal pouch-anal anastomosis (IPAA). The etiology of pouchitis is still unknown, but several theories have been proposed, such as genetic susceptibility, a possible novel third form of inflammatory bowel disease (IBD) in the pouch, recurrence of UC in the pouch, misdiagnosis of Crohn's disease, ischemic complication of surgery, fecal stasis, and bacterial overgrowth. Recent studies have reported HCMV infection as a cause of pouchitis in 3 immunocompetent patients[7,8]. The diagnosis of this specific infectious agent as a possible cause of pouchitis is crucial before initiating immune modifier therapy, fecal diversion, or pouch excision. We explored the presence of viral gene products and proteins in the pouches of a series of patients who have undergone proctocolectomy with IPAA.

MATERIALS AND METHODS

Patients

Enrolled in this study were 34 Japanese patients (17 females, 17 males) who underwent proctocolectomy

with IPAA at the Department of General and Digestive Surgery, Niigata University Hospital between 1990 and 2003. The patients' age ranged from 24 to 68 years (mean 34.8 ± 15.4 years). Oral and written informed consent was obtained from each patient. The study protocol adhered to the ethical guidelines of the 1975 Declaration of Helsinki and was approved by the institution's ethical committee. We reviewed the clinical and endoscopic records of all the enrolled patients. The patients had a history of UC between 1 to 5 years and underwent the operation in two or three steps. The diagnosis of pouchitis was based on clinical and endoscopic criteria according to the modified pouchitis disease activity index (mPDAI)[9] and the Japanese classification of pouchitis (JCP)[10]. JCP defines pouchitis as a condition with severe endoscopic findings, or with two or more clinical symptoms and moderate endoscopic findings. Eighty-six endoscopies were performed in 34 patients. Twenty-eight endoscopies were performed in patients complaining of symptoms, 46 endoscopies were carried out in routine controls after surgery, and 12 were performed during pouchitis follow-up. Biopsies were performed both in areas with pathological findings (edema, granularity, friability, erythema, loss of vascular pattern, mucous exudates, erosion or ulceration) and in areas with mucosa of normal appearance.

Immunohistochemistry (IHC)

Immunostaining for HCMV was performed on paraffin-embedded sections with a cocktail of two monoclonal mouse antibodies against human cytomegalovirus (clone CCH2 & DDG9, Dako Cytomation, CA, USA) at a dilution of 1:100. All paraffin-embedded samples from each patient were used for IHC. According to the company specifications, antibody CCH2 reacts with an early nuclear protein identical with non-structural DNA-binding protein p52 (UL44), whereas antibody DDG9 reacts with an immediate-early nuclear protein with a molecular weight of about 76 kDa. For both antibodies, the reactivity persists also at later stages during HCMV infection where the localization is less distinctly nuclear and appears to be in the cytoplasm. Five-μm thick sections were deparaffinized and rehydrated using graded alcohol concentrations, then the sections were digested with trypsin (Sigma Chemicals, Germany) at 37℃ for 20 min. After endogenous peroxidase was blocked by incubation with 30 mL/L hydrogen peroxide for 20 min, the sections were incubated overnight at 4℃ with the cocktail of anti-human cytomegalovirus antibodies. Control slides from the same biopsy block were incubated with PBS without the primary antibody. They were then incubated at room temperature for 30 min with goat anti-mouse immunoglobulin conjugated to a peroxidase-labeled amino-acid polymer, Simple Stain Max PO (Nichirei Histofine, Tokyo, Japan). The sections were reacted with diaminobenzidine in 50 mol/L Tris-HCL (pH 7.5) with 0.3% (vol/vol) hydrogen peroxide for 5 min and counterstained with hematoxylin.

Polymerase chain reaction (PCR) and PCR sequencing

To confirm that our probe was specific for HCMV nucleic acids, DNA samples were extracted from two paraffin sections 20 μm in size, and cut from the same biopsy specimens described above with a QIAamp DNA minikit (Qiagen, Tokyo, Japan). From each sample, 200 ng of DNA was amplified by PCR with the primer 5'-TGCAGTTTGGTCCCTTAAAG-3' and 5'-AAGAATCCTCACCTGGCTTA-3' from the HCMV large structural phosphoprotein (UL32) and the primer 5'-TCCAACACCCACAGTACCCGT-3' and 5'-CGGAAACGATGGTGTAGTTCG-3' from the HCMV glycoprotein B (UL55), using a method specific for UL32 gene[11] and UL55 gene[12]. The amplified DNA products were visualized on 2% agarose gel (NuSieve GTG agarose, FMC Bio Products, Rockland, USA) stained with 0.01% (vol/vol) ethidium bromide and visualized under ultraviolet light. The bands of UL32 gene were cut out and the DNA was analyzed by automated sequencing (ABI Prism 310 Diagnostics Systems, Applied Biosystems, Tokyo, Japan). The HCMV sequence was confirmed by NCBI Blast, and found to be identical to that of UL32. To avoid potential PCR contamination, all preparations were processed masked, no positive controls were used in any PCR reactions and a separated room was used for the preparation of the reaction mixture. The distilled water control gave negative results in each assay run, and confirmed the efficiency of these preventive measures. When IHC and/or PCR were positive, the sample was considered to be HCMV-positive, and when both of them were negative, the sample was considered to be HCMV-negative.

Statistical analysis

The results of HCMV detection are expressed in numbers of patients and percentages. The results of the cumulative-life steroid dose are given as means ± SD. Statistical significance was calculated with SPSS 13 (SPSS Inc., Chicago, IL, USA) using Fisher's exact test and Student's *t*-test when appropriate, and the results were considered significant at $P \leqslant 0.05$.

RESULTS

Twenty-eight endoscopies were performed in patients complaining of symptoms and 46 endoscopies were performed in routine controls at different time points after surgery. Four hundred and seventy-three specimens were evaluated, 103 from patients with pouchitis and 370 from patients with a normal pouch. We detected HCMV in samples from 12 endoscopies using IHC and PCR. These endoscopies were performed because the patients were complaining of symptoms (8 endoscopies) or during routine controls after surgery (4 endoscopies). Immunoreactivity was observed in the submucosal layer with predominant nuclear staining of cells (Figure 1). There were not any differences in the staining pattern between the HCMV-positive patients with and without pouchitis either using mPDAI or JCP. We performed PCR for all samples, and amplified products from both genes were detected in the same sample with positive IHC (Figure 2). No HCMV was detected in the distilled water control that was run through the same PCR reaction.

HCMV was significantly detected in endoscopies of patients diagnosed with pouchitis (5 of 12, 41.6%)

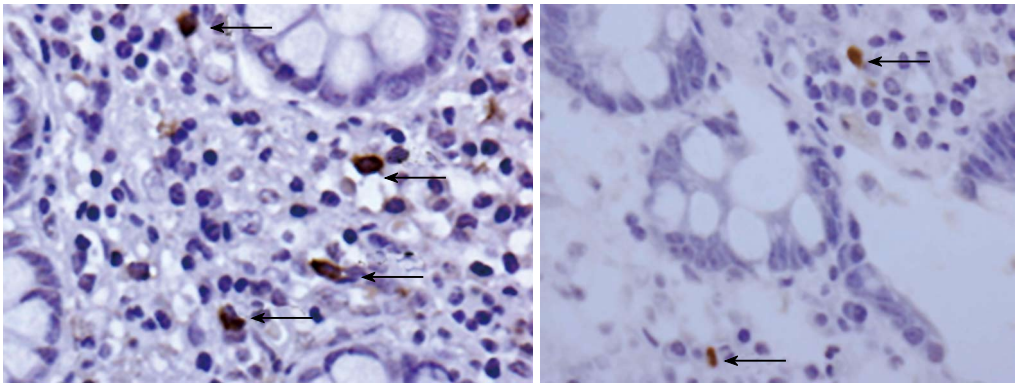

Figure 1 Immunohistochemical staining for HCMV of biopsy samples from ileoanal pouch. Cells in the submucosa (arrows) show strong nuclear staining. Original magnification x 600.

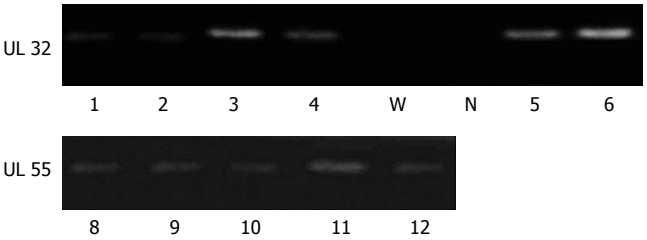

Figure 2 Agarose gel showing UL32 gene products (lanes 1-4, 5 and 6) and UL 55 gene products (lanes 8-12). W: Water; N: HCMV-negative patient.

Table 1 HCMV detection during endoscopic examinations of UC patients with proctocolectomy and ileal pouch-anal anastomosis *n* (%)

	HCMV positive	HCMV negative	*P*
mPDAI[10]			
Pouchitis	3 (27.2)	8 (72.7)	NS
No pouchitis	9 (14.2)	54 (85.7)	
JCP[11]			
Pouchitis	5 (41.6)	7 (58.3)	0.021
No pouchitis	7 (11.2)	55 (88.7)	

mPDAI: modified pouchitis disease activity index; JCP: Japanese classification of pouchitis, NS: not significant.

compared to those with normal pouch (7 of 62, 11.2%; $P = 0.021$, Table 1). According to mPDAI, HCMV was more frequently detected in patients with pouchitis (3 of 11, 27.2%) than in those with normal pouch (9 of 63, 14.2%), but this result was not statistically significant. In all patients with pouchitis in which the HCMV was detected in endoscopy, it was the first episode of pouchitis. In these patients HCMV was not detected in biopsies taken in previous normal endoscopies. The odds ratio suggested that the presence of HCMV was 5 times more frequent in patients with episodes of pouchitis than in patients without.

There was not correlation between the presence of HCMV and the duration of UC, the period of pouchitis, the number of operations, the age, and the gender of the patients. There was no significant difference between the cumulative-life steroid dose and HCMV presence. The mean of the cumulative-life steroid dose was 17152.5 mg ± 16999.0 mg in HCMV-negative patients, and 13347.8 mg ± 12966.7 mg in HCMV-positive patients ($P = 0.52$). After the diagnosis of pouchitis, all patients began treatment with oral metronidazole (500 mg/d). During the follow-up, 2 patients diagnosed with pouchitis were lost and one of them was HCMV-positive. In the samples from 12 endoscopies performed during follow-up, HCMV was detected using IHC and PCR in 4 (4 of 10, 40%) patients. One of these patients had recurrent pouchitis and 3 showed improvement of pouchitis episodes but persistent positive endoscopic findings.

DISCUSSION

It has been suggested that HCMV plays a role in the onset, exacerbation and complication of inflammatory bowel disease (IBD)[2-6,13-18]. However, the etiology of pouchitis is still unknown and the role of HCMV as a possible etiologic factor has not been studied yet. This is the first report exploring the correlation between HCMV and pouchitis in a group of patients with UC who underwent proctocolectomy with IPAA. There are three possible causes for this association: (1) the virus is a simple bystander in the inflammatory process of the pouch, (2) the virus takes part in the inflammatory process after reactivation and productive infection due to another pathogen infection, (3) the virus induces the inflammatory process after infection.

The differentiation of latently infected monocytes[19-23] into tissue macrophages, as occurs with intercurrent infections, could lead to the productive infection and dissemination of HCMV in the digestive tract mucosa of infected patients. No single identifiable causative organism has been detected as the cause of pouchitis, but the infiltration of neutrophils and the proven response to antibacterial therapy suggest that pouchitis could have a bacterial cause[24-27]. However, different facts suggest that HCMV is a real gastrointestinal pathogen and that it can be partly related to the development of pouchitis in some patients. HCMV is often detected in the absence of other pathogens, and some UC complications have been associated with the presence of HCMV[3,5,6]. Moreover, colitis and pouchitis caused by HCMV infection are known to respond to antiviral therapy[8,9,15], and immediate-early HCMV gene products enhance cytokine production and cytokine gene expression[28,29] which *in vivo* would lead to the pronounced inflammation in UC

and pouchitis. Although the pathway of HCMV infection and inflammation is still unclear, the increased production of different cytokines and arachidonic acid, as well as the increased activity of cyclooxygenase 2 after HCMV infection[30-34], could explain the inflammatory response in IBD and pouchitis. In our study on a small series of patients with pouchitis, we hypothesized that HCMV may have played an important role in the etiology of pouchitis in those cases. We detected by IHC an early protein and an immediate-early protein present during an early stage of viral infection. This result corresponds to the detection by PCR of genes that appear early after infection and then frequently decline to undetectable levels with the passage of time[35]. The presence of HCMV turned positive in the episode of pouchitis. However, other factors such as bacterial overgrowth and fecal hydrogen sulfide production[36] could also be implicated in the etiology of pouchitis episode in patients with no detectable HCMV.

The true incidence of HCMV infection in pouchitis as well as in IBD may be underestimated, as diagnostic evaluation for HCMV is not pursued in many of these patients. In our series, the patients did not receive antiviral therapy and HCMV antigenemia was not measured because a diagnosis of HCMV pouchitis was not sought on the occasion of endoscopy. However, after the antibacterial treatment, HCMV persisted in 4 patients with positive endoscopic findings, confirming the possibility of a possible role of HCMV in the etiology of pouchitis in those patients. Since multiple factors play a role in pouchitis, the clinician must exclude HCMV infection as the cause of pouchitis, especially in patients resistant to treatment, before performing fecal diversion, or pouch excision. Concomitant evaluation of the presence of HCMV may be a clinically significant component of the successful treatment of pouchitis.

In conclusion, the presence of HCMV in pouchitis could partly explain the inflammatory response in some patients with UC who have undergone proctocolectomy with IPAA. Therefore, prospective studies with a large number of patients and an analysis of the correlation between antigenemia of HCMV and immunohistological data are definitely needed to identify the specific role of this virus.

ACKNOWLEDGMENTS

The authors thank Mr. Takashi Hatano for his technical assistance. DC is in receipt of a grant from the Ministry of Education, Culture, Sports, Science and Technology of Japan.

REFERENCES

1 **Diepersloot RJ**, Kroes AC, Visser W, Jiwa NM, Rothbarth PH. Acute ulcerative proctocolitis associated with primary cytomegalovirus infection. *Arch Intern Med* 1990; **150**: 1749-1751
2 **Lortholary O**, Perronne C, Leport J, Leport C, Vildé JL. Primary cytomegalovirus infection associated with the onset of ulcerative colitis. *Eur J Clin Microbiol Infect Dis* 1993; **12:** 570-572
3 **Berk T**, Gordon SJ, Choi HY, Cooper HS. Cytomegalovirus infection of the colon: a possible role in exacerbations of inflammatory bowel disease. *Am J Gastroenterol* 1985; **80**: 355-360
4 **Surawicz CM**, Myerson D. Self-limited cytomegalovirus colitis in immunocompetent individuals. *Gastroenterology* 1988; **94**: 194-199
5 **Cooper HS**, Raffensperger EC, Jonas L, Fitts WT. Cytomegalovirus inclusions in patients with ulcerative colitis and toxic dilation requiring colonic resection. *Gastroenterology* 1977; **72**: 1253-1256
6 **Eyre-Brook IA**, Dundas S. Incidence and clinical significance of colonic cytomegalovirus infection in idiopathic inflammatory bowel disease requiring colectomy. *Gut* 1986; **27:** 1419-1425
7 **Moonka D**, Furth EE, MacDermott RP, Lichtenstein GR. Pouchitis associated with primary cytomegalovirus infection. *Am J Gastroenterol* 1998; **93**: 264-266
8 **Muñoz-Juarez M**, Pemberton JH, Sandborn WJ, Tremaine WJ, Dozois RR. Misdiagnosis of specific cytomegalovirus infection of the ileoanal pouch as refractory idiopathic chronic pouchitis: report of two cases. *Dis Colon Rectum* 1999; **42**: 117-120
9 **Shen B**, Achkar JP, Connor JT, Ormsby AH, Remzi FH, Bevins CL, Brzezinski A, Bambrick ML, Fazio VW, Lashner BA. Modified pouchitis disease activity index: a simplified approach to the diagnosis of pouchitis. *Dis Colon Rectum* 2003; **46:** 748-753
10 **Inflammatory bowel disease study group**. Atlas of endoscopic diagnosis of pouchitis. Tokyo: Kyoubundou, 2003
11 **Ashshi AM**, Klapper PE, Cooper RJ. Detection of human cytomegalovirus, human herpesvirus type 6 and human herpesvirus type 7 in urine specimens by multiplex PCR. *J Infect* 2003; **47:** 59-64
12 **Kühn JE**, Wendland T, Eggers HJ, Lorentzen E, Wieland U, Eing B, Kiessling M, Gass P. Quantitation of human cytomegalovirus genomes in the brain of AIDS patients. *J Med Virol* 1995; **47**: 70-82
13 **Cottone M**, Pietrosi G, Martorana G, Casà A, Pecoraro G, Oliva L, Orlando A, Rosselli M, Rizzo A, Pagliaro L. Prevalence of cytomegalovirus infection in severe refractory ulcerative and Crohn's colitis. *Am J Gastroenterol* 2001; **96**: 773-775
14 **Loftus EV**, Alexander GL, Carpenter HA. Cytomegalovirus as an exacerbating factor in ulcerative colitis. *J Clin Gastroenterol* 1994; **19:** 306-309
15 **Papadakis KA**, Tung JK, Binder SW, Kam LY, Abreu MT, Targan SR, Vasiliauskas EA. Outcome of cytomegalovirus infections in patients with inflammatory bowel disease. *Am J Gastroenterol* 2001; **96**: 2137-2142
16 **Pfau P**, Kochman ML, Furth EE, Lichtenstein GR. Cytomegalovirus colitis complicating ulcerative colitis in the steroid-naive patient. *Am J Gastroenterol* 2001; **96:** 895-899
17 **Vega R**, Bertrán X, Menacho M, Domènech E, Moreno de Vega V, Hombrados M, Cabré E, Ojanguren I, Gassull MA. Cytomegalovirus infection in patients with inflammatory bowel disease. *Am J Gastroenterol* 1999; **94:** 1053-1056
18 **Maté del Tío M**, Peña Sánchez de Rivera JM, Larrauri Martínez J, Garcés Jiménez MC, Barbado Hernández FJ. Association of cytomegalovirus colitis and the 1st episode of ulcerative colitis in an immunocompetent patient. *Gastroenterol Hepatol* 1996; **19**: 206-207
19 **Dankner WM**, McCutchan JA, Richman DD, Hirata K, Spector SA. Localization of human cytomegalovirus in peripheral blood leukocytes by in situ hybridization. *J Infect Dis* 1990; **161:** 31-36
20 **Ibanez CE**, Schrier R, Ghazal P, Wiley C, Nelson JA. Human cytomegalovirus productively infects primary differentiated macrophages. *J Virol* 1991; **65:** 6581-6588
21 **Sinzger C**, Plachter B, Grefte A, The TH, Jahn G. Tissue macrophages are infected by human cytomegalovirus in vivo. *J Infect Dis* 1996; **173:** 240-245
22 **Taylor-Wiedeman J**, Sissons JG, Borysiewicz LK, Sinclair JH. Monocytes are a major site of persistence of human cytomegalovirus in peripheral blood mononuclear cells. *J Gen*

Virol 1991; **72** (Pt 9): 2059-2064
23 **Yurochko AD**, Huang ES. Human cytomegalovirus binding to human monocytes induces immunoregulatory gene expression. *J Immunol* 1999; **162:** 4806-4816
24 **Iwaya A**, Iiai T, Okamoto H, Ajioka Y, Yamamoto T, Asahara T, Nomoto K, Hatakeyama K. Change in the bacterial flora of pouchitis. *Hepatogastroenterology* 2006; **53**: 55-59
25 **Lim M**, Sagar P, Finan P, Burke D, Schuster H. Dysbiosis and pouchitis. *Br J Surg* 2006; **93**: 1325-1334
26 **Abdelrazeq AS**, Kelly SM, Lund JN, Leveson SH. Rifaximin-ciprofloxacin combination therapy is effective in chronic active refractory pouchitis. *Colorectal Dis* 2005; **7**: 182-186
27 **Gosselink MP**, Schouten WR, van Lieshout LM, Hop WC, Laman JD, Ruseler-van Embden JG. Eradication of pathogenic bacteria and restoration of normal pouch flora: comparison of metronidazole and ciprofloxacin in the treatment of pouchitis. *Dis Colon Rectum* 2004; **47**: 1519-1525
28 **Geist LJ**, Monick MM, Stinski MF, Hunninghake GW. The immediate early genes of human cytomegalovirus upregulate tumor necrosis factor-alpha gene expression. *J Clin Invest* 1994; **93**: 474-478
29 **Iwamoto GK**, Monick MM, Clark BD, Auron PE, Stinski MF, Hunninghake GW. Modulation of interleukin 1 beta gene expression by the immediate early genes of human cytomegalovirus. *J Clin Invest* 1990; **85:** 1853-1857
30 **Rahbar A**, Boström L, Lagerstedt U, Magnusson I, Söderberg-Naucler C, Sundqvist VA. Evidence of active cytomegalovirus infection and increased production of IL-6 in tissue specimens obtained from patients with inflammatory bowel diseases. *Inflamm Bowel Dis* 2003; **9**: 154-161
31 **Compton T**, Kurt-Jones EA, Boehme KW, Belko J, Latz E, Golenbock DT, Finberg RW. Human cytomegalovirus activates inflammatory cytokine responses via CD14 and Toll-like receptor 2. *J Virol* 2003; **77**: 4588-4596
32 **Redman TK**, Britt WJ, Wilcox CM, Graham MF, Smith PD. Human cytomegalovirus enhances chemokine production by lipopolysaccharide-stimulated lamina propria macrophages. *J Infect Dis* 2002; **185**: 584-590
33 **Zhu H**, Cong JP, Yu D, Bresnahan WA, Shenk TE. Inhibition of cyclooxygenase 2 blocks human cytomegalovirus replication. *Proc Natl Acad Sci USA* 2002; **99**: 3932-3937
34 **Nokta MA**, Hassan MI, Loesch K, Pollard RB. Human cytomegalovirus-induced immunosuppression. Relationship to tumor necrosis factor-dependent release of arachidonic acid and prostaglandin E2 in human monocytes. *J Clin Invest* 1996; **97:** 2635-2641
35 **Greijer AE**, van de Crommert JM, Stevens SJ, Middeldorp JM. Molecular fine-specificity analysis of antibody responses to human cytomegalovirus and design of novel synthetic-peptide-based serodiagnostic assays. *J Clin Microbiol* 1999; **37**: 179-188
36 **Ohge H**, Furne JK, Springfield J, Rothenberger DA, Madoff RD, Levitt MD. Association between fecal hydrogen sulfide production and pouchitis. *Dis Colon Rectum* 2005; **48**: 469-475

S- Editor Wang J **L- Editor** Wang XL **E- Editor** Ma WH

PO Box 2345, Beijing 100023, China
www.wjgnet.com
wjg@wjgnet.com

World J Gastroenterol 2007 February 21; 13(7): 1090-1097
World Journal of Gastroenterology ISSN 1007-9327

RAPID COMMUNICATION

Frequent loss of heterozygosity in two distinct regions, 8p23.1 and 8p22, in hepatocellular carcinoma

Tomoe Lu, Hiroshi Hano, Chenxi Meng, Keisuke Nagatsuma, Satoru Chiba, Masahiro Ikegami

Tomoe Lu, Hiroshi Hano, Chenxi Meng, Keisuke Nagatsuma, Satoru Chiba, Masahiro Ikegami, Department of Pathology, Jikei University School of Medicine, Tokyo, Japan
Supported by The Jikei University Research Fund
Correspondence to: Tomoe Lu, MD, PhD, Department of Pathology, The Jikei University School of Medicine, 3-25-8 Nishishinbashi, Minato-ku, Tokyo 105-8461, Japan. luwei@jikei.ac.jp
Telephone: +81-3-34331111-231 Fax: +81-3-54720700
Received: 2006-11-25 Accepted: 2007-01-18

Abstract

AIM: To identify the precise location of putative tumor suppressor genes (TSGs) on the short arm of chromosome 8 in patients with hepatocellular carcinoma (HCC).

METHODS: We used 16 microsatellite markers informative in Japanese patients, which were selected from 61 published markers, on 8p, to analyze the frequency of loss of heterozygosity (LOH) in each region in 33 cases (56 lesions) of HCC.

RESULTS: The frequency of LOH at 8p23.2-21 with at least one marker was 63% (20/32) in the informative cases. More specifically, the frequency of LOH at 8p23.2, 8p23.1, 8p22, and 8p21 was 6%, 52%, 47%, and 13% in HCC cases. The LOH was significantly more frequent at 8p23.1 and 8p22 than the average (52% *vs* 22%, $P = 0.0008$; and 47% *vs* 22%, $P = 0.004$, respectively) or others sites, such as 8p23.2 (52% *vs* 6%, $P = 0.003$; 47% *vs* 22%, $P = 0.004$) and 8p21 (52% *vs* 13%, $P = 0.001$; 47% *vs* 13%, $P = 0.005$) in liver cancer on the basis of cases. Notably, LOH frequency was significantly higher at *D8S277*, *D8S503*, *D8S1130*, *D8S552*, *D8S254* and *D8S258* than at the other sites. However, no allelic loss was detected at any marker on 8p in the lesions of nontumor liver tissues.

CONCLUSION: Deletion of 8p, especially the loss of 8p23.1-22, is an important event in the initiation or promotion of HCC. Our results should be useful in identifying critical genes that might lie at 8p23.1-22.

Key words: Loss of heterozygosity; Chromosome; Hepatocarcinogenesis; Hepatocellular carcinoma; 8p

Lu T, Hano H, Meng C, Nagatsuma K, Chiba S, Ikegami M. Frequent loss of heterozygosity in two distinct regions, 8p23.1 and 8p22, in hepatocellular carcinoma. *World J Gastroenterol* 2007; 13(7): 1090-1097

http://www.wjgnet.com/1007-9327/13/1090.asp

INTRODUCTION

Primary liver cancer is one of the most frequent neoplasms worldwide, with both an incidence and a mortality rate that are increasing markedly. According to a recent report, the global number of new cases annually rose from 437 400 to 564 000 between 1990 and 2000, and is expected to continue to rise in the future[1-4].

Hepatocellular carcinoma (HCC), the predominant histological subtype of primary liver cancer, mostly arises against a background of chronic liver disease, usually in association with cirrhosis. Several risk factors for HCC have been reported, such as chronic infection with hepatitis B virus (HBV), and C virus (HCV) or both, alcohol-induced liver injury, and dietary exposure to aflatoxin B1 and others. Prolonged exposure to these risk factors is thought to cause an accumulation of chromosomal aberrations and altered gene expression, and eventually results in hepatocarcinogenesis[4-6]. In Japan, more than 70% of HCCs develop in patients with chronic infections with HCV[7]. Carcinogenesis is mainly researched based on virology and the viral gene itself. However, the mechanisms by which inflammation and cirrhosis contribute to tumor development and/or progression remain unclear. After the human genome was sequenced, the mechanism of generation and subsequent progression was researched at a molecular level for HCC. Histological findings suggest that the initiation and subsequent development of HCC are multistep processes involving qualitative and quantitative changes in sequentially expressed genes, especially the inactivation of tumor suppressor genes (TSGs) related to the deletion of chromosomal regions critical for hepatocarcinogenesis[8,9]. A typical alteration in many TSGs, the mutation of one allele, can be detected as a loss of heterozygosity (LOH) with informative markers in TSG regions. Therefore, LOH assays have been widely used as an indirect approach in the search for a new TSG[10]. In the last few years, genetic approaches to the detection of genome-wide LOH using microsatellite markers and chromosomal aberrations detected by comparative genomic hybridization (CGH) have indicated that frequent allelic loss in many different chromosomal regions, including 1p[11,12], 3p[13],

4q[14], 6q[15], 8p[16-19], 9p[20], 10p[21], 13q[22], 22q[23], 16q, 17p and Xq[24,25] , is closely associated with the tumorigenesis of HCC.

We have performed a genome-wide search for LOH with human genetic markers in several types of human cancer and confirmed that loss of 8p is the most frequent chromosomal alteration in prostate cancer, especially allelic loss at 8p22, which not only is an important event in the initiation of tumor, but also is closely associated with the progression of primary cancer to metastatic cancer[26].

In our comprehensive allelotyping, less than 30% of microsatellite markers located at 8p21-23, were recognized as informative for Japanese patients. We therefore undertook an allelotype based study of 33 HCCs using the selected informative markers to obtain a comprehensive view of the LOH on the most frequent altered chromosome, and to identify the location of the putative TSGs in HCC.

MATERIALS AND METHODS

Tissue collection, histopathology, and DNA extraction

Thirty-three patients with hepatocellular carcinoma who underwent liver resection were included in this study. Of these, fifty six tumor lesions and 33 adjacent morphological non-tumor lesions were obtained from surgically resected specimens. All specimens were formalin-fixed, and paraffin wax-embedded tissues were processed with routine histological methods. Use of the tissues was approved by the Ethics Committee of the Jikei University School of Medicine before the study. The study group included 26 men and 7 women, ranging in age from 31 to 76 years. Of the 33 patients, 24 (73%) had a chronic infection with HCV, HBV or both and 15 (45%) had cirrhosis in the background liver tissues. Histological diagnoses were made according to the WHO Histological Classification of Tumors of the Liver and Intrahepatic Bile Ducts (2000). According to histological grade, HCC was classified into well differentiated (WD), moderately differentiated (MD), and poorly differentiated (PD) types. In this study, clinicopathological characteristics were also classified, such as solitary or multiple tumor, growth pattern of tumor (expansive or infiltrative), infiltration of capsule or not, histological grading of tumor (well, moderately or poor differentiation), and with or without vascular and bile duct infiltration. Simultaneously, we also compared LOH frequency and etiological factors, such as chronic hepatitis with HCV or HBV infection, and cirrhosis in the background liver tissues. Fibrosis degree was classified as F1, F2, F3, and F4 according to the histological grading and staging of chronic hepatitis. In this system, liver cirrhosis was classed as F4, which is the end-stage form of liver fibrosis. Of the 33 patients who underwent liver resection, 18 had a solitary tumor nodule and 15 had multiple tumor nodules. All lesions from each case were selected and reviewed by two pathologists in order to confirm the original diagnosis. The tumor (T) and corresponding non-tumor hepatocytes (H), and remaining nonhepatocytes that were portal vein lesions (*P*) were micro-dissected from 15-μm tissue specimens after deparaffinization and nuclear staining. Normal tissues were obtained from the gallbladder or lymph nodes collected from the same patients (Figure 1). DNA was extracted using the standard phenol/chloroform method as described previously[26].

LOH analysis

Matched tumors, corresponding non-tumor liver tissues, and normal tissue DNAs were analyzed for LOH by amplification of polymorphic microsatellite markers using the polymerase chain reaction (PCR). Sixty-one published microsatellite markers, located at 8p23.3, 8p23.2, 8p23.1, 8p22, and 8p21, were selected from the Genome Database (available at http: //www. gdb. org). A total of 16 microsatellite markers were identified as informative in Japanese patients and used (Table 1).

DNA amplification was performed in 10-μL volumes containing 100 ng of genomic DNA as a template. Each PCR mixture contained 1.5 mmol/L $MgCl_2$, 100 μmol/L forward and reverse primers, 200 μmol/L each of dATP, dGTP, dTTP and dCTP, 10 μCi of [α-^{32}P] dCTP (6000 Ci/mmol, Amersham, Biosciences Corp., Piscataway, NJ), 1 U of Taq DNA polymerase (Wako Pure Chemical Industries, Ltd., Osaka, Japan), and 1 × PCR buffer. After the initial denaturation at 94℃, 35 PCR cycles, each consisting of denaturation at 94℃ for 30 s, annealing at 65℃ -50℃ for 30 s, elongation at 72℃ for 1 min, and a final extension at 72℃ for 5 min, were performed in a 96-well Hybaid thermocycler (Gene Amp PCR System 9600, Takara, Tokyo, Japan). Ten microliters of PCR products were denatured with 30-60 μL of dye solution (95% formamide, 10 mmol/LEDTA (pH 8.0), 0.2% xylene cyanol FF, and 0.02% bromophenol blue) at 95℃ for 3 min and then cooled on ice immediately. Three microliters of denatured products were separated on a 6% urea-formamide-polyacrylamide gel and electrophoresed at 40 W for 2-3 h at room temperature. The dried gel was exposed to Hyperfilm MP (Amersham Biosciences Corp.) for 3-7 d and reexposed to another film for 2-3 wk.

Criteria for LOH

A pair of regular and longer-exposed autoradiographs was reviewed independently by two of the authors (T. L. and CX. M.). Informative pairs were judged by visual inspection to show LOH, no loss or to be noninformative.

LOH was defined as a loss of intensity of 60% or greater in 1 or more alleles in the tumor (T) or corresponding hepatocytes (H) compared with the identical allele in the normal tissue (N) (Figure 1).

Statistical analysis

The differences in LOH frequency between tumor, nontumor and normal tissues for individual markers and background values were determined with Fisher's exact test.

RESULTS

The distribution of the frequency of LOH at 8p23.2, 8p23.1, 8p22 and 8p21 for hepatocellular carcinoma is shown in Table 2. Allelic loss at 8p23.2-21 was detected with at least 1 marker in 18 of 32 (56%) cases of liver cancer. More specifically, the frequency of LOH at 8p23.2, 8p23.1, 8p22, and 8p21 with at least 1 marker was 6% (1

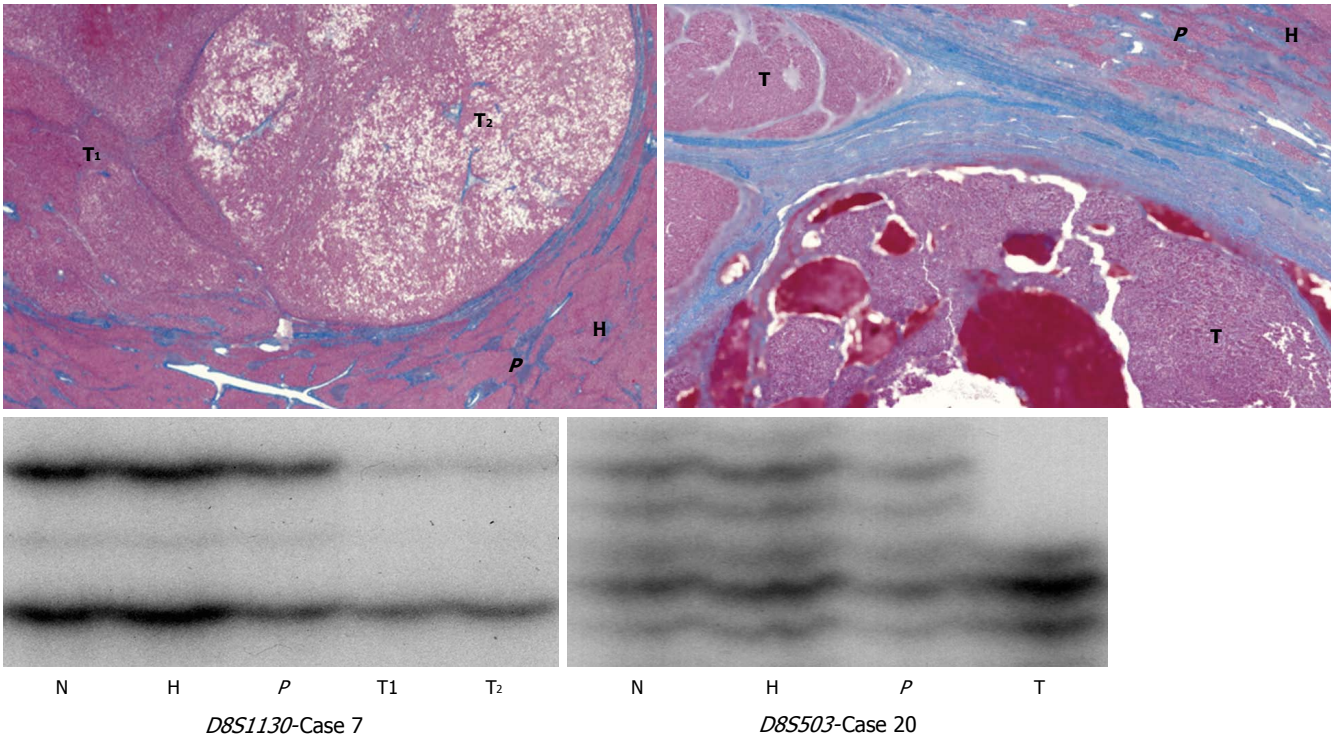

Figure 1 Representative examples of LOH in two cases of hepatocellular carcinoma (N: normal; H: hepatocytes; P: portal vein; T: tumor; number beside T indicates different lesion): case 7 showing partial loss of upper alleles in lesions of tumor 1 and tumor 2 but not in lesions of hepatocytes and portal vein at *D8S1130*; case 20 showing complete loss of upper alleles in lesion of tumor but not in surrounding non-tumor tissues at *D8S503*.

of 16), 52% (16 of 31), 47% (15 of 32), and 13% (4 of 32) for liver cancer cases respectively (Table 2). A similar result was obtained in the lesion-to-lesion comparison (data not shown). In contrast, no allelic loss at any markers on 8p was detected in the background liver tissue. The average frequency of LOH at 8p23.2-21 was 22% (58 of 264) in informative cases. We found that LOH at the 8p23.1 and 8p22 loci was significantly higher than the average in HCC cases ($P = 0.0008$, and $P = 0.004$, respectively). But allelic loss at 8p23.2 and 8p21, the loci on either side of the 8p23.1-22 region, tended to be lower than the average. On the other hand, no allelic loss (0 of 52 lesions) was detected at any informative markers on 8p23.2-21 in the surrounding liver tissues. Moreover, allelic loss at *D8S277, D8S503, D8S1130, D8S552, D8S1109, D8S254*, and *D8S258* was 25%, 42%, 39%, 43%, 24%, 43% and 50%, respectively, significantly higher than that elsewhere and the average frequency at 8p.

Correlations between LOH frequency and clinicopathological variables are summarized in Table 3. To determine whether allelic loss at 8p was associated with clinicopathological characteristics and reveal its biological role in the initiation and/or progression of tumors, we compared the frequency of LOH based on almost all of the clinicopathological findings. Corresponding to the result described above, the LOH frequency tended to be higher at 8p23.1 and 8p22 loci than at 8p23.2 and 8p21 loci for all clinicopathological findings, but no significant difference in LOH frequency was found between the liver cancer positive or negative for malignant factors. In other words, no association was detected between the deletion of 8p23.1-22 and subsequent progression of the tumors.

The distribution of LOH frequency based on the fibrosis (F) of background liver tissues, which is usually thought to be associated with hepatocarcinogenesis, was also analyzed. The frequency of LOH at 8p23.1 or 8p22 in F1, F2, F3, and F4 was 75% (3 of 4), 78% (7 of 9), 20% (1 of 5), and 38% (5 of 13), or 100% (2 of 2), 56% (5 of 9), 40% (2 of 5), and 46% (6 of 13), respectively. No statistically significant difference in LOH frequency was found on the basis of the fibrosis staging at 8p. Allelic loss at 8p even tended to be slightly more frequent in cases of tumor with earlier-stage fibrosis than in cases with advanced stage fibrosis of the background liver tissues.

DISCUSSION

Previous studies of LOH have reported that allelic loss of 8p is the most frequent chromosomal alteration in a variety of human cancers and have suggested that one or several tumor suppressor genes (TSGs) may lie within the short arm of chromosome 8[16-19]. To further identify the precise location of the putative TSGs that might potentially be involved in the tumorigenesis of HCC, we performed a high-density LOH study of HCC at 8p using recently developed microsatellite markers. Only 16 of 61 (less than 30%) were identified as informative for Japanese patients. Furthermore, among the informative markers, the informative cases for all specimens were usually lower (from 20% to 70%) for Japanese than for Westerners. The same-general tendency has been found in various other types of cancer, possibly because Japan is not multiracial like Western countries. This has led us to suggest that using this characteristic might be more efficient for identifying

Table 1 Informative microsatellite markers were selected and used in this study

No.	Locus	Markers	Genetic map (cM)	Forward	Reverse	PCR product size (bp)	result[1]
1	8p23.3	D8S7	Not listed	ACCCTGACAGCAGAGGTTTC	ACCCTGACGTTCTCCCAGTA	250-252	ni
2	8p23.2	D8S1164	Not listed	CACAAATCAGATTTTTGAAGTTGC	GGGTTAGACGGACAACCTCA	225	ni
3	8p23.2	D8S264	0.7	ACATCTGCGTCGTCTTCATA	CCAACACCTGAGTCAGCATA	121-145	in
4	8p23.2	D8S262	4.3	AGCTCAAAAGCGAAGGTGAT	GGCAACAAAGTGAGATCCTG	114-128	in
5	8p23.1	sts-X53793	Not listed	TCGACTACCCAGTGGTCTTG	GTTCAAAATGCTTGCTCGC	127	ni
6	8p23.1	D8S1742	Not listed	CCCCCACCAAGACACA	CTCAAGGGATATGAAGGGCA	130	in
7	8p23.1	D8S277	8.2	GATTTGTCCTCATGCAGTGT	ACATGTTATGTTTGAGAGGTCTG	121	in
8	8p23.1	D8S1918	Not listed	GAATGTCATGCTGGGAACG	GTAGCTCTCAAAGCAAATTATGAGC	108	ni
9	8p23.1	D8S1819	10	TCACTGAGGGACTTGGC	CGTGCTGAGAATGAGACC	207	in
10	8p23.1	D8S1140	Not listed	GACAACATCCGATAATGCTG	GAGGACATCTAGATAATTGGAAGA	378	ni
11	8p23.1	D8S503	16.2	GGTTACGAGTTTTGTCCTTTG	GAAACAAACCAATGTAGGAGTG	136	in
12	8p23.1	D8S1672	Not listed	AACTGAGATCACGCCACTCC	CCCATTGGTTTTAGAGTGGC	149	ni
13	8p23.1	AFM234ve1	Not listed	TACCGCAAAACACACCA	GCAGCCTTAGTTGACAACA	245	ni
14	8p23.1	D8S2045	Not listed	CCGATTGCTTCATCGGGAC	CGCCTCCTCCTCTGAAATCCT	120	ni
15	8p23.1	D8S1130	22.4	GAAGATTTGGCTCTGTTGGA	TGTCTTACTGCTATAGCTTTCATAA	145	in
16	8p23.1	D8S1946	Not listed	GCACAAGATCAGAGAGGTTGTG	GAGGAGAGATGGTGTTGGGA	102	ni
17	8p23.1	D8S1640	Not listed	TGCAGTCTGCGGGAGTTC	AGCAGGGTGACTGTAAAGAAGG	175	ni
18	8p23.1	D8S2060	Not listed	CTCTCCGGGAATGTAATACTGC	GAGCTGGGAGTTACTGCCTG	256	ni
19	8p23.1	D8S552	26.4	CCTGTACCATACCCCTGTATC	AAGGTTTGAATCTCTCAGTGG	132	in
20	8p23.1	D8S1109	26.4	TTCTCAGAATTGCTCATAGTGC	TCAGCTCCTCTTCTGCTGAT	241	in
21	8p23.1	D8S2066	Not listed	TTTTCTCCATCCGGTGACTC	CCAACTACGGCATGGTTTCT	175	ni
22	8p23.1-22	D8S1106	26.5	TTGTTTACCCCTGCATCACT	TTCTCAGAATTGCTCATAGTGC	149	ni
23	8p22	D8S1451	Not listed	AACCTAAGGTTCTGTGCTACATCA	AACTTACCAAGGCCGTTTAGG	149	ni
24	8p22	EST465487	Not listed	TTTGTTTGGGTGGAGGACTC	TGGACATCTGCCTAGGTCCT	250	ni
25	8p22	D8S1647	Not listed	CCAGAATTTTGAAATAGATTCATCC	AAATTTTGTAAATATCAGTGTTCCG	174	ni
26	8p22	stSG29388	32	GCAGTGAGATTTTGCTTCTGG	ATGAACATTCAATGAATCAGCA	125	ni
27	8p22	D8S1713	Not listed	CAGGGGCTGATTGTCAGAAC	GTGGCTGTCACCAAGGTCTC	113	ni
28	8p22	SGC33312	Not listed	AGGGCCTTGGGAACACTC	TCAGTTTAAATGGATGGTTTTTACT	137	ni
29	8p22	D8S2080	Not listed	GACTCAAAGAGAACCTGCCG	TAGGTTGGTGAGCACACGTC	132	ni
30	8p22	D8S2081	Not listed	ACCCAGTTACAGCACTGTAATATCA	CTCTACCCCGAAATGATGGA	147	ni
31	8p22	SHGC-24261	Not listed	AAGCAGAGATAAGCCCGACA	TTTCTTTAGATGGAGTCCATTGC	123	ni
32	8p22	SHGC-52401	Not listed	ACAGGATAGTGTTAGGCTCACATG	CATTCTCTGTATCTTTTGGGGG	120	ni
33	8p22	D8S254	Not listed	TGCCGGACATACATTAGTGA	TTGTAAACACCACAAGCAGG	65-75	in
34	8p22	D8S2001	Not listed	GACATTGAATTCCAGTATTTGTGC	GGACAAATGCCACTGCAAC	138	ni
35	8p22	SHGC-5873	Not listed	GACACACACATACAGAAAACCA	CTTACCATGAATGGAGCTTG	225	ni
36	8p22	D8S261	35.8	TGCCACTGTCTTGAAAATCC	TATGGCCCAGCAATGTGTAT	128	in
37	8p22	AFM234vf4	Not listed	GGGCACAGGCATGTGT	GGCTGCATTCTGAAAGGTTA	260-272	ni
38	8p22	D8S1948	Not listed	TTACAAAACATACCCAGTGTTTGG	CTTTTTAGTGCTTGAGACTGTCTCC	110	ni
39	8p22	D8S2028	Not listed	TCAAAAGTTTTGTTTCTATTCAGGG	TTTTTTCTGTTCCCCTCCG	178	ni
40	8p22	D8S258	40.3	CTGCCAGGAATCAACTGAG	TTGACAGGGACCCACG	144-154	in
41	8p22	D8S1949	Not listed	TGTCTTACAGCTCTCCCTCTCC	CAGTAAGGATCACCAAGACAAGG	106	ni
42	8p22	D8S1983	Not listed	ATTGGAAGAGGCAAATGGTG	TATGTACTGGATGAAGCAGGACA	175	ni
43	8p22	D8S1786	Not listed	CGAAAGATTGAGACCCCAT	GTTTCCACACCGAAGCC	209	ni
44	8p22	D8S298	42.7	AGGCTTACACCCATGGACC	ACGCAGCACACAACATCAT	155-167	in
45	8p21.3	D8S2050	Not listed	TGCCAATATCAGTGGAAGAGG	TCCTTTTTCCCTTGTTGCC	162	ni
46	8p21.3	D8S1752	Not listed	TCCTGGATCAGGCAGAAA	TCAGAGTTGGGTGAGCGA	140	in
47	8p21.3	D8S1734	44.9	GCTATCCACTTGTCCCAGA	AGCCCAGAAATAAACCCTC	114	in
48	8p21.2	D8S2256	Not listed	GTGTCTTGAGATACTGGTGA	GAGAAATGTCTTTGTTGAGG	101	ni
49	8p21.2	D8S2259	Not listed	TGAAAGCCTGTTTAGAGAGA	CTATTGCCCTGTGTTTTGCC	105	ni
50	8p21.2	D8S1220	Not listed	TTCCGTATACACATGCACCC	TAGCAGCCAGACACAGGAGC	90	ni
51	8p21.1	D8S1445	Not listed	GCAACAGAGCGAGACTCCGTC	AAGCTTACATTCTGGGTGAC	117-139	in
52	8p21.1	D8S2261	Not listed	GTATTTATTCCACAAGCATCTTA	CAACCCCATCAGTCTCTCTAAT	204	ni
53	8p21.1	D8S1444	Not listed	TTCTTCTAGATTTCCTACTA	CATTTGTTAAAAGTACAACC	91	x
54	8p21	D8S2249	Not listed	TCCACCCATTTCAGCCTTTC	CTAAAACATTTAACTTTCATT	101	ni
55	8p21	D8S2248	Not listed	ATACAGGTAGGTGAGGGCAA	TTCTGATGCTCTTCTGGAGT	136	ni
56	8p21	D8S2247	Not listed	CATTGTGGTGGAGGTCGGAG	TTCCCCCATCCCATCTGAG	122	ni
57	8p21	D8S2262	Not listed	ATGTTTTGTTCATGGGTCTTT	AAGAAAAAGGGAAGGGGCAGT	98	ni
58	8p21	D8S339	Not listed	TAGATGTTACCATTTCAC	GATTAGATCTTGGATCAG	162	ni
59	8p21	D8S2245	Not listed	CCTCTTTATCCCACTTTTCAG	CATTTTACGAATATAAGCATCC	138	ni
60	8p21	D8S2244	Not listed	ACAACTAAAGGACTTAAAGG	GACAAGAAAAGAACAAATGG	145	ni
61	8p21	D8S2246	Not listed	TAACCTGTGAATGAGAATAC	TGACAGTTTTGAGAGAATCC	169	ni

[1]ni: noninformative; in: informative.

candidate regions of deletion at 8p.

In this study, LOH at 8p was detected in 56% of informative cases of HCC. However, no allelic loss was found in corresponding hepatocytes including 18 lesions of morphogenetic non-tumor tissues and 14 lesions of cirrhotic liver tissues at any markers, the latter usually considered a

Table 2 LOH status for the 8p23.2, 8p23.1, and 8p22 in hepatocellular carcinoma

Case	Age	Sex	St/Mt	Grading	Etiology	D8S264	D8S262	8p23.2	D8S1742	D8S277	D8S1819	D8S503	D8S1130	D8S552	D8S1109	8p23.1	D8S254	D8S261	D8S258	D8S298	8p22	D8S1752	D8S1734	D8S1445	8p21	8p23.2-21
12	60	M	Mt	MD	Alcoholic	ni	ni	ni	ni	ni	ni	ni	○	ni	ni	○	○	○	●	○	●	○	○	○	○	●
11	64	M	St	MD	CH(C)+, LC	ni	ni	ni	○	○	ni	○	○	ni	○	○	○	ni	●	ni	●	○	○	○	○	●
1	42	M	St	PD	CH(B)+	ni	ni	ni	ni	○	○	ni	○	ni	●	●	●	○	ni	ni	●	○	○	○	○	●
2	59	M	St	MD	CH(-)	○	○	○	ni	ni	ni	○	○	ni	●	●	●	○	ni	○	●	ni	○	○	○	●
27	69	M	Mt	PD	CH(C)+	ni	ni	ni	○	○	ni	ni	ni	ni	●	●	○	○	○	ni	○	○	○	○	○	●
26	58	M	St	MD	CH(C)+, LC	○	ni	○	○	○	○	●	○	ni	○	●	○	○	ni	○	○	○	ni	○	○	●
15	31	F	Mt	MD	CH(C)+	ni	ni	ni	ni	ni	ni	●	ni	ni	ni	●	ni	ni	●	ni	●	○	ni	○	○	●
29	73	M	St	WD	CH(C)+	ni	ni	ni	ni	ni	ni	ni	●	ni	○	●	●	ni	●	●	●	○	○	○	○	●
6	72	M	St	MD	CH(C)+	ni	ni	ni	ni	ni	○	ni	●	ni	ni	●	○	ni	●	○	●	○	○	○	○	●
20	65	M	St	WD	Alcoholic, LC	ni	○	○	●	●	●	●	●	●	●	●	●	●	●	ni	●	●	○	○	●	●
8	74	M	Mt	MD	CH(-)	ni	○	○	●	●	ni	ni	●	ni	○	●	●	ni	ni	●	●	●	ni	ni	●	●
7	59	M	Mt	WD	CH(B)+, (C)+	○	○	○	○	●	●	ni	●	ni	ni	●	○	ni	ni	○	○	○	●	●	●	●
19	50	M	Mt	MD	CH(B)+, LC	○	●	●	●	○	ni	●	●	●	○	●	ni	ni	●	○	●	●	●	○	●	●
28	58	M	Mt	MD	CH(B)+	ni	○	○	ni	○	ni	○	●	●	○	●	●	ni	ni	ni	●	ni	○	○	○	●
5	51	M	Mt	MD	CH(B)+	ni	ni	ni	ni	ni	○	ni	●	ni	ni	●	●	ni	ni	ni	●	ni	○	○	○	●
10	71	F	Mt	MD	CH(C)+, LC	ni	ni	ni	○	○	○	●	ni	ni	ni	●	●	○	●	ni	●	○	○	○	○	●
4	57	M	Mt	MD	CH(C)+, LC	○	○	○	ni	●	○	○	○	○	○	●	○	ni	○	○	○	○	○	○	○	●
13	74	M	Mt	MD	CH(-)	ni	ni	ni	○	ni	ni	ni	●	ni	ni	●	ni	ni	ni	ni	ni	○	ni	○	○	●
18	51	M	St	WD	CH(B)+, LC	ni	ni	ni	ni	ni	○	ni	ni	○	ni	○	●	○	ni	ni	●	○	○	○	○	●
16	54	M	Mt	MD	Alcoholic, LC	ni	ni	ni	○	ni	ni	○	○	ni	ni	○	●	ni	○	ni	●	○	ni	○	○	●
25	71	M	St	MD	CH(B)+, (C)+	ni	○	○	○	ni	ni	ni	○	ni	ni	○	ni	ni	ni	ni	ni	○	ni	○	○	○
30	56	M	St	MD	CH(C)+	ni	○	○	○	○	ni	○	ni	ni	○	○	ni	ni	ni	○	○	ni	ni	○	○	○
9	57	M	St	WD	CH(C)+	ni	ni	ni	○	ni	ni	ni	○	ni	ni	○	○	ni	ni	ni	ni	○	○	○	○	○
3	51	M	St	MD	CH(B)+	ni	ni	ni	○	○	○	ni	○	ni	○	○	○	ni	○	ni	○	ni	○	○	○	○
32	54	F	St	MD	CH(B)+, LC	○	ni	○	○	○	ni	○	○	○	○	○	○	○	○	ni	○	○	○	○	○	○
21	67	M	St	WD	CH(C)+, LC	ni	ni	ni	ni	○	ni	ni	ni	ni	ni	○	ni	ni	○	○	○	ni	ni	○	○	○
33	76	F	St	WD	CH(C)+, LC	○	○	○	○	ni	ni	ni	○	ni	○	○	○	ni	ni	○	○	○	○	○	○	○
23	71	M	Mt	MD	CH(-)	ni	ni	ni	ni	ni	ni	ni	○	ni	ni	○	ni	ni	○	ni	○	ni	○	○	○	○
22	65	M	Mt	MD	CH(C)+	ni	ni	ni	ni	ni	○	ni	ni	ni	ni	○	○	ni	ni	○	○	○	○	○	○	○
31	65	F	Mt	MD	CH(C)+, LC	ni	ni	ni	○	ni	○	ni	○	○	○	○	ni	ni	ni	ni	ni	ni	○	○	○	○
17	37	F	Mt	MD	CH(B)+, LC	ni	ni	ni	ni	ni	ni	ni	ni	ni	ni	ni	ni	○	ni	ni	○	ni	ni	○	○	○
24	60	M	Mt	MD	CH(-), LC	ni	○	○	ni	○	ni	ni	ni	ni	○	○	○	ni	○	ni	○	○	○	○	○	○
LOH ●						0	1	1	3	4	2	5	9	3	4	16	10	1	8	2	15	3	2	1	4	20
Informative (32/33)						8	13	16	17	16	12	12	23	7	17	31	23	10	16	13	32	23	23	31	32	32
LOH/Informative (58/264 = 22%)						0%	8%	6%[a]	18%	25%	17%	42%	39%	43%	24%	52%[b]	43%	10%	50%	15%	47%[c]	13%	9%	3%	13%[d]	63%[e]

A total of 32 informative liver cancer cases were analyzed for LOH at the sixteen microsatellite markers. The number of informative cases and frequency of LOH was shown at the bottom. St: solitary tumor; Mt: multiple tumor; WD: well differetiation; MD: moderately differretiation; PD: poorly differentiation; CH: chronic hepatitis; LC: liver cirrhosis. ● LOH; ○ retention of heterozygosity; ni: noninformative. Significant different from the average, 52% *vs* 22%, [b]$P = 0.0008$; 47% *vs* 22%, [c]$P = 0.004$; 63% *vs* 22%, [e]$P = 0.007$; No statistically significant different from the average, 6% *vs* 22%, [a]$P = 0.207$; 13% *vs* 22%, [d]$P = 0.257$.

premalignant liver lesion. Our result suggests that allelic loss at 8p is an important event in the initiation or promotion of HCC.

Furthermore, among the informative regions 8p23.2, 8p23.1, 8p22, and 8p21, allelic loss was significantly more frequent at 8p23.1 and 8p22 than at 8p23.2 and 8p21 on both sides of the loci. Several minimal regions adjacent to frequently deleted markers were also identified, such as *D8S277, D8S503, D8S1130,* and *D8S552* at 8p23.1, and *D8S254* and *D8S258* at 8p22. On the basis of the minimal regions of overlapping deletions at 8p, we identified two sites, 8p23.1 and 8p22, possibly containing TSGs involved in human liver carcinogenesis. That is to say, the commonly deleted regions were restricted to 8p23.1-22 suggesting that the key genes exist in two distinct regions that might be closely related to the carcinogenesis of

Table 3 Distribution of LOH frequency at 8p in hepatocellular carcinoma cases by clinicopathological variables

Clinicopathological Variables	D8S 264	D8S 262	8p23.2	D8S 1742	D8S 277	D8S 1819	D8S 503	D8S 1130	D8S 552	D8S 1109	8p23.1	D8S 254	D8S 261	D8S 258	D8S 298	8p22	D8S 1752	D8S 1734	D8S 1445	8p21	8p23.2-21
Tumor size (mm)																					
> 50	0/4	0/4	0/5 (0%)	0/6	1/5	0/6	2/4	4/12	0/1	3/8	10/14 (71%)	4/10	0/5	3/7	1/6	6/13 (46%)	0/10	0/10	0/15	0/15 (0%)	10/15 (67%)
< 50	0/3	1/7	1/8 (13%)	3/11	3/11	2/6	3/7	5/11	3/6	1/9	6/17 (35%)	6/13	1/7	5/9	1/7	9/16 (56%)	3/11	2/14	1/15	4/15 (27%)	10/17 (59%)
Tumor number																					
St	0/2	0/3	0/5 (0%)	1/9	1/8	1/5	2/6	3/12	1/3	3/10	6/15 (41%)	9/18	1/6	4/7	1/7	4/13 (31%)	3/20	2/18	1/24	4/24 (17%)	17/24 (71%)
Mt	0/5	1/10	1/10 (10%)	2/7	3/8	1/6	3/6	6/11	2/4	1/7	10/16 (63%)	1/4	0/4	4/9	1/6	5/13 (38%)	0/2	0/5	0/7	0/7 (0%)	2/7 (29%)
Growth Pattern																					
Eg	0/8	1/13	1/15 (7%)	3/16	4/13	2/11	4/11	9/22	3/7	3/15	14/28 (50%)	8/20	1/8	7/14	2/13	13/26 (50%)	3/20	2/21	1/29	4/29 (14%)	18/29 (62%)
Ig	0/1	0/1	0/1 (0%)	0/1	0/3	0/2	1/1	0/1	0/0	1/2	2/5 (40%)	2/2	0/2	1/2	0/0	2/2 (100%)	0/2	0/2	0/2	0/2 (0%)	2/2 (100%)
Formation of capsule																					
Fc-	0/6	1/8	1/10 (10%)	2/3	1/4	1/4	2/3	4/7	3/4	2/5	5/6 (83%)	3/4	1/3	3/3	0/3	5/5 (100%)	2/5	1/5	0/5	2/5 (40%)	5/5 (100%)
Fc+	0/2	0/6	0/6 (0%)	1/14	3/12	1/8	3/9	5/17	0/3	2/12	11/25 (44%)	7/18	0/7	5/13	2/10	10/23 (43%)	1/18	1/18	1/26	2/26 (8%)	15/26 (58%)
Infiltration to capsule																					
Fc-Inf-	0/6	1/8	1/10 (10%)	1/5	1/7	0/7	3/5	3/8	0/4	2/8	7/11 (64%)	3/10	0/5	4/9	0/3	7/15 (47%)	1/10	1/12	0/15	1/15 (7%)	10/15 (67%)
Fc-Inf+	0/1	0/3	0/3 (0%)	1/8	1/3	0/2	1/4	3/10	0/0	1/5	5/13 (38%)	5/9	0/3	3/5	2/7	6/11 (55%)	1/10	0/8	0/13	1/13 (8%)	7/13 (54%)
Septal formation																					
Sf-	0/0	0/3	0/3 (0%)	1/7	2/6	1/7	3/5	3/8	1/4	2/5	7/13 (54%)	5/9	0/5	5/9	1/4	7/15 (47%)	1/12	0/12	0/16	1/16 (6%)	9/16 (56%)
Sf+	0/6	1/9	1/10 (10%)	2/8	1/5	0/3	1/4	3/10	1/1	2/7	5/12 (42%)	4/10	0/3	3/6	1/6	7/11 (64%)	2/9	1/9	0/12	2/12 (17%)	8/12 (67%)
Grading																					
WD	0/3	0/3	0/4 (0%)	1/4	2/4	2/4	1/2	4/6	1/4	1/2	4/8 (50%)	3/6	1/2	3/5	1/5	3/7 (43%)	1/7	1/7	1/7	2/7 (29%)	4/7 (57%)
MD	1/7	0/9	1/13 (8%)	2/13	2/12	1/9	4/12	5/17	1/12	3/6	11/21 (52%)	6/13	1/8	5/11	1/13	10/18 (56%)	2/12	1/13	0/21	2/21 (10%)	13/21 (62%)
PD	0/0	0/1	0/1 (0%)	0/1	0/3	0/1	0/1	1/3	2/3	0/1	2/3 (67%)	1/2	1/3	0/1	0/0	1/2 (50%)	0/2	0/2	0/2	0/2 (0%)	2/2 (100%)
pT																					
pT1	0/1	0/2	0/2 (0%)	0/2	0/1	0/1	0/1	1/2	0/3	0/2	0/5 (0%)	2/6	0/1	2/3	1/2	3/6 (50%)	0/6	0/6	0/6	0/6 (0%)	3/6 (50%)
pT2	1/7	0/7	1/10 (10%)	2/6	1/7	1/3	4/6	4/5	2/5	3/3	7/11 (64%)	5/8	1/4	5/7	0/4	7/11 (64%)	2/8	1/9	0/11	2/11 (18%)	8/11 (73%)
pT3	0/2	0/2	0/3 (0%)	1/4	2/2	1/3	0/2	3/8	1/5	0/1	5/8 (63%)	2/4	0/1	0/2	1/4	2/5 (40%)	1/5	1/5	1/8	2/8 (25%)	5/8 (63%)
pT4	0/0	0/0	0/0 (0%)	0/0	0/1	0/1	0/0	0/1	1/1	0/0	1/1 (100%)	1/1	0/2	0/0	0/0	1/2 (50%)	0/1	0/1	0/2	0/2 (0%)	1/2 (50%)
pN																					
pN-	1/8	0/10	1/12 (8%)	3/7	3/7	2/4	3/5	6/9	1/8	0/1	5/12 (42%)	4/9	0/0	6/7	2/7	8/13 (62%)	3/11	2/10	1/13	4/13 (31%)	9/13 (69%)
pNx	0/0	0/3	0/3 (0%)	0/6	1/5	0/4	1/4	2/9	2/6	1/5	6/12 (50%)	2/4	0/6	1/5	0/1	2/4 (50%)	0/5	0/5	0/7	0/7 (0%)	4/7 (57%)
pM																					
pM-	1/6	0/11	1/13 (8%)	2/7	1/5	1/2	3/5	3/10	3/8	2/4	6/14 (43%)	3/7	1/5	5/9	1/6	6/11 (55%)	2/10	1/11	0/13	2/13 (15%)	7/13 (54%)
pMx	0/0	0/0	0/0 (0%)	0/0	2/3	0/2	0/1	2/2	0/2	1/1	3/4 (75%)	5/6	0/1	0/1	0/0	5/7 (71%)	1/5	0/5	0/8	1/8 (13%)	7/8 (88%)
Vascular infiltration																					
V-	0/7	1/10	1/13 (8%)	2/10	3/10	1/8	4/9	6/13	2/6	2/9	9/20 (45%)	6/15	0/5	7/13	0/7	11/20 (55%)	2/16	2/18	1/21	3/21 (14%)	14/21 (67%)
V+	1/7	0/2	1/9 (11%)	1/7	1/6	1/4	1/3	3/10	1/1	2/8	7/11 (64%)	4/6	1/5	1/3	2/6	4/7 (57%)	1/6	0/5	0/9	1/9 (11%)	5/9 (56%)
Bile duct infiltration																					
B-	0/10	1/13	1/17 (6%)	3/18	4/15	2/11	4/13	10/24	3/9	3/17	15/28 (54%)	7/18	2/9	8/15	2/12	11/24 (46%)	2/19	2/20	1/27	3/27 (11%)	16/27 (59%)
B+	0/1	0/1	0/2 (0%)	0/3	0/3	1/4	1/3	0/4	1/3	1/4	3/4 (75%)	3/5	1/5	0/1	0/4	4/5 (80%)	1/4	0/4	0/5	1/5 (20%)	4/5 (80%)
Liver cirrhosis																					
LC-	0/2	0/6	0/6 (0%)	1/8	2/7	1/6	1/4	7/14	1/1	3/8	11/18 (61%)	6/11	0/4	4/7	2/8	9/16 (56%)	1/10	1/13	1/18	2/18 (11%)	12/18 (67%)

LC+	0/5	1/5	1/7 (14%)	2/9	2/9	1/6	4/8	2/9	2/6	1/9	5/13 (38%)	4/10	1/6	4/9	0/5	6/13 (46%)	2/11	1/11	0/14	2/14 (14%)	8/14 (57%)
Chronic hepatitis																					
CH-	0/1	0/3	0/4 (0%)	2/3	2/3	1/1	1/2	3/7	1/1	2/4	4/8 (50%)	4/6	1/3	2/5	1/3	5/7 (71%)	2/6	0/5	0/8	2/8 (25%)	6/8 (75%)
CH+	0/6	1/7	1/9 (11%)	1/13	2/13	1/11	4/9	6/16	2/6	2/13	12/23 (52%)	6/17	0/7	6/11	1/10	10/22 (45%)	1/17	2/19	1/24	2/24 (8%)	14/24 (58%)

Eg: expansive growth; Ig: infiltrative growth; St: solitary tumor; Mt: multiple tumor; LC: liver cirrhosis; CH: chronic hepatitis.

HCC. Our results are consistent with previously reported patterns of molecular change in HCC and other epithelial tumors. No statistically significant differences were detected in the candidate regions 8p23.1 and 8p22 between the frequency of LOH and any clinicopathologic characteristics, including etiological factors considered to contribute to tumorigenesis, and malignant factors usually important to the subsequent progression of tumors. These results led us to the hypothesis that loss of 8p is not essential for the subsequent development or progression of HCC.

Moreover, with respect to the results of allelotyping, several genes, such as angiopintin 2 (ANGPT2), AGPAT5, LOC648814, DEFB 137 and DEFB 136, LONRF1, and FLJ36980, which were adjacent to the candidate markers D8S277, D8S503, D8S1130, D8S552, and D8S1109 at 8p23.1, respectively, were analyzed for somatic mutations or expression by single nucleotide polymorphisms (SSCPs) and the reverse transcription polymerase chain reaction (RT-PCR) methods. However, no significant mutation or absence of expression of these adjacent genes was found (data not shown), indicating that alterations of those genes may not be closely related to the carcinogenesis[16-19,26]. Several new candidate cancer-susceptibility genes at 8p22, such as deleted in breast cancer 2 (DBC2), leucine zipper tumor suppressor 1 (LZTS1), and deleted in liver cancer 1 (DLC1), and mitochondrial tumor suppressor 1 (MTUS1) have been cloned[27-30]. We have analyzed these genes in the same HCC samples, but a somatic mutation or absence of expression of these candidate genes is rare in Japanese patients (data not shown), indicating that these well-known candidate genes are not the main targets of the observed LOH at 8p22. Although no significant genetic alterations were detected in HCC in the present study, it could not be denied that they had already had some epigenetic change during the pre-cancer stage or earlier in the carcinogenesis. Although detailed data have not been published, the present results strongly suggest that other unknown genes in the region 8p22-23.1 play an important role in HCC. Further studies are needed to identify critical oncogenes or TSGs, including those in 8p22-23.1. Our results should be useful for identifying the targets of deletion at 8p.

ACKNOWLEDGMENTS

We thank Miss Kana Tamura and Ms. Michiko Kasai for their help in collecting samples, Mrs. Misako Shirai and Mrs. Mamiko Owada for technique help, and Miss Michiko Takagi for photographic help.

REFERENCES

1 **Parkin DM**, Pisani P, Ferlay J. Estimates of the worldwide incidence of 25 major cancers in 1990. *Int J Cancer* 1999; **80**: 827-841
2 **Pisani P**, Bray F, Parkin DM. Estimates of the world-wide prevalence of cancer for 25 sites in the adult population. *Int J Cancer* 2002; **97**: 72-81
3 **Bosch FX**, Ribes J, Díaz M, Cléries R. Primary liver cancer: worldwide incidence and trends. *Gastroenterology* 2004; **127**: S5-S16
4 **Bruix J**, Boix L, Sala M, Llovet JM. Focus on hepatocellular carcinoma. *Cancer Cell* 2004; **5**: 215-219
5 **Feitelson MA**, Sun B, Satiroglu Tufan NL, Liu J, Pan J, Lian Z. Genetic mechanisms of hepatocarcinogenesis. *Oncogene* 2002; **21**: 2593-2604
6 **Thorgeirsson SS**, Grisham JW. Molecular pathogenesis of human hepatocellular carcinoma. *Nat Genet* 2002; **31**: 339-346
7 **Minister's Secretariat**, Ministry of Health, Labor and Welfare, Statistics and Information Dept, Vital Statistics of Japan. Age-adjusted death rates of malignant neoplasms by site, sex and calendar year (1970-2001). 2001
8 **Ng IO**, Guan XY, Poon RT, Fan ST, Lee JM. Determination of the molecular relationship between multiple tumour nodules in hepatocellular carcinoma differentiates multicentric origin from intrahepatic metastasis. *J Pathol* 2003; **199**: 345-353
9 **Maggioni M**, Coggi G, Cassani B, Bianchi P, Romagnoli S, Mandelli A, Borzio M, Colombo P, Roncalli M. Molecular changes in hepatocellular dysplastic nodules on microdissected liver biopsies. *Hepatology* 2000; **32**: 942-946
10 **Vogelstein B**, Fearon ER, Hamilton SR, Kern SE, Preisinger AC, Leppert M, Nakamura Y, White R, Smits AM, Bos JL. Genetic alterations during colorectal-tumor development. *N Engl J Med* 1988; **319**: 525-532
11 **Gisin J**, Perren A, Bawohl M, Jochum W. Rare allelic imbalances, but no mutations of the PRDX1 gene in human hepatocellular carcinomas. *J Clin Pathol* 2005; **58**: 1229-1231
12 **Mori T**, Nomoto S, Koshikawa K, Fujii T, Sakai M, Nishikawa Y, Inoue S, Takeda S, Kaneko T, Nakao A. Decreased expression and frequent allelic inactivation of the RUNX3 gene at 1p36 in human hepatocellular carcinoma. *Liver Int* 2005; **25**: 380-388
13 **Tischoff I**, Markwarth A, Witzigmann H, Uhlmann D, Hauss J, Mirmohammadsadegh A, Wittekind C, Hengge UR, Tannapfel A. Allele loss and epigenetic inactivation of 3p21.3 in malignant liver tumors. *Int J Cancer* 2005; **115**: 684-689
14 **Bando K**, Nagai H, Matsumoto S, Koyama M, Kawamura N, Onda M, Emi M. Identification of a 1-cM region of common deletion on 4q35 associated with progression of hepatocellular carcinoma. *Genes Chromosomes Cancer* 1999; **25**: 284-289
15 **Okabe H**, Ikai I, Matsuo K, Satoh S, Momoi H, Kamikawa T, Katsura N, Nishitai R, Takeyama O, Fukumoto M, Yamaoka Y. Comprehensive allelotype study of hepatocellular carcinoma: potential differences in pathways to hepatocellular carcinoma between hepatitis B virus-positive and -negative tumors. *Hepatology* 2000; **31**: 1073-1079
16 **Kahng YS**, Lee YS, Kim BK, Park WS, Lee JY, Kang CS. Loss of heterozygosity of chromosome 8p and 11p in the dysplastic nodule and hepatocellular carcinoma. *J Gastroenterol Hepatol* 2003; **18**: 430-436
17 **Chan KL**, Lee JM, Guan XY, Fan ST, Ng IO. High-density allelotyping of chromosome 8p in hepatocellular carcinoma and clinicopathologic correlation. *Cancer* 2002; **94**: 3179-3185
18 **Pineau P**, Nagai H, Prigent S, Wei Y, Gyapay G, Weissenbach J, Tiollais P, Buendia MA, Dejean A. Identification of three

distinct regions of allelic deletions on the short arm of chromosome 8 in hepatocellular carcinoma. *Oncogene* 1999; **18**: 3127-3134

19 **Piao Z**, Park C, Park JH, Kim H. Allelotype analysis of hepatocellular carcinoma. *Int J Cancer* 1998; **75**: 29-33

20 **Anzola M**, Cuevas N, Lopez-Martinez M, Martinez de Pancorbo M, Burgos JJ. p16INK4A gene alterations are not a prognostic indicator for survival in patients with hepatocellular carcinoma undergoing curative hepatectomy. *J Gastroenterol Hepatol* 2004; **19**: 397-405

21 **Kremer-Tal S**, Reeves HL, Narla G, Thung SN, Schwartz M, Difeo A, Katz A, Bruix J, Bioulac-Sage P, Martignetti JA, Friedman SL. Frequent inactivation of the tumor suppressor Kruppel-like factor 6 (KLF6) in hepatocellular carcinoma. *Hepatology* 2004; **40**: 1047-1052

22 **Chen CF**, Yeh SH, Chen DS, Chen PJ, Jou YS. Molecular genetic evidence supporting a novel human hepatocellular carcinoma tumor suppressor locus at 13q12.11. *Genes Chromosomes Cancer* 2005; **44**: 320-328

23 **Zhu GN**, Zuo L, Zhou Q, Zhang SM, Zhu HQ, Gui SY, Wang Y. Loss of heterozygosity on chromosome 10q22-10q23 and 22q11.2-22q12.1 and p53 gene in primary hepatocellular carcinoma. *World J Gastroenterol* 2004; **10**: 1975-1978

24 **Nishida N**, Fukuda Y, Komeda T, Ito T, Nishimura T, Minata M, Kuno M, Katsuma H, Ikai I, Yamaoka Y, Nakao K. Prognostic impact of multiple allelic losses on metastatic recurrence in hepatocellular carcinoma after curative resection. *Oncology* 2002; **62**: 141-148

25 **Yeh SH**, Chen PJ, Shau WY, Chen YW, Lee PH, Chen JT, Chen DS. Chromosomal allelic imbalance evolving from liver cirrhosis to hepatocellular carcinoma. *Gastroenterology* 2001; **121**: 699-709

26 **Lu W**, Takahashi H, Furusato B, Maekawa S, Ikegami M, Sudo A, Egawa S, Hano H. Allelotyping analysis at chromosome arm 8p of high-grade prostatic intraepithelial neoplasia and incidental, latent, and clinical prostate cancers. *Genes Chromosomes Cancer* 2006; **45**: 509-515

27 **Knowles MA**, Aveyard JS, Taylor CF, Harnden P, Bass S. Mutation analysis of the 8p candidate tumour suppressor genes DBC2 (RHOBTB2) and LZTS1 in bladder cancer. *Cancer Lett* 2005; **225**: 121-130

28 **Seng TJ**, Low JS, Li H, Cui Y, Goh HK, Wong ML, Srivastava G, Sidransky D, Califano J, Steenbergen RD, Rha SY, Tan J, Hsieh WS, Ambinder RF, Lin X, Chan AT, Tao Q. The major 8p22 tumor suppressor DLC1 is frequently silenced by methylation in both endemic and sporadic nasopharyngeal, esophageal, and cervical carcinomas, and inhibits tumor cell colony formation. *Oncogene* 2007; **26**: 934-944

29 **Di Benedetto M**, Pineau P, Nouet S, Berhouet S, Seitz I, Louis S, Dejean A, Couraud PO, Strosberg AD, Stoppa-Lyonnet D, Nahmias C. Mutation analysis of the 8p22 candidate tumor suppressor gene ATIP/MTUS1 in hepatocellular carcinoma. *Mol Cell Endocrinol* 2006; **252**: 207-215

30 **Di Benedetto M**, Bièche I, Deshayes F, Vacher S, Nouet S, Collura V, Seitz I, Louis S, Pineau P, Amsellem-Ouazana D, Couraud PO, Strosberg AD, Stoppa-Lyonnet D, Lidereau R, Nahmias C. Structural organization and expression of human MTUS1, a candidate 8p22 tumor suppressor gene encoding a family of angiotensin II AT2 receptor-interacting proteins, *ATIP*. *Gene* 2006; **380**: 127-136

S- Editor Liu Y **L- Editor** Zhu LH **E- Editor** Lu W

PO Box 2345, Beijing 100023, China
www.wjgnet.com
wjg@wjgnet.com

World J Gastroenterol 2007 February 21; 13(7): 1098-1102
World Journal of Gastroenterology ISSN 1007-9327

RAPID COMMUNICATION

KIT-negative gastrointestinal stromal tumors with a long term follow-up: A new subgroup does exist

Katerina Kontogianni-Katsarou, Constantina Lariou, Eugenia Tsompanaki, Christina Vourlakou, Evi Kairi-Vassilatou, Costas Mastoris, Georgia Pantazi, Agatha Kondi-Pafiti

Katerina Kontogianni-Katsarou, Evi Kairi-Vassilatou, Agatha Kondi-Pafiti, Department of Pathology, Athens Medical School, Areteion University Hospital, 76, Vas. Sophias Ave., Athens 11528, Greece
Constantina Lariou, Christina Vourlakou, Costas Mastoris, Georgia Pantazi, Department of Pathology, Evaggelismos General Hospital, Ipsiladou 45-47, Athens 10676, Greece
Eugenia Tsompanaki, Department of Statistics, School of Economics and Business, Athens University, Patision 76, Athens 10434, Greece
Supported by Hellenic State Scholarship Foundation, Department of Science Promotion, No. 19366/2005
Correspondence to: Katerina Kontogianni-Katsarou, MD, PhD, Department of Pathology, Athens Medical School, Areteion University Hospital, 1b, Agias Annis Str. 145 63, Kifisia, Greece. k.kontogianni@m2k.gr
Telephone: +30-210-8018624 Fax: +30-210-8018624
Received: 2006-10-27 Accepted: 2007-01-12

Abstract

AIM: To investigate the incidence of KIT immunohostochemical staining in (GI) stromal tumors (GISTs), and to analyze the clinical manifestations of the tumors and prognostic indicators.

METHODS: We retrospectively analyzed 50 cases of previously diagnosed GISTs. Tissue samples were assessed with KIT (CD117 antigen), CD34, SMA, desmin, S-100, NSE, PCNA, Ki-67, and BCL-2 for immunohistochemical study and pathological characteristics were analyzed for prognostic factors.

RESULTS: Fifteen tumors (30%) were negative in KIT staining. A significant association was observed between gender (male patients: 14/15) and KIT-negative staining (P = 0.003).The patients's mean age was 56.6 years. Tumors developed in stomach (n = 8), small intestine (n = 5), large intestine (n = 1) and oesophagus (n = 1). The mean tumor size was 5.72 cm. The mitotic count ranged from 0-29/50 HPF (mean: 3.4) and 73% of tumors showed no necrosis. The majority of the tumors (67%) had dual or epithelioid differentiation. Tumors were classified as very low or low risk (n = 7), intermediate risk (n = 5), and high risk (n = 3) groups. Twelve (80%) patients were alive without evidence of residual tumor for an average period of 40.25 mo (12-82 mo); three patients developed metastatic disease to the liver and eventually died within 2-12 mo (median survival: 8.6 mo).

CONCLUSION: A small subgroup of GISTs fulfils the clinical and morphological criteria of these tumors, and lacks KIT expression. These tumors predominantly developed in the stomach, being dual or epithelioid in morphology, which are classified as low risk tumors and presented a better survival status than KIT-positive tumors. The ability to diagnose GISTs still depends on immunohistochemical staining but the research should extend in gene mutations.

Key words: Gastrointestinal stromal tumors; CD 117 antigen; Immunohistochemistry; Survival

Kontogianni-Katsarou K, Lariou C, Tsompanaki E, Vourlakou C, Kairi-Vassilatou E, Mastoris C, Pantazi G, Kondi-Pafiti A. KIT-negative gastrointestinal stromal tumors with a long term follow up: A new subgroup does exist. *World J Gastroenterol* 2007; 13(7): 1098-1102

http://www.wjgnet.com/1007-9327/13/1098.asp

INTRODUCTION

Most gastrointestinal mesenchymal neoplasms are gastrointestinal stromal tumors (GISTs). Their definitions follow the WHO histological classification where the term GIST is now used for a specific group of tumors comprising the majority of all gastrointestinal stromal tumors[1]. Typically, GISTs are immunohistochemically positive for KIT tyrosine kinase receptor which is perhaps their single best defining feature[2]. Most GISTs are positive for KIT (CD117 antigen), which may show membrane, diffuse cytoplasmic or a perinuclear accentuation pattern.

Histological assessment of malignancy is essentially based on mitotic counts, the size of the lesion and presence or absence of metastasis[3-5]. A proportion of GISTs, especially the malignant tissues show mutations in the regulatory juxtamembrane domain (exon 11) of the KIT gene[6]. Until now, the treatment with selective tyrosine kinase inhibitors, such as imatinib mesylate, for patients with GISTs has hinged on the KIT positive immunostaining tumors. Although the KIT positivity by immunohistochemistry becomes invaluable in the diagnosis of GISTs, some authors believe that a small subgroup of these tumors fulfils the clinical and morphological criteria

of GISTs, and lacks KIT expression. The biological features of these tumors have rarely been addressed.

Our aim was to investigate the incidence of KIT immunohostochemical staining in 50 cases of previously diagnosed GI stromal tumors, to carried out a comprehensive examination of GISTs that are negative in CD117 expression, and to analyze the clinical manifestations and prognostic indicators of the tumors.

MATERIALS AND METHODS

Using the database of Surgery and Pathology Departments of "Evaggelismos" General Hospital and Areteion University Hospital, we collected records with a pathologic diagnosis of stromal tumor of GI tract. Fifty patients with the diagnosis of GIST between 1994-2004 were retrieved from the archives. Patient age, gender, clinical manifestations, tumor size, pathological characteristics, the presence of distant metastasis and the outcome were recorded.

Tumor specimens were fixed in 10% buffered formalin after gross examination and embedded in paraffin. Histologic sections stained with hematoxylin and eosin were evaluated for all cases. Tumors were classified as very low risk, low risk, intermediate or high risk groups based on histological parameters according to NIH Consencus Guidelines for Grading[4].

Immunohistochemistry

The tumor samples from all 50 cases were examined for various markers using commercially available immunohistochemical antibodies against KIT (CD117 antigen), (A4502, polyclonal, Dako, USA; 1:50 dilution), CD34 (clone QBEnd/10) (Novocastra Labs; 1:50), S-100 (clone S1/61/69) (Novocastra Labs; 1:40), smooth-muscle actin (SMA) (clone asm-1) (Dako; 1:200), desmin (clone DE-R-11) (Novocastra Labs; 1:100), neuron-specific enolase (NSE) (clone 5E2) (Novocastra Labs; 1:100), neurofilament protein (NFL) (clone NR4) (Novocastra Labs; 1:50), bcl-2 (clone 124) (Dako; 1:40), proliferating cell nuclear antigen (PNA) (clone PC10) (Novocastra Labs; 1:200), Ki-67 (clone MM1) (Novocastra Labs; 1:200) by a standard three-step immunoperoxidase procedure (APAAP, DAKO, Glostroup, Danmark). Appropriate positive controls were run concurrently for all antibodies tested. According to the percentage of tumor cells showing an immunopositive reaction among the total tumor cells, tumors were reported as negative ($\leqslant$ 10%) or positive (> 10%).

Statistical methods

Data was analyzed using statistical software SPSS version 12.0. Chi-square test or Fisher's exact test was done for categorical variables to assess differences among baseline patient features. Overall survival was computed by the Kaplan-Meier method. Comparison of survival between subgroups was performed by the log-rank test. The relative importance of prognostic factors for the survival was analyzed with Cox's proportional hazard model. Statistical significance would be inferred at a two-tailed P value < 0.05.

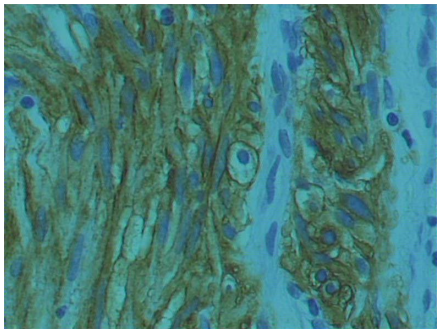

Figure 1 Histological section of GIST showing positive immunostaining for KIT (CD117 antigen) × 400.

RESULTS

Clinical and pathological data of patients with GISTs

Thirty-one (62%) patients were male and 19 (38%) female. Their age at diagnosis ranged from 26 to 89 years (mean: 62 ± 14.5). The most common symptoms were abdominal pain (72%). The most common anatomic sites of tumor origin were the small intestine (n = 23) and the stomach (n = 19). Three tumors were located in oesophagus and 5 tumors in large intestine.

The size of the tumor ranged from 0.2 cm to 30 cm (mean: 4.58 ± 5.2). The mitotic count was 0-29 per 50 HPF (× 400) (mean: 4.25 ± 2). Necrosis was present in 13 (26%) tumors. Twenty-four (48%) tumors showed evidence of dual differentiation toward smooth muscle and neural elements. Reactivity for either SMA or desmin (epithelioid features) was observed in 8 (16%) cases. There was neural differentiation (spindled features) in 7 (14%) cases. No evidence of differentiation toward either cell type, was formed even after exhaustive immunohistochemistry in 11 (22%) cases. Of the 50 tissues tested, 35 (70%) were positive for KIT staining (Figure 1), while 15 (30%) tumors lacked KIT expression. The high incidence of KIT-positive staining (57%) was in tissues diagnosed as "high risk" tumors. Twenty-four (48%) tumors were CD34 positive. The proliferative activity (PCNA labeling index) was high (> 10% labeled nuclei) in 62% of our specimens. Only 6 (12%) cases were characterized by high (> 20% labeled nyclei) Ki-67 immunoreactivity percentages. Bcl-2 protein was positively expressed in the cytoplasm of tumor cells in 26 (52%) specimens.

Complete information on patients' clinical course could be obtained in 50 (100%) cases. According to the available follow-up, patients with KIT-positive staining tumors were alive without evidence of residual tumor for an average period of 32.3 mo (12-82 mo). Tumor location, mitotic counts, risk group and metastasis seem to be related to survival, since partial likelihood ratio test of Cox regression for each of these patient's feature was less than 0.05 (Figure 2, Figure 3, Figure 4). There was an indication of association between tumor size and mitoses (P = 0.055, Fisher's Exact test).

Clinicopathological features of KIT (CD117) negative GISTs

Of the 50 tissues tested, a small subgroup of tumors (n = 15) fulfiled the clinical and morphological criteria of GISTs and lacked KIT antigen immunoexpression. The clinicopathological features of KIT-negative cases

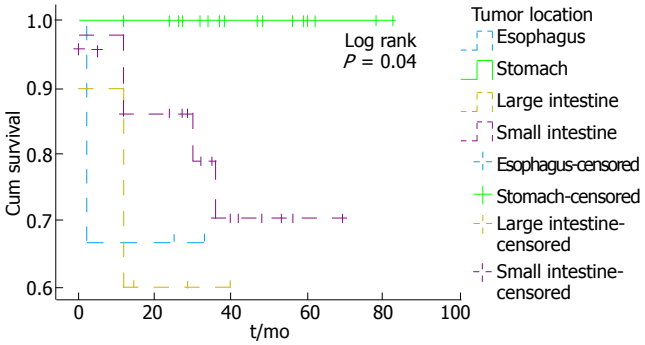

Figure 2 Cumulative survival for patients with GISTs based on tumor location.

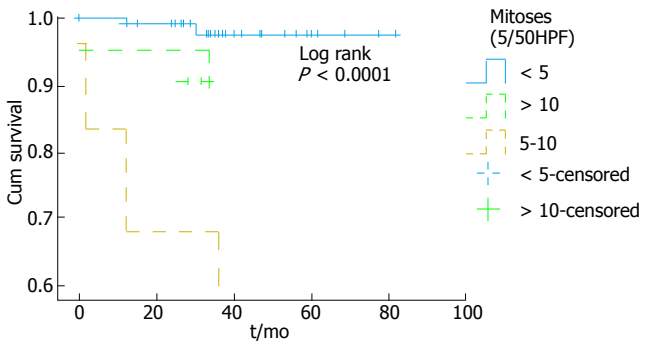

Figure 3 Cumulative survival for patients with GISTs based on mitotic counts.

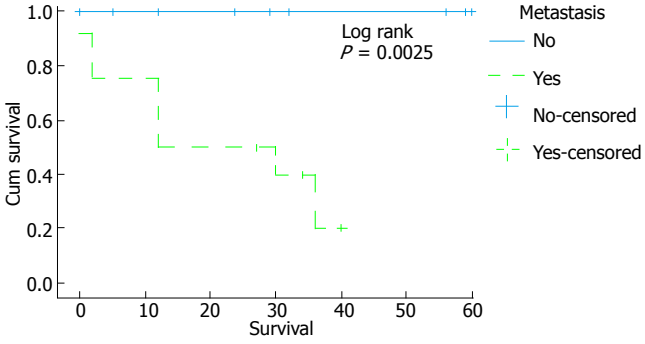

Figure 4 Cumulative survival for patients with GISTs based on metastasis status.

are shown in Table 1. A highly significant association was observed between gender and CD117 staining ($P = 0.003$). All, except one, KIT-negative tumors were observed in male patients, while the majority of female patients (18/19) expressed CD117 immunostaining (Table 2).

Patients' age at diagnosis ranged from 26 to 82 years (mean: 56.6). The majority of them (11/15) presented at the hospital with symptoms, as abdominal pain. KIT-negative GISTs developed in stomach ($n = 8$), small intestine ($n = 5$), large intestine ($n = 1$) and oesophagus ($n = 1$) (Table 3).

Tumors size ranged from 0.5 cm to 30 cm (mean: 5.72). The majority of tumors were smaller than 5 cm (9/15), and only one was > 10 cm. The mitotic count ranged from 0-29 per 50 HPF (× 400) (mean: 3.4). Twelve (80%) tumors contained less than 5/50 HPF mitoses, 2 (13%) tumors contained mitoses between 5 and 10/50 HPF and 1 (7%) tumor contained mitoses > 10/50 HPF. Absence of necrosis was present in 73% (11/15) of tumors.

Of the 15 KIT-negative samples, 6 (40%) cases had dual differentiation showing histologically mixed spindled and epithelioid type features, four (27%) cases showed histologically predominantly epithelioid type features, two (13%) cases spindled type features, and 3(20%) cases were classified as anaplastic (Table 4).

KIT-negative tumors were diagnosed as "very low" and "low risk" (benign) ($n = 7$), "intermediate risk" (uncertain malignant potential) ($n = 5$), and "high risk" tumors (malignant potential) ($n = 3$).

The clinical status was primary presentation in 12 patients. According to the available follow-up, twelve patients (80%) were alive without evidence of residual tumor for an average period of 40.25 mo (12-82 mo); three patients developed metastatic disease to the liver and eventually died within 2-12 mo (median survival: 8.6 mo).

DISCUSSION

The classification of GISTs has been a continually evolving process reflecting our increasing understanding of the biological nature of these tumors. One of the most important concepts of the recent years is that GISTs show the differentiation of the interstitial cells of Cajal (ICC)[2]. Mesenchymal tumors of GI can be identified based on the features of ICCs and can therefore designated as GISTs[4].

Histological and immunohistochemical advances, and molecular genetics provide a new era for GISTs. KIT, a type Ⅲ tyrosine kinase growth factor receptor, is the common denominator in most GISTs[7-9]. CD117, the epitope for KIT, is introduced as a new phenotypic marker for distinguishing between GISTs and non-GIST spindle cell tumors of the GI. A small subgroup of GISTs that fulfill the clinical and morphological criteria of these tumors is essentially KIT-negative by immunohistohemistry. The biological features of these tumors have rarely been addressed. In the absence of CD117 immunopositivity, the diagnosis of GISTs is challenging.

Based on this and using the latest clinical and histological criteria, we screened 50 cases of gastrointestinal stromal tumors with a long term follow-up. Generally, as it was expected, tumor location, mitotic counts, risk group and metastasis were significantly associated with survival. Of the 50 tissues tested, 35 (70%) were positive for CD117 staining and 15 (30%) were negative. A significant association was observed between gender and KIT (CD117) immunostaining. KIT-negative tumors were observed in male patients, while the majority of female patients expressed CD117 immunostaining.

The majority of KIT-negative tumors developed in stomach while KIT-positive tumors developed in small intestine. This finding is in accordance with recent studies[10]. The majority of KIT-negative tumors were smaller than 5 cm (9/15), and 80% contained mitoses less than 5/50 HPF.

Of the 15 CD117-negative samples, 6 cases had evidence of dual differentiation, 4 cases showed histologically epithelioid type features, two had spindle type features, and 3 cases were negative for all markers,

Table 1 Clinicopathological features of KIT-negative cases

Case No.	Sex	Age (yr)	Symptoms	Site	Size (cm)	Mitoses (/50 HPF)	Presence of necrosis	Morphology	Risk category	Clinical status	Survival data/mo
1	M	60	Yes	Small Intestine	4.30	1	No	Epithelioid	Low risk	Primary	Alive/12
2	M	46	No	Stomach	0.50	0	No	Mixed	Very low risk	Primary	Alive/24
3	M	50	No	Small Intestine	0.50	0	No	Anaplastic	Very low risk	Primary	Alive/24
4	M	64	Yes	Large Intestine	4.50	10	Yes	Epithelioid	High risk	Liver metastasis	Dead/12
5	M	78	Yes	Small Intestine	7.00	1	Yes	Mixed	Intermediate risk	Liver metastasis	Dead/12
6	F	53	Yes	Stomach	5.00	0	No	Spindled	Low risk	Primary	Alive/47
7	M	43	Yes	Esophagus	7.00	0	No	Mixed	Intermediate risk	Primary	Alive/25
8	M	51	Yes	Small Intestine	6.00	2	Yes	Epithelioid	Intermediate risk	Primary	Alive/12
9	M	69	No	Stomach	2.00	0	No	Mixed	Very low risk	Primary	Alive/37
10	M	54	Yes	Stomach	3.50	0	No	Spindled	Low risk	Primary	Alive/62
11	M	70	Yes	Stomach	6.00	0	No	Anaplastic	Intermediate risk	Primary	Alive/82
12	M	42	Yes	Stomach	6.00	2	No	Anaplastic	Intermediate risk	Primary	Alive/56
13	M	26	No	Stomach	0.50	0	No	Epithelioid	Very low risk	Primary	Alive/78
14	M	82	Yes	Stomach	30.00	6	Yes	Mixed	High risk	Primary	Alive/82
15	M	61	Yes	Small Intestine	3.00	29	No	Mixed	High risk	Liver metastasis	Dead/2

M = male; F = female.

Table 2 Correlation between gender and CD117 expression in patients with GISTs

		CD117 expression		
		Negative	Positive	Total
Gender	Male	14	17	31
		45.20%	54.80%	100%
	Female	1	18	19
		5.30%	94.70%	100%
Total		15	35	50

Table 3 Correlation between tumor location and CD117 expression in patients with GISTs

Tumor location	CD117 expression		
	Negative	Positive	Total
Esophagus	1	2	3
	33.30%	66.70%	100%
Stomach	8	11	19
	42.10%	57.90%	100%
Small intestine	5	18	23
	21.70%	78.30%	100%
Large intestine	1	4	5
	20%	80%	100%
Total	15	35	50
	30%	70%	100%

Table 4 Immunohistohemical findings of patients with KIT-negative GISTs

Case No.	CD117	Immunohistochemistry				CD34
		α-SMA	Desmin	S-100	NSE	
1	Negative	Positive	Positive	-	-	Positive
2	Negative	-	Positive	Positive	-	-
3	Negative	-	-	-	-	Positive
4	Negative	Positive	-	-	-	Positive
5	Negative	Positive	-	-	Positive	-
6	Negative	-	-	Positive	Positive	-
7	Negative	Positive	Positive	Positive	-	-
8	Negative	Positive	-	-	-	Positive
9	Negative	Positive	Positive	-	Positive	-
10	Negative	-	-	Positive	Positive	Positive
11	Negative	-	-	-	-	Positive
12	Negative	-	-	-	-	Positive
13	Negative	Positive	Positive	-	-	-
14	Negative	Positive	-	-	Positive	Positive
15	Negative	Positive	-	Positive	-	-

but positive for CD34 staining. Our findings support previously published data[10,11], suggesting that there is a subgroup of KIT–negative GISTs that exhibit the same clinical and morphological features as the KIT-positive tumors.

The majority of KIT-negative tumors were diagnosed as "very low" or "low risk" tumors, while the highest incidence of KIT-positive staining was found in "high risk" tumors. The majority of patients with KIT-negative tumors (80%) were alive without evidence of residual tumor for an average period of 40.25 mo and presented a better survival status than the patients with KIT-positive tumors.

Benign and malignant GISTs carry mutations in KIT gene. It is still not clear whether mutations are independent prognostic factors[12,13]. We believe that a search for gene mutation, as the c-kit gene, in KIT-negative staining tumors might clarify the diagnosis status (unpublished observations), as other authors believe that KIT mutations[11] or intragenic platelet-derived growth factor-alpha (PDGFR-a) activating mutations are present in some of these tumors[10]. The pharmaceutical development and therapeutic implications of protein tyrosine kinase inhibitors has refocused the attention on GIST. Until recently, no patient with complete response to therapy was reported[14]. Is there any value in separating these tumors with epithelioid or dual differentiation because they are often KIT-antigen negative[15]? Is this going to be the result of a better differentiation status, detection of certain molecular alterations or it may be related to more traditional criteria as size and mitosis rate? There is still challenge to identify those patients who would benefit

from receiving the new therapy.

In conclusion, our study confirms that traditional histologic criteria alone are not enough to confirm GISTs diagnosis, but are still the only criteria to estimate biological behavior in these tumors. A small subgroup of GISTs fulfils the clinical and morphological criteria of these tumors, and lacks KIT expression. These tumors predominantly develop in stomach, showing dual or epithelioid morphology; they are classified as "low risk" tumors, and present with a better survival status than KIT-positive staining tumors. The ability to diagnose GISTs still depends on the immunohistochemical staining but the research should expand in gene mutations.

REFERENCES

1 **Miettinen M**, Lasota J. Gastrointestinal stromal tumors: review on morphology, molecular pathology, prognosis, and differential diagnosis. *Arch Pathol Lab Med* 2006; **130**: 1466-1478
2 **Kindblom LG**, Remotti HE, Aldenborg F, Meis-Kindblom JM. Gastrointestinal pacemaker cell tumor (GIPACT): gastrointestinal stromal tumors show phenotypic characteristics of the interstitial cells of Cajal. *Am J Pathol* 1998; **152**: 1259-1269
3 **Miettinen M**, El-Rifai W, H L Sobin L, Lasota J. Evaluation of malignancy and prognosis of gastrointestinal stromal tumors: a review. *Hum Pathol* 2002; **33**: 478-483
4 **Fletcher CD**, Berman JJ, Corless C, Gorstein F, Lasota J, Longley BJ, Miettinen M, O'Leary TJ, Remotti H, Rubin BP, Shmookler B, Sobin LH, Weiss SW. Diagnosis of gastrointestinal stromal tumors: A consensus approach. *Hum Pathol* 2002; **33**: 459-465
5 **Berman J**, O'Leary TJ. Gastrointestinal stromal tumor workshop. *Hum Pathol* 2001; **32**: 578-582
6 **Kitamura Y**, Hirota S, Nishida T. Molecular pathology of c-kit proto-oncogene and development of gastrointestinal stromal tumors. *Ann Chir Gynaecol* 1998; **87**: 282-286
7 **Koay MH**, Goh YW, Iacopetta B, Grieu F, Segal A, Sterrett GF, Platten M, Spagnolo DV. Gastrointestinal stromal tumours (GISTs): a clinicopathological and molecular study of 66 cases. *Pathology* 2005; **37**: 22-31
8 **Hirota S**, Isozaki K, Moriyama Y, Hashimoto K, Nishida T, Ishiguro S, Kawano K, Hanada M, Kurata A, Takeda M, Muhammad Tunio G, Matsuzawa Y, Kanakura Y, Shinomura Y, Kitamura Y. Gain-of-function mutations of c-kit in human gastrointestinal stromal tumors. *Science* 1998; **279**: 577-580
9 **Miettinen M**, Lasota J. KIT (CD117): a review on expression in normal and neoplastic tissues, and mutations and their clinicopathologic correlation. *Appl Immunohistochem Mol Morphol* 2005; **13**: 205-220
10 **Debiec-Rychter M**, Wasag B, Stul M, De Wever I, Van Oosterom A, Hagemeijer A, Sciot R. Gastrointestinal stromal tumours (GISTs) negative for KIT (CD117 antigen) immunoreactivity. *J Pathol* 2004; **202**: 430-438
11 **Tzen CY**, Mau BL. Analysis of CD117-negative gastrointestinal stromal tumors. *World J Gastroenterol* 2005; **11**: 1052-1055
12 **Rubin BP**. Gastrointestinal stromal tumours: an update. *Histopathology* 2006; **48**: 83-96
13 **Miettinen M**. Gastrointestinal stromal tumors: parameters that determine biological potential and guide therapy from a surgical pathologist point of view. Society for Ultrastructural Pathology. *USCAP Meeting;* 2003: 16-20
14 **Demetri GD**. Identification and treatment of chemoresistant inoperable or metastatic GIST: experience with the selective tyrosine kinase inhibitor imatinib mesylate (STI571). *Eur J Cancer* 2002; **38** Suppl 5: S52-S59
15 **Herrera GA**. Histological perspective: a journey through evolution of classification schemes. Society for Ultrastructural Pathology. *USCAP Meeting;* 2003: 1-6

S- Editor Liu Y **L- Editor** Ma JY **E-Editor** Lu W

PO Box 2345, Beijing 100023, China
www.wjgnet.com
wjg@wjgnet.com

World J Gastroenterol 2007 February 21; 13(7): 1103-1107
World Journal of Gastroenterology ISSN 1007-9327

RAPID COMMUNICATION

NCB-02 (standardized Curcumin preparation) protects dinitrochlorobenzene-induced colitis through down-regulation of NFκ-B and iNOS

MV Venkataranganna, Md Rafiq, S Gopumadhavan, Ghouse Peer, UV Babu, SK Mitra

MV Venkataranganna, Md Rafiq, S Gopumadhavan, Ghouse Peer, UV Babu, SK Mitra, R&D Center, The Himalaya Drug Company, Bangalore-562 123, India
Correspondence to: MV Venkataranganna, PhD, Senior Research Scientist, R&D Center, The Himalaya Drug Company, Makali, Bangalore-562 123, India. venkataranganna@himalayahealthcare.com
Telephone: +91-80-23714444 Fax: +91-80-23714471
Received: 2006-10-07 Accepted: 2007-01-12

Abstract

AIM: To evaluate the efficacy and mechanism of action of NCB-02, a standardized Curcumin preparation, against 2, 4-dinitrochlorobenzene (DNCB)-induced ulcerative colitis in rats.

METHODS: Ulcerative colitis was induced in male rats by sensitizing with topical application of DNCB in acetone for 14 d and intra-colonol challenge with DNCB on day 15. A separate group of animals with vehicle treatment in similar fashion served as control group. Colitis rats were divided into different groups and treated with NCB-02 at doses of 25, 50 and 100 mg/kg b.wt p.o. for 10 d. Sulfasalazine at a dose of 100 mg/kg b.wt for 10 d served as a reference group. On day 10 after respective assigned treatment, all the animals were euthanized and the length of the colon, weight of entire colon and distal 8 cm of the colon were recorded. The distal part of the colon was immediately observed under a stereomicroscope and the degree of damage was scored. Further distal 8 cm of the colon was subject to the determination of colonic myeloperoxidase (MPO), lipid peroxidation (LPO) and alkaline phosphatase (ALP) activities. A small piece of the sample from distal colon of each animal was fixed in 10% neutral buffered formalin and embedded in paraffin wax and sectioned for immunohistochemical examination of NFκ-B and iNOS expression.

RESULTS: NCB-02 showed a dose dependent protection against DNCB-induced alteration in colon length and weight. NCB-02 treatment also showed a dose dependent protection against the elevated levels of MPO, LPO and ALP, induced by DNCB. NCB-02 demonstrated a significant effect at a dose of 100 mg/kg b.wt., which was almost equipotent to 100 mg/kg b.wt. of sulfasalazine. Treatment with sulfasalazine and curcumin at a dose of 100 mg/kg b.wt. inhibited the DNCB-induced overexpression of NFκ-B and iNOS in the colon.

CONCLUSION: Curcumin treatment ameliorates colonic damage in DNCB-induced colitic rats, an effect associated with an improvement in intestinal oxidative stress and downregulation of colonic NFκ-B and iNOS expression.

Key words: Curcumin; Colitis; Dinitrochlorobenzene; NFκ-B; iNOS

Venkataranganna MV, Rafiq Md, Gopumadhavan S, Peer G, Babu UV, Mitra SK. NCB-02 (standardized Curcumin preparation) protects dinitrochlorobenzene-induced colitis through down-regulation of NFκ-B and iNos. *World J Gastroenterol* 2007; 13(7): 1103-1107

http://www.wjgnet.com/1007-9327/13/1103.asp

INTRODUCTION

Inflammatory bowel disease (IBD), including Crohn's disease and ulcerative colitis (UC), is a chronic and relapsing inflammatory disease caused by the inflammation and sores in the lining of large intestine and characterized clinically by recurrent episodes of bloody diarrhea, cramping, abdominal pain and histologically by mucosal inflammation and injury[1]. Conventional therapy for UC includes sulfasalazine and other 5-aminosalicylic acid (5-ASA) type of compounds, and in more persistent and/or severe cases, oral, rectal and parenteral corticosteroids and immunosuppressants are administered[2]. All of these have significant toxicities and are partly or completely ineffective in significant numbers of patients[3].

Several agents used in the management of IBD, such as corticosteroids, sulfasalazine and 5-ASA, have documented regulation of Nuclear Factor Kappa-B (NFκ-B) function[2]. Given the importance of inflammatory cell activation involved in the development of IBD, there is a need for a treatment modality against IBD that can block the inflammatory processes. There is substantial evidence for the involvement of oxidative stress and profound alterations in the biosynthesis of the labile free

radical nitric oxide from L-arginine in the pathogenesis of colitis[4]. The use of medicinal plants or their active components has become an increasingly attractive approach for the treatment of UC. Curcumin, the active principle in turmeric, is a polyphenolic antioxidant and a natural yellow orange dye. Turmeric contains three curcumin analogues based on the number of hydroxyl groups present in the parent molecule. They are Curcumin (Curcumin I), demethoxy curcumin (Curcumin Ⅱ) and bis-demethoxy curcumin (Curcumin Ⅲ). Curcumin is a active constituent of *Curcuma longa*, whose anti-inflammatory properties are related in part to inhibition of the activities of the cyclooxygenase, lipoxygenase and NFκ-B in several cell systems[5-9]. Many experimental studies have demonstrated the important role of Curcumin in the attenuation of IBD and colonic cancer and it is also known to exhibit a variety of beneficial effects including antitumor, anti-HIV, antioxidant, anticataract development, septic shock, promotion of wound healing in normal and diabetic conditions, anti-asthmatic, anti-colitis, anti-fibrosis, reduction of mucosal damage, prevention of UV damage to skin, inhibition of development of cancers of the skin, stomach, colon, prostate, oral cavity and liver. Furthermore, Curcumin could also inhibit tumor metastases, pancreatitis, drug or alcohol-induced liver fibrosis, cystic fibrosis and Alzheimer's disease[10,11].

NCB-02 is a standardized extract of *Curcuma longa* containing 78% curcuminoids, 72% of which is Curcumin, 18.08% demethoxy curcumin and 9.42% bis-demethoxy Curcumin. This study was designed to evaluate its efficacy and mechanism of action against 2, 4-dinitrochloro-benzene (DNCB)-induced ulcerative colitis in rats.

MATERIALS AND METHODS

Animals

Laboratory bred Wistar male rats weighing between 220-250 g were used for the experiments. The animals were housed and acclimatized to a constant temperature of 22 ± 3℃ and were exposed to 12 h day and night cycle. The animals were fed with synthetic diet and water *ad libitum*.

Effect of NCB-02 on UC in rats induced by DNCB[12]

Forty-eight rats were divided into six groups of eight animals each and, the nape hair was depleted. About 300 μL DNCB in acetone (20 g/L) was dropped to the nape of the rats once a day for 14 d. On the 15th day, animals of Groups Ⅱ-Ⅵ were subject to intracolonol challenge of DNCB. Intra-colon challenge was done by infusing 0.25 mL of 0.1% DNCB in 50% alcohol into colon by a nylon catheter (3 mm in diameter), which was inserted into the colon at the site of 8 cm from the anus. Group I served as normal control and received 50% alcohol instead of DNCB. The animals were kept in Trendelenburg position for 1 min after DNCB administration and maintained in cages with free access to water and food.

Rats of Groups I and Ⅱ served as normal and positive controls respectively and were administered with water (vehicle) at a dose of 10 mL/kg b.wt. p.o. and Group Ⅲ rats with 100 mg/kg b.wt. p.o. of reference drug, sulfasalazine. Rats of groups Ⅳ-Ⅵ received 25, 50 and 100 mg/kg b.wt. p.o. of NCB-02, respectively. The treatment was carried out for 10 d, after challenge with DNCB. On d 10, after assigned treatment, all the animals were euthanized by exsanguinations. The entire length of the colon starting from the ceacal end was excised, opened and gently rinsed with ice-cold saline. The colon was kept flat with the mucosal surface upward on a plate prechilled to 4℃. The length of the colon, weight of entire colon and distal 8 cm of the colon were recorded. The distal part of the colon was immediately observed under stereomicroscope to note any visible damage. The degree of damage was scored macroscopically on a 0-5 scale by independent observers[13]. Further distal 8 cm of the colon was subject to the determination of colonic myeloperoxidase[14], lipid peroxides[15] and ALP activity. A small piece of the sample from distal colon of each animal was fixed in 10% neutral buffered formalin and embedded in paraffin wax and sectioned for immunohistochemical examination[16].

Myeloperoxidase (MPO) activity

MPO is an enzyme found in cells of myeloid origin, and has been used extensively as a biochemical marker of granulocyte (mainly neutrophil) infiltration into gastrointestinal tissues[14]. Samples of distal colon were homogenized in 10 mmol/L potassium phosphate buffer, pH 7.0 containing 0.5% hexadecyltrimethylammonium bromide and centrifuged for 30 min at 20000 × *g* at 4℃. An aliquot of the supernatant was then allowed to react with a solution of 1.6 mmol/L O-dianisidine and 0.1 mmol/L H_2O_2. The rate of change in absorbance was measured spectrophotometrically at 650 nm. One unit of myeloperoxidase activity was defined as degrading 1 mmol of H_2O_2 per min at 37℃ and was expressed as units per milligram of tissue sampled (U/mg tissue).

Estimation lipid peroxidation and ALP

The tissue was homogenized at a concentration of 10% w/v in 0.15 mol/L potassium chloride using a glass homogenizer. The homogenate was centrifuged at 800 × *g* and the supernatants were used for the estimation of lipid peroxides[15] and alkaline phosphatase (ALP) using Boheringer Mannheim kit.

Immunohistochemistry for NFκ-B and inducible nitric oxide synthase (iNOS)[16]

Colon sections were deparaffinized in xylene, for 2-5 min and dehydrated with 100% ethanol for 2-3 min followed with 95% ethanol for 1 min, then rinsed in distilled water. Tissue sections were incubated with primary antibody at appropriate dilution in phosphate buffered saline (PBS) for 1 h at room temperature, then incubated in biotinylated secondary antibody in PBS for 1 h at room temperature. After rinsing in PBS for 3 changes of 2 min each, sections were incubated in freshly prepared peroxidase substrate solution for 10 min at room temperature and counterstained with weak haematoxylin for 10 min after rinsing with PBS.

Table 1 Various biomarkers of colitis

	Ulcer index	Colon length	Colon Wt. (Total) (gm)	Distal Colon wt. (last 8 cm) (gm)	MPO Units/gm of tissue	LPO nmol/L per 100 mg	ALP IU/100 mg
Control	0.00 ± 0.00	19.88 ± 0.41	1.46 ± 0.05	0.52 ± 0.02	2.98 ± 0.42	145.75 ± 13.78	26.63 ± 3.45
Positive control	4.50 ± 0.25[b]	15.75 ± 0.39[b]	2.18 ± 0.13[b]	1.33 ± 0.10[b]	5.63 ± 0.46[b]	296.23 ± 23.98[b]	252.13 ± 33.69[d]
Sulfasalazine (100 mg/kg)	2.75 ± 0.39[f]	18.13 ± 0.37[h]	1.76 ± 0.05[j]	0.84 ± 0.05[h]	3.60 ± 0.29[j]	211.54 ± 32.23[j]	136.38 ± 17.69[j]
NCB-02 (25mg/kg)	3.75 ± 0.23	15.13 ± 0.37	1.98 ± 0.14	1.22 ± 0.13	4.27 ± 0.45	259.38 ± 28.71	232.38 ± 33.79
NCB-02 (50mg/kg)	3.00 ± 0.18[j]	16.50 ± 0.31	1.88 ± 0.15	1.09 ± 0.09	3.90 ± 0.32	205.69 ± 22.09[j]	186.88 ± 24.86
NCB-02 (100mg/kg)	2.63 ± 0.25[f]	18.13 ± 0.45[h]	1.69 ± 0.07[j]	0.90 ± 0.06[j]	3.73 ± 0.30[j]	174.84 ± 13.06[h]	153.13 ± 20.23[j]

[b]$P < 0.001$, [d]$P < 0.01$ *vs* control; [f]$P < 0.001$, [h]$P < 0.01$, [j]$P < 0.05$ *vs* positive control.

Statistical analysis

The values were expressed as mean ± SE. The results were analyzed statistically using one-way ANOVA followed by Dunnet's multiple comparison test using GraphPad Prism software package (Version 4.0) to find the level of significance. The minimum level of significance is fixed at $P < 0.05$.

RESULTS

Rats sensitized and challenged with DNCB showed ulcers with severe macroscopic inflammation in the colon as assessed by the colonic damage score. Colon length was significantly reduced with a significant increase in total and distal colon weight in colitic rats as compared with non-colitic control rats. There was also a significant increase in colonic MPO, LPO and ALP activity as compared with non-colitic rats (Table 1). Treatment with NCB-02 showed a dose dependent protection against DNCB-induced colonic damage as indicated by normalization of colon length, reduction in colon weight (total and distal) and decrease in the levels biochemical markers such as MPO, LPO and ALP. NCB-02 at a dose of 100 mg/kg b.wt. p.o. showed a significant effect on various parameters (Table 1). Reference drug sulfasalazine presented with a significant reversal of DNCB-induced alterations at a dose of 100 mg/kg b.wt. p.o. (Table 1).

Sulfasalazine treatment resulted in significant protection with the mean ulcer score of 2.75 ± 0.39 and NCB-02 had a dose dependent protection at 25, 50 and 100 mg/kg b.wt. with ulcer scores of 3.75 ± 0.23, 3.00 ± 0.18 and 2.63 ± 0.25 ($P < 0.001$), respectively (Table 1).

Myeloperoxidase activity is an established marker for inflammatory cell (mainly neutrophils) infiltration in rodent models of colitis, and was thus examined. MPO activity was significantly increased in colitis rats as compared with the control. NCB-02 treatment inhibited DNCB-induced MPO activity in a dose dependent manner. Both sulfasalazine and NCB-02 at a dose of 100 mg/kg b.wt. significantly protected DNCB-induced elevation of MPO activity (Table 1).

High level expression of iNOS and NFκ-B were observed in colitis rats, which is revealed by immunohistochemistry (Figures 1 and 2). This immunohistochemistry for NFκ-B and iNos expression revealed that NCB-02 at a dose 100 mg/kg b.wt. inhibited the DNCB-induced expression of these pro-inflammatory mediators of ulcerative colitis.

From the various parameters evaluated it was observed that 100 mg/kg b.wt. of NCB-02 was almost equipotent to sulfasalazine at 100 mg/kg b.wt.

DISCUSSION

In the present investigation, the beneficial effects observed with NCB-02 (Standardized Curcumin preparation) treatment were assessed based on the improvement of colon weight and length, and histologically by preservation of the colon architecture in comparison with the rats from the non-treated colitic group. The biochemical assays, such as MPO and ALP, performed in the colonic specimens confirmed the anti-inflammatory effect exerted by Curcumin at a dose of 100 mg/kg, since it was associated with significant reduction in MPO and ALP activities. MPO activity has been widely used to detect and follow intestinal inflammation, and a reduction in the activity of this enzyme can be interpreted as a manifestation of the anti-inflammatory activity of a given compound. Alkaline phosphatase activity is considered as one of the sensitive markers of inflammation in the intestine, as this enzyme activity is invariably augmented in these experimental conditions of colitis. The results obtained in this study confirm the intestinal anti-inflammatory effect previously demonstrated for Curcumin[9,17].

Earlier studies provided evidence of significantly elevated activation of NFκ-B in ulcerative colitis and Crohn's disease[18,19]. Several therapeutic agents with NFκ-B inhibitory activity, such as sulfasalazine, mesalamine, and corticosteroids have been used for the treatment of IBD. They have sundry defects such as steroid dependence and steroid resistance, decreasing glucose tolerance, hepatotoxicity and pancreatitis[2]. Now, more potent and selective treatment strategies for IBD aim at preventing NFκ-B activation in mucosal macrophages and T lymphocytes.

According to the well-described role of NFκ-B in inflammatory regulation and iNOS expression, the degree of NFκ-B expression was determined in the colonic tissue samples from animals subjected to DNCB sensitization and challenge. The inflammatory status induced by DNCB was associated with increased colonic NFκ-B expression when compared to normal tissues. Curcumin treatment resulted in inhibition of NFκ-B expression and similar

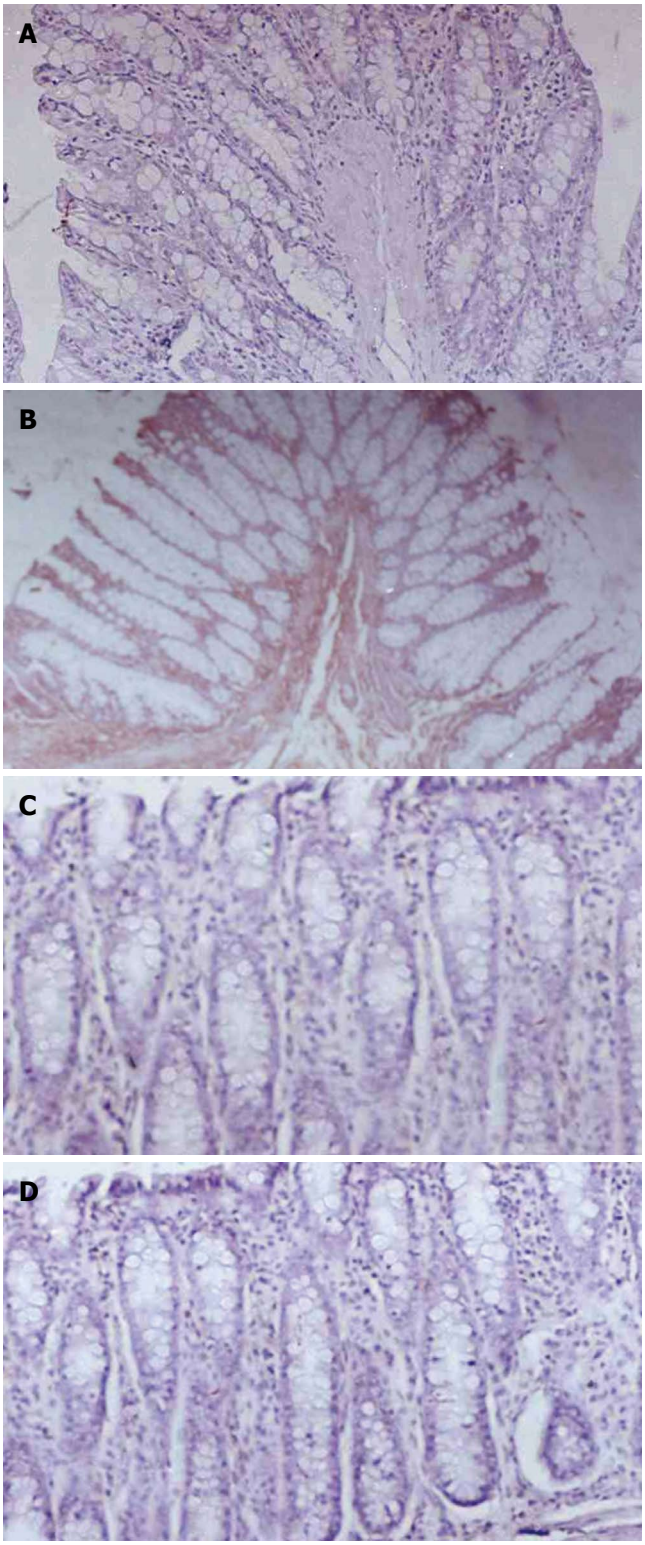

Figure 1 **A**: Section of colon in normal control showing normal structure and architecture (immunohistochemistry, 40 x); **B**: Section of colon in DNCB control showing extensive NFκ-B (brown) expression in tissue (immunohistochemistry, 40 x); **C**: Section of colon in sulfasalazine treated group showing limited NFκ-B (brown) expression (immunohistochemistry, 40 x); **D**: Section of colon in NCB-02 treated group showing minimal NFκ-B (brown) expression (immunohistochemistry, 40 x).

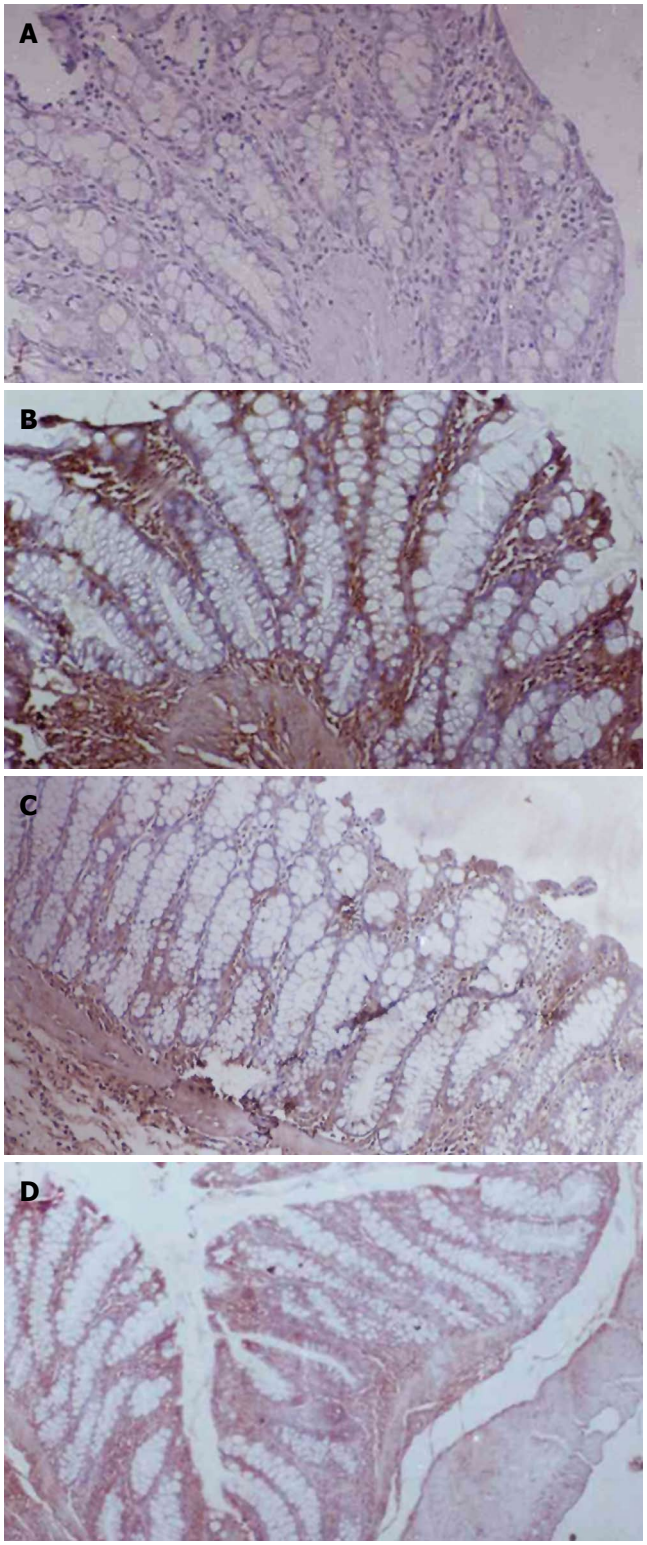

Figure 2 **A**: Section of colon in normal control showing normal structure and architecture (immunohistochemistry, 40 x); **B**: Section of colon in DNCB control showing extensive iNos (brown) expression in tissue (immunohistochemistry, 40 x), **C**: Section of colon in sulfasalazine treated group showing limited iNos (brown) expression (immunohistochemistry, 40 x); **D**: Section of colon in NCB-02 treated group showing minimal iNos (brown) expression (immunohistochemistry, 40 x).

response was observed with sulfasalazine treatment.

Nitric oxide is one of the important pro-inflammatory mediators, which plays a key role in the pathogenesis of IBD. In our study, we evaluated the effect of Curcumin on colonic iNOS activity in the DNCB-induced model of experimental colitis. DNCB administration increased colonic iNOS activity expression in rats, as detected by immunohistochemistry (Figure 2B). The intestinal anti-

inflammatory effect exerted by NCB-02, was associated with a reduction of iNOS expression (Figure 2D) when compared with DNCB control animals.

Myeloperoxidase is an enzyme found in cells of myeloid origin, and has been used extensively as a biochemical marker of granulocyte (mainly neutrophil) infiltration into gastrointestinal tissues. Our study showed that DNCB raised the levels of colonic MPO, which was ameliorated in NCB-02 and sulfasalazine treated groups.

In addition, our study gives some evidence about the mechanisms involved in the intestinal anti-inflammatory effect of Curcumin. One of the mechanisms could be its inhibition of free radical generation and antioxidant properties, which is evident from several earlier observations[9,10]. This activity may play a crucial role in the intestinal anti-inflammatory effect of the Curcumin, because intense oxidative insult is a common feature in human IBD and in the different experimental models of rat colitis, such as the trinitrobenzene sulfonic acid (TNBS) and the DNCB models in rats, and is an important mechanism for tissue damage during chronic intestinal inflammation[18].

In the last decade, it became increasingly clear that NO overproduction by iNOS is deleterious to intestinal function, which contributes significantly to gastrointestinal immunopathology in the chronic inflammatory events in IBD[16,18]. The important role attributed to NO in these intestinal conditions prompted us to study whether the beneficial effects of Curcumin on DNCB-induced colitis could be related to an effect on colonic NO production. The results in this study reveal that colonic inflammation is associated with a higher colonic iNOS expression, as evidenced by immunohistochemistry. Treatment of colitic rats with NCB-02 effectively inhibited the upregulated colonic iNOS expression.

The present study revealed that oral treatment of NCB-02 in colitic rats significantly inhibited the NFκ-B pathway, which is reported to be activated as a consequence of the intestinal inflammatory process induced by DNCB. The molecular mechanism involved in the suppressive effects of Curcumin on NFκ-B could be due to the inhibition of NFκ-B by acting as antioxidants, since NFκ-B is a redox-sensitive transcription factor and activated by oxidative stress in the inflamed intestinal mucosa via blocking the phosphorylation and degradation of IkB protein, as previously reported *in vitro* and *in vivo*[7,19].

In conclusion, Curcumin treatment ameliorates colonic damage in DNCB-induced colitic rats, an effect associated with an improvement in intestinal oxidative stress and a downregulation in colonic iNOS and NFκ-B expression. Therefore, Curcumin (NCB-02) may hold promise for the treatment of inflammatory bowel disease.

REFERENCES

1 **Furrie E**, Macfarlane S, Cummings JH, Macfarlane GT. Systemic antibodies towards mucosal bacteria in ulcerative colitis and Crohn's disease differentially activate the innate immune response. *Gut* 2004; **53**: 91-98

2 **Nikolaus S**, Fölscn U, Schreiber S. Immunopharmacology of 5-aminosalicylic acid and of glucocorticoids in the therapy of inflammatory bowel disease. *Hepatogastroenterology* 2000; **47**: 71-82

3 **Farrell RJ**, Kelleher D. Glucocorticoid resistance in inflammatory bowel disease. *J Endocrinol* 2003; **178**: 339-346

4 **Barbosa DS**, Cecchini R, El Kadri MZ, Rodríguez MA, Burini RC, Dichi I. Decreased oxidative stress in patients with ulcerative colitis supplemented with fish oil omega-3 fatty acids. *Nutrition* 2003; **19**: 837-842

5 **Han SS**, Keum YS, Seo HJ, Surh YJ. Curcumin suppresses activation of NF-kappaB and AP-1 induced by phorbol ester in cultured human promyelocytic leukemia cells. *J Biochem Mol Biol* 2002; **35**: 337-342

6 **Pan MH**, Lin-Shiau SY, Lin JK. Comparative studies on the suppression of nitric oxide synthase by curcumin and its hydrogenated metabolites through down-regulation of IkappaB kinase and NFkappaB activation in macrophages. *Biochem Pharmacol* 2000; **60**: 1665-1676

7 **Zhang F**, Altorki NK, Mestre JR, Subbaramaiah K, Dannenberg AJ. Curcumin inhibits cyclooxygenase-2 transcription in bile acid- and phorbol ester-treated human gastrointestinal epithelial cells. *Carcinogenesis* 1999; **20**: 445-451

8 **Jobin C**, Bradham CA, Russo MP, Juma B, Narula AS, Brenner DA, Sartor RB. Curcumin blocks cytokine-mediated NF-kappa B activation and proinflammatory gene expression by inhibiting inhibitory factor I-kappa B kinase activity. *J Immunol* 1999; **163**: 3474-3483

9 **Singh S**, Aggarwal BB. Activation of transcription factor NF-kappa B is suppressed by curcumin (diferuloylmethane) [corrected] *J Biol Chem* 1995; **270**: 24995-25000

10 **Ruby AJ**, Kuttan G, Babu KD, Rajasekharan KN, Kuttan R. Anti-tumour and antioxidant activity of natural curcuminoids. *Cancer Lett* 1995; **94**: 79-83

11 **Aggarwal BB**, Kumar A, Bharti AC. Anticancer potential of curcumin: preclinical and clinical studies. *Anticancer Res* 2003; **23**: 363-398

12 **Jiang XL**, Cui HF. A new chronic ulcerative colitis model produced by combined methods in rats. *World J Gastroenterol* 2000; **6**: 742-746

13 **Fan H**, Qiu MY, Mei JJ, Shen GX, Liu SL, Chen R. Effects of four regulating-intestine prescriptions on pathology and ultrastructure of colon tissue in rats with ulcerative colitis. *World J Gastroenterol* 2005; **11**: 4800-4806

14 **Perner A**, Andresen L, Normark M, Fischer-Hansen B, Sørensen S, Eugen-Olsen J, Rask-Madsen J. Expression of nitric oxide synthases and effects of L-arginine and L-NMMA on nitric oxide production and fluid transport in collagenous colitis. *Gut* 2001; **49**: 387-394

15 **Mitra SK**, Venkataranganna MV, Sundaram R, Gopumadhavan S. Antioxidant activity of AO-8, a herbal formulation *in vitro* and *in vivo* experimental models. *Phytother Res* 1999; **13**: 300-303

16 **Dong WG**, Liu SP, Yu BP, Wu DF, Luo HS, Yu JP. Ameliorative effects of sodium ferulate on experimental colitis and their mechanisms in rats. *World J Gastroenterol* 2003; **9**: 2533-2538

17 **Ukil A**, Maity S, Karmakar S, Datta N, Vedasiromoni JR, Das PK. Curcumin, the major component of food flavour turmeric, reduces mucosal injury in trinitrobenzene sulphonic acid-induced colitis. *Br J Pharmacol* 2003; **139**: 209-218

18 **Monteleone G**, Mann J, Monteleone I, Vavassori P, Bremner R, Fantini M, Del Vecchio Blanco G, Tersigni R, Alessandroni L, Mann D, Pallone F, MacDonald TT. A failure of transforming growth factor-beta1 negative regulation maintains sustained NF-kappaB activation in gut inflammation. *J Biol Chem* 2004; **279**: 3925-3932

19 **Jian YT**, Mai GF, Wang JD, Zhang YL, Luo RC, Fang YX. Preventive and therapeutic effects of NF-kappaB inhibitor curcumin in rats colitis induced by trinitrobenzene sulfonic acid. *World J Gastroenterol* 2005; **11**: 1747-1752

S- Editor Liu Y **L- Editor** Ma JY **E- Editor** Ma WH

PO Box 2345, Beijing 100023, China
www.wjgnet.com
wjg@wjgnet.com

World J Gastroenterol 2007 February 21; 13(7): 1108-1111
World Journal of Gastroenterology ISSN 1007-9327

RAPID COMMUNICATION

Primary duodenal neoplasms: A retrospective clinico-pathological analysis

Amanjit Bal, Kusum Joshi, Kim Vaiphei, JD Wig

Amanjit Bal, Kusum Joshi, Kim Vaiphei, JD Wig, Departments of Histopathology and General Surgery, Post Graduate Institute of Medical Sciences and Research, Sector-12, Chandigarh 160012, India
Correspondence to: Dr. Amanjit Bal, MD, Assistant Professor, Department of Histopathology, Post Graduate Institute of Medical Sciences and Research, Chandigarh 160012, India. docaman5@hotmail.com
Telephone: +91-172-2755136
Received:2006-12-10 Accepted: 2007-01-29

Abstract

AIM: To analyze the clinico-pathological spectrum of primary duodenal neoplasms.

METHODS: A total of 55 primary duodenal neoplasms reported in the last 10 years after excluding ampullary and periampullary tumors were included in the study. Clinical details were noted and routine hematoxylin and eosin stained paraffin sections were studied for histological subtyping of the tumors.

RESULTS: On histopathological examination primary duodenal neoplasms were categorized as: epithelial tumor in 27 cases (49.0%) including 10 cases of adenoma, 15 cases of adenocarcinoma, and 2 cases of Brunner gland adenoma; mesenchymal tumor in 9 cases (16.3%) consisting of 4 cases of gastrointestinal stromal tumor, 4 cases of smooth muscle tumor and I case of neurofibroma; lymphoproliferative tumor in 12 cases (21.8%), and neuroendocrine tumor in 7 cases (12.7%).

CONCLUSION: Although non-ampullary/periampullary duodenal adenocarcinomas are rare, they constitute the largest group. Histopathological examination of primary duodenal tumors is important for correct histological subtyping.

Key words: Duodenum; Adenocarcinoma; Stromal tumor; Neuroendocrine tumor; Lymphoma

Bal A, Joshi K, Vaiphei K, Wig JD. Primary duodenal neoplasms: A retrospective clinico-pathological analysis. *World J Gastroenterol* 2007; 13(7): 1108-1111

http://www.wjgnet.com/1007-9327/13/1108.asp

INTRODUCTION

Although the small intestine constitutes 75% of the gastrointestinal tract, tumors arising from it are rare. Small intestine tumors account for about 5% of all alimentary tract tumors and the duodenum has a higher proportion of these tumors than the jejunum and ileum[1]. Duodenal carcinomas account for 20%-25% of all small bowel malignancies, whereas sarcomas, carcinoid and lymphomas are less common[2]. Duodenal tumors pose diagnostic difficulties because of their rarity, non-specific signs and symptoms and the fact that duodenum is usually overlooked during upper gastrointestinal endoscopy. The present study was undertaken to analyze the clinico-pathological spectrum of primary duodenal neoplasms reported in the last 10 years.

MATERIALS AND METHODS

A retrospective analysis of duodenal tumors retrieved from the Department of Histopathology, PGIMER, over a period of 10 years (1997-2006) was done. A total of 60 duodenal neoplasms after excluding 163 ampullary/periampullary carcinomas were retrieved from the records. All the clinical details like age, sex, presenting symptoms were noted from the patient record files. Relative laboratory and radiological findings were obtained. The specimens were fixed in buffered formalin and processed for paraffin sections. Routine hematoxylin and eosin-stained paraffin sections were studied for histological subtyping of the tumors. Histochemical stains like periodic acid Schiff (PAS), mucicarmine and immunohistochemical stains like c-kit, smooth muscle antigen (SMA), leukocyte common antigen (LCA), CD3, CD20, cytokeratin (CK) and chromogranin, were performed wherever required for exact categorization of the tumors.

RESULTS

Of the 60 duodenal neoplasms retrieved from records, 2 metastatic tumors and 3 with direct infiltration into duodenum from the subjacent site were excluded from the study. The study comprised of 55 cases of primary duodenal neoplasm. The age of the patients ranged from 7 to 70 years and the male to female ratio was 1.9:1. On histopathological examination primary duodenal neoplasms were categorized as: epithelial tumor, mesenchymal tumor, lymphoproliferative tumor, and neuroendocrine tumor (Table 1).

Table 1 Histopathological sub-classification of primary duodenal tumors (excluding ampullary and peri-ampullary tumors)

Pathological diagnosis	Cases *n* (%) *n* = 55
Epithelial tumors	27 (49.0)
Adenoma	10
Adenocarcinoma	15
Brunneroma	2
Mesenchymal tumors	9 (16.3)
GIST	4
Benign	1
Borderline	1
Malignant	2
Smooth muscle tumors	4
Leiomyoma	2
Leiomyosarcoma	2
Neurofibroma	1
Lymphoproliferative tumors	12 (21.8)
Non-Hodgkin's lymphoma	12
B-Cell lymphoma	10
T Cell lymphoma	2
Neuroendocrine tumors	7 (12.7)
Carcinoid	5
Gastrinoma	1
Neuroendocrine carcinoma	1

Epithelial tumor

There were 27 cases (49.0%) of epithelial tumor including 10 cases of adenoma, 15 cases of adenocarcinoma, and 2 cases of Brunner gland adenoma.

Adenoma: The age range of patients with adenoma was 10-60 years and the male to female ratio was 1:2.3. All adenomas were seen in D1-D2 portion of the duodenum and classified as flat adenoma in 1 case, tubular adenoma in 4 cases, tubulovillous adenoma in 3 cases (Figure 1A), and villous adenoma in 2 cases. Two cases were associated with multiple polyposis coli.

Adenocarcinoma: The age range of patients with adenocarcinoma was 38-70 years and the male to female ratio was 2:1. Of the 15 cases, 10 were found to have adenocarcinoma in D1-D2 portion of the duodenum and 5 were found to have adenocarcinoma in D3-D4 portion of the duodenum. Adenocarcinomas were sub-categorized as well-differentiated adenocarcinoma in 8 cases, moderately-differentiated adenocarcinoma in 2 cases, poorly-differentiated adenocarcinoma in 2 cases, and signet ring cell type adenocarcinoma in 3 cases. One adenocarcinoma was documented to be arising from pre-existing adenoma (Figure 1B).

Brunner gland adenoma: They were both seen in males and in D1 portion of the duodenum. The size of tumor ranged from 3 to 4 cm and microscopic examination showed lobules of Brunner glands separated by fibrovascular septa (Figure 1C).

Mesenchymal/stromal tumor

Nine cases (16.3%) were included in this group including 4 cases of gastrointestinal stromal tumor, 4 cases of smooth muscle tumor and 1 cases of neurofibroma. The age of the patients ranged from 32 to 70 years and the male to female ratio was 1.2:1.

Gastrointestinal stromal tumor (GIST): On pathological examination of 4 cases of GIST, 2 cases were diagnosed as malignant GIST based on the mitotic count of > 10/50HPF and tumor deposits in the omentum. One case was categorized as borderline GIST (5 cm in diameter) with its mitotic count of < 5/50HPF and one case was labeled as benign GIST (Figure 1D). All the cases were positive for c-kit immunostain and negative for SMA and S-100.

Smooth muscle tumor: Leiomyoma was found in 2 cases and leiomyosarcoma in 2 cases, respectively. Leiomyosarcoma showed high mitotic count of > 5/10HPF and areas of necrosis. All the tumors were positive for SMA and negative for c-kit.

Neural tumor: There was a single case of plexiform neurofibroma positive for S-100 immunostain.

Lymphoproliferative tumor

Twelve cases (21.8%) of non-Hodgkin's lymphoma (NHL) were included in this group (Figure 1E). Their age ranged from 7 to 85 years and the male to female ratio was 5:1. All the cases were found to have primary duodenal lymphoma because of the absence of disease in other organs. On immunohistological examination of 12 cases, B-cell phenotype was documented in 10 cases (83.3%) and T-cell phenotype in 2 cases (16.6%). B-cell lymphomas were further categorized as diffuse large cell lymphoma in 8 cases and MALT lymphoma in 2 cases. T-cell duodenal lymphomas were not associated with enteropathy as there was no histologic evidence of villous atrophy.

Neuroendocrine tumor

Seven tumors (12.7%) were located in this histologic category. Of the 7 tumors, 5 were benign and labeled as carcinoid based on their characteristic organoid pattern, granular cytoplasm, salt and pepper nuclear chromatin as well as chromogranin positivity (Figure 1F). One case was suggestive of gastrinoma based upon serum gastrin levels and was associated with parathyroid and adrenal hyperplasia. However, confirmation was not possible on histopathological sections because of non-availability of gastrin immunostain. One case was labeled as malignant as it had metastatic tumor deposits in lymph nodes.

DISCUSSION

Primary neoplasms of the small intestine constituting 90% of mucosal surface area of the gastrointestinal tract are extremely rare. Duodenum constituting only 4% of the small intestine has a relatively high proportion of all the tumors as compared to the jejunum and ileum. Primary malignant duodenal tumors are uncommon accounting for only 0.3% of all gastrointestinal tumors but about 50% of all small intestinal malignancies[3]. Many hypotheses have been proposed for the low incidence of small intestinal tumors as compared to large intestine including greater fluidity of contents in the small intestine which are less irritating as compared to solid contents, rapid transit

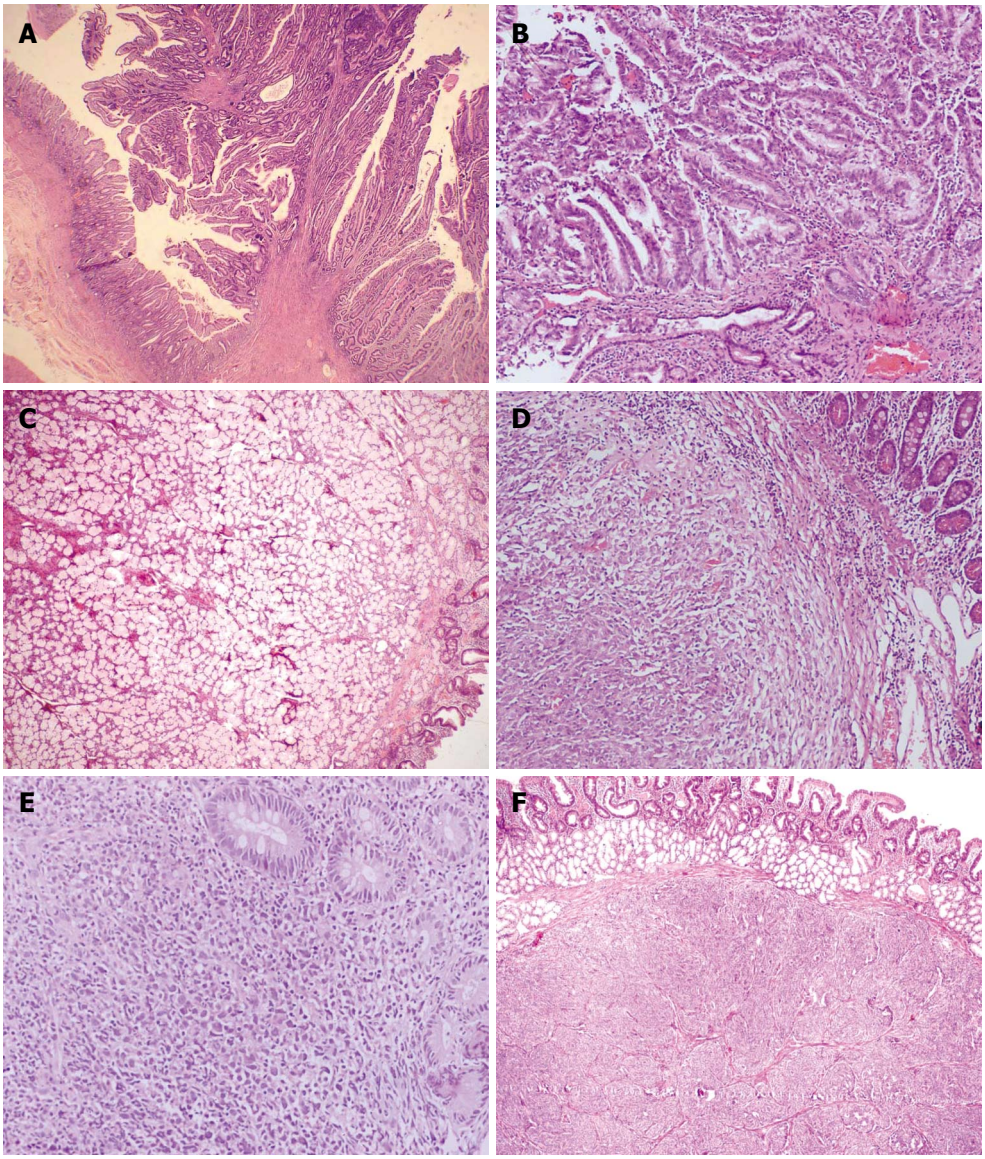

Figure1 Photomicrograph showing tubulovillous adenoma of the duodenum (**A**) (HE × 100), adenocarcinoma arising in tubulovillous adenoma of the duodenum (**B**) (HE × 200), Brunner glands separated by fibrovascular septa in Brunner gland adenoma of the duodenum (**C**) (HE × 40), spindle cell gastrointestinal stromal tumour in submucosa of the duodenum (**D**) (HE × 100), non-Hodgkin's lymphoma showing diffuse monotonus population of large cells infiltrating duodenal glands (**E**) (HE × 100), and circumscribed tumour nodule with tumour cells arranged in organoid pattern in carcinoid of the duodenum (**F**) (HE × 40).

time through small intestine thus reducing exposure to potential carcinogens, low bacterial population producing carcinogens and high concentration of lymphoid tissue producing IgA immunoglobulins[4]. It is often difficult to diagnose early duodenal tumors because of their non-specific and insidious presentation.

Adenomas are the most common duodenal tumors including adenomatous polyps and Brunner adenoma. Adenomatous polyps are more common at gastroduodenal junction and have 3%-5% risk of developing adenocarcinoma in life time[5]. Brunner gland adenomas are very rare tumors and less than 150 cases have been reported in the English literature[6]. Size of the tumor is important in differentiating adenoma from Brunner gland hyperplasia. The size less than 1 cm is referred to as Brunner gland hyperplasia. Adenocarcinoma of the duodenum not originating from the region of ampulla is an uncommon neoplasm. Since it was first described in 1746 by Hamburgur, approximately 800 cases have been described in the literature. However in these cases there is a mix of ampullary and peri-ampullary carcinomas[7]. Because of rarity of these tumors, the exact etiological factors have not been defined. Patients with familial adenomatous polyposis and Crohn's disease or celiac disease have a higher risk of developing duodenal carcinoma[8]. In the present study, there were no such associations. Only one case was arising in the background of adenoma and two cases of tubulovillous adenoma were associated with polyposis coli. Heniford *et al*[8] reported that D3-D4 is the most common site of primary duodenal adenocarcinoma. However, in the present study 10/15 adenocarcinomas were seen in D1-D2 region. D3-D4 carcinomas have better prognosis as compared to D1-D2 carcinomas because the former behave like hind gut tumors and the latter as foregut tumors[9].

The relative frequency of duodenal stromal tumors is not known. Only one study has presented a series of 190 duodenal stromal tumors[10]. According to their findings, gastrointestinal stromal tumors (GIST), the c-kit positive primary mesenchymal tumor, constitute the largest group of mesenchymal tumors in contrast to smooth muscle tumors i.e. leiomyoma and leiomyosarcoma which are now thought to be rare in the duodenum. In the present series, there were an equal number of GISTs and smooth muscle

tumors. However, the number of cases was too small to comment on the relative frequency of these tumors in duodenum. Neural tumors are extremely rare in duodenum and we encountered only one case of neurofibroma. Subclassification into benign, borderline and malignant stromal tumors based upon size, mitosis, necrosis and metastasis must be made for prognosis[11,12].

Gastrointestinal tract is the most common extranodal site of involvement by non-Hodgkin's lymphoma (NHL). Primary lymphomas of the small intestine are relatively rare and account for 4%-12% of all NHLs and 19%-38% of small bowel malignancies[13]. In the present study, duodenal lymphomas accounted for 21.8% all duodenal tumors. Recently reports have emerged about the increasing frequency of primary MALT lymphomas in the small intestine and it is proposed that small intestinal MALTs are of gastric origin due to the probable role of *H pylori*. In this review of duodenal tumors, only two cases were of MALT lymphomas, the remaining were of diffuse large B cell type and T cell lymphomas. It was reported that intestinal T cell lymphomas are more common in small intestine and a term "enteropathy associated T-cell lymphoma" (EATL) has been introduced based upon their existence in coelic disease[14]. However, no such association was seen in our cases. Histopathological examination and exact immunophenotyping of NHLs based on WHO classification are important from the prognosis point of view as T cell lymphomas have poor prognosis as compared to B cell lymphomas. MALT lymphomas in B cell group have a better prognosis.

Duodenal neuroendocrine tumors (NETs) comprise 2%-3% of all gastrointestinal endocrine tumors including gastrinoma, somatostatinoma, nonfunctional NET, and poorly-differentiated NE carcinoma and their frequency is increasing[15]. Although the majority of these tumors are nonfunctional, they can cause Zollinger-Ellison syndrome and other clinical hormonal syndromes. Gastrinomas defined as gastrin secreting tumors are associated with Zollinger-Ellison syndrome (ZES) and hereditary gastrinomas, which are associated with endocrine neoplasia type 1 (MEN1) syndrome. In the present study, there was only one case of gastrinoma associated with parathyroid and adrenal hyperplasia.

In conclusion, although non-ampullary/periampullary duodenal adenocarcinomas are rare, they constitute the largest group. Histopathological examination of primary duodenal tumors is important for the correct histological subtyping of these tumors and collecting prognostic information which influences the management.

REFERENCES

1 **Zollinger RM. Primary neoplasms of the small intestine.** *Am J Surg* 1986; **151**: 654-658
2 **Kaminski N**, Shaham D, Eliakim R. Primary tumours of the duodenum. *Postgrad Med J* 1993; **69**: 136-138
3 **Kerremans RP**, Lerut J, Penninckx FM. Primary malignant duodenal tumors. *Ann Surg* 1979; **190**: 179-182
4 **Negri E**, Bosetti C, La Vecchia C, Fioretti F, Conti E, Franceschi S. Risk factors for adenocarcinoma of the small intestine. *Int J Cancer* 1999; **82**: 171-174
5 **Ryder NM**, Ko CY, Hines OJ, Gloor B, Reber HA. Primary duodenal adenocarcinoma: a 40-year experience. *Arch Surg* 2000; **135**: 1070-1074; discussion 1074-1075
6 **Rocco A**, Borriello P, Compare D, De Colibus P, Pica L, Iacono A, Nardone G. Large Brunner's gland adenoma: case report and literature review. *World J Gastroenterol* 2006; **12**: 1966-1968
7 **Rose DM**, Hochwald SN, Klimstra DS, Brennan MF. Primary duodenal adenocarcinoma: a ten-year experience with 79 patients. *J Am Coll Surg* 1996; **183**: 89-96
8 **Heniford BT**, Iannitti DA, Evans P, Gagner M, Henderson JM. Primary nonampullary/periampullary adenocarcinoma of the duodenum. *Am Surg* 1998; **64**: 1165-1169
9 **Tocchi A**, Mazzoni G, Puma F, Miccini M, Cassini D, Bettelli E, Tagliacozzo S. Adenocarcinoma of the third and fourth portions of the duodenum: results of surgical treatment. *Arch Surg* 2003; **138**: 80-85
10 **Miettinen M**, Kopczynski J, Makhlouf HR, Sarlomo-Rikala M, Gyorffy H, Burke A, Sobin LH, Lasota J. Gastrointestinal stromal tumors, intramural leiomyomas, and leiomyosarcomas in the duodenum: a clinicopathologic, immunohistochemical, and molecular genetic study of 167 cases. *Am J Surg Pathol* 2003; **27**: 625-641
11 **Goldblum JR**, Appelman HD. Stromal tumors of the duodenum. A histologic and immunohistochemical study of 20 cases. *Am J Surg Pathol* 1995; **19**: 71-80
12 **Winfield RD**, Hochwald SN, Vogel SB, Hemming AW, Liu C, Cance WG, Grobmyer SR. Presentation and management of gastrointestinal stromal tumors of the duodenum. *Am Surg* 2006; **72**: 719-722; discussion 722-723
13 **Kohno S**, Ohshima K, Yoneda S, Kodama T, Shirakusa T, Kikuchi M. Clinicopathological analysis of 143 primary malignant lymphomas in the small and large intestines based on the new WHO classification. *Histopathology* 2003; **43**: 135-143
14 **Harris NL**, Jaffe ES, Stein H, Banks PM, Chan JK, Cleary ML, Delsol G, De Wolf-Peeters C, Falini B, Gatter KC. A revised European-American classification of lymphoid neoplasms: a proposal from the International Lymphoma Study Group. *Blood* 1994; **84**: 1361-1392
15 **Mullen JT**, Wang H, Yao JC, Lee JH, Perrier ND, Pisters PW, Lee JE, Evans DB. *Carcinoid tumors of the duodenum. Surgery* 2005; **138**: 971-977; discussion 977-978

S- Editor Liu Y **L- Editor** Wang XL **E- Editor** Ma WH

PO Box 2345, Beijing 100023, China
www.wjgnet.com
wjg@wjgnet.com

World J Gastroenterol 2007 February 21; 13(7): 1112-1118
World Journal of Gastroenterology ISSN 1007-9327

RAPID COMMUNICATION

Aqueous suspension of anise "*Pimpinella anisum*" protects rats against chemically induced gastric ulcers

Ibrahim A Al Mofleh, Abdulqader A Alhaider, Jaber S Mossa, Mohammed O Al-Soohaibani, Syed Rafatullah

Ibrahim A Al Mofleh, Department of Medicine, College of Medicine, King Saud University, Riyadh, Saudi Arabia
Abdulqader A Alhaider, Department of Pharmacology, College of Medicine, King Saud University, Riyadh, Saudi Arabia
Mohammed O Al-Sohaibani, Department of Pathology, College of Medicine, King Saud University, Riyadh, Saudi Arabia
Jaber S Mossa, Syed Rafatullah, Department of Pharmacognosy and Medicinal, Aromatic and Poisonous Plants Research Center, College of Pharmacy, King Saud University, Riyadh, Saudi Arabia
Supported by King AbdulAziz City for Science and Technology, Riyadh, Saudi Arabia, Spices Project No. AR-16-37
Correspondence to: Professor Ibrahim Abdulkarim Al Mofleh, College of Medicine, King Saud University, PO Box 2925 (59), Riyadh 11461, Saudi Arabia. iamofleh@yahoo.com
Telephone: +966-1-4671215 Fax: +966-1-4671217
Received: 2006-12-02 Accepted: 2007-01-23

Abstract

AIM: To substantiate the claims of Unani and Arabian traditional medicine practitioners on the gastroprotective potential effect of a popular spice anise, "*Pimpinella anisum* L." on experimentally-induced gastric ulceration and secretion in rats.

METHODS: Acute gastric ulceration in rats was produced by various noxious chemicals including 80% ethanol, 0.2 mol/L NaOH, 25% NaCl and indomethacin. Anti-secretory studies were undertaken using pylorus-ligated Shay rat technique. Levels of gastric non-protein sulfhydryls (NP-SH) and wall mucus were estimated and gastric tissue was also examined histologically. Anise aqueous suspension was used in two doses (250 and 500 mg/kg body weight) in all experiments.

RESULTS: Anise significantly inhibited gastric mucosal damage induced by necrotizing agents and indomethacin. The anti-ulcer effect was further confirmed histologically. In pylorus-ligated Shay rats, anise suspension significantly reduced the basal gastric acid secretion, acidity and completely inhibited the rumenal ulceration. On the other hand, the suspension significantly replenished ethanol-induced depleted levels of gastric mucosal NP-SH and gastric wall mucus concentration.

CONCLUSION: Anise aqueous suspension possesses significant cytoprotective and anti-ulcer activities against experimentally-induced gastric lesions. The anti-ulcer effect of anise is possibly prostaglandin-mediated and/or through its anti-secretory and antioxidative properties.

Key words: Spice; Anise; *Pimpinella anisum*; Cytoprotection; Gastric ulcer; Gastric secretion; Sulfhydryls; Gastric wall mucus

Al Mofleh IA, Alhaider AA, Mossa JS, Al-Sohaibani MO, Rafatullah S. Aqueous suspension of anise "*Pimpinella anisum*" protects rats against chemically induced gastric ulcers. *World J Gastroenterol* 2007; 13(7): 1112-1118

http://www.wjgnet.com/1007-9327/13/1112.asp

INTRODUCTION

Peptic ulcer is one of the most common gastrointestinal diseases. Nowadays proton pump inhibitors and H_2-recptor antagonists are the most widely used drugs to treat peptic ulcer disease. However, the use of these anti-secretory drugs may be associated with adverse events and ulcer relapse[1]. Thus, there is a need for more effective, less toxic and cost-effective anti-ulcer agents. In recent years, a widespread search has been launched to identify new anti-ulcer drugs from natural sources. Spices comprising the most important products used for flavouring foods and medicinal herbs are considered nowadays as potential bioactive agents that can interfere positively or negatively with different cellular processes. They are extensively used in medicine, pharmaceuticals, perfumery and cosmetics. Additionally they possess antioxidant, antispasmodic, carminative, anti-inflammatory and other properties[2]. A number of spices, namely large cardamom[3], black pepper[4], caraway[5], cardamom[6], clove[7], coriander[8], ginger[9], peppermint[10], saffron[11], turmeric[12] among others have been shown to possess significant gastroprotective activities. The fruits of anise plant, *pimpinella anisum* L. are locally known as aniseed and yansoon. The powder and concoction of anise in hot water are used as carminatives, antiseptics, diuretics, digestives, aphrodisiacs, and as a remedy for insomnia and constipation[13]. Furthermore, anise is used to promote digestion, improve appetite, alleviate cramps and nausea, and relieve flatulence and colic. In Unani and Arabian traditional medicine, anise fruit and its oil have been used for the treatment of various conditions including dyspepsia, nausea, abdominal colic,

seizures and epilepsy[14]. The phytotherapeutic applications of anise are based on its digestive, carminative, diuretic and expectorating action[15]. It has been recently reported that the essential oil of anise is highly effective as both larvicidal and ovicidal agents[16]. The principal constituents of anise are volatile oil, coumarins, fatty acids, flavonoid glycosides, proteins and carbohydrates. Among others, anise oil contains anethole and caryophyllene[17]. Since we have not come across a scientific report on potential gastroprotective claims of anise aqueous suspension, the present study was carried out to assess its effect on chemically induced gastric ulcers in rats.

MATERIALS AND METHODS

Plant material and preparation of aqueous suspension

Seeds of anise "*Pimpinella anisum* L" (family, Apiaceae) were purchased from local herb shops in Riyadh and identified by an expert taxonomist. The sample was preserved (voucher # Sp.Pr.17-16-37) at the herbarium of Department of Pharmacognosy, College of Pharmacy, King Saud University, Riyadh, for future reference. The seeds were ground to very fine powders (75 micron), and used as an aqueous suspension for treatment in different experiments.

Animals

Wistar albino rats of either sex, approximately at the same age, weighing 150-200 g were obtained from Animal Care Center, College of Pharmacy, King Saud University, and maintained under standard conditions of temperature, humidity and light (12 h dark, 12 h light) with free access to Purina chow and water. Before testing, the animals were fasted for 36 h with access to water *ad libitum*. The conduct of experiments and the procedure of sacrifice (using ether) were approved by the Ethics Committee of the Experimental Animal Care Society, College of Pharmacy, King Saud University, Riyadh, Saudi Arabia.

Dose selection and route of administration

The doses (250 and 500 mg/kg, body weight) selected for the experiments were based on the maximum tolerable dose value (MTD) (30 g/kg, body weight) and the preliminary experiments conducted on the pharmacological activity of anise. The aqueous suspension was administred intragastrically (i.g.) through gastric intubation in all experiments, unless stated otherwise intraperitoneally (i.p.) in anti-secretory studies.

Gastric lesions induced by necrotizing agents

The rats were administered ig 1 mL of different necrotizing agents (80% ethanol, 0.2 mol/L NaOH and 25% NaCl)[18]. Anise suspension was given 30 min before the administration of necrotizing agents. One hour after the administration of ethanol and alkalis, the rats were sacrificed and examined for lesions in the stomach. The scoring of lesions, assays of gastric wall mucus and sulfhydryls as well as histological changes in the stomach were observed as follows. The patchy lesions of stomach induced by ethanol were scored according to the method described by Schiantarelli *et al*[19] using the following scale: 0 = normal mucosa, 1 = hyperemic mucosa or up to 3 small patches, 2 = 4 to 10 small patches, 3 = more than 10 small or up to 3 medium-sized patches, 4 = 4 to 6 medium-seized patches, 5 = more than 6 medium-sized or up to 3 large patches, 6 = 4 to 6 large patches, 7 = 7 to 10 large patches, 8 = more than 10 large patches or extensive necrotic zones. "Small" was defined as up to 2 mm across (max. diameter), "medium-sized" between 2 and 4 mm across and "large" more than 4 mm across.

Histopathological evaluation

Gastric tissue samples were fixed in neutral buffered formalin for 24 h. Sections of gastric tissue were histopathologically examined to study the ulcerogenic and/or anti-ulcerogenic activity of anise. The tissues were fixed in 10% buffered formalin and processed using a VIP tissue processor. The processed tissues were embedded in paraffin blocks and sections of about 5 μm thickness were cut by employing an American optical rotary microtome. These sections were stained with haematoxylin and eosin using routine procedures[20]. The slides were examined microscopically for pathomorphological changes such as congestion, hemorrhage, edema and erosions using an arbitrary scale for severity assessment of these changes.

Gastric lesions induced by indomethacin

Indomethacin was suspended in 1.0% carboxy-methylcellulose (CMC) in water (6 mg/mL) and administered orally to the rats fasted for 36 h at a dose of 30 mg/kg, body weight. Control rats were treated similarly with an equivalent amount of the vehicle[21]. The animals were sacrificed 6 h after the treatment. Stomachs of the animals were excised off the body, rinsed with normal saline and studied accordingly [22].

Estimation of non-protein sulfhydryls

Gastric mucosal non-protein sulfhydryls (NP-SH) were measured according to the method of Sedlak and Lindsay[23]. The glandular part of the stomach was homogenized in ice-cold 0.02 mmol/L ethylenediam inetetraacetic acid (EDTA). Aliquots of 5 mL of the homogenates were mixed in 15 mL test tubes with 4 mL of distilled water and 1 mL of 50% trichloroacetic acid (TCA). The tubes were shaken intermittently for 10 min and centrifuged at 3000 *g*. Two milliliters of supernatant was mixed with 4 mL of 0.4 mol/L Tris buffer at pH 8.9, 0.1 mL of 5, 5'-dithio-bis- (2-nitrobenzoic acid) (DTNB) was added and the sample was shaken. The absorbance was measured within 5 min after addition of DTNB at 412 nm against a reagent blank.

Pylorus-ligated rats (anti-secretory studies)

The rats were fasted for 36 h with access to water *ad libitum* before the pylorus was ligated under ether anesthesia and care was taken to avoid bleeding and occlusion of blood vessels [24]. Anise suspension was administered immediately after pylorus ligation (Shay) by ip route. The rats were sacrificed at 6 h after the pylorus ligation. The stomachs were removed, with the contents collected, volumes measured, centrifuged and analyzed for titratable acidity

Table 1 Effect of aqueous anise suspension on gastric lesions induced by various necrotizing agents (mean ± SD)

Group serial	Treatment	Dose (mg/kg, i.g.)	Ulcer index		
			80% EtOH	0.2 mol/L NaOH	25% NaCl
1	Control (distilled water)	-	7.16 ± 0.40	8.00 ± 0.0	7.66 ± 0.33
2	*Pimpinella anisum*	250	6.00 ± 0.51[b]	4.66 ± 0.80[d]	6.00 ± 0.44[d]
3	*Pimpinella anisum*	500	4.00 ± 0.44[d]	3.66 ± 0.66[d]	4.00 ± 0.51[d]

Six rats were used in each group. [b]$P < 0.01$, [d]$P < 0.001$ *vs* control (distilled water) group, Student' *t*-test.

Table 2 Effect of aqueous anise suspension on ethanol-induced histopathological changes in rat stomach

Group serial	Treatment and dose (mg/kg, body weight/day)	Histopathological changes							
		Congestion	Haemorrhage	Edema	Necrosis	Inflammatory changes	Dysplastic changes	Erosions	Ulceration
1	Control (distilled water) (1 mL/rat)	-	-	-	-	-	-	-	-
2	Ethanol, 80% (1 mL/rat)	++	+++	++	++	+	+	+++	+
3	Pimpinella anisum (250) + ethanol, 80% (1 mL/rat)	+	+	+	-	-	-	+	-
4	Pimpinella anisum (500) + ethanol, 80% (1 mL/rat)	+	+	+	-	-	-	+	-

-: normal, +: moderate, ++: severe, +++: intensely severe.

against 0.01 mol/L NaOH (pH 7) and the titratable acidity was calculated.

Determination of gastric wall mucus

Gastric wall mucus was determined according to the modified procedure of Corne *et al*[25]. The glandular segment of the stomach was separated from the rumen of the stomach, weighed, and transferred immediately to 10 mL of 0.1% w/v Alcian blue solution (in 0.16 mmol/L sucrose solution buffered with 0.05 mL sodium acetate at pH 5). Tissue was stained for 2 h in Alcian blue, and excess dye was removed by two successive rinses with 10 mL of 0.25 mmol/L sucrose, first for 15 min and then for 45 min. Dye complexed with the gastric wall mucus was extracted with 10 mL of 0.5 mmol/L magnesium chloride which was intermittently shaken for 1 min at 30 min intervals for 2 h. Four milliliters of blue extract was then vigorously shaken with an equal volume of diethyl ether. The resulting emulsion was centrifuged at 4000 r/min for 10 min and the absorbance of aqueous layer was recorded at 580 nm. The quantity of Alcian blue extracted from per gram of wet glandular tissue was then calculated.

Statistical analysis

The readings shown are means ± SD. The mean determination of treatment groups was compared statistically with that of control group using *t*.

RESULTS

Effect of anise suspension on gastric lesions induced by necrotizing agents

The treatments of rats with 80% ethanol, 0.2mol/L NaOH and 25% NaCl produced extensive gastric lesions mainly confined to glandular part of the stomach in all the control (only necrotizing agents treated) animals. The ulcer index in ethanol, sodium hydroxide and sodium chloride treatment groups was 7.16 ± 0.40, 8.00 ± 0.0 and 7.66 ± 0.33, respectively. Pretreatment of rats with anise suspension at the dose of 250 mg/kg significantly prevented gastric mucosal lesions induced by all necrotizing agents used. The ulcer index was 6.00 ± 0.51 ($P < 0.01$), 4.66 ± 0.80 ($P < 0.001$), 6.00 ± 0.44 ($P < 0.001$), respectively. In stomach of rats treated with 500 mg/kg of anise suspension, the ulcer index was 4.00 ± 0.44 ($P < 0.001$), 3.66 ± 0.66 ($P < 0.001$) and 4.00 ± 0.51 ($P < 0.001$) in ethanol, sodium hydroxide and sodium chloride groups respectively (Table 1).

Effect of anise suspension on histopathological changes

Histological examination of gastric mucosa showed various histopathological changes including congestion, haemorrhage, edema, necrosis, inflammatory and dysplastic changes, erosions and ulcers in ethanol-treated rats. The histological indices such as necrosis, inflammatory and dysplastic changes and ulceration were completely inhibited in rats pretreated with both doses of anise suspension (Table 2).

Effect of anise suspension on gastric lesions induced by indomethacin

To study the anti-ulcerogenic effects of anise suspension on indomethacin-induced gastric lesions in rats, two does of anise were used (250 and 500 mg/kg). Data on ulcer index in rats pretreated with both doses are reported in Table 3. The increased ulcer index in the gastric mucosa of

Table 3 Effect of aqueous anise suspension on indomethacin-induced gastric mucosal lesions (mean ± SD)

Group serial	Treatment	Animals (*n*)	Dose (mg/kg, i.g.)	Ulcer index
1	Control (indo only)	6	-	32.16 ± 5.22
2	*Pimpinella anisum* + indo	6	250	9.66 ± 1.96[d]
3	*Pimpinella anisum* + indo	6	500	6.00 ± 2.68[d]

[d]$P < 0.001$ *vs* control (indo only) group. Indo: indomethacin.

Table 4 Effect of aqueous anise suspension on the levels of non-protein sulfhydryles (NP-SH) in glandular stomach of rats treated with 80% ethanol (mean ± SD)

Group serial	Treatment and dose (mg/kg, body weight)	NP-SH concentration (μmol/100 mg wet tissue)
1	Control (distilled water, 1 mL/rat)	11.70 ± 0.86
2	Control (80% ethanol, 1 mL/rat)	6.31 ± 0.23[b]
3	*Pimpinella anisum* (250) + 80% ethanol (1 mL/rat)	6.71 ± 0.33
4	*Pimpinella anisum* (500) + 80% ethanol (1 mL/rat)	7.68 ± 0.37[a]

Six rats were used in each group. [a]$P < 0.05$ *vs* control (80% ethanol) group, [b]$P < 0.01$ *vs* control (distilled water) group.

Table 5 Effect of anise suspension on gastric secretion, acidity and gastric lesion index in pylorus-ligated Shay rats (mean ± SD)

Group serial	Treatment	Dose (mg/kg, i.g)	Volume of gastric content (mL)	Titratable acid (mEq/L)	Ulcer index
1	Control (distilled water)	-	7.83 ± 0.38	127.21 ± 2.64	0.66 ± 0.21
2	*Pimpinella anisum*	250	3.00 ± 0.51[b]	109.33 ± 4.64[d]	0.00[d]
3	*Pimpinella anisum*	500	0.33 ± 0.33[d]	108.33 ± 5.00[d]	0.00[d]

Six rats were used in each group. [b]$P < 0.01$, [d]$P < 0.001$ *vs* control (distilled water) group.

Table 6 Effect of aqueous anise suspension on ethanol-induced gastric wall mucus concentration changes (mean ± SD)

Group serial	Treatment	Dosage (mg/kg,i.g.)	Gastric wall mucus (μg Alcian blue of wet glandular tissue)
1	Control (distilled water)	-	474.98 ± 13.86
2	80% ethanol only	-	307.92 ± 10.69[d]
3	*Pimpinella anisum* 80% ethanol	250	372.75 ± 20.87[a]
4	*Pimpinella anisum* 80% ethanol	500	391.60 ± 20.19[b]

[a]$P < 0.05$, [b]$P < 0.01$ *vs* 80% ethanol group only; [d]$P < 0.001$ *vs* control (distilled water) group.

indomethacin-treated rats (control) decreased significantly in animals treated with lower and higher anise doses (32.16 ± 5.22 *vs* 9.66 ± 1.96 and 6.00 ± 2.68, $P < 0.001$), respectively.

Effect of anise suspension on ethanol-induced mucosal NP-SH *depletion*

The level of NP-SH in the gastric mucosa of control rats was 11.70 ± 0.86 mmol/g of tissue, significantly decreased to 6.31 ± 0.23 mmol/g following the administration of ethanol. Pretreatment of rats with anise suspension at a higher dose (500 mg/kg) significantly replenished the ethanol-induced depletion of NP-SH ($P < 0.05$, Table 4).

Effect of anise suspension on gastric secretion in pylorus-ligated rats

In control rats, pylorus ligation for 6 h resulted in an accumulation of 7.83 ± 0.38 mL of gastric secretions, titratable acidity 127.21 ± 2.64 in mEq/L and an ulcer index 0.66 ± 0.33 (Table 5). The volume of gastric secretion in the rats treated with 250 and 500 mg/kg of anise suspension significantly reduced to 3.00 ± 0.51 and 0.33 ± 0.33 mL, respectively ($P < 0.001$). A significant decrease in titratable acid was also observed in the rats treated with 250 mg/kg (109.33 ± 4.64 mEq/L) and 500 mg/kg (108.33 ± 5.00 mEq/L) ($P < 0.001$). A complete inhibition of rumenal ulcers was noted in both groups of rats treated with anise suspension as compared to control group (Table 5).

Effect of anise suspension on ethanol-induced changes in gastric wall mucus

The treatment of rats with ethanol significantly decreased the Alcian blue binding capacity of gastric wall mucus (307.92 ± 10.69 μg Alcian blue/g of tissue) as compared to control rats (474.98 ± 13.86 μg/g). Pretreatment of rats with anise suspension at 250 mg/kg (372.75 ± 20.87 μg/g) and 500 mg/kg (391.60 ± 20.19 μg/g) significantly enhanced Alcian blue binding capacity of gastric mucosa ($P < 0.05$, $P < 0.01$), respectively (Table 6).

DISCUSSION

Anise spice is added to foods in several forms as whole spice, as ground spice or as isolates from its extracts and volatile oils[26]. We adopted the suspension dosage form in our experiments. In necrotizing agents-induced gastric ulcers, the lesions were characterized by multiple haemorrhage red bands of different sizes along the longitudinal axis of the glandular stomach. This model is extensively used to screen drugs for cytoprotection[27]. This study provided a substantial evidence for anti-ulcer and

anti-secretory effects of an aqueous suspension of anise. Anise suspension significantly inhibited the ulcerative lesions in all animals treated with necrotizing agents, which was further confirmed by histological findings in which necrosis, inflammatory, dysplastic changes and ulcers were abolished in rats pretreated with anise suspension. The ability of gastric mucosa to resist injury by endogenous secretions (acid, pepsin and bile) and ingested irritants (e.g., alcohol), can be attributed to a number of factors that have been referred to collectively as mucosal defense[28]. Gastric mucosal lesions induced by necrotizing agents such as ethanol and strong alkalis are due to depression of the gastric defensive mechanisms[29]. Although ethanol-induced ulcers are not inhibited by anti-secretory agents such as cimetidine, they are inhibited by agents that enhance mucosal defensive factors such as prostoglandins[30]. The current results suggest that the anti-ulcerogenic effect of anise suspension may be related to its cytoprotective activity.

Gastroduodenal ulceration is a major limitation to the use of non-steroidal anti-inflammatory drugs (NSAIDs)[31]. NSAIDs can cause damage to the gastroduodenal mucosa via several mechanisms, including their topical irritant effect on the epithelium, impairment of the mucosal barrier function, suppression of gastric prostaglandin synthesis, reduction of gastric mucosal blood flow and interference with the repair of superficial injury. The presence of acid in the lumen of stomach also contributes to the pathogenesis of NSAIDs-induced ulcers and bleeding by impairing the restitution process, interfering with haemostasis and inactivating several growth factors that are important in mucosal defence and repair[32,33]. In the present study, indomethacin-induced gastric lesions were extensively prevented by anise suspension.

Sulfhydryl compounds have been significantly implicated in the maintenance of gastric integrity, particularly when reactive oxygen species are involved in the pathophysiology of tissue damage[34]. Since anise suspension significantly enhances gastric tissue NP-SH concentration, it is conceivable that it is endowed with antioxidant properties accounting for its gastroprotective action. Hence, it may be presumed that the replenishing potential of sulfhydryl levels might play an important role in the gastroprotective activity of anise suspension-treated rats. Furthermore, the ability of anise suspension to protect against ulcers in NSAID-induced gastric damage may be due to the enhanced synthesis of mucus, bicarbonates and prostaglandins, as well as reduced acid output. Consequently these activities can promote the inhibition of basal gastric acid secretion as observed in our pylorus-ligated shay rat model[35,36]. On the other hand, it is also important to note that NSAIDs can increase gastric acid secretion, through prostaglandin inhibitory effects on parietal cells[37,38]. In the present study, anise aqueous suspension treatment significantly reduced basal gastric acid volume, titratable acidity and completely inhibited ulcer formation in rats. However, to date it is still controversial about relationship between the acid output and the genesis of acute gastric mucosal lesions (AGML). Our results support this correlation as anise suspension significantly reduced basal gastric secretion and prevented the occurrence of AGML in pylorus-ligated rats and thus, supporting the hypothesis of "no acid no ulcer" [39]. It has been postulated that histamine may be involved in the formation of pylorus-ligated ulcers and play a mediating role in the gastric secretion stimulated by gastrin, vagal stimulation, and cholinergic agents[40]. The correlation between gastric mucus and acid secretions in our experiments, clearly demonstrated that the gastric protective activity observed may be associated with correction or normalization of the altered balance between erosive action of acid and gastric mucosal defence. Gastric wall mucus is thought to play an important role as a defensive factor against gastric mucosal damage[41]. The determined gastric wall mucus is used as an indicator for gastric wall mucus secretion[42]. In the present investigation, anise suspension caused a significant enhancement of ethanol-induced gastric wall mucus depletion in rats, which further confirms the ability of anise to prevent and/or ameliorate the effects of damaging agents. These findings indicate that anise suspension preserves gastric mucus secretion and strengthens gastric mucosa defense factors in experimental rats[43,44].

The chemical constituents of anise responsible for its anti-ulcer activity are not known. However, chemical studies demonstrated that anise contains estrarole[45], anethol[46], eugenol[47], anisaldehyde, methylchanicol[48], coumarins[49] and terpenes[50] among others as the major compounds. Anise and its compounds have been identified as free radicals or active oxygen scavengers[51]. In addition, the ability of anise suspension to protect gastric mucosa against lesions induced by chemical irritants is likely by maintaining the structural integrity of gastric epithelium and balance of aggressive factors and inherent protective mechanisms[52]. Furthermore, the mucus gel and its bicarbonate gradient seem to be an important first-line defense against harmful stimuli [53].

In conclusion, anise suspension exhibits an anti-ulcer potential activity through at least one or more possible mechanisms including inhibition of basal gastric secretion, stimulation of mucus secretion, endogenous gastric mucosal prostaglandin synthesis and possible antioxidative activity.

REFERENCES

1 **Wolfe MM**, Sachs G. Acid suppression: optimizing therapy for gastroduodenal ulcer healing, gastroesophageal reflux disease, and stress-related erosive syndrome. *Gastroenterology* 2000; **118**: S9-S31

2 **Nalini N**, Sabitha K, Viswanathan P, Menon VP. Influence of spices on the bacterial (enzyme) activity in experimental colon cancer. *J Ethnopharmacol* 1998; **62**: 15-24

3 **Rafatullah S**, Galal AM, Al-Yahya MA, Al-Said MS. Gastric and duodenal antiulcer and cytoprotective effects of *Afromomum melegueta* in rats. *Int J Pharmacogn* 1995; **33**: 311-316

4 **Al-Mofleh IA**, Alhaider AA, Mossa JS, Al-Sohaibani MO, Rafatullah S, Qureshi S. Inhibition of gastric mucosal damage by *piper nigrum* (Black pepper). *Phcog Mag* 2005; **1**: 64-68

5 **Alhaider AA**, Al-Mofleh IA, Al-Sohaibani MO, Rafatullah S and Qureshi S. Effect of *Carum carvi* on experimentally induced gastric mucosal damage in wistar albino rats. *Intl J Pharmacol* 2006; **2**: 309-315

6 **Alhaider AA**, Al-Mofleh IA, Mossa JS, Al-Sohaibani MO, Qureshi S, Rafatullah S. Pharmacological and safety evaluation studies on "Cardamom" *Elettaria cardamomum*: An important ingredient of Gahwa (Arabian coffee). *Arab J Pharm Sci* 2005; **3**: 47-58

7 **Al-Mofleh IA**, Alhaider AA, Mossa JS, Al-Sohaibani MO, Qureshi S, Rafatullah S. Pharmacological studies on 'Clove' *Eugenia caryophyllata*. *Phcog Mag* 2005; **1**: 105-109

8 **Al-Mofleh IA**, Alhaider AA, Mossa JS, Al-Sohaibani MO, Rafatullah S, Qureshi S. Protection of gastric mucosal damage by *Coriandrum sativum* L. pretreatment in Wistar albino rats. *Environ Toxicol Pharmacol* 2006; **22**: 64-69

9 **al-Yahya MA**, Rafatullah S, Mossa JS, Ageel AM, Parmar NS, Tariq M. Gastroprotective activity of ginger zingiber officinale rosc., in albino rats. *Am J Chin Med* 1989; **17**: 51-56

10 **Al-Mofleh IA**, Alhaider AA, Mossa JS, Al-Sohaibani MO, Qureshi S, Rafatullah S. Antisecretagogue, antiulcer and cytoprotective effects of 'Peppermint' *Mentha piperita* L. in laboratory animals. *J Med Sci* 2006; **6**: 930-936

11 **Al-Mofleh IA**, Alhaider AA, Mossa JS, Al-Sohaibani MO, Qureshi S, Rafatullah S. Antigastric ulcer studies on "Saffron" *Crocus sativus* L. in rats. *Pakistan J Biol Sci* 2006; **9**: 1009-1013

12 **Rafatullah S**, Tariq M, Al-Yahya MA, Mossa JS, Ageel AM. Evaluation of turmeric (*Curcuma longa*) for gastric and duodenal antiulcer activity in rats. *J Ethnopharmacol* 1990; **29**: 25-34

13 **Kreydiyyeh SI**, Usta J, Knio K, Markossian S, Dagher S. Aniseed oil increases glucose absorption and reduces urine output in the rat. *Life Sci* 2003; **74**: 663-673

14 **Said HM**, Saeed A, D'Silva LA, Zubairy HN, Bano Z. Medicinal herbal: A textbook for medical students and doctors. Pakistan: Hamdard Foundation Pakistan, 1996: 1-82

15 **Besharati-Seidani A**, Jabbari A, Yamini Y. Headspace solvent microextraction: a very rapid method for identification of volatile components of Iranian *Pimpinella anisum* seed. *Anal Chim Acta* 2005; **530**: 155-161

16 **Prajapati V**, Tripathi AK, Aggarwal KK, Khanuja SP. Insecticidal, repellent and oviposition-deterrent activity of selected essential oils against Anopheles stephensi, Aedes aegypti and Culex quinquefasciatus. *Bioresour Technol* 2005; **96**: 1749-1757

17 **Leung AY**. Encyclopedia of common natural ingredients used in food, drugs and cosmetics. New York: John Wiley and Sons Inc, 1980: 409

18 **Robert A**, Nezamis JE, Lancaster C, Davis JP, Field SO, Hanchar AJ. Mild irritants prevent gastric necrosis through "adaptive cytoprotection" mediated by prostaglandins. *Am J Physiol* 1983; **245**: G113-G121

19 **Schiantarelli P**, Cadel S, Folco GC. Gastroprotective effects of morniflumate, an esterified anti-inflammatory drug. *Arzneimittelforschung* 1984; **34**: 885-890

20 **Culling CFA**. Handbook of Histopathological and Histochemical Techniques. 3rd ed. London: Butterworth and Company, 1974: 126-159

21 **Bhargava KP**, Gupta MB, Tangri KK. Mechanism of ulcerogenic activity of indomethacin and oxyphenbutazone. *Eur J Pharmacol* 1973; **22**: 191-195

22 **Szabo S**, Trier JS, Brown A, Schnoor J, Homan HD, Bradford JC. A quantitative method for assessing the extent of experimental gastric erosions and ulcers. *J Pharmacol Methods* 1985; **13**: 59-66

23 **Sedlak J**, Lindsay RH. Estimation of total, protein-bound, and nonprotein sulfhydryl groups in tissue with Ellman's reagent. *Anal Biochem* 1968; **25**: 192-205

24 **Shay H**, Komarov SA, Fels SS, Meranza D, Grunstein M, Siplet H. A simple method for uniform production of gastric ulceration in rat. *Gastroenterology* 1945; **5**: 43-61

25 **Corne SJ**, Morrissey SM, Woods RJ. Proceedings: A method for the quantitative estimation of gastric barrier mucus. *J Physiol* 1974; **242**: 116P-117P

26 **Suhaj M**. Spice antioxidants isolation and their antiradical activity: a review. *J Food Compos Anal* 2006; **19**: 531-537

27 **Robert A**, Nezamis JE, Lancaster C, Hanchar AJ. Cytoprotection by prostaglandins in rats. Prevention of gastric necrosis produced by alcohol, HCl, NaOH, hypertonic NaCl, and thermal injury. *Gastroenterology* 1979; **77**: 433-443

28 **Wallace JL**. Pathogenesis of NSAID-induced gastroduodenal mucosal injury. *Best Pract Res Clin Gastroenterol* 2001; **15**: 691-703

29 **Kinoshita M**, Noto T, Tamaki H. Effect of a combination of ecabet sodium and cimetidine on experimentally induced gastric lesions and gastric mucosal resistance to ulcerogenic agents in rats. *Biol Pharm Bull* 1995; **18**: 223-226

30 **Morimoto Y**, Shimohara K, Oshima S, Sukamoto T. Effects of the new anti-ulcer agent KB-5492 on experimental gastric mucosal lesions and gastric mucosal defensive factors, as compared to those of teprenone and cimetidine. *Jpn J Pharmacol* 1991; **57**: 495-505

31 **Wallace JL**. How do NSAIDs cause ulcer disease? *Baillieres Best Pract Res Clin Gastroenterol* 2000; **14**: 147-159

32 **Toma W**, Hiruma-Lima CA, Guerrero RO, Brito AR. Preliminary studies of Mammea americana L. (Guttiferae) bark/latex extract point to an effective antiulcer effect on gastric ulcer models in mice. *Phytomedicine* 2005; **12**: 345-350

33 **Whittle BJ**. Gastrointestinal effects of nonsteroidal anti-inflammatory drugs. *Fundam Clin Pharmacol* 2003; **17**: 301-313

34 **Blandizzi C**, Fornai M, Colucci R, Natale G, Lubrano V, Vassalle C, Antonioli L, Lazzeri G, Del Tacca M. Lansoprazole prevents experimental gastric injury induced by non-steroidal anti-inflammatory drugs through a reduction of mucosal oxidative damage. *World J Gastroenterol* 2005; **11**: 4052-4060

35 **Kimura M**, Goto S, Ihara Y, Wada A, Yahiro K, Niidome T, Aoyagi H, Hirayama T, Kondo T. Impairment of glutathione metabolism in human gastric epithelial cells treated with vacuolating cytotoxin from *Helicobacter pylori*. *Microb Pathog* 2001; **31**: 29-36

36 **Loguercio C**, Romano M, Di Sapio M, Nardi G, Taranto D, Grella A, Del Vecchio Blanco C. Regional variations in total and nonprotein sulfhydryl compounds in the human gastric mucosa and effects of ethanol. *Scand J Gastroenterol* 1991; **26**: 1042-1048

37 **Ligumsky M**, Goto Y, Debas H, Yamada T. Prostaglandins mediate inhibition of gastric acid secretion by somatostatin in the rat. *Science* 1983; **219**: 301-303

38 **Soll AH**. Mechanisms of action of antisecretory drugs. Studies on isolated canine fundic mucosal cells. *Scand J Gastroenterol Suppl* 1986; **125**: 1-8

39 **Melo JR**, de Araújo GK, da Luz MM, da Conceição SA, Lisboa FA, Moraes-Santos T, Cunha-Melo JR. Effect of acid secretion blockade on acute gastric mucosal lesions induced by Tityus serrulatus scorpion toxin in anaesthetized rats. *Toxicon* 2006; **48**: 543-549

40 **Blandizzi C**, Mengozzi G, Intorre L, Natale G, Soldani G, Del Tacca M. Inhibitory cholinergic effects of esaprazole on gastric secretion and plasma gastrin levels in the dog. *Pharmacology* 1993; **46**: 231-240

41 **Marhuenda E**, Martin MJ, De La Alarcon Lastra C. Antiulcerogenic acitivity of aescine in different experimental models. *Phytother Res* 1993; **7**: 13-16

42 **Mersereau WA**, Hinchey EJ. Role of gastric mucosal folds in formation of focal ulcers in the rat. *Surgery* 1982; **91**: 150-155

43 **Lukie BE**, Forstner GG. Synthesis of intestinal clycoproteins. Inhibition of (I- 14 C)glucosamine incorporation by sodium salicylate *in vitro*. *Biochim Biophys Acta* 1972; **273**: 380-388

44 **Davenport HW**. Destruction of the gastric mucosal barrier by detergents and urea. *Gastroenterology* 1968; **54**: 175-181

45 **Zargari A**. Medicinal plants. Tehran, Iran: Tehran University Press, 1989: 519-521

46 **Andarwulan N**, Shetty K. Phenolic content in differentiated tissue cultures of untransformed and Agrobacterium-transformed roots of anise (Pimpinella anisum L.). *J Agric Food Chem* 1999; **47**: 1776-1780

47 **Monod C**, Dortan D. Eugenol in anise oil. *Chem abstr* 1950; **45**: 3124A

48 **Reichling J**, Kemmerer B, Sauer-Gürth H. Biosynthesis of pseudoisoeugenols in tissue cultures of Pimpinella anisum. Phenylalanine ammonia lyase and cinnamic acid 4-hydroxylase activities. *Pharm World Sci* 1995; **17**: 113-119
49 **Kartnig V**, Moeckel H, Maunz B. The occurrence of cumarins and sterols in tissue-cultures of roots of Anethum graveolens and Pimpinella anisum (author's transl). *Planta Med* 1975; **27**: 1-13
50 **Burkhardt G**, Reichling J, Martin R, Becker H. Terpene hydrocarbons in Pimpinella anisum L. *Pharm Weekbl Sci* 1986; **8**: 190-193
51 **Gülçin İ**, Oktay M, Kireçci E, Küfrevioğlü Öİ. Screening of antioxidant and antimicrobial activities of anise (*Pimpinella anisum* L.) seed extracts. *Food Chem* 2003; **83**: 371-382
52 **Hills BA**, Butler BD, Lichtenberger LM. Gastric mucosal barrier: hydrophobic lining to the lumen of the stomach. *Am J Physiol* 1983; **244**: G561-G568
53 **Allen A**, Garner A. Mucus and bicarbonate secretion in the stomach and their possible role in mucosal protection. *Gut* 1980; **21**: 249-262

S- Editor Liu Y **L- Editor** Wang XL **E- Editor** Ma WH

PO Box 2345, Beijing 100023, China
www.wjgnet.com
wjg@wjgnet.com

World J Gastroenterol 2007 February 21; 13(7): 1119-1122
World Journal of Gastroenterology ISSN 1007-9327

RAPID COMMUNICATION

H pylori are associated with chronic cholecystitis

Dong-Feng Chen, Lu Hu, Ping Yi, Wei-Wen Liu, Dian-Chun Fang, Hong Cao

Dong-Feng Chen, Lu Hu, Ping Yi, Wei-Wen Liu, Dian-Chun Fang, Hong Cao, Department of Gastroenterology, Daping Hospital,Third Military Medical University, Chongqing 400042, China
Supported by the National Natural Science Foundation of China, No. 39970039
Correspondence to: Dr. Dong-Feng Chen, Department of Gastroenterology, Research Institute of Surgery, Daping Hospital, Third Military Medical University, Chongqing 400042, China. dfchen9@hotmail.com
Telephone: +86-23-68757362 Fax: +86-23-68813806
Received: 2005-08-05 Accepted: 2007-01-23

Abstract

AIM: To study whether *H pylori* are associated with chronic cholecystitis.

METHODS: The subjects were divided into three groups: *H pylori*-infected cholecystitis group, *H pylori*-negative cholecystitis group and control group. Pathologic changes of the gallbladder were observed by optic and electronic microscopes and the levels of interleukin-1, 6 and 8 (IL-1, 6 and 8) were detected by radioimmunoassay.

RESULTS: Histological evidence of chronic cholecystitis including degeneration, necrosis, inflammatory cell infiltration, were found in the region where *H pylori* colonized. Levels of IL-1, 6 and 8 in gallbladder mucosa homogenates were significantly higher in *H pylori*-infected cholecystitis group than those in *H pylori*-negative cholecystitis group and control group.

CONCLUSION: *H pylori* infection may be related to cholecystitis.

Key words: *H pylori*; Chronic cholecystitis; Interleukin; Colonization; Gallbladder mucosa

Chen DF, Hu L, Yi P, Liu WW, Fang DC, Cao H. *H pylori* are associated with chronic cholecystitis. *World J Gastroenterol* 2007; 13(7): 1119-1122

http://www.wjgnet.com/1007-9327/13/1119.asp

INTRODUCTION

H pylori have definite pathogenic action and related to gastritis, peptic ulcer and gastric carcinoma[1-3]. Previous studies have demonstrated that *H pylori* correlate with diseases of the extra-gastrointestine, the liver and the cholecyst[4-8]. We have isolated *H pylori* from the gallbladder and cultured *H pylori*, and preliminarily proved that there exist live *H pylori* in the gallbladder. In the present study, we carried out electron microscopic observation and immunohistochemistry to the relationship between *H pylori* and chronic cholecystitis.

MATERIALS AND METHODS

Subjects

A total of 81 cases with chronic cholecystitis were divided into *H pylori*-negative group (n = 59) and *H pylori*-infected group (n = 22), based on previous studies, PCR amplification and culture results for *H pylori*. Besides, a control group was used including another 20 cases who were proved to have no obvious inflammation in the gallbladder mucosa except polyps or *H pylori* infection after a cholecystectomy due to a gallbladder polyp.

Investigation of gastric mucosa metaplasia of epithelial cells of gallbladder mucosa

By histochemical staining of AB/PAS mucus, and based on histology of mucosal epithelial cells and characteristics of cells secreting mucus, an observation was made on gastric mucosa metaplasia of epithelial cells of gallbladder mucosa and colonization of *H pylori* in the epithelial cells of gallbladder mucosa. The relationship between *H pylori* and the epithelial cells of the gallbladder was observed by optic microscopy, W-S silver stain and immunohistochemical stain using anti-*H pylori* antibodies. The resected gallbladder specimens from cases with chronic cholecystitis were immobilized with 3% glutaral, embedded and sliced for transmission electron microscopic investigation.

Relationship between H pylori and cholecystitis

Inflammatory changes of epithelial cells of the gallbladder mucosa in regions where *H pylori* colonized were observed by optic microscopy and ultrastructural changes of epithelial cells of the gallbladder were observed by electron microscopy.

Assay of interleukins in homogenates of gallbladder mucosa

The radio-immune analytical reagent kits including IL-1, IL-6 and IL-8 were purchased from Dongya Research Institute of Biotechnology, Beijing. About 1 g of resected

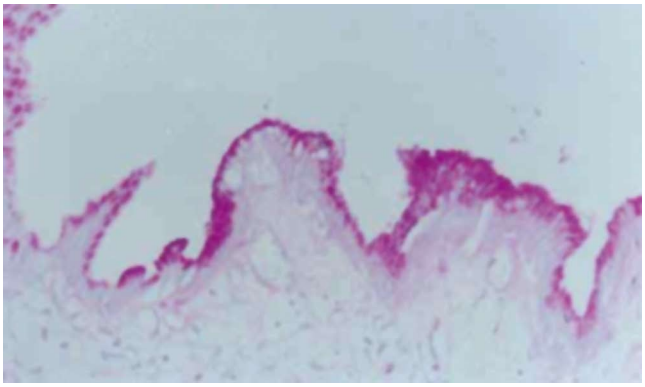

Figure 1 Specimens of chronic cholecystitis. Many positive PAS materials appear in epithelial cells of gallbladder mucosa (PAS × 200).

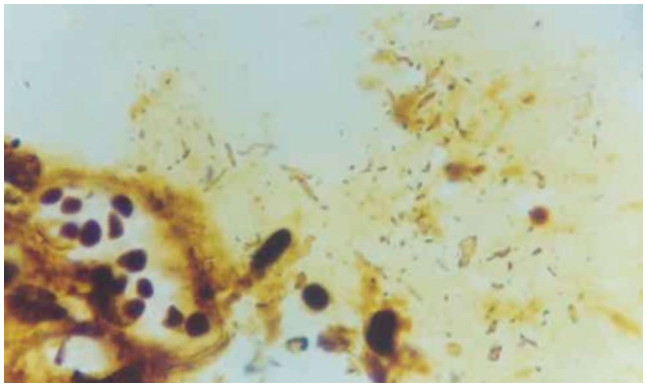

Figure 2 Helicobacter-like bacteria and inflammatory cells in mucus on gallbladder mucosa (WS × 200).

Table 1 Gastric metaplasia of gallbladder mucosa in cases with chronic cholecystitis

Group	*n*	Gastric metaplasia positive (*n*)	Gastric metaplasia negative (*n*)
Control	20	0	20
Chronic cholecystitis			
Positive *H pylori*	22	18	4
Negative *H pylori*	59	7	52

gallbladder mucosa was added into ultrapure water (Center of Molecular Biology, Research Institute of Surgery, Daping Hospital, Third Military Medical University, Chongqing) and homogenized in an IS-l homogenizer (Medical Machine Factory, Zhejiang) and the homogenates were centrifuged at 4000 r/min for l5 min, after which the supernatants were collected and frozen at -70℃. The EC-l200 radio-immune auto-γ counting device (Zhongjia Corporation of ChinaAcademy of Sciences) was employed for radio-immune assay and a fully automatic biochemical assay device of Beckman Synchron CX (USA) was used for quantification of proteins of gallbladder mucosa homogenates.

Statistical analysis

Data were expressed as mean ± SD and processed with Chi-square test and Student's t-test. $P < 0.05$ was considered significant.

RESULTS

Metaplasia of gastric mucosa in gallbladder

In cases with a gallbladder polyp, no mucus stained positive for PAS was found in gallbladder mucosa in the region beyond the polyp, nor was positive substance of PAS, i.e., metaplasia of gastric mucosa, found in epithelial cells of mucosa. In cases with chronic lithic cholecystitis, the epithelium of gallbladder mucosa was column-like. AB/PAS stain showed that neutral mucus was positive, with metaplasia of epithelial cells of gastric mucosa (Figure 1).

Gastric metaplasia of gallbladder mucosa appeared in 25 cases, accounting for 30.86% (25/81) of all cases with chronic cholecystitis, however, it was not found in the control group (Table 1). This suggested that gallbladder mucosa was apt to gastric metaplasia in cases with chronic lithiasis cholecystitis, especially in those with *H pylori* infection in the gallbladder, of gastric metaplasia of gallbladder mucosa (18/22, 81.82%) was significantly higher than that in cases with negative *H pylori* (7/59, 11.86%, $P < 0.01$). It indicated that gastric metaplasia of gallbladder mucosa might relate to *H pylori* infection in the gallbladder.

Colonization of H pylori in gallbladder and its relation to cholecystitis

The optic microscopy showed that *H pylori* were scattered or aggregated on, or located within certain distance from the epithelial cells of gallbladder mucosa and that individual *H pylori* distributed inside epithelial cells or existed in intercellular space. At the regions with *H pylori,* column-like cells secreted neutral mucus by AB/PAS stain, indicating that the gallbladder mucosa had gastric metaplasia and that gastric mucosa were absent in some regions where *H pylori* located. Electron microscopy showed that *H pylori* were located on, stuck to, or entered the epithelial cells of gallbladder mucosa, where, however, no tight junction or adhesiveness could be seen. Moreover, optic microscopy revealed degeneration of the epithelial cells of gallbladder mucosa, infiltration and exudation of inflammatory cells, exfoliation of the epithelial cells, or chronic inflammation such as mucous layer shrinkage, decrease or even disappearance of epithelial cells and glands at sites where *H pylori* were present. Sometimes, there could be seen that inflammatory cells aggregated around *H pylori* and the latter were swallowed (Figure 2). On the other hand, only a few inflammatory cells infiltrated the mucosa, with intact epithelial cells, in most cases with chronic cholecystitis without *H pylori* infection. Exceptionally, even in these cases, there emerged acute inflammatory manifestations including infiltration of large numbers of inflammatory cells, degeneration, apoptosis and exudation of epithelial cells or chronic inflammatory manifestations including atrophy of glands. In the gallbladder epithelial cells that were proved to have

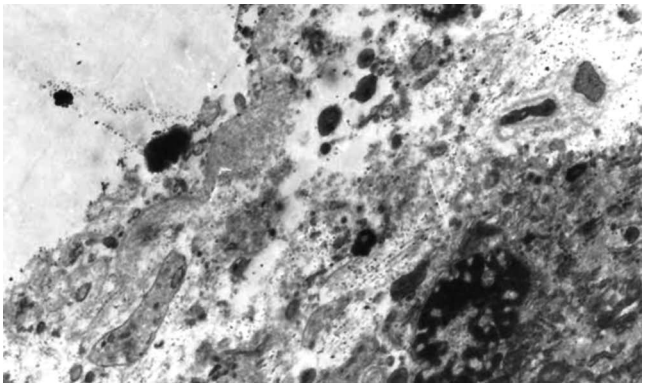

Figure 3 Electron microscopic images of *H pylori* on the epithelial cells of gallbladder (× 6000).

H pylori infection by electron microscopy, changes such as destructed epithelial cell membranes, loose cellular connection, dilatation of mitochondria, decrease or disappearance of crest, and dilatation of endoplasmic reticulum could be seen, which were severer compared with those without *H pylori* infection (Figure 3). The levels of IL-l, IL-6 and IL-8 of gallbladder mucosa homogenates were expressed as ng/g protein, and are shown in Table 2.

In cases with chronic cholecystitis, the levels of IL-l, IL-6 and IL-8 in gallbladders in both negative *H pylori* group and positive *H pylori* group were significantly higher than those in control group ($P < 0.01$). Moreover, there was a significant difference between positive *H pylori* group and negative *H pylori* group in levels of IL-1, IL-6 and IL-8 in the gallbladder ($P < 0.01$).

Table 2 Levels of IL-l, IL-6 and IL-8 of gallbladder mucosa homogenates (ng/g protein)

Groups	*n*	IL-1	IL-6	IL-8
Control	20	21.65 ± 4.28	77.10 ± 10.56	101.35 ± 19.39
Chronic cholecystitis				
Negative *H pylori*	59	68.76 ± 15.08[b]	159.54 ± 37.65[b]	152.10 ± 46.57
Positive *H pylori*	22	142.68 ± 25.41[b,d]	241.50 ± 80.60[b,d]	593.18 ± 93.59[b,d]

[b]$P < 0.01$ *vs* control group; [d]$P < 0.01$ *vs* negative *H pylori* group.

DISCUSSION

The gallbladder and stomach are originated from endoblasts and have similar tissue structures, with the mucosa covered with a slime layer [9-11]. AB/PAS stain showed that the epithelial cells of gallbladder mucosa secreted neutral mucus, with gastric metaplasia, in about 31% (25/81) of cases with cholecystolithiasis. Caselli *et al*[12-14] also demonstrated that the epithelial cells of gallbladder mucosa had gastric metaplasia in cases with cholecystolithiasis. Roa *et al*[15,16] found that pepsinogen I , Ⅱ were expressed in the epithelial cells of the gallbladder. The significance of gastric metaplasia of gallbladder mucosa lies in that the gastric metaplasia provides conditions for *H pylori* colonization in the gallbladder. The results of our study showed that compared with cases without *H pylori* infection in the gallbladder, there was a significantly higher incidence rate of gastric metaplasia in epithelial cells of gallbladder mucosa in cases with *H pylori* infection. It also proved that the gastric metaplasia of gallbladder mucosa closely correlated with *H pylori* infection in the gallbladder. Nevertheless, there were cases with *H pylori* infection but without gastric metaplasia in the gallbladder; meanwhile, there were cases with gastric metaplasia but without *H pylori* infection. These findings indicate that there is no absolute causality between gastric metaplasia and *H pylori* infection in the gallbladder. We hypothesize that many epithelial cells of the gastrointestinal tract have receptors for *H pylori* colonization factors. Therefore, *H pylori* can colonize on the epithelial cells of the gallbladder mucosa with no gastric metaplasia[17].

We also found that *H pylori* were separated from or adhered to the epithelial cells of gallbladder mucosa and that some *H pylori* penetrated through epithelial cells of the gallbladder. It that *H pylori* had a weak ability to pass through cells. At sites where *H pylori* aggregated, the epithelial cells of gallbladder mucosa were degenerated, erosive and even apoptotic. In some parts, inflammatory cells infiltrated, which became more obvious with increases in the number of *H pylori*. Electron microscopy revealed that at sites infected with *H pylori*, the integrity of the cell membrane of epithelial cells was destructed, with swelling of mitochondria and dilatation of endoplasmic reticulum. It showed that colonization of *H pylori* in the gallbladder cause inflammation of the gallbladder, mainly chronic nonsuppurative inflammation, which in turn provides an important condition for *H pylori* as one of the etiological factors leading to cholecystitis. Damage of the epithelial cells of gallbladder mucosa caused by *H pylori* may relate to specific virulence factors of *H pylori* such as cytotoxin-associated protein (CagA) and vacuoles toxin (VacA) , as well as urease, lipopolysaccharides and mucus enzyme of *H pylori*[18].

H pylori can also damage the epithelial cells of gallbladder mucosa through mediating inflammation and immunoreaction. The levels of IL-l, IL-6 and IL-8 in gallbladder mucosa homogenates in both *H pylori* negative and positive groups were significantly higher than those in control group ($P < 0.01$). It indicates that chronic lithic cholecystitis is associated with these three cytokines. We also found that in cholecystitis specimens with or without *H pylori* infection, levels of IL-1, IL-6 and IL-8 were significantly higher than those in control group, indicating that these interleukins may participate in pathogenesis of chronic cholecystitis. This may accord with the function of IL in *H pylori*-related gastritis and gastric ulcer[19,20]. After infection with *H pylori*, the urease, lipase and heat shock proteins secreted by *H pylori* can activate regional epithelial cells of mucosa and vascular endothelial cells expressing IL-1, IL-6 and other cytokines such as ICAM-I, hence stimulating and chemotaxy intravascular lymphocytes and monocytes to shift to *H pylori*-infected sites. IL-6 can activate and induce differentiation of T cells through other cytokines and enhance the function of

monocytes and NK cells, resulting in inflammation and injury at sites infected with *H pylori*. Our study verified that CagA of *H pylori* exerted strong action in stimulating epithelial cells and other cells expressing IL-8, which can activate and chemotactic neutrophils and lymphocytes[21]. In cases with chronic cholecystitis infected with *H pylori*, levels of IL-1, IL-6 and IL-8 of gallbladder mucosa were significantly higher than those in cases without *H pylori* infection. It suggests that *H pylori* participate in and aggravate cholecystitis, destruction of epithelial cells of the gallbladder and atrophy of the gallbladder[22]. Taken together, our study indicates that *H pylori* infection in the gallbladder may be one of the etiological factors leading to cholecystitis. The precise mechanism requires further verifications.

REFERENCES

1 **Tsuji S**, Kawano S. Peptic ulcer recurrence and Helicobacter pylori: evidence from Japan. *J Gastroenterol* 2003; **38**: 410-411

2 **Apostolov E**, Al-Soud WA, Nilsson I, Kornilovska I, Usenko V, Lyzogubov V, Gaydar Y, Wadström T, Ljungh A. Helicobacter pylori and other Helicobacter species in gallbladder and liver of patients with chronic cholecystitis detected by immunological and molecular methods. *Scand J Gastroenterol* 2005; **40**: 96-102

3 **Guo XL**, Wang LE, Du SY, Fan CL, Li L, Wang P, Yuan Y. Association of cyclooxygenase-2 expression with Hp-cagA infection in gastric cancer. *World J Gastroenterol* 2003; **9**: 246-249

4 **Ohara T**, Kanoh Y, Higuchi K, Arakawa T, Morisita T. Eradication therapy of Helicobacter pylori directly induces apoptosis in inflammation-related immunocytes in the gastric mucosa--possible mechanism for cure of peptic ulcer disease and MALT lymphoma with a low-grade malignancy. *Hepatogastroenterology* 2003; **50**: 607-609

5 **Gibbons AH**. Helicobacter pylori: a clinician's view. *Hosp Med* 2003; **64**: 535-538

6 **D'Elios MM**, Amedei A, Del Prete G. Helicobacter pylori antigen-specific T-cell responses at gastric level in chronic gastritis, peptic ulcer, gastric cancer and low-grade mucosa-associated lymphoid tissue (MALT) lymphoma. *Microbes Infect* 2003; **5**: 723-730

7 **Konturek PC**, Brzozowski T, Konturek SJ, Kwiecień S, Pajdo R, Drozdowicz D, Stachura J, Karczewska E, Hahn EG. Functional and morphological aspects of Helicobacter pylori-induced gastric cancer in Mongolian gerbils. *Eur J Gastroenterol Hepatol* 2003; **15**: 745-754

8 **Randi G**, Franceschi S, La Vecchia C. Gallbladder cancer worldwide: geographical distribution and risk factors. *Int J Cancer* 2006; **118**: 1591-1602

9 **Tsukanov VV**, Grishchenko NN. Association of Helicobacter pylori with chronic cholecystitis. *Eksp Klin Gastroenterol* 2003; (6):80-82

10 **Osadchuk MA**, Geras'kina TB. Chronic cholecystitis--some lithogenic aspects. *Ter Arkh* 1997; **69**: 27-30

11 **Pradhan SB**, Dali S. Relation between gallbladder neoplasm and Helicobacter hepaticus infection. *Kathmandu Univ Med J* (KUMJ) 2004; **2**: 331-335

12 **Peng XN**, Fan XG, Huang Y, Wang ZM, Cheng YP. The study on relationship between helicobacter infection and primary liver carcinoma. *Shijie Huaren Xiaohua Zazhi* 2002; **10**: 902-906

13 **Jiao JZ**, Nie QH, Zhao CL, Wu YS, Wen SX, Wu Q. Clinical relationship between Helicobacter pylori infection and chronic hepatopathy. *Shijie Huaren Xiaohua Zazhi* 2003; **11**: 851-853

14 **Huang C**, Wu ZM, Zheng ZX. Clinical significance of 13C breath test in preoperative examination for patients with cholecystolithiasis cholecystitis. *Shijie Huaren Xiaohua Zazhi* 2002; **10**: 1336-1338

15 **Chen W**, Li D, Cannan RJ, Stubbs RS. Common presence of Helicobacter DNA in the gallbladder of patients with gallstone diseases and controls. *Dig Liver Dis* 2003; **35**: 237-243

16 **Leong RW**, Sung JJ. Review article: Helicobacter species and hepatobiliary diseases. *Aliment Pharmacol Ther* 2002; **16**: 1037-1045

17 **Monstein HJ**, Jonsson Y, Zdolsek J, Svanvik J. Identification of Helicobacter pylori DNA in human cholesterol gallstones. *Scand J Gastroenterol* 2002; **37**: 112-119

18 **Roa I,** Araya JC, Shiraishi T, Yatani R, Wistuba I, Villaseca M, de Aretxabala X. Immunohistochemical demonstration of pepsinogens I and II in the gallbladder. *Rev Med Chil* 1992; **120**: 1351-1358

19 **Straubinger RK**, Greiter A, McDonough SP, Gerold A, Scanziani E, Soldati S, Dailidiene D, Dailide G, Berg DE, Simpson KW. Quantitative evaluation of inflammatory and immune responses in the early stages of chronic Helicobacter pylori infection. *Infect Immun* 2003; **71**: 2693-2703

20 **Kamangar F**, Limburg P, Taylor P, Dawsey S. Re: Helicobacter pylori and interleukin 1 genotyping: an opportunity to identify high-risk individuals for gastric carcinoma. *J Natl Cancer Inst* 2003; **95**: 760; author reply 760-761

21 **Morland CM**, Fear J, Joplin R, Adams DH. Inflammatory cytokines stimulate human biliary epithelial cells to express interleukin-8 and monocyte chemotactic protein-1. *Biochem Soc Trans* 1997; **25**: 232S

22 **Amieva MR**, Vogelmann R, Covacci A, Tompkins LS, Nelson WJ, Falkow S. Disruption of the epithelial apical-junctional complex by Helicobacter pylori CagA. *Science* 2003; **300**: 1430-1434

S- Editor Liu Y **L- Editor** Zhu LH **E- Editor** Ma WH

PO Box 2345, Beijing 100023, China
www.wjgnet.com
wjg@wjgnet.com

World J Gastroenterol 2007 February 21; 13(7): 1123-1128
World Journal of Gastroenterology ISSN 1007-9327

RAPID COMMUNICATION

Effect of parenteral and early intrajejunal nutrition on pancreatic digestive enzyme synthesis, storage and discharge in dog models of acute pancreatitis

Huan-Long Qin, Zhen-Dong Su, Lei-Guang Hu, Zai-Xian Ding, Qing-Tian Lin

Huan-Long Qin, Zhen-Dong Su, Lei-Guang Hu, Zai-Xian Ding, Qing-Tian Lin, Institute of Parenteral Nutrition and Enteral Nutrition, Department of Surgery, Shanghai Jiaotong University Affiliated Sixth People's Hospital, Yishan Rd. 600, Shanghai 200233, China
Supported by grant from the Morning Star Fund of Shanghai, China, No. 99QB14010
Correspondence to: Dr. Huan-Long Qin, Institute of Parenteral Nutrition and Enteral Nutrition, Department of Surgery, Shanghai Jiaotong University Affiliated Sixth People's Hospital, Yishan Rd. 600, Shanghai 200233, China. hlqin@sjtu.edu.cn
Telephone: +86-21-64942226 Fax: +86-21-64368920
Received: 2006-10-17 Accepted: 2007-01-04

Abstract

AIM: To study the effect of early intrajejunal nutrition on enzyme-protein synthesis and secretion during acute pancreatitis.

METHODS: Fifteen dogs were randomly divided into parenteral nutrition (n = 7) and early intrajejunal nutrition groups (n = 8). An acute pancreatitis model was induced by injecting 5% sodium taurocholate and trypsin into the pancreas via the pancreatic duct. Intrajejunal nutrition was delivered with a catheter via a jejunostomy tube after the model was established for 24 h. On d 1 and 7 and at the beginning of nutritional support, radioactive tracing and electron microscopes were used to evaluate the enzyme-protein synthesis in acinar cells, the subcellular fractionation and the change in zymogen granules after 1.85 × 10^6 Bq L-^{3}H phenylalanine was infused at 30, 60, 120, and 180 min.

RESULTS: The ^{3}H radioactivity in pancreatic acinar cells reached its peak level at 60 min, and the contents in the early intrajejunal nutrition group were higher than those in the parenteral nutrition group, which were then decreased. The mean number and area of zymogen granules did not show any significant statistical difference in both groups on d 1 or on d 7 (P > 0.05).

CONCLUSION: Early intrajejunal nutrition might be effective in dogs with acute pancreatitis.

Key words: Parenteral nutrition; Enteral nutrition; Digestive enzyme; Acute pancreatitis

Qin HL, Su ZD, Hu LG, Ding ZX, Lin QT. Effect of parenteral and early intrajejunal nutrition on pancreatic digestive enzyme synthesis, storage and discharge in dog models of acute pancreatitis. *World J Gastroenterol* 2007; 13(7): 1123-1128

http://www.wjgnet.com/1007-9327/13/1123.asp

INTRODUCTION

Beneficial effects of total enteral nutrition (TEN) have been noted in a number of diseases, such as burn, trauma, and sepsis. In comparison with parenteral nutrition (PN), TEN can reduce nosocomial infection, multiple organ failure (MOF), and the length of hospitalization[1-4]. Early enteral nutritional (EEN) support in patients with acute pancreatitis (AP) has been evaluated by some authors who reported that it can moderate the acute phase response and improve disease severity and clinical outcome[5-10]. However, the commonly encountered problems of gastric atony and outlet obstruction have limited the successful delivery of enteral nutrition to patients with severe acute pancreatitis. In addition, many surgeons believe that EEN may lead to recurrence of symptoms and delayed complications, because EEN may increase the release of digestive enzymes and lysosomal hydrolases. This action of digestive enzymes and lysosomal hydrolases may be important in the development of acute pancreatitis, as lysosomal enzymes such as cathepsin B, are known to be capable of activating trypsinogen and intracellular digestive enzymes that may trigger the autodigestive phenomenon of the pancreas[11]. However, these problems may be overcome if enteral nutrition is delivered to the jejunum as distal as possible from Treitz's ligament, thereby avoiding stimulation of the cephalic and gastric phase. Therefore, it is necessary to investigate the effect of early intrajejunal nutrition (EIN) on pancreatic acinar cell uptake of ^{3}H phenylalanine, digestive enzyme synthesis, storage and discharge in dogs with AP.

MATERIALS AND METHODS

Materials

^{3}H phenylalanine (5mCi/mL) was obtained from Amersham. CBZ-arginine-napthalamide , thymus DNA

and RNA-napthalamide, cytochrome c, 3- (N-morphplino) propanesulfonic acid (MOPS), phenylmethyl- sulfonyl fluoride (PMSF), and Triton X-100 were from Sigma Chemical. All other commercially available reagents were of the highest purity.

Animal model

Twenty-two dogs weighing 18-22 kg had free access to water. After fasting for 12-14 h, all dogs were anesthetized by intramuscular injection of ketamine (10 mL/kg) and intravenous injection of sodium pentobarbital (30 mg/kg). Under sterile conditions, middle laparotomy and duodenotomy were performed. An AP model was induced by injecting 1mg/kg of a combined solution of 5% sodium taurocholate and trypsin 8000-10000 BAEF units/mL into the pancreatic duct at a pressure of 30 cm H_2O. The common biliary duct was clamped. A catheter was placed at 30 cm distal to Treitz's ligament *via* jejunostomy. After the AP model was established, the duodenum and abdomen were closed. The neck regions of dogs were shaved and prepared in a sterile manner for catheterization. A silastic catheter (1.0 mm in inner diameter, 1.5 mm in outer diameter) was inserted through the external jugular vein to reach the superior vena cava and connected to the infusion solution. Fifteen dogs with AP survived after 7 d, and the death rate was 32% (7/22). The study was approved by our Institutional Animal Committee.

Experimental groups and nutritional solution preparation

Fifteen dogs with AP were randomly divided into PN group (n = 7) and EIN group (n = 8). The two groups were isocaloric and isonitrogenous. PN solutions consisted of 7% Vamin (SSPC, 9.4 g/1000 mL), 20% intralipid (SSPC), and 50% glucose (GS). Non-protein calorie was 50 kC (209.2 kJ/kg) and nitrogen was 0.3 g/kg.d. The total volume of solution infused was 70 mL/kg.d. The energy index supported with glucose and fat emulsion was 1:1. Multivitamins and electrolytes were also included in TPN solutions. The 0.9% saline solution was infused at 250 mL/kg during operation and postoperatively for 8 h, thereafter at 125 mL/kg. The nutrient solution was infused at a constant infusion rate by a pump (100-120 mL/h).

The EIN solution was Nutrison (Nutricia). The jejunum was infused through a jejunostomy catheter with 250 mL Nutrison and 500 mL 0.9% saline at 24 h after AP was induced, 500 mL Nutrison and 250mL 0.9% saline were infused after 48 h and continued for 7 d. The infusion rate was controlled by microcomputer-pump (Nutricia). During the EIN support period, the insufficient amount of calorie and nitrogen was supplemented by partial parenteral nutrition[4] (Table 1).

Table 1 Calories, nitrogen and liquid supplemented between two groups

Group	20% Intralipid (mL/kcal)	50% glucose (mL/kcal)	Vamin (9.4g/L) (mL/g)	0.9% saline (mL)	Nutrison (1 kal/mL)
PN group (1-7 d)	227/500	500/500	640/6.0	2500	0
EIN group (1 d)	170/375	187.5/375	468/4.4	1750	250 mL (1.6 g) + NS500 mL
EIN group (2-7 d)	113.6/250	125/250	298/2.8	1750	500 mL (3.2 g) + NS 250 mL

NS: natural saline.

Amino acid uptake

Dogs with AP were infused with radioactive ^3H phenylalanine (1.85×10^6 Bq) at beginning of PN or EIN on d 1 and 7, respectively. The abdomen was opened twice and partial pancreas was rapidly removed at 30, 60, 120 and 180 min after ^3H phenylalanine pulse infusion. After rinsed with a cold homogenization buffer containing 5 mmol/L MOPS (pH 7.0), 250 mmol/L sucrose, 1 mmol/L $MgSO_4$, and 0.1 mmol/L PMSF and trimmed of fat, the pancreas was homogenized in this cold buffer using a Brinkman polytron. The homogenate was centrifuged at 150 × g for 15 min at 4℃ to pellet unbroken cells and the resulting supernatant was used to measure ^3H phenylalanine uptake. For this purpose, an aliquot of the supernatant was mixed with an equal volume of cold 20% trichloroacetic acid (TCA) and centrifuged at 4000 × g for 15 min. The remaining radioactive ^3H phenylalanine in the resulting supernatant was quantified using a Packard liquid scintillation counter.

Protein synthesis

The pancreas was sampled at the above fixed time points. The pancreas was rinsed in cold homogenization buffer, trimmed of fat, and divided into small fragments, which were homogenized in 8 mL of homogenization buffer using 5 full up- and down strokes of a motorized glass-Teflon homogenizer. The homogenate was centrifuged at 150 × g for 15 min at 4℃ to remove unbroken cells and debris. An aliquot was mixed with an equal volume of cold 20% TCA. After incubation on ice for 1 h to precipitate proteins, the sample was centrifuged at 4000 × g for 15 min at 4℃. The pellet was washed twice in 2 mL of 10% TCA. The final pellet was dissolved using a Packard liquid scintillation counter after addition of 10 mL of Beckman Ready-Solv.

Subcellular fractionation

The pancreas was removed, homogenized and subcellularly fractionated using the method of Tartakoff and Jamieson[12] with some modifications by DeLisle *et al*[13]. Briefly, the pancreas was divided into fragments, homogenized in 8 mL homogenization buffer by 5 full up- and -down strokes of a motorized glass-Teflon homogenizer, unbroken cells and debris were removed by centrifugation at 150 × g for 15 min at 4℃. The resulting supernatant was considered to be the entire sample for later calculation and to contain 100% of all measured components, and centrifuged at 1300 × g for 15 min at 4℃, yielding the "zymogen granule" pellet and a supernatant. The latter was harvested and centrifuged at 12000 × g for 12 min at 4℃ to obtain the "lysosome-mitochondria" pellet and a 12000 × g supernatant. This supernatant was centrifuged at 105000 × r/min for 60 min at 4℃

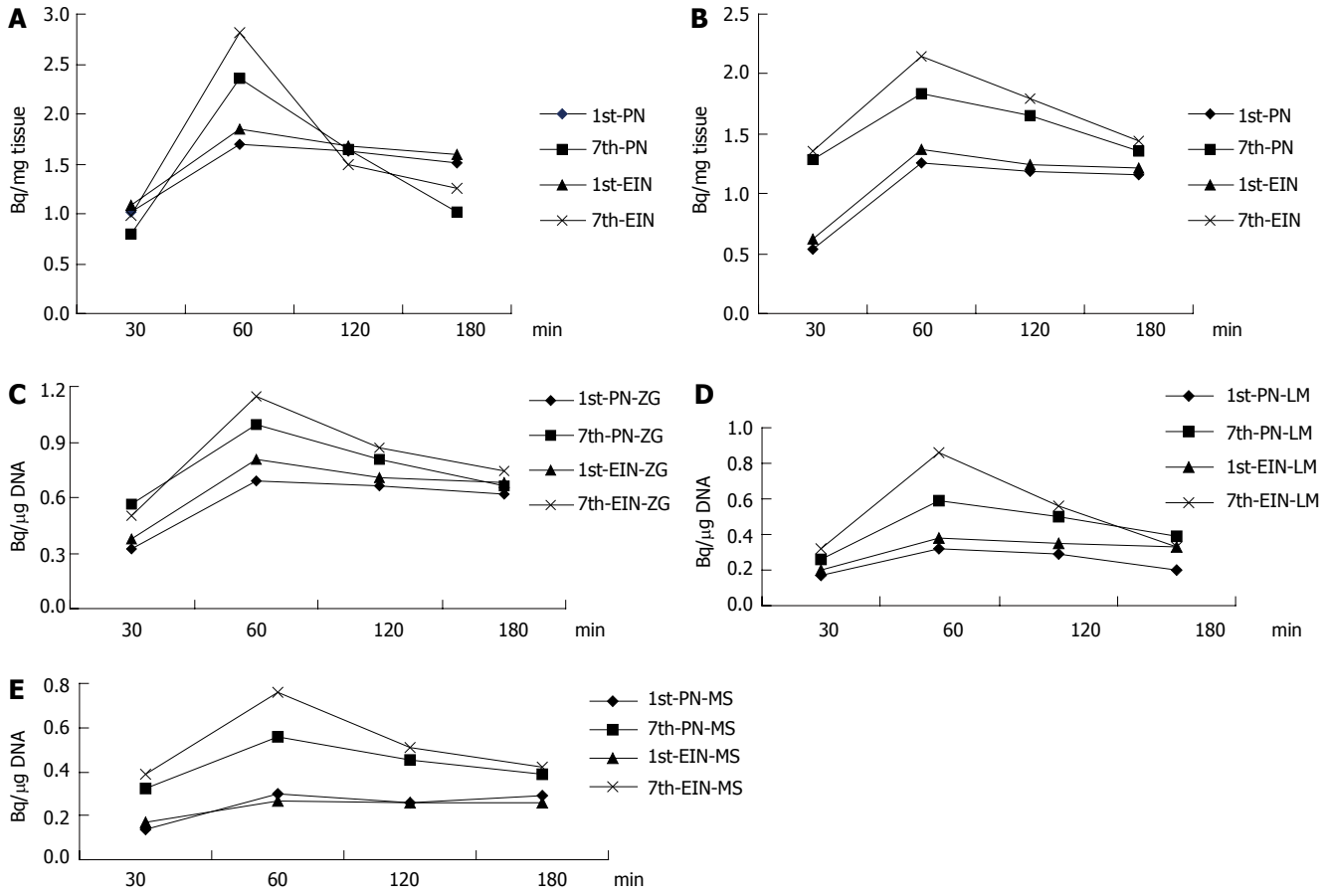

Figure 1 Change of ^{3}H radioactivity in acinar cell uptake (**A**), enzyme-protein synthesis (**B**), zymogen granules (**C**), lysosomal mitochondria (**D**), and microsomal (**E**) at different time points in two groups.

to produce a "microsomal" pellet and postmicrosomal or soluble fraction. The pellets described above were individually resuspended in 2 mL of homogenization buffer prior to measurement of marker enzymes and DNA. To measure the content of newly synthesized protein in each fraction, an aliquot of the sample or the resuspended pellet was mixed with an equal volume of 20% TCA, incubated for 1 h at 4℃ and centrifuged at 4000 × *g*. The pellet was washed as described above prior to measurement of TCA-precipitable radioactivity.

Electron microscopy

The fixation procedure used for conventional thin-section electron microscopy involved incubation with OsO4 alone (1% or 2% in phosphate buffer) at 0℃ for 30 min. After fixation, the sample was washed extensively in Veronal acetate buffer (90 mmol/L, ph 6.0), stained by incubation at 0℃ for 60 min in uranyl-magnesium acetate (0.5%) in the same buffer, washed again, dehydrated and embedded. Thin sections were doubly stained with uranyl acetate and lead nitrate, and examined under Philip EM 400 electron microscope.

A systematic randomized protocol was used to select tissue areas for morphometric analysis[14]. In each grid, 10 pictures were taken by one operator at a magnification of 150 for a total of ten negatives per sample. Two hundred and thirty pictures (PN group, n = 110; EIN group, n = 120) were printed and observed by one operator with a semi automated method using a digitizing tablet and pen, and a PC with dedicated software (Image Measure, Microscince, USA). The interstitial and vascular space, nonexocrine cells, exocrine cell nuclei, and acinar lumen space were not considered. The cross-sectional cytoplasmic area (mm^2) of exocrine cells and mature exocrine enzyme granules was directly measured on prints. In each group of samples, the mean zymogen granular number and area were obtained.

Statistical analysis

The data were collected by two blinded observers and presented as mean ± SE for multiple determinations. The statistical significance of observed changes was evaluated by t test using SPSS 10.0 statistical-software. $P < 0.05$ was considered statistically significant.

RESULTS

Pancreatic exocrine secretion stimulation test (PESST) on the first day

Acinar cell uptake of ^{3}H phenylalanine: The pancreatic acinar cell uptake of ^{3}H phenylalanine was evaluated at 60 min after the start of pulse infusion, and ^{3}H radioactivity in the EIN group was higher than that in PN group ($P < 0.05$), and then gradually decreased. There was no statistical difference between the two groups (Figure 1A).

Enzyme-protein synthesis: The maximal values for

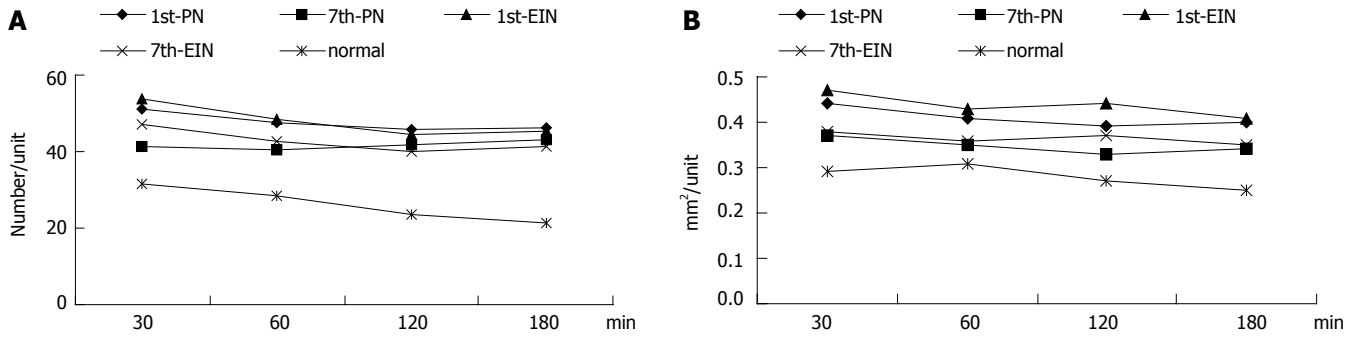

Figure 2 Change of MZGA in EIN group (**A**) and PN group (**B**) at different time points.

both groups were similar in acinar cell uptake of ^{3}H phenylalanine. The incorporation of ^{3}H-phenylalanine into enzyme protein was maximal at 60 min in both groups, and then gradually decreased. There was no difference between the two groups at 180 min (Figure 1B).

Intracellular transport of newly synthesized protein: The peak level of ^{3}H radioactivity was reached in the three subcellular fractionations at 60 min, and ^{3}H radioactivity in zymogen granules in the EIN group was higher than that in the PN group at 60min ($P < 0.05$). ^{3}H radioactivity in lysosomal-mitochondria and the microsomal subcellular fractionation did not reach statistical difference at the fixed time between the two groups, and then gradually decreased, the changes did not reach statistical difference (Figure 1C-E).

Electron microscopy

There was no difference in the submicroscopic cytology of acinar cells between the two groups. In particular, the fine structure of mature secretory granules was consistently similar. The electron density of membrane-bound mature exocrine granules had no change in this study in both PESST determinations. However, the mean zymogen granule number (MZGN) and mean zymogen granule area (MZGA) were not apparently changed on d 1 and 7 in either group, and the change in their number and unit area at different time points did not reach statistical difference (Figure 2A and B).

DISCUSSION

Traditionally, enteral nutrition is implemented after a 2-3 wk period of parenteral nutritional support[15]. This clinical strategy has been developed to provide a sufficient time period for the pancreas to rest and rehabilitate. The concept of pancreatic rest stems from the belief that stimulation of pancreatic exocrine function in patients with acute pancreatitis releases large quantities of proteolytic enzymes which result in autodigestion of the pancreas and peripancreatic tissues, causing deterioration in the patient's condition. The presence of food in the stomach and duodenum elicits gastropancreatic and duodenopancreatic reflexes that result in the stimulation of pancreatic exocrine secretion. However, these effects are insignificant when nutrients are delivered directly into the jejunum[16-25]. Kaushik *et al*[26] reported that enteral feeding can be given without stimulating pancreatic trypsin secretion provided it is delivered into the mid-distal jejunum, because the avoidance of trypsin stimulation may optimize enteral feeding in patients with acute pancreatitis.

It is known that digestive proteins and lysosomal enzymes are synthesized by polyribosomes binding to the cytoplasmic surface of endoplasmic reticulum (ER) membrane, and then transferred to the lumen of ER cisternae[27]. They are transported together to the Golgi, and normally separated from each other in the Golgi complex and condensing vacuole (CV) stage of intracellular transport. Normally, digestive enzymes and lysosomal hydrolases, which are synthesized in ribosomes attaching to the rough-surfaced endoplasmic reticulum and migrating to the Golgi complex and CV, are separated from each other by a complex sorting mechanism. Eventually, they are targeted for inclusion in distinct organelles: zymogen granules and lysosomes. In order to evaluate the effect of EIN on pancreatic acinar cell uptake of ^{3}H-phenylalanine and incorporation into zymogen protein in acute pancreatitic dogs, morphological changes were observed by determining the process of amino acid uptake, enzyme-protein synthesis, intracellular transport, and discharge of newly synthesized proteins from the pancreas within 3 h after beginning of PN and EIN on the first day. The results showed that ^{3}H phenylalanine radioactivity due to amino acid uptake and the extent of incorporation into newly synthesized proteins reached its peak level at 60 min in both groups. The parameters in the EIN group were higher than those in the PN group ($P < 0.05$), and then gradually decreased. To further analyze the effect of EIN on uptake of amino acids and enzyme-protein synthesis in subcellular fractions on the first day, we used differential and density-gradient centrifugation to determine the ^{3}H radioactivity in zymogen granules, lysosome-mitochondria and microsomal subcellular fractionation. In this study, the maximal values were obtained at 60 min in each of these fractions in lysosomes (cathepsin B), mitochondria (cytochrome oxidase) and zymogen granules (amylase), and then gradually decreased. These results suggest that the EIN alters neither amino acid uptake nor the extent of incorporation of ^{3}H radioactivity into newly synthesized proteins.

To study the possibility of recurrent pancreatitis,

PESST was performed to determine whether EIN increases ^{3}H radioactivity in lysosomes, mitochondria, and zymogen granules during AP. The results showed that the ^{3}H radioactivity in amino acid uptake, enzyme-protein synthesis, and subcellular fractionation reached its peak level at 60 min in both groups, which was higher in the EIN group than in the PN group ($P < 0.05$), and then gradually decreased. The content of ^{3}H in zymogen granules, lysosome-mitochondria and microsomal subcellular fractionation were consistent with the changes of amino acid uptake. The peak level of radioactivity on d 7 was higher than that on d 1. The tissue level of pulse-labeled proteins declined as expected due to secretion of labeled digestive zymogens into the duodenum via the pancreatic duct system. These results suggest that 7 d continuous intrajejunal nutrition can neither over-stimulate acinar cell uptake of ^{3}H nor enhance enzyme-protein synthesis and release. Cell fractionation studies indicated that intracellular transport of granules was not affected by EIN stimulation. Indeed, disappearance of pulse-labeled proteins from 10 500 × *g* pellet (total microsomal fraction enriched in rough endoplasmic reticulum elements and expected to contain Golgi elements as well) and their appearance in the 1300 × *g* pellet (enriched in zymogen granules and presumably condensing vacuoles) were not significantly different in EIN stimulation.

It is known that stored zymogens granules and lysosomal enzymes could play a key role in the development of pancreatitis and may, in fact, explain the intrapancreatic activation of digestive enzymes occurring in the course of many forms of pancreatitis[28]. Secretory proteins, on the other hand, progressively increase their concentration within the dilated Golgi cisternal rims and/or CV. The CV ultimately matures to ZG which is transported to the luminal plasmalemma and releases its contents by exocytosis. The large vacuoles containing both secretory and lysosomal enzymes in acute pancreatitis suggest that AP stimulates the process of CV maturation. Therefore, theoretically, EIN might increase intracellular transport and expand the CV compartment (formation of large vacuoles). To quantitatively assess the effect of EIN on the secretory granule cell compartment, ultrastructural morphometrical study of the pancreas under electron microscope was designed. The results showed that more ZG was accumulated in the interstitial space. The number and area of ZG were higher than those in normal. However, no gross difference in acinar cell ultrastructure was observed. These findings did not reach statistical difference between the two groups on d 1 and 7 during the nutritional support period, suggesting that EIN does not promote pancreatic acinar cell enzyme protein synthesis and release. The precise mechanism of EIN-stimulating acinar cells is unclear. However, some results indicate that receptor-triggered events of transmembrane signaling (rise of cytoplasmic Ca^{2+}) and the responsiveness and sensitivity to gastrointestinal hormones in pancreatic acinar cells are significantly inhibited[29].

In conclusion, early intrajejunal nutrition might be effective in dogs with acute pancreatitis. However, further study is needed to evaluate the effects of EIN and PN in patients with AP.

REFERENCES

1 **MacFie J**. Enteral versus parenteral nutrition. *Br J Surg* 2000; **87**: 1121-1122
2 **Neoptolemos JP**, Raraty M, Finch M, Sutton R. Acute pancreatitis: the substantial human and financial costs. *Gut* 1998; **42**: 886-891
3 **Al-Omran M**, Groof A, Wilke D. Enteral versus parenteral nutrition for acute pancreatitis. *Cochrane Database Syst Rev* 2003; (1): CD002837
4 **Qin HL**, Su ZD, Hu LG, Ding ZX, Lin QT. Effect of early intrajejunal nutrition on pancreatic pathological features and gut barrier function in dogs with acute pancreatitis. *Clin Nutr* 2002; **21**: 469-473
5 **Saluja A**, Saito I, Saluja M, Houlihan MJ, Powers RE, Meldolesi J, Steer M. In vivo rat pancreatic acinar cell function during supramaximal stimulation with caerulein. *Am J Physiol* 1985; **249**: G702-G710
6 **Abou-Assi S**, Craig K, O'Keefe SJ. Hypocaloric jejunal feeding is better than total parenteral nutrition in acute pancreatitis: results of a randomized comparative study. *Am J Gastroenterol* 2002; **97**: 2255-2262
7 **Oláh A**, Pardavi G, Belágyi T, Nagy A, Issekutz A, Mohamed GE. Early nasojejunal feeding in acute pancreatitis is associated with a lower complication rate. *Nutrition* 2002; **18**: 259-262
8 **Chen QP**. Enteral nutrition and acute pancreatitis. *World J Gastroenterol* 2001; **7**: 185-192
9 **Hallay J**, Kovács G, Szatmári K, Bakó A, Szentkereszty Z, Lakos G, Sipka S, Sápy P. Early jejunal nutrition and changes in the immunological parameters of patients with acute pancreatitis. *Hepatogastroenterology* 2001; **48**: 1488-1492
10 **McGregor CS**, Marshall JC. Enteral feeding in acute pancreatitis: just do it. *Curr Opin Crit Care* 2001; **7**: 89-91
11 **Sanabria A**. Randomized controlled trial of the effect of early enteral nutrition on markers of the inflammatory response in predicted severe acute pancreatitis. *Br J Surg* 2001; **88**: 728
12 **Tartakoff AM**, Jamieson JD. Subcellular fractionation of the pancreas. *Methods Enzymol* 1974; **31**: 41-59
13 **De Lisle RC**, Schulz I, Tyrakowski T, Haase W, Hopfer U. Isolation of stable pancreatic zymogen granules. *Am J Physiol* 1984; **246**: G411-G418
14 **Falconi M**, Caldiron E, Zancanaro C, Benati D, Talamini G, Bassi C, Pederzoli P. In vivo octreotide administration acutely reduces exocrine granule size in the human pancreas. *Pancreatology* 2001; **1**: 30-35
15 **Oláh A**, Belágyi T, Issekutz A, Gamal ME, Bengmark S. Randomized clinical trial of specific lactobacillus and fibre supplement to early enteral nutrition in patients with acute pancreatitis. *Br J Surg* 2002; **89**: 1103-1107
16 **Takács T**, Hajnal F, Németh J, Lonovics J, Pap A. Stimulated gastrointestinal hormone release and gallbladder contraction during continuous jejunal feeding in patients with pancreatic pseudocyst is inhibited by octreotide. *Int J Pancreatol* 2000; **28**: 215-220
17 **Eckerwall G**, Andersson R. Early enteral nutrition in severe acute pancreatitis: a way of providing nutrients, gut barrier protection, immunomodulation, or all of them? *Scand J Gastroenterol* 2001; **36**: 449-458
18 **Eatock FC**, Brombacher GD, Steven A, Imrie CW, McKay CJ, Carter R. Nasogastric feeding in severe acute pancreatitis may be practical and safe. *Int J Pancreatol* 2000; **28**: 23-29
19 **Lehocky P**, Sarr MG. Early enteral feeding in severe acute pancreatitis: can it prevent secondary pancreatic (super) infection? *Dig Surg* 2000; **17**: 571-577
20 **Erstad BL**. Enteral nutrition support in acute pancreatitis. *Ann Pharmacother* 2000; **34**: 514-521
21 **Duerksen DR**, Bector S, Yaffe C, Parry DM. Does jejunal

feeding with a polymeric immune-enhancing formula increase pancreatic exocrine output as compared with TPN? A case report. *Nutrition* 2000; **16**: 47-49

22 **Sahin M**, Ozer S, Vatansev C, Aköz M, Vatansev H, Aksoy F, Dilsiz A, Yilmaz O, Karademir M, Aktan M. The impact of oral feeding on the severity of acute pancreatitis. *Am J Surg* 1999; **178**: 394-398

23 **Windsor AC**, Kanwar S, Li AG, Barnes E, Guthrie JA, Spark JI, Welsh F, Guillou PJ, Reynolds JV. Compared with parenteral nutrition, enteral feeding attenuates the acute phase response and improves disease severity in acute pancreatitis. *Gut* 1998; **42**: 431-435

24 **Lobo DN**, Memon MA, Allison SP, Rowlands BJ. Evolution of nutritional support in acute pancreatitis. *Br J Surg* 2000; **87**: 695-707

25 **Kalfarentzos F**, Kehagias J, Mead N, Kokkinis K, Gogos CA. Enteral nutrition is superior to parenteral nutrition in severe acute pancreatitis: results of a randomized prospective trial. *Br J Surg* 1997; **84**: 1665-1669

26 **Kaushik N**, Pietraszewski M, Holst JJ, O'Keefe SJ. Enteral feeding without pancreatic stimulation. *Pancreas* 2005; **31**: 353-359

27 **Rosenfeld MG**, Kreibich G, Popov D, Kato K, Sabatini DD. Biosynthesis of lysosomal hydrolases: their synthesis in bound polysomes and the role of co- and post-translational processing in determining their subcellular distribution. *J Cell Biol* 1982; **93**: 135-143

28 **Watanabe O**, Baccino FM, Steer ML, Meldolesi J. Supramaximal caerulein stimulation and ultrastructure of rat pancreatic acinar cell: early morphological changes during development of experimental pancreatitis. *Am J Physiol* 1984; **246**: G457-G467

29 **Powers RE**, Saluja AK, Houlihan MJ, Steer ML. Aberration in stimulus-secretion coupling caused by a choline deficient 0.5% ethionine containing (CDE diet) (Abstract). *Federation Proc* 1985; **44**: 535

S- Editor Wang J **L- Editor** Wang XL **E- Editor** Ma WH

PO Box 2345, Beijing 100023, China
www.wjgnet.com
wjg@wjgnet.com

World J Gastroenterol 2007 February 21; 13(7): 1129-1134
World Journal of Gastroenterology ISSN 1007-9327

RAPID COMMUNICATION

Mechanisms involved in ceramide-induced cell cycle arrest in human hepatocarcinoma cells

Jing Wang, Xiao-Wen Lv, Jie-Ping Shi, Xiao-Song Hu

Jing Wang, Research Center for Eco-Environmental Sciences, The Chinese Academy of Sciences, Beijing 100085, China
Xiao-Wen Lv, Feed Research Institute, Chinese Academy of Agricultural Sciences, Beijing 100081, China
Jie-Ping Shi, Xiao-Song Hu, College of Food Science and Nutritional Engineering, China Agricultural University, Beijing, China
Correspondence to: Xiao-Song Hu, Research Center for Eco-Environmental Sciences, The Chinese Academy of Sciences, Haidian District, Beijing 100085, China. wangjing@rcees.ac.cn
Telephone: +86-10-62849321
Received: 2006-10-12 Accepted: 2007-01-18

Abstract

AIM: To investigate the effect of ceramide on the cell cycle in human hepatocarcinoma Bel7402 cells. Possible molecular mechanisms were explored.

METHODS: [3- (4, 5)-dimethylthiazol-2-yl]-2, 5-diphenyltetrazolium bromide (MTT) assay, plasmid transfection, reporter assay, FACS and Western blotting analyses were employed to investigate the effect and the related molecular mechanisms of C2-ceramide on the cell cycle of Bel7402 cells.

RESULTS: C2-ceramide was found to inhibit the growth of Bel7402 cells by inducing cell cycle arrest. During the process, the expression of p21 protein increased, while that of cyclinD1, phospho-ERK1/2 and c-myc decreased. Furthermore, the level of CDK7 was downregulated, while the transcriptional activity of PPARγ was upregulated. Addition of GW9662, which is a PPARγ specific antagonist, could reserve the modulation action on CDK7.

CONCLUSION: Our results support the hypothesis that cell cycle arrest induced by C2-ceramide may be mediated *via* accumulation of p21 and reduction of cyclinD1 and CDK7, at least partly, through PPARγ activation. The ERK signaling pathway was involved in this process.

Key words: Ceramide; Cell cycle arrest; Human hepatocarcinoma cells; P21; CyclinD1; CDK7; PPARγ; ERK

Wang J, Lv XW, Shi JP, Hu XS. Mechanisms involved in ceramide-induced cell cycle arrest in human hepatocarcinoma cells. *World J Gastroenterol* 2007; 13(7): 1129-1134

http://www.wjgnet.com/1007-9327/13/1129.asp

INTRODUCTION

Ceramide has emerged as a novel lipid second messenger with specific roles in mediating cell growth, differentiation, stress responses and apoptosis[1-3]. Ceramide is generated through the hydrolysis of sphingomyelin by the activation of sphingomyelinase (SMase). A number of stimuli have been reported to activate SMase[4-6]. Exogenously administered synthetic ceramide mimicked the action of these inducers in the regulation of various cell functions. Ceramide mediates numerous cellular functions such as differentiation, growth arrest, apoptosis and proliferation[7,8]. Ceramide is thought to be involved in modulating ceramide-activated protein kinase (CAPK), mitogen-activated protein kinase (MAPK), ceramide-activated protein phosphatase (CAPP) and phospholipaseA2 (PLA2), *etc*[9]. Apoptosis induction by ceramide is associated with Bcl-2 phosphorylation, SAPK/JNK and caspase pathway activation[10]. On the other hand, activation of PKC and Bcl-2 expression can inhibit the ceramide signal pathway[11,12]. However, the link between ceramide signaling and the cell cycle is poorly understood.

To exploit the effect of ceramide on the cell cycle, human hepatocarcinoma Bel7402 cells were employed and treated with C2-ceramide. Hepatocarcinoma occurs with high incidence in southern China and southeast Asia. Radiation is one of the agents that activates ceramide signaling[13], and therefore, it is of interest in investigating the effect of ceramide on Bel7402 cells. In this study, we observed inhibition of cell proliferation and cell cycle arrest in the G1 phase following C2-ceramide treatment in Bel7402 cells. Subsequent studies suggested that modulation might be mediated *via* accumulation of p21 and reduction of cyclinD1 and CDK7, at least partly, through PPARγ activation. The ERK signaling pathway was also involved in this process.

MATERIALS AND METHODS

Materials

C2-ceramide was purchased from Sigma. Co (St Louis Mo, USA); mouse monoclonal anti-p21, anti-cyclinD1,

anti-CDK7, anti-p-ERK and anti-c-myc were purchased from Santa Cruz Biotechnology, Inc (CA, USA); antibody of PE-E-cadherin was purchased from DAKO Co. Horseradish peroxidase-conjugated secondary antibodies were purchased from Jackson Immuno-Research Laboratories, Inc (West Grove, PA, USA). Lipofectamine and lipofectin reagents were from Gibco, Inc. RNaseA, MTT, propiudium iodide and other chemicals were all from Sigma.

Cell culture

Bel7402 cells were provided by the Institute of Zoology, Chinese Academy of Sciences, China. Cells were maintained in Dulbecco's minimal essential medium (DMEM) supplemented with 10% fetal bovine serum (FBS) in a humidified atmosphere of 95% air/5% CO_2 at 37℃. A subculture of cells was processed by enzymatic digestion (trypsin/EDTA solution: 0.25/0.02%). C2-ceramide dissolved in ethanol was used without filtration. The final concentration of ethanol in culture medium was < 0.3%.

MTT assay

Bel7402 cells were seeded onto 96-well plates at a concentration of 2.5×10^3 cells/well in DMEM plus 5% FBS. The stock of C2-ceramide was diluted with medium, and then added to wells for desired final concentrations. After exposure to C2-ceramide for the desired time, 10 μL of 5 mg/mL MTT was added to each well and incubated for 4 h, and the liquid in wells was evaporated. To dissolve the formazam, 100 μL of DMSO was added. The absorbance was determined with a microplate reader model 550 at the wavelength of 570 nm.

Cell cycle analysis

The proportions of cells in G0-G1, S, and G2-M were determined by flow cytometric analysis of DNA content. Briefly, cells were obtained by trypsinization following treatment with C2-ceramide, and then washed twice with PBS. Cells were then incubated with RNase at a concentration of 0.25 mg/mL at 37℃ for 1 h following incubation with PI (50 μg/mL in PBS) for 30 min at 4℃ in the dark. Before flow cytometry, samples were syringed through a 25-gauge needle to prevent nuclear clumping. PI was excited at 488 nm, and fluorescence was analyzed at 620 nm. All measurements were carried out under the same instrumental settings.

PE-E-cadherin labeling

Cells were washed once with cold PBS, and centrifuged to collect the cell pellet (350 g × 5 min) following treatment with C2-ceramide.The cell pellet was resuspended in cold PBS (4℃) and PE-E-cadherin and the corresponding isotype antibodies were added to the cell suspension and mixed gently. The tube was then incubated for 30-60 min in the dark at room temperature prior to flow cytometry. PE-E-cadherin binding was analyzed by flow cytometry collecting the fluorescence of 10 000 cells using a FACScan (Becton Dickinson) according to the manufacturer's instructions. All experiments were replicated three times.

Western blot analysis

To determine the expression levels of E-cadherin, p21, cyclinD1, CDK7 and c-myc, cells were lysed in buffer (150 mmol/L NaCl, 1% NP-40, 0.5% sodium deoxycholate, 0.1% SDS, 50 mmoL/L Tris, pH 8.0, 1 mmoL/L phenylmethylsulfonyl fluoride (PMSF), and 10 μg/mL aprotinin). To determine the level and phosphorylation state of ERK, cells were harvested in lysis buffer containing 50 mmol/LTES (N-tris [hydroxymethyl] methyl-2-aminoethane sulfonic acid) (pH 7.4), 2 mmol/L EGTA, 1 mmol/L EDTA, 250 mmol/L sucrose, 40 mmol/L phenylphosphate, 1 mmol/L $MgCl_2$, 2 mmoL/L Na_3VO_4, 10 mmol/L $Na_4P_2O_7$, 100 mmol/L NaF, 5 μg/mL aprotinin, 1 mmol/L PMSF, 1 μg/mL leupeptin, 5 mmol/L benzamidine, and 10 mmol/L dithiothreitol. Protein (40-80 μg) was separated by 12%-15% SDS-polyacrylamide gel in the separation buffer (25 mmol/L Tris, 250 mmol/L Glycine, 0.1% SDS). Total proteins were transferred onto a PVDF membrane after electrophoresis. Western blot analyses using anti-p21, anti-cyclinD1, anti-CDK7, anti-c-myc, anti-phospho-p42/p44ERK and anti-totalERK antibodies were performed. As an internal control, mouse monoclonal anti-β-actin antibody was used.

Transient transfection and luciferase assay for PPARγ activity

Bel7402 cells were seeded at a concentration of 1×10^5 cells/35 mm dish. After 12 h, the medium was changed from complete medium to DMEM without antibiotic. Transfection was done using LipofectAMINE reagent mixed with 2 μg of acyl-CoA oxidase promoter-luciferase plasmid pAOXPPREluc and the control pAOXBluc basic vector (kindly donated by Dr. Osumi) for 8 h. After the transfection mixture was replaced by a medium containing 10% FBS, cells were then incubated with or without different concentrations of ceramide for a desired time. Luciferase activity was measured according to the manufacturer's protocol (Promega).

Statistical analysis

All statistical analyses were performed with SPSS 10.0 statistical package for Microsoft Windows. Data were expressed as mean ± SE for all measurements. $P < 0.05$ was considered statistically significant.

RESULTS

Ceramide inhibited proliferation by halting the cell cycle in Bel7402 cells

Treatment with different concentrations of C2-ceramide for 24 h exhibited significant inhibition of cell proliferation of human hepatocarcinoma Bel7402 cells as suggested by MTT assay. Under concentrations of 0, 5, 10, 15, 30 and 60 μmmo/L, inhibitory rates were 0, 21.5% ± 1.3%, 52.7% ± 0.9%, 69.3% ± 1.2%, 77.2% ± 0.8% and 83.8% ± 1.2%, respectively (Figure 1A). Cytotoxicity was further indicated by determination of E-cadherin, which is a marker for many tumor cells with high expression. PE-E-cadherin antibodies were stained with cells to determine

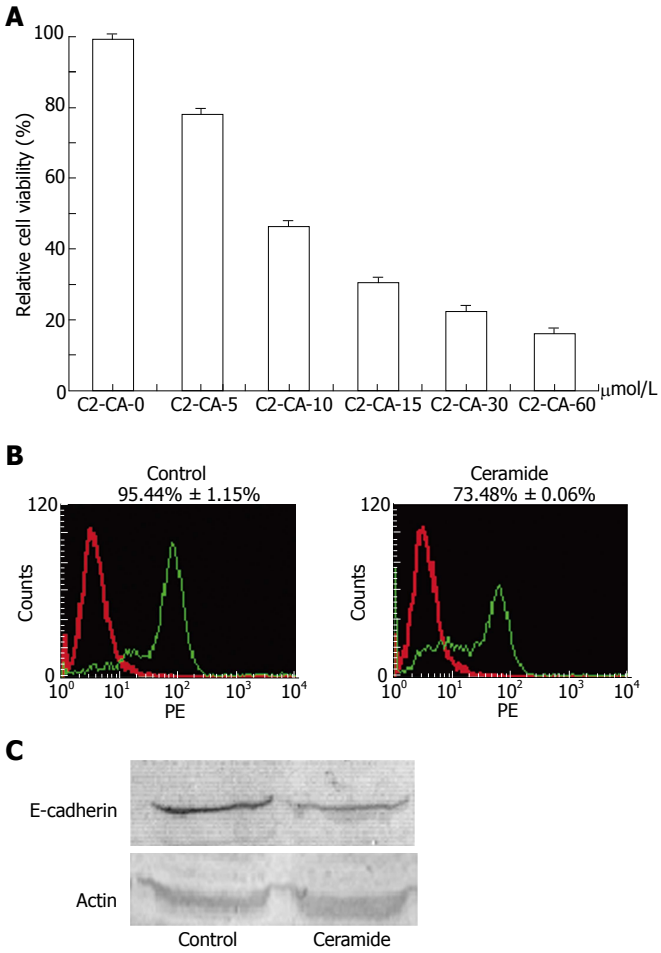

Figure 1 Ceramide inhibited proliferation by halt of cell cycle in Bel7402 cells. **A**: ceramide inhibited cell proliferation in Bel7402 cells. Cells were cultured in the medium with different concentrations of C2-ceramide for 24 h. Cell viability was analyzed by MTT assay and presented as cell proliferative rates. The results show the mean ± SE (n = 3-4); **B** and **C**: ceramide down-regulated the expression of E-cadherin. Bel7402 cells were incubated with or without 30 μmmo/L of ceramide for 24 h. Cells were then harvested and stained with anti-E-cadherin directly labeled by PE. The protein levels of E-cadherin were determined by flow cytometry. Data was represented by the mean ± SE of 3 or 4 separate experiments (**B**). Bel7402 cells were incubated with or without 30 μmmo/L of ceramide for 24 h. Cells were then harvested, lysed and resolved in 12% SDS-PAGE. The expression of E-cadherin was determined by Western blot. Actin was used as a control. Data represent the results of three separate experiments (**C**).

the expression of E-cadherin on the cell surface. Flow cytometry analysis results indicated that E-cadherin was significantly down-regulated by C2-ceramide (Figure 1B), which was also suggested by blot assay (Figure 1C). To test whether the cytotoxicity was derived from the effect on the cell cycle, flow cytometry analysis was applied following treatment with different concentrations of C2-ceramide at 0, 5, 15, 30 and 60 μmol/L. As shown in Table 1, the cell cycle was halted in the G1 phase, and the percentage of cells in the G1 phase was 35.3% ± 0.7%, 36.8% ± 1.2%, 43.9% ± 1.2%, 57.2% ± 0.6% and 76.2% ± 1.3%, respectively.

Ceramide up-regulated the expression of p21$^{WAF1/BIP1}$ and down-regulated that of cyclinD1

In order to elucidate whether molecules were involved in the G1/S transition following C2-ceramide treatment,

Table 1 Ceramide halted cell cycle in Bel7402 cells (mean ± SE, n = 3)

Ceramide (μmol/L)	G_0/G_1 (%)	S (%)	G_2/M
0	35.3 ± 0.7	44.3 ± 0.3	20.4 ± 0.1
5	36.8 ± 1.2	43.9 ± 0.4	19.3 ± 1.8[a]
15	43.9 ± 1.2[a]	41.9 ± 0.7[a]	14.2 ± 0.8[a]
30	57.2 ± 0.6[a]	28.8 ± 0.5[a]	14.0 ± 0.5[a]
60	76.2 ± 1.3[a]	8.2 ± 0.2[a]	15.6 ± 1.3[a]

[a]$P < 0.05$ *vs* control.

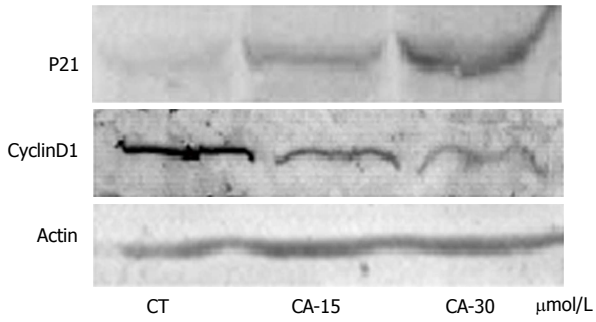

Figure 2 Ceramide up-regulated the expression of p21$^{WAF1/BIP1}$ and down-regulated that of cyclinD1. Bel7402 cells were incubated with different concentrations of ceramide as indicated for 24 h. Cells were harvested, lysed and resolved in 15% SDS-PAGE. The expression of p21 and cyclinD1 were determined by Western blot. Actin was used as a control. Data represent the results of three separate experiments.

cell extracts were prepared from Bel7402 cells treated with different concentrations of C2-ceramide. Protein expression was indicated by blot using anti-p21 and anti-cyclinD1 antibodies, respectively. As shown in Figure 2, C2-ceramide increased the expression of p21 protein, but decreased that of cyclinD1 protein.

CDK7 and PPARγ pathways involved in cell cycle arrest induced by C2-ceramide

In our previous study, we reported that C2-ceramide could activate PPARγ transcription activity in human colon cancer HT29 cells[14]. In this study, as shown in Figure 3A, C2-ceramide could also markedly activate the transcriptional activity of PPARγ in hepatocarcinoma Bel7402 cells.

Cyclin-dependent kinase 7 (CDK7) is critical for cell cycle and transcriptional programs[15]. Therefore, we investigated the expression of CDK7 by blotting. It was observed that CDK7 expression decreased following treatment with 30 μmmo/L C2-ceramide for 24 h. However, addition of the PPARγ specific antagonist GW9662 markedly reversed the inhibition (Figure 3B).

Ceramide inhibited the activation of ERK1/2 in Bel7402 cells

ERK plays a key role in cell survival in many cells. To examine whether ceramide inhibited the activation of ERK, Bel7402 cells were treated with different concentrations of C2-ceramide and phospho-ERK1/2 was determined. As shown in Figure 4, the expression of p-ERK decreased significantly with the treatment of

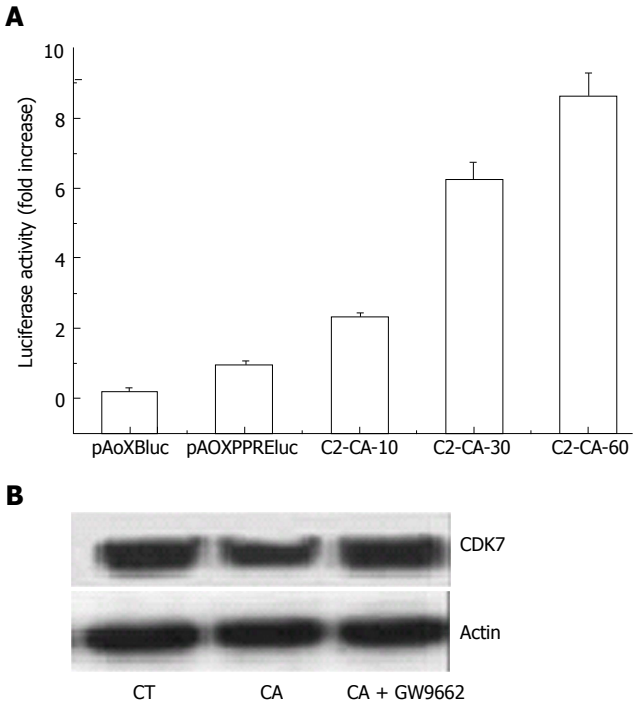

Figure 3 CDK7 and PPARγ pathways involved in cell cycle arrest induced by C2-ceramide. **A**: activation of PPARγ transcriptional activity induced by C2-ceramide. Bel7402 cells were transiently transfected with the PPAR responsive element (PPRE) reporter construct (pAOXPPREluc) or the promoter-less control vector pAOXBluc following the treatment of different concentrations of C2-ceramide as indicated, PPARγ transcriptional activity was measured as described. The bar represents the relative fold increase of luciferase activity. The results show means ± SE (n = 3); **B**: C2-ceramide down-regulated the expression of CDK7, which was blocked by GW9662. Bel7402 cells were cultured with 30 μmol/L C2-ceramide in the presence or absence of GW9662, which was claimed as a specific PPARγ antagonist for 24 h. Total proteins were extracted and resolved on SDS-PAGE followed by Western blot assay using anti-CDK7 antibody. Data represents the results of three separate experiments.

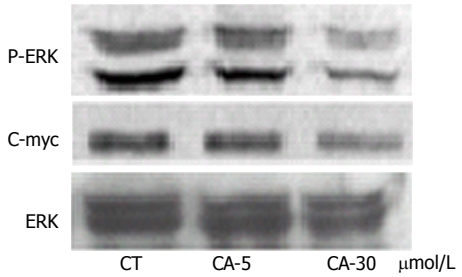

Figure 4 Ceramide inhibited activation of ERK pathway in Bel7402. Bel7402 cells were incubated with different concentrations of ceramide as indicated. Total proteins were extracted and resolved on SDS-PAGE. Phospho-ERK1/2 and c-myc were normalized to total Erk1/2 and internal standard actin was determined by Western blot. Data represents the results of three separate experiments.

C2-ceramide, while total ERK protein expression was unaffected.

To complete the study of the MAPK pathway, c-myc content was also indicated by blot using anti-c-myc antibodies. As shown in Figure 4, the modulation pattern on the expression of c-myc induced by C2-ceramide was similar to that of p-ERK.

DISCUSSION

Since ceramide was affirmed as an important lipid second messenger in 1994, the importance of ceramide in cell metabolism has been broadly investigated. Ceramide has shown inhibition of cell growth *via* apoptosis in a variety of cancers. However, the link between ceramide signaling and the cell cycle is poorly understood. The present work demonstrates that C2-ceramide halted the distribution of cell cycles in G1 phase, and the mechanisms involved were explored.

As displayed in Table 1, C2-ceramide induced cell cycle arrest in the G1 phase. Accordingly, down-regulation of E-cadherin, a marker for many tumor cells with high expression, suggested that C2-ceramide inhibited cancer cell growth (Figure 1B).

In order to elucidate the mechanisms involved in cell cycle arrest following treatment with C2-ceramide in Bel7402 cells, we firstly investigated whether the cell cycle control genes; i.e., cyclin D1 and the cyclin-dependent kinase inhibitor p21, are involved in ceramide-mediated cell cycle regulation in Bel7402 cells.

Cell cycle progression is regulated by interactions between cyclins and cyclin-dependent kinases, which are modulated by a family of negative cell cycle regulators; i.e., cyclin-dependent kinase inhibitors, which are especially involved in controlling the transition from G1 to S-phase[16,17]. The latter includes two families, the CIP/KIP family and the INK4 family. p21 is a member of the CIP/KIP family and plays a crucial role in growth arrest by a variety of mechanisms[18]. Consistent with this idea, we showed that C2-ceramide up-regulated the expression of p21 protein concomitant with inhibition of cyclin D1 protein (Figure 2).

PPARγ is clearly involved in lipid metabolism and is essential for cell differentiation[19,20]. Activation of PPARγ by its ligands can induce growth inhibition and cytotoxicity in human prostate cancer cells, colon cancer cells and liposarcoma cells, and their biological activities are attributed to inhibition of proliferation and induction of apoptosis by PPARγ[21,22]. We have previously shown C2-ceramide could induce apoptosis *via* a PPARγ dependent pathway in human colon cancer HT29 cells[14]. To examine whether the PPARγ pathway was involved in the modulation of cell cycle arrest induced by ceramide in human hepatocarcinoma Bel7402 cells, the luciferase reporter of PPRE3x-tk-luc was transfected and luciferase activity was assayed. The result shown in Figure 3A suggested that ceramide activated the transcriptional activity of PPARγ in a dose-dependent manner.

CDK7 distributes normally throughout the nucleus and cytoplasm, and in the nucleus, it attaches to a DNA template with other TFⅡH subunits initiating gene transcription[23], which is very important in modulating cell proliferation. Participating in basal transcription by phosphorylating the carboxy-terminal domain of the largest subunit of RNA polymerase Ⅱ, CDK7 is critical for the cell cycle and transcriptional programmes, which also phosphorylate other CDKs as an essential step for their activation[24,25]. Often, phosphorylation of NRs by kinases that are associated with general transcription factors (e.g. CDK7 within TFⅡH), or activated in response to a variety of signals (MAPKs, Akt, PKA, PKC),

facilitates the recruitment of coactivators or components of the transcription machinery and, therefore, cooperates with the ligand to enhance transcription activation.

Though there is much to be explored, data have shown that C2-ceramide inhibited cell proliferation through attenuation of CDK7 (Figure 3B). However, GW9662, which is a PPARγ specific antagonist, could markedly block this action. These data suggested that CDK7 was related to PPARγ, which was consistent with the opinion described above.

ERK signaling plays a key role in cell survival, and Erk1/2 are proteins belonging to the MAPK pathway, whose members are active when phosphorylated. Consequently, dephosphorylation of these proteins inhibits their activity and the transcription factor c-myc. The increase of PP2A, which is a serine/threonine phosphatase causing dephosphorylation of MAPKs[26], is one of the causes of Erk1/2 dephosphorylation. Indeed, the ERK1/2 pathway, that regulates cellular growth and proliferation, has been shown to be pro[27-30] or anti-apoptotic[31-33], depending on experimental conditions and/or cell types. To examine whether C2-ceramide can inhibit activation of ERK, phospho-ERK was determined. It was found that phospho-ERK decreased with the treatment of C2-ceramide in Bel7402 cells, however, the expression level of total ERK protein was unaffected. Accordingly, the protein expression of c-myc also decreased (Figure 4).

In summary, with consideration that there is much to be explored, it was concluded that C2-ceramide plays an important role in the inhibition of cell growth in Bel7402 cells. Our results showed that there is p21 accumulation in accordance with decreased cyclinD1, inactivation of the ERK pathway, downregulation of CDK7 and stimulation of PPARγ transcriptional activity. As such, our results support the hypothesis that suppression of hepatocarcinoma cell growth through cell cycle arrest induced by C2-ceramide may be mediated *via* accumulation of p21 and reduction of cyclinD1 and CDK7, at least partly, through PPARγ activation. The ERK signaling pathway was involved in this process.

REFERENCES

1 **Obeid LM**, Linardic CM, Karolak LA, Hannun YA. Programmed cell death induced by ceramide. *Science* 1993; **259**: 1769-1771
2 **Hannun YA**, Obeid LM. The Ceramide-centric universe of lipid-mediated cell regulation: stress encounters of the lipid kind. *J Biol Chem* 2002; **277**: 25847-25850
3 **Mathias S**, Peña LA, Kolesnick RN. Signal transduction of stress via ceramide. *Biochem J* 1998; **335** (Pt 3): 465-480
4 **Tavarini S**, Colombaioni L, Garcia-Gil M. Sphingomyelinase metabolites control survival and apoptotic death in SH-SY5Y neuroblastoma cells. *Neurosci Lett* 2000; **285**: 185-188
5 **Tomassini B**, Testi R. Mitochondria as sensors of sphingolipids. *Biochimie* 2002; **84**: 123-129
6 **Jaffrézou JP**, Levade T, Bettaïeb A, Andrieu N, Bezombes C, Maestre N, Vermeersch S, Rousse A, Laurent G. Daunorubicin-induced apoptosis: triggering of ceramide generation through sphingomyelin hydrolysis. *EMBO J* 1996; **15**: 2417-2424
7 **Levade T**, Malagarie-Cazenave S, Gouazé V, Ségui B, Tardy C, Betito S, Andrieu-Abadie N, Cuvillier O. Ceramide in apoptosis: a revisited role. *Neurochem Res* 2002; **27**: 601-607
8 **Haimovitz-Friedman A**, Kolesnick RN, Fuks Z. Ceramide signaling in apoptosis. *Br Med Bull* 1997; **53**: 539-553
9 **Hannun YA**. Functions of ceramide in coordinating cellular responses to stress. *Science* 1996; **274**: 1855-1859
10 **Raisova M**, Goltz G, Bektas M, Bielawska A, Riebeling C, Hossini AM, Eberle J, Hannun YA, Orfanos CE, Geilen CC. Bcl-2 overexpression prevents apoptosis induced by ceramidase inhibitors in malignant melanoma and HaCaT keratinocytes. *FEBS Lett* 2002; **516**: 47-52
11 **Zhang J**, Alter N, Reed JC, Borner C, Obeid LM, Hannun YA. Bcl-2 interrupts the ceramide-mediated pathway of cell death. *Proc Natl Acad Sci USA* 1996; **93**: 5325-5328
12 **Sawai H**, Okazaki T, Takeda Y, Tashima M, Sawada H, Okuma M, Kishi S, Umehara H, Domae N. Ceramide-induced translocation of protein kinase C-delta and -epsilon to the cytosol. Implications in apoptosis. *J Biol Chem* 1997; **272**: 2452-2458
13 **Haimovitz-Friedman A**, Kan CC, Ehleiter D, Persaud RS, McLoughlin M, Fuks Z, Kolesnick RN. Ionizing radiation acts on cellular membranes to generate ceramide and initiate apoptosis. *J Exp Med* 1994; **180**: 525-535
14 **Wang J**, Lv X, Shi J, Hu X. Ceramide induces apoptosis via a peroxisome proliferator-activated receptor gamma-dependent pathway. *Apoptosis* 2006; **11**: 2043-2052
15 **Xiao D**, Singh SV. Phenethyl isothiocyanate-induced apoptosis in p53-deficient PC-3 human prostate cancer cell line is mediated by extracellular signal-regulated kinases. *Cancer Res* 2002; **62**: 3615-3619
16 **Fang JY**, Lu YY. Effects of histone acetylation and DNA methylation on p21 (WAF1) regulation. *World J Gastroenterol* 2002; **8**: 400-405
17 **Chellappan SP**, Giordano A, Fisher PB. Role of cyclin-dependent kinases and their inhibitors in cellular differentiation and development. *Curr Top Microbiol Immunol* 1998; **227**: 57-103
18 **Kim JS**, Lee S, Lee T, Lee YW, Trepel JB. Transcriptional activation of p21 (WAF1/CIP1) by apicidin, a novel histone deacetylase inhibitor. *Biochem Biophys Res Commun* 2001; **281**: 866-871
19 **Rosen ED**, Sarraf P, Troy AE, Bradwin G, Moore K, Milstone DS, Spiegelman BM, Mortensen RM. PPAR gamma is required for the differentiation of adipose tissue in vivo and in vitro. *Mol Cell* 1999; **4**: 611-617
20 **Barak Y**, Nelson MC, Ong ES, Jones YZ, Ruiz-Lozano P, Chien KR, Koder A, Evans RM. PPAR gamma is required for placental, cardiac, and adipose tissue development. *Mol Cell* 1999; **4**: 585-595
21 **Chinetti G**, Griglio S, Antonucci M, Torra IP, Delerive P, Majd Z, Fruchart JC, Chapman J, Najib J, Staels B. Activation of proliferator-activated receptors alpha and gamma induces apoptosis of human monocyte-derived macrophages. *J Biol Chem* 1998; **273**: 25573-25580
22 **Takahashi N**, Okumura T, Motomura W, Fujimoto Y, Kawabata I, Kohgo Y. Activation of PPARgamma inhibits cell growth and induces apoptosis in human gastric cancer cells. *FEBS Lett* 1999; **455**: 135-139
23 **Chen J**, Larochelle S, Li X, Suter B. Xpd/Ercc2 regulates CAK activity and mitotic progression. *Nature* 2003; **424**: 228-232
24 **Bushnell DA**, Westover KD, Davis RE, Kornberg RD. Structural basis of transcription: an RNA polymerase II-TFIIB cocrystal at 4.5 Angstroms. *Science* 2004; **303**: 983-988
25 **Oelgeschläger T**. Regulation of RNA polymerase II activity by CTD phosphorylation and cell cycle control. *J Cell Physiol* 2002; **190**: 160-169
26 **Westermarck J**, Li SP, Kallunki T, Han J, Kähäri VM. p38 mitogen-activated protein kinase-dependent activation of protein phosphatases 1 and 2A inhibits MEK1 and MEK2 activity and collagenase 1 (MMP-1) gene expression. *Mol Cell Biol* 2001; **21**: 2373-2383
27 **Garg TK**, Chang JY. Oxidative stress causes ERK phosphorylation and cell death in cultured retinal pigment epithelium: prevention of cell death by AG126 and 15-deoxy-delta 12, 14-PGJ2. *BMC Ophthalmol* 2003; **3**: 5
28 **Choi YJ**, Lim SY, Woo JH, Kim YH, Kwon YK, Suh SI, Lee

SH, Choi WY, Kim JG, Lee IS, Park JW, Kwon TK. Sodium orthovanadate potentiates EGCG-induced apoptosis that is dependent on the ERK pathway. *Biochem Biophys Res Commun* 2003; **305**: 176-185

29 **Wang X**, Martindale JL, Holbrook NJ. Requirement for ERK activation in cisplatin-induced apoptosis. *J Biol Chem* 2000; **275**: 39435-39443

30 **Calabrese C**, Frank A, Maclean K, Gilbertson R. Medulloblastoma sensitivity to 17-allylamino-17-demethoxygeldanamycin requires MEK/ERKM. *J Biol Chem* 2003; **278**: 24951-24959

31 **Johnson GL**, Lapadat R. Mitogen-activated protein kinase pathways mediated by ERK, JNK, and p38 protein kinases. *Science* 2002; **298**: 1911-1912

32 **Smalley KS**. A pivotal role for ERK in the oncogenic behaviour of malignant melanoma? *Int J Cancer* 2003; **104**: 527-532

33 **Zheng B**, Fiumara P, Li YV, Georgakis G, Snell V, Younes M, Vauthey JN, Carbone A, Younes A. MEK/ERK pathway is aberrantly active in Hodgkin disease: a signaling pathway shared by CD30, CD40, and RANK that regulates cell proliferation and survival. *Blood* 2003; **102**: 1019-1027

S- Editor Liu Y **L- Editor** Lutze M **E- Editor** Lu W

PO Box 2345, Beijing 100023, China
www.wjgnet.com
wjg@wjgnet.com

World J Gastroenterol 2007 February 21; 13(7): 1135-1137
World Journal of Gastroenterology ISSN 1007-9327

CASE REPORT

Pancreatic metastasis of leiomyosarcoma in the right thigh: A case report

Yang Seok Koh, Jung Chul, Chol Kyoon Cho, Hyun Jong Kim

Yang Seok Koh, Jung Chul, Chol Kyoon Cho, Hyun Jong Kim, Division of Hepatobiliary & Pantreatic Surgery, Department of Surgery, Chonnam National University Medical School, Gwangju 501757, Korea
Correspondence to: Jung Chul Kim, Division of Hepatobiliary & pantreatic Surgery, Department of Surgery, Chonnam University Medical School, Hakdong 8, Donggu, Gwangju 501757, Korea. 3rdvivace@hanmail.net
Telephone: +82-62-2206456 Fax: +82-62-2271635
Received: 2006-12-07 Accepted: 2007-01-29

Abstract

Pancreatic tumors are primary in most of the cases. Pancreatic metastases associated with other primary malignancies, especially pancreatic metastasis of leiomyosarcoma, are uncommon. A 66-year-old woman underwent surgical resection of malignant mesenchymoma (70% osteosarcoma and 30% leiomyosarcoma) in the right thigh. In the postoperative period, a pancreatic mass was identified radiologically by abdominal computed tomography. Pylorus-preserving pancreaticoduodenectomy was performed. The surgical specimen revealed leiomyosarcoma metastasized to the pancreas. A metastatic nodule on the remnant pancreatic tail was discovered 9 mo after the first pancreatic resection, and distal pancreatectomy was performed. Cases of pancreatic metastasis from leiomyosarcoma are extremely rare, especially when the tumor was resectable. We report here a unique case of pancreatic metastasis from a leiomyosarcoma in the right thigh that had been treated surgically.

Key words: Pancreatic tumor; Leiomyosarcoma; Metastasis

Koh YS, Chul J, Cho CK, Kim HJ. Pancreatic metastasis of leiomyosarcoma in the right thigh: A case report. *World J Gastroenterol* 2007; 13(7): 1135-1137

http://www.wjgnet.com/1007-9327/13/1135.asp

INTRODUCTION

The occurrence of metastatic lesions in the pancreas is very uncommon. The incidence of metastatic pancreatic tumors is 1.6%-11% at autopsy[1,2]. The majority of patients with pancreatic metastasis have widespread diseases. Isolated, potentially resectable pancreatic metastasis is detected infrequently. Therefore, resection of metastatic tumors of the pancreas has been occasionally reported, and its role in improving the survival or quality of life is not clearly defined[3,4]. However, some recent studies have reported that surgical resection can be performed in selected patients with isolated pancreatic metastases, achieving long-term survival and good palliation[1,5]. We report here a case of pancreatic metastatic from leiomyosarcoma of the right anterior thigh, which was treated by surgical resection, and review the literature about pancreatic metastasis.

CASE REPORT

A 66-year-old woman was referred to our hospital with a mass in the right thigh (Figure 1). In September 2005, she had undergone surgical resection for this mass. Malignant mesenchymoma (70% osteosarcoma and 30% leiomyosarcoma) was diagnosed histologically. In the postoperative period, abdominal computed tomography (CT) identified a pancreatic mass. The patient complained of non-specific abdominal discomfort. Laboratory findings were all within normal limits. The levels of the tumor markers including carcinoembryonic agent and carbohydrate antigen 19-9, were within the normal ranges. Abdominal CT revealed a mass at the head of the pancreas. Magnetic resonance imaging of the abdomen showed a low-intensity mass on T1-weighted images and a non-homogeneous high-intensity mass on T2-weighted images. No evidence of other distant metastases was seen (Figure 1). At laparotomy, a fixed mass of 4 cm or so in length was palpated at the head of the pancreas, displacing the surrounding duodenum. Therefore, pylorus-preserving pancreaticoduodenectomy was performed. Macroscopic examination of the operative specimen showed a 4 cm × 3 cm lobulated solid mass with a thin wall. Microscopic examination revealed a malignant neoplasm with predominance of spindle cells. The tumor cells were immunoreactive for desmin. Metastatic leiomyosarcoma was diagnosed histologically (Figure 2). The postoperative course was uneventful. We recommended systemic chemotherapy to the patient, but she declined. Nine months after the first pancreatic resection, a follow-up abdominal CT showed development of a new 1-cm mass in the remnant tail of the pancreas (Figure 1). Distal

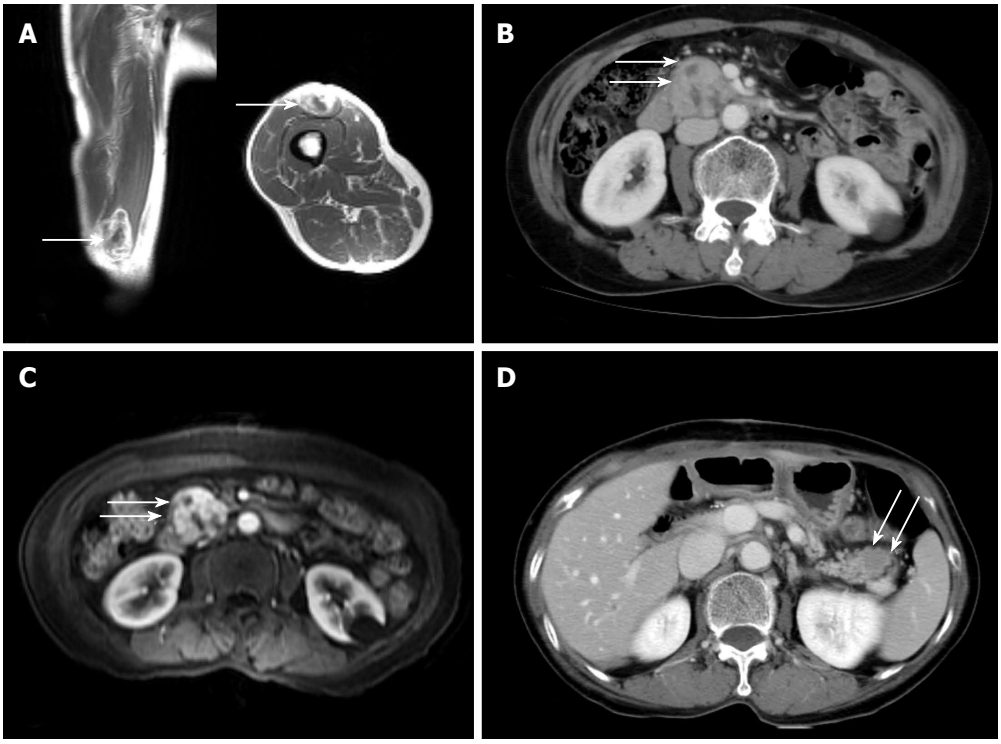

Figure 1 Radiological findings. **A**: Gadolinium-enhanced T1 weighted image showing a soft tissue tumor in the muscle of the anterior thigh; **B**: Contrast-enhanced abdominal CT scan showing a heterogeneously enhanced mass at the head of the pancreas; **C**: Gadolinium-enhanced T1 weighted image showing a well-enhanced mass with necrotic foci at the head of the pancreas; **D**: Follow-up CT obtained after 10 mo showing a low attenuated mass in the tail of the pancreas.

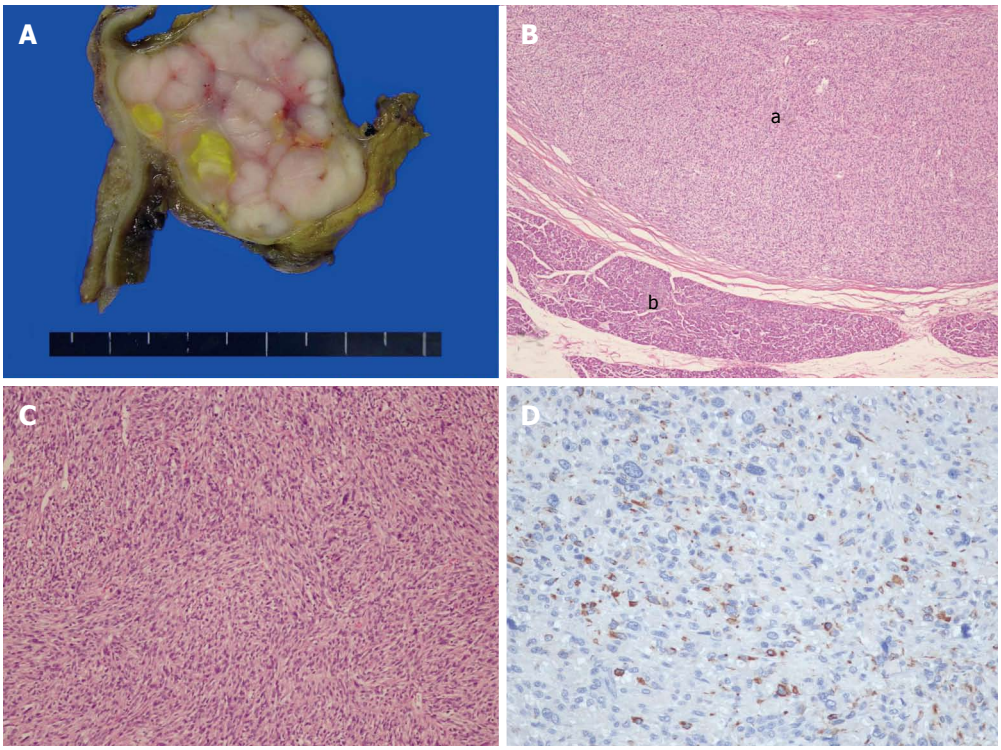

Figure 2 Gross and microscopic findings for metastatic leiomyosarcoma. **A**: The section reveals a whitish solid tumor with a lobulated pattern and a yellowish necrotic portion, abutting duodenal wall on the left side, and compressed pancreatic head tissue on the right side; **B**: Low-power view displaying eosinophilic intersecting fascicles circumscribed by a fibrous capsule (a) and adjacent normal pancreatic tissue (b) (hematoxylin and eosin stain × 40); **C**: Cellular proliferation of atypical spindle tumor cells is accompanied by nuclear atypia and hyperchromasia (hematoxylin and eosin stain × 200); **D**: Tumor cells show immunoreactivity for desmin.

pancreatectomy was performed. The tumor showed the same microscopic findings, and leiomyosarcoma was also diagnosed histologically.

DISCUSSION

Metastatic lesions in the pancreas are uncommon. Adsay *et al*[1] reviewed pathological specimens from 4955 adult autopsy cases in an attempt to identify tumors that had metastasized to the pancreas. There were only 81 (1.6%) cases of metastatic tumors, the majority of which were of epithelial origin, and the most common sites of the primary lesions were the lung, kidney, and gastrointestinal tract. However, a few cases of leiomyosarcoma with metastases to the pancreas have been reported. Primary sites of leiomyosarcomas included the uterus[6,7], ovary[8], veins[9], spermatic cord[10], intestine[3,10], retroperitoneum[2,11], and soft tissue[11,12]. To the best of our knowledge, including the present case, only 16 cases of pancreatic metastasis from leiomyosarcoma have been reported to

date in the English language literature[7,8,12].

The differential diagnosis between a solitary metastatic tumor and primary pancreatic carcinoma may be very difficult as signs and symptoms are similar for both primary and secondary tumors, and radiological imaging is unable to differentiate primary from secondary pancreatic lesions[13]. In our case, non-specific abdominal pain appeared to be the most common symptom. The symptoms of pancreatic metastases often include pain, weight loss, obstructive jaundice, and duodenal obstruction, which are very similar to the symptoms of primary pancreatic cancer[1,3,9]. Therefore, pre-operative diagnosis is challenging, and considerable caution is needed for patients with a previous history of non-pancreatic neoplastic disease. The pre-operative diagnosis of our case was primarily a non-functioning islet cell tumor of pancreas, although the patient had previously undergone surgical treatment for mesenchymoma of the left leg. Various diagnostic tools have been used to assess tumors. In recent years, 18-FDG-PET has proven to be useful for the accurate staging of tumors[3]. Percutaneous fine-needle aspiration (FNA) is found helpful in establishing the correct preoperative diagnosis, especially in patients who are not amenable to surgery, and in assisting in decisions related to the possibility and type of chemotherapy[3]. However, with the exception of postoperative histology, there is no definitive method for unambiguous diagnosis.

Metastatic tumors of the pancreas are usually diagnosed at an advanced stage, and solitary resectable metastasis occurs less frequently. Therefore, metastatic tumors of the pancreas are rarely treated surgically. Sperti *et al*[3] reported that 8/259 (3%) pancreatic resections were performed for pancreatic metastases. Therefore, our patient represents a very unusual case.

Only a few cases of pancreatic metastasis from sarcomas have been reported. Experience is limited, and the effectiveness of surgery for these types of lesions has not been clearly established. However, long-term survival may be conferred by "curative" resection for pancreatic metastasis from visceral or soft tissue sarcoma[3,7,9,14]. It is clear that surgical excision has the potential to improve prognosis if the primary site and other metastases are well-controlled. In the present unique case, pancreatic metastasis from leiomyosarcoma was diagnosed, and the patient underwent pancreatectomy twice in 10 mo. An attempt at complete tumor resection can offer patients the best hope of prolonged survival.

REFERENCES

1 **Crippa S**, Angelini C, Mussi C, Bonardi C, Romano F, Sartori P, Uggeri F, Bovo G. Surgical treatment of metastatic tumors to the pancreas: a single center experience and review of the literature. *World J Surg* 2006; **30**: 1536-1542

2 **Adsay NV**, Andea A, Basturk O, Kilinc N, Nassar H, Cheng JD. Secondary tumors of the pancreas: an analysis of a surgical and autopsy database and review of the literature. *Virchows Arch* 2004; **444**: 527-535

3 **Sperti C**, Pasquali C, Liessi G, Pinciroli L, Decet G, Pedrazzoli S. Pancreatic resection for metastatic tumors to the pancreas. *J Surg Oncol* 2003; **83**: 161-166; discussion 166

4 **Roland CF**, van Heerden JA. Nonpancreatic primary tumors with metastasis to the pancreas. *Surg Gynecol Obstet* 1989; **168**: 345-347

5 **Hiotis SP**, Klimstra DS, Conlon KC, Brennan MF. Results after pancreatic resection for metastatic lesions. *Ann Surg Oncol* 2002; **9**: 675-679

6 **Iwamoto I**, Fujino T, Higashi Y, Tsuji T, Nakamura N, Komokata T, Douchi T. Metastasis of uterine leiomyosarcoma to the pancreas. *J Obstet Gynaecol Res* 2005; **31**: 531-534

7 **Falconi M**, Crippa S, Sargenti M, Capelli P, Pederzoli P. Pancreatic metastasis from leiomyosarcoma of the broad ligament of the uterus. *Lancet Oncol* 2006; **7**: 94-95

8 **Nasu M**, Inoue J, Matsui M, Minoura S, Matsubara O. Ovarian leiomyosarcoma: an autopsy case report. *Pathol Int* 2000; **50**: 162-165

9 **Le Borgne J**, Partensky C, Glemain P, Dupas B, de Kerviller B. Pancreaticoduodenectomy for metastatic ampullary and pancreatic tumors. *Hepatogastroenterology* 2000; **47**: 540-544

10 **Wernecke K**, Peters PE, Galanski M. Pancreatic metastases: US evaluation. *Radiology* 1986; **160**: 399-402

11 **Nakamura E**, Shimizu M, Itoh T, Manabe T. Secondary tumors of the pancreas: clinicopathological study of 103 autopsy cases of Japanese patients. *Pathol Int* 2001; **51**: 686-690

12 **Boudghène FP**, Deslandes PM, LeBlanche AF, Bigot JM. US and CT imaging features of intrapancreatic metastases. *J Comput Assist Tomogr* 1994; **18**: 905-910

13 **Ishigure K**, Kaneko T, Takeda S, Inoue S, Kawase Y, Nakao A. Pancreatic metastasis from leiomyosarcoma in the back. *Hepatogastroenterology* 2003; **50**: 1675-1677

14 **Nakajima Y**, Kakizaki S, Kanda D, Shimada Y, Sohara N, Sato K, Takagi H, Mori M, Watanabe H. Pancreatic and gastric metastases of leiomyosarcoma arising in the left leg. *Int J Clin Oncol* 2005; **10**: 342-347

S- Editor Liu Y **L- Editor** Ma JY **E- Editor** Ma WH

PO Box 2345, Beijing 100023, China
www.wjgnet.com
wjg@wjgnet.com

World J Gastroenterol 2007 February 21; 13(7): 1138-1140
World Journal of Gastroenterology ISSN 1007-9327

CASE REPORT

A prophylactic approach for bone marrow transplantation from a hepatitis B surface antigen-positive donor

Abhasnee Sobhonslidsuk, Artit Ungkanont

Abhasnee Sobhonslidsuk, Artit Ungkanont, Department of Medicine, Faculty of Medicine, Ramathibodi Hospital, Mahidol University, Bangkok, Thailand
Correspondence to: Abhasnee Sobhonslidsuk, MD, Department of Medicine, Ramathibodi hospital, 270 Praram 6 Road, Rajathevee, Bangkok 10400, Thailand. teasb@mahidol.ac.th
Telephone: +66-2-2011304 Fax: +66-2-2011387
Received: 2006-12-14 Accepted: 2007-01-08

Abstract

It has been accepted that bone marrow transplantation (BMT) is the only curative therapeutic option for certain hematologic malignancies. The southeast Asia region is an endemic area of hepatitis B virus (HBV) infection; thus, BMT using a hepatitis B surface antigen (HBsAg)-positive donor is occasionally unavoidable. Organ transplantation using a HBsAg-positive donor can lead to post-transplantation de novo HBV infection and severe HBV-related hepatitis if no effective prophylactic measures are taken prior to and after transplantation. In this report, a four-level approach was designed for a patient with chronic myeloid leukemia, beginning with a booster HBV vaccination before performing BMT with a HBsAg-positive donor. Prior to BMT, the HBV viral load of the donor was reduced to an undetectable level by antiviral therapy. After BMT, hepatitis B immunoglobulin was administered intramuscularly for 1 wk together with a long-term antiviral drug, lamivudine. One year after discontinuation of lamivudine, the patient is still free of HBV infection.

Key words: Bone marrow transplantation; Hepatitis B virus; Vaccination; Hepatitis B immunoglobulin; Lamivudine.

Sobhonslidsuk A, Ungkanont A. A prophylactic approach for bone marrow transplantation from a hepatitis B surface antigen-positive donor. *World J Gastroenterol* 2007; 13(7): 1138-1140

http://www.wjgnet.com/1007-9327/13/1138.asp

INTRODUCTION

Certain hematologic malignancies can only be cured by bone marrow transplantation (BMT). In the southeast Asian region, hepatitis B virus (HBV) infection is highly prevalent. BMT from donors exhibiting the hepatitis B surface antigen (HBsAg) is therefore occasionally unavoidable. Intensive chemotherapeutic drugs used in a conditioning regimen and post-transplantion immunosuppressive drugs are required to suppress host immunity and to prevent graft versus host disease (GVHD). Using grafts with HBsAg-positive hematopoietic stem cells is associated with severe liver injury and a high mortality rate[1-3]. In this report, we present a long-term follow-up study of a seronegative patient who underwent BMT with a HBsAg-positive donor in which a four-level approach for the prevention of HBV infection was utilized.

CASE REPORT

A thirty-seven year old man, a known case of chronic myeloid leukemia with positive Philadelphia chromosome in chronic phase, was previously treated with hydroxyurea. The patient planned to receive BMT from his sole HLA-identical sibling, his sister, who had been a known hepatitis B carrier. She was anti-HBe positive and had an HBV viral load of 5260 copies/mL, as indicated by the Amplicor HBV Monitor Test (Roche Diagnostics, NJ, USA). Lamivudine (100 mg/d) was initiated to suppress HBV DNA; and 3 mo later, her HBV viral load became undetectable. His antibody to HBsAg (anti-HBs) was firstly positive at a level of 10.3 mIU/mL. A booster dose of hepatitis B vaccine was given to him, and the subsequent anti-HBs level rose to 83 mIU/mL. A conditioning regimen for BMT containing busulfan (16 mg/kg) and cyclophosphamide (120 mg/kg) was started before the initiation of BMT. GVHD was prevented using methotrexate and tacrolimus. Lamivudine (100 mg/d) was initiated 7 d prior to BMT and was continued thereafter. From the day of BMT to the 7th d post-BMT, hepatitis B immunoglobulin (HBIg) 800 IU was injected intramuscularly daily in order to maintain the anti-HBs level > 1000 IU/L. From the 7th d post-BMT, the anti-HBs level was persistently over 1000 IU/L without HBIG administration. One month after BMT, while on tacrolimus for GVHD suppression and lamivudine for HBV prophylaxis, the patient's blood test results were as follows: HBsAg negative, anti-HBs positive (at 400 mIU/mL), anti-HBc positive, HBV viral load < 200 copies per ml and HBV PCR positive. HBV PCR became negative by 6 mo after BMT. The patient had only grade I acute GVHD and limited chronic GVHD. Tacrolimus was gradually tapered

off and then discontinued at the 15th mo post-BMT, and lamivudine was stopped 3 mo later. Two and a half years after BMT or 1 year after discontinuation of lamivudine, the patient felt well, and his blood tests indicated that he was HBsAg negative, anti-HBc positive, anti-HBs positive (at 14 mIU/mL) and HBV PCR negative.

DISCUSSION

The Asia-Pacific region is an endemic area of HBV infection, with a prevalence of more than 8%[4]. Most transplantation centers have regarded HBV infection as a relative contraindication for organ transplantation[5,6]. BMT with HBsAg-positive donors has been reported to be associated with an increased incidence of HBV-related hepatitis, severe liver-related complications, fatal liver failure and death[1,2,6-11]. However, a few reports show that HBsAg might be present transiently in some patients after receiving bone marrow graft from HBsAg-positive donors[1,2]. High HBV viral load in BMT donors and the absence of anti-HBs in BMT patients are two important risk factors predisposing a patient to the development of HBV-related hepatitis post-BMT[1,2]. Oral antiviral drugs are suitable to decrease the HBV viral load of the HBsAg-positive BMT donor. Lamivudine seems to be an appropriate antiviral drug in this situation because it causes rapid viral load reduction and because HBV resistance rarely occurs in a short period of lamivudine treatment[12]. Before BMT, the anti-HBs level in the present case report was increased to 83 mIU/mL by a booster dose of HBV vaccination. In general, the persistence of anti-HBV activity after BMT may be caused by residual recipient lymphocytes that have survived intensive conditioning regimens[3]. We decided to administer HBIg intramuscular injection from d 0 to d 8 post-BMT because the residual number of patient lymphocytes was uncertain. Anti-HBs level monitoring during the early post-BMT period showed that anti-HBs levels were over 1000 mIU/mL, resulting in the decision to discontinue HBIg 7 d post-BMT. HBIg was injected intramuscularly according to the protocol employed in HBV-related liver transplantation[13]. The mechanisms by which HBIg prevents graft re-infection are not completely understood. They may decrease the spread of HBV infection by neutralizing circulating viral particles and by inducing lyses of infected cells through pathways such as antibody-dependent cellular cytotoxicity[13]. Combination therapy of HBIg and lamivudine offers synergistic protection against HBV infection and appears to be more effective than a single agent for prophylaxis after HBV-related liver transplantation[13]. A recent study proposed a three-level approach when hematopoietic stem cell transplantation (HSCT) was performed with a HBV-positive donor[6]. The three-level approach consisted of a pre-HSCT reduction of HBV viral replication in donors by lamivudine, a pre-HSCT enhancement of the recipient's anti-HBV immunity by HBV vaccination, and finally, a post-HSCT suppression of HBV viral replication in recipients with lamivudine[6]. In that paper, patients received lamivudine for 52 wk after HSCT; however, our patient received lamivudine for 72 wk, and treatment with this drug was stopped 12 wk after the discontinuation of tacrolimus. A flare of HBV infection and severe hepatitis was reported if antiviral drug was withdrawn in patients with immunosuppressive status or upon completion of chemotherapy[14]. Continuing lamivudine for at least 3 mo after completion of chemotherapy or immunosuppressive drugs has been recommended by a recent practice guideline[15]. The HBV viral load, as determined by the Amplicor HBV monitor test used in this report, is far more sensitive than the Digene Hybrid Capture assay used in a previous report[6,16]. De novo HBV infection might appear in the long-term follow-up of antiviral-prophylactic BMT patients with HBV-positive donors whose viral load was determined to be negative using a low sensitivity assay. An additional benefit of post-transplantion HBIg may be anticipated in hematopoietic stem cell transplantation. Recently, HBIg and lamivudine treatment during BMT in a child who received BMT from her HBsAg-positive mother has been reported[17]. The child received lamivudine only 1 d before BMT and continued the drug for 102 d. The details of HBV viral load and HBV PCR, however, were not mentioned in that paper[17]. The authors suggested that HBIg and lamivudine combination may be useful during the early period of BMT[17]. Intramuscular injection of HBIg sometimes requires the correction of thrombocytopenia or changing the route of administration from intramuscular to intravenous injection. Due to the large dosage of intravenous HBIg and its high cost, it may not be affordable for all patients. Our strategies for using BMT from HBsAg-positive donors will require multicenter studies with a large number of patients and a longer follow-up before this costly, four-level prophylactic approach can be put into practice.

REFERENCES

1 **Locasciulli A**, Alberti A, Bandini G, Polchi P, Arcese W, Alessandrino P, Bosi A, Testa M, Bacigalupo A. Allogeneic bone marrow transplantation from HBsAg+ donors: a multicenter study from the Gruppo Italiano Trapianto di Midollo Osseo (GITMO). *Blood* 1995; **86**: 3236-3240

2 **Lau GK**, Lie AK, Kwong YL, Lee CK, Hou J, Lau YL, Lim WL, Liang R. A case-controlled study on the use of HBsAg-positive donors for allogeneic hematopoietic cell transplantation. *Blood* 2000; **96**: 452-458

3 **Hui CK**, Cheung WW, Chan SC, Lo CM, Lau GK. Hepatitis B vaccination and preemptive treatment of hepatitis B virus in liver transplantation. *Curr Opin Organ Transplant* 2006; **11**: 594-598

4 **Lesmana LA**, Leung NW, Mahachai V, Phiet PH, Suh DJ, Yao G, Zhuang H. Hepatitis B: overview of the burden of disease in the Asia-Pacific region. *Liver Int* 2006; **26** Suppl 2: 3-10

5 **Guideline on the microbiological safety of human organs, tissues and cells used in transplantation: Advisory committee on the microbiological safety of board and tissues for transplantation**. United Kingdom Department of Health. August 2000

6 **Hui CK**, Lie A, Au WY, Ma SY, Leung YH, Zhang HY, Sun J, Cheung WW, Chim CS, Kwong YL, Liang R, Lau GK. Effectiveness of prophylactic Anti-HBV therapy in allogeneic hematopoietic stem cell transplantation with HBsAg positive donors. *Am J Transplant* 2005; **5**: 1437-1445

7 **McIvor C**, Morton J, Bryant A, Cooksley WG, Durrant S, Walker N. Fatal reactivation of precore mutant hepatitis B

virus associated with fibrosing cholestatic hepatitis after bone marrow transplantation. *Ann Intern Med* 1994; **121**: 274-275

8 **Caselitz M**, Link H, Hein R, Maschek H, Böker K, Poliwoda H, Manns MP. Hepatitis B associated liver failure following bone marrow transplantation. *J Hepatol* 1997; **27**: 572-577

9 **Cooksley WG**, McIvor CA. Fibrosing cholestatic hepatitis and HBV after bone marrow transplantation. *Biomed Pharmacother* 1995; **49**: 117-124

10 **Lau GK**, Liang R, Chiu EK, Lee CK, Lam SK. Hepatic events after bone marrow transplantation in patients with hepatitis B infection: a case controlled study. *Bone Marrow Transplant* 1997; **19**: 795-799

11 **Martin BA**, Rowe JM, Kouides PA, DiPersio JF. Hepatitis B reactivation following allogeneic bone marrow transplantation: case report and review of the literature. *Bone Marrow Transplant* 1995; **15**: 145-148

12 **Liaw YF**, Leung N, Guan R, Lau GK, Merican I, McCaughan G, Gane E, Kao JH, Omata M. Asian-Pacific consensus statement on the management of chronic hepatitis B: a 2005 update. *Liver Int* 2005; **25**: 472-489

13 **Villamil FG**. Prophylaxis with anti-HBs immune globulins and nucleoside analogues after liver transplantation for HBV infection. *J Hepatol* 2003; **39**: 466-474

14 **Hui CK**, Cheung WW, Au WY, Lie AK, Zhang HY, Yueng YH, Wong BC, Leung N, Kwong YL, Liang R, Lau GK. Hepatitis B reactivation after withdrawal of pre-emptive lamivudine in patients with haematological malignancy on completion of cytotoxic chemotherapy. *Gut* 2005; **54**: 1597-1603

15 **Keeffe EB**, Dieterich DT, Han SH, Jacobson IM, Martin P, Schiff ER, Tobias H, Wright TL. A treatment algorithm for the management of chronic hepatitis B virus infection in the United States: an update. *Clin Gastroenterol Hepatol* 2006; **4**: 936-962

16 **Lok AS**, McMahon BJ. Chronic hepatitis B: update of recommendations. *Hepatology* 2004; **39**: 857-861

17 **Tavil B**, Kuşkonmaz B, Kasem M, Demir H, Cetin M, Uçkan D. Hepatitis B immunoglobulin in combination with lamivudine for prevention of hepatitis B virus reactivation in children undergoing bone marrow transplantation. *Pediatr Transplant* 2006; **10**: 966-969

S- Editor Wang J **L- Editor** Ma JY **E- Editor** Ma WH

PO Box 2345, Beijing 100023, China
www.wjgnet.com
wjg@wjgnet.com

World J Gastroenterol 2007 February 21; 13(7): 1141-1143
World Journal of Gastroenterology ISSN 1007-9327

CASE REPORT

Lipoma within inverted Meckel's diverticulum as a cause of recurrent partial intestinal obstruction and hemorrhage: A case report and review of literature

Güldeniz Karadeniz Cakmak, Ali Ugur Emre, Oge Tascilar, Sibel Bektaş, Bulent Hamdi Uçan, Oktay Irkorucu, Kemal Karakaya, Yucel Ustundag, Mustafa Comert

Güldeniz Karadeniz Cakmak, Ali Ugur Emre, Oge Tascilar, Bulent Hamdi Uçan, Oktay Irkorucu, Kemal Karakaya, Mustafa Comert, Department of Surgery, Zonguldak Karaelmas University, School of Medicine, Kozlu-Zonguldak, Turkey
Sibel Bektaş, Department of Pathology, Zonguldak Karaelmas University, School of Medicine, Kozlu-Zonguldak, Turkey
Yucel Ustundag, Department of Gastroenterology, Zonguldak Karaelmas University, School of Medicine, Kozlu-Zonguldak, Turkey
Correspondence to: Dr. Güldeniz Karadeniz Cakmak, Zonguldak Karaelmas Universitesi, Arastirma ve Uygulama Hastanesi Bashekimligi, Kozlu-Zonguldak 67600, Turkey. gkkaradeniz@yahoo.com
Telephone: +90-372-2610159
Received: 2006-11-24 Accepted: 2007-01-15

Abstract

Lipoma within an inverted Meckel's diverticulum presenting with hemorrhage and partial intestinal obstruction is an exceptional clinical entity. We report a case of 47-year-old male with a history of recurrent episodes of partial intestinal obstruction and melena due to a subserosal lipoma located in the base of an inverted Meckel's diverticulum. According to our knowledge, this is the first case of a lipoma within a Meckel's diverticulum giving rise to this clinical scenario without the existence of heterotrophic gastric or pancreatic tissues.

Key words: Meckel's diverticulum; Lipoma; Inversion; Intestinal obstruction; Hemorrhage

Karadeniz Cakmak G, Emre AU, Tascilar O, Bektaş S, Ucan BH, Irkorucu O, Karakaya K, Ustundag Y, Comert M. Lipoma within inverted Meckel's diverticulum as a cause of recurrent partial intestinal obstruction and hemorrhage: A case report and review of literature. *World J Gastroenterol* 2007; 13(7): 1141-1143

http://www.wjgnet.com/1007-9327/13/1141.asp

INTRODUCTION

Tumor of Meckel's diverticulum occurs infrequently. Moreover, the association of a lipoma within the inverted Meckel's diverticulum as a leading point of bleeding and recurrent episodes of partial intestinal obstruction is such an unusual circumstance that might be considered quite impossible.

Meckel's diverticulum is the most prevalent congenital anomaly of the gastrointestinal tract, which is reported to occur in 1%-3% of the general population and autopsy series[1,2]. However, the lifetime risk of complication development in patients with Meckel's diverticulum was proposed to be less than 5% in recent investigations[3]. These complications included intestinal obstruction, intussusceptions, inflammation and bleeding.

Lipomas are the rare benign tumors of the small intestine with no malignant potential and mostly encountered incidentally during investigation of the gastrointestinal tract for another reason, since they are usually asymptomatic[4]. As small intestinal lipoma is relatively infrequent, it is even a rarer source of gastrointestinal bleeding.

We present a case of a 47-year-old man with fatigue, chronic abdominal pain and tarry stool due to an inverted Meckel's diverticulum with a subserosal lipoma. This is a special case that has not appeared in literature over the past 4 decades. Although the incidence of Meckel's diverticulum is high, inversion is a scarsely diagnosed entity and the association of a lipoma within the inverted Meckel's diverticulum as a leading point of lower gastrointestinal hemorrhage without the existence of heterotopic gastric and pancreatic tissues and recurrent partial intestinal obstruction is an exceptional case.

CASE REPORT

A 47-year-old man was admitted to our clinic with fatigue, recurrent episodes of constipation and abdominal pain. Melena was mentioned on admission. He denied vomiting, fever, or chills. He had had symptoms intermittently for about 4 mo, leading to several hospital visits. Over the previous 2 mo, the episodes of pain became more pronounced with radiation to his back. The patient was not using any specific medication and his medical history did not suggest a major disease. Physical examination revealed a temperature of 37℃, a pulse rate of 90 beats per minute (bpm), a blood pressure of 110/70 mmHg, and a respiration rate of 18 breaths per minute. The

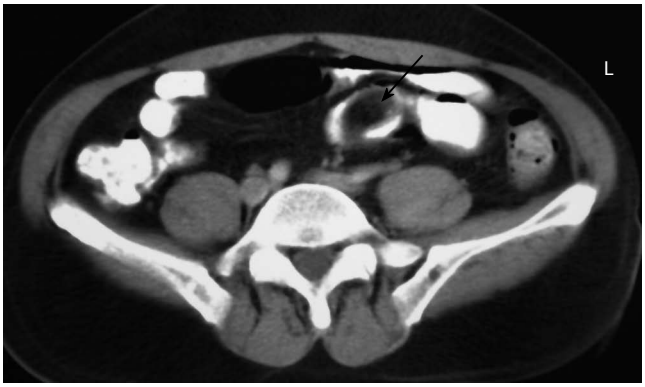

Figure 1 Contrast enhanced CT shows a hypodens, regular contoured, polypoid, 4 cm × 2 cm mass lesion with fatty density.

Figure 2 A pedinculated mass lesion within the inverted Meckel's diverticulum.

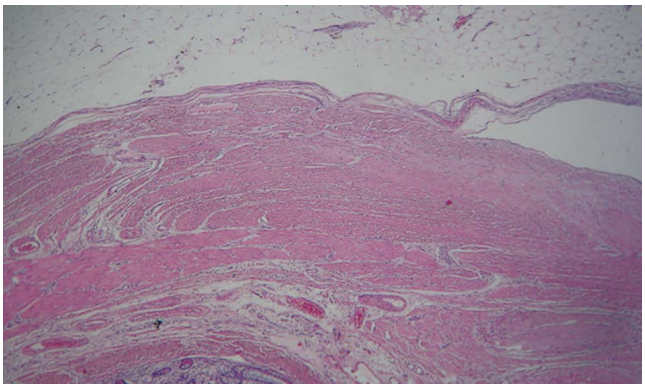

Figure 3 Microscopic appearance of a subserosal lipoma within the inverted Meckel's diverticulum (HE).

patient was pale-looking without abdominal tenderness, guarding or rebound and norm active bowel sounds were auscultated. Examination of heart and lungs revealed no abnormal findings. Rectal examination revealed tarry fecal content. Clear gastric content was obtained on nasogastric aspiration. The initial laboratory workup was as follows: hematocrit, 33%; hemoglobin, 11.2 g/dL; white blood cells, 10 500/mm^3 with a normal differential count; platelets, 195 000/mm^3; blood glucose, 87 mg/dL; blood urea, 25 mg/dL; creatinine, 0.8 mg/dL; SGOT, 32 IU/L; SGPT,25 IU/L; LDH, 54 IU/L; total bilirubin, 0.4 mg/dL; direct bilirubin, 0.2 mg/dL; and Na+, 138 meq/L; andK+, 3.7meq/L. Fecal occult blood test was positive. A gastrointestinal cause was sought in order to explain the patient's hemorrhage. He had received upper and lower gastrointestinal tract endoscopic examinations without identification of a specific bleeding etiology except a little amount of blood residue in terminal ileum. A computed tomography (CT) scan of the abdomen and pelvis revealed mildly dilated loops of proximal small bowel and a polypoid, 4 cm × 2 cm mass lesion with fatty density localized in the left lower quadrant and a suspicious filling defect in cecum (Figure 1). A pedinculated lipoma was assumed to be the underlying cause of recurrent partial intestinal obstruction and bleeding. He was taken to the operating room with the diagnosis of symptomatic small bowel lipoma. At surgery, an inverted Meckel's diverticulum induced by a pedinculated subserosal lipomatous solid mass nearly obstructing the lumen with ulcer and hemorrhage was found 40 cm from the ileocecal valve (Figure 2). Segmental resection of the ileal loop harboring the lesion was carried out and an end-to-end ileo-ileal anastomosis was performed. The lipoma within the inverted Meckel's diverticulum as a leading point of obstruction and bleeding was 5 cm long and 3 cm in diameter. Pathologic evaluation of the specimen confirmed the diagnosis of a subserosal lipoma within the inverted Meckel's diverticulum and revealed neither heterotrophic gastric and pancreatic tissue nor signs of malignancy (Figure 3). Five days after intervention, the patient was discharged from the hospital without any complication.

DISCUSSION

The omphalomesenteric duct connects the mid gut and yolk sac in seven weeks of gestation and during the eighth week, it normally undergoes obliteration[5]. Under circumstances of failure or incomplete vitelline duct obliteration, a spectrum of abnormalities appears, the most common of which is Meckel's diverticulum. Omphalomesenteric fistula, enterocysts or a fibrous band connecting the small intestine to the umbilicus are the other pathologies that can be encountered. As the location of the Meckel's diverticulum varies among individuals, they are usually detected in the antimesenteric side of the ileum within 100 cm of ileocecal valve. Meckel's diverticulum possesses various complication risks including intestinal obstruction, intussusception, inflammation and bleeding. Inversion of a Meckel's diverticula is a scarse entity with a potential of intestinal obstruction due to direct luminal obliteration or causing a lead point for intussusception[6-8]. The pathophysiology of the disease process leads to a complicated and confusing clinical picture of recurrent obstructive symptoms, chronic abdominal pain and lower gastrointestinal bleeding that may cause a delay in diagnosis and waste time. In our case, we have detected a lipoma as a leading point of inversion which causes partial obstruction and bleeding. Recurrent partial obstructive periods and abdominal pain of our patient might be attributed to luminal obstruction due to inversion

of Meckel's diverticulum which might be induced by lipomatous development. An other possible mechanism for this symptomatology might be the probable intussusseptions according to the inverted diverticulum, which has been reported as a lead point previously[6,7]. Intestinal obstruction due to intussusception as a result of a lipoma within Meckel's diverticulum has only been reported twice in literature[9,10]. Primary pathophysiologic process responsible for bleeding in Meckel's diverticulum is the ileal mucosal ulceration due to the existence of heterotrophic gastric or pancreatic tissues which has not been verified in our patient; instead a subserosal lipoma has been demonstrated with ulceration and hemorrhage.

Lipomas of the small intestine are the second most common benign tumors next to leiomyomas[11]. Their location and the peak age vary, however approximately 50% were found in the ileum, and the sixth to seventh decades of life were considered to be the most risky period[4,11]. In general, lipomas are defined to originate in the submucosal layer and are usually solitary, with variable sizes ranging from 1 cm to 30 cm[12]. They usually appear as a sessile protrusion into the lumen of the intestine. Due to motor activity of underlying muscularis propria, they tend to extrude into the bowel wall or through the luminal area progressively, which might be the responsible reason for the inversion of the Meckel's diverticulum in our case. In this manner, a pseudopedicle is formed, providing a polypoid appearance to the lesion. Although the majority of these lesions are asymptomatic and detected incidentally during the routine examinations or in surgical specimen removed for various other reasons, on rare occasions they might present with symptoms depending on their size and location. Lipomas smaller than 1 cm are generally incapable of producing symptoms, however 75% of lipomas with a size > 4 cm might give rise to gastrointestinal symptoms. Intestinal obstruction is one of the major result due to the occlusion of lumen by a large protruding lesion. Hemorrhage which is an other possible consequence might be based on an ulceration of the overlying mucosa caused by direct pressure from the lipoma or due to intussusception per se[4,12]. Preoperative diagnosis of small intestinal lipomas can be established by means of endoscopic and radiologic evaluation. Radiolucency and the so-called "squeeze sign" implying an altered configuration during peristalsis are suggestive findings observed in small intestinal series. Detection of fatty tissue density within the mass on CT scans supports the diagnosis. The "naked fat sign" which can be defined as the protrusion of fat through mucosal disruption following multiple biopsy sampling of the submucosal mass during endoscopic examination is believed to be pathognomonic[4,11].

Although more common in children, the complications of Meckel's diverticulum have also been described in adults. Gastrointestinal bleeding and intestinal obstruction are the two most common clinical problems associated with Meckel's diverticulum. Tumor within a Meckel's diverticulum is a scarce clinical entity with a reported incidence of only 2%[13]. Intestinal obstruction caused by a lipoma within the Meckel's diverticulum is so uncommon that we could only find three cases in the literature, two of which were due to intussusception[9,10], and one case of direct lumen occlusion by a large protruding lesion[14]. Moreover, the association of gastrointestinal hemorrhage and recurrent episodes of partial intestinal obstruction caused by a subserosal lipoma within an inverted Meckel's diverticulum without the existence of heterotrophic gastric or pancreatic tissue is an exceptional case, which has not been reported over the last 40 years in literature.

REFERENCES

1 **Soderlund S**. Meckel's diverticulum. A clinical and histologic study. *Acta Chir Scand Suppl* 1959; Suppl **248**: 1-233
2 **Yahchouchy EK**, Marano AF, Etienne JC, Fingerhut AL. Meckel's diverticulum. *J Am Coll Surg* 2001; **192**: 658-662
3 **Leijonmarck CE**, Bonman-Sandelin K, Frisell J, Räf L. Meckel' s diverticulum in the adult. *Br J Surg* 1986; **73**: 146-149
4 **Fernandez MJ**, Davis RP, Nora PF. Gastrointestinal lipomas. *Arch Surg* 1983; **118**: 1081-1083
5 **DeBartolo HM**, van Heerden JA. Meckel's diverticulum. *Ann Surg* 1976; **183**: 30-33
6 **Dujardin M**, de Beeck BO, Osteaux M. Inverted Meckel's diverticulum as a leading point for ileoileal intussusception in an adult: case report. *Abdom Imaging* 2002; **27**: 563-565
7 **Steinwald PM**, Trachiotis GD, Tannebaum IR. Intussusception in an adult secondary to an inverted Meckel's diverticulum. *Am Surg* 1996; **62**: 889-894
8 **Konstantakos AK**. Meckel's diverticulum-induced ileocolonic intussusception. *Am J Surg* 2004; **187**: 557-558
9 **Ahmed HU**, Wajed S, Krijgsman B, Elliot V, Winslet M. Acute abdomen secondary to a Meckel's lipoma. *Ann R Coll Surg Engl* 2004; **86:** W4-W5
10 **Formejster I**, Mattern R. Ileus due to ileo-cecal intussusception caused by lipoma coexistent with Meckel's diverticulum. *Wiad Lek* 1971; **24**: 1101
11 **Olmsted WW**, Ros PR, Hjermstad BM, McCarthy MJ, Dachman AH. Tumors of the small intestine with little or no malignant predisposition: a review of the literature and report of 56 cases. *Gastrointest Radiol* 1987; **12**: 231-239
12 **Zografos G**, Tsekouras DK, Lagoudianakis EE, Karantzikos G. Small intestinal lipoma as a cause of massive gastrointestinal bleeding identified by intraoperative enteroscopy. A case report and review of the literature. *Dig Dis Sci* 2005; **50**: 2251-2254
13 **Williams RS**. Management of Meckel's diverticulum. *Br J Surg* 1981; **68**: 477-480
14 **Krespis EN**, Sakorafas GH. Partial intestinal obstruction caused by a lipoma within a Meckel's diverticulum. *Dig Liver Dis* 2006; **38**: 358-359

S- Editor Liu Y **L- Editor** Ma JY **E- Editor** Ma WH

PO Box 2345, Beijing 100023, China
www.wjgnet.com
wjg@wjgnet.com

World J Gastroenterol 2007 February 21; 13(7): 1144
World Journal of Gastroenterology ISSN 1007-9327

ACKNOWLEDGMENTS

Acknowledgments to Reviewers of *World Journal of Gastroenterology*

Many reviewers have contributed their expertise and time to the peer review, a critical process to ensure the quality of *World Journal of Gastroenterology*. The editors and authors of the articles submitted to the journal are grateful to the following reviewers for evaluating the articles (including those were published and those were rejected in this issue) during the last editing period of time.

Akira Andoh, MD
Department of Internal Medicine, Shiga University of Medical Science, Seta Tukinowa, Otsu 520-2192, Japan

Taku Aoki, MD
Division of Hepato-Biliary-Pancreatic and Transplantation Surgery, Department of Surgery, Graduate School of Medicine, University of Tokyo,7-3-1 Hongo, Bunkyo-ku, Tokyo, 113-8655, Japan

Hitoshi Asakura, Director, Emeritus Professor
International Medical Information Center, Shinanomachi Renga Bldg.35, Shinanomachi, Shinjukuku, Tokyo 160-0016, Japan

Olivier Barbier
CHUQ-CHUL Research Center, 2705 Laurier Boulevard, Québec G1V 4G2, Canada

Yusuf Bayraktar, Professor
Department of Gastroenterology, School of Medicine, Hacettepe University, Ankara 06100, Turkey

Flavia Bortolotti, Dr
Clinica Medica 5, Via Giustiniani 2, 35100 Padova, Italy

Katja Breitkopf, Dr
Department of Medicine II, University Hospital Mannheim, University of Heidelberg, Theodor-Kutzer-Ufer 1-3, 68167 Mannheim, Germany

Paolo Del Poggio, Dr
Hepatology Unit, Department of Internal Medicine, Treviglio Hospital, Piazza Ospedale 1, Treviglio Bg 24047, Italy

Olivier Detry, Dr
Department of Abdominal Surgery and Transplantation, University of Liège, CHU Sart Tilman B35, B-4000 Liège, Belgium

Curt Einarsson, Professor
Department of Medicine, Karolinska institute, Karolinska University Hospital Huddinge, Dept of Gastroenterology and Hepatology, K 63, Huddinge SE-141 86, Sweden

Nikolaus Gassler, Professor
Institute of Pathology, University Hospital RWTH Aachen, Pauwelsstrasse 30, 52074 Aachen, Germany

Pietro Invernizzi, Dr
Division of Internal Medicine, Department of Medicine, Surgery, Dentistry, San Paolo School of Medicine, University of Milan, Via Di Rudinfi 8, 20142 Milan, Italy

Jonathan D Kaunitz, MD
Building 114, Suite 217, West Los Angeles VA Medical Center, 11301 Wilshire Boulevard, Los Angeles, California 90073, United States

Zahariy Krastev, Professor
Department of Gastroneterology, Universiti Hospital "St. Ivan Rilski",#15, blvd "Acad. Ivan Geshov", Sofia 1431, Bulgaria

Michael Kremer, MD
Skipper Bowles Center for Alcohol Studies, CB# 7178, 3011 Thurston-Bowles Building, University of North Carolina, Chapel Hill, NC 27599, United States

John K Marshall, MD, Associate Professor of Medicine
Division of Gastroenterology (4W8), McMaster University Medical Centre, 1200 Main Street West, Hamilton, Ontario L8N 3Z5, Canada

Samuel Babafemi Olaleye, Dr
Department of Physiology, University of Ibadan, Ibadan, Nigeria, Ibadan 022, Nigeria

Satoshi Osawa, MD
First Department of Medicine, Hamamatsu University School of Medicine, 1-20-1 Handayama, Hamamatsu, 431-3192, Japan

Bo-Rong Pan, Professor
Outpatient Department of Oncology, The Fourth Military Medical University, 175 Changle West Road,Xi'an 710032, Shaanxi Province, China

Richard A Rippe, Dr
Department of Medicine, The University of North Carolina at Chapel Hill, Chapel Hill, NC 27599-7038, United States

Luis Rodrigo, Professor
Gastroenterology Service, Hospital Central de Asturias, c/ Celestino Villamil, s.n., Oviedo 33.006, Spain

Manuel Romero-Gómez, MD, Professor
Hepatology Unit, Hospital Universitario de Valme, Ctra de Cádiz s/n, Sevilla 41014, Spain

Heitor Rosa, Professor
Department of Gastroenterology and Hepatology, Federal University School of Medicine, Rua 126 n.21, Goiania - GO 74093-080, Brazil

Shawn David Safford, Dr
Department of Surgery, Duke University Medical Center, 994 West Ocean View Avenue, Norfolk VA23503, United States

Manfred V Singer, Professor
Department of Medicine II, University Hospital at Mannheim, Theodor-Kutzer-Ufer 1-3, Mannheim 68167, Germany

Zsuzsa Szondy, Professor
Department of Biochemistry and Molecular Biol, University of Debrecen, Debrecen H-4012, Hungary

Wei Tang, MD, EngD, Assistant Professor
H-B-P Surgery Division, Artificial Organ and Transplantation Division, Department of surgery, Graduate School of Medicine, The University of Tokyo, Tokyo 113-8655, Japan

Andrzej Tarnawski, Professor
VA Medical Center/University of California-Irvine, 5901 East 7th St, Long Beach, CA 90822-5201, United States

Harald Vogelsang, Professor
Gastroenterology, AKH- KIM IV, Wahringer G. 18-20, Vienna A-1090, Austria

Stefan Wirth, Professor Dr
Children's Hospital, Heusnerstt. 40, Wuppertal 42349, Germany

Daniel Lindsay Worthley, Dr
Department of Gastroenterology and Hepatology, Flinders Medical Centre, Room 3D230, Bedford Park, SA 5042, Australia

PO Box 2345, Beijing 100023, China
www.wjgnet.com
wjg@wjgnet.com

World J Gastroenterol 2007 February 21; 13(7): 1145
World Journal of Gastroenterology ISSN 1007-9327

Meetings

MAJOR MEETINGS COMING UP

Meeting Falk Research Workshop: Morphogenesis and Cancerogenesis of the Liver
25-26 January 2007
Goettingen
symposia@falkfoundation.de

Meeting Canadian Digestive Diseases Week (CDDW)
16-20 February 2007
Banff-AB
cagoffice@cag-acg.org
www.cag-acg.org/cddw/cddw2007.htm

Meeting Falk Symposium 158: Intestinal Inflammation and Colorectal Cancer
23-24 March 2007
Sevilla
symposia@falkfoundation.de

Meeting BSG Annual Meeting
26-29 March 2007
Glasgow
www.bsg.org.uk/

NEXT 6 MONTHS

Meeting 42nd Annual Meeting of the European Association for the Study of the Liver
11-15 April 2007
Barcelona
easl2007@easl.ch
www.easl.ch/liver-meeting/

Meeting Falk Symposium 159: IBD 2007 - Achievements in Research and Clinical Practice
4-5 May 2007
Istanbul
symposia@falkfoundation.de

Meeting European Society for Paediatric Gastroenterology, Hepatology and Nutrition Congress 2007
9-12 May 2007
Barcelona
espghan2007@colloquium.fr

Digestive Disease Week
19-24 May 2007
Washington Convention Center, Washington DC

Meeting Gastrointestinal Endoscopy Best Practices: Today and Tomorrow, ASGE Annual Postgraduate Course at DDW
23-24 May 2007
Washington-DC
tkoral@asge.org

Meeting ESGAR 2007 18th Annual Meeting and Postgraduate Course
12-15 June 2007
Lisbon
fca@netvisao.pt

Meeting Falk Symposium 160: Pathogenesis and Clinical Practice in Gastroenterology
15-16 June 2007
Portoroz
symposia@falkfoundation.de

Meeting ILTS 13th Annual International Congress
20-23 June 2007
Rio De Janeiro
www.ilts.org

Meeting 9th World Congress on Gastrointestinal Cancer
27-30 June 2007
Barcelona
meetings@imedex.com

EVENTS AND MEETINGS IN 2007

Meeting Falk Research Workshop: Morphogenesis and Cancerogenesis of the Liver
25-26 January 2007
Goettingen
symposia@falkfoundation.de

Meeting Canadian Digestive Diseases Week (CDDW)
16-20 February 2007
Banff-AB
cagoffice@cag-acg.org
www.cag-acg.org/cddw/cddw2007.htm

Meeting Falk Symposium 158: Intestinal Inflammation and Colorectal Cancer
23-24 March 2007
Sevilla
symposia@falkfoundation.de

Meeting BSG Annual Meeting
26-29 March 2007
Glasgow
www.bsg.org.uk/

Meeting 42nd Annual Meeting of the European Association for the Study of the Liver
11-15 April 2007
Barcelona
easl2007@easl.ch
www.easl.ch/liver-meeting/

Meeting Falk Symposium 159: IBD 2007 - Achievements in Research and Clinical Practice
4-5 May 2007
Istanbul
symposia@falkfoundation.de

Meeting European Society for Paediatric Gastroenterology, Hepatology and Nutrition Congress 2007
9-12 May 2007
Barcelona
espghan2007@colloquium.fr

Meeting Gastrointestinal Endoscopy Best Practices: Today and Tomorrow, ASGE Annual Postgraduate Course at DDW
23-24 May 2007
Washington-DC
tkoral@asge.org

Meeting ESGAR 2007 18th Annual Meeting and Postgraduate Course
12-15 June 2007
Lisbon
fca@netvisao.pt

Meeting Falk Symposium 160: Pathogenesis and Clinical Practice in Gastroenterology
15-16 June 2007
Portoroz
symposia@falkfoundation.de

Meeting ILTS 13th Annual International Congress
20-23 June 2007
Rio De Janeiro
www.ilts.org

Meeting 9th World Congress on Gastrointestinal Cancer
27-30 June 2007
Barcelona
meetings@imedex.com

Meeting 15th International Congress of the European Association for Endoscopic Surgery
4-7 July 2007
Athens
info@eaes-eur.org
congresses.eaes-eur.org/

Meeting 39th Meeting of the European Pancreatic Club
4-7 July 2007
Newcastle
www.e-p-c2007.com

Meeting XXth International Workshop on Heliobacter and related bacteria in cronic degistive inflammation
20-22 September 2007
Istanbul
www.heliobacter.org

Meeting Falk Workshop: Mechanisms of Intestinal Inflammation
10 October 2007
Dresden
symposia@falkfoundation.de

Meeting Falk Symposium 161: Future Perspectives in Gastroenterology
11-12 October 2007
Dresden
symposia@falkfoundation.de

Meeting Falk Symposium 162: Liver Cirrhosis - From Pathophysiology to Disease Management
13-14 October 2007
Dresden
symposia@falkfoundation.de

American College of Gastroenterology Annual Scientific Meeting
12-17 October 2007
Pennsylvania Convention Center
Philadelphia, PA

Meeting APDW 2007 - Asian Pacific Digestive Disease Week 2007
15-18 October 2007
Kobe
apdw@convention.co.jp
www.apdw2007.org

15th United European Gastroenterology Week, UEGW
27-31 October 2007
Le Palais des Congrès de Paris, Paris, France

Meeting The Liver Meeting® 2007 - 57th Annual Meeting of the American Association for the Study of Liver Diseases
2-6 November 2007
Boston-MA
www.aasld.org

Gastro 2009, World Congress of Gastroenterology and Endoscopy London, United Kingdom 2009

PO Box 2345, Beijing 100023, China
www.wjgnet.com
wjg@wjgnet.com

World J Gastroenterol 2007 February 21; 13(7): 1146-1148
World Journal of Gastroenterology ISSN 1007-9327

Instructions to authors

GENERAL INFORMATION

World Journal of Gastroenterology (*WJG, World J Gastroenterol* ISSN 1007-9327 CN 14-1219/R) is a weekly journal of more than 48 000 circulation, published on the 7th, 14th, 21st and 28th of every month.

Original Research, Clinical Trials, Reviews, Comments, and Case Reports in esophageal cancer, gastric cancer, colon cancer, liver cancer, viral liver diseases, *etc.*, from all over the world are welcome on the condition that they have not been published previously and have not been submitted simultaneously elsewhere.

Indexed and abstracted in

Current Contents®/Clinical Medicine, Science Citation Index Expanded (also known as SciSearch®) and Journal Citation Reports/Science Edition, *Index Medicus*, MEDLINE and PubMed, Chemical Abstracts, EMBASE/Excerpta Medica, Abstracts Journals, *Nature Clinical Practice Gastroenterology and Hepatology*, CAB Abstracts and Global Health. ISI JCR 2003-2000 IF: 3.318, 2.532, 1.445 and 0.993.

Published by

The WJG Press

SUBMISSION OF MANUSCRIPTS

Manuscripts should be typed double-spaced on A4 (297 mm × 210 mm) white paper with outer margins of 2.5 cm. Number all pages consecutively, and start each of the following sections on a new page: Title Page , Abstract, Introduction, Materials and Methods, Results, Discussion, acknowledgements, References, Tables, Figures and Figure Legends. Neither the editors nor the Publisher is responsible for the opinions expressed by contributors. Manuscripts formally accepted for publication become the permanent property of The WJG Press, and may not be reproduced by any means, in whole or in part without the written permission of both the authors and the Publisher. We reserve the right to put onto our website and copy-edit accepted manuscripts. Authors should also follow the guidelines for the care and use of laboratory animals of their institution or national animal welfare committee.

Authors should retain one copy of the text, tables, photographs and illustrations, as rejected manuscripts will not be returned to the author(s) and the editors will not be responsible for the loss or damage to photographs and illustrations in mailing process.

Online submission

Online submission is strongly advised. Manuscripts should be submitted through the Online Submission System at: http://www.wjgnet.com/index.jsp. Authors are highly recommended to consult the ONLINE INSTRUCTIONS TO AUTHORS (http://www.wjgnet.com/wjg/help/instructions.jsp) before attempting to submit online. Authors encountering problems with the Online Submission System may send an email you describing the problem to wjg@wjgnet.com for assistance. If you submit your manuscript online, do not make a postal contribution. A repeated online submission for the same manuscript is strictly prohibited.

Postal submission

Send 3 duplicate hard copies of the full-text manuscript typed double-spaced on A4 (297 mm × 210 mm) white paper together with any original photographs or illustrations and a 3.5 inch computer diskette or CD-ROM containing an electronic copy of the manuscript including all the figures, graphs and tables in native Microsoft Word format or *.rtf format to:

Editorial Office

World Journal of Gastroenterology
Editorial Department: Apartment 1066, Yishou Garden,
58 North Langxinzhuang Road,
PO Box 2345, Beijing 100023, China
E-mail: wjg@wjgnet.com
http: //www.wjgnet.com
Telephone: +86-10-85381892
Fax: +86-10-85381893

MANUSCRIPT PREPARATION

All contributions should be written in English. All articles must be submitted using a word-processing software. All submissions must be typed in 1.5 line spacing and in word size 12 with ample margins. The letter font is Tahoma. For authors from China, one copy of the Chinese translation of the manuscript is also required (excluding references). Style should conform to our house format. Required information for each of the manuscript sections is as follows:

Title page

Full manuscript title, running title, all author(s) name(s), affiliations, institution(s) and/or department(s) where the work was accomplished, disclosure of any financial support for the research, and the name, full address, telephone and fax numbers and email address of the corresponding author should be included. Titles should be concise and informative (removing all unnecessary words), emphasize what is new, and avoid abbreviations. A short running title of less than 40 letters should be provided. List the author(s)' name(s) as follows: initial and/or first name, middle name or initial(s) and full family name.

Abstract

An informative, structured abstract of no more than 250 words should accompany each manuscript. Abstracts for original contributions should be structured into the following sections: AIM: Only the purpose should be included. METHODS: The materials, techniques, instruments and equipments, and the experimental procedures should be included. RESULTS: The observatory and experimental results, including data, effects, outcome, *etc.* should be included. Authors should present *P* value where necessary, and the significant data should accompany. CONCLUSION: Accurate view and the value of the results should be included.

The format of structured abstracts is at: http://www.wjgnet.com/wjg/help/11.doc

Key words

Please list 5-10 key words that could reflect content of the study mainly from *Index Medicus*.

Text

For most article types, the main text should be structured into the following sections: INTRODUCTION, MATERIALS AND METHODS, RESULTS and DISCUSSION, and should include in appropriate Figures and Tables. Data should be presented in the body text or in Figures and Tables, but not in both.

Illustrations

Figures should be numbered as 1, 2, 3 and so on, and mentioned clearly in the main text. Provide a brief title for each figure on a separate page. No detailed legend should be involved under the figures. This part should be added into the text where the figures are applicable. Digital images: black and white photographs should be scanned and saved in TIFF format at a resolution of 300 dpi; color images should be saved as CMYK (print files) but not as RGB (screen-viewing files). Place each photograph in a separate file. Print images: supply images of size no smaller than 126 mm × 85 mm printed on smooth surface paper; label the image by writing the Figure number and orientation using an arrow. Photomicrographs: indicate the original magnification and stain in the legend. Digital Drawings: supply files in EPS if created by freehand and illustrator, or TIFF from photoshops. EPS files must be accompanied by a version in native file format for editing purposes. Existing line drawings should be scanned at a resolution of 1200 dpi and as close as possible to the size where they will appear when printed. Please use uniform legends for the same subjects. For example: Figure 1 Pathological changes of atrophic gastritis after treatment. A: ...; B: ...; C: ...; D: ...; E: ...; F: ...; G: ...

Tables

Three-line tables should be numbered as 1, 2, 3 and so on, and mentioned clearly in the main text. Provide a brief title for each table. No detailed legend should be included under the tables. This part should be added into the text where the tables are applicable. The information should complement but not duplicate that contained in the text. Use one horizontal line under the title, a second under the column heads, and a third below the Table, above any footnotes. Vertical and italic lines should be omitted.

Notes in tables and illustrations

Data that are not statistically significant should not be noted. $^{a}P<0.05$, $^{b}P<0.01$ should be noted ($P>0.05$ should not be noted). If there are other series of *P* values, $^{c}P<0.05$ and $^{d}P<0.01$ are used. Third series of *P* values can be expressed as $^{e}P<0.05$ and $^{f}P<0.01$. Other notes in tables or under

illustrations should be expressed as ^1F, ^2F, ^3F; or some other symbols with a superscript (Arabic numerals) in the upper left corner. In a multi-curve illustration, each curve should be labeled with ●, ○, ■, □, ▲, △, *etc.* in a certain sequence.

Acknowledgments

Brief acknowledgments of persons who have made genuine contributions to the manuscripts and who endorse the data and conclusions are included. Authors are responsible for obtaining written permission to use any copyrighted text and/or illustrations.

REFERENCES

Coding system

The author should code the references according the citation order in text in Arabic numerals, put references codes in square brackets, superscript it at the end of citation content or the author name of the citation. For those citation content as the narrate part, the coding number and square brackets should be typeset normally. For example, Crohn's disease (CD) is associated with increased intestinal permeability[1,2]. If references are directly cited in the text, they would be put together with the text, for example, from references [19,22-24], we know that...

When the authors code the references, please ensure that the order in text is the same as in reference part and also insure the spelling accuracy of the first author's name. Do not code the same citation twice.

PMID requirement

PMID roots in the abstract serial number indexed by PubMed (http://www.ncbi.nlm.nih.gov/entrez/query.fcgi?db=PubMed). The author should supply the PMID for journal citation. For those references that have not been indexed by PubMed, a printed copy of the first page of the full reference should be submitted.

The accuracy of the information of the journal citations is very important. Through reference testing system, the authors and editor could check the authors name, title, journal title, publication date, volume number, start page, and end page. We will interlink all references with PubMed in ASP file so that the readers can read the abstract of the citations online immediately.

Style for journal references

Authors: the first author should be typed in bold-faced letter. The surname of all authors should be typed with the initial letter capitalized and followed by their name in abbreviation (For example, Lian-Sheng Ma is abbreviated as Ma LS, Bo-Rong Pan as Pan BR). Title of the cited article and italicized journal title (Journal title should be in its abbreviation form as shown in PubMed), publication date, volume number (in black), start page, and end page [PMID: 11819634]

Note: The author should test the references through reference testing system (http://www.wjgnet.com/cgi-bin/index.pl)

Style for book references

Authors: the first author should be typed in bold-faced letter. The surname of all authors should be typed with the initial letter capitalized and followed by their name in abbreviation (For example, Lian-Sheng Ma is abbreviated as Ma LS, Bo-Rong Pan as Pan BR) Book title. Publication number. Publication place: Publication press, Year: start page and end page.

Format

Journals

English journal article (list all authors and include the PMID where applicable)

1 **Grover VP**, Dresner MA, Forton DM, Counsell S, Larkman DJ, Patel N, Thomas HC, Taylor-Robinson SD. Current and future applications of magnetic resonance imaging and spectroscopy of the brain in hepatic encephalopathy. *World J Gastroenterol* 2006; **12**: 2969-2978 [PMID: 16718775]

Chinese journal article (list all authors and include the PMID where applicable)

2 **Lin GZ**, Wang XZ, Wang P, Lin J, Yang FD. Immunologic effect of Jianpi Yishen decoction in treatment of Pixu-diarrhoea. *Shijie Huaren Xiaohua Zazhi* 1999; **7**: 285-287

In press

3 **Tian D**, Araki H, Stahl E, Bergelson J, Kreitman M. Signature of balancing selection in Arabidopsis. *Proc Natl Acad Sci U S A* 2006; In press

Organization as author

4 **Diabetes Prevention Program Research Group**. Hypertension, insulin, and proinsulin in participants with impaired glucose tolerance. *Hypertension* 2002; **40**: 679-686 [PMID: 12411462]

Both personal authors and an organization as author

5 **Vallancien G**, Emberton M, Harving N, van Moorselaar RJ; Alf-One Study Group. Sexual dysfunction in 1, 274 European men suffering from lower urinary tract symptoms. *J Urol* 2003; **169**: 2257-2261 [PMID: 12771764]

No author given

6 21st century heart solution may have a sting in the tail. *BMJ* 2002; **325**: 184 [PMID: 12142303]

Volume with supplement

7 **Geraud G**, Spierings EL, Keywood C. Tolerability and safety of frovatriptan with short- and long-term use for treatment of migraine and in comparison with sumatriptan. *Headache* 2002; **42** Suppl 2: S93-99 [PMID: 12028325]

Issue with no volume

8 **Banit DM**, Kaufer H, Hartford JM. Intraoperative frozen section analysis in revision total joint arthroplasty. *Clin Orthop Relat Res* 2002; (**401**): 230-238 [PMID: 12151900]

No volume or issue

9 Outreach: bringing HIV-positive individuals into care. *HRSA Careaction* 2002; 1-6 [PMID: 12154804]

Books

Personal author(s)

10 **Sherlock S**, Dooley J. Diseases of the liver and billiary system. 9th ed. Oxford: Blackwell Sci Pub, 1993: 258-296

Chapter in a book (list all authors)

11 **Lam SK**. Academic investigator's perspectives of medical treatment for peptic ulcer. In: Swabb EA, Azabo S. Ulcer disease: investigation and basis for therapy. New York: Marcel Dekker, 1991: 431-450

Author(s) and editor(s)

12 **Breedlove GK**, Schorfheide AM. Adolescent pregnancy. 2nd ed. Wieczorek RR, editor. White Plains (NY): March of Dimes Education Services, 2001: 20-34

Conference proceedings

13 **Harnden P**, Joffe JK, Jones WG, editors. Germ cell tumours V. Proceedings of the 5th Germ Cell Tumour Conference; 2001 Sep 13-15; Leeds, UK. New York: Springer, 2002: 30-56

Conference paper

14 **Christensen S**, Oppacher F. An analysis of Koza's computational effort statistic for genetic programming. In: Foster JA, Lutton E, Miller J, Ryan C, Tettamanzi AG, editors. Genetic programming. EuroGP 2002: Proceedings of the 5th European Conference on Genetic Programming; 2002 Apr 3-5; Kinsdale, Ireland. Berlin: Springer, 2002: 182-191

Electronic journal (list all authors)

Morse SS. Factors in the emergence of infectious diseases. Emerg Infect Dis serial online, 1995-01-03, cited 1996-06-05; 1(1): 24 screens. Available from: URL: http//www.cdc.gov/ncidod/EID/eid.htm

Patent (list all authors)

16 **Pagedas AC**, inventor; Ancel Surgical R&D Inc., assignee. Flexible endoscopic grasping and cutting device and positioning tool assembly. United States patent US 20020103498. 2002 Aug 1

Inappropriate references

Authors should always cite references that are relevant to their article, and avoid any inappropriate references. Inappropriate references include those that are linked with a hyphen and the difference between the two numbers at two sides of the hyphen is more than 5. For example, [1-6], [2-14] and [1, 3, 4-10, 22] are all considered as inappropriate references. Authors should not cite their own unrelated published articles.

Statistical data

Present as mean ± SD or mean ± SE.

Statistical expression

Express *t* test as *t* (in italics), *F* test as *F* (in italics), chi square test as χ^2 (in Greek), related coefficient as *r* (in italics), degree of freedom as γ (in Greek), sample number as *n* (in italics), and probability as *P* (in italics).

Units

Use SI units. For example: body mass, m (B) = 78 kg; blood pressure, *p*(B) = 16.2/12.3 kPa; incubation time, t (incubation) = 96 h, blood glucose concentration, c (glucose) 6.4 ± 2.1 mmol/L; blood CEA mass concentration, p (CEA) = 8.6 24.5 μg/L; CO_2 volume fraction, 50 mL/L CO_2 not 5% CO_2; likewise for 40 g/L formaldehyde, not 10% formalin; and mass fraction, 8 ng/g, *etc.* Arabic numerals such as 23, 243, 641 should be read 23 243 641.

The format about how to accurately write common units and quantum is at: http://www.wjgnet.com/wjg/help/15.doc

Abbreviations
Standard abbreviations should be defined in the abstract and on first mention in the text. In general, terms should not be abbreviated unless they are used repeatedly and the abbreviation is helpful to the reader. Permissible abbreviations are listed in Units, Symbols and Abbreviations: A Guide for Biological and Medical Editors and Authors (Ed. Baron DN, 1988) published by The Royal Society of Medicine, London. Certain commonly used abbreviations, such as DNA, RNA, HIV, LD50, PCR, HBV, ECG, WBC, RBC, CT, ESR, CSF, IgG, ELISA, PBS, ATP, EDTA, mAb, can be used directly without further mention.

Italics
Quantities: *t* time or temperature, *c* concentration, *A* area, *l* length, *m* mass, *V* volume.
Genotypes: *gyr*A, *arg* 1, *c myc*, *c fos*, *etc.*
Restriction enzymes: *Eco*RI, *Hin*dI, *Bam*HI, *Kbo* I, *Kpn* I, *etc.*
Biology: *H pylori, E coli, etc.*

SUBMISSION OF THE REVISED MANUSCRIPTS AFTER ACCEPTED

Please revise your article according to the revision policies of *WJG*. The revised version including manuscript and high-resolution image figures (if any) should be copied on a floppy or compact disk. Author should send the revised manuscript, along with printed high-resolution color or black and white photos, copyright transfer letter, the final check list for authors, and responses to reviewers by a courier (such as EMS) (submission of revised manuscript by e-mail or on the *WJG* Editorial Office Online System is NOT available at present).

Language evaluation
The language of a manuscript will be graded before sending for revision. (1) Grade A: priority publishing; (2) Grade B: minor language polishing; (3) Grade C: a great deal of language polishing; (4) Grade D: rejected. The revised articles should be in grade B or grade A.

Copyright assignment form
Please downloaded CAF from http://www.wjgnet.com/wjg/help/9.doc.

We certify that the material contained in this manuscript:

Ms:

Title:

is original, except when appropriately referenced to other sources, and that written permission has been granted by any existing copyright holders. We agree to transfer to WJG all rights of our manuscript, including: (1) all copyright ownership in all print and electronic formats; (2) the right to grant permission to republish or reprint the stated material in whole or in part, with or without a fee; (3) the right to print copies for free distribution or sale; (4) the right to republish the stated material in a collection of articles or in any other format. We also agree that our article be put on the Internet.

Criteria for authorship: The WJG requests and publishes information about contributions of each author named to the submitted study. Authorship credit should be based on (1)direct participation in the study, including substantial contributions to conception and design of study, or acquisition of data, or analysis and interpretation of data; (2) manuscript writing, including drafting the article, or revising it critically for important intellectual content; (3)supportive work, including statistical analysis of data, or acquisition of funding, or administration, technology and materials support, or supervision, or supportive contributions. Authors should meet at least one of the three conditions. The WJG does not publish co-first authors and co-corresponding authors.

We hereby assign copyright transfer to WJG if this paper is accepted.

Author Name in full (Full names should be provided, with first name first, followed by middle names and family name at the last, eg, Eamonn MM Quigley). Handwritten names are not accepted.

Author Name in abbreviation (Family name is put first in full, followed by middle names and first name in abbreviation with first letter in capital, eg, Quigley EMM). Handwritten names are not accepted.

1 Full Name: _____
Abbreviation Name: _____
Signed: _____
Date: _____

2 Full Name: _____
Abbreviation Name: _____
Signed: _____
Date: _____

3 Full Name: _____
Abbreviation Name: _____
Signed: _____
Date: _____

4 Full Name: _____
Abbreviation Name: _____
Signed: _____
Date: _____

5 Full Name: _____
Abbreviation Name: _____
Signed: _____
Date: _____

6 Full Name: _____
Abbreviation Name: _____
Signed: _____
Date: _____

7 Full Name: _____
Abbreviation Name: _____
Signed: _____
Date: _____

8 Full Name: _____
Abbreviation Name: _____
Signed: _____
Date: _____

9 Full Name: _____
Abbreviation Name: _____
Signed: _____
Date: _____

10 Full Name: _____
Abbreviation Name: _____
Signed: _____
Date: _____

Final check list for authors
The format is at: http://www.wjgnet.com/wjg/help/13.doc

Responses to reviewers
Please revise your article according to the comments/suggestions of reviewers. The format for responses to the reviewers' comments is at: http://www.wjgnet.com/wjg/help/10.doc

Proof of financial support
For paper supported by a foundation, authors should provide a copy of the document and serial number of the foundation.

Publication fee
Authors of accepted articles must pay publication fee.
EDITORIAL and LETTERS TO THE EDITOR are free of change.